ADVANCES IN
QUANTUM CHEMISTRY

EDITED BY

PER-OLOV LÖWDIN

DEPARTMENT OF QUANTUM CHEMISTRY
UPPSALA UNIVERSITY
UPPSALA, SWEDEN
AND
QUANTUM THEORY PROJECT
UNIVERSITY OF FLORIDA
GAINESVILLE, FLORIDA

VOLUME 11—1978

ACADEMIC PRESS New York · San Francisco · London
A Subsidiary of Harcourt Brace Jovanovich, Publishers

ACADEMIC PRESS, INC.
111 Fifth Avenue, New York, New York 10003

United Kingdom Edition published by
ACADEMIC PRESS, INC. (LONDON) LTD.
24/28 Oval Road, London NW1 7DX

LIBRARY OF CONGRESS CATALOG CARD NUMBER: 64-8029

ISBN 0-12-034811-X

PRINTED IN THE UNITED STATES OF AMERICA

LIST OF CONTRIBUTORS

Numbers in parentheses indicate the pages on which the authors' contributions begin.

Sadhan Basu, Department of Chemistry, University College of Science, Calcutta-700 009, India (33)

R. A. Bonham, Department of Chemistry, University of Indiana, Bloomington, Indiana 47401 (1)

Dennis Caldwell, Department of Chemistry, University of Utah, Salt Lake City, Utah 84112 (93)

G. Drukarev, Leningrad State University, Leningrad, USSR (251)

Henry Eyring, Department of Chemistry, University of Utah, Salt Lake City, Utah 84112 (93)

Kenichi Fukui, Department of Hydrocarbon Chemistry, Faculty of Engineering, Kyoto University, Kyoto, Japan (195)

Christian Klixbüll Jørgensen, Département de Chimie Minérale, Analytique et Appliquée, Université de Geneve, CH 1211 Geneva 4, Switzerland (51)

R. Kennerly, Department of Chemistry, University of Indiana, Bloomington, Indiana 47401 (1)

J. S. Lee, Department of Chemistry, University of Indiana, Bloomington, Indiana 47401 (1)

F. A. Matsen, Departments of Physics and Chemistry, University of Texas, Austin, Texas 78712 (223)

Jens Oddershede, Department of Chemistry, Odense University, DK-5230 Odense M, Denmark (275)

Pekka Pyykkö, Department of Physical Chemistry, Åbo Akademi, SF-20500 Åbo (Turku), Finland (353)

Eolo Scrocco, Laboratorio di Chimica Quantistica ed Energetica Molecolare del Concilio Nationale delle Ricerche, Pisa, Italia (115)

Gunnar Sperber*, Quantum Chemistry Group, University of Uppsala, Box 518, S-751 20 Uppsala, Sweden (411)

---

* *Present Address:* Åkervagen 2, S-752 51 Uppsala, Sweden.

W. ST. JOHN, Department of Chemistry, University of Indiana, Bloomington, Indiana 47401 (1)

AKITOMO TACHIBANA, Department of Hydrocarbon Chemistry, Faculty of Engineering, Kyoto University, Kyoto, Japan (195)

JACOPO TOMASI, Laboratorio di Chimica Quantistica ed Energetica Molecolare del Concilio Nationale delle Ricerche, Pisa, Italia (115)

TOKIO YAMABE, Department of Hydrocarbon Chemistry, Faculty of Engineering, Kyoto University, Kyoto, Japan (195)

PREFACE

In investigating the highly different phenomena in nature, scientists have always tried to find some fundamental principles that can explain the variety from a basic unity. Today they have not only shown that all the various kinds of matter are built up from a rather limited number of atoms, but also that these atoms are constituted of a few basic elements of building blocks. It seems possible to understand the innermost structure of matter and its behavior in terms of a few elementary particles: electrons, protons, neutrons, photons, etc., and their interactions. Since these particles obey not the laws of classical physics but the rules of modern quantum theory of wave mechanics established in 1925, there has developed a new field of "quantum science" which deals with the explanation of nature on this ground.

Quantum chemistry deals particularly with the electronic structure of atoms, molecules, and crystalline matter and describes it in terms of electronic wave patterns. It uses physical and chemical insight, sophisticated mathematics, and high-speed computers to solve the wave equations and achieve its results. Its goals are great, but perhaps the new field can better boast of its conceptual framework than of its numerical accomplishments. It provides a unification of the natural sciences that was previously inconceivable, and the modern development of cellular biology shows that the life sciences are now, in turn, using the same basis. "Quantum biology" is a new field which describes the life processes and the functioning of the cell on a molecular and submolecular level.

Quantum chemistry is hence a rapidly developing field which falls between the historically established areas of mathematics, physics, chemistry, and biology. As a result there is a wide diversity of backgrounds among those interested in quantum chemistry. Since the results of the research are reported in periodicals of many different types, it has become increasingly difficult for both the expert and the nonexpert to follow the rapid development in this new borderline area.

The purpose of this serial publication is to try to present a survey of the current development of quantum chemistry as it is seen by a number of the internationally leading research workers in various countries. The authors have been invited to give their personal points of view of the subject freely and without severe space limitations. No attempts have been made to avoid overlap—on the contrary, it has seemed desirable to have certain important research areas reviewed from different points of view. The response from the authors has been so encouraging that a twelfth volume is now being prepared.

The editor would like to thank the authors for their contributions which give an interesting picture of the current status of selected parts of quantum chemistry. The topics covered in this volume include studies of atomic and molecular structure, collision phenomena, electronic and photoelectron spectra, as well as method developments including the extended use of the unitary group, propagator theory, and relativistic considerations. Some of the papers emphasize studies in fundamental quantum theory and quantum statistics, and others applications to comparatively complicated systems.

It is our hope that the collection of surveys of various parts of quantum chemistry and its advances presented here will prove to be valuable and stimulating, not only to the active research workers but also to the scientists in neighboring fields of physics, chemistry, and biology, who are turning to the elementary particles and their behavior to explain the details and innermost structure of their experimental phenomena.

PER-OLOV LÖWDIN

ADVANCES IN QUANTUM CHEMISTRY, VOLUME 11

Experimental Measurements of Charge and Momentum Densities, Generalized Oscillator Strengths, and Excitation Frequencies

R. A. BONHAM, J. S. LEE, R. KENNERLY, and W. St. JOHN*
Department of Chemistry
University of Indiana
Bloomington, Indiana

I. Introduction

This paper deals exclusively with the application of high-energy electron impact spectroscopy (HEEIS) to obtain information on charge and momentum densities and generalized oscillator strengths (GOS). It should be noted that the HEEIS method is not the only means of obtaining information on charge densities using electrons as the probe. For example, Fink and co-workers (1976) in Austin, Konaka (1972) in Kimura's laboratory in Sapporo, and Jaeglé *et al.* (1971) in Rouault's laboratory in Orsay have perfected measurements of total electron-scattering cross-section differential with respect to angle. The main theoretical basis for the analysis of such data in terms of charge densities within the framework of the first Born approximation of scattering theory was laid down by Tavard (1965) and by Tavard and Roux (1965). A summary of the early development in this field

---

* The authors gratefully acknowledge the support of this work by the Donors of the Petroleum Research Fund, administered by the American Chemical Society, and by Grant No. GP-41983X the National Science Foundation.

ISBN 0-12-034811-X

can be found in book form (Bonham and Fink, 1974). The most recent and precise information in this field has been presented by M. Fink *et al.* (1976).

Here we are restricted to those experiments in which both the scattering angle and the energy loss of the projectile electron to the target are measured. In such experiments, it is usually possible also to observe the "pure" elastic scattering. We discuss one aspect of this feature of the energy loss spectrum in this paper.

In Fig. 1 a typical set of experimental results is shown. The experimental details are described in the literature (Bonham and Wellenstein, 1973; Wellenstein, 1973; Schmoranzer *et al.*, 1975; Wellenstein *et al.*, 1975). A small-diameter high-energy electron beam impinges upon a narrow gas jet at right angles to the direction of gas flow. Scattered electrons are usually observed at an angle (scattering angle) fixed with respect to the incident electron beam direction by use of collimating slits. The angle-selected scattered electrons are then admitted to an energy analyzer where the energy loss spectrum is recorded. The experiment is then repeated at other angle

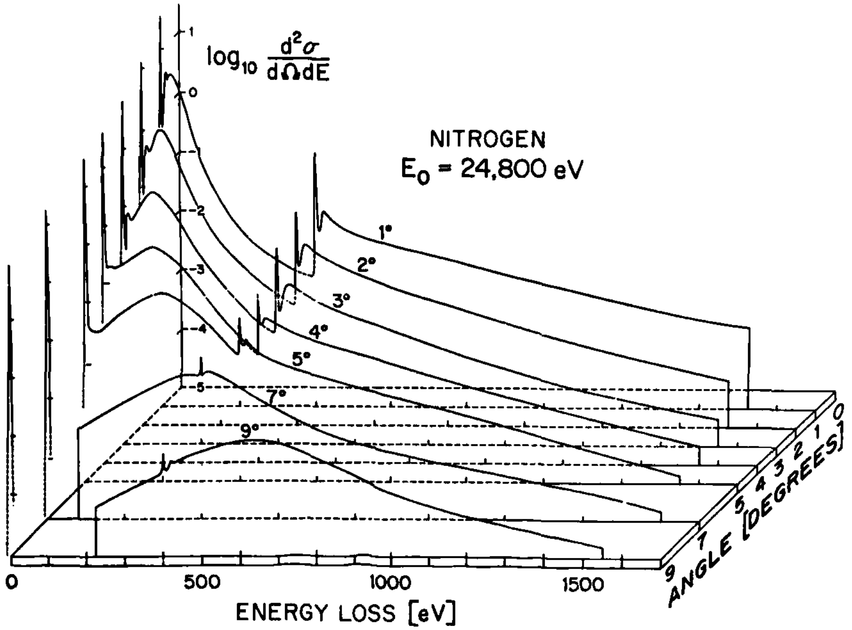

Fig. 1. The cross-section differential with respect to detected solid angle and energy lost to the target on a relative scale for N_2 using 25-keV incident electrons as a function of scattering angle (in degrees) and energy loss (in volts).

settings. The results for molecular nitrogen as a gas target using a 24.8-keV incident electron beam are displayed in Fig. 1. The first sharp feature occurring in each constant-angle cross section of the spectrum at zero energy loss is, of course, the elastic scattering. The most prominent features in the inelastic scattering include: the main dipole-allowed transition at 12.9 eV, which rapidly diminishes in intensity with increasing scattering angle; the valence shell continuum starting at 14.6 eV, whose center of gravity moves to greater-energy loss with increasing scattering angle (we often refer to the shape of this continuum, which is a common feature of all energy loss vs. scattering angle surfaces, as the Bethe ridge); and the strong nitrogen *K*-shell preionization and ionization features at energy losses of 400 and 410 eV, respectively. The bound-state-like preionization peak at 400 eV has usually been attributed to excitation of a single electron from a $1s\sigma_u$ molecular orbital in N_2 to the lowest unoccupied molecular orbital ($2p\pi_g$) (Wight *et al.*, 1972–1973).

Whenever the first Born theory is applicable, we may use it to predict the elastic scattering from a knowledge of the one-electron charge density (Bonham and Fink, 1974) (diagonal first-order charge-density matrix). The total inelastic scattering (integrated over all energy losses) at small angles ($<6°$) can be computed from a knowledge of the one-electron charge density and the electron-pair correlation function (Bonham and Fink, 1974) (diagonal second-order charge-density matrix with origin transferred from the nucleus or center of mass to one of the two electrons and integrated over the remaining electron–nuclear coordinate). On the other hand, for larger scattering angles the shape of the Bethe ridge can be related to the momentum distribution (diagonal first-order momentum density matrix) of target electrons by use of an impulse or binary-encounter-type theory (Bonham and Fink, 1974). The details of these connections are outlined in the following sections. It suffices here to point out that in a single experiment a great deal of detailed and potentially useful information can be obtained about quantities directly derivable from quantum mechanical calculations.

Recently, a great deal of theoretical effort has been devoted to equations-of-motion-type theories (cf. McCurdy and McKoy, 1974) that produce transmission probabilities and excitation frequencies as their primary output as opposed to the usual wavefunctions and state energies. Such approaches should be encouraged since their products are directly observable by experiment without recourse to what are sometimes tedious calculations of the appropriate transition matrices using the necessarily complex initial- and final-state wavefunctions. It thus appears appropriate in this paper also to review our experimental progress and current capabilities in this area. This seems especially pertinent since some of the information now available and the corresponding areas of deficiencies in the theoretical understanding of new experimental techniques are not yet widely appreciated by the quantum chemistry fraternity. In this connection, sections are included in this paper on observation of forbidden transitions by study of the angular or momentum transfer dependence of spectral intensities, observation and interpretation of extended X-ray absorption fine structure (EXAFS), and pulsed electron beam time-of-flight (TOF) observation of secondary electron spectra.

II. The Bethe–Born Theory of Inelastic Electron Scattering and the Bethe Surface

The Bethe–Born theory has recently been reviewed by Inokuti (1971). Further applications of the theory to charge-density determinations can be found in Bonham and Fink (1974). The theory is entirely equivalent to treating the scattering of an incident electron by an atom or molecule by first-order Rayleigh–Schrödinger perturbation theory with the zeroth-order wavefunction chosen as a plane wave in the incident direction. The nonrelativistic scattering cross-section differential with respect to the solid angle of observation Ω and the energy E transferred to the target in the scattering process is, with neglect of exchange, given in this approximation by

$$\frac{d^2\sigma}{d\Omega\, dE} = \frac{4k_n}{k_0 K^4} \left| \langle \Psi_0 | \sum_{i=1}^{N} e^{i\mathbf{K}\cdot\mathbf{r}_i} | \Psi_n \rangle \right|^2, \tag{1}$$

k_0 and k_n $[k_n = (k_0^2 - E)^{1/2}]$ are the magnitudes of the initial and final momenta of the scattered electron, K is the magnitude of the momentum transferred to the target ($K^2 = k_0^2 + k_n^2 - 2k_0 k_n \cos\theta$, where θ is the scattering angle), Ψ_0 and Ψ_n represent the initial- and final-state wavefunctions describing the target before and after the collision, and $\mathbf{r}_i$ is the instantaneous position of the ith of N target electrons. All units here and in the remainder of this paper are Rydberg atomic units.

For some purposes it is convenient to write Eq. (1) as

$$\frac{d^2\sigma}{d\Omega\, dE} = \frac{k_n}{k_0} \left(\frac{d\sigma}{d\Omega}\right)_R \left(\frac{K^2}{E}\right) \begin{cases} f(K,E) \\ \dfrac{df(K,E)}{dE} \end{cases}, \tag{2}$$

where $(d\sigma/d\Omega)_R = 4/K^4$ is the Rutherford cross section and

$$f(K,E) = E \left| \langle \Psi_0 | \sum_{i=1}^{N} e^{i\mathbf{K}\cdot\mathbf{r}_i} | \Psi_n \rangle \right|^2 / K^2 \tag{3}$$

is the GOS for bound-state transitions. For the continuum

$$\frac{df(K,E)}{dE} = \sum_l E_l \left| \langle \Psi_0 | \sum_{i=1}^{N} e^{i\mathbf{K}\cdot \mathbf{r}_i} | \Psi_l \rangle \right|^2 \delta(E - E_l)/K^2, \tag{4}$$

where $df(K, E)/dE$ is the GOS per unit energy loss and the sum over l is over all possible excitation processes that can be excited by the energy transfer E, with energy conservation imposed by the Dirac delta function $\delta(E - E_l)$. Equation (2) is an especially convenient form since it allows comparisons to be made with the corresponding Born theory for X-ray or γ-ray photon scattering, for which the same cross section can be written as (Bloch and Mendelsohn, 1974)

$$\left(\frac{d^2\sigma}{d\Omega\, dE}\right)_{XR-\gamma} = \frac{E_n}{E_0}\left(\frac{d\sigma}{d\Omega}\right)_T \left(\frac{K^2}{E}\right)\frac{df(K,E)}{dE}, \tag{5}$$

where (E_n/E_0) is the ratio of scattered to incident X-ray energy, $(d\sigma/d\Omega)_T = (1/c^4)[\frac{1}{2}(1 + \cos^2\theta)]$ is the Thompson cross section for scattering of an unpolarized X-ray beam by an electron with θ the scattering angle and c the velocity of light. Note that only the continuum case has been considered in Eq. (5). The ratio of X-ray or γ-ray scattering to electron scattering is nearly the ratio of the Thompson to Rutherford cross sections for small-to-medium energy losses and high incident energies. This ratio is about 10^{-9}–10^{-4} over the momentum transfer range $1 < K < 10$ a.u. This illustrates one of the main advantages of using electrons rather than photons as a structural probe for gas phase studies.

In the limit as the scattering angle shrinks to zero, which is almost synonymous with $K = 0$ for high incident electron energies ($k_0^2 > 500$ eV), Eq. (2) (to first order in E/k_0^2) reduces to

$$\frac{d^2\sigma}{d\Omega\, dE} = \frac{16k^2}{E^3}\begin{cases} f(E) \\ \dfrac{df(E)}{dE}, \end{cases} \tag{6}$$

where the oscillator strengths are given as

$$f(E) = E\left| \langle \Psi_0 | \sum_{i=1}^{N} z_i | \Psi_n \rangle \right|^2 \tag{7}$$

and

$$\frac{df(E)}{dE} = \sum_l E_l \left| \langle \Psi_0 | \sum_{i=1}^{N} z_i | \Psi_l \rangle \right|^2 \delta(E - E_l) \tag{8}$$

in terms of transition dipole matrix elements with the direction of momentum transfer **K** selected as the z axis. For small-energy losses this direction is almost perpendicular to the direction of propagation of the electron beam. For photon absorption, the cross section in Rydberg units is (Fano and Cooper, 1968)

$$\frac{d\sigma}{dE} = \frac{\pi}{c}\left\{\begin{array}{l} f(E) \\ \dfrac{df(E)}{dE}. \end{array}\right. \tag{9}$$

We note that Eqs. (6) and (9) are somewhat similar and can be compared providing we integrate Eq. (6) over the detector acceptance angle. The ratio of photon absorption to electron impact intensity is approximately $\pi E^3/16k^2c\, d\Omega$, which favors the electron impact case for high incident electron energies and small-energy losses provided that the detector solid angle is not too small. The photon absorption process is definitely favored at high-energy losses, but the ready availability of electron sources that are 10^5–10^6 times brighter than the most intense, currently available, synchrotron radiation sources gives the intensity advantage to the electron method for energy losses as large as 1 keV.

Another advantage of the GOS formalism, besides facilitating comparisons with photon experiments, becomes obvious when one attempts to calculate the total cross sections. For example, the total cross section for bound states, or differential with respect to energy loss for continuum states, is given by

$$\left.\begin{array}{l} \sigma \\ \dfrac{d\sigma}{dE} \end{array}\right\} = \frac{4\pi}{k^2E}\int_{K^2_{\min}}^{K^2_{\max}} d(\ln K^2)\left\{\begin{array}{l} f(K, E) \\ \dfrac{df(K, E)}{dE}, \end{array}\right. \tag{10}$$

where $K^2_{\min}$ and $K^2_{\max}$ are the minimum and maximum values of allowed momentum transfer. For total excitation cross sections for bound-state transitions, Eq. (10) suggests that a plot of the GOS vs. E and $\ln K^2$ would be useful. Such a plot defines a surface, called the Bethe surface, from which a great deal of useful information about the target system can be obtained (Inokuti, 1971). The characteristics of the GOS are such that a cross section at constant E of the Bethe surface lends itself to the calculation of accurate cross sections even when only partial experimental data are available (Inokuti, 1971).

If one desires the total inelastic cross section at energy losses lying in the continuum differential with respect to the solid angle of the detector, then, since

$$\frac{d\sigma}{d\Omega} = \frac{k_n}{k} K^2 \left(\frac{d\sigma}{d\Omega}\right)_R \int_{1/E_{\max}}^{1/E_{\min}} d\left(\frac{1}{E}\right) E \frac{df}{dE}(K, E), \tag{11}$$

a plot of $E(df(K, E)/dE)$ vs. $1/E$ for constant K appears appropriate. Such a plot, termed a Platzman plot (Kim, 1975), is also useful in bringing out subtle features in the energy loss spectrum not obvious in plots of df/dE vs. E.

Other important features of the Bethe surface are certain energy moments of the GOS that are derivable from it. These are defined by

$$S(K, k) = \sum_n E_n^k f(K, E_n) + \int dE E^k \frac{df}{dE}(K, E), \tag{12}$$

where the sum is over all bound states and the integral is over the continuum. For $k = -1$, 0, 1, and 2, Eq. (12) can be reduced exactly to ground-state expectation values (Inokuti, 1971). Perhaps the most useful of these sums are the $k = -1$ and 0 sums, which can be written

$$S(K, -1) = \frac{S(K)}{K^2} \tag{13}$$

and

$$S(K, 0) = N, \tag{14}$$

where $S(K)$ is the X-ray incoherent scattering factor defined as (Bonham and Fink, 1974)

$$S(K) = N - F(K)^2 + \langle \Psi_0 | \sum_{i \neq j} \sum e^{i\mathbf{K} \cdot \mathbf{r}_{ij}} | \Psi_0 \rangle \tag{15}$$

with $F(K) = \langle \Psi_0 | \sum_{i=1}^N e^{i\mathbf{K} \cdot \mathbf{r}_i} | \Psi_0 \rangle$, the X-ray coherent scattering factor. Both $F(K)$ and $S(K)$ can be rewritten in terms of radial charge densities as $S(K) = N - F(K)^2 + \int_0^\infty dr P(r) j_0(Kr)$ and $F(K) = \int_0^\infty dr D(r) j_0(Kr)$, where $j_0(Kr)$ is a zero-order spherical Bessel function, $P(r)$ is the electron-pair correlation function, defined in terms of the diagonal second-order density matrix as

$$P(r) = r_{12}^2 \int d\Omega_{\mathbf{r}_{12}} \int d\mathbf{r}_1 \Gamma^{(2)}(\mathbf{r}_1, \mathbf{r}_{12} - \mathbf{r}_1) \tag{16}$$

and $D(r)$ is the electron radial distribution function given as

$$D(r) = r_1^2 \int d\Omega_{\mathbf{r}_1} \Gamma^{(1)}(\mathbf{r}_1) \tag{17}$$

in terms of the diagonal first-order density matrix. The sum rule in Eq. (14) is called the Bethe sum rule and is a generalization of the Thomas–Kuhn–Reike (TKR) sum rule for the optical oscillator strength (Fano and Cooper, 1968). Equation (14) plays an important part in our work since we use it exclusively to place our experimental relative intensity measurements on an absolute scale.

Extensive Bethe surfaces have been reported in the literature for a number of systems (Inokuti, 1971; Wellenstein *et al.*, 1973; Ulsh *et al.*, 1974) and the Bethe surface for molecular H_2 is reproduced in Fig. 2 as an example. Some of the energy moments of experimentally determined Bethe surfaces have also been given (Wellenstein *et al.*, 1973; Ulsh *et al.*, 1974).

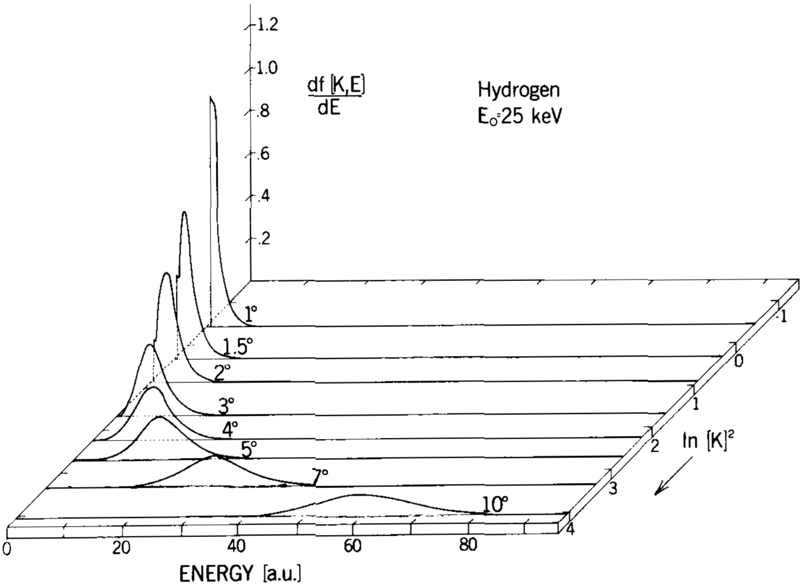

Fig. 2. Bethe surface for H_2 obtained by use of 25-keV incident electrons. (Units are Rydberg atomic units, 1 a.u. of energy = 13.6 eV.)

III. Elastic Scattering and One-Electron Charge Densities

In the first Born approximation the elastic cross section is given by

$$\frac{d\sigma}{d\Omega} = \left(\frac{d\sigma}{d\Omega}\right)_R |f(K)|^2, \tag{18}$$

where for atomic scattering the square of the elastic form factor $f(K)$ averaged over all angles of orientation is given in terms of the one-electron density, $\rho(\mathbf{r})$, and the electron radial distribution, $D(r)$, as

$$\langle |f(K)|^2 \rangle = Z^2 - 2Z \int_0^\infty dr D(r) j_0(Kr) + \int d\mathbf{r}\rho(\mathbf{r}) \int d\mathbf{r}'\rho(\mathbf{r}') j_0(K|\mathbf{r} - \mathbf{r}'|). \tag{19}$$

Tavard (1965) showed that there was a direct connection between certain parts of the average potential energy for the target and the square of the structure factor shown in Eq. (19). This can be most easily observed by considering the integral of the difference between $\langle|f(K)|^2\rangle$ and Z^2 over all values of K as

$$\frac{1}{\pi}\int_0^\infty dK[\langle|f(K)|^2\rangle - Z^2] = -Z\int_0^\infty \frac{dr\,D(r)}{r} + \frac{1}{2}\int d\mathbf{r}\int d\mathbf{r}'\,\frac{\rho(\mathbf{r})\rho(\mathbf{r}')}{|\mathbf{r}-\mathbf{r}'|}$$
$$= \bar{V}_{\mathrm{en}} + \bar{V}^{\mathrm{c}}_{\mathrm{ee}}, \qquad (20)$$

where the upper limit on the integral over K can be extended to ∞ provided that $\langle|f(K)|^2\rangle$ effectively approaches the limiting value Z^2 within the experimental K range, $\bar{V}_{\mathrm{en}}$ is the average electron-nuclear attractive potential energy [the term involving $D(r)$], and $\bar{V}^{\mathrm{c}}_{\mathrm{ee}}$ is the average Coulomb electron-electron repulsive potential energy.

The molecular counterpart of Eq. (19) is

$$\langle|f(K)|^2\rangle = \sum_{l=1}^{M} Z_l^2 + \sum_{l=1}^{M}\sum_{l\neq k}^{M} Z_l Z_k j_0(KR_{lk}) - 2\sum_{l=1}^{M} Z_l\int d\mathbf{r}\,\rho(\mathbf{r})j_0(K|\mathbf{r}-\mathbf{R}_l|)$$
$$+ \int d\mathbf{r}\,\rho(\mathbf{r})\int d\mathbf{r}'\,\rho(\mathbf{r}')j_0(K|\mathbf{r}-\mathbf{r}'|) \qquad (21)$$

and the molecular version of Tavard's theorem follows in the same way as in the atomic case with the addition of a new term for the nuclear-nuclear repulsive energy. Of course, all quantities in Eq. (21) must now be averaged over the molecular vibrational motions (Bonham and Fink, 1974).

A number of experiments (Bonham and Fink, 1974) have been reported on the measurement of quantities related to the function

$$N(K) = \langle|f(K)|^2\rangle - \sum_{l=1}^{M}\sum_{k=1}^{M} Z_l Z_k\langle j_0(KR_{lk})\rangle$$

but only one experiment has so far been reported that is a direct measurement of $N(K)$ (Ulsh *et al.*, 1974). A number of calculations of $N(K)$ functions for various diatomic molecules using near-Hartree–Fock (HF) wavefunctions have been given by Kohl and Bartell (1969). The normal manner for presentation of data, in order to place them on a more sensitive scale, is to compute a molecular difference function $\Delta N(K) = N(K)_{\mathrm{expt}} - N(K)_{\mathrm{IAM}}$, where the model $N(K)_{\mathrm{IAM}}$ function is based on the independent atom model (IAM) consisting of a sum of HF ground-state atomic densities averaged over all orientations in space in which these atoms are positioned in the appropriate ground molecular state geometry. The computed and observed difference functions all tend to have qualitatively different shapes.

The most interesting point concerning the observation of $N(K)$ functions is that, unlike X-ray gas scattering, they still possess information concerning the three-dimensional (3-D) nature of the one-electron charge density. This can be observed by expanding $\rho(\mathbf{r})$ and $j_0(K|\mathbf{r}-\mathbf{R}_{kl}|)$ in the third term on the right of the equal sign in Eq. (21) in spherical harmonics and averaging the result over all angles of orientation. The possibility of recovering the 3-D information has been discussed, but the situation is not encouraging because of the slow convergence of spherical harmonic expansions of 3-D charge densities about their centers of mass.

Recently, Stewart and Bentley (1975; Bentley and Stewart, 1975) have published a more detailed analysis of the Kohl–Bartell approach to expanding 3-D charge densities in the context of X-ray scattering. This analysis exhibits a number of properties that make it appear ideal as a possible solution to our problem of extracting 3-D densities from electron elastic scattering. Stewart was able to show that, if 3-D molecular densities for diatomic molecules (and presumably polyatomics) are expanded in spherical harmonics about each nuclear center, then the resulting expansion converges to a high degree of accuracy using only three terms per center. Furthermore, labeling the successive terms monopole, dipole, and quadrupole, the monopole density term appears to be rather close in shape to the HF spherical atom density for the atomic center under expansion. The Fourier transform of the dipole and quadrupole terms are very similar in shape to the gross features observed in $\Delta N(K)$ plots. With these encouraging signs we are led to suggest that the Stewart approach be utilized in the analysis of $N(K)$ experimental data. Because it is known that the value for the higher electric moments depend increasingly on configuration interaction effects, it is tempting to speculate that the monopole density should be the density component most accurately determined by Hartree–Fock calculations. With these ideas in mind we propose the following extensions of Stewart's work to the analysis of elastic electron scattering.

By using Stewart's notation the $N(K)$ function for a diatomic molecule possessing two centers a and b can be written through quadrupole terms as

$$\begin{aligned} N(K) = & -2[Z_a + Z_b j_0(KR_{ab})]f_{a,0}(K) \\ & -2[Z_b + Z_a j_0(KR_{ab})]f_{b,0}(K) \\ & -2Z_b \sum_{j=1}^{2} j_j(KR_{ab}) f_{a,j}(K) \\ & -2Z_a \sum_{k=1}^{2} (-1)^k j_k(KR_{ab}) f_{b,k}(K) \end{aligned}$$

$$
\begin{aligned}
&+ \sum_{j=0}^{2} \frac{1}{(2j+1)} [f^{2}_{a,j}(K) + f^{2}_{b,j}(K)] + 2j_0(KR_{ab}) f_{a,0}(K) f_{b,0}(K) \\
&+ \tfrac{2}{3}[j_0(KR_{ab}) - 2j_2(KR_{ab})] f_{a,1}(K) f_{b,1}(K) \\
&+ 2j_1(KR_{ab})[f_{a,0}(K) f_{b,1}(K) - f_{a,1}(K) f_{b,0}(K)] \\
&+ 2j_2(KR_{ab})[f_{a,0}(K) f_{b,2}(K) + f_{a,2}(K) f_{b,0}(K)] \\
&+ \tfrac{2}{5}[2j_1(KR_{ab}) - 3j_3(KR_{ab})][f_{a,1}(K) f_{b,2}(K) - f_{a,2}(K) f_{b,1}(K)] \\
&+ \tfrac{2}{5}[j_0(KR_{ab}) - \tfrac{10}{7} j_2(KR_{ab}) + \tfrac{18}{7} j_4(KR_{ab})] f_{a,2}(K) f_{b,2}(K) \qquad (22)
\end{aligned}
$$

with all vibrational averaging understood. The generalized scattering factors are defined as

$$
f_{b,k}(K) = \int_0^\infty dr_b\, r_b^2 \rho_{b,k}(r_b) j_k(Kr_b), \qquad (23)
$$

where $\rho_{b,k}(r_b)$ is the kth expansion term of the density about center b. Stewart describes techniques for extracting these density expansion terms from molecular wavefunctions by use of a least squares technique.

In terms of the Stewart model, for $N(K)$ the IAM model yields the expression

$$
\begin{aligned}
N(K)_{IAM} = &-2Z_a f^{HF}_{a,0}(K) - 2Z_a j_0(KR_{ab}) f^{HF}_{b,0}(K) \\
&-2Z_b f^{HF}_{b,0}(K) - 2Z_b j_0(KR_{ab}) f^{HF}_{a,0}(K) \\
&+ (f^{HF}_{a,0}(K))^2 + (f^{HF}_{b,0}(K))^2 + 2 f^{HF}_{a,0}(K) f^{HF}_{b,0}(K) j_0(KR_{ab}), \qquad (24)
\end{aligned}
$$

where the superscript HF labels the atomic, Hartree-Fock, zero-order, generalized scattering factors [i.e., Eq. (23) with $\rho_{b,0}(r) = \rho_b^{HF}(r)$]. Equation (24) can be subtracted from Eq. (22), and a $\Delta N(K)$ model based on this analysis, which might be expected to be approximately given by the leading terms

$$
\begin{aligned}
\Delta N(K) \simeq &-2Z_b j_1(KR_{ab}) f_{a,1}(K) \\
&- 2Z_a j_1(KR_{ab}) f_{b,1}(K) - 2Z_b j_2(KR_{ab}) f_{a,2}(K) \\
&-2Z_a j_2(KR_{ab}) f_{b,2}(KR_{ab}), \qquad (25)
\end{aligned}
$$

can be obtained. This expectation arises from the assumption of a near cancellation of the monopole and IAM terms according to the observation by Stewart that monopole generalized scattering factors are often quite similar to HF atomic structure factors. Equation (23) also relies on the assumption that all terms involving products of two generalized atomic scattering factors can be neglected. To the extent that $\Delta N(K)$ is given by a single-pole contribution in Eq. (25), the weighted sum $Z_b \rho_{a,i}(r) + Z_a \rho_{b,i}(r)$ can be approximately obtained by Fourier–Bessel transform, where $i = 1$ or 2, depending on which pole is dominant.

Further, Stewart's work showed that the dipole and quadrupole generalized scattering factors for heteronuclear diatomics were of opposite sign and tended to have maxima at different values of the momentum transfer K. In fact, the maximum value of $f_{a,2}(K)$ appears to be at a K value almost twice that for the dipole peak value. Hence we can expect to observe a natural separation of the main contributions from dipole and quadrupole terms into different ranges of momentum transfer K. Also it was noted by Stewart that the dipole term in the case of molecular N_2 tended to be very small and the quadrupole was the dominant term. Since new experiments are under way in which only the elastic component will be measured, the analysis proposed here should prove useful.

IV. Inelastic Scattering and the Electron Pair Correlation Function

In principle the electron-pair correlation function, $P(r)$, is indirectly observable by use of the $S(K, -1)$ sum rule from a knowledge of the energy loss dependence of the GOS at constant momentum transfer [see Eq. (13)]. It has been pointed out that the sum rule approach is the most accurate means for obtaining the incoherent X-ray scattering factor, $S(K)$. The connection between $P(r)$, the one-electron density, and $S(K)$ is given in Eqs. (15)–(17). It is only through measurement of the total X-ray scattering that $P(r)$, or in the molecular case its average over all angles of orientations $P_0(r)$, can be obtained directly (Bonham and Fink, 1974).

It is instructive to note that Tavard's theorem for the difference $S(K) - N$ yields

$$\frac{2}{\pi}\int_0^\infty dK[S(K) - N] = \int_0^\infty dr\,\frac{P(r)}{r} - \int d\mathbf{r}\,\rho(\mathbf{r})\int d\mathbf{r}'\,\frac{\rho(\mathbf{r}')}{|\mathbf{r}-\mathbf{r}'|} = \overline{V}_{ee} - \overline{V}_{ee}^{c} = V_{ee}^{ex}, \tag{26}$$

where $\overline{V}_{ee}$ is the total average electron–electron potential energy of the target system, $\overline{V}_{ee}^{c}$ is the average Coulomb electron–electron potential energy, and $\overline{V}_{ee}^{ex}$ is by definition the exchange potential energy. Although an analysis of $P(r)$ may not be possible with inelastic electron data, it is well known that the X-ray coherent scattering factor $S(K)$ is sensitive to the effects of electron correlation (Kohl and Bonham, 1967; Peixoto *et al.*, 1969). Further, $S(K)$ indicates in a very direct manner how energetic contributions to the exchange energy are distributed in momentum space.

So far only two experimental studies have been reported for $S(K)$ by use of electron-scattering techniques (Wellenstein *et al.*, 1973; Ulsh *et al.*, 1974). Work of this type is currently under way in several laboratories. If the analysis suggested in the preceding section bears fruit, it might prove possible to correct experimental $S(K)$ values for the Coulomb contribution and to obtain some estimate of the electron-pair correlation function. The possibility of combining direct elastic and inelastic measurements with total scattering data in the effort to untangle the various contributions might also prove helpful.

V. Forbidden Transitions and High-Momentum Transfer Spectroscopy

In an analysis of a Bethe surface, all possible spectral features within the energy resolution of the experiment are observed at the incident electron energy under study. We have observed in several investigations a number of well-known valence state transitions that are known to be dipole forbidden. What has been surprising, however, is that we have been able to measure several transitions at high-momentum transfer and energy loss that have not apparently been previously reported.

The best-studied example of what we have found is the broad band centered at 31.4 eV in molecular nitrogen (Lee *et al.*, 1975), which is only visible in the energy loss spectrum at momentum transfers greater than about 2 a.u. This feature has been tentatively assigned as a transition from the ${}^1\Sigma_g^+$ ground state to the $(2s\sigma_g)^{-1}$ $(2p\pi_g)^1$ ${}^1\Pi_g$ excited hole state. In an example of close collaboration between theorists and experimentalists, H.-L. Hsu and R. Pitzer (private communication) were able to confirm the existence of our proposed state, in excellent agreement with our observed energy loss value using *a priori* methods, before we had completed our manuscript reporting the observation. The only loose end in this particular case is the large width observed for the peak ($\sim$4.5 eV) which appears to be about 3 times the theoretical value. Possibly other states exist in this region or there is significant interaction with the underlying ionization continuum.

Since the first observation of this type, preliminary observations have been made on transitions that show a similar angular behavior in O_2, NO, and CO_2. In addition, anomalous behavior of known dipole transitions at high-momentum transfer in atoms such as N_2, Ne, and Ar (Wong *et al.*, 1975) appears to suggest the existence of underlying quadrupole bands or possible failure of the first Born approximation of scattering theory. Work is underway to document these qualitative observations and to attempt to make definite spectral assignments.

VI. Compton Profile Measurements and Momentum Distributions

The shape of the Bethe ridge for constant K approximates that of the Compton profile in X-ray scattering, especially as K increases to larger values. The quantitative connection between the GOS and the Compton profile can be shown to be

$$\lim_{K\to\infty} J_{\mathrm{eff}}(q, K) = \lim_{K\to\infty} \frac{2K^3}{E}\frac{df(K, E)}{dE} = J(q) = 2\pi \int_0^\infty dpp\rho(P), \qquad (27)$$

where $\rho(p)$ is the diagonal first-order momentum density averaged over all orientations in space. Equation (27) is equally valid for both atoms and molecules provided that the rotationally averaged molecular momentum density is also averaged over all vibrational degrees of freedom.

A large number of Compton profiles have been measured with X-rays (Williams, 1977). One of the advantages of the X-ray method is that Compton profiles can be obtained for oriented single crystals, thus making it possible to observe asymmetries related to nonspherical effects in the three-dimensional momentum density. Obviously for investigations on bulk properties of solids or liquids the X-ray or γ-ray methods are to be preferred.

Electrons were first used as a probe to investigate Compton profiles by Hughes and Mann (1938). This technique was revived over 30 years later through the use of modern technology (Wellenstein and Bonham, 1973). It has now been shown that reliable values of Compton profiles and momentum densities can be obtained from electron-scattering information (Wellenstein and Bonham, 1973; Bonham and Tavard, 1973). Several recent studies have been carried out in this laboratory on He, H_2, and D_2 (Lee, 1978). In Tables I–III the results for the finite moments of the momentum density (all seven) and the momentum density and its curvature at zero momentum transfer are presented. Tables I and II indicate the reproducibility of our present experiments. The measured Compton profile data were fitted to an analytic expression of the form

$$J(q) = \sum_{n=1}^{M} \frac{a_n}{(q^2 + \xi_n^2)^{2+n}}. \qquad (28)$$

Equation (28) enables us to obtain analytic expressions for the momentum density and its moments in a trivial fashion. In Tables IV and V the average values of the final least-squares parameters for the a_n's and ξ_n's are presented. The successive terms in Eq. (28) represent the leading terms for s, p, d, etc., atomic orbitals at large-target electron momenta (i.e., large q). Care was

TABLE I

Results for the Compton Profile of He at ~ 10°[a]

	Experimental						Theoretical[b]		
	Trial								
Parameters	1	2	3	4	Average		Correlated	RHF	HF[c]
$\langle p^{-2}\rangle$	4.090	4.114	4.138	4.119	4.115	0.020	4.114	4.093	—
$\langle p^{-1}\rangle$	2.128	2.129	2.128	2.128	2.128[d]	0.50×10^{-3}	2.1370[e]	2.141[e]	2.141
$\langle p^{0}\rangle$	1.998	2.001	1.990	1.990	1.995	0.56×10^{-2}	1.997[3]	2.000[e]	—
$\langle p^{1}\rangle$	2.836	2.830	2.825	2.821	2.828	0.64×10^{-2}	2.818	2.798	2.799
$\langle p^{2}\rangle$	5.867	5.757	5.838	5.809	5.818	0.047	5.799[e]	5.709[e]	5.723
$\langle p^{3}\rangle$	17.63	16.59	17.22	17.01	17.11	0.43	17.64	17.78	—
$\langle p^{4}\rangle$	75.79	64.47	64.61	63.35	67.05	5.9	82.0	100.9	105.86
$f(0)$	0.447	0.462	0.463	0.455	0.457	0.74×10^{-2}	0.448	0.440	—
$f''(0)$	−1.74	−2.18	−1.975	−1.821	−1.927	0.190	−1.713	−1.62	—
$\sigma^2 \times 10^6$	4.328	6.785	5.994	3.228	—	—	1.0068×10^{-2}	4.436×10^{-5}	—

[a] Moments were obtained by fitting the Compton profile with five terms of the form $\sum_{n=1}^{5} a_n/[1 + (q/\xi_n)^2]^{n+2}$.

[b] Moments were obtained by fitting the results of R. Benesch (private communication) using a correlated wavefunction that gives an energy for the ground state of 2.9303 (Kohl and Bonham, 1966).

[c] Moments calculated by Sahni *et al.* (1975) using a six-parameter analytic Hartree–Fock wavefunction of P. S. Bagus and T. L. Gilbert.

[d] It should be pointed out here that the average value of $J(0)$ from the interpolated $J(q)$ is 1.069. The discrepancy between the fitted and the average interpolated results may be due to some kind of systematic error that produces a 2–3% fluctuation at the top of the Compton peak even though the statistical uncertainty of the data is less than 1%.

[e] The $\langle p^0\rangle$, $\langle p^2\rangle$, $J(0) = \frac{1}{2}\langle p^{-1}\rangle$, given by the authors in footnote *b*, are 1.997, 5.803, 1.068_5 for the correlated case and 2.000, 5.680, and 1.0705 for the RHF case (function of Clementi).

TABLE II

RESULTS FOR THE COMPTON PROFILE OF H_2 AT ~10° [a]

Parameters	Trial					Average		Theoretical[b]
	1	2	3	4	5			
$\langle p^{-2}\rangle$	8.312	8.308	8.326	8.348	8.302	8.319	.018	8.022
$\langle p^{-1}\rangle$	3.075	3.080	3.085	3.077	3.078	3.079[c]	.004	3.058[d,e]
$\langle p^{0}\rangle$	1.995	1.997	1.995	1.986	1.990	1.993	.005	2.000
$\langle p^{1}\rangle$	1.864	1.861	1.859	1.835	1.850	1.854	.012	1.857
$\langle p^{2}\rangle$	2.370	2.358	2.378	2.277	2.345	2.346	.040	2.342[d]
$\langle p^{3}\rangle$	4.092	4.067	4.244	3.751	4.088	4.048	.181	4.126
$\langle p^{4}\rangle$	10.51	10.55	12.12	8.68	11.06	10.58	1.25	12.02
$\rho(0)$	1.257	1.250	1.246	1.272	1.244	1.254	.011	1.149
$\rho''(0)$	−9.20	−8.99	−8.69	−9.69	−8.77	−9.07	.40	−7.058
$\sigma^2 \times 10^{+5}$	2.578	4.356	5.645	3.020	1.659	—	—	0.0132

[a] Moments were obtained by fitting the Compton profile with a two-term function of the form $\sum_{n=1}^{2} a_n/[1 + (q/\xi_n)^2]^{n+2}$. The average X-ray incoherent scattering factor from the five sets of data is $S(K) = 1.996$.

[b] Moments were obtained by fitting the results of Brown and Smith (1972). Note that their values do not include vibrational corrections.

[c] It should be pointed out here that the average of the interpolated $J(0) = \frac{1}{2}\langle p^{-1}\rangle$ values of the five sets of data is 1.546. The discrepancy between the fitted and the average interpolated results may be due to some kind of systematic error which produces a 2–3% fluctuation at the top of the Compton peak even though the statistical uncertainty of the data is less than 1%.

[d] The values of $J(0) = \frac{1}{2}\langle p^{-1}\rangle$ and $\langle p^2\rangle$ given by the authors of footnote *b* are 1.529 and 2.348, respectively.

[e] A calculated value for $\langle J(0)\rangle_0$ using the Bowen Liu wavefunction for H_2 with a vibrational correction yields the result $\langle J(0)\rangle_0 = 1.5467$ (V. H. Smith, Jr., private communication).

TABLE III

THE COMPTON PROFILE FOR D_2 AT 8° SCATTERING ANGLE ($K = 6$ a.u.)

$\langle p^{-2} \rangle$	8.381	$\langle p^3 \rangle$	4.129
$\langle p^{-1} \rangle$	3.054	$\langle p^4 \rangle$	10.70
$\langle p^0 \rangle$	1.966	$\rho(0)$	1.294
$\langle p^1 \rangle$	1.840	$\rho''(0)$	−9.971
$\langle p^2 \rangle$	2.360	$\sigma^2 \times 10^5$	1.553

TABLE IV

AVERAGE COEFFICIENTS OF THE POLYNOMIAL USED IN FITTING OF THE H_2 COMPTON PROFILE

	Experimental		Theoretical[a]	
n	a_n	ξ_n	a_n	ξ_n
1	1.0012	0.9896	0.9228	1.1237
2	0.5383	1.5566	0.6061	1.3080

[a] See footnote *b* of Table II.

TABLE V

AVERAGE COEFFICIENTS OF THE POLYNOMIAL USED IN FITTING OF THE He COMPTON PROFILE

	Experimental		Theoretical[a]	
n	a_n	ξ_n	a_n	ξ_n
1	−0.0956	2.157	0.03013	1.285
2	0.05137	4.159	0.02196	4.7388
3	0.1342	3.520	0.32592	2.9482
4	0.7316	2.395	0.64227	1.9826
5	0.2426	1.573	0.075317	1.5140

[a] See footnote *b* of Table I.

taken to make sure that a true minimum was obtained and the same fits were made to theoretical data as shown in Tables I and II. In spite of the similar standard deviations (a factor of about 5 difference in the standard deviation for the fit), the nature of the functional dependence for He and H_2 are obviously quite different. This suggests the feasibility of extracting different types of information from Compton profile data by use of judicious choices for the form of the analytic model.

Recently, Lassettre (1976) has considered the constraints imposed on the analytic form for the one-electron momentum density if one adopts an atomic or molecular orbital description of the target in which each orbital is itself a solution of a one-electron Schrödinger equation with an effective local potential. The applicability of such a model to real systems is suggested by the success of the $X\alpha$ model and by electron-spectroscopy chemical analysis (ESCA) and (e, 2e) experiments. Lassettre has shown that in the molecular case, the momentum density for the jth molecular orbital (MO) can be written in the form

$$\rho_j(\mathbf{P}) = \frac{1}{(P^2 + P_j^2)^4} \sum_{m=1}^{M} \sum_{n=1}^{M} C_m^*(\mathbf{P}) C_n(\mathbf{P}) e^{i \mathbf{P} \cdot \mathbf{R}_{mn}}, \tag{29}$$

where P_j^2 is the binding energy of an electron in the jth MO. The sum in Eq. (29) is carried out over the M nuclear centers in the molecule, and $\rho_j(\mathbf{P})$ must be averaged over all angles of orientation of the molecule in order to account for rotationally inelastic scattering (Iijima *et al.*, 1963). In addition, an average over the molecular vibrational motion is required. The dependence of the coefficients $C_m(\mathbf{P})$ on $\mathbf{P}$ is directly related to the choice of the effective potential and, of course, to the molecular symmetry. The quality of the data presented here suggest that least-squares fits of analytic models derived from appropriate effective local potentials may prove useful.

The data presented in Tables I–III also settle a long-standing controversy between experiment and theory concerning the momentum density for the H_2 molecule. Early X-ray, γ-ray, and (e, 2e) experiments all indicated a certain degree of mutual consistency for both He and H_2. These results agreed with theory for He but not for H_2. Since the discovery of this disagreement, the (e, 2e) work was repeated and an error in the original experiment was uncovered. The new results are now in substantial agreement with theory (Dey *et al.*, 1975). The results presented here are also in substantial agreement with theory, and we are forced to conclude that the error analysis used in our earlier study did not properly consider all possible sources of systematic uncertainty, thus leading to error estimates that were unrealistically small. The present work takes advantage of several instrumental improvements but even with increased precision the uncertainties as judged by experimental reproducibility are not much better than 1% in the best cases. The X-ray work has not yet been repeated, but it is assumed that the basic cause of the discrepancy in our work (failure to account for all sources of systematic error properly) may also apply to the X-ray work.

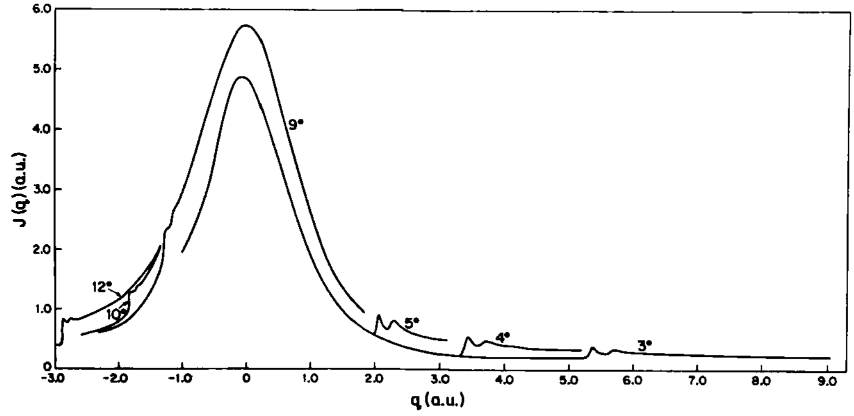

Fig. 3. Compton profiles for N_2 as a function of momentum transfer (scattering angle) as given in Wong *et al.* (1975) using 25-keV incident electrons.

In arriving at the results quoted in Tables I–III some care was exercised in making certain that the binary encounter limit is reached. This was done by measuring $J_{\text{eff}}(q, K)$ as a function of K and making certain that the effective profile value for a given value of q had, indeed, reached its binary encounter limit.

In Figs. 3 and 4, plots of $J_{\text{eff}}(q, K)$ vs. q as a function of K for N_2 and

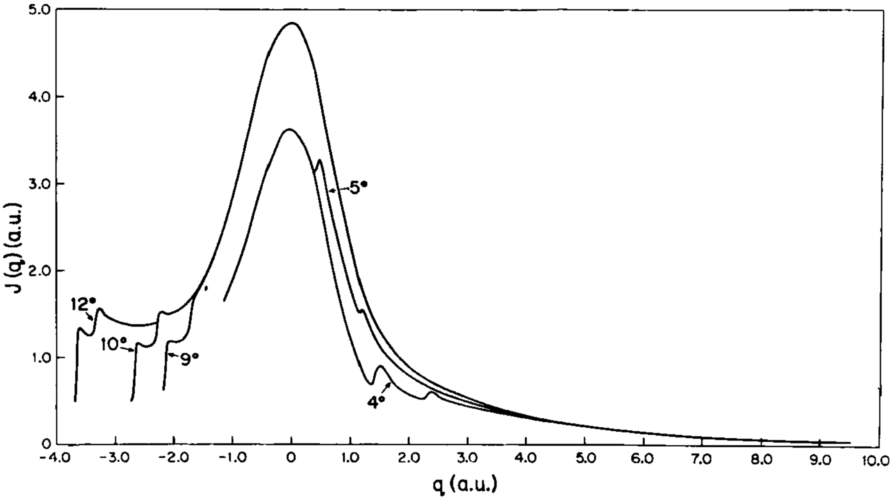

Fig. 4. Compton profiles for Ar as a function of momentum transfer (scattering angle) as given in Wong *et al.* (1975) using 25-keV incident electrons.

Ar are presented. These more complicated targets have more than one electronic shell, and the figures illustrate the striking dependence of $J_{\mathrm{eff}}(q, K)$ on the shell structure. Basically what happens is that the natural separation in energy loss of the spectral contributions from different shells enables us to define separate Compton profiles (or regions thereof) for the cumulative sum of the shells of the target system provided that the shell-binding energies are well separated. For example, Fig. 2 clearly displays an effective valence shell Compton profile at small momentum transfer (scattering angles of 3°–5°), and the valence plus core or total Compton profile at higher momentum transfer. In the case of Ar one observes (see Fig. 4) the M shell and $M + L$ shell Compton profiles. It would appear that it should be possible to use the results of (e, $2e$) experiments at the same K values to correlate with our results. So far this has not been done.

Our analysis of valence or cumulative shell Compton profiles in terms of the predictions of theory using ground-state momentum densities shows that experiments agree with theory only at about the 5% accuracy level. It is significant that the experimental profiles are always sharper than those predicted by theory. This is important because our previous problems with H_2 demonstrated that all known systematic experimental errors have the opposite effect. It is interesting to note that calculations employing the GOS with Coulomb wave simulation of the ejected electron and near-Hartree–Fock wavefunction descriptions of the final ion state yield results for the separate shell Compton profiles that are in much better agreement with experiment (1–2%) (Bloch and Mendelsohn, 1974). We are thus forced to conclude that, whereas plateau behavior in $J_{\mathrm{eff}}(q, K)$ vs. K at fixed q exists, the effective Compton profile in a given plateau region still retains some explicit dependence on the nature of the final states involved in the ionization process.

VII. Inner-Shell Spectroscopy and Extended X-Ray Absorption Fine Structure

In the case of molecular inner-shell ionization, the region above an ionization edge can display a wealth of spectroscopic features. In focusing on small momentum transfer energy loss spectra, analogous to photoabsorption spectra, we already know from many years of X-ray spectral studies that the features above an X-ray edge are divided roughly into two regions. The first such region extending from the edge itself to about 50 eV above the edge is termed the Kössel region (Dey *et al.*, 1975) and the remaining region, the Kronig (1931, 1932) or extended X-ray absorption fine structure region (EXAFS). In the molecular case, ionization of an electron with energy loss in the Kössel region produces an ejected electron with low kinetic energy (0–50 eV), which, since it comes from an inner shell, has a localized point of origin. If the emitting or ionized atom is surrounded by neighbors, the low-energy ejected electron may encounter a potential barrier hindering escape to the outside world. As is well known from quantum mechanics, electrons trapped in wells, even metastable ones, tend to exhibit the phenomena of state formation. In the case of metastable wells, such states are called shape resonances, and a reasonable description of such resonances can be made in lowest order by assuming a simple one-electron model. Hence we can differentiate mechanistically between such shape resonances and the two-electron shake-up and shake-off peaks found in ESCA studies (Carlson and Nestar, 1973). Figures 5–7 show the *K* and *L* ionization for S in SF_6 and the *K* edge for F in the same molecule. These data were recently obtained in this laboratory (St. John *et al.*, 1978). Note the rich and prominent structure in the Kössel region. Dehmer (1972) has discussed the systematics of such shape resonances and has pointed out that they can be used to define the valence state of the observed atom. We intend to pursue these observations experimentally. Although the subject of EXAFS as an analytic tool is currently a "hot" subject, it appears that

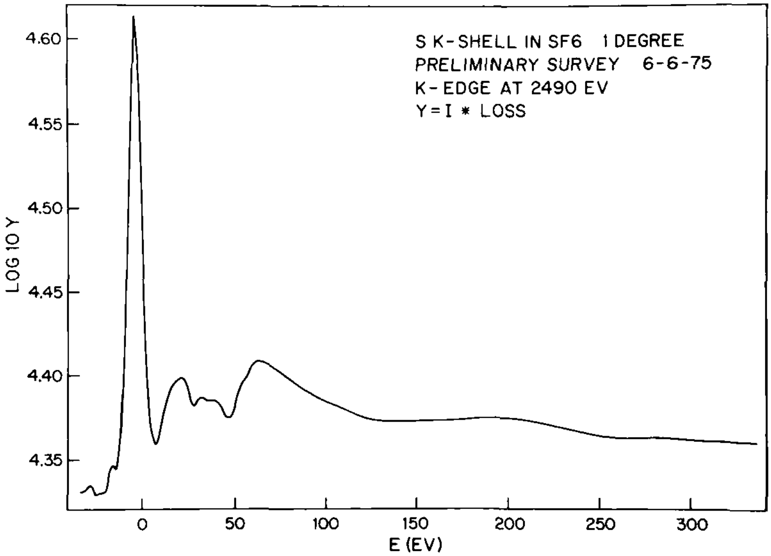

Fig. 5. The small-angle energy loss spectrum (0.5°) of SF_6 obtained with 25-keV incident electrons for the *S-K* shell energy loss range 2,400–2,800 eV. Note that the vertical scale is arbitrary but the intensity has been leveled by multiplication by the energy loss *E*, and the horizontal scale is given in terms of the kinetic energy of the ejected electron in electron volts relative to the *S-K* edge.

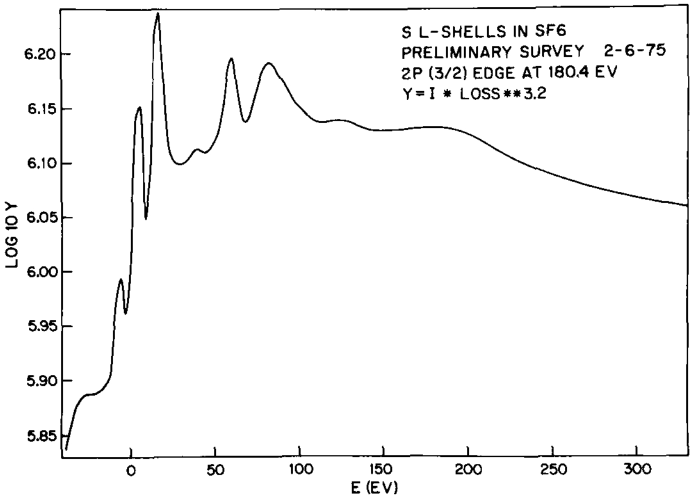

Fig. 6. The small-angle energy loss spectrum (0.5°) of SF_6 obtained with 25-keV incident electrons for the *S-L* shell energy loss range 180–500 eV. Note that the vertical scale is arbitrary but the intensity has been leveled by multiplication by the energy loss raised to the 3.2 power, and the horizontal scale is given in terms of the kinetic energy of the ejected electron in electron volts relative to the *S-L* edge.

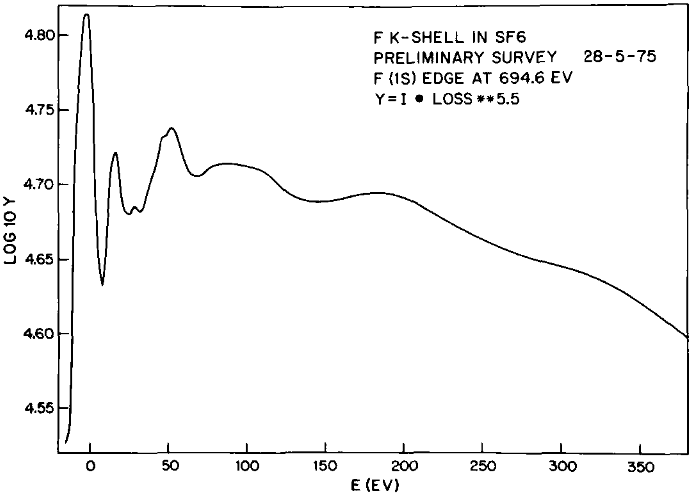

Fig. 7. The small-angle energy loss spectrum (0.5°) of SF_6 obtained with 25-keV incident electrons for the *F-K* shell energy loss range 690–1100 eV. Note that the vertical scale is arbitrary but the intensity has been leveled by multiplication by the energy loss raised to the 5.5 power, and the horizontal scale is given in terms of the kinetic energy of the ejected electron in electron volts relative to the *F-K* edge.

the equally interesting and considerably more intense shape resonances in the Kössel region have gone without much attention.

It is true that EXAFS in principle can lead to definitions of certain molecular structure parameters (nearest-neighbor distances) and that the shape resonances will probably not be equally sensitive to such parameters. On the other hand, the resonances will be more sensitive to the detailed shape of the hindering potential and certainly easier to observe experimentally.

If one investigates the Kronig region in Figs. 5–7, it is clear that there exist several maxima and minima separated by more than 50 eV. These data constitute the first observations of EXAFS by use of incident electrons on gaseous targets. Previously, Isaacson (1972) and Schnatterly and co-workers (Ritsko *et al.*, 1974) had reported similar observations using incident electrons transmitted through thin films. What is the EXAFS? It is in fact just another manifestation of a shape resonance. In the simplest theory one assumes that the only important contribution to EXAFS comes from the elastic scattering of the ejected electron by a neighbor atom at an angle of 180°. If one replaces the emitting atom and the neighbor in question by a particle-in-a-box model, then it is clear that resonance states may form whenever the ejected electron wavelength is an integral or half-integral divisor of the box length. Such a simple model predicts that the energy separation between successive EXAFS maxima would increase but that such maxima plotted as a function of the ejected electron momentum (the square root of the ejected electron kinetic energy given by $E - I$, with I the ionization edge energy) would appear to be periodic. Such is indeed the case. This led Stern and co-workers (Sayers *et al.*, 1971) to develop a theory making it possible to obtain the radial distribution of nearest-neighbor distances from the excited atom by Fourier transformation of EXAFS data. This is an exciting new structural probe since the information can be extracted from any phase of matter (liquid, gas, amorphous, solid, and crystal) by use of X-ray radiation.

One of the major problems in the general application of this technique is the oversimplified nature of the theoretical model needed to extract structural parameters from experimental data. In other words, How accurate are EXAFS bond lengths? A second problem is the need at present to use synchrotron radiation sources to obtain data. For many, this makes the technique difficult to use. This last problem may be solved, however, by creation of a national center for synchrotron radiation research or the possible development of a tunable X-ray laser.

Further applications of the electron method will probably be devoted to investigations on a variety of simple systems with well-characterized molecular geometries in an attempt to provide stringent experimental tests of existing and new theories for EXAFS.

So far most EXAFS studies have been confined to central atom *K*-shell spectra. We note here that we have observed such structure (previously observed in X-ray studies but not discussed in the EXAFS context) in other shells (*L*) in the central atom and also in peripheral atom *K*-shell spectra (*F*). Such observations are important since understanding EXAFS in other shells offers an alternative approach in structural work when interferences occur in the *K*-shell region. Also such studies can supply a confirmation of *K*-shell data. Further, *L*-shell spectra when available are more intense than *K*-shell spectra and easier to obtain experimentally. There is of course the problem in the heavier elements that *L*-shell spectra may be strongly split leading to overlapping EXAFS, which might be difficult to interpret. Data from noncentral atoms have not been extensively analyzed so far (except for atoms in diatomic molecules), and such data should provide a stringent test of theory as well as an opportunity to obtain new information on the nature of the structure.

One new area of EXAFS research not open to investigation using photon sources is the momentum dependence of EXAFS features. Professor Schaich in our Physics Department has developed a simple theory of EXAFS momentum dependence (W. Schaich, private communication), and we intend to carry out experiments to test his conclusions. An understanding of the momentum transfer dependence not only offers the possibility of refining EXAFS theories but also the possibility of obtaining additional structural data.

VIII. Pulsed Electron Beam Time-of-Flight Spectroscopy

During the past year we have successfully developed a pulsed electron beam time-of-flight (TOF) capability that has extended the range of our investigations of electron impact phenomena to energies below 0.5 eV. We have succeeded in making a pulsed electron beam source with a pulse width of less than 150 psec with 10^3–10^4 electrons per pulse and a pulse repetition rate up to 4×10^5 pulses/sec over the incident electron energy range of about 200 eV to 3 keV. This source has been successfully used to scatter electrons from gaseous and solid targets. The scattered and ejected electrons are then energy analyzed by measuring the flight time over a drift distance of 45 cm. A timing accuracy of 240 psec has been obtained as judged by the time FWHM of a 2-keV elastic scattering line for Ar. This experiment is similar to that of Baldwin, but because of improved detector technology the present apparatus can investigate a wider range of electron energies with a much higher-energy resolution capability in the higher energy region (Baldwin and Friedman, 1967). Numerous experiments can be made with such a system but so far only one application has been investigated in detail and is described below.

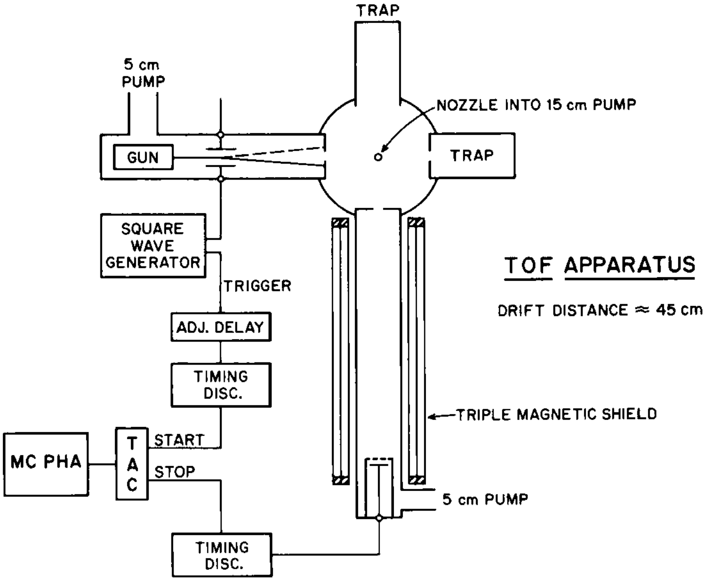

Fig. 8. Diagrammatic view of the pulsed electron beam: time-of-flight (TOF) spectrometer.

In this application the flight time between target and detector of electrons scattered and ejected by the target to be studied is measured over the time range of 0 to 10 μsec. The apparatus is shown in Fig. 8, and a TOF spectrum of He is shown in Fig. 9 for a 90° ejection angle. The data in Fig. 9 constitute a measurement of $d^2\sigma/dt\,d\Omega$ vs. t and can be easily transformed to the more conventional plot of $d^2\sigma/d\Omega\,dE$ vs. E as shown in Fig. 10. The characteristic shape of TOF spectra is quite different from its energy counterpart and thus some features can be more easily observed in one type of spectrum than the other. The peak at 35 eV, due to autoionized electrons from the decay of the 2s2p excited state, is clearly more visible in the TOF He spectrum than is its energy counterpart (Kennerly and Bonham, 1976). In Fig. 11, a plot of the energy resolution of the TOF spectrometer as a function of the detected energy is given. The timing resolution is fixed so that the longer the flight time the better the energy resolution. There are, however, two other limiting factors. When using a gas target the width of the target is on the order of 1 mm, which means that, with a flight path of 45 cm, the energy resolution cannot be better than about 0.25% of the detected energy. In addition, the Doppler broadening present in the use of gas targets can result in as much as a 2-meV lower limit to the energy resolution. (Note that we have not discussed the energy spread in the incident electron beam, which has only a minor and negligible effect in the pulsed TOF approach.)

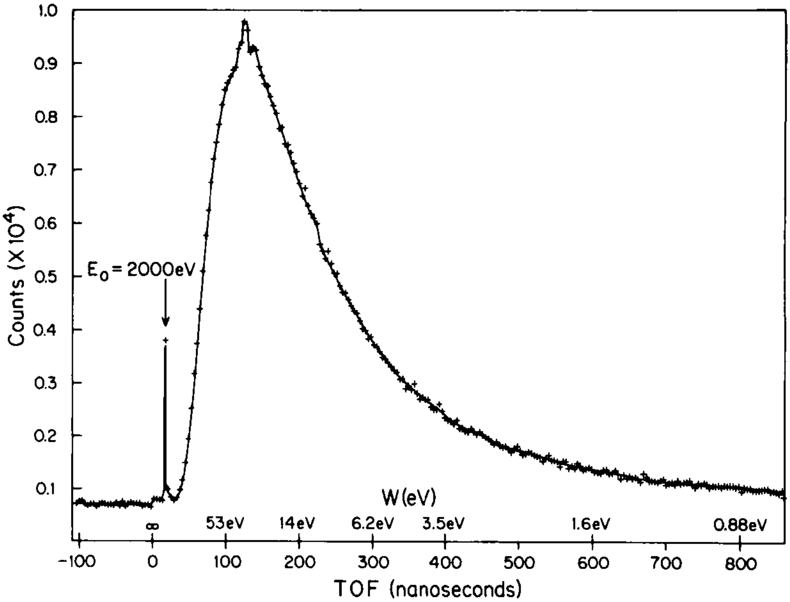

Fig. 9. Pulsed electron beam: time-of-flight spectrum for He obtained with 2-keV incident electrons at an angle of 90° to the incident direction.

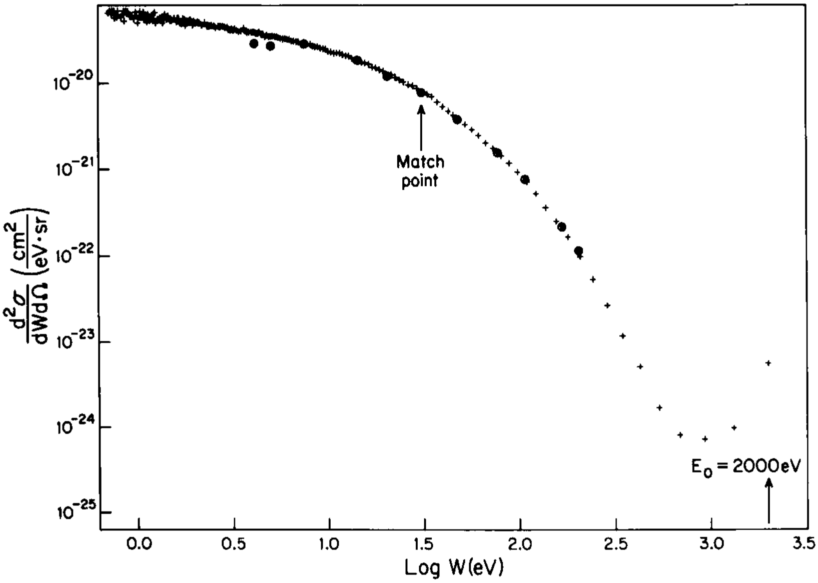

Fig. 10. A plot of the cross-section differential with respect to detected solid angle and detected electron kinetic energy for He. This graph is obtained from the data given in Fig. 9. The circles are the data of Opal, Beatty, and Peterson (1972).

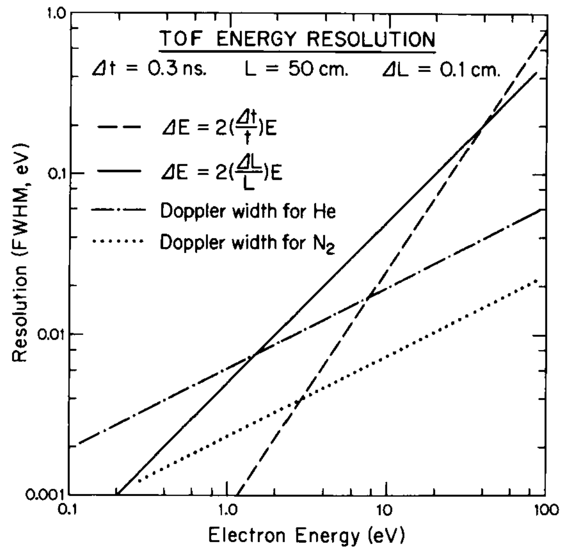

Fig. 11. Graph of limiting energy resolution of the time-of-flight (TOF) method. The dashed line, yielding the lower-energy resolution limit above 25 eV, is due to the resolving time of the experiment. The solid line, giving the lower-energy resolution limit between 25 and 1 eV, is due to the spatial spread of the target. Below 1 eV, the lower-energy resolution limit is determined by Doppler broadening in the target gas.

Our experience with this method indicates that we can obtain energy resolution for electrons of less than 10 eV in detected electron energy that is comparable or superior to the best conventional methods so far in use (Kennerly, 1977). Our absolute energy values are not subject to arbitrary adjustment to correct for contact potentials but can be calculated directly and absolutely from measured experimental quantities. In addition, the method is easy to set up and use, the data collection time is reasonable (usually less than 6 hours) and relatively independent of short-term and long-term fluctuations in experimental parameters such as incident beam energy and intensity.

In the spectrum shown in Fig. 9 the data correspond to all scattered and ejected electrons detected in a cone of angle 2° at a direction of 90° to the incident beam. Our first primitive attempts to measure such spectra are locked into this particular ejection angle because of the apparatus construction. A new apparatus that will make it possible to measure over the angular range of $20° < \theta < 160°$ is under construction.

Note that, as mentioned previously, we measure all electrons, scattered and ejected (secondaries). It is a fortunate situation that theory tells us that almost all detected electrons with energy less than half the incident energy result from secondary electron-producing processes. In fact, it is common experimental practice to define secondary electrons as all those detected with energy less than one-half the incident energy.

Clearly to obtain data of maximum utility we must be able to measure the secondary distribution over an extended angular range and to be able to place it on an accurate absolute scale. Because the elastic line is a prominent feature of our spectra and because accurate measurements and theoretical calculations of elastic cross-section differential with respect to detected solid angle exist, we have found it possible to place our data on an absolute scale with an accuracy of better than 5%.

Kim (1972) has proposed that the mechanism for production of most secondaries by electron impact is analogous to that encountered in photoionization, so that the angular dependent cross section can be written as

$$\frac{d^2\sigma}{d\Omega\, dE} = \frac{1}{4\pi}\left(\frac{d\sigma}{d\Omega}\right)[1 + \beta P_2(\cos\theta)] + \text{small corrections,} \qquad (30)$$

where β is an asymmetry parameter depending only on the incident electron energy and the nature of the process producing the ejected electron; for example, ionization of electrons for s states yields a value of $\beta = 2$, independent of the incident energy. Further, at the two angles where $P_2(\cos\theta) = 0$ the cross section on an absolute scale, as determined by the elastic scattering normalization, should agree with the integration of the complete range of angular data. Disagreement might give important information on the nature of the correction terms. In Fig. 12, a Platzman plot of the He TOF data is used to compare theory and experiment in a sensitive manner. The theoretical results of Kim (1972) are for $d\sigma/dE$ rather than for the measured $d^2\sigma/dE\, d\Omega$ (90°). The comparison indicates that the angular, dependent cross-section data must be reasonably isotropic. The experimental results of Opal *et al.* (1972) agree well with the present results but show deficiencies at energies below 10 eV. This is presumably the result of the electrostatic fields encountered in the use of conventional energy analyzers. The theoretical results of Burnett *et al.* (1976) agree well at the lower energies but show large deviations at high energy. The theoretical data of Manson *et al.* (1975) display the opposite behavior. It is thus of interest to consider the differences in these two calculations. Both calculations are carried out within the framework of the first Born approximation. In the Burnett *et al.* case, the wavefunctions describing the ground and excited states included significant electron correlation effects, but the partial wave expansion of the continuum wavefunction was terminated at $l = 4$. Manson *et al.*, on the other hand, used wavefunctions based on the Hartree–Fock–Slater approximation but included up to sixteen partial waves in their treatment. The results indicate that the use of highly

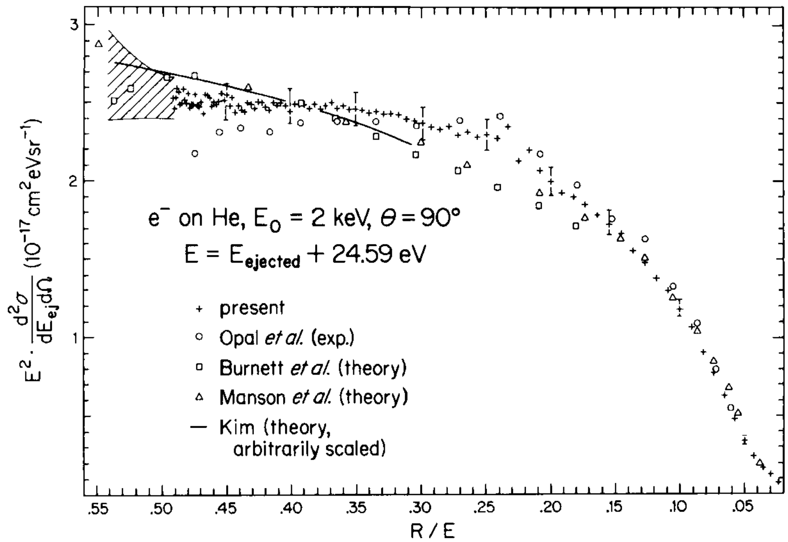

Fig. 12. Platzman plot of absolute, secondary electron spectrum at 90° for 2-keV incident electron energy. The theory of Kim is actually a plot of the total cross section arbitrarily scaled to our data and indicates that the shape of the 90° data is quite similar to that of the differential cross section integrated over all angles. In other words the low-energy ejected electrons are fairly isotropically emitted by the target.

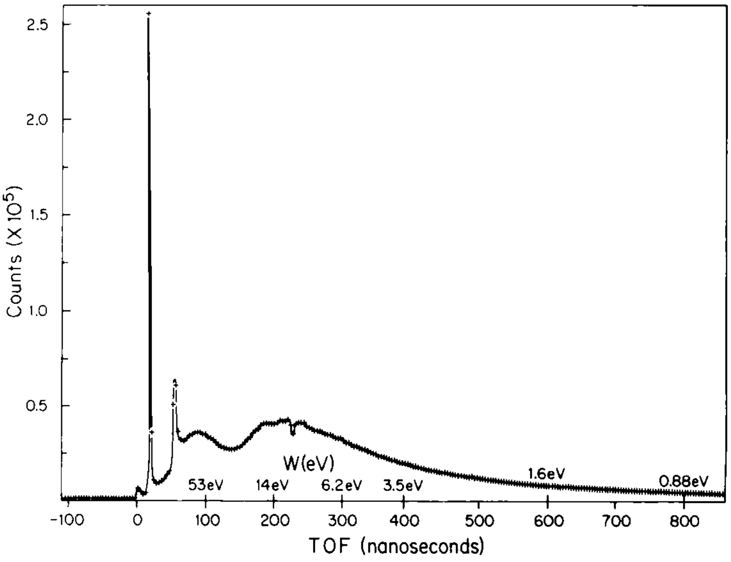

Fig. 13. Pulsed electron beam, time-of-flight (TOF) spectrum for Ar obtained with 2-keV electrons.

correlated wavefunctions is essential for low secondary electron energy, whereas a relatively poorer description of the wavefunction suffices for high ejection energy provided that convergence of the partial wave sum is maintained. Note that in the intermediate region, which contains the $2s^2$, $2p^2$, 2s2p, etc., autoionizing structure, both calculations fail badly. Presumably extensive interaction between the underlying continuum wavefunctions and the bound-state configurations corresponding to these states must be allowed for.

As a by-product of secondary electron studies, it is possible to observe Auger and autoionizing features of the spectrum. In Fig. 13, the TOF spectrum of Ar is shown. In Fig. 14, the transformed spectrum in energy is shown with the Auger line at 200 eV blown up in the upper right inset. The resolution here is only a mediocre 5 eV. In the lower left inset, the 3s autoionizing states are shown at an energy resolution of about 200 meV. In Fig. 15, a newer spectrum of the same region at 100 meV resolution

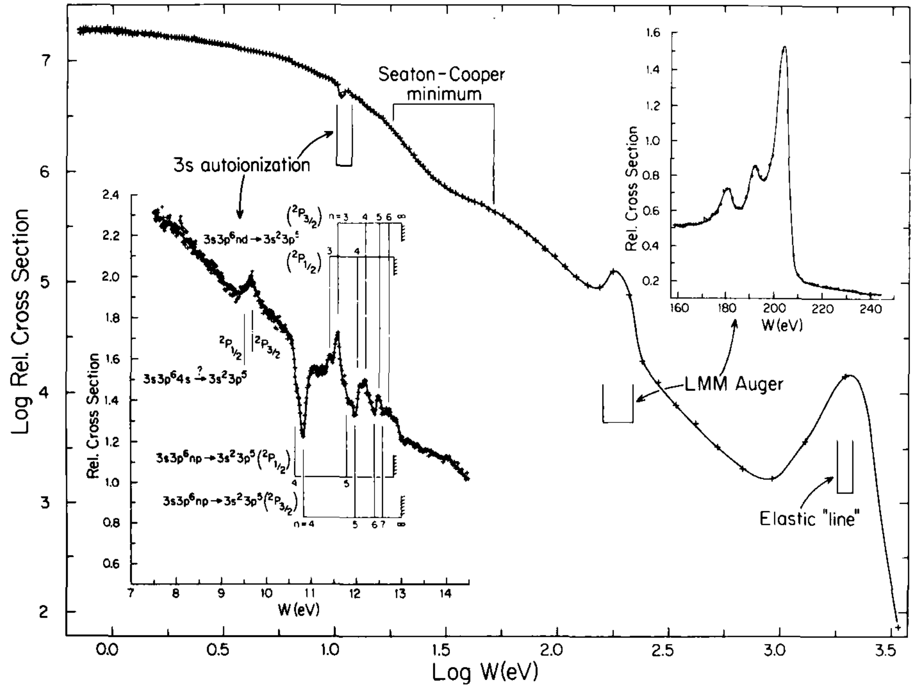

Fig. 14. Cross-section differential with respect to detected solid angle and energy for Ar from the data given in Fig. 13. The upper right inset shows detail in the 200-eV Auger region, and the lower left inset shows the 10-eV autoionizing region. The incident electron energy was 2 keV and the ejection angle was 90°.

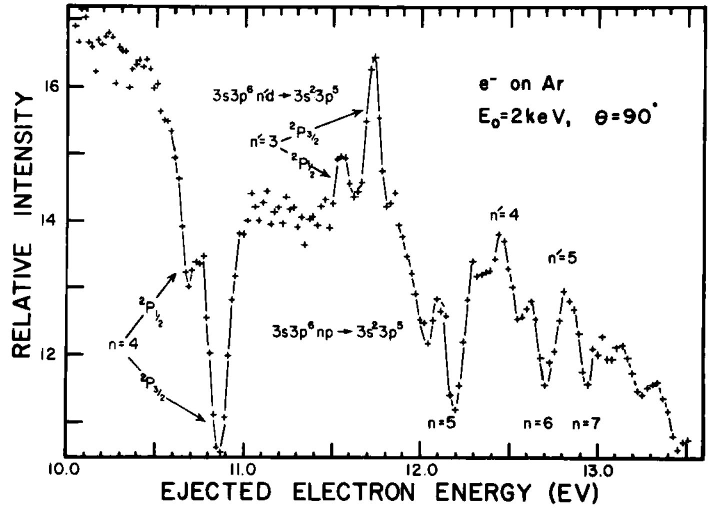

Fig. 15. The 10-eV autoionizing region in Ar shown at high detected energy resolution. The incident electron energy was 2 keV and the ejection angle was 90°.

gives an even clearer view of the spectrum. This work establishes our abilities to observe fine structure, which at 10 eV and below is competitive with the best previously published high-resolution results. There is one important difference, however; that is, we can obtain these high-resolution results in the same experiments that yield the best measurements of the absolute total measured intensity so far recorded. Thus, we have an unsurpassed technique for obtaining absolute spectral line intensities. This fact should be of special interest to theorists.

REFERENCES

Baldwin, G. C., and Friedman, S. I. (1967). *Rev. Sci. Instrum.* **38**, 519.

Bentley, J., and Stewart, R. F. (1975). *J. Chem. Phys.* **63**, 3794.

Bloch, B. J., and Mendelsohn, L. B. (1974). *Phys. Rev. A* **9**, 129.

Bonham, R. A., and Fink, M. (1974). "High Energy Electron Scattering." Van Nostrand-Reinhold, Princeton, New Jersey.

Bonham, R. A., and Tavard, C. (1973). *J. Chem. Phys.* **59**, 4691.

Bonham, R. A., and Wellenstein, H. F. (1973). *J. Appl. Phys.* **44**, 2631.

Brown, R., and Smith, V. (1972). *Phys. Rev. A* **5**, 5.

Burnett, T., Rountree, S. P., Doolen, G., and Robb, W. D. (1976). *Phys. Rev. A* **13**, 626.

Carlson, T. A., and Nestar, C. W., Jr. (1973) *Phys. Rev. A* **8**, 2887.

Dehmer, J. L. (1972). *J. Chem. Phys.* **56**, 4496.

Dey, S., McCarthy, I. E., Teubner, P. J. O., and Weigold, E. (1975). *Phys. Rev. Lett.* **34**, 782.

Fano, U., and Cooper, J. W. (1968). *Rev. Mod. Phys.* **40**, 441

Fink, M., Gregory, D., and Moore, P. G. (1976). *Phys. Rev. Lett.* **37**, 15.

Hughes, A. L., and Mann, M. M., Jr. (1938). *Phys. Rev.* **53**, 50.

Iijima, T., Bonham, R. A., and Ando, T. (1963). *J. Phys. Chem.* **67**, 1472.

Inokuti, M. (1971). *Rev. Mod. Phys.* **43**, 297.

Isaacson, M. (1972). *J. Chem. Phys.* **56**, 1813.

Jaeglé, A., Duguet, A., and Bouchard, R. (1971). *J. Chim. Phys.* **68**, 1159, and earlier works.

Kennerly, R. E. (1977). *Rev. Sci. Instrum.* **48**, No. 2, 48.

Kennerly, R. E., and Bonham, R. A. (1976). *Chem. Phys. Lett.* **43**, 245.

Kim, Y.-K. (1972). *Phys. Rev. A* **6**, 666.

Kim, Y.-K. (1975). *Radiat. Res.* **61**, 21.

Kohl, D. A., and Bartell, L. S. (1969). *J. Chem. Phys.* **51**, 2891 and 3896.

Kohl, D. A., and Bonham, R. A. (1966). *J. Chem. Phys.* **45**, 2471.

Kohl, D. A., and Bonham, R. A. (1967). *J. Chem. Phys.* **47**, 1634.

Konaka, S. (1972). *Jpn. J. Appl. Phys.* **11**, 1199.

Kössel, W. (1920a). *Z. Phys.* **1**, 119.

Kössel, W. (1920b). *Z. Phys.* **2**, 470.

Kronig, R. de. L. (1931). *Z. Phys.* **70**, 317.

Kronig, R. de L. (1932). *Z. Phys.* **75**, 191 and 468.

Lassettre, E. N. (1976). *J. Chem. Phys.* **64**, 4375.

Lee, J. S. (1978). *J. Chem. Phys.* **66**, 4906.

Lee, J. S., Wong, T. C., and Bonham, R. A. (1975). *J. Chem. Phys.* **63**, 1643.

McCurdy, C. W., Jr., and McKoy, V. (1974). *J. Chem. Phys.* **61**, 2820.

Manson, S. T., Toburen, L. H., Madison, D. H., and Stolterfoht, N. (1975). *Phys. Rev. A* **12**, 60.

Opal, C. B., Beaty, E. C., and Peterson, W. K. (1972). *At Data* **4**, 209.

Peixoto, E. M. A., Bunge, C. F., and Bonham, R. A. (1969). *Phys. Rev.* **181**, 322.

Ritsko, J. J., Schnatterly, S. E., and Gibbons, P. G. (1974). *Phys. Rev. Lett.* **32**, 671.

Sahni, V., Krieger, J. B., and Gruenebaum, J. (1975). *Phys. Rev. A* **12**, 768.

St. John, W., Kennerly, R., and Bonham, R. A. (1978). To be published.

Sayers, D. E., Stern, E. A., and Lytle, F. W. (1971). *Phys. Rev. Lett.* **27**, 1204.

Schmoranzer, H., Wellenstein, H. F., and Bonham, R. A. (1975). *Rev. Sci. Instrum.* **46**, 89.

Stewart, R. F., and Bentley, J. (1975). *J. Chem. Phys.* **63**, 3786.

Tavard, C. (1965). *Cah. Phys.* **20**, 397.

Tavard, C., and Roux, M. (1965). *C. R. Hebd. Seances Acad. Sci.* **260**, 4933.

Ulsh, R. C., Wellenstein, H. F., and Bonham, R. A. (1974). *J. Chem. Phys.* **60**, 103.

Wellenstein, H. F. (1973). *J. Appl. Phys.* **44**, 3669.

Wellenstein, H. F., and Bonham, R. A. (1973). *Phys. Rev. A* **7**, 1568.

Wellenstein, H. F., Bonham, R. A., and Ulsh, R. C. (1973). *Phys. Rev. A* **8**, 304.

Wellenstein, H. F., Schmoranzer, H., Bonham, R. A., Wong, T. C., and Lee, J.-S. (1975). *Rev. Sci. Instrum.* **46**, 92.

Wight, G. R., Brion, C. E., and van der Wiel, M. J. (1972–1973). *J. Electron Spectrosc. Relat. Phenom.* **1**, 457.

Williams, B., ed. (1977). "Compton Scattering." McGraw-Hill, New York.

Wong, T. C., Lee, J.-S., Wellenstein, H. F., and Bonham, R. A. (1975). *Phys. Rev. A* **12**, 1846.

Convergence Limit in the Electronic Spectra of Linear Polyenes

SADHAN BASU
Department of Chemistry
University College of Science
Calcutta, India

I. Introduction

What a number of organic molecules, ranging from the carotenoids to organic dyes, have in common is that they all contain a polyene chain with alternate double and single bonds. The whole series of these molecules has become known through the work of Hausser and Kuhn (1935) on its absorption spectra. Among other things, they found that the longest-wavelength absorption band in the spectrum of these molecules shifts to longer wavelengths if more —C=C— units are added to the polyene chain. These experiments confirmed that light is absorbed by the molecule as a whole, and this concept served as the basis for many theories such as "conjugation across a double bond," and "colour and constitution."

Bayliss (1948), Kuhn (1948), and Simpson (1948) calculated electronic spectra of polyenes by simple free-electron theory. According to this method the π-electrons are considered to move along the chain of the —C=C— bonds in the molecule in a constant potential field, and the MO's therefore resemble the solution of the well-known "particle-in-a-box" problem. The wavefunction is given as

$$\phi_n = \sqrt{\frac{2}{L}}\sin\left(\frac{n\pi x}{L}\right) \qquad (n = 1, 2, \ldots), \tag{I.1}$$

ISBN 0-12-034811-X

and the energies as

$$e_n = \frac{n^2h^2}{8mL^2} \tag{I.2}$$

for a carbon chain of length L. For a chain of $2n(N)$ carbon atoms, the energy of the longest-wavelength transition is

$$e_f - e_g = \frac{(N+1)h^2}{8ml^2N}, \tag{I.3}$$

where l is the length of the C—C bond. This analysis shows that as the length of the chain goes to infinity, the transition energy goes to zero.

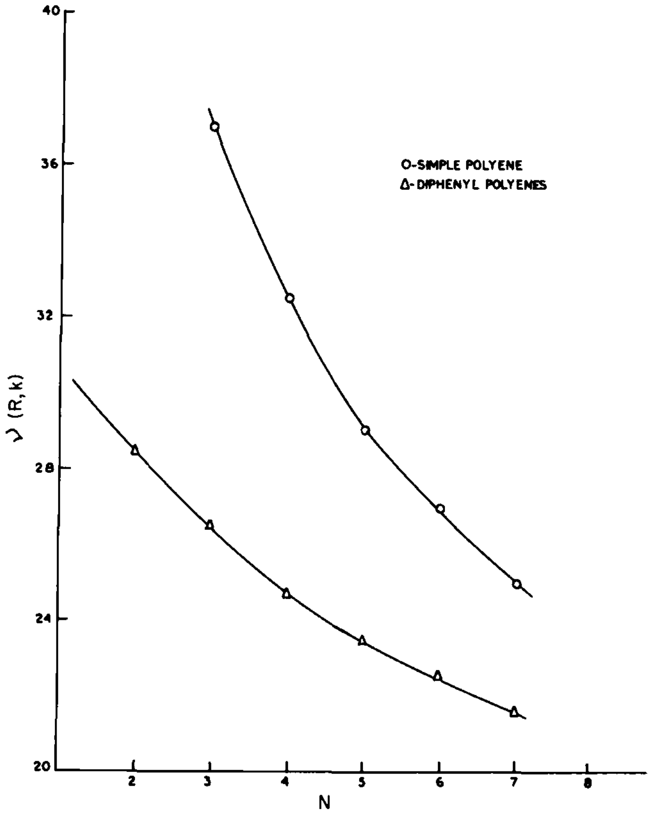

Fig. 1. Frequency vs. chain length plot for polyenes. Plotted from data in Hausser and Kuhn (1935) and Araki and Murai (1952).

In the case of LCAO–MO's, the orbital energies of a linear polyene C_NH_{2N+2} are given by (Salem, 1966)

$$e_j = 2\beta \cos\left(\frac{j\pi}{N+1}\right) \qquad (j = 0, 1, 2, \ldots), \tag{I.4}$$

where β is the resonance integral of the C—C bond. The transition from the occupied top to the empty bottom orbital has the energy

$$e_f - e_g = -4\beta \sin\left(\frac{\pi}{2(N+1)}\right), \tag{I.5}$$

which also shows that as the length of the chain goes to infinity the transition energy goes to zero.

These calculations predicted that for each addition of a vinyl group the wavelength of the absorption band should increase by 1000 + 50 Å. This prediction is not borne out by experimental results. Figure 1 gives the ν vs. N plots for simple polyenes and diphenyl polyenes, showing that the curves tend to a finite limit of about 18,000 cm^{-1} for an "infinite" polyene chain, the convergence being more rapid for the diphenyl polyenes (Hausser and Kuhn, 1935; Araki and Murai, 1952).

II. Bond Alternation and Brillouin Gap

There are many theories concerning whether or not the configuration with alternate long and short bonds is stable for conjugated systems (Tsuji *et al.*, 1960; Ooshika, 1957; Salem and Longuet-Higgins, 1959, 1960). If the configuration with alternating bonds is more stable than the configuration with equal bonds, then the results in Section I will not be valid because the alternating bonds generate a potential with a period of two bond lengths, which perturbs the MO's and introduces a Brillouin gap between the highest occupied and the lowest unoccupied level.

In dealing with this phenomenon, we have to consider the local variations of electron density. First, we assume that n positive charges are embedded in the π-electron cloud in an equal spacing. These positive point charges represent the carbon core in the conjugated chain. Local variations of electron density should generate a field that displaces these positive charges.

The potential energy of the unit positive charge is given by

$$U(a) = \int \rho(x) G(|x - a|)\, dx, \tag{II.1}$$

where a denotes the coordinate of the positive charge, $\rho(x)$ represents the density of electrons, and $G(|x - a|)$, the potential function between positive and negative charges. We assume that $G(u)$ becomes a constant $G(0)$ in the region $u < \delta$. Then $U(a)$ becomes

$$U(a) = U_1(a) - U_2(a) = \int_{a-\delta}^{a+\delta} G(0)\rho(x)\,dx - \int_{|x-a|>\delta} G(|x-a|)\rho(x)\,dx$$
$$= 2\delta G(0)\rho(a) - U_2(a). \tag{II.2}$$

The first term, $U_1(a)$, represents a potential that depends on the local variation of π-electron density. The second term, $U_2(a)$, represents a potential that depends on the density of π-electrons but is independent of its local variation. Because $G(0)$ is a negative quantity, $U_1(a)$ is in inverse phase with the variation of π-electron density.

For $2n(N)$ electrons in a box of length L, the density of electrons in the ground state is given by

$$\rho(x) = 2\sum_{j=1}^{n} |\phi_j(x)|^2$$
$$= \frac{N}{L} - \frac{1}{L}\left[\frac{\sin(N\pi x/L)}{\sin(\pi x/L)} - 1\right]. \tag{II.3}$$

In the neighborhood of the middle of the box, the local density variation is given approximately by

$$\rho(x) = -\frac{1}{L}\cos(N\pi x/2L). \tag{II.4}$$

The coordinates of positive charges are given by

$$a = \frac{L}{N}(m - \tfrac{1}{2}) \qquad m = 1, 2, \ldots, N. \tag{II.5}$$

Then maxima and minima of the electron density are situated alternately in the middle points between neighboring positive charges. According to potential U_1, the positive charges are displaced and the distances between positive charges increase or decrease alternately; that is, a bond alternation is generated.

Once the bond alternation is generated in the conjugated chain, it gives rise to a potential

$$V(x) = V_0\cos(N\pi x/L). \tag{II.6}$$

This potential is known as the Kuhn potential (Kuhn, 1949). It perturbs the wavefunction of the π-electrons, and the density of the π-electrons varies. Using the free-electron molecular orbital (FEMO) (I.1) as the zeroth approximation, we get the following matrix elements for the Kuhn potential:

$$\int \phi_i(x)V(x)\phi_j(x)\,dx = \begin{cases} -\frac{1}{2}V_0 & |i+j| = N \\ +\frac{1}{2}V_0 & |i-j| = N. \\ 0 & \text{otherwise} \end{cases} \qquad \text{(II.7)}$$

When N becomes large, we have

$$e_{n+1} - e_n = V_0 \qquad \text{(Brillouin gap).} \qquad \text{(II.8)}$$

Thus, due to bond alternation, the difference between the energies of the topmost occupied and lowest unoccupied orbital for infinitely long chains becomes V_0 instead of zero. The experimentally observed convergence limit in the electronic spectra of polyenes is thereby explained.

In the LCAO–MO formulation, the different lengths r_1 (long) and r_2 (short) in alternate bonds is taken account of by two different resonance integrals (Dewar, 1952) β_1 and β_2 with $\beta_2 \leq \beta_1 < 0$. The orbital energies are given by

$$e_j = \pm[\beta_1^2 + \beta_2^2 + 2\beta_1\beta_2 \cos(2\pi j/N)]^{1/2} \qquad (j = 0, 1, 2, \ldots). \qquad \text{(II.9)}$$

The energy gap and, hence, the convergence limit becomes evident when we compare this expression with Eq. (I.4) for all bonds equal.

III. Electronic Spectra of Mono- and Dinegative Ions of Polyenes: Incompleteness of Bond Alternation Theory

Recent achievements in the research on hydrocarbon ions are in the first place characterized by a close coordination of experimental investigations and quantum-mechanical calculations. Electronic spectra of negative ions of aromatics have been measured by Paul, Lipkin, and Weissman (1956) and by Balk, Hoijtink, and Schreurs (1957a). The spectra received a very reasonable interpretation in the calculations of Balk, De Bruin, and Hoijtink (1957b, 1958). Paramagnetic resonance spectra of mononegative ions of aromatics were obtained by Weissman *et al.* (1953). The observed hyperfine splittings were in good agreement with calculated spin densities.

Van Der Meij (1958) have prepared mono- and dinegative ions of a series of α,ω-diphenyl polyenes ranging from 1,2-diphenylethene to 1,12-diphenyldodecahexane. In Fig. 2 (Coulon, 1938) are plotted the longest-wavelength electron transitions vs. the number of conjugated double bonds for mono- and dinegative diphenyl polyene ions. It may be observed that, although the spectrum of the mononegative ion is nonconvergent, the spectrum of the dinegative ion is convergent. Further, the next higher transition in the mononegative ion is convergent.

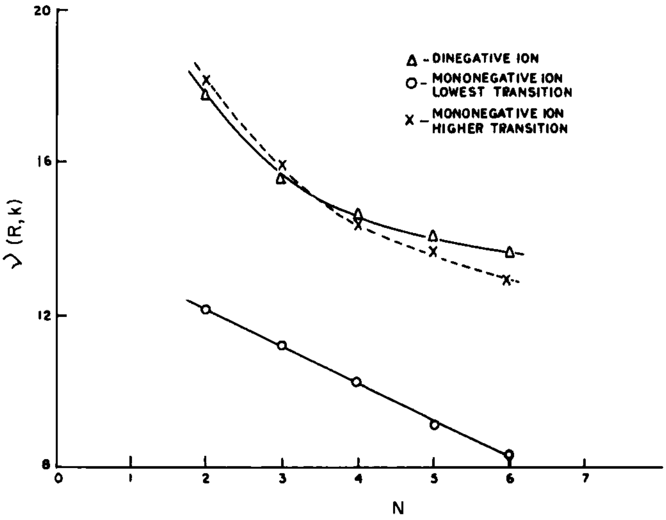

Fig. 2. Frequency vs. chain length plot for mono- and dinegative ions of diphenyl polyenes. Plotted from data in Van der Meij (1958).

The bond orders of neutral, mono-, and dinegative ions calculated with Hückel coefficients are given in Tables I and II for diphenylethene and diphenyloctatetraene. The data in these tables enable the following conclusions to be drawn:

1. The carbon–carbon bonds of the polyene chain have alternately a less and a more double-bond character.

2. The same sequence holds for mononegative ions.

3. For dinegative ions, the shorter bond in the neutral molecule becomes longer in ions but the alternation persists.

Platt (1956) has shown that alternation of single and double bonds becomes even more pronounced if self-consistent functions are used instead

TABLE I

HÜCKEL BOND-ORDER FOR 1,2-DIPHENYLETHENE

	C—C bond				
	1-2	2-3	3-4	4-5	5-6
R	0.6566	0.6814	0.6010	0.4310	0.7188
R^-	0.6318	0.7030	0.5415	0.5260	0.6270
R^{2-}	0.6071	0.7247	0.4821	0.6210	0.4353

TABLE II

HÜCKEL BOND ORDER FOR 1,8-DIPHENYLOCTATETRAENE

	C—C bond							
	1-2	2-3	3-4	4-5	5-6	6-7	7-8	8-9
R	0.6544	0.6842	0.5927	0.4520	0.6598	0.5394	0.7248	0.5548
R^-	0.6487	0.6897	0.5764	0.4828	0.5906	0.6609	0.6343	0.6245
R^{2-}	0.6430	0.6953	0.5602	0.5135	0.5241	0.7217	0.5493	0.6983

TABLE III

SCF-CI BOND ORDERS FOR 1,8-DIPHENYLOCTATETRAENE[a]

	C—C bond							
	1-2	2-3	3-4	4-5	5-6	6-7	7-8	8-9
R	0.6586	0.6790	0.6044	0.4326	0.8024	0.4758	0.7806	0.4772
R^{2-}	0.6540	0.6875	0.5794	0.4935	0.5532	0.7399	0.5265	0.7503

[a] SCF-CI, self-consistent field-configuration interaction.

of Hückel functions. This is shown in Table III, where bond orders of various links in diphenyloctatetraene are calculated from Pariser and Parr configuration interaction (CI) functions.

It has already been mentioned that the alternation in bond lengths of the polyenes give rise to an alternating potential, which has been shown by Kuhn to be responsible for convergence in spectral frequency with length of the conjugated chain. Kuhn's idea was opposed by Bayliss and Riviere (1951). These authors pointed to the qualitative nature of Kuhn's calculation and brought forward calculations of Lennard-Jones (1937) who, using the simple LCAO-MO's, had found that the alternating bonds should become more nearly equal as the number of bonds in the chain increases. The above calculation introduces some new arguments into this discussion. Configuration leads to a more explicit alternation of bond lengths, and the effects of CI is strongest in large systems. As a consequence, even for large molecules, a marked alternation of bonds persists contrary to the Lennard-Jones prediction. But, inspite of bond alternation, mononegative ions show no convergence, whereas the spectrum of dinegative ion is convergent. The crucial point is not whether the bonds of the molecule are equal in length or not or whether the molecule is neutral or charged, but whether or not the electrons in the molecule are paired.

IV. Many-Electron System and Hartree–Fock–Boglyubov Equation Gap

In the usual treatment of the many-electron problem, each particle is supposed to move independently, the effect of the interaction between particles being simply replaced by an average force field. This treatment does not take interparticle correlation into account. A step toward the improvement of the method so as to include correlation was taken by Euler (see Boglyubov, 1958), who calculated the effect of interparticle interaction (which causes the correlation) by perturbation theory assuming the interaction to be small. This type of calculation is carried out in the following manner. In the zeroth approximation, each particle is in a one-particle quantum state, which we consider a "level." Let us consider the lowest state for the sake of definiteness. In this state, all levels up to some highest, which we call the Fermi maximum (λ), are each filled by the particle. The perturbation energy due to the interparticle force has nonvanishing matrix elements that cause virtual transitions to states in which particles are excited to levels higher than the Fermi maximum. The state resulting from the interparticle force is, thus, a superposition of zero-order state and various excited states. Such a mixture of states give rise to correlation between particles.

By accepting the preceding model, we may approach the problem of π-electronic spectra of long-chain polyenes in a different way. In the single-particle level scheme of "electron in a box," the levels up to λ are occupied and the levels above are empty. The state obtained by exciting a particle from an occupied level to an unoccupied level is called a one particle–one hole state, because in this excitation process a vacancy (hole) is left in the occupied level and a "particle" is produced in one of the unoccupied levels. If we use single-particle creation and destruction operators in the treatment of the many-body Hamiltonian, then we will be able to obtain the elementary excitation energy for a hole–particle pair or a quasi particle.

The physics and mathematics of quasi particles have been rigourously developed and applied with great success in nuclear physics (Tomonaga, 1950) and the theory of superconductivity (Bardeen *et al.*, 1957). In what follows we apply this method to polyenes, a many π-electron system (Basu, 1975).

The second quantized version of the many-body Hamiltonian is given as

$$H = \sum_{\alpha\beta} \langle\alpha|T|\beta\rangle c_\alpha^+ c_\beta + \tfrac{1}{2} \sum_{\alpha\beta\gamma\delta} \langle\alpha\beta|v|\gamma\delta\rangle c_\alpha^+ c_\beta^+ c_\gamma c_\delta, \qquad \text{(IV.1)}$$

where c_α^+ is the creation operator for state α, and c_β is the destruction operator for the state β.

According to Weak's theorem, which holds for any product of a set of creation and destruction operators, we can write the following identities:

$$
\begin{aligned}
c_\alpha^+ c_\beta &= \,: c_\alpha^+ c_\beta : + \langle c_\alpha^+ c_\beta \rangle \\
c_\alpha^+ c_\beta^+ c_\gamma c_\delta &= \,: c_\alpha^+ c_\beta^+ c_\gamma c_\delta : + : c_\alpha^+ c_\beta^+ : \langle c_\gamma c_\delta \rangle + \langle c_\alpha^+ c_\beta^+ \rangle : c_\gamma c_\delta : \\
&\quad + : c_\alpha^+ c_\gamma : \langle c_\beta^+ c_\delta \rangle + \langle c_\alpha^+ c_\gamma \rangle : c_\beta c_\delta : - : c_\alpha^+ c_\delta : \langle c_\beta^+ c_\gamma \rangle \\
&\quad - \langle c_\alpha^+ c_\delta \rangle : c_\beta^+ c_\gamma : + \langle c_\alpha^+ c_\beta^+ \rangle \langle c_\delta c_\gamma \rangle + \langle c_\alpha^+ c_\gamma \rangle \langle c_\beta^+ c_\delta \rangle \\
&\quad - \langle c_\alpha^+ c_\delta \rangle \langle c_\beta^+ c_\gamma \rangle. \qquad \text{(IV.2)}
\end{aligned}
$$

(The angular brackets denote the expectation value and the pairs of colons, the normal products.) The sign must be plus or minus, depending on the even or odd nature of the permutation. The expectation value of the Hamiltonian takes the form

$$
\begin{aligned}
\langle H \rangle = \sum_{\alpha\beta} \langle a | T | \beta \rangle \langle c_\alpha^+ c_\beta \rangle + \tfrac{1}{2} \sum_{\alpha\beta\gamma\delta} \langle \alpha\beta | v | \gamma\delta \rangle [\langle c_\alpha^+ c_\beta^+ \rangle \langle c_\gamma c_\delta \rangle \\
+ \langle c_\alpha^+ c_\gamma \rangle \langle c_\beta^+ c_\delta \rangle - \langle c_\alpha^+ c_\delta \rangle \langle c_\beta^+ c_\gamma \rangle. \qquad \text{(IV.3)}
\end{aligned}
$$

Since γ and δ are summation symbols, we can interchange them in the last term, which when combined with its predecessor gives us the Coulomb term and exchange term, i.e., the self-consistent Hartree–Fock (HF) potential V. There is an extra term in the potential, namely $\langle c_\alpha^+ c_\beta^+ \rangle \langle c_\delta c_\gamma \rangle$. Now the expectation value of the product of creation and destruction operators is expressed in terms of density function ρ (Pal, 1970):

$$
\langle \beta | \rho | \alpha \rangle = \langle \psi_0 | c_\alpha^+ c_\beta | \psi_0 \rangle = \langle c_\alpha^+ c_\beta \rangle. \qquad \text{(IV.4)}
$$

We introduce the definition of a pairing density $K_{\delta\gamma} = \langle c_\delta c_\gamma \rangle$ such that

$$
K_{\beta\alpha}^* = \langle c_\alpha^+ c_\beta^+ \rangle = \langle c_\beta c_\alpha \rangle^*. \qquad \text{(IV.5)}
$$

Since the destruction operators anticommute with each other, we have

$$
K_{\gamma\delta} = \langle c_\gamma c_\delta \rangle = -\langle c_\delta c_\gamma \rangle = -K_{\delta\gamma}. \qquad \text{(IV.6)}
$$

We, therefore, write the extra term in the Hamiltonian as

$$
\tfrac{1}{2} \sum_{\alpha\beta\gamma\delta} \langle \alpha\beta | v | \gamma\delta \rangle \, K_{\beta\alpha}^* \tfrac{1}{2}(K_{\delta\gamma} - K_{\gamma\delta}) = \tfrac{1}{4} \sum_{\alpha\beta\gamma\delta} \langle \alpha\beta | v | \gamma\delta \rangle K_{\beta\alpha}^* K_{\delta\gamma}. \qquad \text{(IV.7)}
$$

If we introduce the definition of a pairing potential,

$$
\Delta_{\alpha\beta} = \tfrac{1}{2} \sum_{\gamma\delta} \langle \beta\alpha | v | \gamma\delta \rangle K_{\delta\gamma}, \qquad \text{(IV.8)}
$$

then we get the Hartree–Fock–Boglyubov Hamiltonian (HFB) as

$$\langle H\rangle = \sum_{\alpha\beta} \{\langle\alpha|T + \tfrac{1}{2}V|\beta\rangle\langle\beta|\rho|\alpha\rangle + \tfrac{1}{2}\,\Delta_{\alpha\beta}K^{*}_{\beta\alpha}\}. \tag{IV.9}$$

We now try to determine the groundstate ψ_0 by minimizing $\langle H(\lambda)\rangle$, i.e., we minimize $\langle\psi_0|H - \lambda\hat{N}|\psi_0\rangle$, where λ is the Lagrangian multiplier and $\hat{N}$ is the operator for the total number of particles:

$$\hat{N} = \sum_{\alpha} c_{\alpha}^{+} c_{\alpha}. \tag{IV.10}$$

The minimization of $H(\lambda)$ without pairing potential gives us energies $(e_i - \lambda)$, where e_i is the HF energy. By introducing the pairing interaction term, we may solve the variation problem by the so-called pairing force model, i.e., the pairing potential is written as

$$\Delta_{j,-j} = -G \sum c_j^{+} c_{-j}^{+} c_j c_{-j}, \tag{IV.11}$$

where G is the strength of pairing force and j is the time-reversed partner of $-j$, i.e., they refer to states having same principal quantum number but the projection quantum numbers are of opposite sign. The elementary excitation of the system is called Bardeen, Cooper, and Scheiffer (BCS) quasi particle. The creation and destruction operators of the quasi particle, b_j^{+} and b_j, are related to particle creation and destruction operators by the Boglyubov–Valantin (1961) transformation

$$b_j^{+} = u_j c_j^{+} - v_j c_{-j}; \qquad b_j = v_j c_j^{+} + u_j c_{-j}, \tag{IV.12}$$

where u_j and v_j are the probability amplitude for occupation and non-occupation of the level j by a pair. Since v_j^2 is the probability of finding a zero coupled pair in the ground state, we have the condition

$$u_j^2 + v_j^2 = 1 = u_j^2 + v_{-j}^2. \tag{IV.13}$$

Since the state $|\mathrm{BCS}\rangle$ is not an eigenstate of the particle number operator $1N$, it does not correspond to a definite number of particles. However, we require that the expectation value of the number operator in $|\mathrm{BCS}\rangle$, which is given by $2\sum_j v_j^2$, equal the actual particle number

$$\langle\mathrm{BCS}|1N|\mathrm{BCS}\rangle = 2\sum_j v_j^2 = N. \tag{IV.14}$$

The probability amplitude u_j and v_j are determined by minimizing the Hamiltonian

$$1H - \lambda 1N,$$

where λ is the Lagrange multiplier. The result is

$$v_j^2 = \frac{1}{2}\left(1 - \frac{e_j - \lambda}{E_j}\right), \tag{IV.15}$$

where e_j is the single-particle HF energy, and E_j is the quasi-particle energy (Basu, 1974), i.e., the single-particle excitation energy

$$E_j = [(e_j - \lambda)^2 + \Delta^2]^{1/2},$$

where

$$\Delta = G \sum u_j v_{-j} = -\left(\frac{\Delta_{j,-j}}{2}\right). \tag{IV.16}$$

Significance of E_j. The term E_j is the energy of a quasi particle, i.e., the energy of the system obtained by taking a particle from the filled band to an empty band. It, therefore, refers to the electronic excitation energy of the system in the independent particle scheme.

Significance of λ. From relation (IV.15), it is evident that when $-E_j$ is much larger than λ, $v_j^2 = 0$, whereas when it is much less than λ, $v_j^2 = 1$, assuming Δ to be small. In the usual description of the π-electron system the levels up to the Fermi maximum are occupied, whereas those above are all empty. So the occupation probability above the Fermi maximum is zero and that below it is unity. This suggests that λ is to be associated with the energy of the Fermi maximum. Hence the electronic excitation energy is given as

$$E_j = \sqrt{(e_j - e_F)^2 + \Delta^2}. \tag{IV.17}$$

V. Convergence Limit and Electron-Pairing Interaction

Equation (4.17) shows that when e_j becomes equal to e_F, the quasi-particle energy is Δ and not zero. If the long-wavelength transition in linear polyene is associated with the electron jump from the topmost filled to the first empty orbital, then in the quasi-particle scheme the energy should go over to Δ, as the energy difference $e_j - e_F$ goes to zero, i.e., as the length of the chain goes to infinity.

In the relation

$$2u_j v_{-j} = \frac{\Delta}{\sqrt{(e_j - e_F)^2 + \Delta^2}}, \tag{V.1}$$

we have for HF state

$$\begin{aligned} u_j &= 1 \quad \text{for a particle state,} \\ &= 0 \quad \text{for a hole state,} \\ v_j &= 1 \quad \text{for a hole state,} \\ &= 0 \quad \text{for a particle state.} \end{aligned}$$

In the HFB case, u_j and v_j deviate from these unique values and will lie between zero and one. This means that even for the HFB case, the product $u_j v_j$ should be positive, i.e., Δ must be a positive quantity. Now Δ has been set equal to $-\Delta_{j,\,-j}/2$, so that $\Delta_{j,\,-j}$ should be negative. The term $\Delta_{j,\,-j}$ is related to pairing potential, and a negative potential indicates an attraction between two particles in states j and $-j$. The j and $-j$ have the same principal quantum number but one has the projection quantum number reversed in sign from the other. In a spherical system characterized by quantum numbers n, l, and m, the states j and $-j$ differ from each other in the sign of m values. In linear polyene, the only good quantum number is n. So the only way that states j and $-j$ can differ from each other is by having spin $+\frac{1}{2}$ and $-\frac{1}{2}$. It is to be remembered, however, that HFB calculations do not take spin into account at any stage. We can only say that there is electron pairing in the same level of polyene, but to satisfy the basic requirements of HFB theory, the two electrons must have opposite projection quantum numbers. But this term does not arise from spin–spin interaction in any way. With this basic prescription, we now analyze the electronic spectra of polyene in greater detail.

NEUTRAL (I) MONONEGATIVE ION (II)

Fig. 3. Energy levels of neutral and mononegative ions.

Let us consider the level schemes for a neutral and a negatively charged polyene (Fig. 3). In Case I, an electron from f (Fermi level) can go to level c, such that $e_c - e_f \geq \Delta$, i.e., the low-lying excited states cannot be populated as the pairing interaction cannot be "broken" by the energy supplied for the low-energy transitions. The minimum amount of energy that the system can absorb is Δ, i.e., the spectrum should converge to Δ. The same argument should hold for the dinegative ion. In Case II, for the mononegative ion, on the other hand, the unpaired electron in level a may be excited to any of the vacant levels as there is no pairing interaction to "break." So this system will show no convergence. For the mononegative ion there may be transitions from level f to higher states. These transitions will be restricted by the pairing interaction in the same way as the neutral and dinegative polyene, so that the higher-frequency transitions will converge. This is borne out by the experimental results, as shown by the dotted curve in Fig. 2. The pairing interaction, therefore, explains fairly well the electronic spectrum of neutral, mono-, and dinegative polyene ions (Szymanski, 1970).

VI. Mechanism of Pairing Interaction

The major factor that determines the appearance of pairing interaction and energy gap is the presence of an attractive force between two electrons. The appearance of such a force in superconductors may be explained in a number of ways. Interaction of electrons with the crystal lattice plays a major role in bringing about such an attraction. An electron moving in the metal deforms the electrical field and polarizes the crystal lattice. The shift in ions in the lattice thus induced is reflected in the state of another electron, since it is now in the field of a polarized lattice with a changed periodic structure. Hence the crystal lattice plays the role of an intermediate medium, the presence of which leads to interelectronic attractions (Kuhn and Huber, 1959). The electron is surrounded by a cloud of positive charges due to deformation of the lattice (Hubbard, 1958; Linderberg and Ohrn, 1968). The magnitude of this charge may exceed that of the electronic charge. The electron, together with the cloud surrounding it, is then a positively charged system that is attracted to another electron. This is the qualitative description of the fundamental mechanism of the physics of superconductors. In the quantum picture, the perturbation of the crystal lattice state can be described as disruption by the moving electron of the condition of "null" vibration of the ionic system. Additional attraction between the electrons in this process is due to exchange of virtual phonons (Kresen, 1967a,b; Ginzburg, 1964).

Similar interaction mechanisms are observed in complex molecules. We shall first consider the interaction of π-electrons with the σ-framework. Virtual transitions of the σ-electron system play the most important role (Hubbard, 1958; Linderberg and Ohrn, 1968). Due to Coulomb interaction, π-electrons cause transitions of a σ-electron. We note that experimentally excitation of σ-electrons (σ–π transitions) are observed corresponding to a frequency of 4×10^4 cm^{-1}. On return of the σ-electrons to the original state, the energy is transmitted to another electron, which leads to an effective interaction between π-electrons.

The Hamiltonian of the system may be written in the form

$$H = H^{\pi} + H^{\sigma} + H^{\sigma\pi}. \tag{VI.1}$$

Within the concept of second quantization, we now write the term H that describes the interaction of the π-electron and σ-electron as

$$H^{\sigma\pi} = \sum_{ij} A^{\pi\sigma}_{\lambda_i \mu_j,\, \lambda_i \mu_j} c^{+}_{\lambda_i} c^{+}_{\mu_j} c_{\lambda_i} c_{\mu_j}, \tag{VI.2}$$

where λ_i and μ_j are the sets of quantum numbers that describe the states of the π- and σ-electrons, respectively. The matrix element $A^{\pi\sigma}_{\lambda_1\mu_1\lambda_2\mu_2}$ is equal to $\langle \lambda_1 \mu_1 | v | \lambda_2 \mu_2 \rangle$. Within the limit of second-order perturbation theory, we arrive at the following effective Hamiltonian of the π-electrons describing its interaction with the σ-framework:

$$H^{\pi} = \sum_{\lambda_i} g_{\lambda_1\lambda_2\lambda_3\lambda_4} c^{+}_{\lambda_1} c^{+}_{\lambda_2} c_{\lambda_3} c_{\lambda_4}, \tag{VI.3}$$

where

$$g_{\lambda_1\lambda_2\lambda_3\lambda_4} = \sum_{\mu_1\mu_2} \frac{A_{\lambda_1\mu_1\lambda_3\mu_2}}{(e^{\pi}_{\lambda_3} - e^{\pi}_{\lambda_1} - \Delta^{\sigma})} \cdot \frac{A_{\lambda_2\mu_1,\, \lambda_4\mu_2}}{(e^{\pi}_{\lambda_4} - e^{\pi}_{\lambda_2} - \Delta^{\sigma})} \cdot n^{\sigma}_{\mu_1}(1 - n^{\sigma}_{\mu_2}), \tag{VI.4}$$

the e^{π}_{λ}'s are the single-particle levels of the π-electron system, Δ^{σ} is the change in the energy of the σ-electron during virtual transition, and factor $n^{\sigma}_{\mu_1}(1 - n^{\sigma}_{\mu_2})$ is associated with the restriction imposed by the Pauli principle. It is apparent that $\Delta^{\sigma} > 0$. It follows from (VI.3) that $g < 0$ for transitions in the π-electron system corresponds to energy change smaller than Δ, i.e., the effective attraction arises in the π-electron system (Kresen, 1967a,b).

Another mechanism that has been proposed for superconductors is associated with the presence of different electron groups in metals and semiconductors. Such groups may be formed by the electrons that are in different energy zones or to different domains of the semiconductors. In this process, attraction of electrons in one zone arise from their Coulombic interaction with the electrons in the other zone, undergoing virtual transitions. In π-electron systems, the attraction between the electrons may arise from the existence of various groups of π-electrons in the molecule. Thus, the virtual transitions of the π-electrons of the phenyl group in diphenylpolyene may bring about an effective attraction in the ground state of the π-electron system of the polyene chain.

The third mechanism arises from the interaction of π-electrons with the vibrational degrees of freedom of the molecule (Kresen, 1967a,b). The appropriate Hamiltonian can be written in the form

$$H_1 = \sum_{ja} v(r_j - R_a),$$

where r_j gives the position of the electron, and R_a that of the nucleus. By expanding H_1 in powers of δR_a, we obtain

$$H_1 = \sum_{ja} v(r_j - R_{a0}) + \sum_{ja} \delta R_a \nabla v(r_j - R_{a0}). \tag{VI.5}$$

By combining the first term of the expansion with H_0 and representing δR_a in the form of superposition of normal vibrations we get the following Hamiltonian for the electrons within the framework of second quantization:

$$H_{\text{int}}^{\pi\pi} = \sum_{\substack{\lambda,\lambda' \\ \lambda_1,\lambda_1'}} g_{\lambda\lambda',\lambda_1\lambda_1'} c_\lambda^+ c_{\lambda_1}^+ c_{\lambda'} c_{\lambda_1'}, \tag{VI.6}$$

where

$$g_{\lambda\lambda',\lambda_1\lambda_1'} = \sum M_{\lambda\lambda'} M'_{\lambda_1\lambda_1'} \frac{\omega}{(e_\lambda - e_{\lambda'})^2 - \omega^2}. \tag{VI.7}$$

Here the λ and λ' refer to vibrational states, and λ_1 and λ_1' to the corresponding electron transitions. It is clear that the values of $e_\lambda - e_{\lambda'} < \omega$, where the change in electronic energy is less than the energy of excitation of the virtual vibrational quanta, correspond to the interelectronic attraction. In this mechanism the superconductivity of metals is associated with the interaction of conductivity electrons with lattice vibrations. It should be noted that the preceding mechanism may be satisfied either due to the existence in a molecule of groups that have a high vibrational frequency or to deviation from the simple adiabetic picture. The second possibility definitely exists for complex organic molecules. Whatever the mechanism for the attractive interaction may be, the electron interaction is responsible for the convergence in the electronic spectra of linear polyenes.

VII. Concluding Remarks

In the foregoing discussion, we have established that the pairing interaction between electrons introduces an energy gap between the highest occupied orbital (homo) and the lowest empty orbital (lemo). We expect convergence with chain length in any physical property that depends on the position of lemo or the energy difference between homo and lemo. The energy of lemo determines the electron affinity of the π-electron system and this is related to the polarographic half-wave potential ($E_{1/2}$). In Fig. 4 is given the plot of $E_{1/2}$ against the number of bonds in diphenylpolyene (Van der Meij, 1958). It may be observed that the curve is, in fact, convergent.

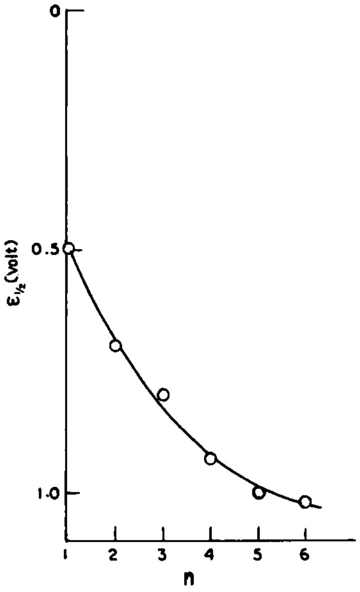

Fig. 4. Plot of $E_{1/2}$ vs. chain length for diphenylpolyene.

The electronic polarizability of a molecule is calculated from the following second-order energy expression:

$$E_2 = \sum_{n \neq 0} \sum_{ij} \frac{\langle \psi_0 | H(i) | \psi_n \rangle \langle \psi_n | H(j) | \psi_0 \rangle}{e_0 - e_n}, \qquad \text{(VII.1)}$$

where 0 and n refer to the ground and excited states. In the simple description, the difference $(e_0 - e_n)$ goes to zero as the length of the chain goes to infinity. The polarizability of a very long-chain molecule is, therefore, very large. Introduction of an energy gap will cause the polarizability to converge. However, this point has not been experimentally tested.

REFERENCES

Araki, G., and Murai, T. (1952). *Prog. Theor. Phys.* **8**, 639.

Balk, P., Hoijtink, G. J., and Schreurs, J. W. H. (1957a). *Recl. Trav. Chim. Pays-Bas* **76**, 813.

Balk, P., De Bruin, S., and Hoijtink, G. J. (1957b). *Recl. Trav. Chim. Pays-Bas* **76**, 860.

Balk, P., De Bruin, S., and Hoijtink, G. J. (1958). *Mol. Phys.* **1**, 151.

Bardeen, J., Cooper, L. N., and Schrieffer, J. R. (1957). *Phys. Rev.* **108**, 117.

Basu, S. (1974). *Bull. Chem. Soc. Jpn.* **47**, 2618.

Basu, S. (1975). *Bull. Chem. Soc. Jpn.* **47**, 735.
Bayliss, N. S. (1948). *J. Chem. Phys.* **16**, 287.
Bayliss, N. S., and Riviere, J. C. (1951) *Aust. J. Sci. Res., Ser. A* **4**, 344.
Boglyubov, N. N. (1958). *Dokl. Akad. Nauk SSSR* **110**, 936.
Coulon, C. A. (1938). *Proc. R. Soc. London, Ser. A* **169**, 413.
Dewar, M. J. S. (1952). *J. Chem. Soc.* p. 3544.
Ginzburg, V. L. (1964). *Zh. Eksp. Teor. Fiz.* **47**, 2318.
Hausser, K. W., and Kuhn, R. (1935). *Z. Phys. Chem., Alt. B* **29**, 363.
Hubbard, J. (1958). *Proc. R. Soc. London, Ser. A* **244**, 199.
Kresen, V. Z. (1967a). *Dokl. Akad. Nauk SSSR* **177**, 1306.
Kresen, V. Z. (1967b). *Phys. Lett. A* **24**, 749.
Kuhn, H. (1948). *Helv. Chim. Acta* **31**, 1441.
Kuhn, H. (1949). *J. Chem. Phys.* **17**, 1198.
Kuhn, H., and Huber, W. (1959). *Helv. Chim. Acta.* **42**, 2618.
Lennard-Jones, J. E. (1937). *Proc. R. Soc. London* **158**, 280.
Linderberg, J., and Ohrn, Y. (1968). *J. Chem. Phys.* **49**, 716.
Ooshika, Y. (1957). *J. Phys. Soc. Jpn.* **12**, 1238.
Pal, M. (1970). IAEA-SMR-6125, p. 566.
Paul, D. E., Lipkin, D., and Weissman, S. I. (1956). *J. Am. Chem. Soc.* **78**, 119.
Platt, J. (1956). *J. Chem. Phys.* **25**, 80.
Salem, L. (1966). "The Molecular Orbital Theory of Conjugated Systems," p. 366. Benjamin, New York.
Salem, L., and Longuet-Higgins, H. C. (1959). *Proc. R. Soc. London, Ser. A* **251**, 172.
Salem, L., and Longuet-Higgins, H. C. (1960). *Proc. R. Soc. London, Ser A* **255**, 435.
Simpson, W. T. (1948). *J. Chem. Phys.* **16**, 1124.
Szymanski, Z. (1970). IAEA-SMR-6125.
Tomonaga, S. (1950). *Prog. Theor. Phys.* **5**, 544.
Tsuji, M., Huzinaga, S., and Hashino, T. (1960). *Rev. Mod. Phys.* **32**, 425.
Valentin, J. G. (1961). *Phys. Rev.* **122**, 1012.
Van der Meij, P. H. (1958). Thesis, Free University, Amsterdam.
Weissman, S. I., Townsend, J., Paul, D. E., and Parke, G. E. (1953). *J. Chem. Phys.* **21**, 2227.

ADVANCES IN QUANTUM CHEMISTRY, VOLUME 11

Kossel Isoelectronic Series and Photoelectron Spectra

CHRISTIAN KLIXBÜLL JØRGENSEN
Département de Chimie Minérale, Analytique et Appliquée
Université de Genève
Geneva, Switzerland

I. Introduction

The paper by Walter Kossel entitled "Über Molekülbildung als Frage des Atombaus," which appeared in the March 1916 issue of *Annalen der Physik* (Kossel, 1916), contained 134 pages (apparently referees then were not the same as what they are today). It is a remarkable attempt to reconcile and connect atomic spectroscopy with chemistry, and, since the Aufbau principle with $(4l + 2)$ electrons in each nl shell was not formulated until 1924, it is also an early unification of X-ray and atomic spectra. It cannot be said that Kossel was the first author to discuss closed shells of electrons: this concept goes back to the planar distribution of electrons in rings proposed by Thomson (cf. the recent review by Heilbron, 1977). It was recognized that noble gas atoms have ionization energies about 4 times that of the atom of the subsequent alkaline metal. Hence, Kossel suggested that certain numbers of electrons confer a particular stability to the atom and that neighboring elements readily gain one (halogen) or two (chalkogens), if their atomic number Z is one or two units below that of the noble gas, whereas higher Z values correspond to a ready loss of electrons.

In a note commemorating the sixtieth anniversary of this idea (Jørgensen, 1976c), it was proposed to call the number of electrons in a given species K, and an *isoelectronic series* is constituted by monatomic entities having the

ISBN 0-12-034811-X

same *K*. This integer is obviously well defined when the system containing only one nucleus can be observed under isolated conditions, but, in gaseous molecules or in condensed matter, it is not evident that each atom has this "quantum number" *K*. Nevertheless, it can be argued (Jørgensen, 1969) that oxidation states in typical inorganic compounds form isoelectronic series. Kossel did not only select noble gas electron configurations, but on his Figure 1 (Kossel, 1916, p. 255) $K = 28$ and 46 are clearly indicated. Actually, long isoelectronic series (containing from seven to twelve members, as discussed in the following) occur in chemistry for

$$K = \mathit{2}, \mathit{10}, \mathit{18}, 28, \mathit{36}, 46, 48, \mathit{54}, 68, 78, 80, \mathit{86}, 100, \ldots \qquad (1)$$

corresponding to the *Aufbau principle* of consecutive closure of the *nl* shells:

$$1s, (2s + 2p), (3s + 3p), 3d, (4s + 4p), 4d, 5s, 5p, 4f, 5d, 6s, 6p, 5f, \ldots \qquad (2)$$

Only the italicized *K* values in Eq. (1) correspond to noble gas atoms. It should not be argued that only *K* values indicating closed shells occur in chemistry. Actually, all integers from $K = 19$ to 99 are also known (Jørgensen, 1969) including the somewhat doubtful case of $K = 77$, based on the existence of (monomeric) gold(II) compounds. However, the profound difference is that only one to four members of the non-closed-shell isoelectronic series usually are known. Somewhat special cases are $K = 24$, having six members from vanadium(−I) to nickel(IV), and $K = 74$, having seven members from tantalum(−I) to gold(V). The octahedral symmetry is particularly suitable for six d electrons and diamagnetic ground state ($S = 0$), and for the last two oxidation states, only one example of each, $Ta(CO)_6^-$ and AuF_6^-, is known, whereas tungsten(0), osmium(II), iridium(III), and platinum(IV) complexes are numerous and mostly octahedral.

Obviously, the Kossel isoelectronic series was originally associated with a rather electrostatic picture of chemical bonding, derived from the ideas of Berzelius. However, we show in the following that oxidation states can be defined as (negative or positive) integers in a multitude of compounds without reference to the numerical questions of whether the binding energies are well described by Madelung expressions and whether the wavefunctions are, indeed, ionic. It is a very valuable result of atomic spectroscopy that the symmetry types and the number of mutually orthogonal states (obtained by permutational theory according to the Pauli exclusion principle) characterize a given electron configuration without the requirement of Slater antisymmetrized determinants implying vanishing correlation effects. This is a rather sophisticated statement: on the one hand, a given *K* value corresponds to very many electron configurations and, on the other hand, there may occur situations (in chemistry) where a certain number of electrons constitutes an undifferentiated background with the behavior characterizing a set of closed shells, without definite localization on each atom. Thus, the tetrahedral molecule VCl_4 contains one 3d-like electron, and octahedral IrF_6 has three 5d-like electrons, irrespective of the molecular orbitals containing eight electrons from each halide delocalized to some extent on the central atom having the oxidation states vanadium(IV) and iridium(VI); these are instances of $K = 19$ $(= 18 + 1)$ and of $K = 71$ $(= 68 + 3)$.

II. Classificatory Aspects of Electron Configurations

The National Bureau of Standards circulars "Atomic Energy Levels" (Moore, 1949, 1952, 1958) are the major source attesting to the conceptual utility of the electron configuration. Most of the monatomic entities have 20–400 J levels (with even or odd parity), which can be assembled in electron configurations according to the rules of vector coupling (Hund, 1927; Condon and Shortley, 1953). Whereas there are hardly any low-lying levels that escape this classification by being obviously superfluous, there are also rather impressive cases of almost complete configurations, such as the 38 out of the predicted 41 J levels of the lowest configuration $[Xe]4f^3$ and 101 among the 107 J levels of the next-lowest $[Xe]4f^2 5d$ that have been identified with certainty in gaseous Pr^{2+} (Sugar, 1963; Trees, 1964).

One might argue that the excellent parametrization in terms of interelectronic repulsion and of spin–orbit coupling may be taken as evidence that these configurations are rather pure (in the sense that the optimized Slater determinant $1s^2$ contributes 0.99 to the squared amplitude of the wavefunction of the ground state of the helium atom). However, this seems highly unlikely in atoms heavier than neon. Atomic number $Z = 10$ constitutes a crossing-point in the sense that as soon as Z is above 10, the ionization of the neutral atom costs less than the correlation energy (relative to the Hartree–Fock function) with opposite sign. A closer analysis (Jørgensen, 1962b, c) of the *Watson effect*, i.e., that the term distances inside a given configuration in an isoelectronic series (*e.g.* $[Ar]3d^3$ of Ti^+, V^{2+}, Cr^{3+}, Mn^{4+}, Fe^{5+}) are decreased by amounts almost independent of the *ionic charge* z (when compared with the prediction from Hartree–Fock results), suggests a major influence of two-electron substitutions on continuum orbitals with positive one-electron energy. To the first approximation, the phenomenological parameter of interelectronic repulsion (separating the terms characterized by the quantum numbers S and L in Russell–Saunders coupling) is $(z + 2)/(z + 3)$ times the Hartree–Fock integrals in the case of a partly filled 3d shell. This does not prevent the lower L values from appearing more depressed by the Watson effect than by high L values. Thus, the terms ^2P and ^2H of $3d^3$ should coincide in the Slater–Condon–Shortley treatment; but ^2P is distinctly lower in the actual ions. The latter type of deviations can be described by Trees parameters, and the physical mechanism (Trees and Jørgensen, 1961) in the example is the interaction (via the two-electron operator) of configurations $[Ne]3s^2 3p^6 3d^q$ and $[Ne]3s^2 3p^4 3d^{q+2}$ (which belong to the continuum so far as the diagonal element of total energy is concerned, but involve orbitals with negative one-electron energy, in contrast to a typical continuum two-electron substitution such as $[Ne]3s^2 3p^6 3d^{q-2}(\infty f)^2$). The deviations from Hartree–Fock results for gaseous ions containing a partly filled 4f shell are even larger, and a model of core-polarization (Morrison, 1972; Caro *et al.*, 1976) explains about one-third of the decrease of parameters of interelectronic repulsion in Pr^{3+}, Dy^{2+}, and Er^{3+}. Many authors speak about a "Coulomb hole" stabilizing terms of low S by a particularly strong correlation effect compared with the ground state having maximum S. This idea is in conflict with experiment in the configurations d^q presenting two terms with S_{max} such as ^3P and ^3F for $q = 2$ and 8, and ^4P and ^4F for $q = 3$ and 7. If anything, the distance between two such terms is shorter (compared with Hartree–Fock results) than it is between the ground term and terms with lower S. It may once more be noted that the numerous terms of $[Xe]4f^q$ agree much better with the Slater–Condon–Shortley theory, as reorganized by Racah (1949) and described in two books (Judd, 1963; Wybourne, 1965), than do the three terms p^2, p^3, and p^4 (Jørgensen, 1969; Katriel and Paunсz, 1977).

One might seek a theoretical explanation for the Watson effect (invariant with z) and the Trees effect [roughly proportional to z like the large contribution to the correlation energy of the ground state of the isoelectronic series ($K = 4$) $Be^0, B^+, C^{2+}, \ldots$ due to interaction between $1s^2 2s^2$ and $1s^2 2p^2$] in a theorem first found by Linderberg and Shull (1960) and later elaborated (Linderberg, 1961). In a given isoelectronic series, the *nonrelativistic* wavefunction for a given S, L term shows the eigenvalue:

$$E = -Z^2 \text{ hartree } (h_0 + h_1 Z^{-1} + h_2 Z^{-2} + \cdots), \tag{3}$$

where the first three coefficients h_0, h_1, and h_2 are predominant in atoms containing at most ten electrons. Actually, h_0 has the *hydrogenic value* obtained by summation over $(\frac{1}{2}n^2)$ for each electron having the principal quantum number n in what the writer (Jørgensen, 1969) calls the *preponderant configuration*, and h_1 has a definite value (generally an infinite decimal fraction) generated by the configurations having the same number of electrons with a given n (Linderberg and Shull, 1960) such as $1s^2 2s^2$ and $1s^2 2p^2$ for the lowest ^1S of $K = 4$. It is obvious that the (generally smaller) Trees effect is mainly expressed by h_1, whereas the Watson effect independent of the ionic charge $z = (Z - K)$ is mainly expressed by h_2.

Equation (3) is a rather unique case in the quantum mechanics of many-electron atoms involving actual wavefunctions and their eigenvalues: less accurate descriptions (such as a Hartree–Fock model) have smaller h_2 and smaller (or more negative) subsequent coefficients $h_3, \ldots$. Thus, the model of the ground state of ($K = 2$) with hydrogenic radial functions (optimized for the Slater screening coefficient, 0.3125) shows the correct values $h_0 = 1$ and $h_1 = -0.625$ with $E = -(Z - \frac{5}{16})^2$ hartree, whereas $h_2 = 0.09765625$. For the optimized Hartree–Fock function, $h_2 = 0.1110\ldots$, and h_3 and the following coefficients have very small values. The fact that the correlation energy is almost invariant (we exclude H^-) as a function of ionic charge z corresponds to the major difference between the Hartree–Fock expression and Eq. (3); in the latter case, $h_2 = 0.1576\ldots$

Unfortunately, the practical utility of Eq. (3) is limited by two features. Coefficients h_3, h_4, ... are rather small (for the low-K values for which they are known), but they do not converge rapidly toward zero and frequently show alternating signs that present additional difficulties for the rapid convergence. The other problem is that the relativistic corrections to Eq. (3) have coefficients times Z^4 (and $Z^6, \ldots$), starting with $-Z^4$ hartree/$137^2 \times 4$ when two 1s electrons are present, 137 being the reciprocal fine-structure constant.

In the following, the experimental data from atomic and photoelectron spectra are considered the raw material for our conclusions. At present, it would be very difficult to provide *ab initio* evidence for the problems discussed here.

III. Arguments Derived from Atomic Spectra

The crossing of different eigenvalues E of Eq. (3) belonging to the same K (but different terms) when the integer Z is varied cannot be prevented. Actually, most isoelectronic series have different ground states for small z, in particular in the d and f transition groups. On the other hand, it is not conceivable that the preponderant ground configuration varies for K at most 18. A major distinction between atomic spectroscopy and chemistry is that, in the former case, anions M^- cannot carry more than one negative charge. Even gaseous O^{2-} loses spontaneously an electron in empty space to form O^-. The *electron affinity* of the neutral M atom is the same quantity as the ionization energy of M^-. It is not reasonable to speak about *negative* electron affinities. Such results are either derived from the heats of formation of crystals (say, oxides), assuming the Born–Haber–Fajans model, or from Hartree–Fock functions constrained to contain equivalent electrons (with identical radial functions) such as $1s^22s^22p^6$ isoelectronic with neon. The problem is that a very large number of other configurations, of the type

$1s^22s^22p^53p$ or $1s^22s^22p^5117d$, are more stable in the latter case. Related problems can occur in species, such as H^-, that are stable in the sense of having a positive ionization energy. Not only is the Slater screening constant model of H^- (7 hartree/256) *less* stable than the hydrogen atom, but H^- does not possess a conventional Hartree–Fock function. The writer is not in favor of the wording "unrestricted Hartree–Fock function" for a mixture of two configurations $(n_1s)^2$ and $(n_2s)^2$ for the wavefunction, which can readily be shown to be algebraically equivalent with two different radial functions being allowed to accommodate each one electron.

Gaseous anions M^- have not attracted much interest among atomic spectroscopists, because they do not possess detectable, excited, discrete states (although the halides show two series limits in absorption just as for the isoelectronic noble gases, corresponding to the two spin-orbit components $j = \frac{3}{2}$ and $\frac{1}{2}$ of the p shell). Berry (1969) and Massey (1976) have reported on recent progress in evaluating ionization energies. About one-quarter of the neutral atoms have zero electron affinity. Outside the transition groups, the M atoms forming M^- with a positive affinity undoubtedly provide a ground state of the same kind as the neutral atom of the subsequent element. In d-group atoms with two external s electrons, normally an additional d electron occurs. Atoms such as Nb, Mo, Tc, Ru, and Rh, having ground states belonging to the configuration $[Kr]4d^q5s$, presumably form M^- of $[Kr]4d^q5s^2$ (Zollweg, 1969). However, it is difficult to evaluate the corresponding low-electron affinities between 0 and 2 eV with experimental or theoretical arguments. It is also probable that the lanthanides form gaseous M^-, with the ground state being the lowest J-level of $[Xe]4f^q5d6s^2$ and not $[Xe]4f^{q+1}6s^2$ as recently suggested (Angelov, 1976), probably in analogy to the eleven (excluding La, Ce, Gd, and Lu) neutral lanthanide atoms, namely, Pr, Nd, Pm, Sm, Eu, Tb, Dy, Ho, Er, Tm, and Yb. Seen from the point of view of an atomic spectroscopist, these atoms are really barides, though one should not neglect the slightly arbitrary character of this classification, when it is realized the two configurations mentioned may be 10–300 times wider than the tiny energy difference between the lowest level of each of the two configurations.

The isoelectronic series $K = 68$ is a typical case of a closed-shell configuration not represented in the neutral atom, but only from Yb^{2+} onward, where the ground state is the only state of $[Xe]4f^{14}$ (Kaufman and Sugar, 1976) corresponding also to the chemical isoelectronic series having seven members, from ytterbium(II) to osmium(VIII). On the other hand, ground state $^3H_6$ of the gaseous erbium atom belongs to $[Xe]4f^{12}6s^2$, and $^3F_4$ of Tm^+ to $[Xe]4f^{13}6s$. The situation is more sophisticated for $K = 67$. As already mentioned, it is likely that the ground state of Dy^- belongs to $[Xe]4f^{10}5d6s^2$, and it is certain that the lowest-level $^4I_{15/2}$ of the holmium atom belongs to $[\mathrm{Xe}]4\mathrm{f}^{11}6\mathrm{s}^2$, and Er^+ to $[\mathrm{Xe}]4\mathrm{f}^{12}6\mathrm{s}$. One would have expected Tm^{2+}, Yb^{3+}, $\mathrm{Lu}^{4+}, \ldots,$ and all the subsequent positive ions to have the lowest-level ${}^2\mathrm{F}_{7/2}$ of $[\mathrm{Xe}]4\mathrm{f}^{13}$. However, Kaufman and Sugar (1976) pointed out that this is only the case up to W^{7+}. Beginning with Re^{8+} and going on to Bi^{16+}, it is easier to remove a 5p electron (from the complete shells of the xenon atom) than to ionize the 4f shell, and the ground state is actually ${}^2\mathrm{P}_{3/2}$ of the configuration $[\mathrm{Kr}]4\mathrm{d}^{10}4\mathrm{f}^{14}5\mathrm{s}^2 5\mathrm{p}^5$. Such a situation was obtained also from Hartree–Fock calculations by Cowan (1973), suggesting the following, most probable, ground configurations (only the occupation of the 5p and the 4f shells is indicated):

M	M^{4+}	M^{5+}	M^{6+}	M^{7+}	M^{8+}	M^{9+}
Nd	$5\mathrm{p}^6 4\mathrm{f}^2$	$5\mathrm{p}^6 4\mathrm{f}$	$5\mathrm{p}^6$	$5\mathrm{p}^4 4\mathrm{f}$	$5\mathrm{p}^3 4\mathrm{f}$	$5\mathrm{p} 4\mathrm{f}^2$
Gd	$5\mathrm{p}^6 4\mathrm{f}^6$	$5\mathrm{p}^6 4\mathrm{f}^5$	$5\mathrm{p}^6 4\mathrm{f}^4$	$5\mathrm{p}^5 4\mathrm{f}^4$	$5\mathrm{p}^3 4\mathrm{f}^5$	$5\mathrm{p}^2 4\mathrm{f}^5$
Er	$5\mathrm{p}^6 4\mathrm{f}^{10}$	$5\mathrm{p}^6 4\mathrm{f}^9$	$5\mathrm{p}^6 4\mathrm{f}^8$	$5\mathrm{p}^5 4\mathrm{f}^8$	$5\mathrm{p}^4 4\mathrm{f}^8$	$5\mathrm{p}^2 4\mathrm{f}^9$

(4)

The concomitant parabolic variation of the number of 4f electrons as a function of the ionic charge for a given element is probably characteristic for this crossing of the 5p and 4f shell energies. All the same, Eq. (4) demonstrates the conceptual difficulty involved in speaking about one-electron energies as if they were additive in the total energy of the configuration, neglecting the parabolic dependence on occupation numbers introduced by interelectronic repulsion, when the shells differ strongly in average radii. This variation can be described quantitatively by the *phenomenological baricenter polynomial* (Jørgensen, 1969, 1973a, 1974a). For sufficiently high ionic charges, the 5s and 5p lose their preferential occupation with respect to 4f, and the hydrogenic order is restored. Then, the isoelectronic series $K = 47$ to 60 contains $(K - 46)$ electrons in the 4f shell, quite in contrast to the position of the lanthanides in the periodic table. Since the validity of the Aufbau principle in the form of Eq. (2) starts with gaseous M^{2+} (with the five exceptions, M = La, Gd, Lu, Ac, and Th, whereas no exceptions are known for M^{3+}, M^{4+}, and M^{5+}), it is likely that the first exceptions for higher ionic charges occur for M^{7+} as in Eq. (4). In other words, the decisive criterium for Eq. (2), which is of great significance for inorganic chemistry (because those compounds having well-defined oxidation states turn out to adopt this Aufbau principle), seems to be the ionic charge below $+7$ (or Re^{8+}) rather than the atomic number. The 5p–4f shell-crossing in photoelectron spectra (Jørgensen, 1976b) occurs between tungsten ($Z = 74$) and osmium ($Z = 76$) almost at the same elements as between gaseous W^{7+} and Re^{8+}.

IV. Closed Shells as the Neutral Element of Vector Coupling

The periodical table was established by Mendeleev in 1869 based on chemical analogies, although some early associations between atomic spectroscopy and chemistry had been made. Thus, the publication of the principles of line spectra in 1860 by Bunsen and Kirchhoff was immediately followed by the discovery of rubidium, cesium, and slightly later by gallium, indium, and thallium. Rydberg pointed out that all five alkaline metals have line spectra of which the wave numbers can be connected via Ritz's combination principle to term values following the Rydberg formula. What is even more important for our purpose is that the spark spectra (i.e., of M^+) of the alkaline-earth metals are quite similar to the isoelectronic alkaline metal atoms in this respect, although they have an apparent Rydberg constant 4 times larger. This result was generalized by multiplying the original Rydberg formula by $(z + 1)^2$. A certain divergence between the chemical and the spectroscopic versions of the periodical table appeared when it was realized that not only Be, Mg, Ca, Sr, Ba, and Ra but also He, Zn, Cd, Yb, and Hg are similar *spectroscopic alkaline-earths* with series of triplet and singlet terms each following the Rydberg formula to a high precision. This development is important for our subject for two reasons: one is the concept that one or two external electrons (*Leuchtelektron*) outside a neutral background of the atomic core (*Atomrumpf*) have no influence on the number of energy levels; the other is the fact that in Russell–Saunders coupling the total-spin quantum number S is an odd positive integer divided by 2 for an *odd* number of electrons, but a nonnegative integer for an *even* number of electrons. This alternation (when removing or adding one electron at a time) is not an approximate result based on the validity of the Russell–Saunders coupling, but it is also present in the quantum number of total angular momentum J which is well defined on condition of spherical symmetry with center of inversion, even with superposed strong relativistic effects (spin–orbit coupling).

Around 1920, the feeling among atomic spectroscopists was that "simple" atoms show *series spectra* (described to a good approximation by the Rydberg formula) as treated by Fowler (1922), whereas the "complicated" atoms (mainly concentrated in the transition groups) show *multiplet spectra.* The first connection between these two categories was the analysis by Paschen (1919) of the spectrum of the neon atom. The numerous lines could be identified with transitions between the four J levels of the next-lowest configuration $1s^2 2s^2 2p^5 3s$ and the ten J levels of each of the configurations such as $1s^2 2s^2 2p^5 3p$ or $1s^2 2s^2 2p^5 4p$. Weaker spectral lines involve transitions from the latter configurations to the twelve J levels of $1s^2 2s^2 2p^5 3d$ or $1s^2 2s^2 2p^5 4d$. Not only was this classification soon extended to the heavier noble gases Ar, Kr, Xe, and Rn, but it also formed the experimental basis for the *vector-coupling model* developed by Hund (1927). Disregarding the somewhat simplistic physical approach of atomic spectroscopists before the Schrödinger equation was introduced, quantum vector coupling is an operation (commutatively symmetric) involving two quantum numbers Q_1 and Q_2 (neither of which is negative),

$$Q_1 \oplus Q_2, \tag{5}$$

producing alternative results (unless at least one of the quantum numbers is zero):

$$(Q_1 + Q_2); (Q_1 + Q_2 - 1); (Q_1 + Q_2 - 2); \\ \ldots; (|Q_1 - Q_2| + 1); |Q_1 - Q_2|. \tag{6}$$

In Russell–Saunders coupling, the individual S, L terms have exactly the levels with $J = S \oplus L$, and the terms of a given electron configuration can be obtained by the operation (5) applied consecutively to each partly filled nl shell. The associative law, $Q_1 \oplus (Q_2 \oplus Q_3) = (Q_1 \oplus Q_2) \oplus Q_3$, allows an arbitrary choice of the order of these operations, and it is only necessary to know the terms of a given number q of electrons in a shell with definite l. *Pauli's hole-equivalence principle* is that the same terms (and, hence, also the same J levels) occur for $(4l + 2 - q)$ and q electrons. Thus, $(4l + 1)$ electrons, or a single electron, have one term with $S = \frac{1}{2}$ and $L = l$. An explicit expression is known for the terms of two "equivalent l electrons" (the wording used by atomic spectroscopists for electrons in the same shell):

$${}^1\text{S}, {}^3\text{P}, {}^1\text{D}, {}^3\text{F}, {}^1\text{G}, {}^3\text{H}, {}^1\text{I}, \ldots, {}^3(2l-1), {}^1(2l). \tag{7}$$

This series, selecting half the terms occurring for two nonequivalent electrons $(n_1 l)(n_2 l)$, also decreases the ratio between triplet and singlet states, $(2S + 1)(2L + 1)$ for each term, to $3l/(l + 1)$ from 3 for the latter, simpler case. Karayianis (1965) found recursive formulas for the terms of l^q, and the practically important results for $l = 1, 2, 3$ have appeared in textbooks for many years.

The number of mutually orthogonal, many-electron wavefunctions, *states*, such as $(2J + 1)$ for each J level, plays an important role in our considerations. The correct number of levels with a given J can be evaluated by coupling schemes, which do not need to be perfectly realistic, because second-order perturbations do not modify the number of states with a given symmetry type. In particular, the well-established correlation effects mixing a given configuration with other configurations (mainly substituted in the orbitals of two of the electrons) do not modify the number and symmetry types (S, L) of the terms of what is now called the "preponderant configuration." Also the number of J levels can be evaluated in Russell–Saunders coupling, though it may be recognized to be an otherwise unsatisfactory approximation in a heavy atom with strong relativistic effects. The other way round, the assignment of electrons ranging from zero to $(2j + 1)$ to each group nlj (where $j = l \pm \frac{1}{2}$ for positive l) also provides the same J levels as Russell–Saunders coupling for a distribution of the same number of electrons on the same nl shells.

Many operations have a *neutral element* Q_0. If the commutative law applies, it means that every Q related to Q_0 by the operation remains invariantly Q. Thus, the neutral element of addition is zero and of multiplication, $+1$. It is interesting to compare these with quantum numbers showing two possible values (Jørgensen, 1971) such as parity, where even (*gerade*) wavefunctions remain invariant by the transformation from a point (x, y, z) to $(-x, -y, -z)$ with the center of inversion at the origin, whereas odd (*ungerade*) wavefunctions are multiplied by (-1); in planar systems (such as molecules having all their nuclei in the xy plane), where "σ" wavefunctions remain unchanged from (x, y, z) to $(x, y, -z)$ and "π" functions (this does not mean $\lambda = 1$ in linear symmetries) are multiplied by (-1); and in the classification of atomic $l\lambda$ orbitals ($\lambda = 0, 1, 2, \ldots, l$) with an additional quantum number ç having the value c when invariant going from (x, y, z) to $(x, -y, z)$ with λ determined around the linear z axis, and having the value s when multiplied by (-1) during such a transformation. In each case, one of the two alternatives corresponds to the neutral element of Hund vector coupling and is possessed by the total symmetry type of the point group considered. It may be mentioned that *atomic* orbitals adapted to spherical symmetry are "σ" if $(l + \lambda)$ is even, and "π" if $(l + \lambda)$ is an odd integer.

The neutral element of the vector coupling [Eq. (5)] combines even parity with $S = L = J = 0$. This is an obvious property of closed-shell systems in spherical symmetry, if each nl shell contains $(4l + 2)$ electrons or is empty. It is less evident whether all even $^1S_0$ states have closed-shell character. In Russell–Saunders coupling for pure configurations, there is one such state [Eq. (7)]; d^4, d^6, f^4, and f^{10} show two ^1S; f^6 and f^8, four; and according to Karayianis (1965), g^q show 3, 7, and 10 such states for $q = 4$, 6, and 8. Frequent features of ^1S states of partly filled shells, can be unusually low seniority number v (Racah, 1949), but it cannot be argued that they are of the type generating Kossel isoelectronic series, in particular because they tend to be among the highest levels of the configuration. (This is not true for all terms with $L = 0$, since ^4S states are fairly low in f^3 and f^{11} and actually coincide with the baricenter of ^4F, the first excited quartet term above ^4I to which the ground state belongs.) However, one may ask the question whether or not the ^1S ground state of the gaseous beryllium atom is a closed-shell system. The preponderant configuration $1s^2 2s^2$ has an amplitude close to 0.957 (Watson, 1960) and is admixed with $1s^2 2p^2$ having an amplitude of about 0.285. It must be admitted that the corresponding squared amplitude, 0.081, is each time the result of one of a series of consecutive ameliorated basis sets, but this kind of quantity tends to converge very rapidly to a fixed value. In the case of high ionic charges of the Kossel series ($K = 4$), Clementi and Veillard (1966) found that the $1s^2 2p^2$ amplitude smoothly decreases with increasing z and is 0.25 for Ne^{6+}. The comparable amplitudes of $1s^2 2p^4$ for $K = 6$ decreases from 0.15 for C to 0.12 for Si^{8+}, and in the case of $K = 8$, the amplitude of $1s^2 2p^6$ decreases smoothly from 0.195 for the oxygen atom to 0.173 for Si^{6+}. Linderberg and Shull (1960) analyzed the reasons why the contributions to the energy tend to enter h_1 in Eq. (3). It is, of course, a matter of taste, whether one considers 6–8% of the squared amplitude (substituting $2s^2$ with two 2p electrons) a sufficient reason not to apply the classification "closed-shell ground state" to the isoelectronic series $K = 4$.

Returning to the simpler behavior first pointed out by Rydberg, there is no doubt that the role of the closed-shell configuration as a neutral element of Hund vector coupling is the major reason for the similarities between atomic spectra of elements in the same column in the periodic table and for the fact that there is no dramatically increasing complication as a function of increasing total number of electrons $K = (Z - z)$. Chemists were happy to learn about this justification for chemical analogies, and perhaps underestimated the discrepancies between the chemical and the spectroscopic versions of the periodic table. They speak about "pseudoisoelectronic species" when the outer valence shells (taken alone) would constitute isoelectronic species in the sense as defined in the following. A better word is *isologous*, and characteristic examples are cyanate NCO^-, thiocyanate NCS^-, and selenocyanate $NCSe^-$ related by the substitution of one atom belonging to the column of chalkogens. On the other hand, cyanate is isoelectronic, not only with its isomer fulminate CNO^- but also with the gaseous molecule NNO. The equilibrium positions of the three nuclei in these species correspond to the point group $C_{\infty v}$ representing linear symmetry without a center of inversion. Other species isoelectronic with cyanate are the azide N_3^- and cyanamide NCN^{2-} anions and the gaseous molecule OCO, all three corresponding to the point group $D_{\infty h}$ with center of inversion. Carbon dioxide is also the prototype of isologous species, such as SCS and SeCSe, retaining the center of inversion, as well as OCS and OCSe belonging to the point group $C_{\infty v}$. Whereas the linear triatomic molecules ClMCl, BrMBr, and IMI (with M = Zn, Cd, and Hg) of which the photoelectron spectra have been much discussed (Jørgensen, 1976b) obviously are isologous, it is to a certain extent a matter of taste whether they are isologous with OCO and SCS, and the uranyl ion OUO^{2+} belongs to a more distant category. To mention a counterexample, $ONpO^{+}$ and $ONpO^{2+}$ are distinctly not isologous with the uranyl ion because of the presence of two or one 5f electron, respectively, on the neptunium atom (Jørgensen and Reisfeld, 1975). On the other hand, the Np(V) complex $ONpO^{+}$ is strictly isoelectronic with the plutonium(VI) complex $OPuO^{2+}$.

V. Chemical Isoelectronic Series

It is striking that the closed-shell (but not necessarily noble gas) K values in the series Eq. (1) are represented by much longer series of isoelectronic chemical species than the intervening K values. This distinction does not show up in atomic spectra, where a given K value may be represented (by species not spontaneously losing electrons) by any element between $Z = (K - 1)$ or K (according to whether or not the gaseous anion is stable) and any higher Z value. It is true that strong relativistic effects become prominent for Z above 120 (Fricke, 1975; Jørgensen, 1971, 1973a, 1979; Fricke and McMinn, 1976) and modify the concept of isoelectronic monatomic species by entirely different *nlj* distributions among the ionization energies of the inner shells. Thus, the element with $Z = 164$ is not closely similar to lead, as one would derive from isologous behavior in the nonrelativistic limit, but rather it is comparable to palladium with a closed-shell configuration of the neutral atom, and divalent compounds containing the partly filled shell $7d^8$ (Penneman *et al.*, 1971).

The idea of isoelectronic chemical species originated in the comparison of *isosteric* anions, neutral molecules, and cations, where the physical properties of the neutral molecule obviously are rather different from the salts. Some organic cases are $B(C_6H_5)_4^-$ and $N(C_6H_5)_4^+$, which are isologous with the series $M(C_6H_5)_4$ (M = Si, Ge, Sn, and Pb) and $M(C_6H_5)_4^+$ (M = P, As, Sb). It is not argued that the central atom is exactly in the state B^-, C, N^+, Si, P^+, ... but only that modifying Z of the central atom by one unit and leaving the total number of electrons constant, modifies the ionic charge of the species by one unit. Similar inorganic examples are octahedral AlF_6^{3-}, SiF_6^{2-}, PF_6^-, SF_6, and ClF_6^+; pyramidal SO_3^{2-} and ClO_3^- isologous with BrO_3^-, IO_3^-, and XeO_3; pyramidal $SnCl_3^-$, $SbCl_3$, and $TeCl_3^+$; and regular tetrahedral PO_4^{3-}, SO_4^{2-}, and ClO_4^- to be compared with the not strictly regular tetrahedral OPF_3, $O_2PF_2^-$, O_3PF^{2-}, O_2SF_2, O_3SF^-, and O_3ClF that contain the same number of electrons as the tetroxo complexes. This is also true for the protonated forms of phosphate O_3POH^{-2}, $O_2P(OH)_2^-$, $OP(OH)_3$ (conventional phosphoric acid), and $P(OH)_4^+$ (found in very strong acids such as nearly anhydrous perchloric acid).

It is not easy to give a clear-cut definition of what makes two species isosteric. It is much more a question of bond angles than of bond lengths (in spite of the much lower "bending" than "stretching" force constants, explaining unusual bond angles such as 60° in cyclopropane and P_4) and somewhat analogous to the point groups of the equilibrium nuclear positions (disregarding rotation and translation). Like in the case of subgroups to higher point groups, a parameter has frequently infinitely many alternatives in the lower symmetry, compared with a few distinct values in the higher symmetry. A typical case is the distinction between *bent* and *linear* shapes of triatomic molecules, where Walsh (1953) discussed the quantum-chemical reasons behind the bending, when molecules isologous with carbon dioxide, such as ONO^+, add one electron (to form ONO) or two electrons (nitrite ONO^- and ozone O_3 isologous with SO_2 in spite of highly different chemical properties). The questions of differing time scales of the experiment opens the possibility for quite legitimate discrepancies between crystallography (or electron diffraction) and various spectroscopic techniques (Jørgensen, 1971). It is generally felt by chemists that two species have to be both isosteric and isoelectronic in order to be genuinely analogous. This argument can be applied the other way round, inferring the oxidation state from the stereochemistry in selected cases. Thus, $HMn(CO)_5$ is octahedral like the undisputed manganese(I) complexes $XMn(CO)_5$ with $X = Cl, Br, I,$ or CH_3. The suggestion of it containing $3d^8$ manganese(−I) was previously based on two arguments. Hieber compared $HMn(CO)_5$ with $Fe(CO)_5$ and $HCo(CO)_4$ with $Ni(CO)_4$ and introduced the idea of "pseudoatoms" HMn and HCo replacing the Fe and Ni atoms. However, such an assumption would only be attractive if the Mn—H internuclear distance was particularly short. It is, indeed, shorter than Mn—Cl in the carbonyl chloride (e.g., in CH_4 compared with CCl_4) but not more than expected for a hydride ligand. The other argument is that the Brønsted acid–base equilibrium,

$$HMn(CO)_5 = H^+_{aq} + Mn(CO)_5^-, \tag{8}$$

is almost instantaneous in aqueous solution, and shows $pK = 7$ just as does the acid $O_2P(OH)_2^-$ in losing a proton to form O_3POH^{-2}. However, already Brønsted pointed out that it is *inevitable* that certain acid–base reactions simultaneously are redox (reduction–oxidation) reactions (e.g., those of hydride with protons forming H_2). Although this particular argument is not based on absolute results of measurements, it seems by far most convenient (Jørgensen, 1969) to ascribe the oxidation state H(I) only to hydrides of F, Cl, Br, I, O, S, Se, Te, and N and to classify all other hydrogen compounds as H(−I). This choice has the consequence that the reactions,

$$\begin{gathered} Be_2C + 4H^+_{aq} + 8H_2O = 2Be(OH_2)_4^{2+} + CH_4, \\ Al_4C_3 + 12H^+_{aq} + 24H_2O = 4Al(OH_2)_6^{3+} + 3CH_4, \end{gathered} \tag{9}$$

involve the oxidation of C(−IV) to C(IV) by H(I) becoming H(−I), whereas Be(II) and Al(III) do not change.

In d-group compounds, chemists also feel that it is a rather necessary condition for species that are analogous to show the same S of the ground state (as discussed in Section IX, Russell–Saunders coupling is a remarkably good approximation) besides being isoelectronic. The isosteric correspondence can go very far. Thus, the gold(I), mercury(II), and thallium(III) complexes $Au(NH_3)_2^+$, $Hg(NH_3)_2^{2+}$, $Hg(CH_3)_2$, and $Tl(CH_3)_2^+$ are strictly isoelectronic and isosteric. This can sometimes be true for species not necessarily possessing oxidation states of the heavy elements (because catenation is taken care of by a pair of electrons of unspecified character) such as the manganese carbonyl $(OC)_5MnMn(CO)_5$ and Adamson's purple dimer $(NC)_5CoCo(CN)_5^{6-}$ of which salts can be precipitated from solutions containing the green, square-pyramidal, cobalt(II) complex (with $S = \frac{1}{2}$) $Co(CN)_5^{3-}$. Also $V(CO)_6^-$, $Cr(CO)_6$, $Fe(CN)_6^{4-}$, and $Co(CN)_6^{3-}$ are strictly isoelectronic and isosteric.

Chemists speak about isoelectronic species (as just mentioned) and isoelectronic *central atoms*. Without necessarily making any assumptions of exclusively electrovalent bonding, the oxidation state z of the central atom in a given polyatomic entity is obtained by subtracting the charges corresponding to a closed-shell *standard state of the ligands* such as neutral H_2O, NH_3, CO, PF_3 or the anions F^-, Cl^-, Br^-, I^-, OH^-, CN^-, CH_3^-, ..., though a small ambiguity shows up in the last carbanion. Not only the nine elements (with relatively high electronegativity) mentioned just before Eq. (9) as forming hydrogen(I) compounds, but also cases such as $Te(CH_3)_3^+$ or $As(CH_3)_4^+$ may inspire questions whether we are in presence of Te(−II) and As(−III) adducts of carbonium cations or of Te(IV) and As(V) carbanion complexes. It is quite characteristic that when N equivalent ligands have the choice between two standard states (Jørgensen, 1969) the oxidation state of the central atom changes by $2N$ units. In any event, for the purpose of constructing Table I, it is sufficient to have one or a few cases showing the definite existence of a given oxidation state combined with ligands in a clear-cut standard state, and it is not necessary to discuss the profound (and not fully understood) reason why most (but not all) complexes can be classified with definite oxidation states (Jørgensen, 1969).

Many chemists give the rather sceptical name "formal oxidation states" to the z values derived from standard states of the more frequent ligands listed in the foregoing. They argue that our system of labeling the compounds may be useful for storage in a cupboard or for an encyclopedia but has no greater intrinsic interest than the calibration of eggs or fruit. However, this point of view neglects that many, otherwise attractive, competing modes of classification lead to corollaries in contradiction with experimental evidence. Thus, neutral ligands H, Cl, I, CH_3, and CN have $S = \frac{1}{2}$ in their ground state and they produce a large number of excited states with a variety of high S values, contrary to the vanishing absorption spectra of colorless compounds. In other words, H_2 should have a low-lying triplet in this picture. It also has, for large internuclear distances (Ammeter, 1975) and it is not unreasonable to use the valence-bond description on *antiferromagnetic* systems. We emphasize that the main motivation for introducing integral oxidation states z and hence $K = (Z - z)$ is not to obtain a fair agreement with the distributions of (not perfectly well-defined) atomic fractional charges, but to obtain a satisfactory description of the symmetry types of the ground state and low-lying excited levels. At this point, it may be worth while to mention that for the monatomic entities M, M^+, M^{2+}, ..., atomic spectroscopists use M I, M II, M III, ... without parentheses and that chemists commit the anachronism to write selenium(−II), iridium(−I), and nickel(0) as if Roman numerals could be negative or zero. By the way, Ni(0) is not used for metallic nickel, nor for the gaseous atom (neither of which are $3d^{10}$ systems) but only for zero-valent compounds such as $Ni(CO)_4$ and $Ni(PF_3)_4$.

The first chemical isoelectronic series ($K = 2$) in Table I starts with H(−I) known from salt-like hydrides. The (He) in parentheses indicates the neutral atom, not a compound. The last member is N(V), which is most stable in the planar nitrate NO_3^- but is also known from more oxidizing tetrahedral species such as ONF_3 and NF_4^+. The next series ($K = 10$) has no less than twelve members. It cannot be argued that B(−V) exists; this would need rather far-fetched postulates such as $B(C_6H_5)_4^-$ having $C_6H_5^+$ ligands. The C(−IV) occurs in the amber-yellow (nonmetallic) beryllium(II) carbide, as shown in Eq. (9), whereas it is more appropriate to let carbon remain C(IV) when burning CH_4 to CO_2. Just as in the oxidation of methane to the intermediate CH_3OH or H_2CO (monomeric formaldehyde) or to formic acid HCO_2H, also in this case it is the hydride ligands that are being oxidized. The N(−III) occurs in solid nitrides, and also in ammonia if it is assumed that the protonation to NH_4^+ is not an oxidation of N(III) to N(V). The subsequent members up to Cl(VII), which are best known from ClO_4^-, are well authenticated. It is conceivable (Jørgensen *et al.*, 1967) that mixtures of argon and oxygen contract to ArO_4 under extremely high pressure; this compound may or may not revert when the pressure is released.

There are many examples of the series ($K = 12$) P(III), S(IV), and Cl(V), but it is rather too short for inclusion in Table I. However, it has the early member Na(−I) obtained in a crystalline salt (Tehan *et al.*, 1974) by disproportionation of metallic sodium in unreactive solvents containing a crown ether (an octadentate cryptate ligand $C_{18}H_{36}N_2O_6$) that forms a

TABLE I

KOSSEL CHEMICAL ISOELECTRONIC SERIES WITH MANY MEMBERS

K	No. of members	Oxidation states
2	Seven	H(−I), (He), Li(I), Be(II), B(III), C(IV), N(V)
10	Twelve	C(−IV), N(−III), O(−II), F(−I), (Ne), Na(I), Mg(II), Al(III), Si(IV), P(V), S(VI), Cl(VII)
18	Twelve	Si(−IV), P(−III), S(−II), Cl(−I), (Ar), K(I), Ca(II), Sc(III), Ti(IV), V(V), Cr(VI), Mn(VII)
28	Eleven	Mn(−III), Fe(−II), Co(−I), Ni(0), Cu(I), Zn(II), Ga(III), Ge(IV), As(V), Se(VI), Br(VII)
36	Thirteen	Ge(−IV), As(−III), Se(−II), Br(−I), (Kr), Rb(I), Sr(II), Y(III), Zr(IV), Nb(V), Mo(VI), Tc(VII), Ru(VIII)
46	Eleven	Ru(−II), Rh(−I), Pd(0), Ag(I), Cd(II), In(III), Sn(IV), Sb(V), Te(VI), I(VII), Xe(VIII)
48	Six	In(I), Sn(II), Sb(III), Te(IV), I(V), Xe(VI)
54	Nine	Sn(−IV), Sb(−III), Te(−II), I(−I), (Xe), Cs(I), Ba(II), La(III), Ce(IV)
68	Seven	Yb(II), Lu(III), Hf(IV), Ta(V), W(VI), Re(VII), Os(VIII)
78	Nine	Re(−III), Os(−II), Ir(−I), Pt(0), Au(I), Hg(II), Tl(III), Pb(IV), Bi(V)
80	?	Au(−I), Hg(0), Tl(I), Pb(II), Bi(III), Po(IV), ...
86	Eleven	Bi(−III), Po(−II), At(−I), (Rn), Fr(I), Ra(II), Ac(III), Th(IV), Pa(V), U(VI), Np(VII)

very strong complex with Na^+. Physical properties (Golden *et al.*, 1966) of the concentrated (not dilute, blue) solution of sodium in liquid ammonia actually indicate the presence of Na^- having an ionic radius comparable to iodide. Also the series $K = 30$ has recently acquired the early member cobalt(−III) in the anion $Co(CO)_3^{3-}$ (Ellis *et al.*, 1977). It is a fascinating question as to what extent the MO's conserve sufficient 3d and 4s character to allow comparison with the isoelectronic zinc atom. Carbonyl complexes obtained by the reaction of carbon monoxide with dispersed metal atoms (say, neodymium or uranium, cf. Slater *et al.*, 1971) in cool matrices (such as solid argon) pose the same problem, but they are not included in this review. It may not be possible to ascribe significant oxidation states to all such cases, because of the fundamental ambiguity of considering totally symmetric MO's to be s-like. The corresponding Rh(−III) and Ir(−III) carbonyl-tris complexes (Ellis *et al.*, 1977) seem to represent $K = 48$ and 80. Hence, the series $K = 12$, 30, and 48 seem to have "holes" in contrast to the uninterrupted series in Table I. There are more examples for the series ($K = 30$) Ga(I), Ge(II), As(III), Se(IV), and Br(V), which has two members more than for the analogous $K = 12$.

Series $K = 18$ starts with Si(−IV), known from a few nonmetallic silicides, and P(−III) from comparable phosphides and from soluble complexes such as PAg_6^{3+}. The twelve members are closely similar to the $K = 10$ cases, the last being Mn(VII), mainly known from permanganate (and not from a fluoride). Compound FeO_4 is not too likely to be prepared. Among the 3d group series not included in Table I may be mentioned ($K = 21$) V(II), Cr(III), and Mn(IV) which is the first series where the most frequent oxidation state of a given element (here chromium) has an *odd* number of electrons (and $S = \frac{3}{2}$). The next odd ($K = 23$) has five members, V(0), Cr(I), Mn(II), Fe(III), and Co(IV). Only Mn(II) and Fe(III) show the typical half-filled shell behavior ($S = \frac{5}{2}$) and are good candidates for the title of the most common oxidation states, whereas the two first members have $S = \frac{1}{2}$ and are represented by rather unique organometallic species such as $V(CO)_6$ and $Cr(C_6H_6)_2^+$. We already discussed the six members of series ($K = 24$), V(−I), Cr(0), Mn(I), Fe(II), Co(III), and Ni(IV), which are mostly octahedral and diamagnetic ($S = 0$) with exception that the majority of iron(II) complexes, and CoF_6^{3-}, have $S = 2$.

The following odd series, $K = 25$, is essentially presented by the high-spin ($S = \frac{3}{2}$) cobalt(II) complexes, and a few Ni(III) with $S = \frac{1}{2}$ or $\frac{3}{2}$. The stereochemical behavior varies in a characteristic fashion with increasing oxidation number in the series $K = 26$, starting with the trigonal-bipyramidic (coordination number $N = 5$) diamagnetic Cr(−II), Mn(−I), Fe(0), and Co(I), then going to a very large number of Ni(II) complexes of highly different N and symmetry, and both $S = 1$ and 0, and finally a few Cu(III) complexes with quadratic ($N = 4$, $S = 0$) and octahedral ($N = 6$, $S = 1$) coordination. In contrast to this six-member series, $K = 27$ is essentially known from a large variety and rather individualistic copper(II) complexes, though a few cases of monomeric Ni(I) have been reported quite recently. In Table I, $K = 28$ has eleven members starting with tetrahedral $Mn(CO)_4^{3-}$ (Ellis and Faltynek, 1975) and ending with perbromate BrO_4^-, whose existence, it was thought for many years, could not be demonstrated. Series $K = 36$ has perhaps the highest possible number (13) of members, if any nonmetallic germanide is perfectly characterized. The other examples, from As(−III) to Ru(VIII) are well known from chemical textbooks. The $4d^3$ series ($K = 39$) contains Mo(III), Tc(IV), Ru(V), and Rh(VI) all with $S = \frac{3}{2}$. The $4d^6$ series ($K = 42$) is very similar to the $3d^6$ series, going from Nb(−I) to Pd(IV), but all species are diamagnetic.

In Table I, the $4d^{10}$ series ($K = 46$) ranges from ruthenium(−II), with the rather unique example of $Ru(PF_3)_4^{2-}$, to xenon(VIII), represented by perxenate XeO_6^{4-} and by the less stable XeO_4. The $4d^{10}5s^2$ series ($K = 48$) has also been included in Table I because all the members In(I) to Xe(VI) have numerous well-established examples. On the other hand, $K = 50$ is not included, because the series Te(II), I(III), and Xe(IV) is so short. A similar situation occurs with $K = 82$, which includes Bi(I) and Po(II) and probably also At(III) and Rn(IV), though these elements are very difficult to study because they only occur as short-lived radioactive isotopes. The series $K = 54$ is shown in Table I to begin with tin(−IV), presumably existing in CaF_2-type Mg_2Sn, which seems to be a semiconductor (and not a metal). However, it stops at cerium(IV), and it can be inferred from photoelectron spectra that Pr(V) compounds cannot exist (Jørgensen, 1974a).

The trivalent lanthanides constitute all the K values from 55 to 67 with $K - 54$ electrons in the partly filled 4f shell. Most of these K values are only represented by one or two oxidation states, but the half-filled $4f^7$ shell ($K = 61$) is represented by europium(II), gadolinium(III), and terbium(IV) compounds. Many textbooks argue that this is a specific property of the half-filled shell, but the parameters of interelectronic repulsion entering the "refined spin-pairing energy theory" produce weaker, but quite perceptible, effects on other numbers of 4f electrons stabilizing M(II) or M(IV) (Jørgensen, 1973b, 1975b, 1976a; Nugent *et al.*, 1973). The series $K = 68$, which we have already discussed for monatomic entities, has seven chemical members from Yb(II) to Os(VIII). The $5d^6$ series ($K = 74$) includes all seven members Ta(−I), W(0), Re(I), Os(II), Ir(III), Pt(IV), and Au(V), ranging from $Ta(CO)_6^-$ to the recently reported AuF_6^- (Leary and Bartlett, 1972) in octahedral, diamagnetic complexes. The $5d^8$ series ($K = 76$) is predominantly represented by quadratic ($N = 4$) complexes of Ir(I), Pt(II), and Au(III) but also by a few instances of trigonal-bipyramidic ($N = 5$) Re(−I) and Os(0).

In Table I, the $5d^{10}$ series ($K = 78$) begins with Re(−III) in the form of $Re(CO)_4^{3-}$ (Ellis and Faltynek, 1975) continues to Os(−II) and Ir(−I), exemplified by $Os(PF_3)_4^{2-}$ and $Ir(PF_3)_4^-$, then passes through Pt(0), with varying $N = 3$ and 4, Au(I), which is almost exclusively linear ($N = 2$) whereas Hg(II) and Tl(III) can assume both $N = 2$ and 4, and Pb(IV) having $N = 4$ and 6. The latter value seems also to apply to Bi(V). There is no safe argument for or against the existence of polonium(VI). Partly as a consequence of the relativistic stabilization of the 6s orbital and of the "lanthanide contraction" (Bagus *et al.*, 1975), the $5d^{10}6s^2$ systems ($K = 80$) are strikingly stable from a chemical point of view. Gold(−I) is best known from the CsCl-type semiconductor CsAu, but even liquid cesium and liquid gold can be "titrated" and shown to have a far smaller electric conductivity at the exact stoichiometric composition (Schmutzler *et al.*, 1975). Mercury(0) seems to occur in certain ligands HgX^- obtained by reacting certain rhodium(III) complexes of multidentate arsines and one hydride ligand with XHgX eliminating HX and forming an RhHgX group. Since the complex remains octahedral, it is more plausibly described as Rh(III) and Hg(0) than as Rh(I) and Hg(II), although it cannot be denied that it may represent a special form of catenation. Thallium(I), lead(II), and bismuth(III) are by far the most stable oxidation states of the three elements. It is not quite easy to know where $K = 86$ begins, but it is known to go on to neptunium(VII). The typical 5f group series in the interval from $K = 87$ to $K = 91$ tends to be represented by about three oxidation states, more than are found in the lanthanides. The ($K = 100$) closed-shell series starts with nobelium(II), which is actually difficult to oxidize to No(III), and may possibly go on to 109(IX) (Jørgensen and Penneman, 1976). The author (Jørgensen, 1979) is preparing a book about the predicted chemistry of translawrencium elements.

It should be emphasized that Kossel did not argue that the specific isoelectronic series [Eq. (1)] necessarily always indicates the most frequent (or the most stable) oxidation state of a given element, if it can attain one (or more) of the closed-shell K values. Thus, neither Mn(−III) nor Mn(VII) is the most persistent oxidation state of manganese, and neither Ru(−II) nor Ru(VIII) of ruthenium. Among the members of the chemical isoelectronic series $K = 68$, the Yb(II) is by no means the most stable oxidation state of ytterbium, which distinctly prefers Yb(III) belonging to $K = 67$ together with the rather exceptional oxidation state thulium(II). The characteristic feature of what is now recognized to be closed-shell K values is that the corresponding chemical isoelectronic series are unusually *long*. Though the distribution on negative and positive oxidation states z is not as extreme as for monatomic entities (where at most one anion is stable for a given element, but $Z - 1$ different ions have positive z), Table I shows only twenty-nine negative z as compared with seventy-five positive values. By the way, the negative z values fall in two categories: the monatomic anions (for $z = -1$, H, F, Cl, Br, I, Au) and complexes (mainly of ligands such as PF_3 and CO) of the transition elements showing negative z.

We turn in Section VIII to the reasons why the evidence (from spectroscopic and magnetic measurements) for a definite oxidation state of an atom in a given compound sometimes can be overwhelming. This is particularly true for the lanthanides. The qualitative trend toward well-defined oxidation states seems to be determined by the ratio between the ionic radius and the average radius of the partly filled shell in the transition groups.

VI. Photoelectron Data for Ionization of Inner Shells

There is no doubt that X-ray absorption and emission spectra (Kossel, 1921) provide a much more unified picture of electronic structure than atomic spectra do, at a first glance. First of all, condensed matter (liquids, amorphous and crystalline solids) show the inner nl shells with essentially the same energies as gaseous atoms or molecules containing the same element. Second, Moseley established in 1913 the atomic number Z from the ionization energy of the strongest bound shell:

$$I(1s) = (Z - Z_s)^2 \text{ rydberg.} \tag{10}$$

It is not generally realized that the *screening constant* Z_s varies with Z, rapidly increasing from 0.3 to a value around 3, where a plateau is reached, and then (because of second-order relativistic effects) decreasing and crossing zero close to ($Z = 90$). In actual compounds from lithium to aluminum, it is a mnemotechnic rule that

$$I(1s) = Z(Z - 1) \times 9.7 \text{ eV}, \tag{11}$$

where the constant 9.7 eV is only 0.71 rydberg. From a formal point of view, the subsequent shells 2s, 2p, 3s, ... can be described by the expression (10) divided by n^2 but the screening constant is large and rapidly varying. The $I(nl)$ always increases going from Z to $(Z + 1)$, but, as already Coster pointed out in 1923, this increase is rather irregular and is smaller in the lanthanides than in the neighbor elements. It is possible to plot the change dI/dZ as a function of Z (Jørgensen, 1973b) and, indeed, this quantity is 10–12 eV smaller in the 4f group than extrapolated from the adjacent elements. The effect is conspicuous on I(4d), which has less than one-third of the interpolated dI/dZ. A similar comparison (Jørgensen, 1974a) has been made for $Z = 10$–60, and dI/dZ does not vary monotonously with Z, but jumps downward at the beginning of the transition groups (at scandium, yttrium, and lanthanum) and upward at the end.

The $I(nlj)$ derived from X-ray spectra have been compiled by Cauchois (1952, 1956) and by Bearden and Burr (1967). An alternative experimental technique *photoelectron spectrometry* (ESCA) was developed by Kai Siegbahn and his group in Uppsala. Contrary to the X-ray emission spectra providing differences between two I values (if we neglect Franck–Condon broadening and complications due to partly filled shells), the I values are obtained directly as the maxima (signals) of the probability distribution of kinetic energy E_{kin} of the ejected photoelectron using Einstein's equation

$$I = h\nu - E_{\text{kin}}, \tag{12}$$

where the photon energies 1253.6 and 1486.6 eV, which are most frequently used, originate in magnesium or aluminium anticathodes. In future, the intense continuous spectrum emitted by synchrotrons is likely to be highly useful.

For metallic samples, most authors indicate I^* relative to the Fermi level. Partly because of the calibration of several commercial instruments available, it is customary to indicate I^* also for nonconducting samples (about 5 eV lower than I relative to vacuum) by reference to metallic gold having I^* (Au $4f_{7/2}$) = 83.8 eV and the corresponding I = 89.1 eV. However, in our Varian IEE-15 apparatus, the typical nonconductors acquire quasi-stationary positive potentials between 2 and 5 volts (the latter value for certain anhydrous fluorides), and we obtain I' corrected for charging effects by defining I'(C1s) of the aliphatic hydrocarbon in electric contact with the sample (powder distributed on 600P one-sided scotch tape from the 3M Company) to be 290.0 eV. This allows an internal consistency around 0.2 eV (Jørgensen and Berthou, 1972, 1973, 1975a) and is more satisfactory than (rather unreliable) attempts to connect the sample electrically to the instrument (Jørgensen, 1977).

Moore (1970) elaborated a revised table of ionization energies for gaseous ions based on the new value of 1 eV = 8065.73 cm^{-1}. Whereas the limits of typical series spectra may be known almost as well as observed wave numbers of spectral lines, and frequently with an accuracy better than 0.1 cm^{-1}, many multiplet spectra allow I to be determined only within a few percent. In the following, we speak about the ionization energy I_{z+1} going from the ground state of M^{+z} to the ground state of M^{+z+1}. With this definition, I_0 is the electron affinity of the neutral atom, and I_1 its first ionization energy. As examples of the uncertainty, it may be mentioned that I_6 of Ta^{5+} within 1 year was devaluated from 97.34 to 94.01 eV.

When comparing I_{z+1} of the loosest-bound shell (the highest of the two j values, if distinguishable) of a gaseous ion with the photoelectron spectra of the same element in the oxidation state $+z$, it is striking that, in the latter case, I is strongly decreased to the extent ΔI. This makes it attractive to evaluate the quantity $\Delta I/z$ for various values of K and z (Jørgensen, 1976c). Table II gives such values. The I_{z+1} data are from the list of Moore (1970) except where specific references are given in the table footnotes. The $I(nl)$ values are mainly taken from the study (Jørgensen and Berthou, 1972) of 600 nonmetallic compounds containing 77 elements. The more recent work also has specific references in the table footnotes. In the case of gaseous molecules, Jolly and Perry (1974) made a comparative study of 144 compounds.

Contrary to original belief (Fadley *et al.*, 1968), the $I(nl)$ of a given element is not predominantly determined by the oxidation state z but rather by the definite nature of the ligating atoms; fluorides show higher I than sulfides. The various origins of this *chemical shift* have already been reviewed in this series (Jørgensen, 1974b) and are further discussed in Section VII. The reasonably well-established extreme limits (excepting metallic alloys) are given as an interval in Table II and are, if possible, I' values corrected for the charging effect. The gaseous molecules are in the fortunate situation that their I values always refer to vacuum, like in atomic spectroscopy.

TABLE II

CHANGES OF IONIZATION ENERGIES $I(nl)$ IN KOSSEL ISOELECTRONIC SERIES

K		nl	I_{z+1} (eV)	Nonmetallic solids (eV)	Gaseous molecules (eV)	$(\Delta I/z)$ (eV)	K		nl	I_{z+1} (eV)	Nonmetallic solids (eV)	Gaseous molecules (eV)	$(\Delta I/z)$ (eV)
2	Li(I)	1s	75.64	60.7–60	—	15.3 ± 0.4	36	Zr(IV)	4p	81.5	39–36	—	11.0 ± 0.4
2	Be(II)	1s	153.89	121–118.5	—	17.0 ± 0.6	36	Nb(V)	4p	102.6	43–41	—	12.1 ± 0.2
2	B(III)	1s	259.37	201–192	202.8–193	20.8 ± 1.7	36	Mo(VI)	4p	126.8	47–45	—	13.5 ± 0.2
2	C(IV)	1s	392.08	298–288	301.8–289.7	24.3 ± 1.7	44	Rh(I)	4d	18.08	—	9.7	8.4
10	F(−I)	2p	3.40	14–11.5	16.5–15	10 ± 2	44	Pd(II)	4d	32.93	10.2–9.7	—	11.0 ± 0.3
10	Ne	2p	21.57	—	—	—	46	Pd	4d	8.34	—	—	—
10	Na(I)	2p	47.29	36–35	—	11.8 ± 0.5	46	Ag(I)	4d	21.49	10.5–10	—	11.2 ± 0.3
10	Mg(II)	2p	80.14	56–54	—	12.6 ± 0.5	46	Cd(II)	4d	37.48	17.4–16.8	19.6–17.3	9.9 ± 0.7
10	Al(III)	2p	119.99	82–79	81.5–79[a]	13.1 ± 0.5	46	In(III)	4d	54	24.3–23	—	10.0 ± 0.2
10	Si(IV)	2p	166.77	109.5–107.5	111.8–105.9	14.8 ± 0.7	46	Sn(IV)	4d	72.28	33–31	34.5–30[c]	10.0 ± 1
10	P(V)	2p	220.43	143.6–138.5	145.6–140	15.9 ± 0.7	46	Sb(V)	4d	108	42.2–40	—	13.4 ± 0.3
10	S(VI)	2p	280.93	175–174	180.4–176.5	17.0 ± 0.5	46	Te(VI)	4d	137	52–48	—	14.5 ± 0.3
10	Cl(VII)	2p	348.28	215–212.5	216.1	19.2 ± 0.3	48	In(I)	5s	18.87	—	9.8–8.8[d]	10.5
18	Cl(−I)	3p	3.61	10–9	12.7–11.1	7 ± 2	48	Sn(II)	5s	30.50	—	10.3–9.8[e]	10.2
18	Ar	3p	15.76	—	—	—	54	Sb(−III)	5p	0	5	—	—
18	K(I)	3p	31.62	23–21.4	—	9.6 ± 0.8	54	Te(−II)	5p	0	6	—	—
18	Ca(II)	3p	50.91	30.6–30	—	10.2 ± 0.2	54	I(−I)	5p	3.06	8.5–8	10.4–8	5.8 ± 1
18	Sc(III)	3p	73.47	39–38	—	11.7 ± 0.2	54	Xe	5p	12.13	—	—	—
18	Ti(IV)	3p	99.22	44–42	—	14.0 ± 0.5	54	Cs(I)	5p	23.17[f]	16–15	(18.3)[g]	8.3 ± 0.5
18	V(V)	3p	128.12	47–44	—	16.5 ± 0.3	54	Ba(II)	5p	35.79[f]	19.5–19	—	8.2 ± 0.2
18	Cr(VI)	3p	161.1	54–52	—	18.0 ± 0.3	54	La(III)	5p	45.95[f]	25–24	—	7.1 ± 0.2

18	Mn(VII)	3p	196.46	61–60	—	19.4	61	Eu(II)	4f	24.70[h]	7–5	—	9.3 ± 0.5
19	Ti(III)	3d	43.27	—	7.9	11.8	61	Gd(III)	4f	44.01[h]	15.5–12	—	10.1 ± 0.6
19	V(IV)	3d	65.28	—	9.4	14.0	61	Tb(IV)	4f	66.46[i]	24.7	—	10.4
24	Mn(I)	3d	(13.8)	—	10.5–9	4	62	Tb(III)	4f	39.37[j]	9.0–6	—	10.6 ± 0.5
24	Fe(II)	3d	30.65	8–7	(6.9)	11.7	63	Dy(III)	4f	41.47[h]	11–8	—	10.7 ± 0.5
24	Co(III)	3d	51.3	10–8	10–8	14.1	65	Er(III)	4f	42.65[h]	12–9	—	10.7 ± 0.5
26	Ni(II)	3d	35.17	9.3–7.7	(6.5)	13.6	66	Tm(III)	4f	42.69[h]	12–8.5	—	10.8 ± 0.6
27	Cu(II)	3d	36.83	11–10	—	13.2 ± 0.3	67	Tm(II)	4f	23.68[h]	4	—	10
28	Ni(0)	3d	(5.8)	—	9.6–8.9	—	67	Yb(III)	4f	43.74[h]	14.2–12	—	10.3 ± 0.4
28	Cu(I)	3d	20.29	8.9	—	11.4	68	Yb(II)	4f	25.05[k]	6	—	9.5
28	Zn(II)	3d	39.72	17–15	19.1–17.0	11.5 ± 1	68	Lu(III)	4f	45.25[k]	15.3–12	—	10.5 ± 0.5
28	Ga(III)	3d	64	26.8–25.6	—	12.5 ± 0.5	68	Hf(IV)	4f	68.37[k]	23.7–22	—	11.3 ± 0.4
28	Ge(IV)	3d	93.5	39–37.5	—	13.8 ± 0.2	68	Ta(V)	4f	94.01[k]	34–31	—	12.3 ± 0.3
28	As(V)	3d	127.6	51–50.5	—	15.5 ± 0.1	68	W(VI)	4f	122.01[k]	42–40.7	46.7	13.1 ± 0.5
28	Se(VI)	3d	155.4	66–65	—	16.5	68	Re(VII)	4f	(150.6)[k]	51.4–50.7	—	14.2
36	Se(−II)	4p	0	7	—	—	78	Au(I)	5d	20.5	10.6	—	10
36	Br(−I)	4p	3.36	9–8.5	11.7–10	6.5 ± 1.5	78	Hg(II)	5d	34.2	14.3–14	16.7–15.0	9.5 ± 1
36	Kr	4p	14.00	—	—	—	78	Pb(IV)	5d	68.8	25–24.4	—	11.0
36	Rb(I)	4p	27.28	19–18.5	—	8.5 ± 0.3	80	Hg	6s	10.44	—	—	—
36	Sr(II)	4p	41.64[b]	25–24.5	—	8.5 ± 0.3	80	Tl(I)	6s	20.43	—	10.8–9.9	10.0 ± 0.5
36	Y(III)	4p	61.8	32–31	—	10.1 ± 0.2	80	Pb(II)	6s	31.94	16–15[l]	10.1	10

[a] Schaaf *et al.*, 1976.

[b] Persson and Valind, 1972.

[c] Avanzino and Jolly, 1976.

[d] Berkowitz and Dehmer, 1972.

[e] Evans and Orchard, 1975.

[f] Reader and Epstein, 1975.

[g] Berkowitz *et al.*, 1973.

[h] Sugar and Reader, 1973.

[i] Sugar, 1975.

[j] Spector and Sugar, 1976.

[k] Kaufman and Sugar, 1976.

[l] Mason and Gerensen, 1976.

It is seen from Table II that the two kinds of intervals are not systematically shifted relative to each other. This is, in part, due to a compensation; the gaseous molecules tend to lower interatomic relaxation effect (and under equal circumstances having higher I) and to be relatively more covalent (decreasing I). Although the volatility of fluorides (frequently representing an isolated high I value) does not necessarily exclude partly electrovalent bonding, it seems rather to be conditioned by the coordination number N not being higher than z and, hence, not needing oligomerization or formation of crystal lattices.

We have a special problem with the *valence region* (say, I below 40 eV) where the loosest-bound nl shell of gaseous halogen compounds appears as several signals corresponding to various *molecular orbitals*. In such a case, the lowest I is given in Table II, typically a nonbonding MO, and mostly taken from the book by Turner *et al.* (1970) though such values have also been discussed by the writer (Jørgensen, 1975c, 1976b) together with 3d-like MO's of gaseous and solid transition-group compounds. In Table II, the parentheses around I_2 for Mn^+ and I_1 for the gaseous nickel atom indicate that the processes $3d^6 \rightarrow 3d^5$ and $3d^{10} \rightarrow 3d^9$ are considered, not involving the ground state of the species to be ionized. The estimate $I_8 = 150.6$ eV for Re^{7+} is the ionization energy to $^2F_{7/2}$ situated about 6.2 eV above the ground state (lacking one 5p electron) $^2P_{3/2}$ of Re^{8+}.

Table II gives the ratio $\Delta I/z$. When an interval is given, it does not mean a statistical uncertainty, but rather the limits obtained by considering both the nonmetallic solids and the gaseous compounds. It is noted that even rather large chemical shifts do not always provide a high percentage variation of this ratio. As discussed in Section VII, this aspect even removes, to a certain extent, the physical significance of some values of the ratio. Thus, gaseous nitrogen compounds have I(N1s) varying between 417.0 eV for ONF_3 and 404.7 eV for $N(CH_3)_3$ (Jolly and Perry, 1974) showing that the oxidation state does not need to be N(V). If $\Delta I/z$ is evaluated by comparison between $I_6 = 552.06$ eV for N^{5+} and I between 412.5 and 412 eV for solid nitrates (Jørgensen and Berthou, 1972), the value 28.0 eV is obtained, as a quite reasonable extrapolation of the values included in Table II. The first series ($K = 2$) has several other unusual characteristics. One might get an impression from Table II that I(B1s) is far more variable than I(Be1s). However, this seems to be owing to the fact that photoelectron spectra of organoberyllium compounds have not been reported, whereas the chemical shift is considerable between gaseous BF_3 and $B(CH_3)_3$ or between solid salts of BF_4^- and $B(C_6H_5)_4^-$. Experimental difficulties (chemical reactivity and very weak signal intensities) have prevented results for solid hydrides, though obviously, I(H1s) is far higher than $I_0 = 0.75$ eV. It was noted

(Jørgensen, 1976c) that for many isoelectronic series, the ratio $\Delta I/z$ in electron volts varies almost as a straight line as a function of z:

$$\begin{array}{ll} K = 2 & 11.0 + 3.3\ z, \\ K = 10 & 10.7 + 1.0\ z, \\ K = 18 & 7.5 + 1.5\ z, \\ K = 28 & 10.0 + 1.0\ z, \\ K = 36 & 7.8 + 0.8\ z, \\ K = 68 & 7.7 + 0.9\ z, \end{array} \tag{13}$$

where the observed value for $z = +1$ tends to be slightly above the straight line, and for $z = -1$, somewhat indeterminate. The situation is rather different for the series $K = 46$, showing a shallow minimum between cadmium(II) and tin(IV). Though it might be argued that I_{z+1} of the corresponding gaseous ions are not known with great precision in this series, it cannot be doubted that the relatively high $\Delta I/z = 11.2$ eV for silver(I) is an example of a more general tendency for "chemically polarizable ions" (Jørgensen, 1975a) to show high values for this ratio, as can be seen from the equal values obtained for rubidium(I) and strontium(II) or from the decrease in value from barium(II) to lanthanum(III). Actually, the post-transitional elements in $K = 78$ and $K = 80$ all tend to have a roughly invariant $\Delta I/z$, close to 10 eV. It may be noted that this ratio in the trivalent lanthanides from terbium ($K = 62$) to thulium ($K = 66$) is marginally larger than one would obtain by interpolation between gadolinium(III) and lutetium(III). This tendency is even more pronounced for partly filled d shells, as exemplified by the high ratios in cobalt(III), nickel(II), and copper(II). These findings create unexpected and interesting problems for the "ligand field" description (Jørgensen, 1974a).

VII. External Screening; Madelung and Relaxation Energies

The electric potential of the charge q distributed uniformly on a spherical surface with radius R_0 is invariantly (q/R_0) inside the sphere and (q/R) at a point (outside the sphere) at a distance R from the center of the sphere. These two expressions were early applied to Eq. (10) to explain the screening constant Z_s (especially for n above 1, where this expression is divided by n^2). Seen from the point of view of an external electron, sufficiently internal electrons might equally well be situated on the nucleus in the center, diminishing its apparent positive charge to $(Z - Z_s)$. However, external electrons also diminish I of inner shells because of what is called *external screening.* If the increase of I from one element (Z) to the next ($Z + 1$) is considered, the hydrogenic expression is $(Z + \frac{1}{2})$ hartrees/n^2, and one would expect external screening to decrease this value by $\langle r^{-1} \rangle$ in atomic units for the additional electron (expressed in reciprocal bohr units and 1 hartree = 27.2116 eV). Whereas the (positive) hydrogenic expression is only appropriate for 1s electrons, but is only about $(Z - 7) \times 4$ eV for the (rather irregular) variation of dI/dZ for I(2p), even the slope being smaller than 6.8 eV (Jørgensen, 1974a), the negative contribution from external screening is a quite satisfactory qualitative explanation of the seemingly irregular variation of dI/dZ as a function of Z. Ha and O'Konski (1969) calculated the chemical shift dI(1s) on a variety of monatomic species (with z between -1 and $+6$) of beryllium, boron, carbon, sulfur, and chlorine and found agreement (mostly within 3% but deviating in both directions) with the sum of $\langle r^{-1} \rangle$ valence shell electrons removed.

Politzer and Daiker (1973) elaborated such calculations for the purpose of comparing the J integral of interelectronic repulsion between an inner and an outer orbital with $\langle r^{-1} \rangle$ of the latter orbital. A characteristic result is that I(Cl2p), known experimentally to be 348 eV for gaseous Cl^{7+}, would be decreased approximately 8 times this parameter (0.67 hartree = 18.2 eV) to 201 eV in gaseous Cl^-, quite close to the photoelectron results for chlorides, whereas a decrease in the neutral atom 7 times 18.2 eV to give 219 eV seems rather too small, in view of the fact that the gaseous Cl_2 molecule has $I = 207.64$ eV (Jolly and Perry, 1974). The J(2p, 3p) varies almost linearly from 0.36 hartree for $Z = 13$ to 0.67 hartree for $Z = 17$. Hence, the results of Politzer and Daiker (1973) suggest a coefficient 0.08 hartree = 2.1 eV for z in Eq. (13) to be compared with the empirical value 1.0 eV for $K = 10$. This agreement is less satisfactory than several other interesting quantities evaluated for the expected behavior of 3d group elements. It may even be taken as an argument that aluminum(III) is further removed from behaving as a neutral atom than is chlorine in chlorine compounds. On the other hand, it is fully confirmed that $\langle r^{-1} \rangle$ is marginally higher than the J integral. The former quantity for 3p electrons increases roughly linearly from 0.379 in Al to 0.733 atomic unit in Cl. It may be noted that the similar increase for 3d electrons is from 0.799 in scandium to 1.531 atomic unit in zinc. Since the 3p and 3d shells have roughly similar average radii [their very different I values are connected with their angular part of the kinetic energy, $l(l + 1)\langle r^{-2} \rangle/2$; cf. Jørgensen, 1975c], the corresponding J(3p, 3d) vary only from 0.642 to 1.152 hartrees, compared with J(2p, 3d) between 0.792 and 1.508 hartrees and J(1s, 3d) between 0.799 and 1.530 hartrees that have almost the values predicted from their $\langle r^{-1} \rangle$. There is no clear-cut relation between J(3p, 3d) and the $\Delta I/z = (7.5 + 1.5\ z)$ eV in Eq. (13) because the additional electron in the chemical series $K = 18$ is not a 3d electron to a good approximation, at least for chlorine to calcium.

Although it is likely that a major part of ΔI in Table II is due to external screening (arriving at quite larger proportions than for the 1s shell), an alternative model may contribute to a certain extent. *If* the compounds were almost electrovalent, the modification ΔI (to the first approximation proportional to z) would represent the *Madelung potential* due to electric charges on the surrounding atoms. This description is plausible in crystalline halides of the alkaline and alkaline-earth metals and provides a potential varying (according to the size of the unit cell) from 12.5 eV in LiF to 6.4 eV in CsI among the alkaline-metal halides, and being 15.3 eV in CaF_2. In all of these cases, the potential is exactly multiplied by (-1) going from anion to cation sites, and increases I in the former case from the low values for gaseous halide anions given in Table II. There are many difficulties in assuming an *exclusive* influence of the Madelung potential (Citrin and Thomas, 1972; Jørgensen and Berthou, 1972; Jørgensen, 1975c). Thus, $I(K2p)$ of various potassium salts vary in a way opposite to the change of the Madelung potential and instead suggest interatomic relaxation effects with the "chemically polarizable" anions (Jørgensen, 1974b, 1975a). The value $\Delta I = 15.3$ eV for lithium(I) is somewhat too large to be readily explained by a Madelung potential (though the order of magnitude in most crystals is indeed z times 8 eV), and it would be difficult to understand why it is so insensitive to the choice of the anion. It is also striking that $\Delta I/3$ for yttrium 4p and trivalent lanthanide 4f ionization only varies between 9.5 and 11.4 eV in all kinds of nonmetallic compounds studied. There may be some inherent tendency in quantum chemistry (Jørgensen *et al.*, 1967; Jørgensen, 1969) within large groups of compounds to obtain almost the same observable results as when the starting hypothesis is ions (with the full charge corresponding to the oxidation state) if the Madelung potential is taken into account; or, the other way round, when strong covalent bonding and almost neutral atoms are assumed. We are speaking about the spherically symmetric part of the Madelung potential. There is no need here to emphasize that the electrostatic model of the "ligand field" invoking the much smaller nonspherical part has been replaced by weak effects of antibonding among the five d-like or seven f orbitals in the *angular overlap model* (Jørgensen *et al.*, 1963; Schäffer, 1968, 1973; Jørgensen, 1971).

It is also clear that a case such as nitrogen(V) discussed in the foregoing (but excluded from Table II) cannot be explained by a Madelung potential due to the fractional charges of the neighbor atoms. Nevertheless, many authors have treated the chemical shift observed in photoelectron spectra as a superposition of (partly compensating) effects of varying fractional atomic charge and of the Madelung potential (Stucky *et al.*, 1972); Jolly and Perry (1974) elaborate the technique of *equilibrated electronegativity* originally suggested by Sanderson and expressed algebraically as the *differential ionization energy* (Jørgensen, 1962c, 1969; Jørgensen *et al.*, 1967). It is perhaps worth while to note that the Madelung potential in a way is a summation over *interatomic* external screening (Berthier, 1974).

It is difficult to be completely convinced by a model superposing fractional atomic charges and the Madelung potential, first of all because the sum of the inferred atomic charges is not always zero in neutral compounds (but appears somewhat positive in diatomic molecules) and, second, because a linear relation between the atomic charges in a linear combination of atomic orbitals (LCAO) model and the observed chemical shifts does not by itself guarantee that all the atomic charges have not been multiplied by some huge factor, say 3 or 0.5. The experimental evidence for *relaxation effects* was reviewed in this series (Jørgensen, 1974b), and the *Manne–Åberg principle* (constituting an analogy to the Franck–Condon principle) seems to be generally valid that the photoelectron I values obtained from Eq. (12) correspond to the eigenvalues of the *new Hamiltonian* operator appropriate after the sudden removal of the electron ejected. In most optical absorption spectra, the vibronic origin is not much stronger than the transitions corresponding to co-excited vibrations, but in photoelectron spectra, except for unusual cases of very strong satellite signals (Jørgensen, 1975c, 1976b) and the configuration interaction between straightforward 4p ionization to $4p^54d^{10}$ and the substituted $4p^64d^84f$ in elements from tellurium to lanthanum (Gelius, 1974; Wendin and Ohno, 1976; Svensson *et al.*, 1976b; Kowalczyk *et al.*, 1976; Jørgensen and Berthou, 1975b; Wendin, 1978), the main signal at lowest I concentrates by itself 50–90% of the total intensity, leaving the rest to rather extended and broad satellite structures. In monatomic entities, the baricenter of intensity is situated close to the Koopmans value (Manne and Åberg, 1970) from Hartree–Fock functions (with minor relativistic corrections), whereas the main signal turns out (Jørgensen, 1974b) to be situated 0.8 eV times the square root of I (in eV) below the Koopmans value for I in the interval from 100 to 1500 eV. This is a typical *intra-atomic* relaxation effect; the final state of the ionization process contains contracted radial functions for all the other electrons. The interatomic relaxation effect is smaller, and probably below 10 eV in most cases, but its variation from one compound to another contributes significantly to the chemical shift. Among the most clear-cut cases are the implantation of neon, argon, krypton, and xenon atoms in metallic copper, silver, and gold (Citrin and Hamann, 1974) and of xenon atoms in iron (Wagner, 1976) where I decreases 3–5 eV relative to the gaseous atom, and the most in neon. A perhaps even more striking case is the condensation of mercury atoms to the metal (Svensson *et al.*, 1976a) showing a decrease of all I values of inner shells 2.7 ± 0.3 eV. The relaxation is more pronounced in metallic elements and alloys, and somewhat more in solids than in gaseous molecules, but until reliable formulas are found for the evaluation of interatomic relaxation energies, these facts make it almost impossible to believe in the consequences of a hypothesis involving only fractional atomic charges and the Madelung potential. It is true, of course, that such a model may give correct results when comparing two solids with exactly the same amount of interatomic relaxation.

If all the inner shells of a given atom show the same chemical shift dI (this is suggested by the well-established observation that X-ray emission lines shift 10 to 20 times less than dI from photoelectron spectra) the *Auger transitions* (having an initial state lacking one electron and a final state lacking two electrons) should produce an Auger electron with the kinetic energy E_{kin} decreased to the extent dI. Since increased I in Eq. (12) also corresponds to E_{kin} of the photoelectron being decreased by dI, Wagner (1976) proposed a new Auger parameter to be the difference between the kinetic energies of the Auger electron and of the corresponding photoelectron produced by initial ionization in the stronger-bound inner shell. Wagner's new parameter should consist almost entirely of the variation of the interatomic relaxation energy and has been used in the discussion of perxenates compared with xenon (Jørgensen and Berthou, 1975b) and of germanium-containing glasses (Reisfeld *et al.*, 1976).

VIII. The Atomic Spectroscopist and Chemical Bonding

Condensed matter and chemical bonding are rather remote from the concepts of atomic spectroscopy for the simple reason that most excited states of monatomic entities have at least one electron in an orbital with relatively large average radius. Many coupling schemes involving one typically external electron and S, L terms or J levels of a definite core configuration are theoretically and empirically known (Racah, 1942, 1960), but the photoelectron spectra have been particularly significant in providing entirely new opportunities of ascertaining the subsistence of such core configurations in solids. It is well known that spherical symmetry is an excellent approximation when ascribing the narrow absorption bands (mainly below 6 eV) of trivalent lanthanides to transitions between the J levels of a configuration containing $q = 1$ to 13 electrons in the 4f shell (Carnall *et al.*, 1968), and the corresponding radiative lifetimes for luminescence and energy transfer from other excited states in glasses and crystals (Reisfeld, 1973, 1975, 1976) have taken over models derived from atomic spectra, as well as the applications of such processes in lasers (Reisfeld and Jørgensen, 1977).

Cox *et al.* (1973) pointed out that the complicated structure in the region with I between 5 and 15 eV (or I^* relative to the Fermi level between 2 and 12 eV) found both in nonmetallic compounds and in the metallic elements, in particular for $q = 8$ to 13, could be ascribed to the accessible J levels of $4f^{q-1}$. The question of detectable ionized states is partly determined by selection rules (J increases or decreases at most $\frac{7}{2}$ units, and in Russell–Saunders coupling, S increases or decreases half a unit and L changes at most by 3) and partly by numerical probabilities determined (Cox, 1975) by the squared *coefficient of fractional parentage* of the ($q - 1$, S', L', J') ionized state in the (q, S, L, J) ground state. After remarkable agreement with the calculated probabilities had allowed the assignment of ionized states of $4f^{q-1}$, it became interesting to compare the J-level energy differences obtained from photoelectron spectra with the isoelectronic M(III) aqua ions of the previous element (Carnall *et al.*, 1968) and if no *nephelauxetic effect* (Jørgensen, 1969) occurred in M(IV) obtained by ionization, one would expect S, L-term distances about 20% higher than in M(III). Both in the metallic element and in the NaCl-type nonmetallic antimonides, the actual increase is about 6% in thulium(IV) and about 12% in terbium(IV). Hence, the nephelauxetic ratio β is fairly close to 1, that is, 0.89 in thulium and 0.94 in terbium. This conclusion has rather profound consequences for "ligand field" theory (Jørgensen, 1975b) because $\frac{1}{2}(1 - \beta)$ gives a *higher limit* to the delocalization of the 4f-like orbitals (β can decrease for other reasons, such as expanded radial functions adapted to a lower fractional atomic charge or a more pronounced Watson effect) and one might have expected a considerable invasion of conduction electron density in the M(IV) suddenly formed in the metal or a considerable extent of covalent bonding in the LCAO model in the antimonides, where the Sb5p shell has $I^* = 1.9$ eV corresponding to I close to 5 eV, invariantly *lower* than the I(4f). In other compounds (such as fluorides and oxides), one can always find trivalent lanthanides, where the lowest I(4f) roughly coincides with I of the loosest-bound orbitals of the adjacent atoms. This paradox has been reviewed by Ferreira (1976) who considers it a specific type of deviation from Koopmans behavior.

The photoelectron spectrometry of solid lanthanide compounds exhibits other interesting ramifications. The time scale of the initial ionization is unusually short, close to 10^{-17} sec. Several compounds such as SmB_6 and $EuCu_2Si_2$ have magnetic properties or Mössbauer spectra suggesting simultaneous coexistence of the conditional oxidation states $4f^5$ Sm[III] and $4f^6$ Sm[II], or $4f^6$ Eu[III], and $4f^7$ Eu[II]. A perhaps more surprising case is the NaCl-type thulium telluride containing (on an instantaneous picture) approximately equal concentrations having the preponderant configurations $4f^{12}$ Tm[III] and $4f^{13}$ Tm[II]. It may be noted that the nephelauxetic ratio β for Tm[IV] in the former case is 0.90 like in TmSb but as high as 0.99 for Tm[III] formed by the ionization in the latter case. Photoelectron evidence for such systems showing "configuration fluctuation" was recently reviewed (Campagna *et al.*, 1976; Wilson, 1977). The confirmation of the hypothesis of the ionized system choosing between eigenstates of the *new* Hamiltonian is rather overwhelming in these cases.

It is also clear that X-ray spectra (as studied already by Kossel) and photoelectron spectra show evidence for individual *nlj* values in condensed matter. It had not always been realized that partly filled shells, when present already in the ground state, produce a large number of *J* levels for each of the ionized levels of a closed-shell system. A typical case are the configurations $3d^9 4f^2$ (containing 910 mutually orthogonal states and 107 *J* levels) and $3d^9 4f^3$ (with 3640 states and 386 *J* levels; $J = 3$ and 4 each is represented by 61 levels) recently calculated (Spector *et al.*, 1976) and compared with the photoelectron spectra of metallic praseodymium and neodymium. For reasons related to the arguments of Cox (1975), the intensities of each of the numerous signals vary strongly. Because of the smaller spin–orbit coupling in the 4d shell, the corresponding configurations $4d^9 4f^q$ show complicated, but rather unresolved structures (Jørgensen and Berthou, 1972; Bonnelle *et al.*, 1972; Signorelli and Hayes, 1973; Lang *et al.*, 1976). Nissan Spector continues extensive calculations in full intermediate coupling along these lines.

Comparable problems occur in the interpretation of Auger spectra where the electron configuration of the final state frequently lacks two electrons in otherwise closed shells. Typical examples (neglecting filled shells) are $3d^8$ and $3p^5 3d^9$ known from metallic copper (Kowalczyk *et al.*, 1973), zinc atoms (Aksela *et al.*, 1974), metallic zinc, and zinc(II) compounds (Wagner, 1976). In particular, the nephelauxetic ratio β in $3d^8$ of metallic copper is 0.66 (compared with Cu^{3+}), higher than 0.54 of CuF_6^{3-} (Allen and Warren, 1971). Another interesting aspect is that the Cu3d photoelectron signals of metallic copper show a structure (like silver and gold; Watson and Perlman, 1975) much broader than the moderate effect of spin–orbit coupling, and usually interpreted as the "density of states" in the energy band picture, multiplied by their probability of being ionized by the high-energy photon. This may or may not be an appropriate description, but the copper atom lacking an electron in an inner shell (such as 2p) seems to function as an "impurity" having its own distinct energy levels, as seen from the similarity of the Auger spectrum (having $3d^8$ final states) with that of the krypton atom. Nevertheless, the $1s^2 2s^2 2p^4$ final states of various fluorides (Jørgensen and Berthou, 1974) show distinct "ligand field" effects from the neighbor atoms, as also seen in various alloys and compounds of heavier elements (Berthou and Jørgensen, 1974, 1977). It is here an experimental advantage that photoelectron spectrometers (using bombardment of the sample with soft X-rays rather than electrons) can be used to obtain reliable Auger spectra of nonconducting solids, as first pointed out by Wagner.

A rather extreme case of invariant behavior of inner shells, when modifying the valence electrons, is the separation $(l + \frac{1}{2})\zeta_{nl}$ between the two components $j = (l - \frac{1}{2})$ and $(l + \frac{1}{2})$, where ζ_{nl} is the *Landé parameter.* This situation is already pronounced in the lanthanides (Jørgensen, 1976a) where the separations between $^2F_{5/2}$ and the ground state $^2F_{7/2}$ of the gaseous $4f^{13}$ systems, 8774 cm^{-1} in Tm^{2+}, 10214 cm^{-1} in Yb^{3+}, and 11793 cm^{-1} in Lu^{4+} are found, within a percent or less; in the gaseous thulium atom, where two 6s electrons are added (8771 cm^{-1}), like in the excited configuration $4f^{13}6s^2$ of Yb$^+$(10149 cm^{-1}); in absorption spectra of Tm(II) and Yb(III) compounds; and in photoelectron spectra of metallic ytterbium and lutetium (Cox *et al.*, 1973) and of lutetium(III) compounds. Quite generally, the nephelauxetic effect on spin–orbit coupling is far smaller than on the interelectronic repulsion in lanthanide compounds. By the same token, the separation between the $2p_{1/2}$ and $2p_{3/2}$ signals of a large number of sulfur compounds is 1.2 eV compared with 1.256 eV in gaseous S^{7+} (Moore, 1970). Only when the 2p shell is depleted for z above +7, does this separation increase, and is 2.97 eV in the one-electron system S^{15+} according to the Sommerfeld formula. There is marginal evidence (Reisfeld *et al.*, 1976) that it is 1.15 eV in crystalline sulfur. However, the 2p separation is perceptibly decreased from 2.91 eV in K^{10+} to 2.65 eV in potassium(I) salts and from 3.72 eV in Ca^{11+} to 3.5 eV in calcium(II) compounds (Jørgensen and Berthou, 1972). The situation is slightly less transparent in the 3d group elements, where the 2p splitting appears to be increased by about 1 eV in compounds with positive S related to structure of the configuration $2p^5 3d^q$ (Jørgensen, 1975c, 1976b). A clear-cut result of the absence of the two 3s, six 3p, and ten 3d electrons can be found in Zn^{21+} (Behring *et al.*, 1976) 24.40 eV compared with the 2p separation of 23.1 eV derived from X-ray spectra (Bearden and Burr, 1967) and 23.15 eV from photoelectron spectra (Jørgensen and Berthou, 1972). By the same token, the 2p separation of 32.66 eV in gaseous Ge^{23+} (Behring *et al.*, 1976) is distinctly larger than 31.1 eV found from X-ray and photoelectron spectra. However, such effects on the spin–orbit coupling are, on the whole, much smaller than the chemical shifts dI, not to speak about the ΔI given in Table II.

A quite interesting case of highly charged gaseous ions belonging to the isoelectronic series $K = 28$ are Sm^{34+}, Gd^{36+}, and Dy^{38+} of which three transitions from each of the two excited configurations [Ar]$3d^9 4f$ and

$[Ar]3d^94p$ to the ground state $[Ar]3d^{10}$ can be observed in a plasma produced by irradiation with a high-power laser (Burkhalter *et al.*, 1974). The order of magnitude of the spin–orbit separation between $3d_{3/2}$ and $3d_{5/2}$ is the same as 25.8(Sm), 32.0(Gd), and 37.6(Dy) eV derived from X-ray spectra (Bearden and Burr, 1967) or the slightly larger values (with uncertainty 0.3 eV) derived from photoelectron spectra, 27.2, 33.5, and 38.7 eV, respectively. It is perhaps more instructive that the best determined (±2 eV) transition (in emission from $4f_{5/2}$ to $3d_{3/2}$) has $h\nu = 1325$ eV in Sm^{34+}, 1452 eV in Gd^{36+}, and 1585 eV in Dy^{38+} compared with the (charge-corrected) $I'(3d_{3/2}) = 1115$ eV in Sm(III), 1225 eV in Gd(III), and 1339 eV in Dy(III) compounds (Jørgensen and Berthou, 1972). The difference $h\nu - I' = 210$, 227, and 246 eV, respectively, has to be corrected for the binding energy of the $4f_{5/2}$ electron in order to allow a reliable estimate of the ionization energy in the gaseous ion. The hydrogenic expression for $I(4f)$ is $(z + 1)^2 \times 0.85$ eV, i.e., 1040 eV for $z = 34$, 1164 eV for $z = 36$, and 1297 eV for $z = 38$. Starting with this hypothesis, $I(3d_{3/2})$ would be 2365, 2616, and 2882 eV in the gaseous ions, from 1250 to 1543 eV higher than the photoelectron values. Such examples are not included in Table II, because several closed shells are removed, but the three values of $(\Delta I/z)$ would be 37.2, 38.3, and 40.6 eV, respectively. This is 1.07 eV times z for comparison with Eq. (13).

In the iron (3d), palladium (4d), and platinum (5d) group compounds, the S,L terms of the partly filled d shell can no longer be recognized [with rare exceptions, such as the $^6S - {}^4G$ distance in manganese(II) and iron(III) complexes], and, in this sense, there is not the approximate spherical symmetry characterizing the 4f and (at least the major part of) the 5f group. Between 1952 and 1962, a large number of absorption bands of the d groups were identified, using the concepts of ligand field theory (Jørgensen, 1962a, 1963, 1969) in a way (at least in hindsight) closely similar to the development of atomic spectra between 1919 and 1929. The octahedral chromophores with the six ligating atoms disposed on Cartesian axes (with the central atom at the origin) were studied in particular, and it is one of the less recognized, but lasting, results of ligand field arguments that nickel(II) in the octahedral *chromophore* $Ni(II)X_6$ has the 45 states of $3d^8$ (of which 30 states have $S = 1$ and 15 states $S = 0$ in Russell–Saunders coupling) distributed on four triplet ($S = 1$) levels (strictly speaking, terms able to split further by spin–orbit coupling) and seven singlet levels, to which the three spin-allowed (but parity-forbidden) and at least four spin-forbidden transitions from the triplet ground state are readily identified. If X is oxygen, then the green aqua ion $Ni(OH_2)_6^{2+}$, all kinds of hexakis complexes of organic ligands (Reedijk *et al.*, 1968), the solutions in concentrated sulfuric and phosphoric acids, silicate and phosphate glasses, mixed oxides such as green $Ni_xMg_{1-x}O$ (and NiO itself) and red, orange, and yellow ilmenites such as $Ni_xCd_{1-x}TiO_3$, $Ni_xMg_{1-x}TiO_3$, and undiluted $NiTiO_3$ (Reinen, 1966) are cases where the chemical information about local symmetry $Ni(II)O_6$ is clear cut. Corresponding chromophores, $Ni(II)F_6$, $Ni(II)Cl_6, \ldots,$ are well established from crystalline materials, and $Ni(II)N_6$, from solution chemistry of complexes of ammonia and organic amines. However, for our purposes, it is more important that the $3d^8$ nickel(II) electron configuration and concomitant oxidation state is perfectly well defined, in spite of evidence (from the nephelauxetic ratio β varying from 0.92 to below 0.70) for deviations from electrovalent bonding, due to decreased fractional atomic charge as well as to delocalization of the two antibonding 3d-like orbitals on the ligands and, perhaps, also to a more pronounced Watson effect.

The analogies between such chromophores and monatomic entities consist in the bunching together of the energy levels belonging to a definite configuration within a few electron volts in such a way that other configurations usually constitute intervals of energy levels at distinctly higher energy (including the electron transfer states of polyatomic entities such as $3d^9$ Ni[I] in the example). Such a distribution of separate configurations can be quite characteristic, such as $5d^5$ iridium(IV) in $IrCl_6^{2-}$ and $IrBr_6^{2-}$ having $5d^6$ Ir[III] electron transfer states with the expected symmetry types (Jørgensen, 1970b), whereas the chemical species $IrCl_6^{3-}$ and $IrBr_6^{3-}$ have $5d^6$ ground states and their electron transfer bands (at considerably higher wave numbers) belong to a configuration containing $5d^7$ Ir[II]. All of these classifications are valid without any reference to the (much less varying) fractional atomic charges, which may very well be *lower* on Ir(IV) than on Ir(III).

It is to be noted that when we speak about the definite, partly filled shell containing between one and $(4l + 1)$ electrons, we do not really need to worry about the electrons that are in filled orbitals [not in the strict sense of vanishing correlation effect, but constituting a single state for the purpose of vector coupling in Eq. (5) and not multiplying the number of states of the partly filled shell]. The opposite side of this statement is that the six halide ligands in the ground state of the hexahalide complex MX_6^{+z-6} are such an effective closed shell (Jørgensen, 1959, 1963, 1970b), whereas the electron transfer bands correspond to excited states involving the 36 states of the *collectively oxidized* set of ligands X_6^{5-} lacking one of the loosest-bound X*n*p electrons. Once more, the distinct character of 36*m* states formed by electron transfer to a central atom having *m* states, when one electron has been added, is confirmed by the absorption spectra, especially with finely resolved transitions in the 5d group. Thus, states where the oxidation state of the central atom has been decreased by *two* units, corresponding to the states obtained be vector coupling from X_6^{4-} have never been detected, but there is no doubt that their excitation energy is considerably higher than twice the conventional electron transfer spectra. By the same token, $4f^{q-2}5d^2$ states of lanthanide compounds would have far higher energy than the conventional $4f^{q-1}5d$ states.

IX. *K* as an Analogy to Russell–Saunders Coupling

Nuclear physicists are accustomed to the idea that quantum numbers Q may represent a concept intermediate between an integral number of constituents (such as members of a parliament or bricks in a wall) and a quantity expressed by an "external" property. When a nucleus has Z positive charges and an integer "mass number" A that is closest to the atomic weight, it is difficult to tell whether it is true that it "consists" of Z protons and $A - Z$ neutrons, and the quantum numbers I of the ground state and of the low-lying excited states (neglecting other types of "rotational" excitation) correspond to *the nuclear shell model* where each nucleon (proton or neutron) in a certain approximation has nlj values for use in the vector-coupling Eq. (6). However, the results differ from atomic spectra in many ways. For a given l, the higher $j = l + \frac{1}{2}$ is the *more* stable, and for the ground state of the nucleus $I = 0$ if both $N = A - Z$ and Z are even, whereas many other nuclei have I equal to j of one "external" nucleon (a proton if Z is odd and a neutron if N is odd) in spite of any conceivable Hartree–Fock behavior. The "magic numbers" of Maria Goeppert-Mayer are either Z or N achieving one of the closed-shell values

$$2,8,14,20,28,40,50,82,126,184,\ldots, \tag{14}$$

where the relatively small Coulombic perturbation from the interprotonic repulsion tend to stabilize other Z values, such as 114 and 164 not yet prepared. There is a conspicuous similarity between the K values in Eq. (1) and Eq. (14), but the analogy is perhaps illustrative also in another direction, namely, that such quantum numbers do not at all pretend to describe well-defined one-particle configurations in nuclei. In the classification of *elementary particles* much more extreme problems occur: almost anything "consists" of nearly everything else (cf. a review on quark-containing species, Jørgensen, 1978).

There is another characteristic of quantum numbers used for classification of nuclei and elementary particles which may help to understand the Kossel isoelectronic series. It is the variation of unconventional parameters. Thus, the first-order similarity between protons and neutrons produces a symmetric distribution of I values for low-lying states of two nuclei (with subscripts 1 and 2), $Z_1 = N_2$ and $N_1 = Z_2$, and it is possible to introduce quantum numbers such as the isospin T. The Linderberg–Shull nonrelativistic Eq. (3) can be used for variation also of Z, though it is always thought of as a positive integer. It is suggested that Z may take fractional values (Dunitz and Ha, 1972), representing cases intermediate between H_2 and HeH^+, only in a model of heteronuclear covalent bonding. Schrödinger's equation for the stationary states of a single electron can be solved for a central field involving nonintegral Z, and it can also be adapted to a different mass of the mobile electron, as used in the description of muonic energy levels close to a nucleus. It is much more a philosophical problem why the *number* of electrons in a many-electron wavefunction is an invariant integer. However, it certainly can be said that the conserved quantum number is the difference between the electron and positron counts in a measurement.

Returning to Eq. (3), there exists an empirical analogy to a variation of energy levels as a function of two parameters (Z and $K = Z - z$) in the *phenomenological baricenter polynomial* (Jørgensen, 1969) keeping K constant. To the first approximation, this polynomial is a parabola with three numerical constants, as also discussed in this series (Jørgensen, 1974b). [By the way, J(d, s) in Eq. (9) on p. 168 of the latter reference should be J(s, s).] The parabolic (and not linear) dependence on the occupation numbers of the configurations of the (observed) baricenter energies is exemplified not only by 3d4s of Sc^+ being 1.15 eV below the baricenter of $3d^2$, but also 1.36 eV below the unique state of $4s^2$. Another example is that the baricenter of $3d^94s$ in the gaseous nickel atom is below both the unique state of $3d^{10}$ and the baricenter of $3d^84s^2$ in spite of the fact that the ground state $^3F_4$ belongs to the latter configuration. It is noted that the analytical functions of the shell occupation numbers constituting the phenomenological baricenter polynomial refer to *observed* configuration baricenters in the classificatory sense. The major interest of such polynomials is that shells with unusually small average radii, such as 4f or 3d, have much higher ionization energy than electron affinity.

For Russell–Saunders coupling in spherical symmetry, the various J levels (for both S and L positive) are fairly close together in the terms each containing $(2S + 1)(2L + 1)$ mutually orthogonal states. In lower symmetries of polyatomic entities, the terms each contain $(2S + 1)m$ states, where $m = 1$ or 2. In cubic point-groups, m can also be 3, and in the special case of icosahedral symmetry, it can be 5 (Griffith, 1961; Jørgensen, 1971). It is consistent to speak about Russell–Saunders coupling in molecules and in condensed matter, insofar as the quantum number S is reasonably well defined. This is much more frequently true for transition group complexes than for monatomic entities, mainly because of a nephelauxetic decrease of the Landé parameter of the partly filled shell. Exceptions are the (usually luminescent) electron transfer states of the uranyl ion (Jørgensen and Reisfeld, 1975) and the $^3P_1$ and $^1P_1$ states of 6s6p in the mercury atom, thallium(I), lead(II), and bismuth(III) (McClure, 1959; Jørgensen, 1962a).

For some reason, both these types of exceptions are particularly important for energy transfer to lanthanides (Reisfeld, 1976; Reisfeld and Jørgensen, 1977). In the great majority of d and 4f group energy levels, S is to a very good approximation one of the values, 0, 1, 2, and 3, for an even number of electrons, or $\frac{1}{2}$, $\frac{3}{2}$, $\frac{5}{2}$, and $\frac{7}{2}$, for an odd number. From a purely practical point of view of the inorganic chemist (Jørgensen, 1969) the two most useful numbers for classifying transition and post-transition group complexes (not only the ground states, but also the excited states) are K defining the oxidation state $z = Z - K$, and S. It is possible to ask the question how many oxidation states (i.e., combinations of Z and z) are known. This is not perfectly well defined. Before the recent preparation of $Mn(CO)_4^{3-}$ establishing $3d^{10}$ Mn(−III), a doubtful example was $Mn(NO)_3CO$ appropriate *if* the ligand is NO^+ isoelectronic with CO and CN^-. In 1968 (Jørgensen, 1969), approximately 238 oxidation states were known from $Z = 21$ (scandium) to $Z = 100$ (fermium), i.e., three per element, in condensed matter (we except diatomic molecules that can be quite abundant in high-temperature vapors, and also can be studied in cool matrices such as solidified argon). The last 10 years have not produced a huge increase of this number; the more conspicuous new cases are Ni(I), Zr(II), Nb(III), Pd(V), W(II), Re(−III), Au(V), and Pu(VII). We only consider monomeric cases without direct bonds between atoms of the same element, as frequently seen in "clusters" and catenated compounds (such as the mercurous ion). The total variability of z for a given element is to a great extent a question of choosing the correct ligands: O^{2-} and F^- stabilize high z, whereas low (and in particular negative) oxidation states are obtained with PF_3 and CO.

It is rather far removed from the spirit of most physicists to compare a quantum number related to a constant of motion, such as S, with a quantity such as K indicating to what isoelectronic series the system belongs. However, the mutual difference of kind between S and K is attenuated to a certain extent when it is realized that S is a good, but not perfect, quantum number of many-electron systems and that the validity of S is not connected with spherical symmetry (as would be the case for L), whereas the interesting uses of K are in polyatomic systems. It is noted that chemists are exclusively interested in K values which, at the same time, follow the Aufbau principle [Eq. (2)]. Thus, the 4s electrons play no role in determining the oxidation state $z = Z - K$ in 3d group complexes (in contrast to monatomic entities) with exceedingly rare exceptions such as the diatomic molecule TiO having an MO configuration closely related to 3d4s (Jørgensen, 1964).

Quantum chemistry presents a manifold of interesting paradoxes (Jørgensen, 1974c), for example, the nonnumerical problem why one of two alternative descriptions, such as an electron configuration of a given energy level, simply is the *best* one, better than all the others; it has even been proposed (Jørgensen, 1970a) to use the word *aristic* for this favorable alternative. The numerical calculations may have tended too much to concentrate interest on the ground state or on another definite energy level, rather than to consider the set of low-lying energy levels at once. Both chemists and atomic spectroscopists need the *preponderant configuration* (Jørgensen, 1969) derived from ideas related to Bertrand Russell's theory of types (i.e., that certain properties of a class, such as being numerous, belong in a solidaric fashion to the class and not to its individual members), and reasonably well-defined quantum numbers (such as K and S) show many of the same characteristics. In particular, they correspond to definite numbers of states.

ACKNOWLEDGMENTS

The author would like to express his gratitude to the late Professor Ebbe Rasmussen, Copenhagen (1901–1959), whose inspired teaching of atomic spectra, in particular in the period between 1943 to 1950, when the author turned from astronomy to chemistry. The author is also grateful to Dr. Hervé Berthou for careful and perspicacious work with photoelectron spectra between 1971 and 1977. The Swiss National Science Foundation provided a grant (No. 2323-70) allowing the purchase of the Varian IEE-15 photoelectron spectrometer.

REFERENCES

Aksela, S., Väyrynen, J., and Aksela, H. (1974). *Phys. Rev. Lett.* **33**, 999.
Allen, G. C., and Warren, K. D. (1971). *Struct. Bonding (Berlin)* **9**, 49.
Ammeter, J. (1975). *Chimia* **29**, 504.
Angelov, B. M. (1976). *Chem. Phys. Lett.* **43**, 368.
Avanzino, S. C., and Jolly, W. L. (1976). *J. Electron Spectrosc. Relat. Phenom.* **8**, 15.
Bagus, P. S., Lee, Y. S., and Pitzer, K. S. (1975). *Chem. Phys. Lett.* **33**, 408.
Bearden, J. A., and Burr, A. F. (1967). *Rev. Mod. Phys.* **39**, 125.
Behring, W. E., Cohen, L., Doschek, G. A., and Feldman, U. (1976). *J. Opt. Soc. Am.* **66**, 376.
Berkowitz, J., and Dehmer, J. L. (1972). *J. Chem. Phys.* **57**, 3194.
Berkowitz, J., Dehmer, J. L., and Walker, T. E. H. (1973). *J. Chem. Phys.* **59**, 3645.
Berry, R. S. (1969). *Chem. Rev.* **69**, 533.
Berthier, G. (1974). *Adv. Quantum Chem.* **8**, 183.
Berthou, H., and Jørgensen, C. K. (1974). *J. Electron Spectrosc. Relat. Phenom.* **5**, 935.
Berthou, H., and Jørgensen, C. K. (1977). *J. Microsc. Spectrosc. Electron.* **2**, 135.
Bonnelle, C., Karnatak, R. C., and Jørgensen, C. K. (1972). *Chem. Phys. Lett.* **14**, 145.
Burkhalter, P. G., Nagel, D. G., and Whitlock, R. R. (1974). *Phys. Rev. A* **9**, 2331.
Campagna, M., Wertheim, G. K., and Bucher, E. (1976). *Struct. Bonding (Berlin)* **30**, 99.
Carnall, W. T., Fields, P. R., and Rajnak, K. (1968). *J. Chem. Phys.* **49**, 4412, 4424, 4443, 4447, and 4450.

Caro, P., Beaury, O., and Antic, E. (1976). *J. Phys. (Paris)* **37**, 671.

Cauchois, Y. (1952). *J. Phys. (Paris)* **13**, 113.

Cauchois, Y. (1956). *J. Phys. (Paris)* **16**, 253.

Citrin, P. H., and Hamann, D. R. (1974). *Phys. Rev. B* **10**, 4948.

Citrin, P. H., and Thomas, T. D. (1972). *J. Chem. Phys.* **57**, 4446.

Clementi, E., and Veillard, A. (1966). *J. Chem. Phys.* **44**, 3050.

Condon, E. U., and Shortley, G. H. (1953). "Theory of Atomic Spectra." Cambridge Univ. Press, London and New York.

Coster, D. (1923). *Naturwissenschaften* **11**, 567.

Cowan, R. D. (1973). *Nucl. Instrum. & Methods* **110**, 173.

Cox, P. A. (1975). *Struct. Bonding (Berlin)* **24**, 59.

Cox, P. A., Baer, Y., and Jørgensen, C. K. (1973). *Chem. Phys. Lett.* **22**, 433.

Dunitz, J. D., and Ha, T. K. (1972). *J. Chem. Soc., Chem. Commun.* p. 568.

Ellis, J. E., and Faltynek, R. A. (1975). *J. Chem. Soc., Chem. Commun.* p. 966.

Ellis, J. E., Barger, P. T., and Winzenburg, M. L. (1977). *J. Chem. Soc., Chem. Commun.* p. 686.

Evans, S., and Orchard, A. F. (1975). *J. Electron Spectrosc. Relat. Phenom.* **6**, 207.

Fadley, C. S., Hagström, S. B. M., Klein, M. P., and Shirley, D. A. (1968). *J. Chem. Phys.* **48**, 3779.

Ferreira, R. (1976). *Struct. Bonding (Berlin)* **31**, 1.

Fowler, A. (1922). "Report on Series in Line Spectra." Fleetway Press, London.

Fricke, B. (1975). *Struct. Bonding (Berlin)* **21**, 89.

Fricke, B., and McMinn, J. (1976). *Naturwissenschaften* **63**, 162.

Gelius, U. (1974). *J. Electron Spectrosc. Relat. Phenom.* **5**, 985.

Golden, S., Guttman, C., and Tuttle, T. R. (1966). *J. Chem. Phys.* **44**, 3791.

Griffith, J. S. (1961). "Theory of Transition-Metal Ions." Cambridge Univ. Press, London and New York.

Ha, T. K., and O'Konski, C. T. (1969). *Chem. Phys. Lett.* **3**, 603.

Heilbron, J. L. (1977). *Phys. Today* 23, April 1977.

Hund, F. (1927). "Linienspektren und Periodisches System der Elemente." Julius Springer, Berlin.

Jolly, W. L., and Perry, W. B. (1974). *Inorg. Chem.* **13**, 2686.

Jørgensen, C. K. (1959). *Mol. Phys.* **2**, 309.

Jørgensen, C. K. (1962a). "Absorption Spectra and Chemical Bonding in Complexes." Pergamon, Oxford.

Jørgensen, C. K. (1962b). *Solid State Phys.* **13**, 375.

Jørgensen, C. K. (1962c). "Orbitals in Atoms and Molecules." Academic Press, London.

Jørgensen, C. K. (1963). *Adv. Chem. Phys.* **5**, 33.

Jørgensen, C. K. (1964). *Mol. Phys.* **7**, 417.

Jørgensen, C. K. (1969). "Oxidation Numbers and Oxidation States." Springer-Verlag, Berlin and New York.

Jørgensen, C. K. (1970a). Colloq. Int. C.N.R.S. **191**, 21.

Jørgensen, C. K. (1970b). *Prog. Inorg. Chem.* **12**, 101.

Jørgensen, C. K. (1971). "Modern Aspects of Ligand Field Theory." North-Holland Publ., Amsterdam.

Jørgensen, C. K. (1973a). *Angew. Chem.* **85**, 1.

Jørgensen, C. K. (1973b). *Struct. Bonding (Berlin)* **13**, 199.

Jørgensen, C. K. (1974a). *Chimia* **28**, 6.

Jørgensen, C. K. (1974b). *Adv. Quantum Chem.* **8**, 137.

Jørgensen, C. K. (1974c). *Theor. Chim. Acta* **34**, 189.

Jørgensen, C. K. (1975a). *Top. Curr. Chem.* **56**, 1.

Jørgensen, C. K. (1975b). *Struct. Bonding (Berlin)* **22**, 49.
Jørgensen, C. K. (1975c). *Struct. Bonding (Berlin)* **24**, 1.
Jørgensen, C. K. (1976a). "Gmelin's Handbuch der anorganischen Chemie," 39 Seltenerdelemente, vol. B1, p. 17.
Jørgensen, C. K. (1976b). *Struct. Bonding (Berlin)* **30**, 141.
Jørgensen, C. K. (1976c). *Chimia* **30**, 490.
Jørgensen, C. K. (1977). *Fresenius Z. Analyt. Chem.* **288**, 161.
Jørgensen, C. K. (1978). *Struct. Bonding (Berlin)* **34**, 19.
Jørgensen, C. K. (1979). "Lanthanides and Elements from Thorium to 184." Academic Press, London and New York.
Jørgensen, C. K., and Berthou, H. (1972). *K. Dan. Vidensk. Selsk., Mat.-Fys. Medd.* **38**, No. 15.
Jørgensen, C. K., and Berthou, H. (1973). *J. Fluorine Chem.* **2**, 425.
Jørgensen, C. K., and Berthou, H. (1974). *Chem. Phys. Lett.* **25**, 21.
Jørgensen, C. K., and Berthou, H. (1975a). *Chem. Phys. Lett.* **31**, 416.
Jørgensen, C. K., and Berthou, H. (1975b). *Chem. Phys. Lett.* **36**, 432.
Jørgensen, C. K., and Penneman, R. A. (1976). *In* "Heavy Element Properties" (W. Müller and H. Blank, eds.), p. 117. North-Holland Publ., Amsterdam.
Jørgensen, C. K., and Reisfeld, R. (1975). *Chem. Phys. Lett.* **35**, 441.
Jørgensen, C. K., Pappalardo, R., and Schmidtke, H. H. (1963). *J. Chem. Phys.* **39**, 1422.
Jørgensen, C. K., Horner, S. M., Hatfield, W. E., and Tyree, S. Y. (1967). *Int. J. Quantum Chem.* **1**, 191.
Judd, B. R. (1963). "Operator Techniques in Atomic Spectroscopy." McGraw-Hill, New York.
Karayianis, N. (1965). *J. Math. Phys.* **6**, 1204.
Katriel, J., and Pauncz, R. (1977). *Adv. Quantum Chem.* **10**, 143.
Kaufman, V., and Sugar, J. (1976). *J. Opt. Soc. Am.* **66**, 1019.
Kossel, W. (1916). *Ann. Phys. (Leipzig)* [4] **49**, 229.
Kossel, W. (1921). "Valenzkräfte und Röntgenspektren." Julius Springer, Berlin.
Kowalczyk, S. P., Pollak, R. A., McFeely, F. R., Ley, L., and Shirley, D. A. (1973). *Phys. Rev. B* **8**, 2387.
Kowalczyk, S. P., Ley, L., Martin, R. L., McFeely, F. R., and Shirley, D. A. (1976). *Discuss. Faraday Soc.* **60**, 7.
Lang, W. C., Padalia, B. D., Watson, L. M., Fabian, D. J., and Norris, P. R. (1976). *Discuss. Faraday Soc.* **60**, 37.
Leary, K., and Bartlett, N. (1972). *J. Chem. Soc., Chem. Commun.* p. 903.
Linderberg, J. (1961). *Phys. Rev.* **121**, 816.
Linderberg, J., and Shull, H. (1960). *J. Mol. Spectrosc.* **5**, 1.
McClure, D. S. (1959). *Solid State Phys.* **9**, 399.
Manne, R., and Åberg, T. (1970). *Chem. Phys. Lett.* **7**, 282.
Mason, M. G., and Gerensen, L. J. (1976). *Chem. Phys. Lett.* **40**, 476.
Massey, H. S. W. (1976). *Endeavour* **35**, 58.
Moore, C. E. (1949). "Atomic Energy Levels," Natl. Bur. Stand. Circ. No. 467, Vol. 1. NBS, Washington, D.C.
Moore, C. E. (1952). "Atomic Energy Levels," Natl. Bur. Stand. Circ. No. 467, Vol. 2. NBS, Washington, D.C.
Moore, C. E. (1958). "Atomic Energy Levels," Natl. Bur. Stand. Circ. No. 467, Vol. 3. NBS, Washington, D.C.
Moore, C. E. (1970). *Natl. Stand. Ref. Data Ser., Natl. Bur. Stand.* No. 34.
Morrison, J. C. (1972). *Phys. Rev. A* **6**, 643.
Nugent, L. J., Baybarz, R. D., Burnett, J. L., and Ryan, J. L. (1973). *J. Phys. Chem.* **77**, 1528.
Paschen, F. (1919). *Ann. Phys. (Leipzig)* [4] **60**, 405.

Penneman, R. A., Mann, J. B., and Jørgensen, C. K. (1971). *Chem. Phys. Lett.* **8**, 321.

Persson, W., and Valind, S. (1972). *Phys. Scr.* **5**, 187.

Politzer, P., and Daiker, K. C. (1973). *Chem. Phys. Lett.* **20**, 309.

Racah, G. (1942). *Phys. Rev.* **61**, 537.

Racah, G. (1949). *Phys. Rev.* **76**, 1352.

Racah, G. (1960). *J. Opt. Soc. Am.* **50**, 408.

Reader, J., and Epstein, G. L. (1975). *J. Opt. Soc. Am.* **65**, 638.

Reedijk, J., Van Leeuwen, P. W. N. M., and Groeneveld, W. L. (1968). *Recl. Trav. Chim. Pays-Bas* **87**, 129.

Reinen, D. (1966). *Theor. Chim. Acta* **5**, 312.

Reisfeld, R. (1973). *Struct. Bonding (Berlin)* **13**, 53.

Reisfeld, R. (1975). *Struct. Bonding (Berlin)* **22**, 123.

Reisfeld, R. (1976). *Struct. Bonding (Berlin)* **30**, 65.

Reisfeld, R., and Jørgensen, C. K. (1977). "Lasers and Excited States of Rare Earths." Springer-Verlag, Berlin and New York.

Reisfeld, R., Jørgensen, C. K., Bornstein, A., and Berthou, H. (1976). *Chimia* **30**, 451.

Schaaf, T. F., Avanzino, S. C., Jolly, W. L., and Sievers, R. E. (1976). *J. Coord. Chem.* **5**, 157.

Schäffer, C. E. (1968). *Struct. Bonding (Berlin)* **5**, 68.

Schäffer, C. E. (1973). *Struct. Bonding (Berlin)* **14**, 69.

Schmutzler, R. W., Fischer, R., Hoshino, H., and Hensel, F. (1975). *Phys. Lett. A* **55**, 67.

Signorelli, A. J., and Hayes, R. G. (1973). *Phys. Rev. B* **8**, 81.

Slater, J. L., Sheline, R. K., Lin, K. C., and Weltner, W. (1971). *J. Chem. Phys.* **55**, 5129.

Spector, N., and Sugar, J. (1976). *J. Opt. Soc. Am.* **66**, 436.

Spector, N., Bonnelle, C., Dufour, G., Jørgensen, C. K., and Berthou, H. (1976). *Chem. Phys. Lett.* **41**, 199.

Stucky, G. D., Matthews, D. A., Hedman, J., Klasson, M., and Nordling, C. (1972). *J. Am. Chem. Soc.* **94**, 8009.

Sugar, J. (1963). *J. Opt. Soc. Am.* **53**, 831.

Sugar, J. (1975). *J. Opt. Soc. Am.* **65**, 1366.

Sugar, J., and Reader, J. (1973). *J. Chem. Phys.* **59**, 2083.

Svensson, S., Mårtensson, N., Basilier, E., Malmquist, P. Å., Gelius, U., and Siegbahn, K. (1976a). *J. Electron Spectrosc. Relat. Phenom.* **9**, 51.

Svensson, S., Mårtensson, N., Basilier, E., Malmquist, P. Å., Gelius, U., and Siegbahn, K. (1976b). *Phys. Scr.* **14**, 141.

Tehan, F. J., Barnett, B. L., and Dye, J. L. (1974). *J. Am. Chem. Soc.* **96**, 7203.

Trees, R. E. (1964). *J. Opt. Soc. Am.* **54**, 651.

Trees, R. E., and Jørgensen, C. K. (1961). *Phys. Rev.* **123**, 1278.

Turner, D. W., Baker, C., Baker, A. D., and Brundle, C. R. (1970). "Molecular Photoelectron Spectroscopy." Wiley (Interscience), New York.

Wagner, C. D. (1976). *Discuss. Faraday Soc.* **60**, 291.

Walsh, A. D. (1953). *J. Chem. Soc.* pp. 2260 and 2266.

Watson, R. E. (1960). *Phys. Rev.* **119**, 170.

Watson, R. E., and Perlman, M. L. (1975). *Struct. Bonding (Berlin)* **24**, 83.

Wendin, G. (1978). *Struct. Bonding (Berlin)* (in press).

Wendin, G., and Ohno, M. (1976). *Phys. Scr.* **14**, 148.

Wilson, J. A. (1977). *Struct. Bonding (Berlin)* **32**, 57.

Wybourne, B. G. (1965). "Spectroscopic Properties of Rare Earths." Wiley (Interscience), New York.

Zollweg, R. J. (1969). *J. Chem. Phys.* **50**, 4251.

ADVANCES IN QUANTUM CHEMISTRY, VOLUME 11

Localized Orbitals in Spectroscopy

DENNIS CALDWELL and HENRY EYRING
Department of Chemistry
University of Utah
Salt Lake City, Utah

I. Introduction

The exact solution to the wave equation for a single electron in the field of a positive charge has provided thus far the essential ingredients for virtually all practical methods in quantum molecular physics. One remarkable feature of the many-body problem has been the successful application of the quasi-independent particle or self-consistent field (SCF) model in which solutions to an $\sum_i H(i) + \sum_{i>j} V(i,j)$ eigenvalue equation are sought as products of one-electron functions, $\chi_A(1) \cdots \chi_N(n)$. In the course of time the Hartree method for atoms has been supplanted by the more general Hartree–Fock equations for molecules.

Observables may be divided into the following categories:

(i) simple ground-state properties, measured by diagonal matrix elements such as $\mathbf{R}_{00}$ for the permanent dipole moment;

(ii) complex ground-state properties, which are related to sums over off-diagonal matrix elements,

$$\sum_{n \neq o} \frac{A_{on} B_{no}}{E_n - E_o},$$

such as the zero-frequency polarizability and NMR coupling constants;

(iii) simple transition properties, proportional to a single product of off-diagonal matrix elements, exemplified by the absorption $\mathbf{R}_{on}^2(E_n - E_o)$ and circular dichroism, $\mathbf{R}_{on} \cdot \mathbf{M}_{no}$, and

(iv) complex transition properties, related to sums over products of matrix elements,

$$\sum_{m \neq n} \frac{A_{on} B_{nm} C_{mo}}{E_m - E_n},$$

such as magnetic circular dichroism.

ISBN 0-12-034811-X

There are other more complex forms as well, all of which can be treated by a general density matrix formalism whereby an observable F is related to the quantity,

$$\langle F\rangle = \operatorname{Tr} \rho F(\hat{\Omega}_1, \ldots, \hat{\Omega}_M; E_i),$$

and F is a functional of the operators $\hat{\Omega}_i$ and possibly the explicit spectral density.

The most general molecular orbital formulation of the problem would require each state $\mathscr{H}_a$ to be represented by a sum over all combinations of Slater determinants for a given one-electron basis, $\{\chi_1, \ldots, \chi_N\}$. For simple ground-state properties the first term in this series, if a closed-shell system is initially assumed, is the determinant,

$$\Psi_G = |\chi_1(1)\bar{\chi}_1(2)\cdots\chi_N(n-1)\bar{\chi}_N(n)|,$$

where $n = 2N$. The electronic energy for this function is given by

$$E_G = 2\sum_{i=1}^{N} \bar{h}_i + \sum_i \sum_j [2\langle ii|jj\rangle - \langle ij|ij\rangle], \tag{1}$$

where $\bar{h}$ is the kinetic plus nuclear attraction energy operator and

$$\langle ij|ij\rangle = \int\int \chi_i(1)\psi_j(1)\frac{1}{r_{12}}\chi_i(2)\chi_j(2)\,d\tau_1\,d\tau_2$$

in the usual manner.

Since both the single and double summations are invariant to a unitary transformation among the orbitals χ_i, there is no *a priori* reason for preferring one basis to another so far as the total attractive or repulsion energy is concerned. On the other hand, consider an ionic crystal such as LiF. As the internuclear separation is increased, Ψ_G will eventually describe an array of isolated Li^+ and F^- ions, and a transformation of the χ_i may be found such that each orbital χ_i' is completely localized about a particular ion.

When the process is reversed and the atoms move closer together, it is found that any attempt to repeat this localization procedure by projecting isolated atomic orbitals from each molecular orbital is frustrated by the appearance of tails from neighboring atoms, which increase in size as the equilibrium lattice dimension is approached. The resulting functions, which may be alternatively described as Löwdin (1950) or Wannier (1937) orbitals, represent the best effort to obtain molecular orbitals that most closely resemble those at infinite separation.

For covalent molecules the situation is more complicated, since the separation into neutral atoms is generally more energetically favored and the restricted Hartree–Fock (RHF) closed-shell model is inadequate for dissociation. This first leads to a consideration of diatomic homopolar molecules, such as H_2, N_2, for which certain of the higher-energy, or valence, orbitals cannot be further localized even to a first approximation. Accordingly, in polyatomic molecules one will seek methods that decompose an arbitrary set of χ_i into partially localized monatomic (inner-shell and nonbonding) and diatomic (bonding) components, as well as those characterized by larger arrays of atoms.

Once an optimum set of localized orbitals has been constructed along these guidelines, there exists a convenient basis for obtaining the remaining terms in the sum of determinants for the exact ground-state function $\mathscr{H}_G$. Following the example of the small number of single and double excitation functions required for a reasonable description of a diatomic molecular dissociation process, the appropriate determinants may be introduced into the configuration interaction (CI) scheme to describe the rupture of all bonds in the molecule, greatly reducing the total number of required configurations, along with gaining a conceptual understanding of their role.

Although such a procedure will generally yield a substantial lowering of the ground-state energy from the $\langle \Psi_G | H | \Psi_G \rangle$ value, a precision comparable with that for simple diatomics is not forthcoming until a considerable number of additional configurations are introduced, so many that it may often be more convenient to deal with the original delocalized orbitals. It is quite possible, however, that a truncated CI based on such localized orbitals may represent an optimum balance between accuracy and intelligibility in SCF–CI calculations.

For excited states the most natural expedient is to start from Ψ_G and first form the single excitation determinants,

$$\Psi_{i \to j^\ddagger} = |\chi_1(1) \cdots \chi_i(\rho - 1)\bar{\chi}_j^\ddagger(p) \cdots \chi_M|,$$

which in general will not correspond individually to the actual excited states Θ_n. A configuration interaction treatment of these functions will have the effect of transforming the occupied or virtual orbitals among themselves, which in certain cases will have a tendency toward localization. If these orbitals are initially localized, the size of the CI may again be reduced, particularly when only one or two excited states are under consideration.

Single excitation CI may be divided into two portions: first, separate transformations on the occupied and virtual orbitals in order to minimize the off-diagonal elements of the CI matrix [this essentially comprises the improved virtual orbital (IVO) calculation], followed by the final diagonalization, which may often be done perturbatively. It will turn out that the initial transformation does not generally lead to orbitals of maximum localization, but there will be a decided tendency toward that direction. This procedure is the underlying basis for excitonic theories of composite absorption bands in polymers. For more accurate work, particularly in high-energy processes, multiple excitations are required.

It is important to distinguish between orbitals that are localized by a unitary transformation of the occupied or virtual space and those obtained by other procedures. In the first case the matrix elements $\langle \psi_G | H | \Psi_{i \to j\ddagger} \rangle$ vanish, whereas in the second they may be substantial. Most commonly the latter consist of maximum localization orbitals without the tails present in the former. In the two cases, the CI analysis follows different courses and the distinctions must be kept in clear focus.

One significant feature of ground-state properties is the additivity of bond energies, a fact that is rather difficult to rationalize from molecular orbital theory. The simplest hypothesis is the assumption that localized orbitals are approximately transferable between similar chemical environments and that correlation energies are primarily dependent on internal single and multiple excitations for each bond, with appropriate modifications for conjugated systems.

As will be discussed in the following, the transferability of individual orbitals is a somewhat more restrictive mechanism than the relative invariance of other more general functionals of the density matrix such as Hartree–Fock matrix elements. Even if this were to apply only to maximum localization orbitals, which are not orthogonal, the solution to the energy equations would still require the explicit use of overlap between orbitals describing different bonds. Although zero differential overlap (ZDO) semi-empirical theories do provide an apparent justification for the transferability mechanism, their implicit foundation on symmetric orthonormalization does not remove the overlap dilemma. Regardless of what will prove to be the most satisfactory formulation of the question, there is no doubt that localized orbitals will play a significant role.

Spectroscopic phenomena may be analyzed by local and nonlocal mechanisms. For example, both UV and IR absorption exhibit a specificity for particular chemical groups or bonds, strongly suggesting some local formulation; however, vibrational mode analysis indicates that, whereas fundamental IR frequencies are characteristic, the vibrational modes themselves are considerably delocalized. The situation with the appropriate CI matrix for UV is similar. It is well established that electronic transitions are appreciably more delocalized than the minimal size of a particular chromophore would indicate. By tacitly assuming maximum localizability, it is possible to construct models that reproduce many of the salient features of absorption spectra. For sensitive phenomena, such as optical activity, it is necessary to have a more detailed picture of the transition density matrix over a region much larger than the formally designated chromophore, even for a qualitative discussion. An important distinction is to be made between matrix elements and matrix eigenvectors.

In the following sections we shall outline the general methods for localizing orbitals, along with particular applications of importance, concluding with an assessment of the strengths and limitations inherent in the method.

II. Localization Methods

One method for classifying orbital localization procedures is according to physical or chemical criteria. Specifically, if some property of the orbitals such as the Coulombic energy or distances between centroids is required to be an extremum, a set of orbitals results that are as spherical or spheroidal in nature as is possible within the constraints imposed by the original basis. On the other hand, much the same result may be obtained by requiring certain functionals of the density matrix to achieve values corresponding to isolated chemical bonds between particular atoms. Both approaches enable us to gain an insight on the quasi-invariant properties of homologous series.

In the expression for the total energy [Eq. (1)], the individual summations for the Coulomb and exchange contributions are invariant to transformation. The partial sums for $i = j$ are not. Returning to the example of the ionic crystal, it is evident that the most localized orbitals will be approximately spherical in nature. From the standpoint of self-interaction energy, a sphere is characterized by a maximum with respect to all other geometrical figures; hence, it would be reasonable to suppose that the maximization of the partial sum, $\sum_i \langle ii|ii\rangle$, would lead to the desired localization. This constitutes the basis of the widely used Edmiston–Ruedenberg (1963) method.

In its most practical form, $\langle ii|ii\rangle + \langle jj|jj\rangle$ is maximized for a pair (χ_i, χ_j) at a time, after the fashion of the Jacobi matrix diagonalization method, until no significant increase in the entire sum is observed. If

$$\chi_i' = \cos\gamma\chi_i + \sin\gamma\chi_j \tag{2a}$$

$$\chi_j' = -\sin\gamma\chi_i + \cos\gamma\chi_j, \tag{2b}$$

then one finds that

$$\langle ii|ii\rangle' + \langle jj|jj\rangle' = \langle ii|ii\rangle + \langle jj|jj\rangle + A_{ij} - A_{ij}\cos 4\gamma + B_{ij}\sin 4\gamma, \tag{3}$$

where

$$A_{ij} = \langle ij|ij\rangle - \tfrac{1}{4}[\langle ii|ii\rangle + \langle jj|jj\rangle - 2\langle ii|jj\rangle],$$

$$B_{ij} = \langle ii|ij\rangle - \langle jj|ij\rangle.$$

The extremum values of the function in Eq. (3) are found by equating the first derivative to zero, which gives

$$\tan 4\gamma = \frac{B_{ij}}{A_{ij}}. \tag{4}$$

The maxima are those values of γ for which the second derivative is negative:

$$16[A_{ij}\cos 4\gamma - B_{ij}\sin 4\gamma] < 0.$$

Certain procedural refinements in the method have been introduced by Barr and Basch (1975), which consist in removing the ambiguities involving the distinction between maxima and minima, along with choosing the rotational angle in Eq. (2) to be the smaller of the two options, thus avoiding transformations that in effect switch χ_i and χ_j.

In principle it is also desirable to have methods that directly lead to localized orbitals from the SCF equations. From Eq. (3) it follows that the localization procedure is complete when $B_{ij} = 0$ for all i, j. The general Hartree–Fock equations,

$$h^F\chi_i = \sum_j \varepsilon_{ji}\chi_j, \tag{5}$$

express the requirement that the result of applying the operator h^F to the set $\{\chi_i\}$ leaves the occupied and virtual spaces invariant, once self-consistency has been achieved. The particular solutions will depend on the constraints put on the ε_{ji}, the most natural being $\varepsilon_{ji} = \delta_{ji}\varepsilon_{ii}$, which leads to the largely delocalized canonical set.

Alternatively, one may replace Eq. (5) with an equivalent equation that contains the desired constraints:

$$[h^F + G(\chi_1 \cdots \chi_N)]\chi_i = \lambda_i\chi_i, \tag{6}$$

where

$$G = \sum_m \sum_n G_{mn}|\chi_m\rangle\langle\chi_n|.$$

Now $G(\chi_1 \cdots \chi_N)$ must be constructed such that after the iterative process

$$h^F_{mn} + G_{mn} = 0, \qquad m \neq n \tag{7a}$$

$$h^F_{nn} + G_{nn} = h^F_{nn}. \tag{7b}$$

Equation (7a) follows from Eq. (6), whereas Eq. (7b) is necessary in order that identification with the h^F matrix be made through N linearly independent relations.

The requirement that $B_{mn} = 0$ is included by adding any even function of B_{mn}, $F(B_{mn})$ which vanishes if and only if $B_{mn} = 0$. This leads to the form,

$$G_{mn} = B^2_{mn} - h^F_{mn} \qquad m \neq n \tag{8a}$$

$$G_{nn} = 0. \tag{8b}$$

The resulting equations may then be solved iteratively:

$$[\mathsf{h}^F(k) + \mathsf{G}(\chi_1^{(k)} \cdots \chi_N^{(k)})]\chi_n^{(k+1)} = \lambda_n^{(k+1)}\chi_n^{(k+1)}, \tag{9}$$

where k is the number of the iteration cycle.

A somewhat simpler though less definitive procedure (Peters, 1969) consists in solving the SCF eigenvalue problem in a subspace that is orthogonal to the space spanned by a preselected $N - 1$ localized orbitals. Letting $\{\psi_1 \cdots \psi_{N-1}\}$ signify the initial localized orbitals and $\{\chi_1 \cdots \chi_M\}$ the orthogonal complement, which includes the single remaining occupied along with all the virtual orbitals, the h^F matrix is formed in the usual manner, and the subunit whose elements are

$$h_{mn}^{F\chi} = \langle \chi_m | \mathsf{h}^F | \chi_n \rangle$$

is diagonalized. The eigenvector with the lowest eigenvalue is taken to be the Nth occupied orbital ψ_N, and the process may be repeated by interchanging this orbital with one of the other ψ_i until self-consistency is obtained.

Each iteration allows a particular localized orbital to mix freely with the virtual space. If the initial choice of the $\{\psi_i\}$ is accurate, the final set $\{\psi_1' \cdots \psi_N'\}$ will remain localized. When this is not the case, there is a fair chance that an inordinate amount of delocalization may occur. This comes about because the process is essentially a metastable one, tending to give orbitals as close as possible to the original within the constraints imposed by the separation of occupied and virtual spaces. If the original $\{\psi_i\}$ are already Hartree–Fock orbitals, no change will be brought about by this procedure, regardless of their degree of localization. The success of the method is rather dependent on the ability to make a good initial separation of the two spaces. Whenever this is possible, it has much in the way of simplicity and efficiency to recommend itself.

A number of variations on the Edmiston–Ruedenberg method are possible in which the quantities,

$$\langle ij | ij \rangle = \int\int \chi_i(1)\chi_j(1)\frac{1}{r_{12}}\chi_i(2)\chi_j(2)\,d\tau_1\,d\tau_2,$$

are replaced by

$$\int\int \chi_i(1)\chi_j(1)\Omega_{12}\,\chi_i(2)\chi_j(2)\,d\tau_1\,d\tau_2,$$

where Ω_{12} is an appropriate two-electron operator. In particular, if $\Omega_{12} = \delta(\mathbf{r}_1 - \mathbf{r}_2)$, there results the density localization procedure of von Niessen (1972a, b), for which the sum of the charge-density overlaps is minimized:

$$\delta D = \delta \sum_{i>j} [ii|jj] = 0, \tag{10}$$

where

$$[ii|jj] = \int \chi_i^2(1)\chi_j^2(1)\,d\tau_1.$$

The algebra of this method exactly parallels the original prototype for the maximum self-energy, and the results have been found to be quite similar. This alternative has the advantage that the overlap integrals $[ii|jj]$ are much easier to evaluate than the Coulomb repulsion terms $\langle ii|jj\rangle$.

Turning to chemical methods, according to the Magnasco–Perico (1967) procedure the normalization integral for a molecular orbital takes the form

$$\begin{gathered}\chi_i = \sum_j C_{ij}\phi_j, \\ \sum_p \sum_q C_{ip}C_{iq}S_{pq} = 1.\end{gathered} \tag{11}$$

If the double summation is restricted to a particular set of atoms Γ_i, a local orbital population is defined by

$$P_i = 2\sum_{p\subset\Gamma_i}\ \sum_{q\subset\Gamma_i} C_{ip}C_{iq}S_{pq}. \tag{12}$$

Once the desired partition into localized regions has been made, it is then natural to seek a simultaneous maximization of these quantities via a localization function,

$$P = \sum_{i=1}^{N} P_i.$$

If the initial choice is propitious, then P may approach the ideal value of $2N$. In practice, P is maximized by an iterative cycle of 2×2 rotations, giving rise to equations similar in nature to the Edmiston–Ruedenberg method.

This procedure is relatively simple and avoids dealing with electron repulsion or charge-density overlap integrals, the only input required being the HF orbitals and the overlap matrix. On the other hand, there is the significant restriction that some chemical knowledge must be included in order that the localization process is properly initiated. In fact, the orbitals themselves are strongly dependent on this choice. Nonetheless, the results of this method have in many cases compared favorably with the intrinsic charge repulsion and overlap methods.

One recurring procedural question in the LCAO–MO method has been the problem of overlap. In most *ab initio* programs the initial orbitals are orthonormalized, generally by the Schmidt procedure, whereas in semiempirical theories either explicit or implicit use of symmetrical orthonormalization is made. The projection technique lends itself rather well to the task of dealing with such nonorthogonal atomic basis functions.

Localized orbitals for individual atoms, bonds, or clusters of atoms may be defined in terms of projection operators (Roby, 1974a, b). Each atom I is represented by the operator

$$\mathsf{P}_I = \sum_i |\phi_{Ai}\rangle \langle \phi_{Ai}|, \tag{13}$$

and the space spanned by a pair of atoms I, J, whose orbitals are not necessarily orthogonal, is given by

$$\mathsf{P}_{IJ} = \sum_i \sum_j |\phi_{IJi}\rangle (\mathsf{S}^{(IJ)})^{-1}_{ij} \langle \phi_{IJj}|, \tag{14}$$

where $|\phi_{IJi}\rangle$ denotes the composite set of orbitals on the two atoms, and $\mathsf{S}^{(IJ)}$ is the overlap matrix.

If $\{\chi_1 \cdots \chi_N\}$ is a set of previously determined molecular orbitals such as the delocalized canonical HF functions, its space is accordingly defined by the projector

$$\mathsf{Q} = \sum_{i=1}^{N} |\chi_i\rangle \langle \chi_i|, \tag{15}$$

the orbitals being assumed orthogonal.

Next the operators, $\mathsf{QP}_I\mathsf{Q}$ and $\mathsf{QP}_{IJ}\mathsf{Q}$, are formed, which ferret out the vectors common to both the HF and the appropriate atomic or polyatomic subspace. The eigenvalues λ_{Ii}, which are equal to the squares of the projection norms (Löwdin, 1965; Amos and Hall, 1961)

$$\langle \psi_{Ii} | P_I | \psi_{Ii} \rangle$$

for the associated eigenvectors, provide a direct criterion for atomic (inner-shell and lone-pair), diatomic, and polyatomic localizability. Values sufficiently close to unity are considered to describe properly localized orbitals.

First the inner shell and lone pairs are determined, followed by the bonding orbitals from the orthogonal complement to the atomic set. This leads to a nonorthogonal localized basis, which spans the original HF occupied space. The resulting vectors may either be subjected to symmetric orthonormalization or remain as they are. In the latter case, one obtains the maximum attainable degree of localization within the occupied HF space; however, it should be recognized that here a biorthogonal basis is applicable, and, although the one set is highly localized, the reciprocal basis may be somewhat delocalized. Such ambiguities are removed by symmetric orthonormalization, although this will introduce tails on neighboring atoms in the usual manner.

This method requires only the original orbitals, their overlap matrix, and the SCF eigenvectors. It has the advantage that quantitative criteria for establishing the localizability of chemical bonds are an inherent feature. Like the Magnasco–Perico method, it does require a series of preselected partitionings to be included in the algorithm for obtaining the orbitals. Again the results of the orthonormal version are quite similar to the other methods.

The density matrix provides an additional insight on the nature of localized orbitals. Although the possibilities have been well recognized (McWeeny, 1960), the utilization of this option has not been particularly widespread. One reason for this is related to the degeneracy problem in that, for closed-shell SCF theory, the eigenvalues are all equal to 2 for occupied orbitals, and 0 for virtual ones. This means that the natural orbitals are not uniquely determined and can properly be said to have any degree of localization.

If the orbitals could be completely localized, then it would be possible to obtain them by diagonalizing subunits of the density matrix and selecting those orbitals with eigenvalues of 2. The smallest partitioning for which this is possible would then represent maximum localization. In practice one first diagonalizes all the monatomic sections $\rho^{(I)}$ to obtain the inner-shell and nonbonding orbitals. The other eigenvectors with lower eigenvalues, <2, will be involved in bonding to other atoms. It does not necessarily follow that they are the desired hybrids.

Next all two-atom density matrices $\rho^{(IJ)}$ are diagonalized and the eigenvalues subjected to the following considerations: if there is one eigenvalue near zero, a single bond may be considered to exist between atoms I and J. The nearly vanishing eigenvalue will be associated with a virtual orbital

$$\psi^{\ddagger}_{IJ} = \sum_{i} C^{IJ\ddagger}_{Ii}\phi_{Ii} + \sum_{i} C^{IJ\ddagger}_{Jj}\phi_{Jj}.$$

The companion bonding orbital will have an eigenvalue near 2, but, if one of the atoms has a nonbonding orbital, a second eigenvalue of 2 will occur, which has a tendency to bring about mixing with the bonding orbital. This problem may be cured by projecting out the nonbonding orbital found in the previous monatomic diagonalization process.

Alternatively, it happens that even in the case of a triple bond with three ~ 0 eigenvalues for $\rho^{(IJ)}$, the different symmetry of the π and σ systems suppresses any mixing of the two; hence, one may select the antibonding orbitals,

$$\psi^{\ddagger}_{IJ1}, \qquad \psi^{\ddagger}_{IJ2}, \qquad \psi^{\ddagger}_{IJ3},$$

and convert them into bonding orbitals according to the prescription

$$\psi_{IJ} = \cos\gamma\tau_I + \sin\gamma\tau_J \tag{16a}$$

$$\psi_{IJ}^{\ddagger} = -\sin\gamma\tau_I + \cos\gamma\tau_J, \tag{16b}$$

where τ_I, τ_J are the appropriate hybrids.

The resulting orbitals are neither mutually orthogonal nor orthogonal to the virtual space. This is remedied by projecting them first into the occupied space with $\mathsf{P}_{\text{occ}} = \sum_{i=1}^{N} |\chi_i\rangle\langle\chi_i|$, followed by the symmetric orthonormalization:

$$\psi'_{IJ} = \mathsf{P}_{\text{occ}}\psi_{IJ}, \qquad \psi''_{IJ} = \mathsf{S}'^{-1/2}\psi'_{IJ}.$$

For the small nonconjugated molecules tested (Caldwell, 1978), eigenvalues of 1.9–2.0 are found for nonbonding orbitals, and ca. 0.1 or less for antibonding. The extension to conjugated systems appears to pose no conceptual problems.

It is more convenient to use the symmetrical density matrix of the orthonormal atomic orbitals, $\mathsf{S}^{1/2}\mathsf{P}^{(0)}\mathsf{S}^{1/2}$, where $P_{pq}^{(0)} = \sum_i C_{pi}C_{qi}$ and the C_{pi} are the coefficients in the original atomic basis; however, the localization is less complete than when matrices $\rho^{(0)}\mathsf{S}$ or $\mathsf{S}\rho^{(0)}$ are used. One must then deal with the problem of diagonalizing subunits of non-Hermitian matrices, which may not have real eigenvalues and eigenvectors.

The density matrix method lends itself to multiconfiguration SCF–CI procedures, since there is no need to make a one-to-one correspondence with HF orbitals nor to maintain separation between occupied and virtual space. In a semiempirical formulation based on localized orbitals the following steps are involved:

1. Construct singly and doubly excited configurations from an initially chosen set of localized orbitals

$$\Psi_G = |\chi_1 \cdots \bar{\chi}_N|,$$

$$\Psi_{i\to j} = |\cdots \chi_i(n-1)\bar{\chi}_j^{\ddagger}(n)\cdots|,$$

$$\Psi_{i\to j,\,k\to l} = |\cdots \chi_i(m-1)\bar{\chi}_j^{\ddagger}(m)\cdots \chi_k(n-1)\bar{\chi}_l^{\ddagger}(n)\cdots|.$$

2. Form the CI matrix from the rules

$$\langle\Psi_{i\to j}|H|\Psi_{i\to k}\rangle = \langle\chi_j|h^F|\chi_K\rangle - (\langle ii|jk\rangle - 2\langle ij|ik\rangle), \text{ etc.}$$

where

$$\langle\chi_j|h^F|\chi_k\rangle = \sum_p\sum_q C_{pj}C_{qk}h_{pq}^F.$$

3. Let

$$h_{pp}^F = h_{pp}^{(0)} + Q_p h'_{pp} \tag{17a}$$

$$h_{pq}^F = G(S_{pq})[h_{pp}^F + h_{pq}^F] \tag{17b}$$

in the usual manner, where Q_p is the net charge on the atom containing orbital p.

4. Compute the density matrix ρ_{ij} after each iteration, and diagonalize the appropriate subunits, taking the N natural localized orbitals according to the procedure described in the foregoing.
5. Repeat the process until self-consistency is attained.

III. General Applications

Irrespective of the advances in computational efficiency that may be forthcoming, localized orbitals are an extremely important conceptual tool in molecular physics. Virtually all zeroth-order theories in spectroscopy and chemical bonding are based on this viewpoint. The following basic considerations are applicable:

1. At the Hartree–Fock level of approximation, a direct comparison can be made between localized orbitals in similar chemical environments. For example, a high degree of transferability has been observed in the alkane series.
2. By localizing SCF orbitals as an intermediate procedure, the efficiency of a CI calculation may be increased through the rejection of configurations with small off-diagonal matrix elements.
3. A direct comparison can be made between contributions that are purely local and largely insensitive to conformation and those which depend on resonance effects extending to nonnearest neighbors.

The categories of properties given in Section I may be illustrated with the examples of (1) bond energies and rotational barriers, (2) NMR coupling constants, (3) absorption and circular dichroism. A suitable starting point for the discussion will be a set of localized occupied and virtual orbitals $\{\chi_1 \cdots \chi_N\}$ $\{\chi_1^{\ddagger} \cdots \chi_M^{\ddagger}\}$ that have either been obtained from a ground-state SCF calculation or from localizing the natural orbitals in a CI calculation. In order to deal conveniently with the CI matrix, it will be necessary to use the partially localized orthogonal orbitals obtained by subjecting the maximum localization set to the $S^{-1/2}$ process. This invariably introduces small contributions into formally localized matrix elements from nonnearest neighbors, which may be explicitly retained throughout the calculations or neglected according to the model and the level of approximation.

One advantage of localized orbitals is that often certain spectroscopic phenomena are insensitive to the presence of remote chemical groups. This allows the use of a model in which charge-transfer transitions are included only for nearest and next nearest neighbors with respect to the region of interest. The validity of the assumption may be tested by increasing the size of the CI region and comparing results. Under favorable circumstances, it is possible to include the neglected terms as a perturbation (Millié and Berthier, 1968; Millié *et al.*, 1972). There is of course no guarantee that even with localized orbitals a truncated CI is stable to the dimension of the system, particularly if conjugation is involved. For the case of metals any such scheme invariably breaks down. On the other hand, when the SCF orbitals for the system can be localized to small regions with little overlap, this procedure can significantly simplify the analysis.

Let the sets $\{\chi_i\}$, $\{\chi_i^\ddagger\}$ be localized bonding and antibonding orbitals with $\{\psi_\alpha\}$ nonbonding. Then the zeroth-order description of the ground state is given by

$$\Psi_G = |\chi_1 \cdots \bar{\chi}_N \psi_1 \cdots \bar{\psi}_m|. \tag{18}$$

Following the example of elementary diatomic molecular theory, one will also require the excited configurations,

$$\Psi_{i\to i\ddagger} = |\cdots \chi_i \bar{\chi}_i^\ddagger \cdots| \tag{19a}$$

$$\Psi_{i\to i\ddagger,\, i\to i\ddagger} = |\cdots \chi_i^\ddagger \bar{\chi}_i^\ddagger \cdots|, \tag{19b}$$

in order to describe bond rupture into the proper fragments in conjunction with the correlation energy determinations.

It has been shown (Politzer, 1976; Ruedenberg, 1977) that the total SCF energy of a molecule is given by

$$\gamma \sum_k n_k \varepsilon_k,$$

where ε_k are the orbital energies, n_k the occupation numbers, and $\gamma \sim 1.5$. In similar chemical environments these local orbital energies tend to be relatively invariant, which in turn leads to the additivity of the total SCF energy as a sum of quantities proportional to the orbital energies. To a first approximation the perturbative terms

$$\Delta E = -\sum_i \frac{\langle i \to i^\ddagger i \to i^\ddagger | H | 0 \rangle^2}{E_{i\to i,\, i\to i\ddagger} - E_o}, \text{etc.} \tag{20}$$

will make the same contributions to a given localized bond in any molecule, and one may accordingly write

$$\varepsilon_{\text{bond}}^{(i)} = \lambda \varepsilon_i. \tag{21}$$

The analysis of NMR coupling constants illustrates a number of points related to localization. The interaction between a nucleus with spin I_N and electrons in contact with it is given by

$$H_C = \frac{8\pi}{3} g\beta g_N \beta_N \sum_k \delta(\mathbf{r}_{KN}) \mathbf{I}_N \cdot \mathbf{S}_k, \tag{22}$$

(Pople *et al.*, 1959) where β, β_N are the Bohr magneton values for electron and nucleus, and g, g_N are the gyromagnetic ratios; $\mathbf{S}_k$ is the vector electron-spin operator, and $\delta(\mathbf{r}_{kN})$ is the charge-density operator at the nucleus N.

The first-order correction to the energy vanishes, whereas after rotational averaging the second order becomes

$$J_{NN'} = \frac{E_c}{h} = \frac{2}{3h}\left(\frac{8\pi g\beta\hbar}{3}\right)^2 \gamma_N\gamma_{N'} \frac{\sum_n \langle 0|\sum_k \delta(\mathbf{r}_{kN})\mathbf{S}_k|n\rangle\langle n|\sum_k \delta(\mathbf{r}_{kN'})\mathbf{S}_k|0\rangle}{E_o - E_n}, \tag{23}$$

where $\gamma_N = g_N\beta_N/\hbar$. If the basis set Ψ_n consists of all triplet single excitations from a closed-shell ground state Ψ_G, the following options are available:

1. A zeroth-order contribution may be found from the canonical (delocalized) occupied and virtual orbitals for which

$$\langle\chi_i|h^F|\chi_j\rangle = 0, \qquad \langle\psi_i^\ddagger|h^F|\psi_j^\ddagger\rangle = 0.$$

If an independent electron, Hückel-type model is assumed, the CI matrix is already diagonal, and the sum in Eq. (23) becomes

$$L_{NN'} = -\frac{3}{2}S_N^2(0)S_{N'}^2(0)\sum_p^{\text{occ}}\sum_q^{\text{virt}}\frac{C_{Np}C_{N'p}C_{Nq}C_{N'q}}{\varepsilon_q - \varepsilon_p}, \tag{24}$$

where $S_N^2(0)$ is the s-orbital density on nucleus N, and C_{NP} is the coefficient of the s orbital on nucleus N in the pth molecular orbital χ_p.

This formula has been used extensively for semiempirical calculations of proton coupling constants. Although the results of the so-called vicinal values, where the two nuclei are separated by three bonds (e.g., H—C—C—H), are reasonably satisfactory, those for the aliphatic geminal (H—C—H) are very poor, being of the wrong sign.

The tendency for Eq. (24) to give positive coupling constants can be seen by summing the numerators, which gives

$$\sum_p^{\text{occ}} C_{NP}C_{N'P} = \rho_{NN'}, \qquad \sum_q^{\text{virt}} C_{Nq}C_{N'q} = -\rho_{NN'},$$

the last following from the fact that

$$\sum_i^{\substack{\text{occ}\\\text{virt}}} C_{Ni}C_{N'i} = \delta_{NN'};$$

hence,

$$L_{NN'} \simeq \tfrac{3}{2}S_N^2(0)S_{N'}(0)\rho_{NN'}^2/\overline{\Delta\varepsilon}. \tag{25}$$

2. The single excitation configurations may be subjected to a CI calculation with the matrix elements determined by the conventional SCF methods, which explicitly take electron interaction into account. If a complete treatment is undertaken, it will be immaterial whether or not the orbitals are localized; however, an illuminating analysis of this point has been made by Ellinger *et al.* (1971a, b, 1973) using perturbation theory on localized orbital configurations.

The lowest-order term is essentially Eq. (24) with the denominator replaced by $\varepsilon_q - \varepsilon_p - \langle qq|pp\rangle$, and the analysis leading to Eq. (25) is appropriate. The second-order term is

$$L^{(1)}_{NN'} = \frac{\begin{aligned}\sum\sum [H_{om}\mathbf{G}_{N,mn}\cdot\mathbf{G}_{N',no} \\ + \mathbf{G}_{N,om}\cdot(H_{mn}\mathbf{G}_{N',no}) + \mathbf{G}_{N,om}\cdot\mathbf{G}_{N',mn}H_{no}]\end{aligned}}{(E_o - E_m)(E_o - E_n)}, \tag{26}$$

where

$$\mathbf{G}_N = \sum_k \delta(\mathbf{r}_{kN})\mathbf{S}_k .$$

An estimation of the terms in Eq. (26) may be obtained from the conventional differential overlap approximations, which give

$$\langle\chi_i(1)|\delta(r_{1N})|\chi_i^{\ddagger}(1)\rangle = C_{Ni}C_{Ni^{\ddagger}}S_N^2(0) \tag{27a}$$

$$\begin{aligned}\langle {}^3\Psi_{ii^{\ddagger}}|H|{}^3\Psi_{jj^{\ddagger}}\rangle &= -\langle ij|i^{\ddagger}j^{\ddagger}\rangle \\ &= -\sum_p\sum_q\sum_r\sum_s C_{pi}C_{qi}C_{ri^{\ddagger}}C_{sj^{\ddagger}}\gamma_{pq,rs},\end{aligned} \tag{27b}$$

where

$$\gamma_{pq,rs} = \int\int \phi_p(1)\phi_q(1)\phi_r(2)\phi_s(2)/r_{12}\, d\tau_1\, d\tau_2 .$$

For geminal C—H bonds, the only term that survives is the middle, giving

$$L^{(1)}_{NN'} = \frac{1}{(E^{\ddagger}_{\text{CH}} - E_o)^2}\langle 0|\mathbf{G}_N|\Psi_{11^{\ddagger}}\rangle\cdot\langle\Psi_{11^{\ddagger}}|H|\Psi_{22^{\ddagger}}\rangle\,\langle\Psi_{22^{\ddagger}}|\mathbf{G}_{N'}|0\rangle, \tag{28}$$

where the two bonds are labeled 1 and 2.

Let ψ_{c_1} and ψ_{c_2} denote the σ-hybrids on the carbon atom; then the molecular orbitals may be written

$$\chi_1 = \cos\alpha_1\psi_{c_1} + \sin\alpha_1\phi_{\text{H}} \tag{29a}$$

$$\chi_1^{\ddagger} = -\sin\alpha_1\psi_{c_1} + \cos\alpha_1\phi_{\text{H}}, \tag{29b}$$

with similar expressions for χ_2, $\chi_2^{\ddagger}$. From the properties of the spin operator it follows that

$$L^{(1)}_{NN'} = -\frac{3}{32}\frac{\sin 2\alpha_1 \sin 2\alpha_2}{(E^{\ddagger}_{\text{CH}} - E_o)^2}\gamma_{c_1c_2}S_N^2(0)S_{N'}^2(0), \tag{30}$$

where

$$\gamma_{c_1c_2} = \int\int \psi_{c_1}(1)\psi_{c_2}(1)\psi_{c_1}(2)\psi_{c_2}(2)/r_{12}\, d\tau_1\, d\tau_2 .$$

This quantity is seen to be positive, and when reasonable estimates are given for γ_{cc} and $E_{\mathrm{CH}}^{\ddagger} - E_o$, it is found to be some 5–10 times larger than the values in Eq. (24) or Eq. (25) and of the opposite sign.

For vicinal hydrogens such as the H—C—C—H linkage in ethane or ethylene, $\langle ij|i^{\ddagger}j^{\ddagger}\rangle$ takes a dramatic downward turn as compared with the geminal value, whereas the bond order contribution of Eq. (24) varies much more slowly and turns out to be the dominant term. This provides a simple model for explaining the success of Eq. (24) with many vicinal systems and its failure for geminal protons. The improvement brought about by using the unrestricted Hartree–Fock (UHF) model can be explained along similar lines, since this method is a form of configuration interaction.

It happens that the exact solution to the 4 × 4 secular determinant for the CH σ–σ^* transitions of methane gives essentially the same result as Eq. (30):

$$\begin{aligned} L_{NN'}^{(1)} &= -\frac{3}{4} S_N^2(0) S_{N'}^2(0) \sin\alpha_1 \cos\alpha_1 \sin\alpha_2 \cos\alpha_2 \\ &\quad \times \left[\frac{1}{E_{\mathrm{CH}}^{\ddagger} + \frac{3}{2}H_{11^{\ddagger},22^{\ddagger}} - E_o} - \frac{1}{E_{\mathrm{CH}}^{\ddagger} - \frac{1}{2}H_{11^{\ddagger},22^{\ddagger}} - E_o}\right] \\ &\cong -\frac{3}{32} \frac{\sin 2\alpha_1 \sin 2\alpha_2 S_N^2(0) S_{N'}^2(0)}{(E_{\mathrm{CH}}^{\ddagger} - E_o)^2} \gamma_{c_1c_2} . \end{aligned} \tag{31}$$

It is interesting to note that the geminal coupling constant for ethylene is opposite to that of methane. In this case the positive bond order term is somewhat larger than for methane and mixing with the triplet π–π^* transition tends to enhance this value, leading to a net positive result. In the CNDO approximation $\gamma_{c_1c_2} = 0$ and σ–π mixing also vanishes, which tends to give too high a positive value. When atomic two-electron integrals such as $\langle sx|sx\rangle$ $\langle xy|xy\rangle$ are considered, a nonzero value of $\gamma_{c_1c_2}$ results. In view of the intricate relations among such integrals it is not surprising that both *ab initio* and semiempirical theories vary widely in their quantitative aspects; however, valuable insights may be obtained by calculating coupling constants with the perturbation method on localized orbitals along with a more rigorous model based on diagonalizing the secular determinant.

3. Further refinements can be made by including higher-order excitations; however, certain concepts of coupling constants appear to be covered by a single excitation theory.

Within the framework of molecular orbital theory, three distinct mechanisms are in evidence:

1. An indirect interaction between nuclei that is propagated through the bonds and is to a first approximation proportional to the square of the bond order.

2. A direct coupling that depends on orbital overlap and is largest when there is an atom in common for the occupied orbitals. For geminal coupling this term predominates over the first, whereas for more distant interactions the through bond mechanism leads to a larger effect than the $1/R^3$ dependence associated with $\langle ij|i^{\ddagger}j^{\ddagger}\rangle$ when there is no common atom.

3. An indirect CI coupling of the σ–π–σ variety, which tends to reduce the cancellations involved in the bond order term.

The dichotomy between localized and nonlocalized orbitals is displayed in an even more intricate manner when optical activity is considered. If orbitals were to be regarded as being completely localized on atoms and atomic pairs, then since four interaction centers are required, only a CI mixing of $\Psi_{ii^{\ddagger}}$ and $\Psi_{jj^{\ddagger}}$ terms will give a nonvanishing result.

Consider four consecutively bonded atoms A, B, C, D with localized bonding and antibonding orbitals given by χ_1, $\chi_1^{\ddagger}$, χ_2, $\chi_2^{\ddagger}$, χ_3, $\chi_3^{\ddagger}$, there being no bond between A and D. The lowest-order term is provided by the direct mixing of the $\Psi_{11^{\ddagger}}$ and $\Psi_{33^{\ddagger}}$ configurations. The required expression is $\boldsymbol{\mu}_{on} \cdot \mathbf{m}_{no}$ (Caldwell and Eyring, 1971); if the transition energies of the bonds are assumed to be quite different this becomes

$$R_{11^{\ddagger}}^{(1)} = \boldsymbol{\mu}_{11^{\ddagger}} \cdot \left(\frac{e}{2mc}\right) \mathbf{R}_{13} \times \mathbf{P}_{33^{\ddagger}} \left[\frac{\langle \Psi_{11^{\ddagger}} | H | \Psi_{33^{\ddagger}} \rangle}{E_{11^{\ddagger}} - E_{33^{\ddagger}}}\right], \tag{32}$$

where $\mathbf{R}_{13}$ is the vector distance between the midpoints of the two bonds and

$$\langle \Psi_{11^{\ddagger}} | H | \Psi_{33^{\ddagger}} \rangle = 2\langle 11^{\ddagger} | 33^{\ddagger} \rangle - \langle 13 | 1^{\ddagger}3^{\ddagger} \rangle,$$

which is to be contrasted with Eq. (27b) for triplet excitations.

Due to the small overlap between nonnearest neighbors, $\langle 13|1^{\ddagger}3^{\ddagger}\rangle$ may be neglected, whereas $\langle 11^{\ddagger}|33^{\ddagger}\rangle$ is approximately given by

$$\langle 11^{\ddagger} | 33^{\ddagger} \rangle = \frac{\mu_{11^{\ddagger}}\mu_{33^{\ddagger}}}{\mathbf{R}_{13}^3} \frac{[\mathbf{b}_1 \cdot \mathbf{b}_2 - 3(\mathbf{b}_1 \cdot \mathbf{R}_{13})(\mathbf{b}_3 \cdot \mathbf{R}_{13})]}{R_{13}^2},$$

where $\mathbf{b}_1$ and $\mathbf{b}_3$ are unit vectors along the bond axes. Unlike the case of vicinal NMR coupling constants, this direct interaction term is larger and compares favorably in magnitude with the data on a large number of nonconjugated aliphatic and olefinic compounds.

There are also second-order terms to be considered such as

$$R^{(2)}_{11\ddagger} = \boldsymbol{\mu}_{11\ddagger} \cdot \langle \chi_2^{\ddagger} | \mathbf{m} | \chi_3 \rangle \left[\frac{\langle \Psi_{11\ddagger} | H | \Psi_{21\ddagger} \rangle \langle \Psi_{21\ddagger} | H | \Psi_{32\ddagger} \rangle}{(E_{11\ddagger} - E_{21\ddagger})(E_{11\ddagger} - E_{32\ddagger})} \right]. \tag{33}$$

The foregoing matrix elements are given for nonpolar bonds by

$$\langle \Psi_{21\ddagger} | H | \Psi_{32\ddagger} \rangle = \tfrac{3}{4}\gamma_{\mathrm{BC}} \tag{34a}$$

$$\begin{aligned} \langle \Psi_{11\ddagger} | H | \Psi_{21\ddagger} \rangle &= -h_{12} - [\langle 1^{\ddagger}1^{\ddagger} | 12 \rangle - 2\langle 1^{\ddagger}1 | 1^{\ddagger}2 \rangle] \\ &= -\tfrac{1}{4}(h_{ss}^{(\mathrm{B})} - h_{pp}^{(\mathrm{B})}) - [\tfrac{3}{4}\gamma_{\mathrm{AB}} - \tfrac{1}{4}\gamma_{\mathrm{BB}}]. \end{aligned} \tag{34b}$$

This term may also make a significant contribution to the CI calculation on localized orbitals; however, if the trend observed in NMR coupling constants is followed, such indirect interactions will be of lesser importance.

If four localized σ-bonds joined to an asymmetric center are considered, a typical term is given by

$$R_{11\ddagger} = \mathbf{r}_{11\ddagger} \cdot \frac{[\Psi_{11\ddagger} | H | \Psi_{12\ddagger} \rangle \langle \Psi_{12\ddagger} | H | \Psi_{32\ddagger} \rangle \langle \Psi_{32\ddagger} | \mathbf{m} | \Psi_o \rangle]}{(E_{11\ddagger} - E_{12\ddagger})(E_{11\ddagger} - E_{32\ddagger})}, \tag{35}$$

where

$$\langle \Psi_{11\ddagger} | H | \Psi_{12\ddagger} \rangle = h_{1\ddagger 2\ddagger} - [\langle 11 || 1^{\ddagger}2^{\ddagger} \rangle - 2\langle 11^{\ddagger} | 12^{\ddagger} \rangle].$$

The first-order direct interaction term vanishes, since any pair of bonds joined to a central atom has a plane of symmetry.

These terms may then be summed over all the possible combinations of orbitals 2, 3, 4 to give the localized CI contribution to the optical activity for this configuration. Considerable cancellations may be expected, and as a result the CD of compounds such as CHFCl CH_3 is small. On the other hand, the analogous case of a central metal atom surrounded by three bridged ligands in a dissymmetric array such as the D_3 symmetry

$$\mathrm{Ni(NH_2{-}CH_2{-}CH_2{-}NH_2)_3^{+3}}$$

leads to a very large rotational strength. Here the prospect of electron delocalization must undoubtedly be investigated.

It happens that for a locally complete set of excitations $\Psi_{i\to j}$ the sum rule,

$$\sum_{i}^{\mathrm{occ}} \sum_{j}^{\mathrm{virt}} R_{i\to j} = 0,$$

is satisfied. This means that, although it may be possible to transform occupied and virtual orbitals so that particular $R_{i\to j}$ values are large, the CI will still be able to produce small values by the appropriate linear combinations of the $\Psi_{i\to j}$ functions.

Consider four hydrogen-like atoms in a dissymmetric configuration with equal bond lengths. A zeroth-order set of orbitals may be written in order of increasing energy as

$$\chi_1 = \tfrac{1}{2}(\phi_1 + \phi_2 + \phi_3 + \phi_4), \tag{36a}$$

$$\chi_2 = \tfrac{1}{2}(\phi_1 + \phi_2 - \phi_3 - \phi_4), \tag{36b}$$

$$\chi_3 = \tfrac{1}{2}(\phi_1 - \phi_2 - \phi_3 + \phi_4), \tag{36c}$$

$$\chi_4 = \tfrac{1}{2}(\phi_1 - \phi_2 + \phi_3 - \phi_4). \tag{36d}$$

If the unit vectors along the three bond axes are designated $\mathbf{b}_{12}$, $\mathbf{b}_{23}$, $\mathbf{b}_{34}$, and the distance given by R with the absolute value of the momentum $|\langle\phi_1|\mathbf{p}|\phi_2\rangle| = |\langle\phi_2|\mathbf{p}|\phi_3\rangle| = |\langle\phi_3|\mathbf{p}|\phi_4\rangle| = p$, then typical terms are

$$\langle\chi_1|\mathbf{p}|\psi_3\rangle = \tfrac{1}{2}(-\mathbf{b}_{12} + \mathbf{b}_{34})p \tag{37a}$$

$$\langle\psi_3|\mathbf{m}|\psi_1\rangle = -\tfrac{1}{2}(\mathbf{b}_{12} + \mathbf{b}_{23}) \times \mathbf{b}_{34} Rp. \tag{37b}$$

This gives for the four configurational rotational strengths,

$$R_{1\to 3} = R^{(0)} \tag{38a}$$

$$R_{1\to 4} = -R^{(0)} \tag{38b}$$

$$R_{2\to 3} = -R^{(0)} \tag{38c}$$

$$R_{2\to 4} = R^{(0)} \tag{38d}$$

where

$$R^{(0)} = \frac{1}{4}\frac{e}{2mc} Rp^2 \mathbf{b}_{12} \cdot \mathbf{b}_{23} \times \mathbf{b}_{34}$$

and the dipole velocity matrix elements have been used instead of the dipole.

Now $R^{(0)}$ proves to be a rather large quantity by optical rotation standards; however, if the Hartree–Fock matrix elements between nearest neighbors are small, then the four bands coalesce into a single one with considerable cancellation resulting. Further light may be thrown on the matter by considering the sum rules for optical activity (Caldwell, 1977), which require that

$$\sum_n R_{on}^{(0)} = 0 \tag{39a}$$

$$\sum_n (E_n - E_o)^2 R_{on} = 0 \tag{39b}$$

$$\tau_n (E_n - E_o)^4 R_{on} = 0 \tag{39c}$$

$$\tau_n (E_n - E_o)^6 R_{on} = R^{(6)} \neq 0 \tag{39d}$$

where $R^{(6)}$ is a quantity that depends on geometry and certain atomic parameters.

This puts a constraint on the particular energies $E_{1\to 3}$, $E_{1\to 4}$, $E_{2\to 3}$, $E_{2\to 4}$, or more properly the final energies of the CI treatment. From the properties of $R^{(6)}$ it can be shown that if the occupied orbitals can be completely localized, then the optical activity results solely from the CI mixing of localized excitations in accord with the previous example. If there is a nonvanishing bond order between the middle atoms or between the first and last, an "inherent" through bond contribution occurs with a particularly large value when ρ_{14} is comparable to unity. From Eq. (36) it is seen that the matrix elements,

$$\langle\chi_1|h^F|\chi_3\rangle \quad \text{and} \quad \langle\chi_2|h^F|\chi_4\rangle,$$

do not vanish, which leads to nonvanishing values of ρ_{23} and ρ_{14}.

As the two diatomic pairs A—B, C—D are brought into closer proximity, the predominant CI or localized coupling term becomes lower in relation to the bond order term. In many cases the two contributions may be comparable, and no model that relies solely on the one or the other is completely reliable. The sixth moment $R^{(6)}$ has both a one- and a two-electron contribution; the former depends on the bond order between the first and last atoms in a chain or on intermediate bond orders connecting the two, whereas the latter depends on the direct–dipole coupling between bonds and is properly considered to be a correlation term.

When a partially localized transition occurs on a particular chromophore such as the carbonyl group, transitions on other groups are partially activated to a degree depending on the transition density matrix. This will occur for both the electric and magnetic dipole variety. In the case of the magnetic transition the CI dipole–dipole coupling term is rather small, but for the electric dipole case the two are comparable. When a high degree of conjugation with an adjacent group occurs, the bond order terms predominate.

We have thus seen how both NMR coupling constants and circular dichroism are sensitive to electron delocalization, which in many instances can be understood by a perturbation theory. Both phenomena seem to be equally sensitive to bond orders between nonnearest neighbors, but optical activity displays a particularly critical dependence on geometry as well.

IV. Conclusions

The concept of localized orbitals is one of the most important links between quantum molecular physics and interpretive physical chemistry. The similarity between orbitals associated with particular bonds in different molecules has been observed on numerous occasions. Most spectroscopic data can be explained by models that resort wholly or in part to localization. A distinction should be made, however, between the transferability of localized orbitals and Hartree–Fock matrix elements. The first case is far more restrictive and implies zero bond order between nonnearest neighbors or atoms that are not in a simple conjugated or aromatic system. Since many spectroscopic and thermodynamic properties have a close dependence on such bond order parameters, it is certain that the complex connectivity of a molecule is also reflected in this manner; hence, the most flexible interpretive methods will require a consideration of more general interatomic parameters. The HF matrix elements have the feature of providing a quantitative transferability scheme for zeroth-order localized orbitals as well as the tails that are responsible for the more subtle observations, discussed above. Much chemistry finds an intelligible explanation through the route of localized orbitals and perturbation theory.

For simple ground-state properties, such as the dipole moment, the one-electron density matrix offers a viable alternative to localized SCF orbitals in situations where a more exact treatment than the Hartree–Fock calculation is required. As discussed in Section II, subunits of the density matrix may be diagonalized to determine localized natural orbitals, and the corresponding Hartree–Fock matrix analogs may be invoked to simplify the analysis of SCF–CI calculations. For complex ground and transition properties, a localization model allows one to correlate a great many phenomena that would be largely unintelligible when analyzed with canonical orbitals (cf. NMR geminal coupling constants). Although it is not certain that localization can significantly simplify the most thorough *ab initio* molecular calculations, it has been rather well demonstrated that the essential features of such treatments are far more readily understood via this approach.

ACKNOWLEDGMENT

The authors wish to thank the National Science Foundation (Grant CHE 76 17836) for their financial support.

REFERENCES

Amos, A., and Hall, G. (1961). *Proc. R. Soc. London, Ser. A* **263**, 483.
Barr, R., and Basch, H. (1975). *Chem. Phys. Lett.* **32**, 537.
Caldwell, D. (1977). *Mol. Phys.* **33**, 495.

Caldwell, D., and Eyring, H. (1971). "The Theory of Optical Activity." Wiley (Interscience), New York.

Caldwell, D., Redington, P., and Eyring, H. (1978). In preparation.

Edmiston, C., and Ruedenberg, K. (1963). *Rev. Mod. Phys.* **35**, 457.

Ellinger, Y., Rassat, A., and Subra, R. (1971a). *J. Chem. Phys.* **68**, 730.

Ellinger, Y., Rassat, A., Subra, R., Berthier, G., and Millié, P. (1971b). *Chem. Phys. Lett.* **11**, 362.

Ellinger, Y., Rassat, A., Subra, R., and Berthier, G. (1973). *J. Am. Chem. Soc.* **95**, 2372.

Löwdin, P.-O. (1950). *J. Chem. Phys.* **18**, 365.

Löwdin, P.-O. (1965). *Phys. Rev. A* **139**, 357.

McWeeny, R. (1960). *Rev. Mod. Phys.* **32**, 335.

Magnasco, V., and Perico, A. (1967). *J. Chem. Phys.* **47**, 971.

Millié, P., and Berthier, G. (1968). *Int. J. Quantum Chem.* **2**, 67.

Millié, P., Lévy, B., and Berthier, G. (1972). *Int. J. Quantum Chem.* **6**, 155.

Peters, D. (1969). *J. Chem. Phys.* **51**, 1559 and 1566.

Politzer, P. (1976). *J. Chem. Phys.* **64**, 4239.

Pople, J., Schneider, W., and Bernstein, H. (1959). "High Resolution Nuclear Magnetic Resonance." McGraw-Hill, New York.

Roby, K. (1974a). *Mol. Phys.* **27**, 81.

Roby, K. (1974b). *Mol. Phys.* **28**, 1441.

Ruedenberg, K. (1977). *Chem. Phys. Lett.* **66**, 375.

von Niessen, W. (1972a). *J. Chem. Phys.* **56**, 4290.

von Niessen, W. (1972b). *Theor. Chim. Acta* **27**, 9.

Wannier, G. (1937). *Phys. Rev.* **52**, 191.

ADVANCES IN QUANTUM CHEMISTRY, VOLUME 11

Electronic Molecular Structure, Reactivity and Intermolecular Forces: An Euristic Interpretation by Means of Electrostatic Molecular Potentials

EOLO SCROCCO and JACOPO TOMASI

Laboratorio di Chimica Quantistica ed Energetica Molecolare
del Consilio Nazionale delle Ricerche,
Pisa, Italia

ISBN 0-12-034811-X

I. Electrostatics and Molecular Interactions

A. Introduction

The chemical bond and the chemical reactivity theories strictly depend on the quantum mechanical theory. Why then insist on an electrostatic picture where some essential aspects of the quantum theory are neglected?

This is a question that can be put not only to the authors of the present paper but also to the numerous researchers who continue to propose and to elaborate electrostatic models. The answers would be different because the terms of the problem change according to the case one is considering. There is, anyway, a common background to the motivations of all such attempts, which deserves a few words of discussion to make clearer the aims (and the limitations) of the specific electrostatic model described here.

A direct and rigorous application of the principles of quantum mechanics to problems of molecular structure and reactivity for large molecules meets with enormous difficulties and with much involved elaboration of the basic principles. In general, the theoretician desires to parallel rigorous derivations aiming at providing reliable predictions of some physicochemical properties, with a search of simple interpretations and simple models of the essential characteristics of the chemical phenomenology. The final justification of resorting to classical electrostatic models lies just in this effort of simplification. A characteristic of electrostatic models is the emphasis given to the charge distribution with respect to the wavefunction. The ready physical interpretability of the one-electron density function suggests that it should be easier to build models in terms of approximate density functions than in terms of approximate wavefunctions.

Such models do not present, in general, any pretension of generality and their field of application is limited to a specific aspect of the chemical phenomenology. The model considered in this paper considers only the interactions between two partners (at least one of which is polar or charged) at given fixed internal geometries, without any attempts to describe deformations of the internal nuclear geometries. Such an approach can be thus considered parallel to, but not overlapping with, the electrostatic models that concern more directly the forces acting on the atoms of a given molecule (molecular vibrations, prevision of the geometrical shape assumed by the molecule, deformations under the action of external agents) and which are the object of active research, full of interesting results.

The present model relies on the knowledge of the molecular electrostatic potential, which generally is derived from a molecular wavefunction by using the usual methods for calculating the mean expectation value of an operator. In its basic premises the model employs quantum mechanics, with only the approximations necessary in molecular quantal calculations. The electrostatic approximation is introduced at a later stage and concerns the representation of the interaction energy between the two partners. Its eventual justification and its limits can be inferred from *post hoc* arguments relying on the examination of the results of the partition of such interaction energy into terms of various origin. We shall pass now to define such partitions operationally in the self-consistent field–molecular orbital method and in the perturbative schemes of representing the interaction energy. Later, we shall define more precisely our model, and we shall discuss its relationships with the Hellmann–Feynman theorem.

B. Molecular Orbital Partition of the Interaction Energy

In the variational MO methods, the interaction energy is obtained as the difference between the energy of the supermolecule AB and that of the two isolate partners: $\Delta E = E_{AB} - (E_A^0 + E_B^0)$. Energies E_{AB} and ΔE depends on the particular conformation assumed by AB (distance between the partners and their mutual orientation). The three energies, E_{AB}, E_A^0, E_B^0 are supposed to be calculated to the same level of approximation, for example, at the SCF one-determinant level. Partitions of ΔE have in any case a certain degree of arbitrariness, but they can be accepted, for euristic purposes, if they couple to a precise operative definition an intuitively acceptable definition of the physical effects accounted for by each term of the partitioned energy.

A partition of ΔE into electrostatic, polarization, exchange, and charge transfer terms, which was proposed by Coulson (1957), is intuitively simple and accepted by many researchers. We report here the formulation given by Morokuma (1971). The partition starts from the definition of a set of approximate wavefunctions and of the corresponding energies:

1. A simple Hartree product between the two wavefunctions Ψ_A^0 and Ψ_B^0 of the separate partners, both internally antisymmetrized,

$$\Psi_1 = \Psi_A^0 \cdot \Psi_B^0. \tag{1}$$

If E_1 is the energy corresponding to Ψ_1 and E^0 is the summation of the energies of the isolated A and B molecules ($E^0 = E_A^0 + E_B^0$), the difference $E_1 - E^0$ can be considered as the electrostatic interaction energy (E_{es}) between the two charge distributions kept rigid.

2. A simple product between two internally antisymmetrized wavefunctions, each optimized in the field of the other,

$$\Psi_2 = \Psi_A \cdot \Psi_B. \tag{2}$$

The difference $E_2 - E_1$ can be considered as the mutual polarization energy (E_{pol}) of two subsystems that still preserve their identity. In a parallel definition, given in precedence by Dreyfus and Pullman (1970), this portion of ΔE is collected together with the charge transfer term defined at the point 4 in the following.

3. A fully antisymmetrized product of the unperturbed wavefunctions of the separate partners,

$$\Psi_3 = \mathrm{A}[\Psi_{\mathrm{A}}^0 \cdot \Psi_{\mathrm{B}}^0]. \tag{3}$$

The difference $E_3 - E_1$ can be assimilated to the nonclassical effect due to the exchange of electrons between A and B (E_{ex}). To make easier the calculation of E_3, the orbitals of Ψ_3 are subjected to an orthogonalization procedure.

4. The wavefunction of the supermolecule

$$\Psi_4 = \Psi_{\mathrm{AB}}. \tag{4}$$

In the SCF approximation, $E_4 - E_0$ is the total interaction energy ΔE.

This interaction energy is then partitioned into four contributions,

$$\Delta E = E_{\mathrm{es}} + E_{\mathrm{pol}} + E_{\mathrm{ex}} + E_{\mathrm{ct}}, \tag{5}$$

where the first three terms have been already defined and the fourth, which corresponds essentially to the effects of charge transfer between A and B, is evaluated as the difference: $E_{\mathrm{ct}} = \Delta E - (E_{\mathrm{es}} + E_{\mathrm{pol}} + E_{\mathrm{ex}}) = E_4 + E_1 - E_2 - E_3$; it includes also all the coupling terms among the other contributions (Kitaura and Morokuma, 1976).

Such partition, which corresponds to easily performed manipulations, obviously is not unique. A minor modification should consist in replacing step 3 with the following one:

3′. A completely antisymmetrized product of the wavefunctions Ψ_{A} and Ψ_{B} obtained in step 2 (Bonaccorsi *et al.*, 1969b),

$$\Psi_{3'} = \mathrm{A}[\Psi_{\mathrm{A}} \cdot \Psi_{\mathrm{B}}]. \tag{6}$$

The exchange term ($E_{\mathrm{ex}} = E_{3'} - E_2$) is in this case calculated on a wavefunction obtained again on the separate manifolds pertaining to A and B, but mutually polarized. With this definition the global interaction energy is given directly as a summation of separate contributions:

$$\begin{aligned}\Delta E &= E_{\mathrm{es}} + E_{\mathrm{pol}} + E_{\mathrm{ex}} + E_{\mathrm{ct}} \\ &= (E_1 - E^0) + (E_2 - E_1) + (E_{3'} - E_2) + (E_4 - E_{3'}) = E_4 - E^0.\end{aligned} \tag{7}$$

Since it is advisable to evaluate first the most important terms, definition 3′ should be preferred in cases where the polarization effects are larger than those due to the exchange. Anyway, we shall use definition 3 throughout this paper, as it is the most widely employed.

Recently, Kitaura and Morokuma (1976) have proposed a new interesting operative definition of the partition of ΔE that has the advantage of allowing an independent evaluation of E_{ct}, placing it on an equal footing with the other three terms. In the partitions of ΔE made recently by Morokuma's group, there appears as a consequence a new term, E_{mix}, that corresponds to the difference between the value of ΔE obtained as $E_4 - E^0$ and the summation of the four contributions. Term E_{mix} has been interpreted as due to the coupling terms plus the extra exchange contribution due to polarization of the A and B wavefunctions in the simple Hartree product approximation. The numerical values of E_{es}, E_{pol}, E_{ex} do not change with respect to the definition of Eq. (5). A partition into only two terms was proposed some years ago by Kollman and Allen (1970). These authors define $E_{es} + E_{ex}$ as "electrostatic" and $E_{pol} + E_{ct}$ as "delocalization" energy. This partition has been employed by various authors. A quite different philosophy is at the basis of the Bond Energy Analysis proposed by Clementi (1967), which relies on the partition of the total energy into two- and three-body contributions.

C. Perturbative Approach to the Partition of the Interaction Energy

The partition we have outlined for the SCF case, since it is amenable to previous knowledge regarding wavefunctions of the noninteracting partners, can be obtained also with a perturbative approach, where the Hamiltonian of the interacting system, H_{AB}, is considered to be composed of an unperturbed part H^0_{AB}, corresponding to the two separated molecules ($H^0_{AB} = H_A + H_B$), and a perturbation V_{AB} responsible for the interaction energy. The perturbative treatment is straightforward when A and B are very distant, because in such cases the overlap between the terms constituting the zeroth-order solution, $\Psi^0_{AB} = \Psi^0_A \cdot \Psi^0_B$, is negligible, but it becomes more complex at intermediate and short distances owing to the fact that H^0_{AB} does not reflect the full permutational symmetry of H_{AB}.

It is not necessary to give here a detailed analysis of this problem, which has been satisfactorily dealt with by many authors (Murrell and Shaw, 1967; Murrell *et al.*, 1965; Sustman and Binsch, 1971; Chipman *et al.*, 1973; Daudey *et al.*, 1974; Basilevski and Berenfeld, 1974). We shall limit ourselves to recall here the essential points of such treatments, following the formulation given by Daudey *et al.* (1974) who adopt the Epstein–Nesbet (Nesbet, 1955) partition of the Hamiltonian, with the perturbative expansion interrupted at the second order. The interaction energy can be written

$$\Delta E = AE_C + \Delta E^{(0)}_{EX} + \Delta E_{POL} + \Delta E_{CT} + \Delta E_{DISP} + \Delta E^{(2)}_{EX} + \Delta E_{COR}. \quad (8)$$

The first two terms of Eq. (8) represent the zeroth-order contribution to ΔE (also in this treatment ΔE corresponds to the extra amount of energy with respect to the energy of the unperturbed molecules $E^0 = E^0_{\mathrm{A}} + E^0_{\mathrm{B}}$) due to the first term Ψ^0_{AB} of a development of the perturbed wavefunction,

$$\Psi_{\mathrm{AB}} = \Psi^0_{\mathrm{AB}} + \sum_K C_K \Psi^K_{\mathrm{AB}}, \tag{9}$$

into determinants built up with the occupied and virtual MO's of the separated molecules A and B [suitably orthonormalized by the Löwdin procedure (1950)].

By taking for Ψ^0_{AB} the colinear function $\mathrm{A}[\Psi^0_{\mathrm{A}} \cdot \Psi^0_{\mathrm{B}}]$, where the MO's have not been subjected to the Löwdin transformation and the operator A concerns only permutations among electrons of A and B ($\mathrm{A} = 1 + \sum_{ij} P_{ij}$, where P_{ij} is a permutation that exchanges at least two electrons between A and B), one has for the zeroth-order energy:

$$\begin{aligned}
&\langle \Psi^0_{\mathrm{AB}} | H_{\mathrm{AB}} | \Psi^0_{\mathrm{AB}} \rangle \\
&\quad = [E^0_{\mathrm{A}} + E^0_{\mathrm{B}} + \langle \mathrm{A}\Psi^0_{\mathrm{A}}\Psi^0_{\mathrm{B}} | V_{\mathrm{AB}} | \Psi^0_{\mathrm{A}}\Psi^0_{\mathrm{B}} \rangle] / \langle \mathrm{A}\Psi^0_{\mathrm{A}}\Psi^0_{\mathrm{B}} | \Psi^0_{\mathrm{A}}\Psi^0_{\mathrm{B}} \rangle \\
&\quad = \left[E^0_{\mathrm{A}} + E^0_{\mathrm{B}} + \langle \Psi^0_{\mathrm{A}}\Psi^0_{\mathrm{B}} | V_{\mathrm{AB}} | \Psi^0_{\mathrm{A}}\Psi^0_{\mathrm{B}} \rangle + \sum_{ij} \langle P_{ij}\Psi^0_{\mathrm{A}}\Psi^0_{\mathrm{B}} | V_{\mathrm{AB}} | \Psi^0_{\mathrm{A}}\Psi^0_{\mathrm{B}} \rangle \right] \\
&\qquad \times [1 - \zeta + \zeta^2 + \cdots],
\end{aligned} \tag{10}$$

where $\zeta = \sum_{ij} \langle P_{ij}\Psi^0_{\mathrm{A}}\Psi^0_{\mathrm{B}} | \Psi^0_{\mathrm{A}}\Psi^0_{\mathrm{B}} \rangle$.

Only three terms of Eq. (10) do not depend on the exchange: E^0_{A} and E^0_{B}, energies of the isolated atoms, and $\langle \Psi^0_{\mathrm{A}}\Psi^0_{\mathrm{B}} | V_{\mathrm{AB}} | \Psi^0_{\mathrm{A}}\Psi^0_{\mathrm{B}} \rangle = \Delta E_C$, which represents the electrostatic interaction energy, equivalent to E_{es} of Eq. (5). All the other terms of Eq. (10), if collected together, give a contribution to ΔE that can be assimilated to E_{ex} of Eq. (5). Because such terms give the exchange contribution to ΔE derived only from the zeroth-order function, they are denoted in Eq. (8) by $\Delta E^{(0)}_{\mathrm{EX}}$ to distinguish them from other exchange contributions arising from higher-order terms.

The remaining terms of Eq. (8) collect the second-order contributions (in the Epstein–Nesbet partition, the first-order contributions are zero). The ΔE_{POL} derives from terms of the expansion (9) corresponding to single excitations inside A (or B); ΔE_{CT} from terms of Eq. (9) corresponding to single excitations where an electron passes from A to the empty orbitals of B (or vice versa); ΔE_{DISP} is connected to double excitation terms allowing simultaneous excitation of one electron from A and one from B to their empty orbitals. Two types of double excitations, the first corresponding to an internal excitation of an electron of A and to the promotion of one electron from A to an empty orbital of B (or vice versa), the second corresponding to two crossed one-electron excitations (from A to B and from B to A), are collected in the term $\Delta E^{(2)}_{\mathrm{EX}}$. Finally, the term ΔE_{COR} collects the contributions of two types of double excitations: the first corresponds to an internal excitation of two electrons of A (or B); the second, to the excitations of two electrons of A (or B) to an empty orbital of A and to an empty orbital of B.

From this short resumé of a possible partition of the perturbative calculation of ΔE, it can be seen that there is not a complete agreement with the analogous partitions of the corresponding SCF quantity (for a numerical comparison between perturbative and SCF partitions of ΔE in the $H_2O \cdot H_2O$ case, see Daudey, 1974). Some contributions to ΔE, such as the London dispersion term ΔE_{DISP} and the correlation term ΔE_{COR}, do not have a physical counterpart in the SCF calculation of ΔE. Terms such as ΔE_{POL} and ΔE_{CT} do not correspond exactly to E_{pol} and E_{ct} because they collect only the single excitation contributions to the mutual polarization of the two separated molecules and to the transfer of electrons between A and B. A more detailed dissection of the one-electron excitation contributions to the second-order energy (see Daudey *et al.*, 1974) shows that actually they give as main terms the contribution described in the preceding but that there are also terms depending on the exchange that can find their place in $E_{\mathrm{EX}}^{(2)}$ (in analogy with what was done with the zeroth-order terms). A part of the double-excitation contributions collected in ΔE_{COR} and $\Delta E_{\mathrm{EX}}^{(2)}$ may be classified also as polarization or charge-transfer contributions. Should one take into consideration also third- and higher-order contributions, the scheme would be even more involved.

D. Electrostatic Interaction Energy and Electrostatic Molecular Potential

From the discussion in Sections I, B and C, it is evident that the possibility of alternative definitions of the other terms of the partition does not affect the electrostatic term to which we shall now limit our attention.

To obtain compact notation, we introduce a first-order charge-density function which includes also the nuclear charges:

$$\gamma_{\mathrm{A}}(\mathbf{r}_1, \mathbf{R}_\alpha) = -\rho_{\mathrm{A}}(\mathbf{r}_1) + \sum_{\alpha \in \mathrm{A}} Z_\alpha \, \delta(\mathbf{r}_1 - \mathbf{R}_\alpha), \tag{11}$$

where $\rho_{\mathrm{A}}(\mathbf{r}_1)$ represents the diagonal element of the first-order electronic density matrix of the molecule A, and $\mathbf{R}_\alpha$ is the vector defining the position of the nucleus α of A, having a charge Z_α, with respect to an arbitrary coordinate system (the same set of coordinates is employed also for molecule B).

By using such notation, one has

$$E_{\mathrm{es}}(\mathrm{AB}) = \int\int \frac{\gamma_{\mathrm{A}}(\mathbf{r}_1, \mathbf{R}_\alpha)\gamma_{\mathrm{B}}(\mathbf{r}_2, \mathbf{R}_\beta)}{|\mathbf{r}_1 - \mathbf{r}_2|} \, d\mathbf{r}_1 \, d\mathbf{r}_2 \tag{12}$$

whose value depends on the distance and the mutual orientations of the molecules A and B, i.e., on the values assumed by the sets of vectors $\mathbf{R}_\alpha$ and $\mathbf{R}_\beta$.

Equation (12) may be also written in the following form:

$$E_{es}(\mathrm{AB}) = \int V_{\mathrm{A}}(\mathbf{r}_2)\gamma_{\mathrm{B}}(\mathbf{r}_2, \mathbf{R}_\beta)\, d\mathbf{r}_2, \tag{13}$$

where

$$V_{\mathrm{A}}(\mathbf{r}_2) = \int \frac{\gamma_{\mathrm{A}}(\mathbf{r}_1, \mathbf{R}_\alpha)}{|\mathbf{r}_1 - \mathbf{r}_2|}\, d\mathbf{r}_1. \tag{14}$$

Here V_{A} is the molecular electrostatic potential mentioned in the title of the present paper.

It is evident that the computation of E_{es} requires a computational effort noticeably smaller than the complete calculation of ΔE. The calculation is not iterative and requires the knowledge of only a small portion of the two-electron repulsion integrals necessary to calculate the supermolecule AB. For the calculation of E_{es}, expressions (12) and (13) are equivalent. Equation (13) opens the way to approximate evaluations of the electrostatic portion of ΔE and to the semiquantitative evaluations of the reactivity of A with respect to ionic or dipolar partners. In fact, as has been remarked in the Introduction, it is easier to build up approximate representations of γ_{B} than of the wavefunction Ψ_{B}. If, for example, one could arrive at obtaining a proper expression of γ_{B} in terms of a distribution of point charges $q_{k\mathrm{B}}$ placed at the points k, the expression of E_{es} could assume the simple form:

$$E_{es}(\mathrm{AB}) = \sum_k V_{\mathrm{A}}(\mathbf{k}) q_{k\mathrm{B}}. \tag{15}$$

We shall examine in one of the following sections what are the practical methods for obtaining appropriate approximations of γ_{B}.

Some information on the reactivity of A can be gained also by the direct examination of V in the whole space surrounding the molecule, and by comparing the shape of V in related molecules. Within the limits of the electrostatic approximation, one obtains directly from $V_{\mathrm{A}}(\mathbf{k})$ the value of the interaction between A and a point charge placed at the point $\mathbf{k}$ (the maps of V that we shall use in the next sections are actually maps of the interaction energy of V with a unit of positive charge). By simple numerical manipulations, one can calculate also the forces acting on a point charge. In this sense the electrostatic potential V can be considered as a static reactivity index that supplements the other static indexes currently employed.

The information one may gain in this way is obviously incomplete and subject to all the limitations of the static indexes. The results obtained by inspection of V should be carefully tested before arriving at any conclusion, but the possibility of getting valuable hints on the reactivity of a molecule by means of a relatively inexpensive method, directly related to the expectation value of a one-electron operator, cannot be discarded *a priori.*

In Sections II and III, we examine V itself, in order to show how the electrostatic potential reflects the characteristics of the electronic distribution of a molecule, and we shall return later to the possibility of using only a portion of the interaction energy and we shall discuss the reliability of V as a reactivity index.

E. Electrostatic Potential and Hellmann–Feynman Theorem

As a sort of appendix to this introductory section, we shall consider here briefly what is the status of the electrostatic potential within the framework of the quantum theory.

A connection between the classical electrostatics and the quantal treatment of the interaction between two molecules can be found in the Hellmann–Feynman (H–F) theorem (Hellmann, 1937; Feynman, 1939). The H–F theorem in its generalized formulation states that if Ψ is an exact eigenfunction of the system and λ is a parameter that appears in the Hamiltonian, the variation of E with respect to changes of λ is given by

$$\partial E/\partial\lambda = \langle\Psi|(\partial H/\partial\lambda)|\Psi\rangle/\langle\Psi/\Psi\rangle. \tag{16}$$

When $\lambda = R_{AB}$ is a parameter denoting the distance between A and B (both being supposedly at fixed internal geometry), one may obtain from Eq. (16) an expression of the mutual force acting on the nuclei of A and B recast into purely classical terms. In fact, the parameter R_{AB} appears only in the nucleus–electron and nucleus–nucleus interaction operators, and the force is obtained as an expectation value of a one-electron operator (of multiplicative type) that can be calculated by the diagonal element of the first-order density matrix. The charge density, which has been obtained by means of rigorous quantal methods, is employed in a classical manner. By integration of the force, one arrives eventually at the computation of the interaction energy.

The H–F theorem is valid for exact eigenfunctions and a naive application of it to approximate wavefunction can lead to very misleading results. Much work has been done to establish the conditions of validity of this theorem for approximate wavefunctions; the reader is referred to the numerous reviews published on this subject (see, for example, Deb, 1973; Goodisman, 1973). We limit ourselves to observing this critical dependency of the actual utilization of the H–F theorem from the quality of the wavefunction.

In order to clarify the connections between the H–F theorem and the electrostatic molecular potential, let us consider the specific case of the interaction of a molecule M with an atom A. It is easy to verify (Anderson, 1974) that the expression assumed by the interaction energy calculated via the integration from ∞ to R_{AM} of the force acting on the nucleus of A (in a reference system fixed with M) is similar to that given in Eq. (13) only if the charge density of MA assumes the form,

$$\gamma_{MA} = \gamma_M(\mathbf{r}_1, \mathbf{R}_\mu) + \gamma_A(\mathbf{r}_2, \mathbf{R}_A), \tag{17}$$

and that it coincides with Eq. (13) only if the charge densities of M and A are identical to the undistorted densities of the partners at infinite distance:

$$\gamma_{MA} = \gamma_M^0(\mathbf{r}_1, \mathbf{R}_\mu) + \gamma_A^0(\mathbf{r}_2, \mathbf{R}_A). \tag{18}$$

Let us suppose now that A is a bare nucleus. The foregoing considerations are still applicable: approximation (17) should be valid in absence of the charge-transfer effects and the conditions of validity of approximation (18) are even more severe, implying in addition that M is not polarized. If we perform the rather unphysical operation of reducing gradually the charge of A, approximations (17) and (18) become more and more valid, and when the charge is infinitesimally small, expression (18) is correct. The classical definition of the electrostatic potential is completely analogous. Stating the problem in these terms, one may say that the H–F theorem gives a quantum mechanical status to the electrostatic potential. The derivation holds its validity also for approximate expressions of ρ_M^0 provided that they derive from Hartree–Fock wavefunctions optimized in all the parameters (Stanton, 1962).

Such a connection between the electrostatic potential (or the electrostatic interaction energy) and the H–F theorem could be exploited by resorting to the conceptual simplicity of this theorem in further manipulations which can be of some interest to our problem. In this context, we recall some considerations put forward by Anderson and Parr in their investigations on the vibrational equilibrium force constants of a molecule. We shall consider the simpler case of a diatomic molecule. The electronic density can be written as the sum of three terms (Anderson and Parr, 1970, 1972; Anderson, 1973):

$$\rho_{\alpha\beta} = \rho_\alpha + \rho_\beta + \rho_{\alpha\beta}^{npf}, \tag{19}$$

where ρ_α is supposed to follow perfectly the nucleus α in its motion, ρ_β follows nucleus β, and $\rho_{\alpha\beta}^{npf}$ is a nonrigid "nonperfectly following" component. It is necessary to state at the same time that $\rho_{\alpha\beta}^{npf}$ is just the term that does not permit the use of Eqs. (17) and (18) in actual calculations of ΔE. Deletion of $\rho_{\alpha\beta}^{npf}$ allows the derivation of a simple electrostatic formula for the calculation of the harmonic force constants, relying only on the value of the density ρ_β at the nucleus $\alpha(\rho_\beta(\alpha))$:

$$k_e = \nabla_\alpha^2 E = 4\pi Z_\alpha \rho_\beta(\alpha), \tag{20}$$

which gives results in good agreement with experience.

Anderson (1974) develops arguments to show that the Laplacian of the energy component corresponding to $\rho_{\alpha\beta}^{npf}$ can be considered equal to zero, and therefore that near the equilibrium the energy can be written in purely electrostatic terms:

$$\Delta E_{\alpha\beta} = Z_\alpha V_\beta(\mathbf{R}_\alpha) + \sum_k \frac{Z_\alpha q_k}{|\mathbf{R}_K - \mathbf{R}_\alpha|}. \tag{21}$$

Anderson's argumentation cannot specify better the value and the location of the charges q_K, which derive from $\rho_{\alpha\beta}^{npf}$, and the extension of the argument to polyatomic molecules is not immediate. This connection between electrostatic models concerning, first, the deformation of the geometry of a stable molecule and, second, the approach of two partners can be, however, of some potential interest and deserves to be mentioned here.

Of direct practical application are the considerations put forward by Srebrenik *et al.* (1973). These authors, by assuming, on the basis of the H–F theorem, the validity of the electrostatic laws and then of the Poisson equation relating the Laplacian of V to the charge density,

$$\nabla^2 V = -4\pi\rho, \tag{22}$$

show that if ρ is expanded in a Gaussian basis, an analytical integration of the left side of Eq. (22) gives an alternative and convenient method for calculating V.

II. The Shape of the Electrostatic Potential and Its Relationship to Electronic Molecular Structure

The deformations of the spherical charge distributions of a set of atoms bound together to form a molecule are quite complex, but from the direct examination of molecular charge distribution maps one may gain significant and useful information on the binding process and on the properties of the molecule.

The maps of V, which we shall examine here, can be considered as a useful supplement to maps of ρ (or $\Delta\rho$) for such analyses, because $V(\mathbf{k})$, though directly related to $\rho(\mathbf{k})$, is a quantity of "integral" type. In other words, the value of V at the point k reflects the effect of all the charges present in the molecule, and it is relatively insensitive to a possible poor description of ρ at this given point k. The possibility of a relatively low accuracy in the local description of the charge distribution is larger for points k placed at the external boundaries of the molecule because the process of optimization of the wavefunction passes through the calculation of the energy, which is more sensitive to the form assumed by ρ in the inner region of the molecule and less sensitive to the asymptotic form of the wavefunction at large distances from the nuclei. Analyses of the form assumed by $V(\mathbf{k})$ in the internal regions of the molecule have never been attempted (to the best of our knowledge), although the values assumed by V or by quantities strictly related to V (for example, the electric field) on the nuclei are currently employed to obtain information on the molecular structure and on some physical properties of the molecule.

In this section, we examine the shape assumed by V in the outer molecular space and will show how the chemist's structural units (bonds, lone pairs, mesomeric forms, etc.) found a counterpart in V. There exists in the literature quite a large quantity of typical examples, and some of these examples have already been collected in a previous review (Scrocco and Tomasi, 1973) and for this reason we can dispense with a systematic documentation of the characteristic shapes that V can assume. We consider only a few examples, selected preferably from those never published, sufficient however to show how the shape assumed by V is related to the commonly accepted interpretations of the molecular electronic distribution.

A. Glycine Tautomers and the Corresponding Anion

As a first example we have selected a system of intermediate complexity, namely, the glycine molecule. The occurrence in this molecule of rotational conformers will allow us to establish directly to what extent the overall shape of V depends on a varied interplay of group contributions that assume different spatial arrangements in the various rotational conformers. Such interplay will become even more evident if one compares the electrostatic potential of the neutral glycine with that of its zwitterionic tautomer and with that of the corresponding anion.

The wavefunctions we have employed to calculate V have been obtained with the minimal STO-3G basis set. Such a basis set is surely quite limited, but it is sufficient to reproduce, in a large number of molecules, the essential features of the shape of V, which remains substantially unaltered when one passes to larger basis set calculations (a discussion on the basis set dependence of V is given later in this section).

The map of Fig. 1a presents negative and positive regions to which it is possible to give an immediate intuitive interpretation. To each X—H bond corresponds a positive region (i.e., a region where the electrostatic potential repels an incoming positive charge). The minima of the negative regions can be

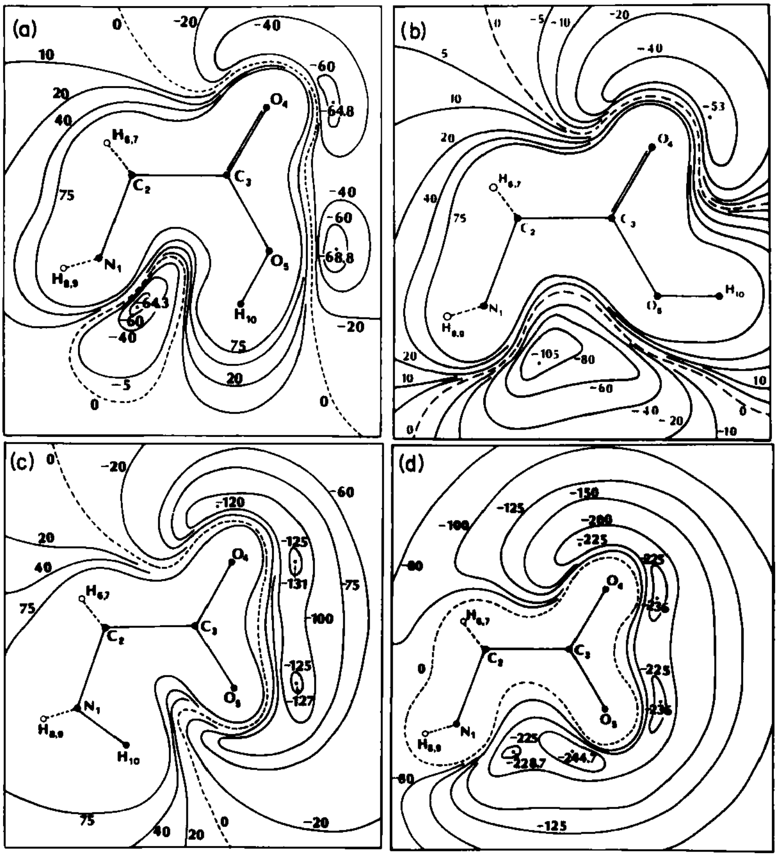

Fig. 1. The electrostatic molecular potential maps for two planar conformations of neutral glycine (a and b), for a planar conformation of the zwitterionic form of the same molecule (c), and for a planar conformation of the glycine anion (d), calculated with a STO-3G basis.

connected with the lone pairs present in the molecule: a first negative well corresponds to the N lone pair (the minimum is just on the plane displayed in Fig. 1a), a second can be related to the two lone pairs of O(4), and a last can be related to the O(5) lone pairs. The asymmetry of the well near O(4) deserves mention: it is due to the asymmetry of the molecular context where the C=O group is placed. It will be shown later that the contributions of the neighboring groups are of decisive importance in giving to *V* its shape.

Let us now consider the same molecule in another planar conformation (Fig. 1b) differing from the preceding one by the orientation of the

O(5)H(10) bond. The comparison of the two maps shows that a decomposition of V into additive local contributions should be able to account for a large portion of the features of V. The negative well at the bottom of the figure is due to the cooperative effects of the lone pairs of N and O(5), and in consequence is decidedly deeper than in the preceding case. The C(3)=O(4) group is now placed in a less asymmetric context and in this conformation two minima related to the two sp^2 lone pairs of O are evident. In the figure only the deeper minimum is marked by a star.

The next figure (1c) concerns a conformation of the zwitterionic tautomer of glycine. The most evident features of this map are due to the dipolar character of this tautomer. At large distances from the molecule the location of the nodal line corresponds to that of a dipole centered in an intermediate point between the CH_2 and the $-CO_2$ groups. At smaller distances the form of V is remarkably complex, and it is quite understandable that it is not possible to approximate its shape by a one-center multipole expansion truncated to a reasonably limited number of terms. Actually, also for molecules of intermediate complexity, such as glycine, the most convenient way to have a sufficiently reliable multipole expansion of the electrostatic potential (or of the charge distribution) consists in adopting a segmentation of the charge distribution with the related multipolar expansions over single bonds, atoms, or chemical groups (Rein, 1973).

Returning now to examine Fig. 1c, it may be remarked that the charge separation between the groups $-CO_2^{(-)}$ and $-NH_3^{(+)}$, with respect to the case shown in Fig. 1a, produces a substantial deepening of the negative zone near the $-CO_2^{(-)}$ group. The passage of the proton H(10) from the acidic head to the aminic group of the amino acid gives rise to a rearrangement of the charge distribution of the $-CO_2$ group where now each O atom has two lone pairs in sp^2 hybridization. A minimum of V is strongly perturbed by the $-NH_3^{(+)}$ group, whereas the other groups maintain approximately the same ratio as they had in the neutral form.

The principal characteristic of the electrostatic potential of the anion (Fig. 1d) are directly amenable to features evidenced in the preceding examples. For instance, the double minimum at the bottom of the figure can be connected to the occurrence of two negative contributions, the first due to the N lone pair, the second to a O(4) lone pair, which in the zwitterionic tautomer was partially masked by the positive charge on the N—H(10) group. The deepening of the minima, with respect to the preceding cases, is quite remarkable and can be intuitively connected with the greater proton affinity of the anion. The occurrence of five distinct minima can lead to the expectation of five preferential channels for the approach of the proton, corresponding to four different conformations of neutral glycine and one of the zwitterion. We examine in a later section to what extent such forecasts are correct also from a quantitative point of view.

The existence in the anion of a net negative charge is evidenced by the form assumed by the nodal surface, which in Fig. 1d is represented by a closed line. At very large distances, the equipotential surfaces show a tendency to assume the spherical shape characteristic of the monopole distribution, but even at relatively large distances the deviations from the spherical symmetry are quite substantial. Also in smaller anions, such as $CNNH^-$ and H_2CO^-, analogous deviations from the spherical symmetry are evident (Hart, 1973; Ellinger *et al.*, 1975; Perahia *et al.*, 1975).

B. Methane, Ethane, Propane

This example concerns very simple molecules, quite homogeneous, and without impressive features in the electrostatic potentials deriving from lone pairs, double bonds, etc. The most interesting feature these compounds present is the occurrence of negative regions in correspondence with the groups CH_3 and CH_2, with minima placed on the axis of local symmetry. We show in Fig. 2 the map of propane, which is representative of the entire set of linear aliphatic hydrocarbons. In the first terms of the set the value of the minima passes from -3.4 kcal/mole in CH_4, to -4.0 kcal/mole in C_2H_6, to -4.1 kcal/mole ($-CH_3$ groups) and -3.1 kcal/mole ($>CH_2$ group) in C_3H_8 (values obtained with STO-3G calculations). Such negative values are not directly amenable to a specific group, as was the case in the preceding example, but rather reflect the rearrangements of the electrons due to the bonding process. A more detailed analysis of these effects is presented in Section III together with an explication of why the $>CH_2$

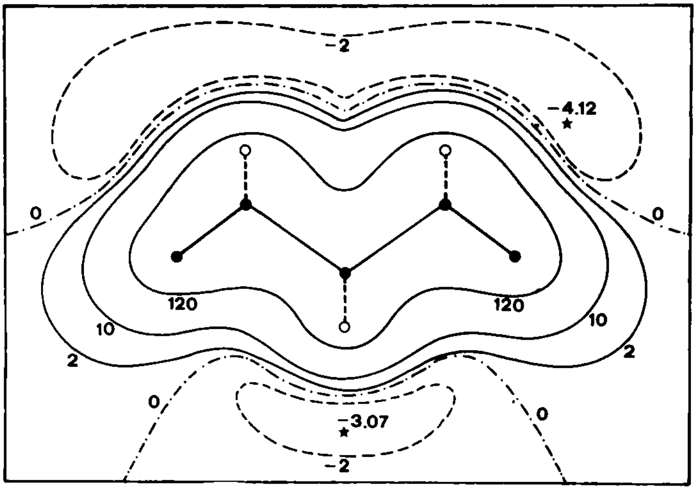

Fig. 2. Map of *V* for the propane molecule (STO-3G basis).

group in glycine does not show a corresponding negative region. We will limit ourselves here to hinting that such minima can give some information about the reactivity of the hydrocarbons.

These negative zones are present also in other hydrocarbons: Politzer and Daiker (1975) have noticed such zones in compounds such as 9,10-dimethyl-1,2-benzanthracene and 20-methylchloranthrene (CNDO/2 calculations). We may add that such minima are present also in smaller aromatic hydrocarbons, such as toluene (the minimum near the $-CH_3$ group is −1.3 kcal/mole in the STO-3G basis set). It should be noticed that toluene and the other aromatic compounds do not present negative zones of this kind near the C—H groups of the ring.

C. Ethylene and Allene

The presence in the ethylene molecule of a double bond introduces in V special features that are shared also by the other olefins and which appear, with the necessary modifications, in compounds containing other types of double bonds. In Fig. 3 is shown the map of V for the parallel and perpendicular planes of symmetry of ethylene. In the molecular plane, the electrostatic potential is everywhere positive, with the exception of a small negative zone on the molecular axis, to which we shall return later. In the perpendicular plane, a large negative zone is evident, with a minimum placed on the median of the C—C bond. This last negative zone can be connected to the presence of a π-bond and reflect the reactivity of ethylene toward positively charged reactants.

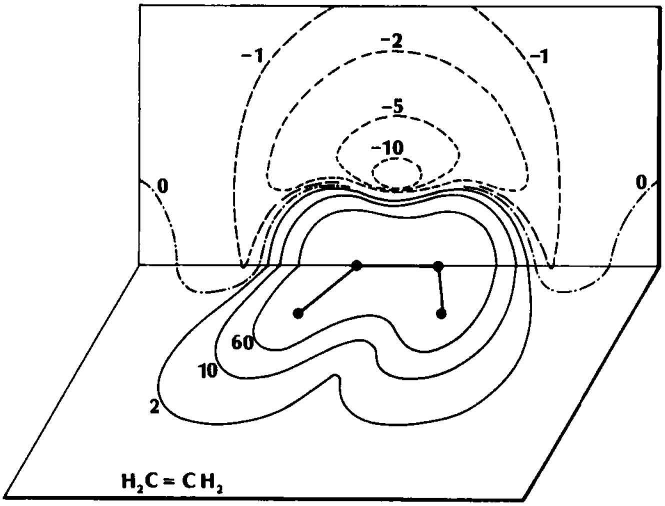

Fig. 3. Map of V for the perpendicular and molecular plane of ethylene (STO-3G basis).

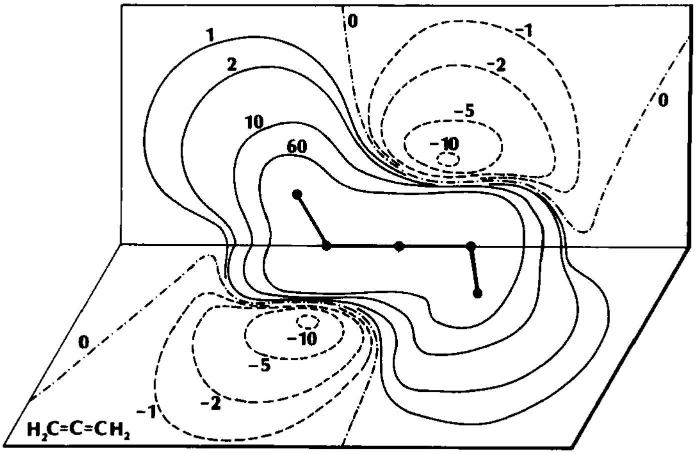

Fig. 4. Map of *V* for the perpendicular and the molecular plane of allene (STO-3G basis).

In the allene molecule (Fig. 4) the two regions each corresponding to a π-bond are only slightly modified with respect to the preceding case. The two regions corresponding to the molecular plane of ethylene present relatively larger changes, which in a first approximation can be related to the substitution of the $=CH_2$ group with the $=C=CH_2$ one. This example evidences the fact that the perpendicular arrangement of the two double bonds minimizes the interactions between the two subunits that compose the molecule (Fischer, 1964).

D. Benzene, Pyridine, and Nucleic Acid Bases

The presence of negative zones related to π-electrons is evident also in aromatic compounds. This characteristic shape of *V* has been the object of different discussions concerning the indications on the chemical reactivity of the ring one may extract from *V* (Berthier *et al.*, 1972; Gelius *et al.*, 1972; Bonaccorsi *et al.*, 1972b, 1974a, 1975; Almlöf *et al.*, 1973a,c; Scrocco and Tomasi, 1973; Politzer *et al.*, 1973; Politzer and Weinstein, 1975; Petrongolo and Tomasi, 1975; Martin *et al.*, 1975; Bertran *et al.*, 1975; Weinstein *et al.*, 1976; Petrongolo *et al.*, 1977; Petrongolo and Kaufman, 1978).

We think that it is not necessary to summarize such discussions here and we shall limit ourselves to giving a few examples. We compare in Fig. 5 the maps for benzene and pyridine drawn for a plane lying at 1.75 Å from the molecular plane. Such maps are taken from a paper by Almlöf *et al.* (1973c) and refer to a basis set larger than the minimal set employed in the other examples of this chapter.

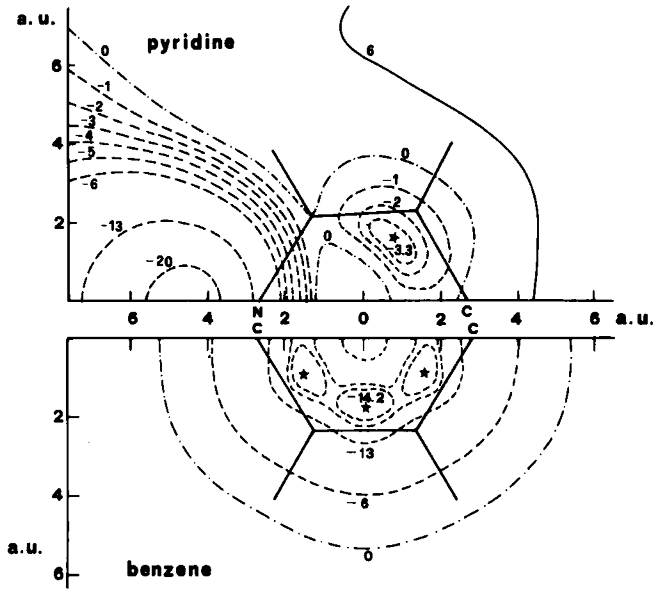

Fig. 5. Maps of V for pyridine and benzene. Both maps refer to a plane parallel to the ring at a distance of 1.75 Å and are calculated with a DZ + P basis set (from Almlöf *et al.*, 1973c).

In benzene the negative region covers (at 1.75 Å from the molecular plane) all the nuclear skeleton and the minima are symmetrically placed at points near the middle of the C—C bonds. This shape of V might suggest the possibility of a bridged carbonium ion as intermediate in electrophilic attacks (Almlöf *et al.*, 1973c).

Passing to pyridine, one finds on the plane shown in Fig. 5 two negative regions: the first is dominated by the N lone pair (the minimum, −82.7 kcal/mole, is on the molecular plane) and the second concerns only a portion of the ring, with local minima above and below the C_β atoms. The shape assumed by V might tentatively be related to the lower reactivity of pyridine (with respect to benzene) toward electrophilic attacks. We can limit here the examination of V in benzene and pyridine to these two planes, but it should be added that in aromatic compounds it is generally advisable to extend the examination also to other maps of V. In fact (see, for example, Scrocco and Tomasi, 1973) the nodal plane can run in some molecules (or in some portion of a molecule) parallel to the ring plane and the comparison of maps of V in different molecules referring to a single plane placed at a fixed distance from the ring can lead to erroneous conclusions.

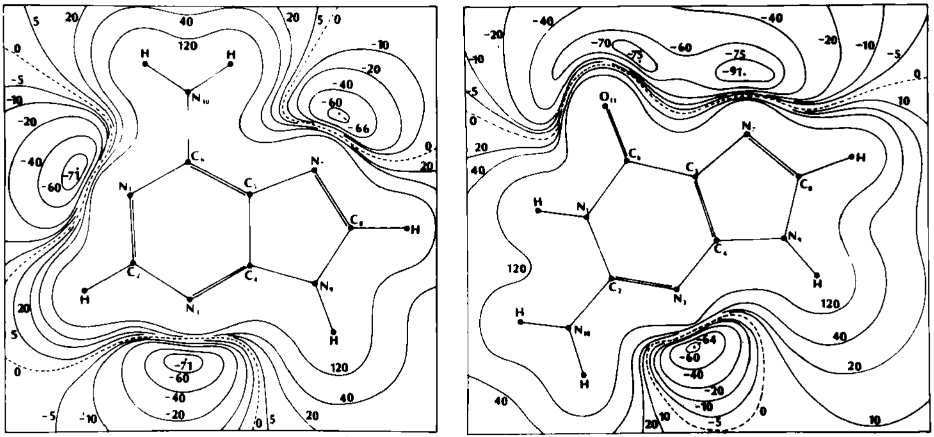

ADENINE GUANINE

Fig. 6. Maps of *V* for the ring plane of adenine and guanine (from Bonaccorsi *et al.*, 1975). (Copyright by Springer-Verlag. Used with permission.)

The last example we give here concerns the two purinic bases of the nucleic acids, guanine and adenine (Bonaccorsi *et al.*, 1975). In this case, we show in Fig. 6 only the maps for the molecular plane [for other maps see the source paper, and for a comparison with thymine and cytosine, see Bonaccorsi *et al.* (1972b) and with uracil, see Perahia *et al.* (1976)].

In the guanine molecule there is a negative region encompassing O(6) and N(7) which prevails on a second negative region concerning N(6). In the adenine molecule, there are three minima corresponding to the N(1), N(3), N(7) atoms. The ordering of the minima within each single molecule is in agreement with what is known about the reactivity of the various heteroatoms with respect to protonation and electrophilic attack by alkylating agents. The minimum near N(7) in guanine is appreciably larger than any of the minima of adenine and this fact is again in agreement with experimental evidence. The maps of Fig. 6 do not show two other important points concerning the reactivity of these two molecules: the amino nitrogens [N(2) in guanine and N(6) in adenine] are far less basic than the ring nitrogens, and the C(8) atom of guanine is decidedly more reactive than the corresponding atom of adenine. These conclusions, which are again in fairly good agreement with the experimental results, have been drawn by the examination of maps of *V* concerning portions of space outside the molecular plane.

E. Nitrous Oxide and Isocyanic Acid

Although simpler than the molecules considered in the preceding section, nitrous oxide and isocyanic acid present a more complex electronic structure.

According to the usual conventions of chemistry, such molecules can be described in terms of resonating structures, e.g.,

$$\underset{\text{(I)}}{N{\equiv}\overset{+}{N}{-}\overset{-}{O}} \qquad \underset{\text{(II)}}{\overset{-}{N}{=}\overset{+}{N}{=}O} \quad \text{and} \quad \underset{\text{(III)}}{H{-}C{\equiv}\overset{+}{N}{-}\overset{-}{O}} \qquad \underset{\text{(IV)}}{H\overset{-}{C}{=}\overset{+}{N}{=}O.}$$

In the alternative picture of the electronic structure given by the localized MO's, the terminal N atom of N_2O is characterized by a single lone pair (with a predominant sp hybridization), the central atom is connected to the first with a set of three bonds, and with a simple σ-bond to the oxygen that has three lone pairs. This description looks similar to the resonance formula I, but a perusal of the shape and polarization of the single localized orbitals shows that some features of the actual electronic distribution are better represented by structure II (C. Ghio, E. Scrocco, and J. Tomasi, unpublished, 1975). The description of the electronic structure of HCNO is qualitatively similar to that of N_2O, the difference being a substitution of a H—C group to the terminal N atom. This substitution of groups will produce changes of quantitative type in the shape and in the polarization of the other localized orbitals.

Let us turn now to the V maps in Fig. 7. There are two regions with negative values of V in N_2O, the first with a single minimum corresponding to the terminal N atom, the second with a toroidal well near the O atom in agreement with the localized description of the lone pairs and with structure I. In the central zone, V has values more positive on the median plane of the N—N bond than on the median plane of the N—O bond; this difference might be tentatively associated with the characteristics of structure I. In the isocyanic acid, the shape assumed by V near the oxygen atom does not differ significantly from that assumed in the preceding molecule: the depth of the toroidal well is now larger. The substitution of the terminal N atom by the H—C group gives rise to noticeable changes: the negative zone has disappeared and the trend of the equipotential lines is completely different. In the central zone the electrostatic potential is now decidedly more positive near the C—N bond than it is near the N—O bond.

It may be of some interest to compare these maps of V with those of the corresponding compounds that do not contain the terminal O atom: N_2 and HCN. The maps are given on the left side of Fig. 7. The shape of V in the region of the N_2 group in N_2O is similar to that of the N_2 molecule. The map of HCN presents noticeable analogies, also from a quantitative point of view, with the portion of the isocyanic map corresponding to the HCN fragment.

In conclusion, such a comparison shows that the addition of a further group (the oxygen atom) does not alter the intrinsic characteristics of NN

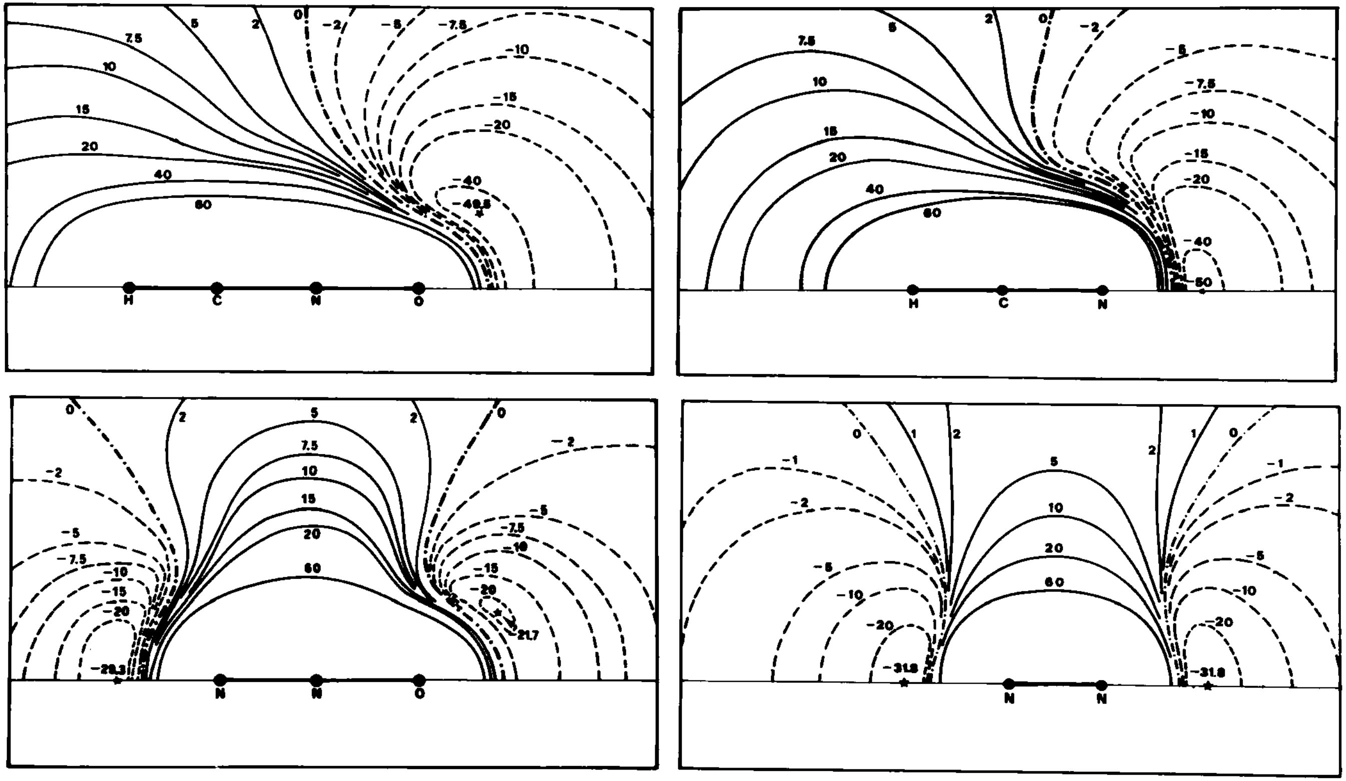

Fig. 7. Maps of V for HCNO, HCN, NNO, and N_2 calculated with the best atom zeta STO basis set (from C. Ghio, E. Scrocco, and J. Tomasi, unpublished 1975).

and HCN, and at the same time that the passage from the "united atom" N to the "separate couple" H—C does not correspond simply to the substitution of a lone pair by a C—H bond, as a quick look at the localized orbitals could suggest, but rather to a more drastic change in the electronic distribution within the molecule.

It may be of some interest to devote a few words to the interpretation of the shape assumed by *V* in these molecules. We shall consider here, as an example, only the simplest one, N_2. The electronic rearrangements due to the formation of the molecule from two isolated N atoms should lead to a piling up of electronic density in the bonding region. Such accumulation should produce a negative electrostatic potential in the median plane perpendicular to the bond. The process of hybridization of the N atom leading to the formation of the bond produces also a lone pair projecting out in the region of space opposite to the bond. Such electron migration partially deshields the nucleus on the side corresponding to the bond, giving thus a positive contribution to *V* on the median plane. This second effect predominates over the first one, and the final result is the occurrence in N_2 of a positive central region surrounded by two negative regions due to the lone pairs.

F. The Dependency of the Shape of *V* on the Accuracy of the Wavefunction

The electrostatic potential, like all the other one-electron observables, is correct to the second order in the Hartree–Fock (HF) approximation. With wavefunctions going beyond the HF approximation, one will of course obtain changes in the shape of *V* (for the H_2CO case, see Daudel *et al.*, 1977), but at present there is not a sufficient quantity of results to permit a profitable discussion on the influence of correlation on the shape of *V*.

We shall limit ourselves to considering the problem of the dependency of *V* on the basis set within the SCF approximation. Such discussion presents also a practical implication because the information on reactivity one can get by employing *V* as an index is only approximate and gains in reliability if it is checked by comparisons over a sufficiently large set of molecules. The practical usefulness of this index would be greatly reduced if it turned out to be necessary to use very sophisticated bases to have reasonable representations of *V*.

Comparisons of values of *V* obtained with different bases on the same molecule are abundant in the literature; some are collected in earlier papers (Scrocco and Tomasi, 1973; Petrongolo and Tomasi, 1975), and it is not necessary to report here all the available material. We shall limit ourselves to the few examples of molecules whose maps we showed in this section.

Figure 8 shows four portions of the maps for the perpendicular plane of ethylene, recently calculated by Almlöf and Støgard (1974), with four

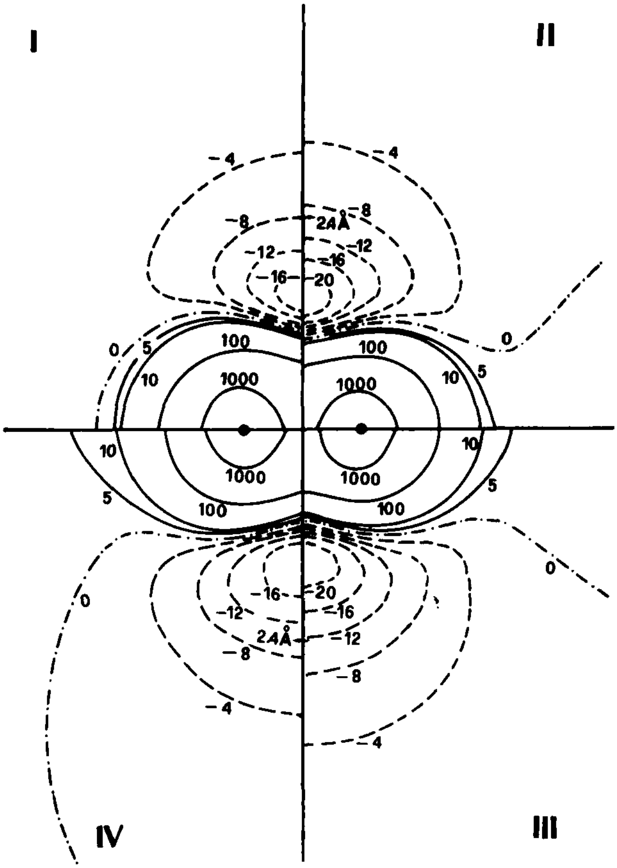

Fig. 8. Comparison of the shape assumed by V in the molecular plane of ethylene according to four different Gaussian basis sets (from Almlöf and Støgart, 1974). (Copyright by North-Holland Publishing Company. Used with permission.)

different bases. The four quadrants of Fig. 8 refer to the following Gaussian basis sets: (I) (7s, 3p/3s) contracted to [2s, 1p/1s]; (II) (7s, 3p/3s) contracted to [4s, 2p/2s]; (III) (9s, 5p/4s) contracted to [4s, 2p/2s]; (IV) (9s, 5p/4s, 1p) contracted to [4s, 2p/2s, 1p]. A fifth basis (9s, 2p, 1d/4s, 1p) contracted to [4s, 2p, 1d/2s, 1p] gives the same V values as basis IV. One may see that the changes of V are remarkable and that changes of basis can lead also to the appearance (or the disappearance) of some secondary features; for example, the position of the nodal curve shows that in case I there is also a small negative zone in the molecular plane (compare with Fig. 3 obtained with the STO-3G basis set, which shows an analogous negative zone on the molecular plane). The results of cases II and III are fairly similar, but this fact depends to a large extent on the substantial likeness of the two uncontracted basis sets. (With another DZ basis set, the 4-31G one, we find for the minimum of V the value of -24.4 kcal/mole instead of -22.9 kcal/mole for case II and -22.5 kcal/mole for case III.) The inclusion of polarization functions (cases IV and V) gives values of V that resemble those of the minimal set I. Changes of the same order of magnitude, or even larger, come out if one passes from a minimal set to another minimal set. For example, in ethylene the minimum of V, according to the STO-3G calculations, is -12.7 kcal/mole instead of the -18.0 kcal/mole given by basis set I. In the glycine zwitterion, if one adopts the minimal basis set proposed by Van Duijneveldt (1971) instead of the STO-3G basis employed in Fig. 1c, one finds a rising of the minima of about 20 kcal/mole (Carozzo, 1976).

A second example concerns the benzene and pyridine molecules for which we have reported in Fig. 5 the results obtained with a (7s, 3p/7s, 3p/4s, 1p) contracted to [4s, 2p/4s, 2p/2s, 1p] basis set. With the STO-3G basis the π negative zones are less deep by a few kilocalories per mole and there is a central shallow minimum instead of six separated minima (this map is reported by Petrongolo and Tomasi, 1975). The same STO-3G basis leads in pyridine to a map at 1.75 Å from the ring which, at first sight, looks different from that of Fig. 5 (see again Petrongolo and Tomasi, 1975): there is only a nodal curve that passes near the C_α atoms and the largest portion of the plane above the ring shows positive values of V. These values are, indeed, very small (around 1 kcal/mole) and the negative minima in correspondence of the C_β atoms are replaced by positive minima (less than $+0.1$ kcal/mole); with the Clementi *et al.* (1967) minimal basis set, such minima are -5 kcal/mole (Scrocco and Tomasi, 1973).

These changes in the values assumed by V and due to changes in the basis set are numerically noticeable, but the overall impression is that they remain practically constant in passing from one member to another of a homogeneous set of molecules (see, for example, Ghio and Tomasi, 1973). The use of V as an index to compare relative reactivities can be thus considered justified, but the comparisons should be made on values obtained from homogeneous basis sets.

The examples shown in this section seem sufficient for us to reach some conclusions. The image that V gives of the electronic distribution is detailed and clear enough. The sensitivity to substitution of groups, to changes in conformation or structure, is evident. It can be seen, at the same time, that, for similar chemical groups, there are corresponding portions of space where the shape of V is reasonably similar and that, for compounds having similar geometrical arrangements of the atoms but different arrangements of the bonds, the *V* maps are quite different. These findings suggest a possible approach for obtaining a rationale of the shape assumed by *V* (a topic that we treat in Section III). For this investigation we shall use, for the reasons outlined in this section, one basis set only, namely, the STO-3G set of Pople and co-workers (Hehre *et al.*, 1969) thus avoiding a possible source of confusion, i.e., comparing things of different quality. It should be borne in mind, however, that the image of *V* thus obtained may suffer to some extent from the limitedness of the basis set and that analogous investigations performed on larger bases could change some of the conclusions.

III. The Electrostatic Molecular Potential in Terms of Local Group Contributions

Several times in the preceding section we have anticipated that an interpretation of the shape of *V* can be obtained by considering *V* as a sum of local contributions, transferable from molecule to molecule.

This transferability may be exploited to get a rationale of the shape of *V* in different molecules and to shed light on the effects of chemical substitution on the values assumed by *V* near a given group in a set of related molecules. In addition to the interpretation of the shape of *V*, the transferability properties of the group contributions open some possibilities of practical utilization. We have not yet checked in this paper whether *V* can be of some use in studying chemical reactivity, but is clear that even in the case of a positive answer to this question the usefulness of *V* will be tempered by the necessity of calculating first the molecular wavefunction and then the expectation value $V(\mathbf{k})$ for a considerable number of space points k. This fact limits the possibility of application to large molecular systems of approximate electrostatic methods for the prediction and the interpretation of their chemical behavior. The introduction of strongly localized and directly transferable group contributions might eliminate such bottlenecks (at the eventual expense of the loss of some accuracy in the results). In fact, if such approximation turns out to give acceptable values of *V*, the calculation of the molecular wavefunction will be no longer necessary, and the elaboration of simplified algorithms to calculate *V* will be much easier.

In this section, we give the definiton of the group contributions we have adopted, and we shall use such partition of the whole observable to gain a better understanding of the shape assumed by *V* in typical molecular contexts. We shall postpone to a subsequent Section the discussion about the possibility of making the calculation of *V* less costly.

A. Definition of Transferable Group Models

For the sake of simplicity, let us consider here only the case of a neutral closed-shell molecule having 2N electrons: the extension to charged or open-shell molecules is straightforward. The first step toward a definition of strictly localized group contributions consists in adopting for the total charge distribution γ_A, an expression equivalent to that of Eq. (11) but having the form of additive neutral contributions with a noticeable (but not complete!) local character. This may be done by replacing in Eq. (11) the canonical molecular orbitals ϕ_i defining ρ_A ($\rho_A = 2\sum_i^{\text{occ}} \phi_i^* \phi_i$) with localized orbitals λ_i and by associating with each electronic contribution $2\lambda_i(1)^*\lambda_i(1)$ a suitable portion of the nuclear charges. If λ_i corresponds to a bond between atoms a and b, this portion of the nuclear charges will consist of a unit positive charge from nucleus a and one from nucleus b; if λ_i corresponds to a lone pair on atom c, the two positive charges will derive from the nucleus c, etc. The expressions for γ_A and $V_A(\mathbf{k})$ will assume the following form:

$$\gamma = \sum_i^{N} \gamma_i \tag{23}$$

$$V_A(\mathbf{k}) = \sum_i^{N} V_i(\mathbf{k}) \tag{24}$$

with explicit expressions for the various V_i of the type,

$$V_{ab}(\mathbf{k}) = -2\int \lambda_{ab}(1)^* \frac{1}{r_{1k}} \lambda_{ab}(1)\, d\tau_1 + \frac{1}{\mathbf{R}_{ak}} + \frac{1}{\mathbf{R}_{bk}}, \tag{25}$$

etc. Of course it is possible to collect more contributions and to consider, for example, all the π-electrons of an aromatic subunit as an entity in itself.

Equation (24) is equivalent to the original expression of the electrostatic potential but does not completely meet the criteria of strong localization and direct transferability, which are very convenient for euristic analyses and necessary for the elaboration of simpler methods for the calculation of V for large molecules. In fact the localized orbitals λ_i have small but not negligible "tails" on the other atoms of the molecule, whatever localization procedure one has adopted. Such tails are in part due to the constraint of maintaining mutual orthogonality between localized orbitals (LO). When the LO are expressed in a linear combination of atomic orbitals (LCAO) form, it is quite easy to eliminate the tails: it is sufficient to set equal to zero all the coefficients corresponding to atomic orbitals not centered on atoms a and b (or c, according to the case) and to normalize the remainder.

For brevity, we will call these normalized LO, without tails, $\bar{\lambda}_i$.[1] The calculation of the mean value of a one-electron quantity by using the $\bar{\lambda}$'s is not convenient because procedures that take into account the nonorthogonality of the $\bar{\lambda}$'s require lengthy manipulations. We have adopted the drastic resolution of discarding such complications by considering as negligible the overlaps among $\bar{\lambda}_i$'s and of calculating V as a simple summation of contributions that are strictly localized. A rather long set of tests, only partially published (Bonaccorsi *et al.*, 1976b) has established that the errors thus introduced are confined into a reasonably narrow range (a maximum of 2–3 kcal/mole on the van der Waals surface and less in the outer space) and, moreover, that the trends of V at particularly significant points (for example the minima) in passing from one molecule to another are conserved to a large degree.

A second conclusion deriving from such tests concerns the transferability of the group contributions expressed in terms of $\bar{\lambda}_i$ orbitals: to a reasonable degree of approximation V_i is independent, in unconjugated molecules, of the molecular context where the a—b bond or the c lone pair is placed. In consequence it is easy to obtain models for each bond or lone pair by averaging among a few examples that are opportunely selected from actual molecules. This averaging process is directly performed on the coefficients of the LCAO expansion of a set of $\bar{\lambda}_i$ orbitals followed by a normalization of the resulting mean coefficients.

We will not expose and analyze here the whole set of controls we have performed, but we shall simply employ such models for a better understanding of the form assumed by V in some typical examples. In Figs. 9–11, we report the maps of V for some simple groups that we shall use in the following discussion. For brevity, we will, when necessary, call the σ-bond between atoms a and b, σ_{ab}, the corresponding π-bond, π_{ab}, a banana bond (i.e., an admixture of σ_{ab} and π_{ab}), β_{ab}, and a lone pair, l_c.

The shape assumed by the group potentials shown in Fig. 9 is easily understandable. For example, in the potential curves of σ_{CC} (which are rigorously symmetrical because of the averaging procedure we have followed), a typical quadrupolar shape is evident; in the potential curves of the X—H groups, one may discern the effect of the vector coupling of the atomic hybrid moment of the heavier atom X with the charge-transfer moment arising from the electronegativity difference between X and H,

---

[1] It should be observed that the orthogonality constraint is not the only reason for the presence of tails (England and Gordon, 1972; Levy, 1976). Anyway, in actual calculations the tails are rather small, as may be verified by examining the value of the square mean deviation $\int |\lambda_i - \bar{\lambda}_i|^2 \, d\tau$ between the localized orbital λ_i and its counterpart without tails $\bar{\lambda}_i$, which is in general less than 0.05 (Bonaccorsi *et al.*, 1968, 1969, 1970, 1971b).

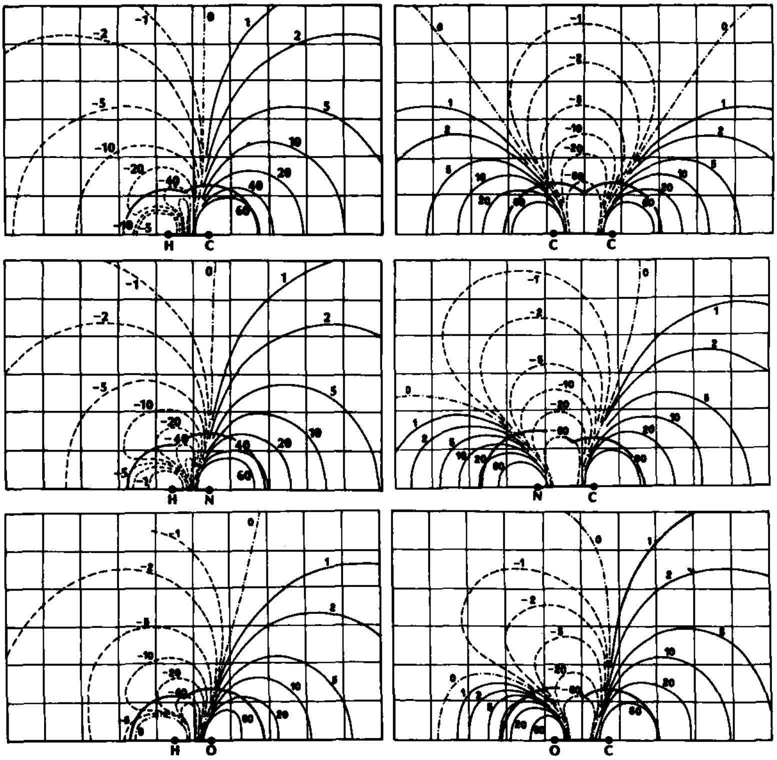

Fig. 9. The shape of V for the transferable localized models of the C—H, N—H, O—H, C—C, C—N, and C—O σ-bonds (in the STO-3G approximation). The grids have a spacing of 1 Å.

which produces a noticeable dipolar component superimposed on the quadrupolar one.

The quality of the results obtainable with such localized contributions can be appreciated by comparing the two maps shown in Fig. 12. Both refer to the same portion of the molecular plane of the fully extended conformation of the 2-formylaminoacetamide molecule: Fig. 12a shows a map calculated directly from a STO-3G SCF wavefunction and Fig. 12b, a map calculated with the transferable group model potentials introduced in this section (Bonaccorsi *et al.*, 1977).

B. Alkylic Groups

The map concerning the σ_{CH} group in Fig. 9 is characterized by the presence of negative values on the side of the H atom. This feature is in apparent contrast to what was found near the CH_2 group in glycine. We

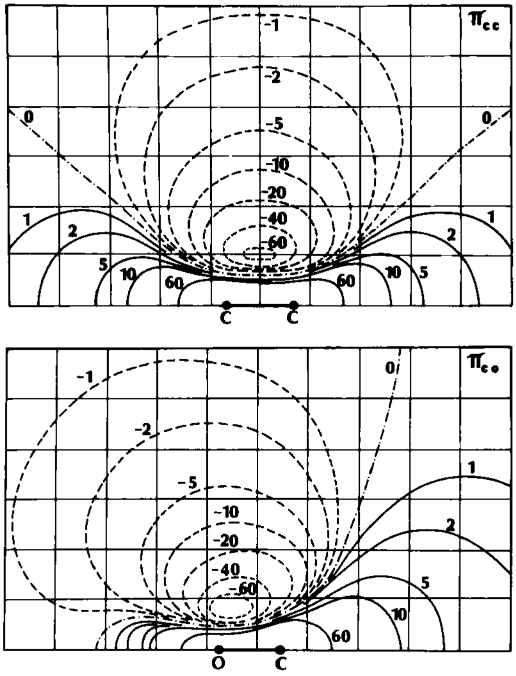

Fig. 10. The shape of V for the transferable localized models of the C—C and C—O π-bonds (in the STO-3G approximation).

will show here how the contributions of more distant groups reverse the sign of V near the CH_3 or the CH_2 groups in a large number of molecules and how the negative contributions due to the C—H bonds can be evidenced in some cases.

When three σ_{CH} groups are juxtaposed at the correct mutual tetrahedral orientation, there is a reinforcement of the negative values of V along the three-fold axis. The additon of the fourth bond (σ_{CH} in methane, σ_{CC} or σ_{C-X} in other compounds containing the methyl group) brings a positive contribution in this region that greatly reduces the entity of the negative zone. The minimum passes from about -50 kcal/mole for the CH_3 group to -3.4 kcal/mole in methane and to about -20 kcal/mole in C—CH_3. The further addition to this last group of three σ_{CH} to form the ethane molecule brings another positive contribution that leads to a final value of -4.0 kcal/mole found in C_2H_6. When the CH_3 group is linked to heteroatoms, the electronegativity difference between C and X leads to a greater positive contribution of the σ_{CX} group in the region of the methyl minimum (compare in Fig. 9 the C—C map with the N—C and O—C maps). This

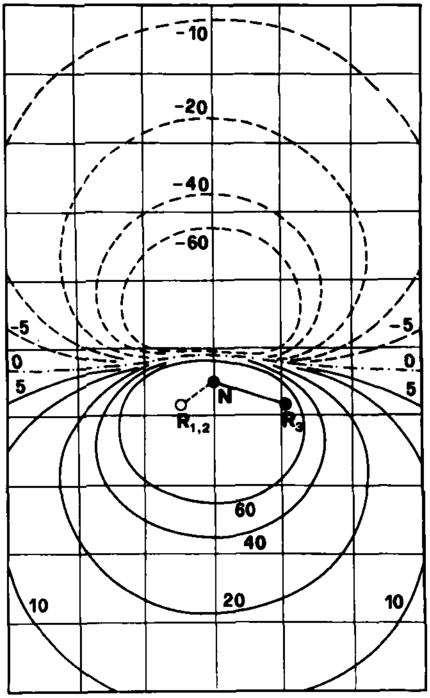

Fig. 11. The shape of *V* for the transferable localized model of the N lone-pair group. To make more evident the spatial relationship of this group with others in actual molecules, we have indicated in the figure also the position of the nearest atoms in trigonal ammonia derivatives.

minimum is depressed to about −16 kcal/mole in N—CH_3 and to −13 kcal/mole in O—CH_3.

Similarly, the inclusion of two C—C bonds in the methylenic group is not sufficient to delete completely the minimum found in CH_2 (the value passes from −112 kcal/mole to −40.2 kcal/mole). We have seen in Section II, B (Fig. 2) that in propane, near the central atom there is a minimum of −3.07 kcal/mole, and we have already remarked that analogous minima are present near CH_3 groups in aromatic hydrocarbons. In methylenic groups linked to one heteroatom (e.g., ethylenimine, ethanol, acetone) or two heteroatoms (e.g., glycine) the polarity of the C—X bonds is sufficient to cancel out such negative regions.

It is relevant to remark that the methyl and methylene minima in the complete molecule are quite small and that their actual occurrence may depend on the basis set employed in the calculations. They are not sufficient, in general, to give a predominant electrostatic contribution to the interaction energy with positively charged reagent, although in some cases (for

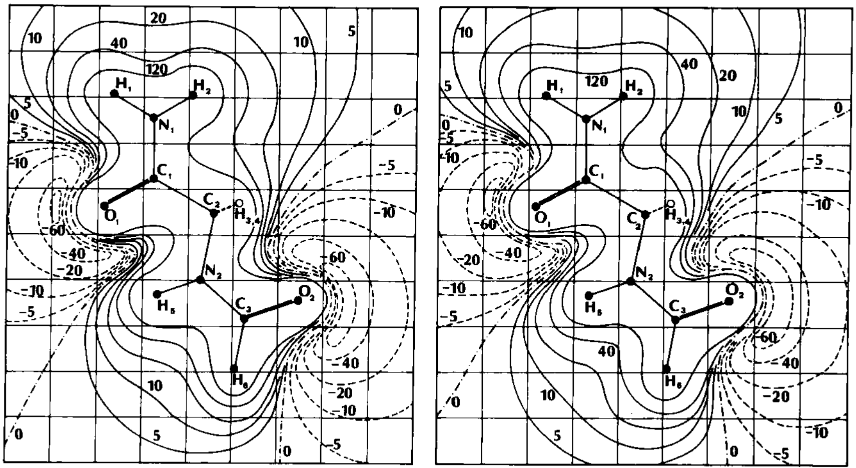

(a) (b)

Fig. 12. A comparison of the in-plane map of the fully extended conformation of 2-formylaminoacetamide calculated (a) directly from a STO-3G SCF wavefunction and (b) by using transferable localized orbital models (from Bonaccorsi *et al.*, 1977). (Reprinted with permission from the Journal of the American Chemical Society. Copyright by the American Chemical Society.)

example, the protonation or similar electrophilic additions in hydrocarbons) they may give a hint regarding the spatial location of the reaction channel, as we have noted in the preceding section.

C. Double Bonds

The C═C double bond can be viewed as a couple of banana bonds or as the result of the juxtaposition of a σ- and a π-bond [this latter representation is given in Figs. 9 (C—C map) and 10 (C—C map)]. The electrostatic potential of the whole C═C group is positive on the nodal π-plane and has two negative regions, symmetric with respect to this plane, with the minimum centered on the median axis orthogonal to the nodal plane. In ethylene the electrostatic potential of the CH_2 group is positive on the C side and presents a negative minimum on the H side, in analogy with what was shown for the methylenic group in tetrahedral arrangement. The juxtaposition of the C═C group and two CH_2 groups produces a substantial lowering of the minimum on the π-region (from -220 to -12.7 kcal/mole) and an analogous reduction of the CH_2 minima (from -86.5 to -1.1 kcal/mole). We have already seen that such a negative zone on the molecular plane occurs in the Almlöf and Støgard (1974) calculations only with the basis set I (see Fig. 8). A change of the basis set can produce variations of a few kilocalories per mole in the V values. These variations can be of minor importance if one looks at positions where V is large, but they are sufficient to delete completely the small minima.

The same type of juxtaposition of group contributions can lead to a rationalization of the shape of V for allene (see Fig. 4). In this case, too, the model pair potentials give deviations from the SCF V values of less than 1 kcal/mole.

The σ_{CC}, σ_{CH}, and π_{CC} electrostatic potentials of Figs. 9 and 10 can be used for a rough estimation of the effects that give rise to the shape of V for benzene (for a more accurate analysis, one should use the actual potential of the six π-electrons): each σ-bond produces a negative contribution on the molecular plane, which is canceled by opposite contributions of the π-electrons and of the other neighboring σ-bonds. In double bonds containing heteroatoms, such as those present in groups C=O, C=N, and N=O, one has also to consider the polarization of the corresponding π- and σ-bonds (see Figs. 9 and 10) and the presence of lone pairs. The potential map of l_N is reported in Fig. 11: its shape is quite similar to that of l_O. All sp, sp^2, and sp^3 lone-pair electrostatic potentials, irrespective of their hybridization (for a discussion, see Bonaccorsi *et al.*, 1976b), have the shape of a finite dipole. Lone-pair contributions and polarization effects produce a complete deletion of the CH_2 minimum in molecules such as $H_2C{=}O$ and $H_2C{=}NH$ also with the same minimal basis sets that produce methylenic minima in $H_2C{=}CH_2$. It should be obvious from the preceding discussion that the local symmetry of groups such as the carbonyl can be remarkably distorted by asymmetries in the neighboring groups: an analysis for the case of the electrostatic potential of formamide (Bonaccorsi *et al.*, 1972a) can be found in a recent paper (Bonaccorsi *et al.*, 1976b).

D. Derivatives of Ammonia and Water

In the ammonia molecule the addition of V_{l_N} to the electrostatic potential of three σ_{NH} has the effect of deleting the negative zone on the side of the hydrogens and of reducing the depth of the negative minimum near the lone pair. This is a direct conclusion and does not require further comment. When hydrogens are substituted by other N—R groups, their effect on the depth of the minima of V near N is due to the difference of the positive contribution such groups give in this region with respect to the analogous positive contribution of σ_{NH}. Substitution of an NH group by NCH_3 increases the minimum of V by about 6 kcal/mole [the minima are -85.5 for NH_3, -79.6 for NH_2CH_3, -72.8 for $NH(CH_3)_2$, and -66.7 for $N(CH_3)_3$ (Bonaccorsi *et al.*, 1976a)]. The effect of the NCH_2CH_3 group is about 2 kcal/mole lower than that due to the methyl group. If one compares the difference of the minima between NH_3 and $NH_2C_2H_5$ and that between CH_4 and $CH_3C_2H_5$, one can see that the transferability of the electrostatic potential of the C_2H_5 group is assured within 0.2 kcal/mole.

In water and its derivatives, the oxygen atom has two lone pairs that can be alternatively described as two sp^3 hybrids or as a sp^2 hybrid and a pure π-orbital. The models respect the substantial equivalence of the two descriptions. The effects of the substituent groups in alcohols and ethers are similar to those shown for the case of primary and secondary amines and do not deserve further discussion.

E. Influence of the Nuclear Conformation on the Shape of V

The changes of V due to rotations around single bonds are fairly well reproduced by the transferable group models. An example is given by the glycine molecule where changes of V due to rotations around the $N_1—C_2$, $C_2—C_3$, and $C_3—O_5$ bonds are accounted for within a few kilocalories per mole on a large portion of the entire set of rotational angles. Variations of V due to changes in geometry corresponding to variations of bond angles can be reproduced, at least semiquantitatively, by the transferable models.

The problem is different if one looks at changes in geometry corresponding to more drastic rearrangements of the electronic cloud. A typical example is given by the diimide molecule [V maps of diimide can be found in Merényi *et al.* (1973) and in Bonaccorsi *et al.* (1976b)]. For this molecule there exist two stable geometries:

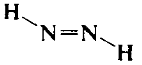

(I)

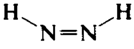

(II)

The group potential models for l_N, σ_{NH}, σ_{NN}, and π_{NN} account for the absolute value of the minima of V in the two molecules within 6 kcal/mole and for their difference (which is of $\simeq 10$ kcal/mole) within 0.5 kcal/mole (Bonaccorsi *et al.*, 1976b). If one considers the rotational path connecting I to II [there is also an inversional path (Baird and Swenson, 1973; Cimiraglia *et al.*, 1977)], the foregoing group models are not able to reproduce the shape of V at the top of the barrier for the obvious reason that at such geometry the π-bond is broken. Another example is given by the occurrence of nuclear conformations corresponding to a specific intramolecular interaction, for example, an intramolecular hydrogen bond. In the glycine molecule, these interactions are particularly strong in some configurations of the zwitterionic form and in such cases the difference between the exact SCF and the model potential can be larger than 10 kcal/mole. The situation is not too different from the case of an intermolecular hydrogen bond: we show in Fig. 13 the potential map of a formamide dimer obtained by using (a) the SCF wavefunction of the dimer

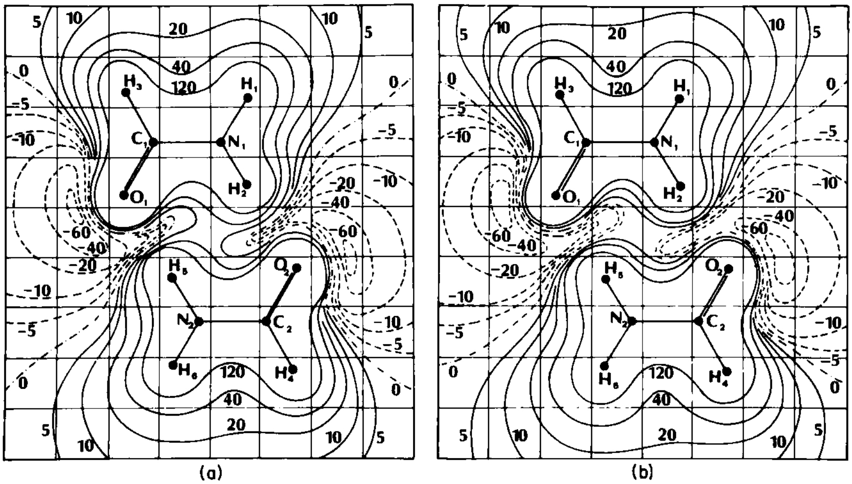

Fig. 13. A comparison of the in-plane map of *V* for a geometry of the formamide dimer calculated (a) by the STO-3G SCF wavefunction of the dimer and (b) by using transferable localized orbital models (from Bonaccorsi *et al.*, 1977). (Reprinted with permission from the Journal of the American Chemical Society. Copyright by the American Chemical Society.)

and (b) the rigid group potential models. The deviations between the two calculations are confined to the regions of the two hydrogen bonds, whereas in the other portions of the space the electrostatic potential maintains a reasonable degree of transferability.

In concluding this section, we would like to stress that these dissections of *V* have mainly an euristic value. The image of *V* given by the STO-3G models of the group potentials are far from completely realistic: first, the basis set is quite poor and the results one may obtain in such a way are valid at the most for comparisons; and, second, the transferability is not complete. Moreover in many cases the interest of the researcher is directed to examine and to rationalize not only the changes due to the direct effect of the other groups of the molecule (which are accounted for, at least partially, by the transferable models) but also the changes due to the mutual polarization of the groups inside the molecule (which are completely discarded by the transferable models).

IV. Electrostatic Potential and Chemical Reactivity

In Section I, D it was shown how the electrostatic potential can be related to one of the terms of the partition of the interaction energy between two molecules A and B. The relative importance of this electrostatic term, E_{es}, changes when the distance (and the orientation) between A and B changes, and changes even more according to the type of reactive interaction one is considering. When at least one of the partners has a net charge or a large dipole moment, E_{es} will be the dominant term at large distances, and it is reasonable to suppose that in such cases E_{es} will determine the approach channel of the two partners. (We consider here, of course, reaction models in which the microscopic structure of the solvent does not play a fundamental role.) We are now interested in discussing the following questions: (*a*) Up to what distances does E_{es} continue to be the most important term? and (*b*) Are there reactions for which E_{es} gives a useful image of ΔE also at distances characterizing the final stages of the elementary reaction (the final product or the transition state)? By a *useful image* we mean an approximation sufficient to give reactivity (or stability) orderings for similar substrates in a given reaction and (or) semiquantitative type of information, at least, on the energetics and the geometry of each single elementary reaction.

It is not possible, of course, to give simple answers of general validity to the two questions we have just posed. The reason for this is due in part to the enormous variety of possible interaction types and in part to the limited amount of energy partition analyses thus far available even for the simplest interaction mechanisms. We are, therefore, compelled to reduce this discussion to quite a limited number of cases and to try to relate these cases to broader classes of reactive interactions. For this purpose we need a taxonomy that does not respect the usual classification of chemical reactions and which does not rely on a *post hoc* knowledge of the results of the interaction energy partition. A possible classification scheme useful for our rather specific point of view could be based on the changes in the internal geometry of A or B during the elementary reaction. We may consider three categories: (*a*) reactions in which the internal geometries of A and B are not significantly affected, (*b*) reactions in which a specific deformation of one of the two partners assumes a decisive meaning, and (*c*) reactions in which changes in geometries are complex and not amenable to simple rules.

a. Association reactions $A + B \rightarrow A \cdot B$, leading to the formation of van der Waals, charge-transfer, and hydrogen bond complexes, may be assigned to this first category. They represent typical examples of chemical interactions where no covalent bonds are formed or broken. This class of reactions can also include other reactions between Lewis acid–base couples with a progressive increase in the magnitude of the interaction energy: a limiting case is given by the primary protonation process $A + H^+ \rightarrow AH^+$, which in some cases (e.g. the gas-phase protonation of heterocycles) can be included in this category. Thus, in this first class there are reactions with low interaction energy (less than 10 kcal/mole) but also reactions with intermediate (~ 50 kcal/mole) or even large (> 100 kcal/mole) interaction energies. Of course, the number of reactions that can be included in this first class decreases as ΔE increases.

b. The second category of reactions partly overlaps the first one; for example, in a large number of protonation processes the changes of geometry play an important role. Typical examples of this second class are numerous electrophilic or nucleophilic substitution reactions which follow S_N2 or S_E2 mechanisms (for example the Walden inversion or the Friedel–Crafts substitution reactions) and the reactions of addition to a double bond. In such cases one can profitably look at distorted geometries of the substrate (or of both partners) in order to gain some information on the transition-state complex by a partition of the energy of the type shown in Section I. Obviously, this type of information relies on a *ceteris paribus* assumption and can be used only to rationalize the trend of the changes occurring in an intermediate transition state, which are due to chemical substitutions in the substrate or in the reagent.

c. A classification of reactions in terms of the entity of the geometry changes of reactants surely is not the best suited to give clearcut and completely satisfying definitions. Consequently, one has to put in this last class the remainder of chemical reactions that have not found their place in the first two classes. These will be reactions that proceed via mechanisms considered in class b as well as other whole classes (for instance the rearrangement and elimination reactions) where simultaneous and complex changes in several geometric parameters and remarkable electron distribution rearrangements occur. In these cases there is no single geometry that can be considered sufficiently representative of the elementary reaction.

The reasons for this particular scheme used in classifying chemical reactions should be evident to the reader who has followed our exposition. In the partitions of ΔE which we have discussed in Section I, changes in the internal geometries of the partners were not included. It is possible, however, to define analogous partitions also for distorted geometries provided that the two partners maintain a separate identity. In the electrostatic contribution the deformation of the internal geometry will correspond to a different shape of V_A (or of γ_B) from what it has in the undistorted geometry. Approximations to E_{es}, which can be straightforward for reactions of the first category, are probably still obtainable for reactions of the second one. One could look, for example, at the electrostatic potential of a substituted methanes CH_3X_i having the three hydrogens in a planar trigonal arrangement, to get information about the S_N2 reactions $Y + CH_3X_i \rightarrow CH_3Y + X_i$ or at the electrostatic potential of an aromatic compound, having an X—H group distorted at a pseudotetrahedral geometry to get information on the transition-state energy of an electrophilic substitution reaction.

The reliability of such information of course depends on the tacit assumption that the portion of the interaction energy responsible for the deformation of the geometry, which is not included in this scheme of approximation, behaves similarly in a set of related molecules. Our neglect of the deformation energy does not mean that it is not possible to develop electrostatic semiclassical procedures to get an approximate determination of such deformations. It is sufficient to recall here the interesting and promising investigations performed by Nakatsuji *et al.* (1973), Fukui *et al.* (1975), Karplus (1973), and others who in different ways calculate forces acting on the nuclei during a reaction making use of the Hellmann–Feynman theorem. A review of the methods employed and of the results thus far obtained would go beyond the limits for the present discussion that we established in Section I.

We do not have sufficient material to cover the rather ambitious classification put forward in the preceding pages. The examples concerning reactions of type b are at present scarce (see, for example, Politzer *et al.*, 1973; Politzer and Weinstein, 1975; Bertran *et al.*, 1975). We shall limit ourselves to a few classes of reaction of type a, chosen only on the basis of the available material.

A. Hydrogen-Bonded Complexes

The partition of the hydrogen bond energy according to the MO schemes discussed in Section I is at present well documented and the available material is sufficient to permit general assessments of the origin and characteristics of this particular type of reactive interaction. Some of these conclusions are summarized in a recent paper of Umeyama and Morokuma (1977).

For hydrogen bonds between electronegative atoms, such as N, O, F, and proton donor groups, such as FH, OH, NH, CH, in neutral molecules (with interaction energies of the order of 1–15 kcal/mole) the changes in the internal geometry of the partners are not essential. However, in ionic hydrogen bonds the changes of geometry can give a noticeable contribution to ΔE: typical cases are the complexes H_2OF^- and FHF^- where the contributions to ΔE due to changes in geometry of HF are, respectively, -3.1 and -7.2 kcal/mole (the overall value of ΔE in the two complexes is -41.7 and -62.7 kcal/mole with the 4-31G basis set) (Alagona *et al.*, 1978). A more detailed discussion for the FHF^- case, comprising an energy decomposition analysis for the entire reaction path and for a stretched geometry of HF can be found in a paper by Umeyama *et al.* (1975).

The decomposition of ΔE in "normal" hydrogen bonds shows that, at distances between the partners larger than that at equilibrium, the interaction energy is dominated by the E_{es} term. Near the equilibrium position the term numerically larger is E_{es}, followed by E_{ex}, which is of opposite

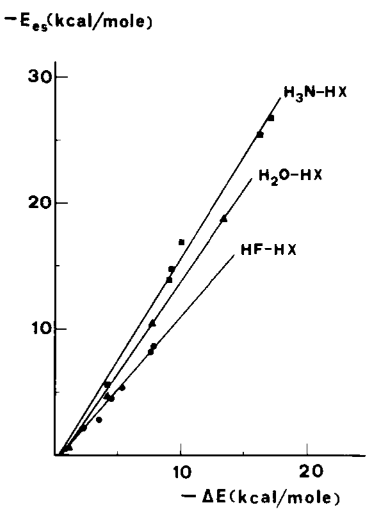

Fig. 14. Plot of E_{es} versus ΔE for some hydrogen-bonded complexes. Calculations with the 4-31G basis performed by Umeyama and Morokuma (1977) and by Kollman (1977).

sign. The other attractive terms (E_{pol}, E_{ct}) have in general a value that partially compensates that of the exchange term, and E_{es} alone represents a reasonable estimate (generally in excess) of ΔE. In Fig. 14, we compare plots of ΔE and E_{es} at the equilibrium distance, which are drawn from data published by Umeyama and Morokuma (1977) and by Kollman (1977). It is evident that within a given set of complexes having in common the proton acceptor (or the proton donor), the correlation between E_{es} and ΔE is sufficiently strict to permit one to consider E_{es} as a useful index for estimating the relative strength of this type of hydrogen bonds.

At shorter distances all contributions to ΔE become larger, and it is no longer possible to put a term in evidence as the dominant one.

In weak hydrogen bonds (for example, those whose proton donor group is CH), the results of the decomposition of ΔE are analogous, but near the equilibrium distance the charge-transfer term is also relatively important. The magnitude of E_{ct} does not change substantially in passing from strong to weak complexes, and its relative weight is larger when ΔE is lower.

For strong hydrogen bonds, involving ionic partners, the importance of E_{es} increases in the whole range of distances.

The conformational potential energy surface, which determines the directionality of the hydrogen bond and the other changes in the mutual orientation of the partners at the equilibrium distance, is essentially ruled by the electrostatic term alone.

This short resumé gives only the main results and it could be enriched with quantitative data. However, it is sufficient for our discussion to have established that for a good number of hydrogen-bonded complexes, it is possible to obtain from E_{es} useful information on the stabilization energy, on their conformation, and on the approach channels of the partners leading to the formation of the complex.

We recall that our goal of getting inexpensive and reliable approximations of E_{es} requires a suitable approximation of γ_B in terms of a set of point charges. This can be done in some cases when B is a small molecule. To this end, it is perhaps better to optimize directly the description of V_B given by such point charges rather than limit the optimization to the reproduction of the lowest electric multipoles of B. To save space, we do not report here actual examples of such an optimization and we limit ourselves to stating that it is possible to get point-charge representations of γ_B for molecules such as H_2O, NH_3, HF with a fairly limited number of charges that reproduce E_{es} to within 0.2–0.8 kcal/mole. Such errors does not change the quality of the correlation between E_{es} and ΔE (an example of which has been given in Fig. 14).

Point-charge representations of good quality can be obtained to simulate electronic distribution of molecules calculated with floating spherical Gaussian orbitals (FSGO) (Frost, 1967) according to the procedure proposed by Hall (1973; Tait and Hall, 1973; McCreery *et al.*, 1976; see also Shipman, 1975; Amos and Joffe, 1975). The Hall model consists of n charges equal to p_{ss} placed at the center of the FSGO χ_s, and of $2n(n-1)$ charges of value $2p_{st}S_{st}$ placed at the point corresponding to the center of the Gaussian resulting from $\chi_s \cdot \chi_t$ (p_{st} is an element of the bond order density matrix, and n is the number of FSGO employed in the calculations). The quality of the conformational curves obtainable either with our model or the Hall one can be appreciated by comparing the conformational energy curves for some formamide–water (Alagona *et al.*, 1973; McCreery *et al.*, 1976) and *N*-methylacetamide–water (Pullman *et al.*, 1974) complexes obtained by SCF calculation on the supermolecule and by using electrostatic models. We do not show here these curves, as they have been reproduced on many occasions.

The possibility of getting at a low cost conformational curves of hydrogen-bonded complexes not too far from the SCF ones could be exploited to get a first approximation estimate of the change of the Gibbs free energy ΔF^0 in the association reaction $A + B \rightarrow AB$. The only example we know of this kind of application was performed by using minimal basis set approximations of V_A and γ_B (Alagona *et al.*, 1972). An error analysis showed that in that case the largest source of error was given by the low quality of the SCF curves (and not by the electrostatic approximation that reproduces these curves): the values of ΔF^0 that are obtainable can be used only for comparing the relative stability of similar complexes. The thermodynamic stability of the complexes can be quite different from the value of ΔE. In two complexes of aziridine with water,

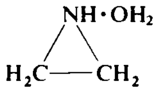
(I)

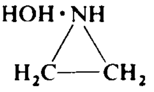
(II)

having H_2O attached in I to the NH bond and in II to the N lone pair, ΔF is -0.05 and 1.42 kcal/mole, whereas ΔE is -7.3 and -7.1 kcal/mole.

Of wide interest is the problem of the interaction of a solute A with water in aqueous solutions. We shall summarize briefly some approaches to this problem that hinge on the electrostatic approximation. The first concerns an investigation at present under way in our laboratory in collaboration with Clementi. The statistical description of solutions (Clementi, 1976) requires, as a first step, the determination of a simple analytical expression of the pair energy for $A \cdot H_2O$ ($\Delta E_{A \cdot H_2O}$), to be used in subsequent Monte Carlo calculations. Such analytical expression must be valid for a large range of distances and for all mutual orientations of A and H_2O. The starting point consists in the computation of ΔE for the supermolecule at a rather generous number of geometries. The analytical expression must minimize the deviation between the set of the SCF values of ΔE and the set of the corresponding values calculated with the analytical expression. It has been found (Carozzo *et al.*, 1977) that such deviations assume decidedly lower values if one extracts and treats separately the E_{es} term and then uses a function built up in terms of atom–atom interactions to fit the residue $\Delta E - E_{es}$. In the zwitterionic forms of glycine and serine, the electrostatic term represents on the average more than 80% of the pair potential (see Table I, where the conformations of the amino acids are denoted according to the standard convention) and the corrections are confined to the region of the short distances.

The supermolecule approach has been coupled to the continuous description of the solvent by McCreery *et al.* (1976) who distinguish between microscopic and macroscopic effects. The effects of the first type concern the interaction of A with specific molecules of water and are treated with the electrostatic representation outlined in the foregoing. Effects of the second type are again dealt with an electrostatic treatment consisting in a calculation of $\frac{1}{2} \int V(r)\rho(r)\,dr$, where $\rho(r)$ is the charge distribution inside a spherical cavity arising from A and from a few H_2O molecules directly bound to A through hydrogen bonds, and $V(r)$ is the electrostatic potential felt by such charges (including also the terms due to the polarized solvent).

TABLE I

MEAN PERCENT DEVIATION OF THE ELECTROSTATIC INTERACTION ENERGY WITH RESPECT TO THE TOTAL SCF INTERACTION ENERGY BETWEEN A WATER MOLECULE AND A MOLECULE OF GLYCINE OR SERINE IN THEIR ZWITTERIONIC FORMS

Amino acid conformation	Mean deviation (%)[a]		
Gly (0, 0)	10.2	12.1	18.6
Gly (60, 0)	14.4		
Ser (0, 0, 180, 0)	19.3	23.9	
Ser (0, 0, 300, 120)	26.8		
Ser (60, 0, 300, 180)	25.8		

[a] These values refer to calculations performed with a minimal basis of contracted Gaussians. The conformational angles (ϕ, ψ) for glycine and (ϕ, ψ, χ', χ'') for serine have been defined according to the convention of Edsall *et al.* (1966). The percent deviation refers to fifty geometries of the complex $M \cdot H_2O$ for each conformation of the amino acid (Corongiu, 1976).

Another technique, put forward by Yamabe *et al.* (1973), consists in performing *ab initio* computations on the solute in presence of a solvent simulated by point dipoles. The interaction energy is thus given by an approximation of E_{es} implemented by a portion of E_{pol} (the polarization of A inside the solute).

Yet another method has been proposed by Noell and Morokuma (1976). The water molecules are represented by a fractional charge model (Noell and Morokuma, 1975) with charges placed on the nuclei. The method allows for an *ab initio* evaluation of E_{es} of A, the solvent of which takes into account the conformational aspects of the solute–solvent interaction and for a partial evaluation of E_{pol} (the polarization of the solute by the solvent).

Returning now to the general argument of the hydrogen bond energies, it may be remarked that all the approximations to E_{es} we have thus far examined rely on an approximate description of γ_B. Kollman *et al.* (1975) made the proposal of using V_A directly as an empirical index to predict the value of ΔE_{AB}. The justification is purely empirical and consists in remarking that, for a set of twelve hydrogen-bonded complexes between first- and second-row hydrides of the type $YH \cdot\cdot NH_3$ and $X \cdot\cdot HF$, the best correlation between ΔE and a specific quantity of the isolated molecule (dipole moment, Mulliken populations, etc.) has been found with the value of V_{YH} and V_X at a given fixed distance from the molecule. We give in Fig. 15 the data employed by Kollman to determine such empirical

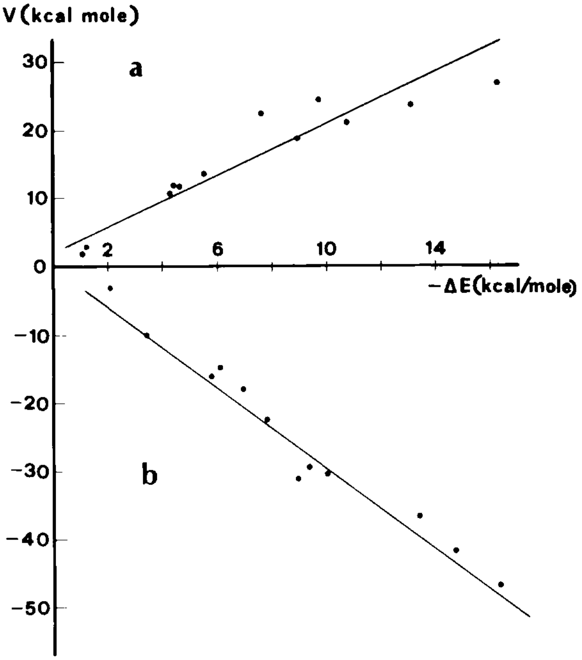

Fig. 15. Plot of V at a selected distance from the proton donor X—H (curve a) or from the proton acceptor Y (curve b) versus ΔE in hydrogen-bonded complexes $XH \cdot NH_3$ and $X \cdot FH$ (Kollman *et al.*, 1975). (Reprinted with permission from the Journal of the American Chemical Society. Copyright by the American Chemical Society.)

relationships, together with the corresponding best least-squares lines: the r^2 value is better in the case of the $X \cdot HF$ complexes than in the case of the $YH \cdot NH_3$ ones. In the same paper, Kollman proposes a simple rule to predict $\Delta E_{X \cdot HY}$ for complexes that do not involve either HF or NH_3, on the basis of the knowledge of V at a given fixed point. Such a rule, which relies on the assumption that it is possible to approximate $\Delta E_{X \cdot HY}$ with a product of two functions, $f(X) \cdot g(HY)$, gives reasonable approximations to ΔE for a large variety of complexes including also π-complexes, but fails when the proton donor is the CH group.

As a last point in this discussion of the hydrogen bond, we mention an interesting and important paper by Allen (1975). We cannot discuss in detail his simple model of the hydrogen bond which aims to give a rationale not only of ΔE but also of other properties such as charge transfer, directionality, stretching force, and IR intensity enhancement. The model is characterized by three monomer quantities, μ_{YH}, the YH bond dipole; ΔI, the difference between the first ionization potentials of the electron donor X and of the corresponding noble gas atom; l, the length of the hydrogen-bonding lone pair. Allen remarks that there exists a close relationship not only between μ_{YH} and V_{NY}, but also between $\Delta I/R_{XY}$ (or $I - I_0$) and V_X. The electrostatic potential appears again as a useful tool for the interpretation of the hydrogen-bonding processes.

B. Other Noncovalent Complexes

The van der Waals and the charge-transfer complexes suggest by their very name what should be the main causes of their stability. Recently, Kollman (1977) extended the analysis of the partition of ΔE (calculated in the SCF approximation) to more than eighty dimers and trimers including van der Waals molecules, charge-transfer complexes, ionic associations, and radical complexes. By coupling Morokuma's (1971) analysis of ΔE to the examination of V of the two partners, Kollman built up a model that allows one to predict semiquantitatively the interaction energy and the geometric structure of such complexes. To this end, an improved version is used (which takes into account also the shape of V in determining the geometry of the complex) of the method proposed by Kollman *et al.* (1975) and discussed in the preceding section. We report in Table II a selection of results, sufficiently representative both for the type of complexes considered in this paper and for the errors in the predictions (which are in some cases quite large). Taking into account the large variety of molecular systems considered in this analysis, the exploratory character of this interesting paper is evident. The exceptions to a simple model relying exclusively on the utilization of V deserve a more detailed examination, and final assessments of the applicability of such very simple models to the whole field

TABLE II

COMPARISON BETWEEN THE VALUES OF ΔE OBTAINED FROM SCF CALCULATIONS ON THE SUPERMOLECULE AND THOSE PREDICTED ON THE BASIS OF THE VALUE ASSUMED BY V AT A GIVEN POINT[a]

Complex	ΔE (SCF 4-31G) (kcal/mole)	ΔE (from V) (kcal/mole)
$Cl_2 \cdot Cl_2$	−0.2	−0.1
$O_2C \cdot OH_2$	−5.6	−4.7
$H_3N \cdot SO_2$	−11.4	−11.5
$F^- \cdot H_2O$	−39.3	−30.2
$Li^+ \cdot OH_2$	−47.2	−62.9
$H_4N^+ \cdot F^-$	−163	−186
$F \cdot HF(^2\pi)$	−1.2	−0.9

[a] Data taken from Kollman (1977).

of noncovalent interactions require further exemplifications and further checks (including also the influence of the basis set).

A whole set of papers has been devoted by Morokuma and co-workers to the examination of the interactions involved in electron donor–acceptor (or charge-transfer) complexes (Lathan and Morokuma, 1975; Lathan *et al.*, 1975; Umeyama and Morokuma, 1976b; Umeyama *et al.*, 1977). We give in Table III a synopsis of the partition of ΔE (at the equilibrium geometry) for some molecules studied in this series of papers. The table gives only a small portion of the valuable information one may obtain from this investigation (other topics are the analysis of the electronic charge distribution, the evaluation of the relative importance of the dispersion terms, the basis effects, the trend of the components of ΔE in function of the distance and orientation of the partners, etc.), but it is sufficient to show that even in such complexes there is a fairly linear relationship between ΔE and E_{es}. In addition, the electrostatic contribution is responsible for the mutual orientation of the partners near the equilibrium geometry. The MO analysis of ΔE [in the Kitaura and Morokuma (1976) version] allows one to classify such complexes according to the importance of the various contributions to ΔE at the equilibrium geometry (see the last column of Table III) and opens the way to a better understanding of these interactive processes. It should be stressed that some of the components of ΔE are more sensitive to the basis-set characteristics than ΔE itself and that the results thus far obtained should be verified by using other basis sets. The general impression, however, is that the main aspects of the question have been correctly evidenced and that further checks will lead only to minor corrections to this picture.

C. Interactions with Protons and Other Cations

Another type of reaction that has been studied in some detail concerns the interaction between a neutral molecule A and a cation B^+ to give AB^+. We shall devote more attention to the ions H^+ and Li^+ for which there exists a larger number of partitions of ΔE.

The results of the partition of ΔE are notably different from those of the noncovalent complexes and differ also among themselves according to the nature of B^+.

In the proton case, the maps of V give directly the electrostatic contribution to ΔE. At the equilibrium distance, E_{es} is only a fraction of the whole interaction energy because the polarization and charge transfer effects are far larger than in the preceding cases. A certain capability to distinguish among alternative protonation sites in a given molecule has been widely evidenced in other papers where the polarization term can be considered approximately constant (Scrocco and Tomasi, 1973; Pullman, 1973). We will indicate here

TABLE III

Energy Components at the Optimized Intermolecular Separation R_e and Qualitative Classification of Some Electron Donor-Acceptor Complexes[a]

Donor-acceptor	Type	R_e (Å)	ΔE (kcal/mole)	ES (kcal/mole)	EX (kcal/mole)	PL (kcal/mole)	CT (kcal/mole)	MIX (kcal/mole)	Classification
H_3N-BF_3	n-σ^*	1.60	−71.5	−142.3	136.3	−42.7	−52.7	29.9	Strong ES
H_3N-BH_3	n-σ^*	1.70	−44.7	−92.9	86.9	−17.2	−27.1	5.6	Strong ES
OC-BH_3	σ-σ^* π^*-π	1.63	−28.5	−60.9	98.9	−61.8	−68.3	63.6	Strong CT-PL-ES
H_3N-ClF	n-σ^*	2.72	−8.2	−11.2	7.4	−1.1	−3.6	0.2	Intermediate ES
H_2O-$OC(CN)_2$	n-π^*	2.70	−8.0	−9.7	4.4	−1.0	−1.8		Intermediate ES
HF-ClF	n-σ^*	2.74	−3.4	−3.6	1.8	−0.2	−1.4	0.1	Weak ES
H_3N-Cl_2	n-σ^*	2.93	−2.9	−4.0	3.9	−0.8	−2.3	0.3	Weak ES-CT
H_3N-F_2	n-σ^*	3.00	−1.1	−0.8	0.6	−0.3	−0.6	0.0	Weak ES-CT
H_2CO-F_2	n-σ^*	2.91	−0.7	−0.4	0.3	−0.1	−0.5	0.0	Weak CT-ES-DISP
H_2CO-C_2H_4	π-π^*	3.75	−0.7	−0.5	0.4	−0.1	−0.5		Weak CT-ES
F_2-F_2	n-σ^* π-σ^*	2.7	−0.2	−0.1	0.3	0.0	−0.4	0.0	Weak DISP-ES

[a] This table is taken from Umeyama *et al.* (1977). The results refer to 4-31G calculations, and the partition of ΔE has been performed according to the scheme of Kitaura and Morokuma (1976).

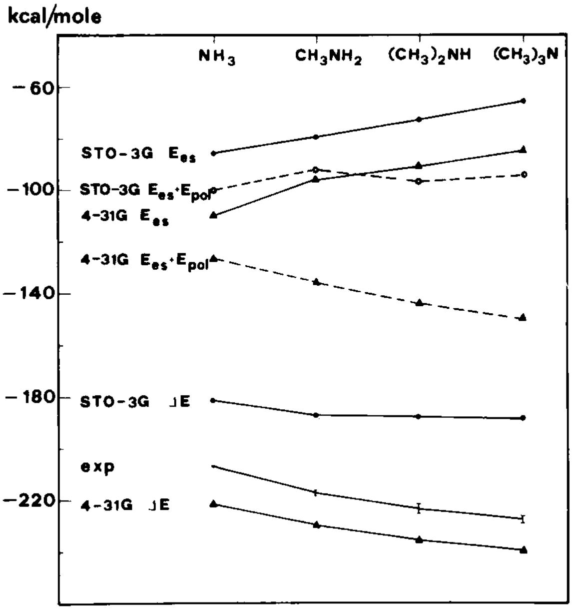

Fig. 16. Trends for ΔE, E_{es}, and $E_{es} + E_{pol}$ in the protonation process of ammonia and methyl derivatives according to STO-3G and 4-31G calculations (Bonaccorsi *et al.*, 1976a; Umeyama and Morokuma, 1976a).

the limitations of such previsions. In Fig. 16, we report trends for V and ΔE in the first terms of the series of the aliphatic amines according to STO-3G and 4-31G calculations (Pullman and Brochen, 1975; Bonaccorsi *et al.*, 1976a; Umeyama and Morokuma, 1976a; Kollman and Rothenberg, 1977) and compared with experimental values (Aue *et al.*, 1972; Henderson *et al.*, 1972; Briggs *et al.*, 1972). The ΔE values of the 4-31G calculations reproduce well the trend of the experimental proton affinities (PA's) and also the STO-3G ΔE values give a passable prediction of such a trend. In both bases the E_{es} values represent less than a half of the total interaction energy and, moreover, the trend of the E_{es} values is exactly opposite to that of the experimental PA's. It is clear that the erroneous predictions one could get from the electrostatic term is not due to spurious effects arising from the limited nature of the basis set in evaluating V, because the E_{es} values run almost parallel in the two sets of calculations. The gradual substitution of H atoms with CH_3 groups increases the number of polarizable electrons with the consequent effect of increasing the value of E_{pol}. In fact, $E_{es} + E_{pol}$ in the 4-31G basis reproduces the trend of the PA's quite well. The STO-3G basis gives more ambiguous results and one should conclude (on the basis of these results alone) that the charge-transfer effects are essential in determining the correct trend. This example illustrates what was said above, i.e., that the components of ΔE are more basis dependent than ΔE itself (or than V).

One could ask why we have considered the collective contribution $E_{es} + E_{pol}$ instead of the $E_{el} + E_{ct}$, E_{ct} being numerically larger than E_{pol}. The main reason is that the correlation of $E_{el} + E_{ct}$ with the experimental values is not very good: the contribution that determines the correct trend is just E_{pol}. This evidence [which is valid also for similar sets of compounds, such as the aliphatic alcohols and ethers (Umeyama and Morokuma, 1976a), and the nucleic acid bases (Pullman and Ambruster, 1977)] is to a certain extent gratifying because E_{pol} can be obtained, as well as V, from the isolated molecule relying only on the subspace spanned by the functions of A. We shall return later to this topic.

A second example concerns the proton affinity of the glycine anion. In the V map of the glycine anion shown in Fig. 1d, there are five minima that may be intuitively connected to five different preferential sites of protonation.

TABLE IV

COMPARISON OF THE PROTONATION ENERGY OF THE GLYCINE ANION IN DIFFERENT SITES WITH THE VALUE OF V AT THE FINAL LOCATION OF THE PROTON AND WITH THE MINIMA OF THE ELECTROSTATIC POTENTIAL OF $H_2N—CH_2—COO^-$[a]

Site[b]	Protonation energy (kcal/mole)	V (kcal/mole)	V_{min} (kcal/mole)
1	−473	−210	−225
2	−476	−226	−236
3	−475	−225	−236
4	−478	−241	−245
5	−395	−205	−229

[a] The identification of the sites can be performed on the basis of Fig. 1d where the values of V_{min} are reported.

[b] Sites 1–4 refer to protonations of the $—CO_2^-$ group, site 5 refers to protonation of the $—NH_2$ group.

We report in Table IV the proton affinities (calculated with a STO-3G basis), the values of V at the final positions of the proton, and the minima of V taken from the map in Fig. 1d. In this case, too, V is less than a half of the total interaction energy, but in the first four cases (which concern the protonation of the anionic head $—CO_2^-$) there exists a fairly linear relationship between the electrostatic and the total interaction energy. In this case, the variations of E_{pol} in the different protonation processes are much smaller than in the preceding example.

In the last protonation process of Table IV, which concerns the protonation of the $-NH_2$ group, there is a different ratio $E_{es}/\Delta E$. The main reason for this difference is due, not so much to changes in E_{pol} and E_{ct}, which are indeed present, as to the effects of the geometry rearrangements, which are larger and internally consistent in the first four cases, where the final product has a

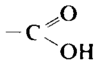
$-C(=O)OH$

group, with respect to the last one, where the anionic head $-CO_2^-$ remains unchanged.

In a set of molecules with a more rigid geometry and a comparable number of electrons, linear relationships between V and ΔE for protonation of different chemical groups are better respected. In Fig. 17, we compare V

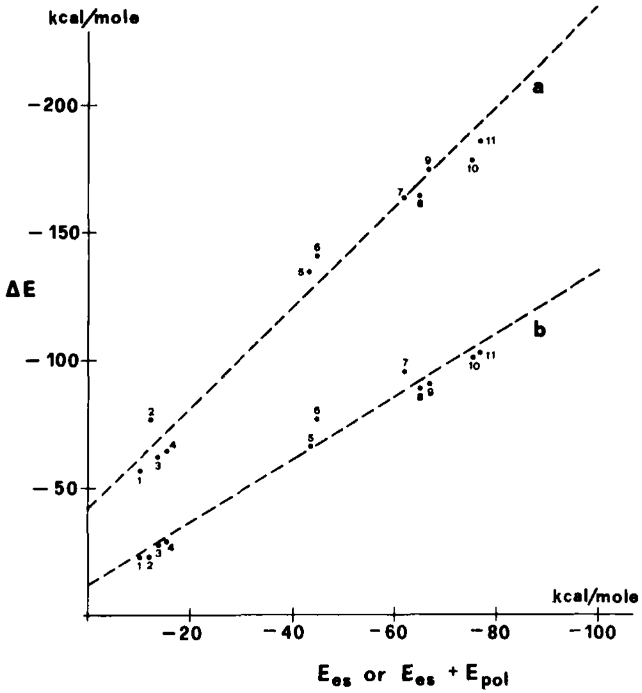

Fig. 17. Plot of ΔE versus E_{es} (curve a) and versus $E_{es} + E_{pol}$ (curve b) for the protonation processes of some three-membered ring compounds; STO-3G calculations (Ghio and Tomasi, 1976).

and ΔE for a set of three-membered rings obtained with a STO-3G basis set (Ghio and Tomasi, 1973) which leads us to conclude, in addition, that the inclusion of E_{pol} does not improve the correlation with ΔE in this case.

From the few examples we have reported it appears that the electrostatic potential does not always represent an index sufficient for the protonation processes. In many cases one may get better results by including also the polarization term in the calculation.[2] A review of the methods proposed and actually employed to evaluate the molecular polarizability cannot be attempted in the present paper, and we confine ourselves to drawing the reader's attention to two practical methods that give approximations of E_{pol} by using the same wavefunction employed to calculate V, allowing thus the adding of quantities obtained at a comparable degree of precision. The first method, proposed by Bartlett and Weinstein (1975), is related to a perturbative expansion simpler than that outlined in Section I (small overlap approximation; Murrell *et al.*, 1965). This perturbative method is extended (by the inclusion of a double perturbation series) to cover the important problem of the simultaneous attack of two point charges, or of a point charge plus a second molecule (Chang *et al.*, 1976), on a molecule containing several reactive sites. This method is readily applicable and, in spite of the limitations imposed by the perturbation techniques, gives useful and interesting results.

The second method, developed in our laboratory (Bonaccorsi *et al.*, 1976a), arrives at an analytical expression of a quantity, $P_A(\mathbf{k})$, which can be directly associated with $V_A(\mathbf{k})$ to give, by means of the expression $qV_A(\mathbf{k}) + q^2 P_A(\mathbf{k})$, the sum of E_{el} and E_{pol} for the interaction with the point charge q. This analytical expression of $P_A(\mathbf{k})$ is valid for all the outer molecular space of A with errors less than 0.4 kcal/mole. The method of obtaining P_A consists in fitting with a suitable expression the results of the SCF values of E_{pol} calculated for a few selected points.[3] The computation time necessary to arrive at maps of $P(\mathbf{k})$ is of the order of $2t$, where t is the time of the normal SCF calculation for one geometry of A.

The interaction with H^+ constitutes a limiting case in the family of the interactions of A with a cation: in most of the examples we have considered in the preceding the protonation process leads to the formation of normal covalent bonds. The interaction of Li^+ with neutral closed-shell molecules gives rise, in most of the cases, to the formation of an adduct, which

---

[2] The charge-transfer term becomes probably more important when one is interested in comparing proton reactivities of different chemical groups, for example, of amines with ketones.

[3] The analytical expression we have chosen has the form of a segmental expansion of the polarizability tensor interacting with charge q placed at point k. Such tensors are located on the charge centers of the localized bonds and lone pairs.

resembles more closely the complexes considered in the preceding sections. The partition of ΔE shows that the charge-transfer term is mostly lower than in the protonation process (this is due to the difference of electronic affinity of Li^+ with respect to H^+) and that at the equilibrium distance the interaction is dominated again by the electrostatic term. We list a few data in Table V to give an idea of the magnitude of the various terms: more details concerning the basis-set dependency of such partitions can be found in a review paper of Schuster *et al.* (1975) who carefully discusses all the available computational data on the interaction between a small ion and the molecules of a solvent (H_2O, NH_3, H_2CO, etc.).

TABLE V

PARTITION OF THE SCF INTERACTION ENERGY OF A FEW $A \cdot Li^+$ COMPLEXES

Energy components	$H_2CO \cdot Li^{+a}$ (kcal/mole)	$H_2O \cdot Li^{+b}$ (kcal/mole)	$H_2O \cdot Li^{+c}$ (kcal/mole)	$(H_2O)_4 \cdot Li^{+d}$ (kcal/mole)
ΔE	−44.0	−43.0	−47.9	−163.7
E_{es}	−39.8	−52.0	−51.1	−151.2
E_{ex}	+9.6	+15.1	+12.7	+8.0
E_{pol}	−13.8[e]	−9.8	−7.8	−19.3
E_{ct}		+3.8	−1.7	−1.2
$R_{O \cdot Li}$(Å)	1.8	1.8	1.80	2.02

[a] Pullman and Schuster (1974); basis set (9, 5/9, 5/7, 1/4) contracted [5, 3/5, 3/3, 1/3].

[b] Schuster *et al.* (1975); same basis set as in footnote *a*.

[c] Kollman (1977); basis set 4-31G (and 5-21G for Li^+).

[d] Noell and Morokuma (1976); same basis set as in footnote *c*.

[e] The terms E_{pol} and E_{ct} are collected together.

Also the interaction of Be^{2+} and Na^+ with neutral molecules gives rise to the formation of complexes that show a similar pattern of the interaction energy decomposition. We show in Table VI a few examples referring to Be^{2+} taken from a paper of Kollman [1977; see Schuster and Preuss (1971) for a different opinion on the $H_2O \cdot Be^{2+}$ complex]. Similar considerations can be extended to other light cations. We confine ourselves to quoting here a dissection of the complex $H_2O \cdot Na^+$ obtained with a (13s, 8p, 1d/9s, 5p/4s) basis set contracted to [7s, 4p, 1d/5s, 3p/3s] (P. Schuster, H. Lischka, and A. Beyer, private communication, 1976): $\Delta E = -27.4$, $E_{es} = -30.3$, $E_{ex} = 15.3$, $E_{pol} = -12.8$, $E_{ct} = 5.2$ kcal/mole, $R_{ONa} = 2.25$ Å.

The paramount importance of the interactions between metallic cations and biomolecules in the life processes (a recent Jerusalem Symposium on Quantum Chemistry and Biochemistry was devoted to this subject, and

TABLE VI

PARTITION OF THE SCF INTERACTION ENERGY ΔE FOR A FEW $A \cdot Be^{2+}$ COMPLEXES[a]

Energy Component	$H_2O \cdot Be^{2+}$ (kcal/mole)	$NH_3 \cdot Be^{2+}$ (kcal/mole)	$N(CH_3)_3 \cdot Be^{2+}$ (kcal/mole)	$H_2NCO \cdot Be^{2+}$ (kcal/mole)
ΔE	−143.7	−164	−191	−197
E_{es}	−124.9	−158	−138	−130
E_{ex}	+28.4	+48	+48	+35
E_{pol}	−44.7	−49	−110	−119
E_{ct}	−2.49	−5	+8	+16
R_{X-Be}(Å)	1.59	1.64	1.64	1.48

[a] Data taken from Kollman (1977); 4-31G basis set.

many relevant papers have been presented at the Sanibel Symposia on Quantum Biology) leads us to suppose that the research actually under way in different laboratories [we refer in particular to the work of the Pullman group (A. Pullman and Pullman, 1975; B. Pullman *et al.*, 1977), and references quoted therein] will shed more light in the near future on the importance of the electrostatic contributions to such processes.

D. Chemical Interactions in Bio-organic Systems

We now add a short digression on the molecular interactions in bio-organic systems. Among the fairly wide variety of reactions that constitute the biochemical cycles or the response of a living organism to a drug, we confine our attention to the highly specific noncovalent interactions between an organic substrate and a portion of a large biomolecule (for example, the receptor of an enzyme). The detailed study of such interactions, from the experimental as well as from the theoretical point of view, constitutes a formidable task, and the contribution that the electrostatic potential may make is certainly modest but not to be discarded *a priori* as irrelevant.

From a microscopic point of view, these interactions must be considered, because of the high specificity of the interaction and of the large dimension of one partner at least, as a situation different from interactions between two small partners, which we have considered in the preceding sections, and from the interactions occurring in free solutions. The change in conformation of the partners presumably plays an important role, and in general information is lacking not only on the actual conformation of the receptor but also on its chemical constitution. The asymmetrical presentation given in Eq. (13) of the electrostatic interaction energy expression may be exploited to infer some information on the process in a devious way. By comparing the shape assumed by the electrostatic potential of different substrates S in different plausible conformations, one may hope to gain some information on the shape of the unknown receptor charge-density distribution γ_R that optimizes the value of

$$E_{es} = \int V_S(\mathbf{r})\gamma_R(\mathbf{r})\,d\mathbf{r}. \qquad (26)$$

In the few cases where the available information on the enzyme is sufficient, one may calculate the electrostatic potential of the enzyme, V_R, and explore the region where the substrate molecule fits better (see Hayes and Kollman, 1976, for the case of carboxypeptidase A). We do not intend to discuss here the considerable number of papers and the further elaborations of this simple approach that have followed the first attempts in this direction (Weinstein *et al.*, 1974; Petrongolo and Tomasi, 1974). This subject deserves in fact a more specific review, and we consider it sufficient to have pointed out that the electrostatic picture of the enzyme–substrate interactions may be a significant step toward the understanding of these processes which are so important from a speculative as well as from a practical point of view.

V. Electrostatics and Effect of a Lattice Field on Properties of a Molecular Ion

In Section IV we touched in passing on two kinds of interactions that may be classified under the heading "environmental effects," namely the interactions of a solvent with a solute and of an enzyme with a substrate. In this section we consider a third type of environmental effect, namely, that due to the interactions among molecular ions within a crystal. We shall pay more attention to the influence that the electrostatic field has in modifying the electronic distribution of an ion and, hence, of its one-electron properties, than to an electrostatic description of the interaction energy (the cohesion energy of the crystal).

In molecular crystals it is possible to put down a series of approximations starting from the exact wavefunction of the entire crystal and terminating in some steps analogous to those we discussed in Section I.

1. A completely antisymmetrized wavefunction expressed in terms of one-determinant wavefunctions of the constituting chemical entities L:

$$\psi_{\text{cryst}} \simeq A \prod_{\mathrm{L}}^{\infty} \psi_{\mathrm{L}}. \qquad (27)$$

2. A wavefunction of the same type but without the antisymmetrizer A, which allows for exchange of electrons between different ions:

$$\psi_{\text{cryst}} \simeq \prod_{\text{L}}^{\infty} \psi_{\text{L}}. \tag{28}$$

3. A wavefunction expressed in terms of the one-determinant wavefunctions of the isolated ions:

$$\psi_{\text{cryst}} \simeq \prod_{\text{L}}^{\infty} \psi_{\text{L}}^{0}. \tag{29}$$

Wavefunctions (27), (28), (29) constitute a generalization of the approximate expressions (3), (2), (1) of a dimer wavefunction employed to define the MO partition of ΔE.

In ionic crystals the series of approximations leading to Eq. (28) is acceptable because the overlap between the component ions of the crystal is in general small (less than 0.005 in the $NaNO_2$ case, which we shall discuss later in more detail). In other terms exchange and charge-transfer effects can be safely discarded in this type of crystal.

Approximation (28), which takes into account the mutual polarization effects, corresponds to the use of effective Hamiltonians of the type:

$$H_{\text{eff}}^{\text{K}} = H_{0}^{\text{K}} + \sum_{\text{L} \neq \text{K}}^{\infty} V_{\text{L}}, \tag{30}$$

where H_0^{K} is the Hamiltonian of the free ion K, and V_{L} is the electrostatic potential generated by another ion of the crystal. Potential V_{L} depends on the charge distribution γ_{L} [see Eq. (14)] which may be approximated by means of a suitable set of fractional point charges selected according to the methods discussed in Section IV, A.

Approximation 3 corresponds to a simple electrostatic picture that can be used to get an appreciation of the Madelung constant (Julg and Létoquart, 1976) and of other quantities like the conformational energy inside the crystal (see, for example, Hullen and Kane, 1974; Smith *et al.*, 1977), but it cannot give a representation of the environmental effects of the crystal lattice on the properties of the ion K.

The use of rigid models of γ_{K} in Eq. (30) implies that only a portion of the polarization effects can be accounted for, i.e., the polarization of K due to the other ions L of the lattice, whereas the reverse polarization of the lattice is neglected. Such approximation has been employed for investigations on the electron charge redistribution within K and on the deformation of the geometry of K inside the crystal (Ghio, 1969; Almlöf and Wahlgren, 1973) and has been extended also to crystals with noncharged components (Almlöf *et al.*, 1972, 1973a; Noell and Morokuma, 1976). In the last case, attention must be paid to the occurrence of specific intermolecular interactions (hydrogen bonding, formation of charge-transfer complexes) that may introduce local charge-transfer or exchange effects.

We shall consider here in more detail some specific points related to the use of the effective Hamiltonian (30), namely the effect of the substitution of a SCF-LCAO representation of γ_L in the V_L terms of Eq. (30) by point-charge models, the influence of the relative validity of such point-charge models on the final results, the effects due to the truncation of the infinite sum in the Hamiltonian, and the effects of the mutual polarization of the ions inside the crystal. To this end we shall resort to calculations performed on a specific crystal, the ferroelectric phase of $NaNO_2$ (Ghio *et al.*, 1976).

We may focus our attention on the NO_2^- ions, neglecting the lattice effects on the less polarizable Na^+ ions. For the description of the crystal field acting on the nitrite ion chosen as central one we shall consider three models for $\gamma_{NO_2^-}$, composed of (*1*) a one-unit negative point charge (model 1P), (*2*) three charges placed at the position of the nuclei of NO_2^- and having values equal to the Mulliken gross atomic charges $Q(N)$ and $Q(O)$ (model 3P), and (*3*) seven charges selected in such way as to minimize the deviation of the description of $V_{NO_2^-}$ that they give with respect to the SCF description and to reproduce the SCF value of the dipole and quadrupole moments (calculated with respect to the mass center) (model 7P). In all cases the Na^+ charge distribution will be approximated by means of a unit point charge.

To appreciate the difference in quality of such models, we show in plane maps of the difference between the SCF and the three point-charge models of $V_{NO_2^-}$ (Fig. 18). The electrostatic potential considered in Fig. 18 refers to an isolated NO_2^- ion: we have, however, reported the position the other ions have in the crystal lattice to make more evident the order of magnitude of the "errors" introduced in the Hamiltonian of Eq. (30) by approximating the SCF description of $V_{NO_2^-}$ for ions lying at increasing distances from the central one.

A correct truncation of the infinite sum of Eq. (30) imposes rather stringent requirements: that portion of crystal must be sufficiently large; it must keep a rigorous electroneutrality; and it must maintain the ferroelectric characteristics of the infinite crystal. An incorrect definition of the boundary surfaces of the crystal specimen can give rise to serious errors, for a discussion of which the reader is referred to the original paper.

We give in the first section of Table VII some properties of the NO_2^- ion calculated *in vacuo* and in the crystal (DZ STO basis set). The crystal calculation (headed in the table as 28 + 7P) refers to a crystal specimen composed of two complete shells of concentric unit crystal cells, where the nearest 28

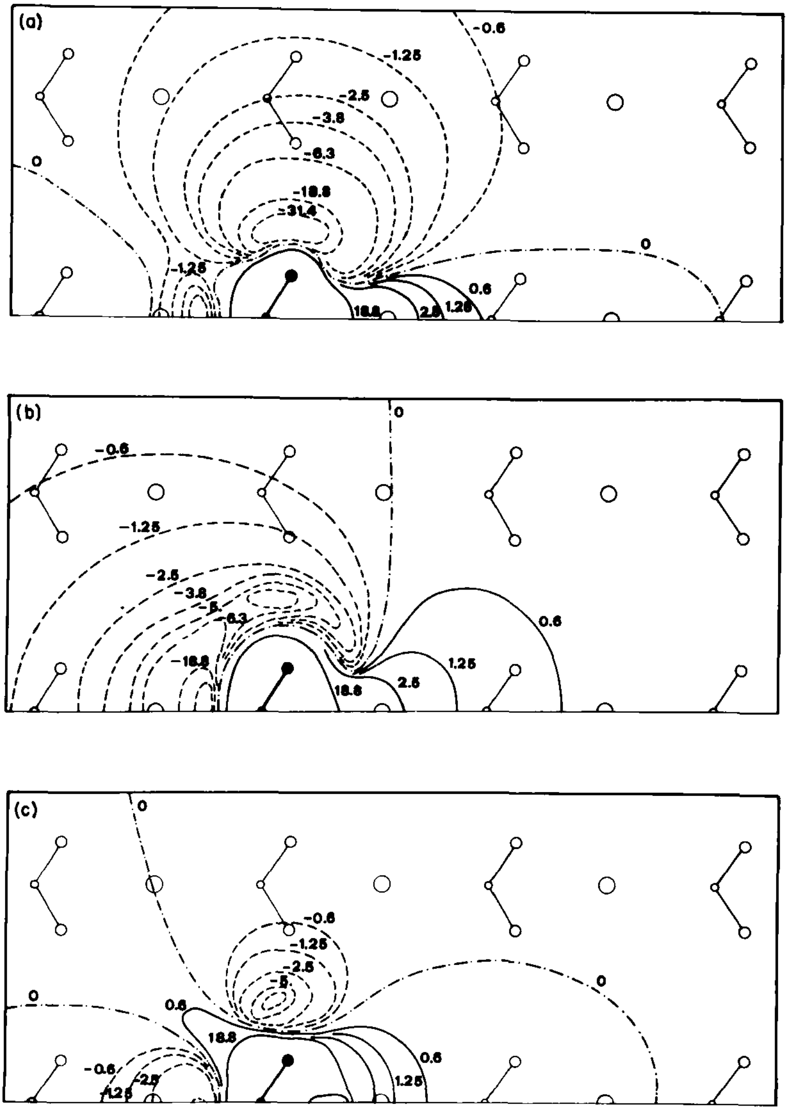

Fig. 18. A comparison of the effectiveness of the 1P, 3P, and 7P models in reproducing the SCF electrostatic potential of NO_2^-. From the top: (a) difference between the SCF and 1P model maps in the NO_2^- plane; (b) difference between the SCF and the 3P model maps; (c) difference between the SCF and the 7P model. In all cases, the position of the other ions in the $NaNO_2$ crystal lattice was also reported.

TABLE VII

Effect of the Lattice Environment in the Ferroelectric Phase of $NaNO_2$ on Some Properties of the NO_2^- Ion[a]

Environment	W[b] (kcal/mole)	$Q(N)$[c]	$Q(O)$[c]	μ_z[d] (debyes)	θ_{xx}[e] (buckinghams)	θ_{yy}[e] (buckinghams)	θ_{zz}[e] (buckinghams)	e^2qQ[f] (MHz)	η[g]
In vacuo	—	0.158	−0.579	−0.60	−7.45	6.00	1.45	6.55	0.65
28 + 7P	−220	0.191	−0.595	−0.65	−7.58	6.07	1.50	6.67	0.69

	ΔW (kcal/mole)	$\Delta Q(N)$	$\Delta Q(O)$	$\Delta\mu_z$ (debyes)	$\Delta\theta_{xx}$ (buckinghams)	$\Delta\theta_{yy}$ (buckinghams)	$\Delta\theta_{zz}$ (buckinghams)	Δe^2qQ	$\Delta\eta$
1P	23	−0.012	0.006	0.051	0.055	−0.002	−0.053	−0.142	0.007
2P	21	−0.001	0.000	0.009	−0.028	0.018	0.010	−0.049	0.004
7P	23	−0.004	0.002	0.011	0.011	−0.007	0.001	−0.022	0.004

[a] Calculations with a DZ STO basis set (Ghio *et al.*, 1976).

[b] Interaction energy between the central ion and the surrounding lattice.

[c] Gross atomic charges (*e* units).

[d] Dipole moment, measured from the center of mass.

[e] Quadrupole moment components measured from the center of mass.

[f] Nuclear quadrupole coupling constant of ^{14}N. For the nuclear quadrupole moment of ^{14}N, we have assumed the value 1.66×10^{-26} e · cm^2 (Bonaccorsi *et al.*, 1969a)

[g] Asymmetry parameter of the nuclear quadrupole coupling constant.

ions ($14NO_2^-$ and $14Na^+$) are described by actual SCF charge distributions[4] and the other ones by the 7P model for NO_2^- and by a unit positive charge for Na^+. Such a dimension of the finite crystal allows us to produce all the quantities reported in Table VII within 3% of the asymptotic value corresponding to an infinite crystal. It may be seen that the effect of the crystal field is not negligible. In the second section of Table VII we report the differences between the values obtained by using the $28 + n$P ($n = 1, 3, 7$) schematization of the crystal and those obtained by also representing the 28 nearest ions with the nP point-charge model. This selection of numerical values has been made on the basis of several checks that have shown that the one-electron properties of the central ion are not particularly sensitive to the quality of the description of the ions lying outside the first 28 neighbors. The differences Δ of Table VII can thus be safely employed to verify the relative goodness of the point-charge models in representing the crystal field contributions due to the other NO_2^- ions of the crystal. The smallest differences for the one-electron observables (and in particular for the nuclear quadrupole coupling constant of ^{14}N, which is the observable most sensitive to changes in the quality of the description of the system) are obtained with the 7P model, in accordance with the better description of the electrostatic contribution to the crystal field given by this model (see Fig. 18). In addition it may be noted that the difference between the nP and the $28 + n$P values of the contribution W to the cohesion energy is practically constant in all the three cases and is relatively larger than the changes in the one-electron observables. This fact is in accordance with the feeling shared by many researchers that electrostatic evaluations of the cohesion energy of molecular ionic crystals do not depend heavily on the goodness of the point-charge representation and, at the same time, that the values obtained in such a way are better suited for comparisons than to obtain absolute values.

The mutual polarization of the ions inside the crystal can be taken into account by means of an iterative procedure (which converges quickly), leading to a coherent description of all the ions inside the crystal that are affected to the same extent by the modifications of their charge distributions induced by the crystal field. This procedure consists in determining the charge distribution of the central nitrite ion ($\gamma^{(1)}_{NO_2^-}$) by means of a SCF calculation relying on an expression of the Hamiltonian Eq. (30), where the models of the V_L terms are taken from the charge distributions of the isolated ions ($V_L^{(0)}$), then in using $\gamma^{(1)}_{NO_2^-}$ to obtain an improved representation of the electrostatic potential of the other ions of the crystal ($V_L^{(1)}$), etc. A parallel procedure must be used for the Na^+ ions.

---

[4] To reduce the computation times, these 28 ions are described by means of a BAZ STO wavefunction.

The influence of the polarization is quite small: the values of the properties of NO_2^- obtained by means of this procedure with the 7P model differ from the values obtained with a rigid 7P model by less than 1–2%. (For example, the $e^2qQ(^{14}N)$ value passes from 6.65 to 6.64 MHz.)

We have focused our attention on the estimate of the changes of the properties of the NO_2^- ion when it is put in the bulk of a regular lattice. The extension of the procedure to the examination of crystals with defects or of ions put on the surface of the crystal leads to interesting results that are too extensive to examine here. As a last point on this subject we would like to remark that the examination of the electrostatic potential of the whole crystal in its outer space parallels the examination we made in this paper of V in the outer space of a molecule (see, for example, Parry, 1975). The potential utility of this approach for obtaining first-order information on numerous absorption phenomena and catalytic processes does not require to be emphasized.

VI. The Electrostatic Potential in Excited Electronic States

We have thus far considered only molecules in the ground closed-shell state. There are no objections, in principle, to extending also to molecules with an odd number of electrons and to electronically excited molecules the motivations justifying the use of V as an auxiliary tool in the study of some properties of the molecular systems. It would be necessary, of course, to verify again for each type of system the limits of validity of the electrostatic approximation and to restate what are the necessary conditions to be fulfilled and what are the precautions to take in order to be reasonably sure that the information extracted from V is valid and useful.

We shall not consider in this paper the ground state of free radicals, but confine ourselves to recalling that a few examples (Ellinger *et al.*, 1975; Cremaschi *et al.*, 1975a,b, 1976) have shown the possibility of using V for considerations on the chemical reactivity of such compounds. A field of investigation that seems to us quite promising concerns the radical anions having a metal cation as counterion. The location of this counterion probably is determined, in a first approximation, by electrostatic effects (Cremaschi *et al.*, 1975a,b; Corvaja *et al.*, 1978). In the present section we shall consider excited states of molecules with an even number of electrons. Discussions on the shape of V of such excited singlets and triplets must take into account an additional parameter with respect to the analogous discussions on the ground-state molecules. In fact, one may consider the one-determinant SCF description of the electron distribution to be in general sufficient for the ground state (and therefore the discussion about the reliability of the results is practically limited to the influence of the basis set), whereas in the excited states one has to check also the reliability of the method employed for calculating the wavefunction from which V is derived.

It may be convenient to make at this point a short digression to examine a recent proposal on answering this question just by using V (Daudel *et al.*, 1978).

A. Potential V as a Test for Judging the Relative Goodness of Wavefunctions

Since V has the characteristics of an observable, it may be employed, like other observables, to obtain numerical tests for judging the relative goodness of different wavefunctions describing the same electronic state. The observables generally used to this end are, apart the energy, one-electron observables such as the electric multipole moments. These one-electron observables give mean values averaged over the entire charge distribution. There may occur compensations between local errors of opposite sign in the description of the charge distribution (with respect to the hypothetical optimal description) or, on the contrary, a summation of local errors of the same sign. Both situations can lead to an erroneous interpretation of the goodness of the wavefunctions. Maps of V are less subject to such possible inconveniences because they give more detailed information. Moreover, because such information mainly regards the outer portions of the molecular space, it is particularly sensitive to the description of the valence shell electrons. Examination of V may be considered a test that supplements well the usual energy test depending heavily on the quality of the description of inner-shell electrons.

We shall give here only one example of such utilization of V. It refers to the $^1(\pi \rightarrow \pi^*)$ and $^3(\pi \rightarrow \pi^*)$ states of formaldehyde, calculated with a split valence shell set supplemented by s and p orbitals on C and O atoms (4-31G + sp basis set). We shall consider only vertical transition states [the most stable geometry for the $^3(\pi \rightarrow \pi)$ state is bent].

We show in Fig. 19 the maps of V in the symmetry perpendicular plane for (*a*) the ground SCF state, (*b*) the description of the $(\pi \rightarrow \pi^*)$ excited states obtained by a simple promotion of one electron from the $1b_1$ orbital to the $2b_1$ virtual one (there is no difference in this approximation between the singlet and triplet state), (*c*) the description of the two excited states obtained by a complete, single excitation, configuration interaction (CSECI), and finally (*d*) the results corresponding to relatively large CI computations [2474 determinants for $^1(\pi \rightarrow \pi^*)$ and 3446 for $^3(\pi \rightarrow \pi^*)$, selected according to the Whitten–Hackmayer (1969) procedure]. In Table VIII we show the values for the minimum of V lying on the molecular plane and for the minimum of V that appears in some calculations on the perpendicular plane considered in Fig. 19. In this table we also give values for intermediate CI calculations from which it is possible to appreciate the convergency of CI processes

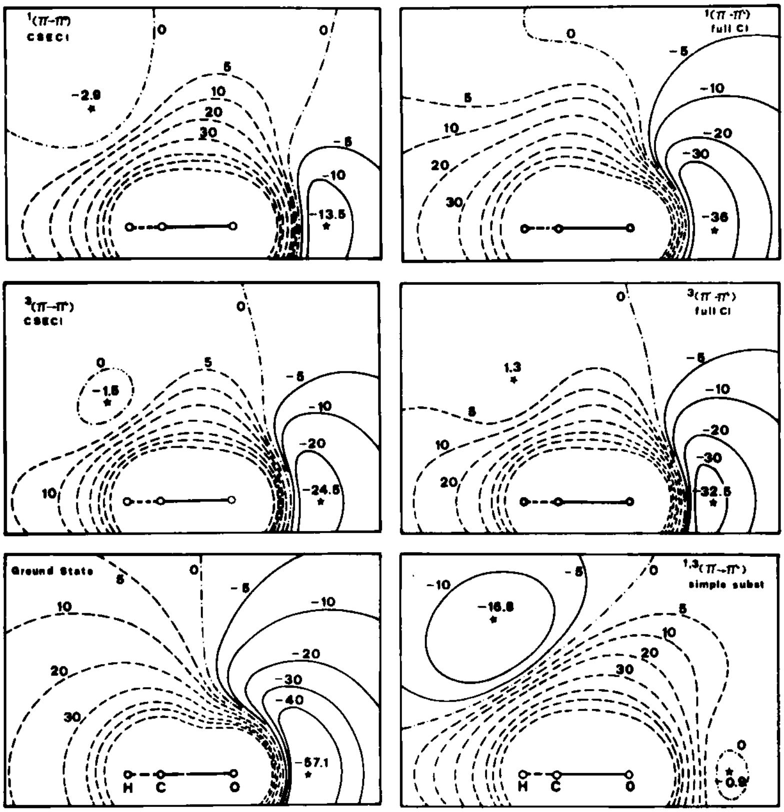

Fig. 19. Electrostatic potential maps of the perpendicular plane of H_2CO: in the ground state (SCF calculation) and in the $^{1,3}(\pi \rightarrow \pi^*)$ states calculated according to different CI approximation; simple excitation to the first virtual MO; CSECI; and full CI treatment including 2474 determinants in the $^1(\pi \rightarrow \pi^*)$ state and 3446 in the $^3(\pi \rightarrow \pi^*)$ state (results on a 4-31G + sp basis; taken from Daudel *et al.*, 1978).

leading to the CSECI and to the final complete CI descriptions. Some conclusions, supported by unpublished analogous calculations made in our Laboratory on other systems, can be drawn from such results.

The simple promotion description gives poor representations of V for excited states (and consequently of the electronic charge distribution). In all cases we have examined, the rearrangements of the charge distribution following the electronic excitation play an essential role. In the triplet state, reasonable results can be obtained with the approximations that can be formulated as single excitation CI's [CSECI, electron-hole potential (EHP) (Morokuma and Iwata, 1972), two-configuration EHP (Iwata and Morokuma, 1974), M-CI (Del Bene *et al.*, 1971), this last not considered in

TABLE VIII

DEPTH AND LOCATION OF THE MINIMA OF V IN THE GROUND AND $^{3,1}A_1$ ($\pi \rightarrow \pi^*$) STATES OF FORMALDEHYDE AND COMPARISON WITH THE DIPOLE MOMENT AND ENERGY[a]

		Molecular plane[c]			Perpendicular plane[d]				
			Location			Location			
Electronic state	Wavefunction[b]	Depth of V (kcal/mole)	r_O (Å)	θ_O (deg)	Depth of V (kcal/mole)	r_C (Å)	θ_C (deg)	Dipole moment (debyes)	Total energy (hartrees)
$^1A_1$ ground	SCF (1)	−60.4	1.23	46	No min.	—	—	3.182	−113.6953
	CI 1 (261)	−51.2	1.22	45	No min.	—	—	2.727	−113.7757
	CI 2 (634)	−50.3	1.24	45	No min.	—	—	2.651	−113.8062
	CI 3 (1188)	−50.2	1.24	45	No min.	—	—	2.646	−113.8249
	CI 3* (2474)	−50.2	1.24	45	No min.	—	—	2.664	−113.8309
$^1A_1$ ($\pi \rightarrow \pi^*$)	Virtual exc. (1)	−1.3	1.56	31	−16.8	2.51	112	−0.778	−113.2540
	CI 1 (261)	−27.8	1.36	32	−5.7	3.02	103	1.406	−113.3747
	CI 2 (634)	−40.9	1.28	36	No min.	—	—	2.137	−113.4074
	CI 3 (1188)	−43.0	1.27	35	No min.	—	—	2.232	−113.4287
	CI 3* (2474)	−40.9	1.27	35	No min.	—	—	2.099	−113.4333
	EHP (1)	−6.4	1.60	25	−14.8	2.37	116	−0.467	−113.2557
	TCEHP (2)	−17.6	1.39	40	−7.4	2.20	119	0.367	−113.2998
	CSECI (63)	−15.4	1.46	33	−2.9	2.33	120	0.323	−113.3334
$^3A_1$ ($\pi \rightarrow \pi^*$)	Virtual exc. (1)	−1.3	1.56	31	−16.8	2.51	112	−0.778	−113.4302
	CI 1 (94)	−34.8	1.35	32	−1.1	2.13	111	1.245	−113.5422
	CI 2 (334)	−33.1	1.30	35	−1.4	2.16	109	1.207	−113.5673
	CI 3 (790)	−36.3	1.29	35	−0.4	2.19	112	1.345	−113.5889
	CI 3* (2008)	−37.0	1.29	35	−0.1	2.21	110	1.416	−113.5957
	CI 4 (1406)	−38.1	1.27	34	0.9	2.22	110	1.464	−113.6003
	CI 4* (3446)	−38.6	1.27	34	1.3	2.22	110	1.505	−113.6066
	EHP (1)	−32.0	1.31	40	−0.6	2.03	118	1.126	−113.5271
	CSECI (63)	−30.0	1.35	40	−1.5	1.92	118	1.084	−113.5306

[a] 4-31G + sp Calculation from Daudel *et al.*, 1978.

[b] The number of determinants included in each wavefunction is given within parenthesis.

[c] The location of the minimum is given with respect to a polar reference frame centered on the O nucleus.

[d] We report here only the local minima (when present) placed near the CH_2 group. The reference frame is centered on the C nucleus.

Table VIII]. Reasonable results of an analogous degree of accuracy can be obtained by using this kind of approximation also for other states, such as the $^{1,3}(n \rightarrow \pi^*)$ ones, in molecules containing the $>\!C{=}O$, $>\!C{=}N\diagdown$, $\diagdown N{=}N\diagup$ chromophores (V maps of such states can be found in Cimiraglia and Tomasi, 1977). It is well known how difficult it is to obtain a satisfactory description of the $^1(\pi \rightarrow \pi^*)$ state of H_2CO (see, e.g., Whitten, 1972). The convergency obtained in the set of CI calculations of Table VIII is worse than in the corresponding triplet state, and the approximate descriptions given by the single excitation CI methods are rather poor.

A detailed discussion of the relative merits of the various methods for obtaining excited state wavefunctions would go beyond the limits of the object of this paper. We confine ourselves to remarking that all the other examples we show in this section refer to wavefunctions calculated with single excitation CI approximations, and especially with the EHP method which gives, with a low computational effort, a description of the excited state with the minimal number of determinants, which in most of the cases checked thus far is not too bad.

B. Vertical Excitations

In Fig. 20 we show the maps of V for the molecular plane of thymine in its ground, $^{1,3}(\pi \rightarrow \pi)$, and $^{1,3}(n \rightarrow \pi^*)$ states (Bonaccorsi *et al.*, 1974a). The corresponding wavefunctions have been calculated by Snyder *et al.* (1970) using for the excited states, four configurations corresponding to a promotion of one electron from the two higher π (or σ) MO's (2M approximation; Del Bene *et al.*, 1971). The changes in the shape of V in passing from the ground to the excited states are quite considerable. In the $(\pi \rightarrow \pi^*)$ states a reduction of the negative zone surrounding the O(2) atom and a corresponding deepening of V in the region outside the molecular plane near the C(5)=C(6) bond is evident. [In this region there is a minimum for V in the ground state of -15 kcal/mole, which is deepened to -24 kcal/mole in the $^3(\pi \rightarrow \pi^*)$ state.] It is relevant to remark that in a first approximation the $(\pi \rightarrow \pi^*)$ states can be classified as arising from the excitation of a π-electron localized on the C(5)=C(6) bond to the corresponding antibonding MO. In the $(n \rightarrow \pi^*)$ states the region surrounding O(2) is completely positive. The negative zone near O(4) is noticeably deeper, and the out-of-plane minimum corresponding to the C(5)=C(6) group reaches values around -85 kcal/mole.

These rather dramatic effects are perhaps emphasized by the smallness of the basis set and by the method chosen for obtaining the wavefunctions of the excited states, but they indicate, at least semiquantitatively, what changes in chemical reactivity one may expect in passing to excited states. In particular, qualitative considerations seem to indicate that a rationale of

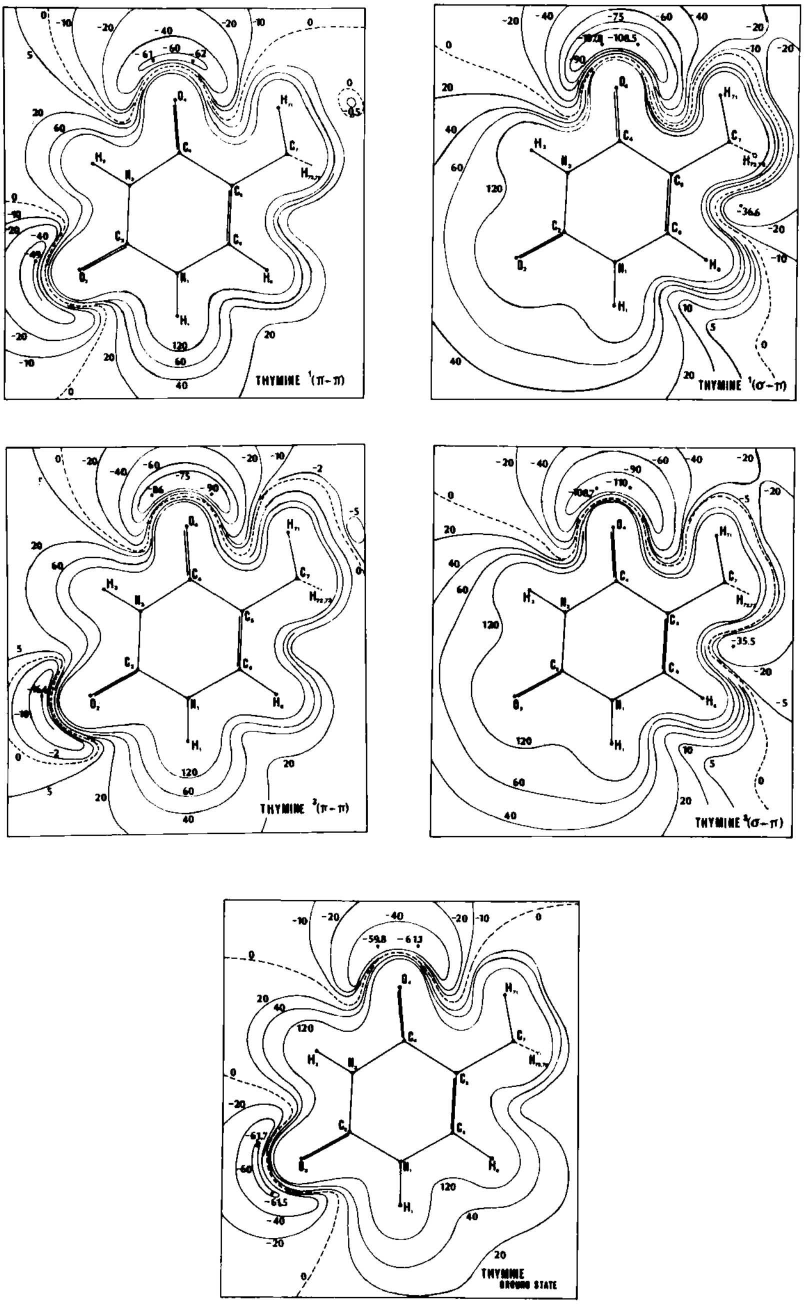

THYMINE $^1(\pi-\pi)$

THYMINE $^1(\sigma-\pi)$

THYMINE $^3(\pi-\pi)$

THYMINE $^3(\sigma-\pi)$

THYMINE GROUND STATE

Fig. 20. In-plane electrostatic potential maps of thymine in its ground and $^{1,3}(\pi \rightarrow \pi^*)$ and $^{1,3}(\sigma \rightarrow \pi^*)$ states. Wavefunctions calculated by Snyder *et al.* (1970), maps reproduced from Bonaccorsi *et al.* (1974a).

the photodimerization process of thymine could be obtained by using electrostatic considerations relying on the shape assumed by *V* in the ground and in the excited state. Another observation that can be made by examining Fig. 20, and which could be extended to other molecules, regards the changes of the organization of the solvent in the first solvation shell for excited states with a sufficiently long lifetime. The maps of *V* make evident that such a reorganization is far from being negligible: its influence on entropic and enthalpic contributions due to the solvent should be taken into account when one compares changes of reaction free energy in the ground and in the excited states.

Other examples of how *V* changes in passing to excited states could be given, and we feel that a rationalization of the shape of *V*, similar to that exposed for the ground states, could be attempted. Such work, however, has not yet been attempted, and rather than multiplying here the examples of shapes of *V* in the vertical transition states, we consider it more convenient to turn to examining another factor that produces changes in the shape of *V* in excited states with respect to the ground state.

C. Changes of *V* Due to Changes in Geometry

The minimum energy geometry in excited states can be in some cases markedly different from that of the ground state. When one considers *V* as a reactivity index (and no longer as a test of the goodness of the wavefunction, as was done in Section VI, A), it will be more interesting to examine the electrostatic potential for states having an appreciable lifetime at the minimum energy geometry rather than at the vertical transition geometry. In such cases the changes of *V* can be roughly divided into effects due to electronic transition and effects due to changes in geometry.

The example of the $^3(n \rightarrow \pi^*)$ state of H_2CO will be sufficient to appreciate the order of magnitude of such effects. In the $^3(n \rightarrow \pi^*)$ state the formaldehyde molecule has a bent geometry, the only symmetry element being a plane bisecting the CH_2 group. We show in Fig. 21 the maps of *V* for such a plane with the equilibrium geometries of the ground state and of the excited one. The wavefunctions have been obtained by the EHP method using the 4-31G + sp basis set already mentioned. The vertical excitation has reduced the negative zone surrounding O. The characteristic shape of *V* near the oxygen atom of symmetrical carbonyls (two minima on the molecular plane symmetrically placed with respect to the C—O axis) is decidedly altered: there are now two relative minima on the vertical plane (−16.4 kcal/mole; see Fig. 21a), whereas on the molecular plane the lowest value of *V* (−15.7 kcal/mole) is just on the C—O axis. In correspondence to the C atom there is now an asymmetric negative region with two minima at −21.5 kcal/mole (see again Fig. 21a). Passing now to the

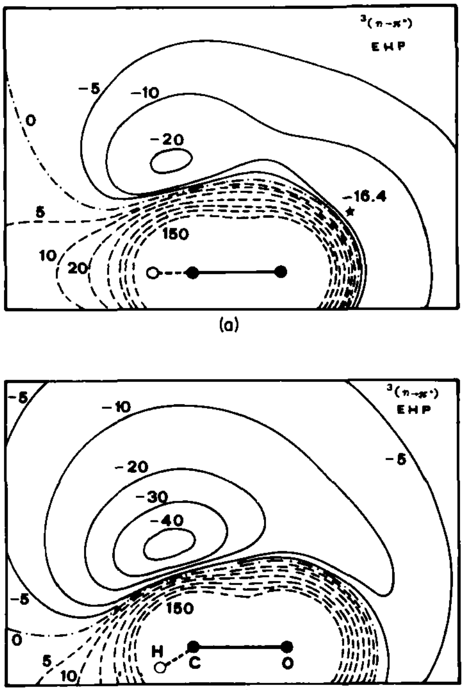

(a)

(b)

Fig. 21. Maps of the $^3(n\text{-}\pi^*)$ state of H_2CO in the (a) planar and (b) bent conformation. Both maps refer to the perpendicular symmetry plane and have been calculated with the EHP method on a 4-31G + sp basis.

stable geometry of the $^3(n \rightarrow \pi^*)$ state (Fig. 21b), it is easy to establish that the bending of the CH_2 group has produced a further lowering of one of the two C minima ($V_{\text{min}} = -47$ kcal/mole) at the expense of the region near the O atom.

What Fig. 21 shows is in agreement with the observed displacement of the reactive zone of the molecule (toward electrophilic agents) from O to CH_2 when one passes from the ground to the $^3(n \rightarrow \pi^*)$ state (Turro *et al.*, 1972). An appreciation of this change of reactivity can be obtained by having recourse to the results published by Iwata and Morokuma (1973) concerning the interaction energy between water and H_2CO. Following the terminology adopted by these authors, we compare in Table IX the hydrogen bond energies (and its electrostatic parts) obtained by adopting a planar (P) or a bent geometry (B) for H_2CO and three different conformations of the H-bonded complex. In every case, H_2O acts as an electron acceptor: in the first conformation, all the nuclei of H_2O lie in the molecular plane of formaldehyde, and the hydrogen bond O ··· HO makes an angle of 60°

TABLE IX

INTERACTION ENERGY ΔE IN THE COMPLEXES $H_2CO \cdot H_2O$ AT VARIOUS GEOMETRIES AND FOR DIFFERENT ELECTRONIC STATES OF H_2CO[a]

Geometry of the $H_2CO \cdot H_2O$ complex[c]	Geometric and electronic state[b]		
	P(G.S.)	P $^3(n \rightarrow \pi^*)$	B $^3(n \rightarrow \pi^*)$
H	−3.4	−0.7	+1.3
	(−4.1)	(+0.2)	(+1.1)
VO	−0.3	+0.1	+0.1
	(−0.7)	(+0.1)	(+0.4)
VC	+0.3	−0.5	−1.2
	(+0.2)	(−0.5)	(−1.4)

[a] From Iwata and Morokuma (1973). Calculations performed with the STO-3G basis set.

[b] In parenthesis are given the corresponding E_{es} values (kcal/mole). P means planar and B means bent geometry of H_2CO.

[c] For the definition of the three geometries (H, VO, and VC) of the complex, see the text.

with the C—O axis (conformation H); in the second one, the nuclei of H_2O lie on the symmetry plane and the hydrogen bond makes an angle of 90° with respect to the C—O axis (conformation VO); in the last one, H_2O is again on the symmetry plane but the hydrogen bond concerns the C atom and the OH · · · C bond makes an angle of 90° with the O—C axis (conformation VC).

The largest stabilization energies correspond to the H conformation of the planar ground state and to the VC conformation of the bent form of $^3(n \rightarrow \pi^*)$. We have discussed in a preceding section the relations among V, ΔE, and E_{es} for the association process with water. It may be noted that the data of Table IX show relationships between ΔE and E_{es} of the same type already found in the ground-state complexes. A larger set of examples of such relationships and an analysis of the basis set dependency of ΔE and of its decomposition into contributions can be found in a series of papers by Morokuma and co-workers (Iwata and Morokuma, 1973, 1975a,b, 1977; Morokuma *et al.*, 1974).

The general impression arising from such data, supported by analogous calculations concerning molecules having the $\gt C{=}N^{\frown}$ chromophore (R. Cimiraglia and J. Tomasi, unpublished results, 1976) is that the decomposition of the interaction energy has a trend quite similar to that found for molecules in the ground state. At distances near the equilibrium one, the electrostatic contribution is dominant and this contribution dictates also the mutual orientation of the partners. The main difference seems to be a somewhat larger dependency of the energy partition on the basis set.

The few examples we have given should be sufficient to show the possibility of using with some profit V as a tool for characterizing chemical reactivity also for the excited states. It is not, however, advisable to go beyond a statement about the possibility of using V for the excited states because the number of checks is quite restricted and limited only to weak interactions. To the best of our knowledge decompositions of the energy for cases where ΔE is larger than a few kilocalories per mole have not yet been performed.

VII. Approximations to Calculation of V and E_{es}

A. The Electrostatic Potential V

There are three factors that determine the computational effort necessary to obtain, via the electrostatic potential, the information on the chemical behavior of a molecule: the time necessary to calculate the wavefunction; the number of points k where $V(\mathbf{k})$ is calculated; and the time necessary to calculate $V(\mathbf{k})$ at a single point.

In large molecules the calculation of the wavefunction can be very long. For this reason a large portion of the calculations of V for molecules of organic or bio-organic interest have been thus far performed on semiempirical wavefunctions [extended Hückel theory (EHT), complete neglect of differential overlap (CNDO), intermediate neglect of differential overlap (INDO)]. One should remember that V is used as a semiquantitative index, and the possibility that a semiempirical approximation of V retains, in some cases at least, the essential part of the information cannot be discarded as uninteresting without a previous accurate examination. An assessment of the reliability of such results requires, however, a detailed analysis, specific for each family of chemical compounds, which would lengthen this paper excessively.

The second factor, the number of points, largely depends on the complexity of the molecule and on its topology. In this paper we have presented V under the form of two-dimensional (2D) maps, but in actual investigations it may be more useful to have three-dimensional (3D) information on smaller portions of space or it may be sufficient to know V at some selected points. The determination of the best strategy for minimizing the number of points necessary to get a 2D map is a rather technical problem that does not deserve a detailed discussion here. In our laboratory we use, according to the case, different techniques: 2D spline interpolation, linear interpolation on grids of variable mesh, and an isopotential line-following procedure.

The third factor, the time necessary to compute $V(\mathbf{k})$ at a given point, constitutes the main subject of this section. According to the definition given in Eq. (14), the calculation of $V(\mathbf{k})$ is performed by following the usual rules for calculating the expectation value of a one-electron operator:

$$V_{\mathrm{A}}(\mathbf{k}) = \int \frac{\gamma_{\mathrm{A}}(\mathbf{r}_1)}{|\mathbf{r}_1 - \mathbf{r}_k|}\, d\mathbf{r}_1 = -\sum_r \sum_s P_{rs}\left(\chi_r \left| \frac{1}{|\mathbf{r}_1 - \mathbf{r}_k|} \right| \chi_s\right) + \sum_\alpha \frac{Z_\alpha}{|\mathbf{r}_k - \mathbf{R}_\alpha|}. \quad (31)$$

The calculation of the electronic part of Eq. (31) increases with the number m of the basis functions as $(m^2 + m)/2$.

For the usual Gaussian basis sets (having also an angular part), the derivation of V by integration of the Poisson equation [see Eq. (22)], proposed by Srebrenick *et al.* (1973), can reduce the computational times by a factor of 3–4. Klöpper and Volkmer (1975) observed that the claim of having brought V to an analytical form in this way is not valid, because in Gaussian bases also the definition Eq. (31) has an analytical form: the observation is correct, but the analytical form obtained by integration of γ is simpler and gives exactly the same numerical results as direct utilization of Eq. (31). There will be, perhaps, other more efficient ways of programming the formulas giving V, but it is not likely that the computation time can be reduced in this way by more than an order of magnitude.

Approximations to the calculations of Eq. (31) have been put forward by Carbò and Martin (1975), following the well-known Mulliken approximation of expressing two-center distributions in terms of the overlap (Mulliken, 1949) or Ruedemberg's alternative version of Mulliken's approximation (Ruedemberg, 1951). In the Mulliken approximation the computational time increase as m, where m is again the number of basis functions.

Approximations of the same kind have been widely applied in CNDO (or INDO) calculations of V. Giessner-Prettre and Pullman (1972) have proposed and discussed a hierarchy of approximations, starting from a crude one where the ZDO approximation is coupled to the other simplifications introduced in the CNDO method, up to complete calculations according Eq. (31) on the deorthogonalized STO set. The interested reader may find further information in a small number of papers on this subject (Giessner-Prettre and Pullman, 1971, 1972, 1974, 1975; Petrongolo and Tomasi, 1973; Caballol *et al.*, 1974).

Another kind of approximation of $V_{\mathrm{A}}(\mathbf{r})$ relies on the multipole expansions of this function. The normal Taylor expansion of $V_{\mathrm{A}}(\mathbf{r})$ about a suitable origin (e.g., the center of mass) leads to the well-known expression (Rein, 1973)

$$V_{\mathrm{A}}(\mathbf{r}) = \frac{q}{r} + \frac{\boldsymbol{\mu}_{\mathrm{A}} \cdot \mathbf{r}}{r^3} + \frac{\mathbf{r} \cdot \mathbf{Q}_{\mathrm{A}} \cdot \mathbf{r}}{r^5} + \cdots, \quad (32)$$

where **q**, **μ**, **Q**, ... are the monopole, dipole, quadrupole, etc. terms of the charge distribution $\gamma_A(\mathbf{r})$. Even for relatively simple polyatomic systems such as H_2O, NH_3, expansion (32) must include at least octupole and even exadecapole terms (Riera and Meath, 1972; Bonaccorsi *et al.*, 1974b): for larger molecules this expansion scheme does not appear practicable. A better convergency can be achieved by using in Eq. (32), for molecules with the appropriate shape, ellipsoidal harmonics instead of the spherical ones (Stiles, 1975; Perram and Stiles, 1976).

Many-center multipolar expansions are more promising. The most extensive applications of this type of expansion have been made by the Rein group (Rabinowitz *et al.*, 1973; Pack *et al.*, 1973; Rein, 1973) who chose to expand the charge distribution and V about the atomic centers [see also Hirshfeld (1977) and Mezei and Campbell (1977)]. One may alternatively expand the total potential V_A (arising from γ_A) or its electronic part: in the last case the monopole term is not canceled by the nuclear contributions, but the convergence appears to be more rapid (Pack *et al.*, 1973). In our laboratory, we have tried to expand the electronic part of V on the charge centers of the localized MO's (Scrocco and Tomasi, 1973; Bonaccorsi *et al.*, 1974b). A comparison between the two methods has been made by Dovesi *et al.* (1974). Both expansions give nearly the same results, but the atomic expansion, though somewhat arbitrary in the partition of the contributions, is in better agreement with the usual chemists' thinking, namely, in terms of atomic contributions; it behaves a little better if the expansion is interrupted at the dipole terms. (For a reasonable representation, the quadrupole terms are however necessary.) The reasons for our choice of the expansion centers will become clearer later.

Also in many-center expansions the substitution of spherical harmonics with other expansion functions can be of some usefulness: we quote here the investigation of Stigter and Schellman (1973) on the use of a tesseral harmonic multipole expansion and on the subsequent expansion of each set of point multipoles by a cluster of discrete charges.

This last proposal can be viewed as an intermediate step toward the limiting case of the many-center expansions that interrupt the expansion at the monopole term and reach the required degree of accuracy by increasing the number of expansion centers. Representations of charge distributions and electrostatic potentials in terms of point charges have a long history, which is not necessary to review here [see, for instance, the well-known model of water proposed by Rowlinson (1951)]. The simplest expressions of this type use the Mulliken atomic charges. With this method one can rapidly find a rough representation of V, which is useful however if one is interested in examining the behavior of V at large distances in a large number of molecules (Fraga and Fraga, 1973).

All the proposals we have thus far reviewed rely on the hypothesis of having the molecular wavefunction at our disposal.[5] Since we have recourse to the models of group potentials described in Section III, we may introduce a set of simplified rules for calculating V that do not even require the calculation of the wavefunction. The first approximation is the one mentioned in Section III employing directly the LCAO expressions of the model group-charge distributions (a few of which are given by Bonaccorsi *et al.*, 1977) to calculate V:

$$V(\mathbf{k}) = \sum_{\alpha} \frac{Z_{\alpha}}{|\mathbf{R}_{\alpha} - \mathbf{r}_k|} - 2 \sum \int \frac{\bar{\lambda}_i^* \bar{\lambda}_i(\mathbf{r})}{|\mathbf{r} - \mathbf{r}_k|} d\mathbf{r}. \tag{33}$$

Because each $\bar{\lambda}$ [which we shall call transferable localized orbitals (TLO's)] is expanded over a set of atomic orbitals centered on one or two atoms only (for lone-pair and bond orbitals, respectively), the computation time increases linearly with the number M of atoms. We have already examined the quality of the results one can obtain in such a way and we shall pass, without further comment, to the next stage of approximation.

The simplicity of the shape of each group contribution to V, of which we have given some examples in Fig. 9–11, makes it easy to obtain suitable point representations of the corresponding charge distributions $\bar{\lambda}_i^* \bar{\lambda}_i$. For example, the following point-charge distributions present a mean deviation of the electrostatic potential that they generate outside the van der Waals surface with respect to that given by the corresponding TLO of less than 0.05 kcal/mole: (*a*) for a σ_{ab} bond, two-unit negative charges symmetrically placed on the AB axis with respect to the electronic charge center P_{ab}; (*b*) for a banana bond β_{AB}, again two-unit negative charges symmetrically placed with respect to the perpendicular axis passing for the charge center P_{ab} (which does not lie on the A-B axis); (*c*) for a lone pair l_{c}, a charge $-2e$ placed at the position of the corresponding TLO charge center. As was stated in Section III, each group is made neutral by including in its charge distribution, two-unit positive charges on nuclei A and B for the bonds and a $+2e$ charge on C for the lone pairs. The overall number of charges necessary for describing a molecule composed of M atoms, n_{l} lone pairs, and n_{b} bonds is thus $M + n_{\mathrm{l}} + 2n_{\mathrm{b}}$.

We show in Fig. 22 some maps obtained with such point charges. To make comparison with Fig. 9 easier, we have superimposed on each set of maps an orthogonal grid with spacings of 1 Å. It should be possible to expand the transferable group potentials in spherical or ellipsoidal harmonics

---

[5] Empirical expansions that use experimental values of the multipole moments have a limited usefulness because the available data concern, in general, only dipole and quadrupole moments, and analogous many-center expansions using partitions of the experimental values into dipole and quadrupole atomic or bond contributions are at present of limited reliability.

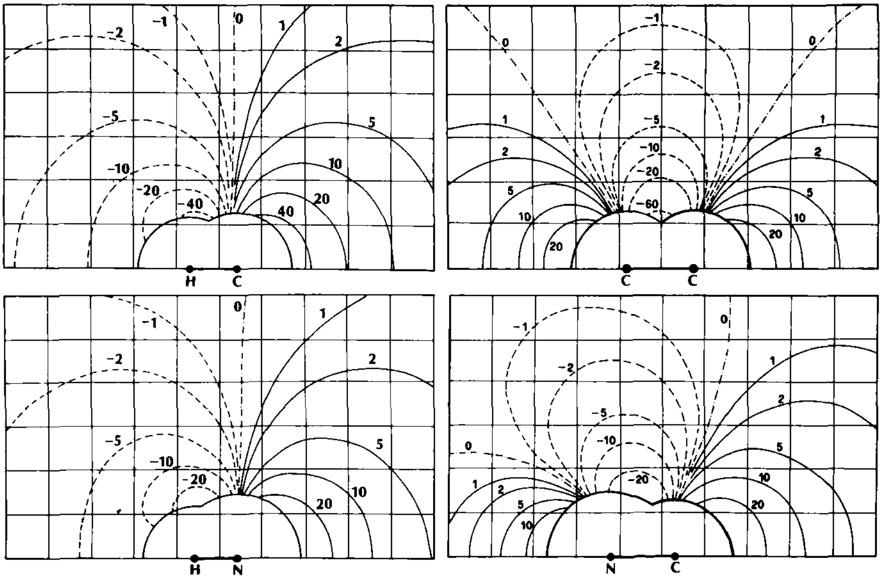

Fig. 22. Electrostatic potential of the point-charge representation of some transferable localized group models. Compare with Fig. 9.

centered on the TLO charge center: the quite limited number of charge points seems to us to indicate that monopole expansions are more practical.

It is of some interest to notice that none of the expansions we have described in the preceding pages is able to reproduce the minima of V that generally lie just within the van der Waals surface. We have seen in Sections II and V what the euristic utility of such minima is, and it would be a pity to lose such interesting information. The extension of multipolar expansions or increasing of the number of fractional point charges until the convergence one has reached assures the reproduction of such value is not a practical way. We have suggested (Bonaccorsi *et al.*, 1977) adopting a mixed representation, in the same spirit as that suggested by Hall (1973) in his point-charge representation of the FSGO wavefunction. Hall defines a set of spheres, and when the point k lies within the envelope of these spheres the point charges are substituted by Gaussians. We suggest using, for the groups immediately near the position of space where V is sampled, the LCAO expression of the group potential and adopting the point-charge representation for all the other groups in the molecule. Checks performed on various molecules indicate that it is sufficient to use the LCAO expression of the group potentials only for the TLO's bounded to the atom directly involved, for example, the lone pairs and the two bananas β_{CO} for a

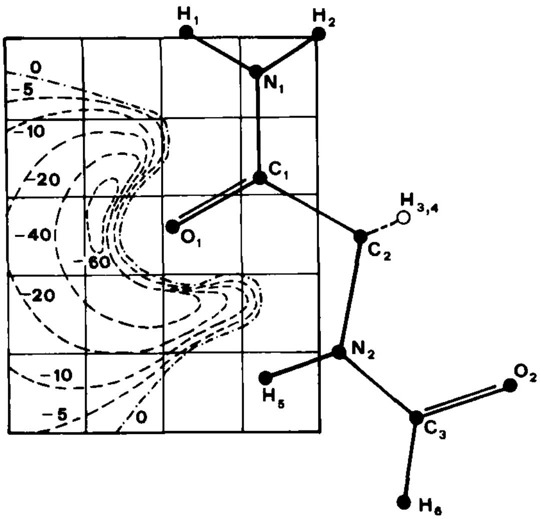

Fig. 23. A portion of the in-plane map of the fully extended form of the 2-formylaminoacetamide molecule obtained by coupling LCAO and point-charge transferable models. Compare with Fig. 12 (from Bonaccorsi *et al.*, 1977). (Reprinted with permission from the Journal of the American Chemical Society. Copyright by the American Chemical Society.)

carbonyl.[6] It is not necessary to remark again that an accurate description of the neighboring groups, like that given by the point models, is necessary to ensure a good description of *V*. We show in Fig. 23 a portion of the map of the fully extended form of 2-formylaminoacetamide near a $>C{=}O$ group, which was obtained in this way and which can be compared with the maps of Fig. 12. For groups more distant, one may also use a simpler point representation of the TLO charge distribution, for instance, the Mulliken subtotal gross population $N(i, \mathrm{K})$ for the TLO i on atom K (Mulliken, 1955). It should be stressed that the use of models with transferable $N(i, \mathrm{K})$'s for groups lying within a sphere with a radius of 4–5 Å centered on point k, where the electrostatic potential is calculated, gives results of decidedly inferior quality (see Fig. 9 in the paper by Bonaccorsi *et al.*, 1977).

B. The Electrostatic Interaction Energy E_{es}

The attempts thus far made for reducing the time of computation of E_{es} overlap to a large extent those for the approximation of *V*, which we have discussed in the preceding. In consequence, we will confine ourselves to only a few comments.

---

[6] We prefer to adopt the banana representation for isolated double bonds. For aromatic compounds, which are at present under examination, we are inclined to treat separately the π-subsystem as a whole, placing couples of fractional charges above and below each nucleus and also at an intermediate point of the bond.

The complete calculation of E_{es} requires the knowledge of $m_A[(m_A + 1)/2] \cdot m_B[(m_B + 1)/2]$ two-electron Coulombic integrals between the m_A basis functions of molecule A and the m_B functions of molecule B. To our knowledge no particular efforts have been devoted to examining whether it is profitable to introduce approximations to such integrals (e.g., the Mulliken one) in the evaluation of E_{es}. Pecul (1977) reduces the number of Coulombic integrals to $N_A \cdot N_B$ by approximating ρ_A and ρ_B as a linear combination of suitable expansion functions F_j (Gaussians or exponentials):

$$\bar{\rho}_A = \sum_{j=1}^{N_A} p_j F_j. \tag{34}$$

The coefficients p_j are determined by requiring the minimization of the square deviation function $\int (\rho_A - \bar{\rho}_A)^2 \, dr$ under the further condition that $\bar{\rho}_A$ should reproduce the first multipole moments.

In general, the approximate expressions of E_{es} avoid the calculations of two-electron Coulombic integrals by resorting to expansions of γ_B of the type we have examined in the parallel expansion of V_A. The observations made in the foregoing about such expansions might be repeated here, but it will be sufficient to remark that it is not strictly necessary to use the same techniques in the two expansions. One may use, for example, a many-center multipolar expansion for V_A and a point-charge expansion for γ_B, or vice versa. A noticeable portion of the E_{es} values concerning the interaction of a molecule A with water have been calculated by using an electrostatic potential without approximations and a point-charge representation of γ_{H_2O} (see, e.g., Bonaccorsi *et al.*, 1971a; Alagona *et al.*, 1972).

We shall report here a few data (Bonaccorsi *et al.*, 1977) concerning the calculation of E_{es} for water complexes $A \cdot H_2O$, where γ_{H_2O} is represented by a set of point charges and V_A is approximated by that combination of LCAO expressions of some group potentials coupled with the point-charge description of others that we have discussed in the preceding section. In Fig. 24 we present three conformational curves for the adduct 2-formylamino-acetamide–water having H_2O bound to the C(1)=O(1) group. The curves refer to rotations of H_2O, placed at the optimal position with respect to the carbonyl group, around three rotation axes. The (0, 0, 0) conformation, ζ, η, ξ, corresponds to a geometry of the adduct having the H_2O molecule on the peptide unit plane, with an OH bond on the line connecting the carbonyl and water oxygens. The water oxygen lies at a distance of 2.815 Å from the carbonyl oxygen and the O—O connecting line makes an angle of 72° with respect to the C—O axis. The η-axis lies on the O—O line, the ξ-axis is perpendicular to the peptide unit plane, and the third is orthogonal to the first two. The presence of two minima in the ξ-curve shows the

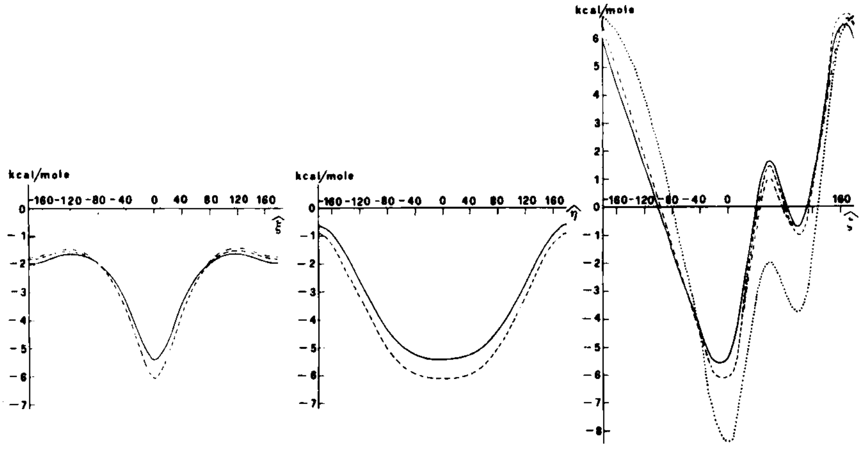

Fig. 24. Conformational curves of the complex of 2-formylaminoacetamide with water at the C(1)=O(1) group. For the definition of the conformational angles, see the text. The (0, 0, 0) conformation corresponds to a geometry of the complex having the H_2O molecule on the peptide unit plane with an OH bond on the line connecting the water and carbonyl oxygen atoms. (———) Calculations using the SCF molecular potential; (---) calculations using the LCAO representation for all the transferable group of the molecule; (-·-·-) calculations using the LCAO representation for the C=O group and the point-charge approximation for the other transferable groups; (···) calculations using the LCA representation for the C=O group and the transferable gross atomic charges for the other groups (Bonaccorsi *et al.*, 1977). (Reprinted with permission from the Journal of the American Chemical Society. Copyright by the American Chemical Society.)

possibility of making a hydrogen bond with both H atoms of H_2O and the deviations of such minima from the values $\hat{\xi} = 0°$ and 104.5° measure the nonlinearity of the two hydrogen bonds. Curve ζ corresponds to displacement of the two H atoms outside the peptide unit plane, and curve η gives information about the rotation of H_2O around the hydrogen bond axis. In the curves of Fig. 24, we report calculations of E_{es} using a point-charge representation of H_2O coupled with (*a*) the exact SCF electrostatic potential of A, (*b*) the LCAO expression of all the transferable group potentials of the molecule, (*c*) the combination of the LCAO expression of the C=O group potential with point-charge expressions of the other group potentials that we have already discussed, and (*d*) the LCAO expression of the C=O group potential with the atomic gross charges of the other groups. We do not report comparison with the exact E_{es} or ΔE values arising from SCF calculations on the supermolecule. The reader can find comparisons of this kind for smaller systems in earlier papers (Bonaccorsi *et al.*, 1971a; Alagona *et al.*, 1973; Pullman *et al.*, 1974). The fairly good agreement among ΔE, E_{es} (exact), E_{es} (approximate) conformational curves may exempt us from the burden of repeating also for the 2-formylaminoacetamide–water complexes the supermolecule calculations. (With the STO-3G basis set, more than 18 minutes is necessary to perform this calculation on an IBM 360/58 computer, and this time is reduced to 1.8 seconds for the approximate calculation of E_{es}: this ratio, 600/1, becomes even more favorable if one uses larger molecules because for a large number of basis functions the computation time for obtaining the SCF energy increases as n^5, whereas the time necessary to get the approximate value of E_{es} increases linearly with the number of electron pairs.)

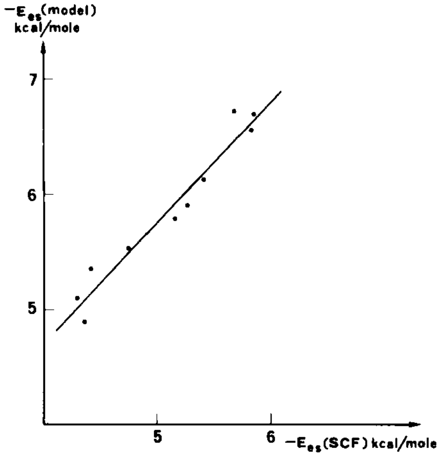

Fig. 25. A comparison of the E_{es} values for complexes A · H_2O, where the water molecule is linked to a C=O group, calculated by using the actual SCF electrostatic potential (E_{es} SCF) and the transferable group electrostatic potential models (E_{es} model). The r^2 value is 0.9728.

As a last numerical example, we compare in Fig. 25 the E_{es} values obtained from SCF calculations of V with those obtained by transferable group contributions (LCAO and point-charge representations) for a few complexes of water with the carbonyl groups of formamide, formamide dimer, acetamide, *N*-methylacetamide, and 2-formylaminoacetamide. The appreciable range of variation of ΔE in the interaction of water with carbonyl groups ($\simeq 2$ kcal/mole) evidences that the effect of the other groups of the molecule in fixing the value of this main contribution to the stabilization energy of the complex is far from negligible. This effect of the substituents may be accounted for with a fairly good approximation by calculations that do not require prior knowledge of any wavefunction.

ACKNOWLEDGMENTS

The authors express their gratitude to all their colleagues at the Laboratory in Pisa who have made substantial contributions to the researchers summarized in this paper, and in particular to Drs. Bonaccorsi, Cimiraglia, and Ghio who have kindly made unpublished results available to them. The authors are indebted to Mr. Palla who performed a part of the actual calculations required for this paper and drew all the figures. A further acknowledgment is due the other researchers who have permitted the reproduction of tables and figures extracted from their papers.

REFERENCES

Alagona, G., Cimiraglia, R., Scrocco, E., and Tomasi, J. (1972). *Theor. Chim. Acta* **25**, 103.
Alagona, G., Pullman, A., Scrocco, E., and Tomasi, J. (1973). *Int. J. Pept. Protein Res.* **5**, 251.
Alagona, G., Scrocco, E., and Tomasi, J. (1978). *Theor. Chim. Acta* **47**, 183.
Allen, L. C. (1975). *J. Am. Chem. Soc.* **97**, 6921.
Almlöf, J., and Støgard, Å. (1974). *Chem. Phys. Lett.* **29**, 418.
Almlöf, J., and Wahlgren, U. (1973). *Theor. Chim. Acta* **28**, 161.
Almlöf, J., Lindgren, J., and Tagenfeldt, J. (1972). *J. Mol. Struct.* **14**, 427.
Almlöf, J., Henriksson-Enflö, A., Kowalewski, J., and Sundbom, M. (1973a). *Chem. Phys. Lett.* **25**, 560.
Almlöf, J., Kvick, Å., and Thomas, J. O. (1973b). *J. Chem. Phys.* **52**, 3901.
Almlöf, J., Johansen, H., Roos, B., and Wahlgren, U. (1973c). *J. Electron Spectrosc. Relat. Phenom.* **2**, 51.
Amos, T. A., and Yoffe, J. A. (1975). *Theor. Chim. Acta* **40**, 221.
Anderson, A. B. (1973). *J. Chem. Phys.* **58**, 381.
Anderson, A. B. (1974). *J. Chem. Phys.* **60**, 2477.
Anderson, A. B., and Parr, R. G. (1970). *J. Chem. Phys.* **53**, 3375.
Anderson, A. B., and Parr, R. G. (1972). *Theor. Chim. Acta* **26**, 301.
Aue, D. H., Webb, H. M., and Bowers, M. T. (1972). *J. Am. Chem. Soc.* **94**, 4726.
Baird, N. C., and Swenson, J. R. (1973). *Can. J. Chem.* **51**, 3097.
Bartlett, R. J., and Weinstein, H. (1975). *Chem. Phys. Lett.* **30**, 441.
Basilevski, M. V., and Berenfeld, M. M. (1974). *Int. J. Quantum Chem.* **8**, 467.
Berthier, G., Bonaccorsi, R., Scrocco, E., and Tomasi, J. (1972). *Theor. Chim. Acta* **26**, 101.
Bertran, J., Silla, E., Carbò, R., and Martin, M. (1975). *Chem. Phys. Lett.* **31**, 267.
Bonaccorsi, R., Scrocco, E., and Tomasi, J. (1968). *J. Chem. Phys.* **48**, 1500.
Bonaccorsi, R., Scrocco, E., and Tomasi, J. (1969a). *J. Chem. Phys.* **50**, 2940.
Bonaccorsi, R., Petrongolo, C., Scrocco, E., and Tomasi, J. (1969b). *Int. Colloc. Chim. Quant. Espr. Lat.* p. 14.
Bonaccorsi, R., Scrocco, E., and Tomasi, J. (1970). *J. Chem. Phys.* **52**, 5270.
Bonaccorsi, R., Petrongolo, C., Scrocco, E., and Tomasi, J. (1971a). *Theor. Chim. Acta* **20**, 331.
Bonaccorsi, R., Scrocco, E., and Tomasi, J. (1971b). *Theor. Chim. Acta* **21**, 17.
Bonaccorsi, R., Pullman, A., Scrocco, E., and Tomasi, J. (1972a). *Chem. Phys. Lett.* **12**, 622.
Bonaccorsi, R., Pullman, A., Scrocco, E., and Tomasi, J. (1972b). *Theor. Chim. Acta* **24**, 51.
Bonaccorsi, R., Scrocco, E., and Tomasi, J. (1974a). *Jerusalem Symp. Quantum Chem. Biochem.* **6**, 387.
Bonaccorsi, R., Cimiraglia, R., Scrocco, E., and Tomasi, J. (1974b). *Theor. Chim. Acta* **33**, 97.
Bonaccorsi, R., Scrocco, E., Tomasi, J., and Pullman, A. (1975). *Theor. Chim. Acta* **36**, 339.

Bonaccorsi, R., Scrocco, E., and Tomasi, J. (1976a). *Theor. Chim. Acta* **43**, 63.

Bonaccorsi, R., Scrocco, E., and Tomasi, J. (1976b). *J. Am. Chem. Soc.* **98**, 4049.

Bonaccorsi, R., Scrocco, E., and Tomasi, J. (1977). *J. Am. Chem. Soc.* **99**, 4546.

Briggs, J. P., Yamdagni, R., and Kebarle, P. (1972). *J. Am. Chem. Soc.* **94**, 5128.

Caballol, R., Gallifa, R., Martin, M., and Carbò, R. (1974). *Chem. Phys. Lett.* **25**, 89.

Carbò, R., and Martin, M. (1975). *Int. J. Quantum Chem.* **9**, 193.

Carozzo, G. (1976). Thesis, Inst. Chem. Phys., University of Pisa.

Carozzo, G., Corongiu, G., Petrongolo, C., and Clementi, E., (1977). *J. Chem. Phys.* **68**, 787.

Chang, S. V., Weinstein, H., and Chou, D. (1976). *Chem. Phys. Lett.* **42**, 145.

Chipman, D. M., Bowman, J. D., and Hirschfelder, J. D. (1973). *J. Chem. Phys.* **59**, 2830.

Cimiraglia, R., and Tomasi, J. (1977). *J. Am. Chem. Soc.* **99**, 1135.

Cimiraglia, R., Riera, J., and Tomasi, J. (1977). *Theor. Chim. Acta* **46**, 223.

Clementi, E. (1967). *J. Chem. Phys.* **46**, 3842.

Clementi, E. (1976). "Determination of Liquid Water Structure," Lecture Notes in Chem. 2. Springer-Verlag, Berlin and New York.

Clementi, E., Clementi, H., and Davis, D. R. (1967). *J. Chem. Phys.* **46**, 4725.

Corongiu, G. (1976). Thesis, Inst. Chem. Phys., University of Pisa.

Corvaja, C., Pasimeni, L., and Ghio, C. (1978), *Chem. Phys.* **31**, 31.

Coulson, C. A. (1957). *Research (London)* **10**, 149.

Cremaschi, P., Gamba, A., Morosi, G., Oliva, C., and Simonetta, M. (1975a). *J. Chem. Soc., Faraday Trans. 2* p. 1829.

Cremaschi, P., Gamba, A., and Simonetta, M. (1975b). *Theor. Chim. Acta* **40**, 303.

Cremaschi, P., Gamba, A., Morosi, G., and Simonetta, M. (1976). *Theor. Chim. Acta* **41**, 177.

Daudel, R., Le Rouzo, H., Cimiraglia, R., and Tomasi, J. (1978). *Int. J. Quantum Chem.* **13**, 537.

Daudey, J. T. (1974). *Int. J. Quantum Chem.* **8**, 29.

Daudey, J. T., Claverie, P., and Malrieu, J. P. (1974). *Int. J. Quantum Chem.* **8**, 1.

Deb, B. M. (1973). *Rev. Mod. Phys.* **45**, 22.

Del Bene, J., Ditchfield, R., and Pople, J. A. (1971). *J. Chem. Phys.* **55**, 2236.

Dovesi, R., Pisani, C., Ricca, F., and Roetti, C. (1974). *J. Chem. Soc., Faraday Trans. 2* p. 1381.

Dreyfus, M., and Pullman, A. (1970). *Theor. Chim. Acta* **19**, 20.

Edsall, J. T., Flory, P. J., Kendrew, J. C., Liquori, A. M., Némety, G. N., Ramachandran, G. N., and Scheraga, H. A. (1966). *Biopolymers* **4**, 121.

Ellinger, Y., Subra, R., Berthier, G., and Tomasi, J. (1975). *J. Phys. Chem.* **79**, 2440.

England, W., and Gordon, M. S. (1972). *J. Am. Chem. Soc.* **94**, 4819.

Feynman, R. P. (1939). *Phys. Rev.* **56**, 340.

Fischer, H. (1964). *In* "The Chemistry of Alkanes" (S. Patai, ed.), p. 1025. Wiley (Interscience), New York.

Fraga, E., and Fraga, S. (1973). "Biomolecules: Structure and Properties." University of Alberta, Edmonton, Canada.

Frost, A. A. (1967). *J. Chem. Phys.* **47**, 3707 and 3714.

Fukui, K., Kato, S., and Fujimoto, H. (1975). *J. Am. Chem. Soc.* **97**, 1.

Gelius, U., Roos, B., and Siegbahn, P. (1972). *Theor. Chim. Acta* **27**, 171.

Ghio, C. (1969). Thesis, Inst. Chem. Phys., University of Pisa.

Ghio, C., and Tomasi, J. (1973). *Theor. Chim. Acta* **30**, 151.

Ghio, C., Scrocco, E., and Tomasi, J. (1976). *Jerusalem Symp. Quantum Chem. Biochem.* **8**, 329.

Giessner-Prettre, C., and Pullman, A. (1971). *C. R. Hebd. Seances Acad. Sci.* **272**, 750.

Giessner-Prettre, C., and Pullman, A. (1972). *Theor. Chim. Acta* **25**, 83.

Giessner-Prettre, C., and Pullman, A. (1974). *Theor. Chim. Acta* **33**, 91.

Giessner-Prettre, C., and Pullman, A. (1975). *Theor. Chim. Acta* **37**, 335.

Goodisman, J. (1973). "Diatomic Interaction Potential Energy," Vol. 1. Academic Press, New York.

Hall, G. G. (1973). *Chem. Phys. Lett.* **6**, 501.

Hart, B. T. (1973). *Aust. J. Chem.* **26**, 461.

Hayes, D. M., and Kollman, P. (1976). *J. Am. Chem. Soc.* **98**, 3335 and 7811.

Hehre, W. J., Stewart, R. F., and Pople, J. A. (1969). *J. Chem. Phys.* **51**, 2657.

Hellmann, H. (1937). "Einführung in der Quantenchemie." Deuticke, Leipzig.

Henderson, W. G., Taagepera, M., Holtz, D., McIver, R. T., Beauchamp, J. L., and Taft, R. W. (1972). *J. Am. Chem. Soc.* **94**, 4728.

Hirshfeld, F. L. (1977). *Theor. Chim. Acta* **44**, 129.

Hüller, A., and Kane, J. W. (1974). *J. Chem. Phys.* **61**, 3599.

Iwata, S., and Morokuma, K. (1973). *J. Am. Chem. Soc.* **95**, 7563.

Iwata, S., and Morokuma, K. (1974). *Theor. Chim. Acta* **33**, 285.

Iwata, S., and Morokuma, K. (1975a). *J. Am. Chem. Soc.* **97**, 966.

Iwata, S., and Morokuma, K. (1975b). *J. Am. Chem. Soc.* **97**, 4786.

Iwata, S., and Morokuma, K. (1977). *Theor. Chim. Acta* **44**, 323.

Julg, A., and Létoquart, D. (1976). *Philos. Mag.* [8] **33**, 721.

Karplus, M. (1973). *J. Am. Chem. Soc.* **95**, 8160.

Kitaura, K., and Morokuma, K. (1976). *Int. J. Quantum Chem.* **10**, 325.

Klöpper, D., and Volkmer, P. (1975). *Chem. Phys. Lett.* **31**, 186.

Kollman, P. (1977). *J. Am. Chem. Soc.* **99**, 4875.

Kollman, P., and Allen, L. C. (1970). *Theor. Chim. Acta* **18**, 399.

Kollman, P., and Rothenberg, S. (1977). *J. Am. Chem. Soc.* **99**, 1333.

Kollman, P., McKelvey, J., Johansson, A., and Rothenberg, S. (1975). *J. Am. Chem. Soc.* **97**, 955.

Lathan, W. A., and Morokuma, K. (1975). *J. Am. Chem. Soc.* **97**, 3615.

Lathan, W. A., Pack, G. R., and Morokuma, K. (1975). *J. Am. Chem. Soc.* **97**, 6624.

Levy, M. (1976). *J. Chem. Phys.* **65**, 2473.

Löwdin, P. O. (1950). *J. Chem. Phys.* **18**, 365.

McCreery, J. H., Christoffersen, R. E., and Hall, G. G. (1976). *J. Am. Chem. Soc.* **98**, 7191 and 7198.

Martin, M., Carbò, R., Petrongolo, C., and Tomasi, J. (1975). *J. Am. Chem. Soc.* **97**, 1338.

Merényi, G., Wettermark, G., and Roos, B. (1973). *Chem. Phys.* **1**, 340.

Mezei, M., and Campbell, E. S. (1977). *Theor. Chim. Acta* **43**, 227.

Morokuma, K. (1971). *J. Chem. Phys.* **55**, 1236.

Morokuma, K., and Iwata, S. (1972). *Chem. Phys. Lett.* **16**, 192.

Morokuma, K., Iwata, S., and Lathan, W. A. (1974). *In* "The World of Quantum Chemistry" (R. Daudel and B. Pullman, eds.), p. 277. Reidel Publ., Dordrecht, The Netherlands.

Mulliken, R. S. (1949). *J. Chim. Phys.* **46**, 500.

Mulliken, R. S. (1955). *J. Chem. Phys.* **23**, 1833.

Murrell, J. N., and Shaw, G. (1967). *J. Chem. Phys.* **46**, 1768.

Murrell, J. N., Randič, M., and Williams, D. R. (1965). *Proc. R. Soc. London, Ser. A.* **284**, 566.

Nakatsuji, H., Kuwata, T., and Yoshida, A. (1973). *J. Am. Chem. Soc.* **95**, 6894.

Nesbet, R. K. (1955). *Proc. R. Soc. London, Ser A* **230**, 312, 922.

Noell, J. O., and Morokuma, K. (1975). *Chem. Phys. Lett.* **36**, 465.

Noell, J. O., and Morokuma, K. (1976). *J. Phys. Chem.* **80**, 2675.

Pack, G. R., Wang, H., and Rein, R. (1973). *Chem. Phys. Lett.* **17**, 381.

Parry, D. E. (1975). *Surf. Sci.* **49**, 333.

Pecul, K. (1977). *Theor. Chim. Acta* (to be published).

Perahia, D., Pullman, A., and Berthod, H. (1975). *Theor. Chim. Acta* **40**, 47.

Perahia, D., Pullman, A., and Pullman, B. (1976). *Theor. Chim. Acta* **42**, 23.

Perram, W. J., and Stiles, P. J. (1976). *Proc. R. Soc. London, Ser. A* **349**, 125.

Petrongolo, C., Preston, H. J. T., and Kaufman, J. J. (1978). *Int. J. Quantum Chem.* **13**, 457.

Petrongolo, C., and Tomasi, J. (1973). *Chem. Phys. Lett.* **20**, 201.

Petrongolo, C., and Tomasi, J. (1974). *Jerusalem Symp. Quantum Chem. Biochem.* **6**, 513.

Petrongolo, C., and Tomasi, J. (1975). *Int. J. Quantum Chem., Quantum Biol. Symp.* **2**, 181.

Petrongolo, C., Macchia, B., Macchia, F., and Martinelli, A. (1977). *J. Med. Chem.* **20**, 1645.

Politzer, P., and Daiker, K. C. (1975). *Chem. Phys. Lett.* **34**, 294.

Politzer, P., and Weinstein, H. (1975). *Tetrahedron* **31**, 915.

Politzer, P., Donnelly, R. A., and Daiker, K. C. (1973). *J. Chem. Soc., Chem. Commun.* p. 617.

Pullman, A. (1973). *Chem. Phys. Lett.* **20**, 29.

Pullman, A., and Ambruster, A. M. (1977). *Theor. Chim. Acta* **45**, 249.

Pullman, A., and Brochen, P. (1975). *Chem. Phys. Lett.* **34**, 7.

Pullman, A., and Pullman, B. (1975). *Q. Rev. Biophys.* **7**, 505.

Pullman, A., and Schuster, P. (1974). *Chem. Phys. Lett.* **24**, 472.

Pullman, A., Alagona, G., and Tomasi, J. (1974). *Theor. Chim. Acta* **33**, 87.

Pullman, B., Gresh, N., Berthod, H., and Pullman, A. (1977). *Theor. Chim. Acta* **44**, 151.

Rabinowitz, J. R., Swissler, T. J., and Rein, R. (1973). *Int. J. Quantum Chem.* **6S**, 353.

Rein, R. (1973). *Adv. Quantum Chem.* **7**, 335.

Riera, A., and Meath, W. J. (1972). *Mol. Phys.* **24**, 1407.

Rowlinson, J. S. (1951). *Trans. Faraday Soc.* **47**, 120.

Ruedemberg, K. (1951). *J. Chem. Phys.* **19**, 1433.

Schuster, P., and Preuss, H. W. (1971). *Chem. Phys. Lett.* **11**, 35.

Schuster, P., Jakubetz, W., and Marius, W. (1975). *Top. Curr. Chem.* **60**, 1.

Scrocco, E., and Tomasi, J. (1973). *Top. Curr. Chem.* **42**, 95.

Shipman, L. L. (1975). *Chem. Phys. Lett.* **31**, 361.

Smith, P. H., Derissen, J. L., and Van Duijneveldt, F. B. (1977). *J. Chem. Phys.* **67**, 275.

Snyder, L. C., Shulman, R. G., and Neumann, D. B. (1970). *J. Chem. Phys.* **53**, 256.

Srebrenik, S., Weinstein, H., and Pauncz, R. (1973). *Chem. Phys. Lett.* **20**, 419.

Stanton, R. E. (1962). *J. Chem. Phys.* **36**, 1298.

Stigter, D., and Schellman, J. A. (1973). *Int. J. Quantum Chem.* **7**, 1.

Stiles, P. J. (1975). *Chem. Phys. Lett.* **30**, 126.

Sustman, R., and Binsch, G. (1971). *Mol. Phys.* **20**, 1.

Tait, A. D., and Hall, G. G. (1973). *Theor. Chim. Acta* **31**, 311.

Turro, N. J., Dalton, J. C., Dawes, K., Farrington, G., Hautala, R., Morton, D., Niemczyk, M., and Schore, N. (1972). *Acc. Chem. Res.* **5**, 92.

Umeyama, H., and Morokuma, K. (1976a). *J. Am. Chem. Soc.* **98**, 4400.

Umeyama, H., and Morokuma, K. (1976b). *J. Am. Chem. Soc.* **98**, 7208.

Umeyama, H., and Morokuma, K. (1977). *J. Am. Chem. Soc.* **99**, 1316.

Umeyama, H., Kitaura, K., and Morokuma, K. (1975). *Chem. Phys. Lett.* **36**, 11.

Umeyama, H., Morokuma, K., and Yamabe, S. (1977). *J. Am. Chem. Soc.* **99**, 330.

Van Duijneveldt, E. (1971). *IBM Res. Rep. R. J.* p. 945.

Weinstein, H., Srebrenik, S., Pauncz, R., Maayani, S., Cohen, S., and Sokolovsky, M. (1974). *Jerusalem Symp. Quantum Chem. Biochem.* **6**, 493.

Weinstein, H., Chou, D., Kang, S., Johnson, C. L., and Green, J. P. (1976). *Int. J. Quantum Chem., Quantum Biol. Symp.* **3**, 135.

Whitten, J. L. (1972). *J. Chem. Phys.* **56**, 5458.

Whitten, J. L., and Hackmayer, M. (1969). *J. Chem. Phys.* **51**, 5584.

Yamabe, S., Kato, S., Fujimoto, H., and Fukui, K. (1973). *Theor. Chim. Acta* **30**, 327.

ADVANCES IN QUANTUM CHEMISTRY, VOLUME 11

Complex Eigenvalue Problems in Atoms and Molecules

TOKIO YAMABE, AKITOMO TACHIBANA, and
KENICHI FUKUI
Department of Hydrocarbon Chemistry
Faculty of Engineering
Kyoto University
Kyoto, Japan

I. Introduction

There are a number of reports that deal with resonances of quantum systems occurring in electron-atom and electron-molecule scattering experiments (Schulz, 1973a,b; Sanche and Schulz, 1973, and references cited therein). In recent years, there have been presented many theories and calculations of the resonant states (Taylor *et al.*, 1966; Chen, 1969; Nicolaides, 1972; Micha, 1974, and references cited therein), and usually the resonances are described by scattering theory (see, e.g., Newton, 1960, 1966).

However, the usual description seems to miss the most striking characteristics of a narrow resonance, which is always associated with a long-living decaying state, a state that physically resembles a true discrete eigenstate (Goldberger and Watson, 1964a; More, 1971a,b). This resemblance is especially close when the lifetime becomes long. Obviously one should choose a description in which this resemblance is clearly exhibited and emphasized. To this purpose it appears favorable to introduce and to study complex eigenvalues $\{\omega_n(E)\}$ and the biorthonormal set of eigenfunctions $\{\Psi_n(\mathbf{r};\ E)\}$ which are both energy dependent. The energy

ISBN 0-12-034811-X

dependency shows that a closed system described by these functions is embedded in continuum. The biorthonormal set is constructed by the eigenfunctions of a suitably defined effective Hamiltonian $H_{\mathrm{eff}}(E)$, and the biorthonormality (Morse and Feshbach, 1953) really brings in absolute advantages for theoretical developments (More and Gerjuoy, 1973).

In the finite-range potential scattering case, the effective Hamiltonian is given by the resonant-state theory of Kapur and Peierls (1938; Peierls, 1948). For a particular value of energy, i.e., the resonance energy E_{res} (one for each resonance), the eigenvalue $\omega_n(E_{\mathrm{res}})$ may provide the "observed" resonance parameters, i.e., the energy level and the width.

On the other hand, there is an intrinsic complex energy W_n to describe the resonance, which is closely connected with the time development of the decay process of the system (Goldberger and Watson, 1964b; Micha, 1974). The complex energy W_n is defined by the pole of the Green's function of the effective Hamiltonian (More and Gerjuoy, 1973). This pole W_n may be called "complex resonance energy" and is not exactly the same as $\omega_n(E_{\mathrm{res}})$. Usually, in recent theoretical works, either $\omega_n(E_{\mathrm{res}})$ or W_n (or only the real part) has been obtained (see, e.g., Miller, 1966; Lippmann and O'Malley, 1970; Froelich and Brändas, 1975). Even in energy-dependent treatments, the energy E as a parameter has been often replaced by a constant value ($\sim E_{\mathrm{res}}$) under the consideration that the energy dependence may not be so strong (O'Malley and Geltman, 1965; Bhatia and Temkin, 1969; Ajmera and Chung, 1974). Recently, the energy dependence has begun to receive attention in the problems of predissociation (Bandrauk and Laplante, 1976a,b), autoionization (Lipsky and Connely, 1976), and Stark broadening (Yamabe *et al.*, 1977a,b; Tachibana *et al.*, 1977). However, the formal discussions of the energy dependence of $\omega_n(E)$ and the application of the energy-dependent eigenfunctions $\{\Psi_n(\mathbf{r}; E)\}$ to the perturbation theory of decaying states are made only in a few papers (Chen, 1969; More and Gerjuoy, 1973; Micha, 1974).

In this brief review, the energy dependence of the complex eigenvalues and the importance of the biorthonormal set of eigenfunctions are emphasized. Subsequently, the Hellmann–Feynman theorem is applied to the complex eigenvalue problem and some of the results are discussed. The difference between $\omega_n(E_{\mathrm{res}})$ and W_n is also estimated in a simple manner. Of many potential applications of the present formalism, only an example of a new type is here illustrated; the effect of an external uniform electrostatic field $\mathbf{F}$ on atomic and molecular systems, that is, the Stark broadening problem. Also comments are made on the newly developed, complex coordinate method (Aguilar and Combes, 1971; Balslev and Combes, 1971; Simon, 1973) with the new type of virial theorem and on the significant relationships between resonant states and virtual orbitals in atoms and molecules. On the other hand, the picture of long-living reaction complexes has been one of the most successful notions in the study of chemical reactions, and rate-determining steps of chemical reactions have often been conveniently ascribed to decaying processes of the reaction complexes (see, for example, Levin and Bernstein, 1974). Indeed, in particular, kinetics of unimolecular fragmentations have been conveniently described by the breakdown of molecular intermediates whose nature is basically equivalent to that of activated complexes (see, for example, Hall and Levin, 1966; Nordholm and Rice, 1975). It may be effective to examine the notion of long-living reaction complexes from the unified viewpoint of resonant states, that is, quasistationary complex-energy states. The dynamics of resonant states in molecular systems will be briefly discussed on the basis of "complex" Heisenberg's equation of motion, where the hypervirial, virial, and Hellmann–Feynman theorems will be formulated in the "complex" form (Tachibana *et al.*, 1978).

II. Kapur–Peierls Eigenvalue Problem

A. Biorthonormal Set of Kapur–Peierls Eigenfunctions

The original resonance theory of Kapur and Peierls (KP) is concerned with the decay of a particle confined at first in a fixed sphere of radius r_0, which contains the major part of the whole potential. The inner channel then corresponds to the interior region of the sphere and the outer channel corresponds to the exterior region. Then, the Hamiltonian is written in two ways [for the radial part $\psi(r)$ of the wavefunction]:

$$H = -(\hbar^2/2\mu)\,\partial^2/\partial r^2 + V_{\text{in}}, \qquad r \le r_0, \tag{1a}$$

$$= -(\hbar^2/2\mu)\,\partial^2/\partial r^2 + V_{\text{out}}, \qquad r \ge r_0. \tag{1b}$$

The effective Hamiltonian $H_{\text{eff}}(E)$, which is defined later in Eq. (5), operates in the inner channel and then, it contains not only the inner part of the true Hamiltonian, but also the effect of decay of the particle into the outer channel (McCarthy, 1968). The decaying nature is represented by introducing the boundary condition operator $L(E)$ (Bloch, 1957; McCarthy, 1968),

$$L(E) = (\hbar^2/2\mu)\,\delta(r - r_0)(\partial/\partial r - g^{(+)}(E)). \tag{2}$$

Here, $g^{(\pm)}(E)$ are the boundary conditions for the outgoing $(+)$ and the incoming $(-)$ waves in the exterior region;

$$(-(\hbar^2/2\mu)\,\partial^2/\partial r^2 + V_{\text{out}})\psi^{(\pm)} = E\psi^{(\pm)}, \tag{3}$$

$$g^{(\pm)}(E) = ((\partial\psi^{(\pm)}/\partial r)/\psi^{(\pm)})_{r_0} \tag{4}$$

Clearly, $g^{(\pm)}(E)$ are complex and energy dependent. The effective Hamiltonian is then given by

$$H_{\text{eff}}(E) = H + L(E), \qquad r \le r_0 \tag{5}$$

and the KP eigenvalue problem is written as

$$H_{\text{eff}}(E)\psi_n(r; E) = \omega_n(E)\psi_n(r; E). \tag{6}$$

Note that the effective Hamiltonian is not Hermitian because of the presence of the complex number $g^{(+)}(E)$. The eigenvalues $\{\omega_n(E)\}$ are, therefore, complex and energy dependent:

$$\omega_n(E) = \varepsilon_n(E) - i\gamma_n(E)/2. \tag{7}$$

Here $\varepsilon_n(E)$ and $\gamma_n(E)$ are real when E is real, corresponding to the resonance energy and the width of the KP resonant state, respectively. The KP eigenfunction has some special properties. If H is invariant under time-reversal operator T,

$$\mathrm{T}H\mathrm{T}^{-1} = H = H^{\dagger}, \tag{8}$$

then the effective Hamiltonian transforms to (McCarthy, 1968)

$$\mathrm{T}H_{\text{eff}}\mathrm{T}^{-1} = H + L^{\dagger} = H^{\dagger}_{\text{eff}}, \tag{9}$$

where $L^{\dagger}$ signifies the incoming-wave boundary condition $g^{(-)}$;

$$L^{\dagger}(E) = (\hbar^2/2\mu)\,\delta(r - r_0)(\partial/\partial r - g^{(-)}(E)). \tag{10}$$

On multiplying Eq. (6) from the left with T and using Eq. (9), one obtains

$$H^{\dagger}_{\text{eff}}\mathrm{T}\psi_n = \omega_n^*(E)\mathrm{T}\psi_n. \tag{11}$$

Thus $\mathrm{T}\psi_n$ is the eigenfunction of $H^{\dagger}_{\text{eff}}$ with the eigenvalue ω_n^*, which is given for real E as

$$\omega_n^*(E) = \varepsilon_n(E) + i\gamma_n(E)/2. \tag{12}$$

Then $\{\psi_n\}$ and $\{\mathrm{T}\psi_n\}$ form a biorthonormal set:

$$\int_0^{r_0} (\mathrm{T}\psi_n)^*\psi_m\,dr = N_n\,\delta_{nm}, \tag{13}$$

where N_n is the normalization constant. The effective Hamiltonian can be diagonalized by this complete set. It should be noted that in the present spinless case the biorthonormality condition becomes

$$\int_0^{r_0} \psi_n\psi_m\,dr = N_n\,\delta_{nm}. \tag{14}$$

and then

$$\int_0^{r_0} \psi_n^*\psi_n\,dr \ne N_n. \tag{15}$$

Also, note that the stationary principle is satisfied for ω_n and ψ_n to be

$$\delta\tilde{\omega}_n = \delta[\langle\tilde{\psi}'_n|H_{\text{eff}}|\tilde{\psi}_n\rangle/\langle\tilde{\psi}'_n|\tilde{\psi}_n\rangle] = 0; \qquad \psi'_n = \mathrm{T}\psi_n. \tag{16}$$

As a corollary, the Hellmann–Feynman theorem is satisfied that yields a formula for $\partial\omega_n(E)/\partial E$:

$$\begin{aligned}\partial\omega_n(E)/\partial E &= \langle\mathrm{T}\psi_n|\partial H_{\text{eff}}/\partial E|\psi_n\rangle/N_n \\ &= \langle\mathrm{T}\psi_n|\partial L(E)/\partial E|\psi_n\rangle/N_n \\ &= -(\hbar^2/2\mu)(\partial g^{(+)}(E)/\partial E)\psi_n(r_0)\cdot\psi_n(r_0)/N_n.\end{aligned} \tag{17}$$

B. Projection Operator Formalism

It is easy to establish the KP eigenvalue problem for the case of a general Hamiltonian H in terms of Feshbach's $P-Q$ projection operator formalism, if one can choose appropriate projection operators Q and $P(=1-Q)$, which project the closed channels and the open channels, respectively (Feshbach, 1962; Chen, 1969; Micha, 1974). This approach has two distinct advantages. First, the annoying channel radius is removed and hence long-range potentials can be treated. Second, it avoids the necessity of making an angular decomposition that makes the theory unnecessarily complicated. In this case, the effective Hamiltonian $H_{\text{eff}}(E)$ is defined in the manifold Q as

$$QH_{\text{eff}}(E)Q = QHQ + QV(E)Q, \tag{18}$$

where the effective potential $QV(E)Q$ is energy-dependent and complex:

$$QV(E)Q = QHP\mathrm{P}(E-PHP)^{-1}PHQ - i\pi QHP\,\delta(E-PHP)PHQ \tag{19}$$

(P means the principal part). It is clear that $QV(E)Q$ acts as $L(E)$ in the original KP theory. All of the KP eigenfunctions $\{Q\psi_n\}$ are obtained in the Q-space by diagonalizing the matrix $QH_{\text{eff}}Q$. If ϕ_n is chosen so as to diagonalize H in the manifold Q, that is,

$$QHQ|\phi_n\rangle = \mathscr{E}_n|\phi_n\rangle, \tag{20}$$

$$\mathscr{E}_n = \langle\phi_n|H|\phi_n\rangle, \tag{21}$$

then one obtains

$$|Q\psi_n\rangle = (1 + QT(\omega_n)QQVQ)|\phi_n\rangle, \tag{22}$$

$$\omega_n = \mathscr{E}_n + \langle\phi_n|QVQ(1 + QT(\omega_n)QQVQ)|\phi_n\rangle, \tag{23}$$

where

$$QT(\omega_n)Q = Q(1 - |\phi_n\rangle\langle\phi_n|)(\omega_n - QH_{\text{eff}}Q)^{-1}(1 - |\phi_n\rangle\langle\phi_n|)Q. \tag{24}$$

The ϕ_n is then considered to be the initial state of the system which decays by the application of the effective potential. The KP eigenvalue clearly holds the imaginary part that represents the decaying property.

In the case of an isolated resonance, one may choose

$$Q = |\phi_n\rangle\langle\phi_n|. \tag{25}$$

One then has a relation,

$$QTQ = 0, \tag{26}$$

which leads to

$$|Q\psi_n\rangle = |\phi_n\rangle, \tag{27}$$

$$\omega_n(E) = \mathscr{E}_n + \langle\phi_n|QV(E)Q|\phi_n\rangle. \tag{28}$$

These equations indicate that the KP state is nothing but ϕ_n keeping the same norm, but with the complex energy. In other words, the surrounding continuum could not alter the "state" but succeeded in changing the "eigenvalue." Then $\omega_n(E)$ is written for real E by the real and the imaginary parts as

$$\varepsilon_n(E) = \mathscr{E}_n + \langle\phi_n|HP\mathrm{P}(E - PHP)^{-1}PH|\phi_n\rangle, \tag{29}$$

$$\gamma_n(E) = 2\pi\langle\phi_n|HP\,\delta(E - PHP)PH|\phi_n\rangle. \tag{30}$$

In order to give the base for the projection operators, it is often convenient to divide the Hamiltonian H into two parts (see, e.g., Lipsky and Russek, 1966; Miller, 1966),

$$H = H_0 + V_0. \tag{31}$$

Here H_0 has both bound and continuum state solutions in the energy range considered. If one chooses a bound state ϕ_n^0 of H_0,

$$H_0\,\phi_n^0 = \mathscr{E}_n^{(0)}\phi_n^0, \tag{32}$$

as the initial state and if one sets the projection operator Q as

$$Q = |\phi_n^0\rangle\langle\phi_n^0|, \tag{33}$$

then one obtains

$$\varepsilon_n(E) = \mathscr{E}_n^{(0)} + \langle\phi_n^0|V_0 + V_0\,G_P(E)V_0\,|\phi_n^0\rangle, \tag{34}$$

$$\gamma_n(E) = 2\pi|\langle\phi_n^0|V_0|P\phi_E\rangle|^2. \tag{35}$$

Here, the Green's function G_P is given by

$$G_P(E) = P\mathrm{P}(E - PHP)^{-1}P, \tag{36}$$

and the continuum $P\phi_E$ (normalized to unit density of E) is given by the solution of

$$(E - PHP)P\phi_E = 0 \tag{37}$$

with the appropriate boundary condition. This equation for $P\phi_E$ can be solved formally as

$$P\phi_E = (1 + G_P(E)V_0)P\phi_E^0 \tag{38}$$

and, therefore,

$$\gamma_n(E) = 2\pi |\langle \phi_n^0 | V_0 + V_0 G_P(E) V_0 | P\phi_E^0 \rangle|^2, \tag{39}$$

where $P\phi_E^0 = \phi_E^0$ is the unperturbed continuum solution of H_0 (normalized to unit density of E). Of course, ϕ_E^0 is orthogonal to ϕ_n^0. If one introduces $\phi_n(E)$ as

$$\phi_n(E) = (1 + G_P(E)V_0)\phi_n^0, \tag{40}$$

then one obtains the alternative expression for the KP eigenvalue:

$$\varepsilon_n(E) = \mathscr{E}_n^{(0)} + \langle \phi_n^0 | V_0 | \phi_n(E) \rangle, \tag{41}$$

$$\gamma_n(E) = 2\pi |\langle \phi_n(E) | V_0 | P\phi_E^0 \rangle|^2. \tag{42}$$

Moreover, expanding the inverse operator G_P in the order of V_0, one has

$$\phi_n(E) = \phi_n^0 + \chi_n^{(1)}(E) + \cdots, \tag{43a}$$

$$\chi_n^{(1)}(E) = \mathrm{PP}(E - H_0)^{-1} P V_0 \phi_n^0, \tag{43b}$$

and therefore

$$\varepsilon_n(E) = \mathscr{E}_n^{(0)} + \mathscr{E}_n^{(1)} + \mathscr{E}_n^{(2)}(E) + \cdots, \tag{44a}$$

$$\mathscr{E}_n^{(1)} = \langle \phi_n^0 | V_0 | \phi_n^0 \rangle, \tag{44b}$$

$$\mathscr{E}_n^{(2)}(E) = \langle \phi_n^0 | V_0 \mathrm{PP}(E - H_0)^{-1} P V_0 | \phi_n^0 \rangle. \tag{44c}$$

It should be noticed here that the energy-dependence of $\varepsilon_n(E)$ appears from the second-order energy in the perturbation series expansion. It follows that from Eqs. (44c) and (43b) one can estimate the energy-dependence as

$$\partial \varepsilon_n(E)/\partial E \sim \partial \mathscr{E}_n^{(2)}(E)/\partial E = -\langle \chi_n^{(1)}(E) | \chi_n^{(1)}(E) \rangle. \tag{44d}$$

Furthermore, if one writes

$$\phi_n(E) = \phi_n^0 + \chi_n(E); \qquad \chi_n(E) = G_P(E) V_0 \phi_n^0, \tag{45}$$

then χ_n is equivalent to the solution of the following equation:

$$(PHP - E)\chi_n(E) + V_0 \phi_n^0 = 0. \tag{46}$$

Then $\varepsilon_n(E)$ is shown to be

$$\varepsilon_n(E) = \mathscr{E}_n^{(0)} + \mathscr{E}_n^{(1)} + \Delta\mathscr{E}_n(E), \tag{47a}$$

$$\Delta\mathscr{E}_n(E) = \langle \phi_n^0 | V_0 | \chi_n(E) \rangle. \tag{47b}$$

Likewise, one has an expression for the imaginary part $\gamma_n(E)$ in the form

$$\gamma_n(E) = 2\pi |\langle \phi_n^0 | V_0 | \phi_E^0 \rangle + \langle \chi_n(E) | V_0 | \phi_E^0 \rangle|^2. \tag{48}$$

For the variational procedure to approximate the wavefunction χ_n Miller's method (1966) is expected to be useful, where the trial functions are able to be chosen as in the case of the usual bound-state calculations in atoms and molecules. However, attention should be given to the energy dependence and to the nonvanishing imaginary part, which are all indispensable to the KP resonant state.

It is now attempted to modify the foregoing formulations to a case such that a more appropriate selection of the asymptotic continuum, which is not the solution of H_0, is significant. This is the case when, e.g., an external uniform electrostatic field is applied to the autoionizing states of atoms; the threshold of the continuum now changes drastically. Then, let us suppose the new asymptotic Hamiltonian H_0' having the same threshold as that of H:

$$H = H_0' + V_0', \tag{49a}$$

being accompanied by the continuum solution

$$(E - H_0')\phi_E^{0\prime} = 0. \tag{49b}$$

Then, the continuum $P\phi_E$ defined by Eq. (37) is rewritten as

$$P\phi_E = (P + G_P(E)V_P')\phi_E^{0\prime}, \tag{50a}$$

where

$$V_P' = PHP - H_0'. \tag{50b}$$

Thus, the matrix element for $\gamma_n(E)$ which appears in Eq. (35) becomes

$$\langle \phi_n^0 | V_0 | P\phi_E \rangle = \langle \phi_n^0 | V_0 | \phi_E^{0\prime} \rangle + \langle \chi_n(E) | V_0' | \phi_E^{0\prime} \rangle - (\varepsilon_n(E) - \mathscr{E}_n^{(0)}) \langle \phi_n^0 | \phi_E^{0\prime} \rangle. \tag{51}$$

Note that the overlap between ϕ_n^0 and $\phi_E^{0\prime}$ is now permitted.

III. Coupled Equations Theory

A. Kapur–Peierls and Siegert Resonant States and the "Extended" Hellmann–Feynman Theorems

1. *General Theory*

It is attempted to extend the preceding treatments of the KP eigenvalue problem by the coupled equations theory (Tachibana *et al.*, 1977). Here, it is not required to introduce the projection operators, Q and $P(=1 - Q)$.

Moreover, there is no need to block-diagonalize the total Hamiltonian H in the complementary manifolds, which, in some cases, will be more effective than the projection operator formalism (Temkin *et al.*, 1972; Bhatia and Temkin, 1976). The original method of coupled equations was introduced by Faddeev (1960) in the problem of three-particle systems and developed extensively by Hahn (1968a,b), Hahn and Watson (1972), Hahn *et al.* (1974), and Kouri and Levin (1975) in the multiple-scattering theory. The coupled equations theory proves effective in a wide class of chemical and physical problems, particularly, as pointed out by Krüger and Levin (1976, 1977), in the bound-state problems of many-electron systems.

Now in coupled equations theories, one identifies the asymptotic Hamiltonian H_{A} of the total Hamiltonian H and writes

$$H = H_{\mathrm{A}} + V_{\mathrm{B}}, \tag{52}$$

so that V_{B} represents the scattering interaction. From the decaying bound-state viewpoint, H is written in a different form by which the bound-state viewpoint is clearly exhibited and emphasized;

$$H = H_{\mathrm{B}} + V_{\mathrm{A}}, \tag{53}$$

where H_{B} is supposed to govern the bound region and V_{A} is the residual potential. (Notice that we consider only real Hermitian operators for these Hamiltonians and potentials.) In other words, the space is divided into two distinct regions. In the first, localized round the atom or molecule, the unperturbed Hamiltonian is H_{B}, and in the second, the asymptotic region, it is H_{A}. For a clear illustration of the situation, let us take the Stark broadening problem; i.e., an external uniform electrostatic field **F** applied to bound electrons in atoms induces not only energy shifts but also broadenings of energy levels. In this case, V_{A} corresponds to the applied field, and, finally, a loosely bound electron is taken away as in the case of field emission from metals. Then, in the final channel one takes an unperturbed Hamiltonian H_{A} as the sum of a free-electron Hamiltonian and that of the residual ion (core), the interaction V_{B} being that of the final free electron with the core. Here, the eigenfunctions of H_{A} and H_{B} are given by

$$(E - H_{\mathrm{A}})\phi_{\mathrm{A}}(E) = 0, \qquad \langle\phi_{\mathrm{A}}(E)|\phi_{\mathrm{A}}(E')\rangle = \delta(E - E'), \tag{54}$$

$$(E_n^{(0)} - H_{\mathrm{B}})\phi_n = 0, \qquad \langle\phi_n|\phi_m\rangle = \delta_{nm}. \tag{55}$$

Then, there exist the bound state ϕ_n of H_{B} and the continuum $\phi_{\mathrm{A}}(E)$ of H_{A} for the energy region $E \sim E_n^{(0)}$. This bound state ϕ_n becomes metastable by V_{A} and decays into the continuum $\phi_{\mathrm{A}}(E)$. Moreover, the overlap is admitted between ϕ_n and $\phi_{\mathrm{A}}(E)$, which may be reasonable from the consideration that the original bound state and the asymptotic continuum may have overlap in the intermediate region. This also gives a large flexibility for the basis sets to be employed. According to the coupled equations theory, it is assumed that the total wavefunction Ψ can be written by the sum of two functions Φ_A and Φ_B, which are projected as follows:

$$\Psi = \Phi_A + \Phi_B, \tag{56}$$

$$\Psi \to \Phi_A \quad \text{as} \quad V_B \to 0, \tag{57a}$$

$$\Psi \to \Phi_B \quad \text{as} \quad V_A \to 0, \tag{57b}$$

where Φ_A represents the unbound region and Φ_B represents the bound region of the decaying state. It is to be noted that, in contrast to the case of Feshbach's projection operator formalism, here the overlap between Φ_A and Φ_B is allowed:

$$\langle \Phi_A | \Phi_B \rangle \neq 0, \tag{58}$$

in accord with the relation between $\phi_A(E)$ and ϕ_n. The Schrödinger equation

$$H\Psi = E\Psi \tag{59}$$

can then be partitioned into two parts:

$$(E - H_A)\Phi_A = V_A \Phi_B, \tag{60}$$

$$(E - H_B)\Phi_B = V_B \Phi_A. \tag{61}$$

It is clear that the limiting properties in Eqs. (57a) and (57b) are automatically incorporated into these coupled equations. The two components, Φ_A and Φ_B, which have thus been governed by the two different Hamiltonians, H_A and H_B, will be coupled to give the exact total wavefunction with the effective way of expression for the limiting properties (Hahn *et al.*, 1974; Krüger and Levin, 1977). Similar type of coupled equations also appear in, e.g., the theory of predissociation (Caplan and Child, 1972; Band and Freed, 1975).

Now, the effective Hamiltonian $H_{\text{eff}}(E)$ for the KP states is readily introduced into Eq. (61), in consequence of the modification of H_B through the inhomogeneous part of the equation. The effective Hamiltonian, which is denoted here by $H_B^+(E)$, is given by

$$H_B^+(E) = H_B + V(E), \tag{62}$$

$$V(E) = V_B G_A^+(E) V_A, \tag{63}$$

where $V(E)$ is the effective potential and $G_A^+(E)$ is the Green's function of H_A defined for real E as

$$G_A^+(E) = \mathrm{P}(E - H_A)^{-1} - i\pi\, \delta(E - H_A). \tag{64}$$

The effective potential is energy dependent and also contains the imaginary part that brings about the decaying nature to the original bound state ϕ_n. It should be noted that the effective potential is not Hermitian and, hence, neither is H_B^+. Thus, H_B^+ has the energy-dependent complex eigenvalues and the biorthonormal set of eigenfunctions. The new KP eigenvalue equations are

$$(\omega_n(E) - H_B^+(E))|\xi_n(E)\rangle = 0, \tag{65}$$

$$\langle\eta_n(E)|(\omega_n(E) - H_B^+(E)) = 0, \tag{66}$$

where $\{\eta_n(E)\}$ are the dual states of the KP resonant states $\{\xi_n(E)\}$. The biorthonormal relations are shown to be

$$\langle\eta_n(E)|\xi_m(E)\rangle = N_n(E)\,\delta_{nm}. \tag{67}$$

Here, for the variational treatment of non-Hermitian operators the bivariational method (Boys, 1969) may be effective. For real energy E, the KP eigenvalue $\omega_n(E) = \varepsilon_n(E) - i\gamma_n(E)/2$ is given by

$$\varepsilon_n(E) = \langle\eta_n^*(E)|H_B + V_B\,\mathrm{P}(E - H_A)^{-1}V_A|\xi_n(E)\rangle/\mu_n(E), \tag{68}$$

$$\gamma_n(E) = 2\pi\langle\eta_n^*(E)|V_B\,\delta(E - H_A)V_A|\xi_n(E)\rangle/\mu_n(E), \tag{69}$$

where

$$\mu_n(E) = \langle\eta_n^*(E)|\xi_n(E)\rangle \neq N_n(E). \tag{70}$$

By using the KP biorthonormal complete set the functions Φ_A and Φ_B are written in the following forms:

$$\Phi_A = \phi_{A\alpha}^{(+)} + G_A^+ V_A \sum_n a_n \xi_n, \tag{71a}$$

$$\Phi_B = \sum_n a_n \xi_n, \tag{71b}$$

where

$$a_n(E) = \langle\eta_n(E)|V_B|\phi_{A\alpha}^{(+)}(E)\rangle/(E - \omega_n(E))N_n(E), \tag{71c}$$

and where $\phi_{A\alpha}^{(\pm)}$ are the outgoing (+) and the incoming (−) wavefunctions of H_A for a channel α. Then the transition matrix $\mathrm{T}_{\beta\leftarrow\alpha}$ is expressed as the sum of the direct amplitude $\mathrm{T}_{\beta\leftarrow\alpha}^{(0)}$ and the resonant amplitude $\mathrm{T}_{\beta\leftarrow\alpha}^{(r)}$:

$$\mathrm{T}_{\beta\leftarrow\alpha} = \mathrm{T}_{\beta\leftarrow\alpha}^{(0)} + \mathrm{T}_{\beta\sim\alpha}^{(r)}, \tag{72a}$$

$$\mathrm{T}_{\beta\leftarrow\alpha}^{(r)} = \sum_n \langle\phi_{A\beta}^{(-)}|V_A|\xi_n\rangle\langle\eta_n|V_B|\phi_{A\alpha}^{(+)}\rangle/(E - \omega_n)N_n. \tag{72b}$$

The nonsymmetric expression of the resonant amplitude is significant in the theory of angular distributions for resonant scattering of electrons by molecules (Read, 1968; Andrick and Read, 1971).

Now the intrinsic complex energy, the "complex resonance energy," is defined by the pole of the Green's function of the effective Hamiltonian (More and Gerjuoy, 1973), i.e., the complex pole of the resonant scattering amplitude. The pole is given by the root of the equation,

$$E = \omega_n(E). \tag{73}$$

The solution $E = W_n$ of this equation is nothing but the Siegert complex energy (Siegert, 1939) which requires the purely outgoing wave boundary condition for Ψ;

$$W_n = E_n - i\Gamma_n/2, \tag{74}$$

where E_n is the (physical) resonance energy and Γ_n is the width. In this case ($E = W_n$), Φ_B is equivalent to the Siegert resonant state or the resonance wavefunction defined by More and Gerjuoy (1973):

$$\Phi_B = \xi_n(W_n) \qquad \text{as } \phi_{A\alpha}^{(+)} = 0. \tag{75}$$

The Siegert states themselves cannot form the orthonormal complete set (More and Gerjuoy, 1973), although the total scattering wavefunction Ψ can be constructed by a linear combination of them (Huestis, 1975). Now, assuming that the pole is simple, one writes

$$E - \omega_n(E) = (E - W_n)R_n(E), \tag{76}$$

where R_n is so defined by this equation, and particularly at $E = W_n$, one has

$$R_n(W_n) = 1 - d\omega_n(W_n)/dW_n. \tag{77}$$

The gradient term is usually supposed to be small compared with unity at the resonance pole W_n, and then $E - \omega_n$ in the denominators of Eqs. (71c) and (72b) may be replaced by $E - W_n$. This makes it easy to estimate the transition matrix and the weight a_n of the KP eigenfunction.

As previously mentioned, it is clear that there are some differences between (i) $\varepsilon_n(E_n)$ and E_n, and (ii) $\gamma_n(E_n)$ and Γ_n. The estimates of the differences are given by

$$\varepsilon_n(E_n) - E_n = (d^2\varepsilon_n(E_n)/dE_n^2)\Gamma_n^2/8 + (d\gamma_n(E_n)/dE_n)\Gamma_n/4 + o(\Gamma_n^4), \tag{78}$$

$$\gamma_n(E_n)/\Gamma_n = 1 - d\gamma_n(E_n)/dE_n + o(\Gamma_n^2). \tag{79}$$

These equations show that the KP eigenvalue is not exactly consistent with the Siegert energy even when the energy E of the system takes the physical resonance energy E_n. These differences may become important when $\varepsilon_n(E)$ or $\gamma_n(E)$ rapidly change as E varies (Bandrauk and Laplante, 1976a,b). The value of W_n may be determined by a formula due to Lagrange, which has been used in perturbation theory by des Cloizeaux (1960), Sack (preprint), and Silverstone and Holloway (1970, 1971).

2. *Hellmann–Feynman Theorems*

The KP complex eigenvalue $\omega_n(E)$ depends on the energy E of the system as a kind of parameter. Therefore, it may be worth while to examine the Hellmann–Feynman theorem (Hellmann, 1937; Feynman, 1939; Epstein *et al.*, 1967). It will be possible to apply the Hellmann–Feynman theorem to the KP resonant state because the KP state is the eigenfunction of the effective Hamiltonian. In this case, the "extended" integral Hellmann–Feynman theorem here defined has the following form for an arbitrary parameter v:

$$\begin{aligned}&[\omega_n(E, v) - \omega_n(E, v')]\langle\eta_n(E, v)|\xi_n(E, v')\rangle \\ &\quad = \langle\eta_n(E, v)|H_B^+(E, v) - H_B^+(E, v')|\xi_n(E, v')\rangle.\end{aligned} \tag{80}$$

Parameter v can be chosen, for instance, as the nuclear coordinate for the molecular resonant state or the field strength F for the Stark broadening problem. In the limit $v' \to v$, one obtains the "extended" differential Hellmann–Feynman theorem:

$$\partial\omega_n(E, v)/\partial v = \langle\eta_n(E, v)|[\partial H_B^+(E, v)/\partial v]|\xi_n(E, v)\rangle/N_n(E, v), \tag{81}$$

$$= \langle\eta_n|[\partial H_B/\partial v]|\xi_n\rangle/N_n + \langle\eta_n|[\partial V(E)/\partial v]|\xi_n\rangle/N_n. \tag{81'}$$

It is interesting to compare this theorem with the usual one pertaining to bound states. The first term is the familiar one where only the bound-state Hamiltonian is differentiated. The second term, being due to the effective potential $V(E)$ defined by Eq. (63), is characteristic of the resonant state. Furthermore, let us find the V_A and V_B dependence of the complex eigenvalue. By supposing the order parameters of $V_{A,B}$ to be $\lambda_{A,B}$, and assuming that V_A and V_B are independent of each other, one gets

$$\partial\omega_n(E)/\partial\lambda_A = \langle\eta_n|V_B G_A^+(E)V_A + V_B G_A^+(E)V_A G_A^+(E)V_A|\xi_n\rangle/\lambda_A N_n, \tag{82}$$

$$\partial\omega_n(E)/\partial\lambda_B = \langle\eta_n|V_B + V_B G_A^+(E)V_A|\xi_n\rangle/\lambda_B N_n. \tag{83}$$

It is interesting to note that the higher-order scattering processes introduced by G_A^+ become sequentially important for the estimates of these quantities. Subsequently, for a different E, which is also characteristic of the present problem, one obtains

$$[\omega_n(E) - \omega_n(E')]\langle\eta_n(E)|\xi_n(E')\rangle = \langle\eta_n(E)|V_B[G_A^+(E) - G_A^+(E')]V_A|\xi_n(E')\rangle, \tag{84}$$

and hence

$$\partial\omega_n(E)/\partial E = \langle\eta_n(E)|V_{\mathrm{B}}[\partial G_{\mathrm{A}}^{+}(E)/\partial E]V_{\mathrm{A}}|\xi_n(E)\rangle/N_n(E), \tag{85}$$

$$= -\langle\eta_n(E)|V_{\mathrm{B}}[G_{\mathrm{A}}^{+}(E)]^2V_{\mathrm{A}}|\xi_n(E)\rangle/N_n(E). \tag{85'}$$

The differential Hellmann–Feynman theorem may be immediately afforded to the estimates of $d\varepsilon_n(E_n)/dE_n$ and $d\gamma_n(E_n)/dE_n$ in Eqs. (78) and (79). These theorems are potentially applicable to various problems of metastable chemical or physical phenomena.

3. *Relationships with Original Bound States*

It is desirable to make clear the relationships between the KP resonant states and the original bound states. The relationships in the frame of Löwdin's wave operator formalism (Löwdin, 1966) will be shown. This formalism has proven useful for the application to the problem of resonant states (Micha and Brändas, 1971). A brief outline is presented here.

Suppose the intermediate normalizations,

$$\langle\phi_n|\xi_n\rangle = \langle\eta_n|\phi_n\rangle = 1. \tag{86}$$

Then, one has the following relationships by introducing a set of wave operators, W_ξ and W_η:

$$|\xi_n\rangle = W_\xi|\phi_n\rangle, \qquad W_\xi = 1 + T(\omega_n)V, \tag{87}$$

$$\langle\eta_n| = \langle\phi_n|W_\eta, \qquad W_\eta = 1 + VT(\omega_n), \tag{88}$$

where V is the effective potential defined by Eq. (63), and T is the reduced resolvent of H_{B}^{+},

$$T(\lambda) = p_n(\lambda - H_{\mathrm{B}}^{+})^{-1}p_n, \tag{89}$$

$$p_n = 1 - |\phi_n\rangle\langle\phi_n|. \tag{90}$$

Then, one obtains

$$\omega_n = E_n^{(0)} + \langle\phi_n|V|\phi_n\rangle + \langle\phi_n|VT(\omega_n)V|\phi_n\rangle, \tag{91}$$

$$= E_n^{(0)} + \langle\phi_n|t(\omega_n)|\phi_n\rangle, \tag{91'}$$

where t is the reaction operator given by

$$t(\lambda) = V + VT(\lambda)V. \tag{92}$$

Additionally,

$$N_n = 1 + \langle\phi_n|VT(\omega_n)^2V|\phi_n\rangle. \tag{93}$$

These are exact functional relationships. It should be noted that the nonsymmetric nature of the effective potential makes it necessary to introduce the additional wave operator W_η for the dual state η_n; this is one of the essential differences compared with the usual wave operator formalism. As a corollary, the differential Hellmann–Feynman theorem for the variation of E can be written by

$$\partial\omega_n/\partial E = \langle\phi_n|[\partial t/\partial E]|\phi_n\rangle. \tag{94}$$

This expression will prove effective if one knows the energy dependence of the reaction operator t, even though in an approximate form.

B. The "Complex" Schrödinger Equation

It has been shown, in Eq. (74), that the energy is "quantized," $E = W_n$, on the complex energy plane. It should be emphasized that the Siegert energy W_n has been recognized as the "complex eigenvalue of H" under the boundary condition of purely outgoing wave for Ψ (Herzenberg *et al.*, 1964; Bardsley *et al.*, 1966; Nicolaides, 1972); that is, it satisfies the "complex" Schrödinger equation,

$$H\Psi(W_n) = W_n\Psi(W_n). \tag{95}$$

Note that $\Psi(W_n)$ could not be normalized in a usual coordinate space (Herzenberg *et al.*, 1964; Nicolaides and Beck, 1977). In our treatment, the Siegert energy defined by the solution of Eq. (73) can also be shown to satisfy the "complex" Schrödinger equation as follows. For real energy E, the KP eigenfunction ξ_n satisfies

$$H(1 + G_\mathrm{A}^+ V_\mathrm{A})\xi_n = \omega_n(1 + G_\mathrm{A}^+ V_\mathrm{A})\xi_n + (E - \omega_n)G_\mathrm{A}^+ V_\mathrm{A}\xi_n. \tag{96}$$

Consequently, after the analytical continuation $E \to W_n$, the wavefunction

$$\Psi(W_n) = (1 + G_\mathrm{A}^+(W_n)V_\mathrm{A})\xi_n(W_n) \tag{97}$$

satisfies the complex Schrödinger equation. The V_A and V_B dependence of the complex eigenvalue W_n may be found from Eqs. (82) and (83) to

$$\partial W_n/\partial\lambda_\mathrm{A} = \langle\eta_n(W_n)|V(W_n)|\Psi(W_n)\rangle/\lambda_\mathrm{A}N_n(W_n), \tag{82$'$}$$

$$\partial W_n/\partial\lambda_\mathrm{B} = \langle\eta_n(W_n)|V_\mathrm{B}|\Psi(W_n)\rangle/\lambda_\mathrm{B}N_n(W_n). \tag{83$'$}$$

Usually, from the decaying bound-state viewpoint, one may choose H_B as the unperturbed Hamiltonian $\mathscr{H}_0$ and V_A as the perturbation $\mathscr{H}'$ and obtain the physical resonance energy E_n perturbationally. This procedure corresponds to solving the complex Schrödinger equation without paying attention to the asymptotic decaying nature of the solution, and then the imaginary part Γ_n can not be obtained. From Eqs. (79) and (91), the imaginary part may be approximated by the Golden-Rule-type formula,

$$\begin{aligned}\Gamma_n &\sim -2\,\mathrm{Im}\langle\phi_n|V(E_n^{(0)})|\phi_n\rangle\\ &= 2\pi\langle\phi_n|V_A\,\delta(E_n^{(0)}-H_A)V_A|\phi_n\rangle\end{aligned}\tag{98}$$

(for the on-shell matrix element one can interchange V_B with V_A).

On the other hand, it is well known that the energy dependent eigenvalue of the kernel $K(E) = G_A^+(E)V_B$ for the Lippmann-Schwinger equation should become unity if $E = W_n$ (Herzenberg *et al.*, 1964; Hall and Levine, 1966; Taylor *et al.*, 1966). Likewise in the present treatment, the relation can be confirmed as follows. The KP eigenfunction ξ_n satisfies

$$(HK - KH)(1 + G_A^+V_A)\xi_n = V_B(K-1)(1 + G_A^+V_A)\xi_n + (E - \omega_n)K\xi_n. \tag{99}$$

At $E = W_n$, the wavefunction from Eq. (97) satisfies

$$(HK - KH)\Psi = V_B(K-1)\Psi. \tag{100}$$

It follows that, if Ψ is the eigenfunction for K with the eigenvalue unity, then Ψ is also that for H with the eigenvalue W_n. Conversely, if Ψ is the simultaneous eigenfunction for K and H, then the eigenvalue for K is unity. Thus one has

$$K(W_n)\Psi(W_n) = \Psi(W_n). \tag{101}$$

Finally, noting that both Eqs. (95) and (101) are valid for the bound states of H, one can see the close similarity between the decaying states and the bound states. The similarity will be discussed again from a different viewpoint in Section IV.

Example

Here an example of the present treatment is shown. Consider decaying states of a hydrogen-like atom under an external uniform electrostatic field—this is the example of the Stark broadening problem. The theory of field ionization of the hydrogen atom was first treated by Oppenheimer (1928), who obtained the Golden-Rule type formula, Eq. (98), for the ionization rate. Lanczos (1030a,b, 1931) and later Rice and Good (1962) treated the problem by the JWKB method. More recent treatments based on numerical methods (Alexander, 1969; Fauchier and Dow, 1974; Hehenberger *et al.*, 1974; Froelich and Brändas, 1975, 1976; Gushina and Nikulin, 1975; Damburg and Kolosov, 1976; Froelich and Brändas, 1976; Reinhardt, 1976; Brändas and Froelich, 1977; Froelich, Hehenberger, and Brändas, 1977) and on analytical approaches (Yamabe, Tachibana, and Silverstone, 1977b; Silverstone, 1978; Damburg and Kolosov, 1978) have more accurately considered the field dependence of the energies, of the widths, and of the intensities of the spectral lines. A different approach was taken by Duke and Alferieff (1966), who neglected the uniform field near the nucleus, and the Coulomb field far away. A one-dimensional model problem also has been treated by Yamabe *et al.* (1977a).

Now, the Hamiltonian of the hydrogen-like atom under the external field $-Fz$ is (atomic units are used)

$$H = -\Delta/2 - Z/r - Fz, \tag{102}$$

where Z is the nuclear charge. In this case, H_A and H_B are

$$H_A = -\Delta/2 - Fz, \tag{103}$$

$$H_B = -\Delta/2 - Z/r, \tag{104}$$

and hence the corresponding potentials are given by

$$V_A = -Fz, \tag{105}$$

$$V_B = -Z/r. \tag{106}$$

The eigenfunctions of H_B are trivial. Whereas the Hamiltonian H_A has the continuous energy spectrum E ranging from $-\infty$ to $+\infty$. The eigenfunction is separated in the cylindrical coordinates (ρ, ϕ, z) as follows (Oppenheimer, 1928):

$$\begin{aligned}\phi_{A(\lambda, m)}(\mathbf{r}; E) &= (2\pi)^{-1/2}\exp(im\phi)J_m(\lambda\rho)\\ &\quad\times (2^{1/2}(2F)^{-1/6})Ai\left(-(2F)^{1/3}\left(z + \frac{E-\varepsilon_\lambda}{F}\right)\right),\end{aligned} \tag{107a}$$

$$\varepsilon_\lambda = \lambda^2/2, \tag{107b}$$

where J_m is the mth-order Bessel function, and Ai is the Airy function (Antosiewicz, 1965). This eigenfunction is normalized for real E as

$$\int_0^\infty \rho\, d\rho \int_0^{2\pi} d\phi \int_{-\infty}^{\infty} dz \phi^*_{A(\lambda, m)}(\mathbf{r}; E)\phi_{A(\lambda', m')}(\mathbf{r}; E) = \delta_{mm'}\, \delta(\varepsilon_\lambda - \varepsilon'_\lambda)\, \delta(E - E'). \tag{108}$$

In this representation, ε_λ corresponds to the propagating energy of the electron along the $\rho = (x^2 + y^2)^{1/2}$ axis. The analytical forms of the Green's functions of H_B (Hostler and Pratt, 1963; L. Hostler, 1964; L. C. Hostler, 1969) and of H_A (Lukes and Somaratna, 1969; Whitcombe, 1971) are also available. Using these, we can solve the KP eigenvalue problem analytically.

Here the decay rate is estimated from the Golden-Rule-type approximation given by Eq. (98). For the initially prepared states the normal $\{n(l, m)\}$

TABLE I

GOLDEN-RULE-TYPE DECAY RATES

Quantum numbers	Decay rates[a]	
	$\Gamma_{n(l,m)}$	$\Gamma^{(z)}_{n(l,m)}$
$n = 3,\ l = 2,\ \lvert m\rvert = 2$	$\frac{\pi}{3a^2} e^{-2/81a^3F}$	0
$\lvert m\rvert = 1$	$\frac{\pi}{2 \cdot 3^4 a^5 F} e^{-2/81a^3F}$	0
$m = 0$	$\frac{\pi}{3^8 a^8 F^2} e^{-2/81a^3F}$	$\frac{2\pi}{3^9 a^9 F^3} e^{-2/81a^3F}$
$l = 1,\ \lvert m\rvert = 1$	$\frac{\pi}{2 \cdot 3^4 a^5 F} e^{-2/81a^3F}$	0
$m = 0$	$\frac{\pi}{3^7 a^8 F^2} e^{-2/81a^3F}$	$\frac{2\pi}{3^8 a^9 F^3} e^{-2/81a^3F}$
$l = 0,\ m = 0$	$\frac{2\pi}{3^8 a^8 F^2} e^{-2/81a^3F}$	$\frac{2^2\pi}{3^9 a^9 F^3} e^{-2/81a^3F}$
$n = 2,\ l = 1,\ \lvert m\rvert = 1$	$\frac{1}{2a^2} e^{-1/12a^3F}$	0
$m = 0$	$\frac{1}{2^3 a^5 F} e^{-1/12a^3F}$	$\frac{1}{2^3 a^6 F^2} e^{-1/12a^3F}$
$l = 0,\ m = 0$	$\frac{1}{2^3 a^5 F} e^{-1/12a^3F}$	$\frac{1}{2^3 a^6 F^2} e^{-1/12a^3F}$
$n = 1,\ l = 0,\ m = 0$	$\frac{\pi}{2a^2} e^{-2/3a^3F}$	$\frac{\pi}{a^3 F} e^{-2/3a^3F}$

[a] Here F is the field strength, and a is the inverse of the nuclear charge.

states are chosen. The leading term of the decay rate (see Table I) is mainly determined by the exponential factor that is dependent on the principal quantum number n and $a = Z^{-1}$;

$$\Gamma_{n(l,m)} \equiv 2\pi \int_0^\infty d\varepsilon_\lambda \lvert \langle \phi_{n(l,m)} \rvert (-Fz) \lvert \phi_{\mathrm{A}(\lambda, m')}(E_n^{(0)}) \rangle \rvert^2 \, \delta_{mm'}, \tag{109a}$$

$$\begin{aligned} &\sim \sigma[2^{2n-2m-2}(n!\,!)^2(2l+1)(l+m)!\,m! \\ &\quad /(n-l-1)!\,(n+1)!\,(l-m)!\,n^{3n-3m-1}F^{n-m-1}]^{-2/3n^3a^3F}, \\ &\qquad\qquad \text{when } F \sim 0, \end{aligned} \tag{109b}$$

where $|m|$ is conveniently replaced by m, and where

$$\sigma = 1 \quad \text{for even } n, \qquad \sigma = \pi/2 \quad \text{for odd } n. \tag{109c}$$

This slightly corrects the result of Oppenheimer's original estimate for the ground state of the hydrogen atom. Moreover, for the electron decaying only along the z axis, one may define and estimate the decay rate as

$$\Gamma^{(z)}_{n(l,m)} \equiv 2\pi \int_0^\infty d\varepsilon_\lambda |\langle \phi_{n(l,m)}|(-Fz)|\phi_{A(\lambda,m)}(E_n^{(0)})\rangle|^2 \, \delta(\varepsilon_\lambda), \tag{110a}$$

$$\sim \delta_{m0}(2/naF)\Gamma_{n(l,0)}, \tag{110b}$$

where the selection rule δ_{m0} holds exactly from Eq. (110a). Particularly, Landau and Lifshitz (1958) have estimated the decay rate for the ground state of the hydrogen atom along the z axis as $(4/F)e^{(-2/3F)}$, which is in close agreement with the present estimate,

$$\Gamma^{(z)}_{1(0,0)} \sim (\pi/F)e^{(-2/3F)}.$$

It should be noted that these estimates are proper to the approximate method employed, even though the general results of the coupled equations theory are exact (see the discussions in the preceding sections). Specifically, the prefactor of the decay rate is very sensitive to the analyticity of the total wavefunction (Yamabe *et al.*, 1977b; Silverstone, 1978), which may be represented by (i) the infinite summation of the perturbation series, and (ii) the modified definitions of V_A and/or V_B to improve the one-term approximation. Also, the general and critical discussion about the difference between the Siegert energy and the particular solution of the KP eigenvalue problem, Eqs. (78) and (79), will be shown by Tachibana *et al.* (1977).

These estimates will also be useful for applications to general tunneling problems of more complex systems.

IV. Comments on Recent Developments

A. Significance of Virtual Orbitals

In the Hartree–Fock theory of many-electron systems, the virtual orbitals have been regarded as the approximate orbitals employed for constructing the excited states of atoms and molecules and have played important roles in the configuration interaction calculation and the perturbation calculation based on the Hartree–Fock solutions. In the theory of charge-transfer complex (Mulliken, 1952) and chemical reactivity (Fukui and Fujimoto, 1968), they are also used as definite orbitals for the electron to be accepted from the electron donor.

Notwithstanding these important roles, there are only a few studies concerning the significance of the virtual orbitals. One of them is the work of Kelly (1963) who demonstrated that, in the Hartree–Fock calculations of neutral atoms and molecules, most of virtual orbitals are in a continuum. The long-range behavior of Hartree–Fock orbitals has also been studied by Handy *et al.* (1969), Weber *et al.* (1970), and Marron *et al.* (1970). Others (Kelly, 1964; Silverstone and Yin, 1968; Hunt and Goddard, 1969; Huzinaga and Arnau, 1970, 1971; Morokuma and Iwata, 1972; Hirao, 1974b; Hirao and Huzinaga, 1977) consider the Hamiltonian for the virtual orbitals, which is modified so as to be appropriate to describe the excited states of the original system. It is thus found that there may be two kinds of virtual orbitals with physical significance, i.e., one for charge transfer and another for excitation. Both may still be called "virtual orbitals" because of their orthogonality to the occupied orbitals. The unified treatment of Hartree–Fock orbitals has been expressed by using projection operators (Huzinaga *et al.*, 1973; Hirao and Nakatsuji, 1973).

Following the implication of the Hartree–Fock V^N potential, the virtual orbital of the first kind is considered to be the orbital for an additional electron that would be placed into this potential field without having any effect on the distribution of occupied orbitals. Therefore, the orbital may be interpreted physically as that of an electron that is far enough outside the atom or molecule so that the distribution of the occupied orbitals (and hence the change of the potential) can be neglected; for instance, an electron in a dipole field (Brown and Roberts, 1967; Coulson and Walmsley, 1967; Jordan and Luken, 1976) or the external electron associated with the formation or autoionization of negative ion (Chen, 1969; Compton and Huebner, 1970; Sanche and Schulz, 1973; Burrow and Jordan, 1975; Jordan *et al.*, 1976; Jordan and Burrow, 1978). Particularly in the low-energy resonance scattering of electrons from molecules, the angle dependence of the scattered electron (Read, 1968; O'Malley and Taylor, 1968; Andrick and Read, 1971) clearly reflects the symmetry of, and therefore the existence of, the virtual orbital of the first kind.

Likewise, the virtual orbital of the second kind may also play an important role for the description of core-excited resonant states (Taylor *et al.*, 1966). Also, if antibonding orbitals take part in the molecular resonance, the cleavage of chemical bond may also occur (dissociative attachment); the theory of dissociative attachment has been developed by Bardsley *et al.* (1964), O'Malley (1966), and Chen (1969).

Following these considerations, the virtual orbital may be a reasonable approximation to the basic constituent of the resonant wavefunction.

Additionally, recent work on the precursor of solvated electron suggests the existence of a "dry electron" that is an almost freely moving electron created in the spur. The dry electron, however, shows an extraordinarily poor reactivity to proton as scavenger (Lam and Hunt, 1975), and the origin is not precisely known (Steen, 1976). Also, from the theory of Regge poles (De Alfaro and Regge, 1965), recall that a pure Coulomb field does not possess the virtual orbital in the continuum. It may be tentatively said that this might be the origin of the poor reactivity: the dry electron shows a poor reactivity to proton since proton itself has no acceptable virtual orbital to allow the stabilization of the electron in the continuum.

Thus, the significance of virtual orbitals has recently been strengthened in the resonant-state theories. The recently developed, extended SCF theories (Hirao, 1974a; Nakatsuji, 1974) may be effective in the study of resonant states.

B. Method of Complex Coordinates

Direct determination of the Siegert complex energy itself can be achieved by complex coordinate method recently established by Aguilar and Combes (1971), Balslev and Combes (1971), and Simon (1973). By this method, the spectra of the Hamiltonian H which are represented in the complex coordinate space are studied. The complex coordinate representation of H is obtained by complex dilatation transformation of coordinates $\mathbf{r} \to e^{i\phi}\mathbf{r}$, $\phi > 0$. The transformed Hamiltonian is written as

$$H(\phi) = e^{-2i\phi}T + \mathscr{V}(\phi), \tag{111}$$

where T is the kinetic operator and $\mathscr{V}$ is the potential. The method is applicable to a large family of dilatation analytic (two-body) potentials, including Coulombic potentials, and hence is more powerful than the usual scattering theory. For the N-body system, in which mass points m_i interact with each other through the two-body interactions $\mathscr{V}_{ij}(\mathbf{r}_i - \mathbf{r}_j)$, the Hamiltonian H is obtained by eliminating the motion of the center of mass from the entire Hamiltonian $\mathscr{H}$ as follows:

$$\begin{aligned} \mathscr{H} &= \sum_{i=1}^{N} (\mathbf{p}_i^2/2m_i) + (1/2)\sum_{i \neq j}^{N} \mathscr{V}_{ij}(\mathbf{r}_i - \mathbf{r}_j) \\ &= \mathbf{P}^2/2M + H; \qquad \mathbf{P} = \sum_{i=1}^{N} \mathbf{p}_i,\ M = \sum_{i=1}^{N} m_i. \end{aligned} \tag{112}$$

Therefore H is the Hamiltonian for the internal motion of the system. Balslev and Combes (1971) have demonstrated that the real discrete eigenvalues for the bound states of H are invariant under the transformation, whereas the continuous spectrum is "rotated" by angle 2ϕ downward from the real axis. Moreover, as ϕ increases, discrete real or complex eigenvalues of the non-Hermitian $H(\phi)$ may be exposed. The real and the imaginary parts of the complex (resonance) eigenvalue give the resonance energy and the width, respectively. The new variational principle is then given by

$$\delta \tilde{W}_n(\theta) = \delta\langle H(\theta)\rangle = 0, \tag{113a}$$

$$\langle H(\theta)\rangle = \langle\tilde{\Psi}'_n|H(\theta)|\tilde{\Psi}_n\rangle/\langle\tilde{\Psi}'_n|\tilde{\Psi}_n\rangle, \tag{113b}$$

where we consider that the case for the general dilatation transformation is applied; $\mathbf{r} \to e^{\theta}\mathbf{r}$, θ is complex (Im $\theta > 0$). As $H(\theta)$ is non-Hermitian, we have a set of eigenvalue equations for the complex eigenvalue $W_n(\theta)$:

$$H(\theta)|\Psi_n(\theta)\rangle = W_n(\theta)|\Psi_n(\theta)\rangle, \tag{114}$$

$$\langle\Psi'_n(\theta^*)|H(\theta) = W_n(\theta)\langle\Psi'_n(\theta^*)|, \tag{115}$$

which satisfy the biorthonormal relations

$$\langle\Psi'_n(\theta^*)|\Psi_m(\theta)\rangle = N_n(\theta)\,\delta_{nm}. \tag{116}$$

It has been shown that the eigenfunctions can be obtained in the Hilbert space (Doolen *et al.*, 1974). Here, the dilatation transformation is governed by an operator $U(\theta)$ that is an element of the dilatation group:

$$U(\theta) = e^{i\theta W/\hbar}, \qquad U(\theta_1 + \theta_2) = U(\theta_1)U(\theta_2). \tag{117}$$

The generator of the group, W, is given by

$$W = \tfrac{1}{2}\sum_i (\mathbf{r}_i\mathbf{p}_i + \mathbf{p}_i\mathbf{r}_i), \tag{118}$$

where the summation is carried over $3(N - 1)$ degrees of freedom for the internal motion. Note that W is invariant under the dilatation transformation:

$$W(\theta) = W. \tag{119}$$

After the variational calculation in the Hilbert space is performed, the approximate wavefunctions may be refined by complex scaling, which is also governed by U:

$$|\tilde{\Psi}_{n,s}(\theta)\rangle = U(\Delta\theta_s)|\tilde{\Psi}_n(\theta)\rangle, \tag{120}$$

$$\langle\tilde{\Psi}'_{n,s}(\theta^*)| = \langle\tilde{\Psi}'_n(\theta^*)|U(\Delta\theta_s)^{-1}, \tag{121}$$

where $\Delta\theta_s$ is the complex scaling parameter. The optimum $\Delta\theta_s$ is then determined by substituting Eqs. (120) and (121) into Eq. (113a) and extremizing the functional about $\Delta\theta_s$. In the case of the Coulombic potentials, the $\Delta\theta_s$ is obtained as

$$e^{\Delta\theta_s} = -\langle\mathcal{V}(\theta)\rangle/2\langle T(\theta)\rangle = -e^{\theta}\langle\mathcal{V}\rangle/2\langle T\rangle, \tag{122}$$

and the scaled result becomes

$$\langle H(\theta)\rangle_s = -\langle \mathscr{V}(\theta)\rangle^2/4\langle T(\theta)\rangle = -\langle \mathscr{V}\rangle^2/4\langle T\rangle. \tag{123}$$

For exact wavefunctions, one may put $\Delta\theta_s = 0$ and finally obtain the "complex" virial theorem,[1] in the form of the hypervirial theorem (Hirschfelder, 1960; Epstein and Hirschfelder, 1961; Hirschfelder and Coulson, 1962):

$$(i/\hbar)\langle WH(\theta) - H(\theta)W\rangle = 0. \tag{124}$$

It is also found that, for an arbitrary parameter v, the "complex" Hellmann–Feynman theorems hold in (i) the integral form,

$$\begin{aligned}[][W_n(\theta, v) - W_n(\theta, v')]\langle \Psi_n'(\theta^*, v)|\Psi_n(\theta, v')\rangle \\ = \langle \Psi_n'(\theta^*, v)|H(\theta, v) - H(\theta, v')|\Psi_n(\theta, v')\rangle,\end{aligned} \tag{125}$$

and (ii) the differential form,

$$\partial W_n(\theta, v)/\partial v = \langle \partial H(\theta, v)/\partial v\rangle. \tag{126}$$

Interestingly, if this differential theorem is applied to the change of θ, then one finds that by virtue of the complex virial theorem

$$\partial W_n(\theta)/\partial\theta = 0. \tag{127}$$

It is concluded, therefore, that all of the complex eigenvalues of $H(\theta)$ are essentially θ independent. This result is a natural extension of the result obtained for only real eigenvalues. Hence, the formal Schrödinger equation $H\Psi = E\Psi$ provides the proper solutions not only for the real eigenvalues of bound states but also for the complex resonance energies of Siegert's resonant states (see the discussions in Section III, B). For real eigenvalue problems, one can then set $\theta = 0$. However, for complex eigenvalue problems, the non-zero imaginary part of θ is indispensable in order to guarantee the square-integrability of the eigenfunctions (Bain *et al.*, 1974). The applications

---

[1] Professor P.-O. Löwdin kindly informed the authors that the referee claimed that precisely the same result about the complex virial theorem and the scaling method was obtained and sent the related preprints, which had not been published, to the authors: (i) Brändas and Froelich (1977); (ii) Froelich, Hehenberger, and Brändas (1977). The authors of these preprints also utilize the complex coordinate method to the variational treatment of the complex eigenvalue problems of resonant states, and obtain an "extended" virial theorem as they call and apply it to the problem of Stark resonance of hydrogen atom, although the potential considered is not dilatation analytic. The extended virial theorem may be, in principle, analogous to the complex virial theorem. But they are not identical because the discussions presented in these preprints are all based on an assumption that $\Psi' = \Psi$; this assumption is different from the general premise, that is, Ψ' and Ψ are distinguished from each other by their mutually complex conjugate boundary conditions, on which premise the complex virial theorem holds.

of the method of complex coordinates are reviewed by Reinhardt (1976); the method opens a direct way to solve the complex eigenvalue problems for the Siegert resonant states in atoms and molecules.

Particularly in the application of the complex coordinate method to the molecular system under the Born–Oppenheimer adiabatic approximation, there arises a question as to which coordinates should be transformed into complex coordinates, electronic or both electronic and nuclear. If one transforms only the electronic coordinates, then one obtains θ-independent adiabatic complex potential energy surface. But if one transforms also the nuclear coordinates at the same time, then one obtains θ-dependent surface $E_{\text{ad}} = E_{\text{ad}}(\theta)$; the θ-dependence is shown to be (Tachibana *et al.*, 1978)

$$\partial E_{\text{ad}}(\theta)/\partial\theta = \sum_{a} e^{\theta}\mathbf{r}_{\text{a}} \cdot (\partial E_{\text{ad}}(e^{\theta}\mathbf{r}'_{\text{a}})/\partial(e^{\theta}\mathbf{r}_{\text{a}})) \tag{128}$$

where $\mathbf{r}_{\text{a}}$ denotes the nuclear coordinate. This is the virial of the external forces inherent to the clamped nuclei system, which is now transformed into the complex coordinate representation. Therefore, one finds an important result that the θ dependence vanishes in this case if the molecular system takes the equilibrium geometry. The dynamics of molecular resonant states will be briefly discussed on the basis of "complex" Heisenberg's equation of motion, where the hypervirial, virial, and Hellmann–Feynman theorems will be formulated in the "complex" form (Tachibana *et al.*, 1978).

Although electronic structure calculations are generally performed with Hermitian Hamiltonians, there are many situations other than shown here where the appropriate operator to be diagonalized is non-Hermitian. With respect to these kinds of problems, Morokuma and George (1973) have developed a general theory for *ab initio* calculations of potential energy surfaces in the complex plane.

REFERENCES

Aguilar, J., and Combes, J. M. (1971). *Commun. Math. Phys.* **22**, 269.

Ajmera, M. P., and Chung, K. T. (1974). *Phys. Rev. A* **10**, 1013.

Alexander, M. H. (1969). *Phys. Rev.* **178**, 34.

Andrick, D., and Read, F. H. (1971). *J. Phys. B* **4**, 389.

Antosiewicz, H. A. (1965). *In* "Handbook of Mathematical Functions" (M. Abramowitz and I. A. Stegun, eds.), p. 435. Nat. Bur. Stand., Washington, D.C.

Bain, R. A., Bardsley, J. N., Junker, B. R., and Sukumar, C. V. (1974). *J. Phys. B* **7**, 2189.

Balslev, E., and Combes, J. M. (1971). *Commun. Math. Phys.* **22**, 280.

Band, Y. B., and Freed, K. F. (1975). *J. Chem. Phys.* **63**, 3382.

Bandrauk, A. D., and Laplante, J. P. (1976a). *J. Chem. Phys.* **65**, 2592.

Bandrauk, A. D., and Laplante, J. P. (1976b). *J. Chem. Phys.* **65**, 2602.

Bardsley, J. N., Herzenberg, A., and Mandl, F. (1964). *In* "Atomic Collision Processes" (M. R. C. McDowell, ed.), p. 415. North-Holland Publ., Amsterdam.

Bardsley, J. N., Herzenberg, A., and Mandl, F. (1966). *Proc. Phys. Soc., London* **89**, 305.

Bhatia, A. K., and Temkin, A. (1969). *Phys. Rev.* **182**, 15.

Bhatia, A. K., and Temkin, A. (1976). *Phys. Rev. A* **13**, 2322.

Bloch, C. (1957). *Nucl. Phys.* **4**, 503.

Boys, S. F. (1969). *Proc. R. Soc. London, Ser. A* **309**, 195.

Brändas, E., and Froelich, P. (1977). *Phys. Rev. A* **16**, 2207.

Brown, W. B., and Roberts, R. E. (1967), *J. Chem. Phys.* **46**, 2006.

Burrow, P. D., and Jordan, K. D. (1975). *Chem. Phys. Lett.* **36**, 594.

Caplan, C. E., and Child, M. S. (1972). *Mol. Phys.* **23**, 249.

Chen, J. C. Y. (1969). *Adv. Radiat. Chem.* **1**, 245.

Compton, R. N., and Huebner, R. H. (1970). *Adv. Radiat. Chem.* **2**, 281.

Coulson, C. A., and Walmsley, M. (1967). *Proc. Phys. Soc., London* **91**, 31.

Damburg, R. J., and Kolosov, V. V. (1976). *J. Phys. B* **9**, 3149.

Damburg, R. J., and Kolosov, V. V. (1978). *J. Phys. B* **11**, 1921.

De Alfaro, V., and Regge, T. (1965). "Potential Scattering." North-Holland Publ., Amsterdam.

des Cloizeaux, J. (1960). *Nucl. Phys.* **20**, 321.

Doolen, G. D., Nuttall, J., and Stagat, R. W. (1974). *Phys. Rev. A* **10**, 1612.

Duke, C. B., and Alferieff, M. E. (1966). *Phys. Rev.* **145**, 583.

Epstein, S. T., and Hirschfelder, J. O. (1961). *Phys. Rev.* **123**, 1495.

Epstein, S. T., Hurley, A. C., Wyatt, R. E., and Parr, R. G. (1967). *J. Chem. Phys.* **47**, 1275.

Faddeev, L. D. (1960). *Zh. Eksp. Teor. Fiz.* **39**, 1459; *Sov. Phys.—JETP* (Engl. *Transl.*) **12**, 1014(1961).

Fauchier, J., and Dow, J. D. (1974). *Phys. Rev. A* **9**, 98.

Feshbach, H. (1962). *Ann. Phys.* (*N.Y.*) **19**, 287.

Feynman, R. P. (1939). *Phys. Rev.* **56**, 340.

Froelich, P., and Brändas, E. (1975). *Phys. Rev. A* **12**, 1.

Froelich, P., and Brändas, E. (1976). *Int. J. Quantum Chem., Symp.* **10**, 353.

Froelich, P., Hehenberger, M., and Brändas, E. (1977). *Int. J. Quantum Chem., Symp.* **11**, 295.

Fukui, K., and Fujimoto, H. (1968). *Bull. Chem. Soc. Jpn.* **41**, 1989.

Goldberger, M. L., and Watson, K. M. (1964a). "Collision Theory." Wiley, New York.

Goldberger, M. L., and Watson, K. M. (1964b). *Phys. Rev.* **136**, B1472.

Gushina, N. A., and Nikulin, V. K. (1975). *Chem. Phys.* **10**, 23.

Hahn, Y. (1968a). *Phys. Rev.* **169**, 794.

Hahn, Y. (1968b). *Phys. Rev.* **175**, 197.

Hahn, Y., and Watson, K. M. (1972). *Phys. Rev. A* **5**, 1718.

Hahn, Y., Kouri, D. J., and Levin, F. S. (1974). *Phys. Rev. C* **10**, 1620.

Hall, G. G., and Levine, R. D. (1966). *J. Chem. Phys.* **44**, 1567.

Handy, N. C., Marron, M. T., and Silverstone, H. J. (1969). *Phys. Rev.* **180**, 45.

Hehenberger, M., McIntosh, H. V., and Brändas, E. (1974). *Phys. Rev. A* **10**, 1494.

Hellmann, H. (1937). "Einführung in die Quantenchemie." Deuticke, Leibzig.

Herzenberg, A., Kwok, K. L., and Mandl, F. (1964). *Proc. Phys. Soc., London* **84**, 477.

Hirao, K. (1974a). *J. Chem. Phys.* **60**, 3215.

Hirao, K. (1974b). *J. Chem. Phys.* **61**, 3247.

Hirao, K., and Huzinaga, S. (1977). *Chem. Phys. Lett.* **45**, 55.

Hirao, K., and Nakatsuji, H. (1973). *J. Chem. Phys.* **59**, 1457.

Hirschfelder, J. O. (1960). *J. Chem. Phys.* **33**, 1462.

Hirschfelder, J. O., and Coulson, C. A. (1962). *J. Chem. Phys.* **36**, 941.

Hostler, L. (1964). *J. Math. Phys.* **5**, 591.

Hostler, L., and Pratt, R. H. (1963). *Phys. Rev. Lett.* **10**, 469.
Hostler, L. C. (1969). *Phys. Rev.* **178**, 126.
Huestis, D. L. (1975). *J. Math. Phys.* **16**, 2148.
Hunt, W. J., and Goddard, W. A., III. (1969). *Chem. Phys. Lett.* **3**, 414.
Huzinaga, S., and Arnau, C. (1970). *Phys. Rev. A* **1**, 1285.
Huzinaga, S., and Arnau, C. (1971). *J. Chem. Phys.* **54**, 1948.
Huzinaga, S., McWilliams, D., and Cantu, A. A. (1973). *Adv. Quantum Chem.* **7**, 187.
Jordan, K. D., and Burrow, P. D. (1978). *Acc. Chem. Res.* (to be published).
Jordan, K. D., and Luken, W. (1976). *J. Chem. Phys.* **64**, 2760.
Jordan, K. D., Michejda, J. A., and Burrow, P. D. (1976). *Chem. Phys. Lett.* **42**, 227.
Kapur, P., and Peierls, R. (1938). *Proc. R. Soc. London, Ser. A* **166**, 277.
Kelly, H. P. (1963). *Phys. Rev.* **131**, 684.
Kelly, H. P. (1964). *Phys. Rev.* **136**, B896.
Kouri, D. J., and Levin, F. S. (1975). *Nucl. Phys. A* **253**, 395.
Krüger, H., and Levin, F. S. (1976). *Phys. Lett. B* **65**, 109.
Krüger, H., and Levin, F. S. (1977). *Chem. Phys. Lett.* **46**, 95.
Lam, K. Y., and Hunt, J. W. (1975). *Int. J. Radiat. Phys. Chem.* **7**, 317.
Lanczos, C. (1930a). *Z. Phys.* **62**, 518.
Lanczos, C. (1930b). *Z. Phys.* **65**, 431.
Lanczos, C. (1931). *Z. Phys.* **68**, 204.
Landau, L. D., and Lifshitz, E. M. (1958). "Quantum Mechanics." Pergamon, Oxford.
Levin, R. D., and Bernstein, R. B. (1974). "Molecular Reaction Dynamics." Oxford Univ. Press, New York and London.
Lippmann, B. A., and O'Malley, T. F. (1970). *Phys. Rev. A* **2**, 2115.
Lipsky, L., and Connely, M. J. (1976). *Phys. Rev. A* **14**, 2193.
Lipsky, L., and Russek, A. (1966). *Phys. Rev.* **142**, 59.
Löwdin, P. O. (1966). *In* "Perturbation Theory and its Applications in Quantum Mechanics" (C. H. Wilcox, ed.), p. 255. Wiley, New York.
Lukes, T., and Somaratna, K. T. S. (1969). *J. Phys. C* **2**, 586.
McCarthy, I. E. (1968). "Introduction to Nuclear Theory." Wiley, New York.
Marron, M. T., Handy, N. C., Parr, R. G., and Silverstone, H. J. (1970). *Int. J. Quantum Chem.* **4**, 245.
Micha, D. A. (1974). *Adv. Quantum Chem.* **8**, 231.
Micha, D. A., and Brändas, E. (1971). *J. Chem. Phys.* **55**, 4792.
Miller, W. H. (1966). *Phys. Rev.* **152**, 70.
More, R. M. (1971a). *Phys. Rev. A* **3**, 1217.
More, R. M. (1971b). *Phys. Rev. A* **4**, 1782.
More, R. M., and Gerjuoy, E. (1973). *Phys. Rev. A* **7**, 1288.
Morokuma, K., and George, T. F. (1973). *J. Chem. Phys.* **59**, 1959.
Morokuma, K., and Iwata, S. (1972). *Chem. Phys. Lett.* **16**, 192.
Morse, P. M., and Feshbach, H. (1953). "Methods of Theoretical Physics." McGraw-Hill, New York.
Mulliken, R. S. (1952). *J. Am. Chem. Soc.* **74**, 811.
Nakatsuji, H. (1974). *J. Chem. Phys.* **61**, 3728.
Newton, R. G. (1960). *J. Math. Phys.* **1**, 319.
Newton, R. G. (1966). "Scattering Theory of Waves and Particles." McGraw-Hill, New York.
Nicolaides, C. A. (1972). *Phys. Rev. A* **6**, 2078.
Nicolaides, C. A., and Beck, D. R. (1977). *Phys. Lett. A* **60**, 92.
Nordholm, S., and Rice, S. A. (1975). *J. Chem. Phys.* **62**, 157.
O'Malley, T. F. (1966). *Phys. Rev.* **150**, 14.

O'Malley, T. F., and Geltman, S. (1965). *Phys. Rev.* **137**, A1344.
O'Malley, T. F., and Taylor, H. S. (1968). *Phys. Rev.* **176**, 207.
Oppenheimer, J. R. (1928). *Phys. Rev.* **31**, 66.
Peierls, R. (1948). *Proc. Cambridge Philos. Soc.* **44**, 242.
Read, F. H. (1968). *J. Phys. B* **1**, 893.
Reinhardt, W. P. (1976). *Int. J. Quantum Chem., Symp.* **10**, 359.
Rice, M. H., and Good, R. H., Jr. (1962). *J. Opt. Soc. Am.* **52**, 239.
Sack, R. A. "Perturbation Theory and Lagrange's Expansion" (preprint).
Sanche, L., and Schulz, G. J. (1973). *J. Chem. Phys.* **58**, 479.
Schulz, G. J. (1973a). *Rev. Mod. Phys.* **45**, 378.
Schulz, G. J. (1973b). *Rev. Mod. Phys.* **45**, 423.
Siegert, A. J. F. (1939). *Phys. Rev.* **56**, 750.
Silverstone, H. J. (1978). To be published.
Silverstone, H. J., and Holloway, T. T. (1970). *J. Chem. Phys.* **52**, 1472.
Silverstone, H. J., and Holloway, T. T. (1971). *Phys. Rev. A* **4**, 2191.
Silverstone, H. J., and Yin, M. L. (1968). *J. Chem. Phys.* **49**, 2026.
Simon, B. (1973). *Ann. Math.* **97**, 247.
Steen, H. B. (1976). *In* "Electron-Solvent and Anion-Solvent Interactions" (L. Kevan and B. C. Webster, eds.), p. 175. Elsevier, Amsterdam.
Tachibana, A., Yamabe, T., and Fukui, K. (1977). *J. Phys. B* **10**, 3175.
Tachibana, A., Yamabe, T., and Fukui, K. (1978). *Mol. Phys.* (in press).
Taylor, H. S., Nazaroff, G. V., and Golebiewski, A. (1966). *J. Chem. Phys.* **45**, 2872.
Temkin, A., Bhatia, A. K., and Bardsley, J. N. (1972). *Phys. Rev. A* **5**, 1663.
Weber, T. A., Handy, N. C., and Parr, R. G. (1970). *J. Chem. Phys.* **52**, 1501.
Whitcombe, A. R. (1971). *J. Phys. C* **4**, 1.
Yamabe, T., Tachibana, A., and Silverstone, H. J. (1977a). *J. Phys. B* **10**, 2083.
Yamabe, T., Tachibana, A., and Silverstone, H. J. (1977b). *Phys. Rev. A* **16**, 877.

ADVANCES IN QUANTUM CHEMISTRY, VOLUME 11

The Unitary Group and the Many-Body Problem*

F. A. MATSEN

Departments of Physics and Chemistry
University of Texas
Austin, Texas

I. Introduction

The unitary group formulation of many-body theory is an alternative to the conventional second-quantized formulation for particle-conserving problems. It differs from the latter by its replacement of products of creation and annihilation operators with infinitesimal generators of the unitary group that generate orbital transformations and by imposing statistics with a selection of invariant subspaces rather than by selection of Lie algebras. The formulation permits *de novo* a spin-free formulation of the many-body problem. In addition, the conventional time-dependent development evaluation of matrix elements by time ordering and Wick's theorem is replaced by a time-independent scheme based on generator commutation and the highest-weight state. The time-dependent evaluation of time-independent particle-hole Green's function is replaced by the equivalent time-independent superoperator formalism, which is also used here for the development of the random-phase approximation.

In the unitary group formulation, there is first specified an orbital space

$$V_\rho^{\square} : \{|r\rangle, r = 1 \text{ to } \rho\} \tag{I.1}$$

such that

$$\langle r|r'\rangle = \delta(r, r'). \tag{I.2}$$

---

* The work reported here was supported by the Robert E. Welch Foundation of Houston, Texas.

ISBN 0-12-034811-X

The unitary group in question is $U(\rho)$, the group of unitary transformations on $V_\rho^{\square}$. The unitary-group many-electron Hamiltonian is

$$\mathbf{H} = \mathbf{H}^0 + \mathbf{V} \tag{I.3}$$

with

$$\mathbf{H}^0 \equiv \overline{\sum_r \sum_s}^{\,\rho} h_{rs}\mathbf{E}_{rs}, \tag{I.4}$$

where

$$h_{rs} \equiv \langle r_i | \mathbf{h}_i | s_i \rangle \tag{I.5}$$

and

$$\mathbf{V} \equiv \tfrac{1}{2} \overline{\sum_r \sum_s \sum_t \sum_u}^{\,\rho} v_{rs,\,tu}(\mathbf{E}_{rs}\mathbf{E}_{tu} - \delta(s, t)\mathbf{E}_{ru}), \tag{I.6}$$

where

$$v_{rs,\,tu} \equiv \langle t_j | \langle r_i | e^2/\mathbf{r}_{ij} | s_i \rangle | u_j \rangle = v_{tu,\,rs} \tag{I.7}$$

and

$$\mathbf{E}_{rs} = \sum_{i=1}^{N} |r_i\rangle \langle s_i|. \tag{I.8}$$

By Eq. (I.8) and orbital orthogonality,

$$[\mathbf{E}_{rs}, \mathbf{E}_{tu}] = \delta(t, s)\mathbf{E}_{ru} - \delta(r, u)\mathbf{E}_{ts} \tag{I.9}$$

therefore the E_{rs} are the (infinitesimal) generators of $U(\rho)$. The Hilbert space of **H** is

$$V_\rho = \sum_{[\lambda]} \oplus V_\rho^{[\lambda]} \tag{I.10}$$

where

$$[\lambda] \equiv [\lambda^1, \lambda^2, \ldots, \lambda^\rho], \qquad \lambda^1 \geq \lambda^2 \geq \cdots \geq \lambda^\rho \tag{I.11}$$

is a partition of a positive integer, say k. A partition is graphically represented by a Young diagram composed of rows of k boxes with λ^i boxes in the ith row. For the orbital space Eq. (I.1), $k = 1$ and $YD[\lambda] = \square$. The spanning of an invariant space is

$$V_\rho^{[\lambda]} : \{|(m)\rangle, \ldots\}, \tag{I.12}$$

where $|(m)\rangle$ denotes a Gel'fand state graphically represented by a Gel'fand tableau, (m) being constructed by inserting N of the ρ orbitals into $YD[\lambda]$

in ascending order along columns and down rows with no orbital occurring more than once in a column. The weight (configuration) of (m) is denoted

$$\{m\} = \{g_1, g_2, \ldots, g_\rho\}, \tag{I.13}$$

where g_r is the occupation number of the rth orbital. The $|(m)\rangle$ is said to lie higher than $|(m')\rangle$ if $g_1 > g'_1$ or, if $g_2 = g'_1$, then $g_2 > g'_2$, etc. The highest-weight state is denoted $|(m^*)\rangle$ with

$$\{m^*\} = \{g_1^*, g_2^*, \ldots, g_\rho^*\} \equiv [\lambda] \tag{I.14}$$

which identifies the invariant space $V_\rho^{[\lambda]}$. A Hilbert subspace $V_\rho^{[\lambda]}$ is invariant under

$$\mathbf{W}(U(\rho)) : \{\mathbf{W}_i\} = \{\mathbf{I}, \mathbf{E}_{rs}, \mathbf{E}_{rs}\mathbf{E}_{tu}, \ldots\}, \tag{I.15}$$

the covering (or enveloping) algebra of $U(\rho)$. In particular the Gel'fand states are eigenvectors to a diagonal generator; i.e.,

$$\mathbf{E}_{rr}|(m)\rangle = g_r|(m)\rangle, \tag{I.16}$$

whereas a nondiagonal generator, E_{rs}, raises (or lowers) the weight for $r < s$ (or $r > s$). Then, since $|(m^*)\rangle$ is the highest-weight state,

$$\mathbf{E}_{rs}|(m^*)\rangle = 0 \qquad \text{for} \quad r < s. \tag{I.17}$$

We note that h_{rs}, $v_{rs,\,tu}$, and $\mathbf{E}_{rs}$ are independent of electron indices and that the particle number N does not appear explicitly in Eq. (I.3) or Eq. (I.9). At this point the theory is independent of particle number. If we now set $k = N$ the particle number, we see that V_ρ is a Fock space. In the unitary group formulation, the particle number, N, is specified *a priori* so that only the N-particle part of this Fock space is used. In this space the unitary group states are then labeled by partitions of the particle number, N, which can in consequence be regarded as a unitary group quantum number.

The only Hilbert subspaces that are physically significant for electrons are those with $[\lambda] = [1^N]$ for fermion orbitals and $[\lambda] = [2^p, 1^{N-2p}]$, $(p = N/2 - S)$ for freon (spin-free) orbitals. The Young diagrams can then have no more than one column for fermions and no more than two columns for freons. By the Gel'fand construction $g_r \leq 1$ for fermions and $g_r \leq 2$ for freons.

The literature on the unitary group is voluminous and only a few selected references can be given: Weyl (1931, 1939), Gel'fand (1950, 1967), Biedenharn (1963), Moshinsky (1963, 1965), and Louck (1970). Recent references on the unitary group and the many-body problem are Harter (1973), Harter and Patterson (1976), Patterson and Harter (1976), Matsen (1974, 1976a,b), and Paldus (1974, 1976). The development in Sections III, IV, and V are due mainly to Rowe (1970) and to Thouless (1972). Other useful many-body texts are Brown (1972), Linderberg and Öhrn (1973), Jones and March (1973), and Feshbach and de Shalit (1974). The concept of the superoperator has been developed mainly in the context of Green's function theory by Linderberg and Ratner (1970), Goscinski and Lukman (1970), Jørgensen (1975), and others.

II. Matrix Element Evaluation

To compute the spectrum and other properties of a many-electron system, it is necessary to evaluate the matrix elements $\langle (m)|\mathbf{H}|(m')\rangle$ of the unitary group Hamiltonian, Eq. (I.3) over the Gel'fand states $|(m)\rangle$ that span $V_\rho^{[\lambda]}$. Since the Hamiltonian is a second-degree polynomial in the generators, we require both $\langle (m)|\mathbf{E}_{rs}|(m')\rangle$ and $\langle (m)|\mathbf{E}_{rs}\mathbf{E}_{tu}|(m')\rangle$. There exist closed forms for the matrix elements of the elementary generators $\mathbf{E}_{rr+1}$ that are sufficient (but not necessarily convenient) for the calculation of $\langle (m)|\mathbf{H}|(m')\rangle$ (see Biedenharn, 1963; Paldus, 1976; Shavit, 1977).

An alternative method makes use of the highest-weight state of $V_\rho^{[\lambda]}$. Let $V_\rho^{\Box}$ be spanned by a set of orbitals numbered in the order of increasing energy. The state of highest weight, Eq. (I.14),

$$|(m^*)\rangle \equiv |\rangle \tag{II.1}$$

is then the state of lowest zero-order energy. We denote by h and p, the orbitals that are occupied and unoccupied, respectively, so that $g_{\mathrm{p}} = 0$ and for fermions $g_{\mathrm{h}} = 1$, whereas for freons $g_{\mathrm{h}} = 1, 2$ for open and closed shells, respectively. We defer the discussion of freon open shells to the end of the section. For closed-shell fermion and freon states,

$$\mathbf{E}_{\mathrm{hh}'}|\rangle = \delta(\mathrm{h}, \mathrm{h}')g_{\mathrm{h}}|\rangle \tag{II.2}$$

and

$$\mathbf{E}_{r\mathrm{p}}|\rangle = 0, \qquad r = \mathrm{h}, \mathrm{p}. \tag{II.3}$$

From this highest-weight (ground) Gel'fand state, we construct generator states as follows:

$$|(G)\rangle = B_{(G)}\mathbf{W}^{\dagger}_{(G)}|\rangle \tag{II.4}$$

where $\mathrm{B}_{(G)}$ is a normalization constant to be determined and where

$$\mathbf{W}^{\dagger}_{(G)} \equiv \mathbf{E}_{\mathrm{ph}}, \mathbf{E}_{\mathrm{ph}}\mathbf{E}_{\mathrm{p'h'}}, \ldots \varepsilon\mathbf{W}(U(\rho)) \tag{II.5}$$

representing single-particle, double-particle, etc., excitations.

Because the Hamiltonian is a polynomial in the generators and because of Eq. (II.4), the Hamiltonian representation is a linear combination of matrix elements of the form $\langle|\mathbf{W}_i|\rangle$, $\mathbf{W}_i \varepsilon \mathbf{W}(U(\rho))$ that are evaluated by repeated application of the commutation relation

$$\mathbf{E}_{rs}\mathbf{E}_{tu} = \mathbf{E}_{tu}\mathbf{E}_{rs} + [\mathbf{E}_{rs}, \mathbf{E}_{tu}] \tag{II.6}$$

and of Eqs. (II.2) and (II.3). For fermion orbitals, we obtain the familiar rule,

$$\langle|\mathbf{W}_i|\rangle = (-1)^{\mathrm{L}+\mathrm{H}}, \tag{II.7}$$

where L is the number of loops and H is the number of hole lines in the appropriate graphs (see Table I). By renumbering the orbitals, the degree of particle excitation can be raised without increasing algebraic labor. For example, if a doubly excited configuration or state vector is renumbered to be a highest-weight state, single- and double-particle excitation operations are sufficient to obtain three- and four-particle excitations as well as the lower-lying states.

We next apply the unitary group formulation to the perturbation calculation of the ground-state energy of for the closed-shell case for both fermions and freons. The graphs and Eq. (II.7) simplify the calculations and lead directly to the familiar diagrams. By Eq. (I.3) the zero-order energy is

$$\begin{aligned} E^{(0)}_{(\theta)} &= \langle|\mathbf{H}^0|\rangle \\ &= \overset{\rho}{\overline{\sum_r \sum_s}} h_{rs} \langle|\mathbf{E}_{rs}|\rangle. \end{aligned} \tag{II.8}$$

By [1.1] of Table I,

$$E^{(0)}_{(0)} = g \sum_{\mathrm{h}} \mathrm{h}_{\mathrm{hh}}. \tag{II.9}$$

By Eq. (I.6), the first-order perturbation energy is

$$\begin{aligned} E^{(1)}_{(0)} &= \langle|\mathbf{V}|\rangle \\ &= \tfrac{1}{2} \overset{\rho}{\overline{\sum_r \sum_s \sum_t \sum_u}} v_{rs,\,tu} \langle|\mathbf{E}_{rs}\mathbf{E}_{tu}|\rangle \\ &\quad - \tfrac{1}{2} \overset{\rho}{\overline{\sum_r \sum_s \sum_u}} v_{rs,\,su} \langle|\mathbf{E}_{ru}|\rangle. \end{aligned} \tag{II.10}$$

TABLE I

MATRIX ELEMENTS FOR THE HIGHEST-WEIGHT STATE

1 = 1	$\langle \| \mathbf{E}_{hh} \| \rangle = g$	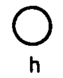	[1.1]
1 = 2	$\langle \| \mathbf{E}_{hh} \mathbf{E}_{h'h'} \| \rangle = g_h g_{h'}$		[2.1]
	$\langle \| \mathbf{E}_{hp} \mathbf{E}_{ph} \| \rangle = g$	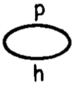	[2.2]
	$\langle \| \mathbf{E}_{co} \mathbf{E}_{oc} \| \rangle = g_c - g_o$	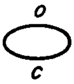	[2.3]
1 = 3	$\langle \| \mathbf{E}_{hp} \mathbf{E}_{h'h} \mathbf{E}_{ph'} \| \rangle = -g$	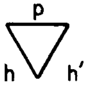	[3.1]
	$\langle \| \mathbf{E}_{hp} \mathbf{E}_{pp'} \mathbf{E}_{p'h} \| \rangle = g$	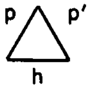	[3.2]
	$\langle \| \mathbf{E}_{hp} \mathbf{E}_{hh} \mathbf{E}_{ph} \| \rangle = g^2 - g$	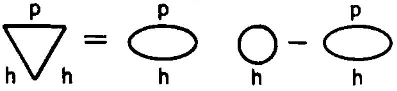	[3.3]
1 = 4	$\langle \| \mathbf{E}_{hp} \mathbf{E}_{h'p'} \mathbf{E}_{p'h'} \mathbf{E}_{ph} \| \rangle = g^2$	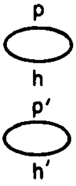	[4.1]
	$\langle \| \mathbf{E}_{h'p} \mathbf{E}_{hp'} \mathbf{E}_{p'h'} \mathbf{E}_{ph} \| \rangle = -g$	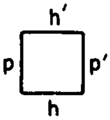	[4.2]
	$\langle \| \mathbf{E}_{hp} \mathbf{E}_{pp'} \mathbf{E}_{p'p} \mathbf{E}_{ph} \| \rangle = g$	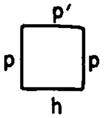	[4.3]

By using [2.1], [2.2], and [1.1] of Table I, we have

$$E^{(1)}_{(0)} = \tfrac{1}{2}\sum_{h}\sum_{h'}\left(g^2 v_{hh,h'h'} \qquad + \sum_{p} g v_{hpph}\right)$$

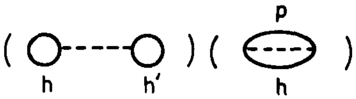

$$-\tfrac{1}{2}\sum_{h}\sum_{s} g v_{hssh} \qquad (s \equiv h', p). \tag{II.11}$$

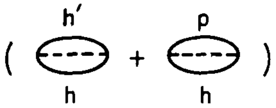

The two terms with diagrams 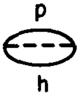 cancel so

$$E^{(1)}_{(0)} = (g/2)\sum_{h} v_{hh}, \tag{II.12}$$

where

$$v_{hh} \equiv \sum_{h'}\left(g v_{hhh'h'} - v_{hh'h'h}\right). \tag{II.13}$$

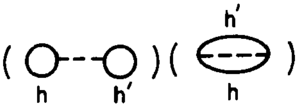

The energy to first order is then

$$E_{(0)} = \langle|\mathbf{H}|\rangle = g\sum_{h}\left(h_{hh} + \tfrac{1}{2}v_{hh}\right). \tag{II.14}$$

The second-order energy is

$$E^{(2)}_{(0)} = -\sum_{(G)}\frac{\langle|\mathbf{V}|(G)\rangle\langle(G)|\mathbf{V}|\rangle}{E^{(0)}_{(G)} - E^{(0)}_{(0)}} \tag{II.15}$$

To simplify the calculation we choose the orbitals to be Hartree–Fock orbitals in which case by Brillouin's theorem the sum over (G) contains no single-particle excitations. Since the remaining terms in V' are quadratic, excitations greater than double particle make no contributions, consequently

$$E^{(2)}_{(0)} = \frac{-1}{g^{L}}\sum_{p}\sum_{p'}\sum_{h}\sum_{h'}\frac{\langle|\mathbf{V}\mathbf{E}_{ph}\mathbf{E}_{p'h'}|\rangle\langle|\mathbf{E}_{h'p'}\mathbf{E}_{hp}\mathbf{V}|\rangle}{\varepsilon(p) + \varepsilon(p') - \varepsilon(h) - \varepsilon(h')}, \tag{II.16}$$

where, by [4.1] and [4.2] of Table I,

$$\langle|\mathbf{V}\mathbf{E}_{\mathrm{ph}}\mathbf{E}_{\mathrm{p'h'}}|\rangle = \tfrac{1}{2}\overset{\rho}{\overline{\sum_{r}\sum_{s}\sum_{t}\sum_{u}}} v_{rs,\,tu}\langle|\mathbf{E}_{rs}\mathbf{E}_{tu}\mathbf{E}_{\mathrm{ph}}\mathbf{E}_{\mathrm{p'h'}}|\rangle$$

$$= \tfrac{1}{2}(g v_{\mathrm{hph'p'}} - v_{\mathrm{hp'h'p}})g$$

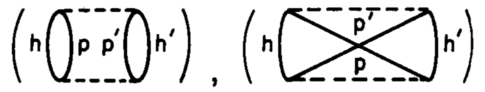

(II.17)

We now remove the restriction to freon closed shells. We divide the h orbitals into two sets, the closed set with h ≡ c, $g_c = 2$ and the open set with h = o, $g_o = 1$. For the highest-weight state of $[\lambda] = [2^{\mathrm{p}}, 1^{N-2\mathrm{p}}]$, $S = N/2 = \mathrm{p}$, the number of closed orbitals is

$$n_c = \mathrm{p}, \tag{II.18}$$

the number of open orbitals is

$$n_o = N - 2\mathrm{p}, \tag{II.19}$$

and the total number of occupied orbitals is

$$n = n_c + n_o = N - \mathrm{p}. \tag{II.20}$$

For singlet states, $n_c = N/2, n_o = 0$; for doublet states, $n_c = (N-1)/2, n_o = 1$; for triplet states, $n_c = (N-2)/2$, $n_o = 2$; etc. Then by [2.1], [2.2], and [2.3] of Table I, the energy of the highest-weight state is

$$\begin{aligned} E_{(0)} &= \langle|\mathbf{H}|\rangle \\ &= \sum_{c} g_c \mathrm{h}_{cc} + \sum_{o} g_o \mathrm{h}_{oo} \\ &\quad + \tfrac{1}{2}\sum_{c}\sum_{c'}(g_c^2 v_{cc c'c'} - g_c v_{cc'c'c}) \\ &\quad + \tfrac{1}{2}\sum_{o}\sum_{o'}(g_o^2 v_{oo o'o'} - g_o v_{oo'o'o}) \\ &\quad + \sum_{c}\sum_{o}(g_c g_o v_{ccoo} - (g_c - g_o)v_{cooc}). \end{aligned} \tag{II.21}$$

III. The Hartree–Fock Theory

The Hartree–Fock orbitals are defined as that set of orbitals which make stationary the energy of the highest-weight state of $V_\rho^{[\lambda]}$. We affect the variation of orbitals by a unitary transformation,

$$|V\rangle = e^{\mathbf{Z}}|\rangle, \tag{III.1}$$

where

$$\mathbf{Z}^{\dagger} \equiv \sum_{\mathrm{p}} \sum_{\mathrm{h}} (Z_{\mathrm{ph}} \mathbf{E}_{\mathrm{ph}} + \bar{Z}_{\mathrm{ph}} \mathbf{E}_{\mathrm{hp}}) \tag{III.2}$$

is skew Hermitian,

$$\mathbf{Z} = -\mathbf{Z}^{\dagger}. \tag{III.3}$$

Its energy is by the Baker–Campbell–Hausdorff expansion

$$\begin{aligned} E(V) &= \langle V|\mathbf{H}|V\rangle \\ &= \langle |e^{-\mathbf{Z}}\mathbf{H}e^{\mathbf{Z}}|\rangle \\ &= \langle |\mathbf{H}|\rangle + \langle |[\mathbf{H}, \mathbf{Z}]|\rangle + \tfrac{1}{2}\langle |[[\mathbf{Z}, \mathbf{H}], \mathbf{Z}^{\dagger}]|\rangle + \cdots. \end{aligned} \tag{III.4}$$

The extremum condition on the variation is

$$\lim_{\mathbf{Z}\to 0} \frac{\partial}{\partial Z_{\mathrm{ph}}} \langle |[\mathbf{H}, \mathbf{Z}]|\rangle = \langle |[\mathbf{H}, \mathbf{E}_{\mathrm{ph}}]|\rangle = 0 \tag{III.5}$$

or

$$\lim_{\mathbf{Z}\to 0} \frac{\partial}{\partial \bar{Z}_{\mathrm{ph}}} \langle |[\mathbf{H}, \mathbf{Z}]|\rangle = \langle |[\mathbf{H}, \mathbf{E}_{\mathrm{hp}}]|\rangle = 0. \tag{III.6}$$

The two conditions are equivalent and constitute Brillouin's theorem. After substitution of **H** [Eq. (I.3)], the commutation rules are applied and the matrix elements worked out as in Section II. Initially we restrict the highest weight to a closed-shell state, with $g = 1$ for fermions and $g = 2$ for freons. Thus

$$\langle |[\mathbf{E}_{\mathrm{hp}}, \mathbf{E}_{rs}]|\rangle = \delta(r, \mathrm{p})\, \delta(s, \mathrm{h}) g_{\mathrm{h}}. \tag{III.7}$$

Further, by commutation

$$\begin{aligned} \langle |[\mathbf{E}_{\mathrm{hp}}, \mathbf{E}_{rs}\mathbf{E}_{tu}]|\rangle &= \langle |[\mathbf{E}_{\mathrm{hp}}, \mathbf{E}_{rs}]\mathbf{E}_{tu}|\rangle + \langle |\mathbf{E}_{rs}[\mathbf{E}_{\mathrm{hp}}, \mathbf{E}_{tu}]|\rangle \\ &= \delta(r, \mathrm{p})\langle |\mathbf{E}_{\mathrm{h}s}\mathbf{E}_{tu}|\rangle - \delta(s, \mathrm{h})\langle |\mathbf{E}_{r\mathrm{p}}\mathbf{E}_{tu}|\rangle \\ &\quad + \delta(t, \mathrm{p})\langle |\mathbf{E}_{rs}, \mathbf{E}_{\mathrm{h}u}|\rangle - \delta(u, \mathrm{h})\langle |\mathbf{E}_{rs}\mathbf{E}_{t\mathrm{p}}|\rangle \end{aligned} \tag{III.8}$$

so

$$\begin{aligned} \langle |[\mathbf{E}_{\mathrm{hp}}, \mathbf{E}_{rs}\mathbf{E}_{tu}]|\rangle = \delta(r, \mathrm{p})[&\delta(s, \mathrm{h})\, \delta(t, u, \mathrm{h}')g^2 \\ &+ \delta(u, \mathrm{h})\, \delta(s, t, \mathrm{p})g] \\ &- \delta(s, \mathrm{h})\, \delta(t, \mathrm{p})\, \delta(r, u, \mathrm{h}')g \\ &+ \delta(t, \mathrm{p})\, \delta(r, s, \mathrm{h}')\, \delta(u, h)g^2. \end{aligned} \tag{III.9}$$

The extremum condition, Eq. (III.5), is then

$$h_{\mathrm{ph}} + v_{\mathrm{ph}} = 0, \tag{III.10}$$

where

$$v_{\mathrm{ph}} \equiv \sum_{\mathrm{h}'} (g v_{\mathrm{phh'h'}} - v_{\mathrm{ph'h'h}}). \tag{III.11}$$

The set of orbitals that diagonalize the Fock operator

$$\mathbf{F} \equiv \sum_{i} \sum_{j} (\mathrm{h}_{ij} + v_{ij}) \mathbf{E}_{ij} \tag{III.12}$$

with

$$v_{ij} = \sum_{\mathrm{h}'} (g v_{ij\mathrm{h'h'}} - v_{i\mathrm{h'h'}j}), \tag{III.13}$$

i.e., the set of orbitals for which

$$\mathrm{h}_{ij} + v_{ij} - \varepsilon(i)\, \delta(i, j) = 0 \qquad i, j = \mathrm{h}, \mathrm{p} \tag{III.14}$$

are Hartree–Fock orbitals since Eq. (III.14) satisfies the extremum condition Eq. (III.10). Let

$$|i\rangle = \sum_{r} |r\rangle\langle r|i\rangle \tag{III.15}$$

be the transformation between the Hartree–Fock and the primary orbitals. With this transformation, Eq. (III.14) becomes

$$\sum_{r} \sum_{s} \langle i|r\rangle(\mathrm{h}_{rs} + v_{rs} - \varepsilon(j)\, \delta(i, j)\langle r|s\rangle)\langle s|j\rangle = 0, \tag{III.16}$$

where

$$v_{rs} = \sum_{\mathrm{h}} (g v_{rs\mathrm{hh}} - v_{r\mathrm{hh}s}) = \sum_{t} \sum_{u} \mathrm{p}_{tu}(g v_{rstu} - v_{ruts}) \tag{III.17}$$

and where

$$\mathrm{p}_{tu} \equiv \sum_{\mathrm{h}} \langle u|\mathrm{h}\rangle\langle \mathrm{h}|t\rangle. \tag{III.18}$$

On multiplying Eq. (III.16) by $\langle t|i\rangle(i = j)$ and summing over i, the extremum condition becomes

$$\sum_{s} (\mathrm{h}_{rs} + v_{rs} - \varepsilon(j)\langle r|s\rangle)\langle s|j\rangle = 0. \tag{III.19}$$

This is solved self-consistently beginning with a guess for $\langle s|j\rangle$, computing v_{rs}, solving Eq. (III.19) for a second approximation to $\langle s|j\rangle$, etc. By Eqs. (II.14) and (III.14), the Hartree–Fock energy is

$$\begin{aligned} E(\mathrm{HF}) = E_{(0)}^{(0)} + E_{(0)}^{(1)} &= g \sum_{\mathrm{h}} (\mathrm{h}_{\mathrm{hh}} + \tfrac{1}{2} v_{\mathrm{hh}}) \\ &= \sum_{\mathrm{h}} g(\varepsilon(\mathrm{h}) - \tfrac{1}{2} v_{\mathrm{hh}}). \end{aligned} \tag{III.20}$$

By Eq. (III.4), the condition that the extremum be a minimum (the stability condition) is

$$\lim_{\mathbf{Z}\to 0} \frac{\partial^2}{\partial Z_{\mathrm{ph}}^2} \langle | [[\mathbf{Z}, \mathbf{H}], \mathbf{Z}^\dagger] | \rangle \geq 0. \tag{III.21}$$

The matrix element in Eq. (III.21) is a superoperator matrix element (see Section IV),

$$\langle | [[\mathbf{Z}, \mathbf{H}], \mathbf{Z}^\dagger] | \rangle \equiv \langle | \mathbf{Z} \hat{\mathbf{H}} \mathbf{Z}^\dagger | \rangle, \tag{III.22}$$

in the random-phase approximation (RPA) and is discussed in Section V.

We now drop the restriction to closed freon shells and decompose h into c (closed) and o (open) orbitals leading to three extremum conditions:

$$\langle | [\mathbf{E}_{\mathrm{co}}, \mathbf{H}] | \rangle = \langle | [\mathbf{E}_{\mathrm{cp}}, \mathbf{H}] | \rangle = \langle | [\mathbf{E}_{\mathrm{op}}, \mathbf{H}] | \rangle = 0 \tag{III.23}$$

and three Fock operators. The details are given by Matsen and Nelin (1978) and Roothaan (1960).

Generally, the matrix elements are formulated in terms of fermions, which are then integrated over the spin coordinate. If the freons form a closed shell, the fermion and spin-free treatments give the same results; this is called restricted Hartree–Fock (RHF). If the freons are not in closed shells, the fermion theory does not produce a pure spin state and is called unrestricted Hartree–Fock (UHF). If UHF is spin-projected into the various spin states (PUHF), the results are the same as for the spin-free treatment.

IV. The Superoperator Theory

The superoperator (or equation of motion) formulation of the many-body problem is a device for the calculation of excited states from a given ground state. It provides a route to the random-phase approximation (RPA), a route that does not require the linearization of quadratic operators. It has application to the Hartree–Fock stability condition, Eq. (III.21) and to time-independent Green's function (Section VI).

In the superoperator formulation (SOF), the Hamiltonian acts as a superoperator on an operator vector space and has as eigenoperators and eigenvalues excitation operators and excitation energies, respectively. Let

$$V_\rho^{[\lambda]} : \{ |0\rangle, \mathbf{W}_i^\dagger |0\rangle ; i = 1 \text{ to } \gamma \} \tag{IV.1}$$

be a Hilbert subspace of H with $|0\rangle$ the exact ground state and $\mathbf{W}_i^\dagger \varepsilon \mathbf{W}(U(\rho))$. Now let

$$\hat{V}_\rho^{[\lambda]} : \{ \mathbf{W}_i, \mathbf{W}_j^\dagger ; i, j = 1 \text{ to } \gamma \} \tag{IV.2}$$

be an operator vector space relative to $V_\rho^{[\lambda]}$ spanned by "primary" operators and let $\hat{\mathbf{S}}$ and $\hat{\mathbf{H}}$ be the unit and Hamiltonian superoperators, respectively.

The metric in the primary basis is defined by

$$[\hat{S}]_W = \begin{bmatrix} C_W & K_W \\ K_W^* & -C_W^* \end{bmatrix} \tag{IV.3}$$

a $2\gamma \times 2\gamma$ matrix with $\gamma \times \gamma$ submatrices defined by

$$\begin{aligned} C_{ij} &\equiv \langle 0|\mathbf{W}_i \hat{\mathbf{S}} \mathbf{W}_j^\dagger|0\rangle \\ &\equiv \langle 0|[\mathbf{W}_i, \mathbf{W}_j^\dagger]|0\rangle \\ &= -\langle 0|[\mathbf{W}_i^\dagger, \mathbf{W}_j]|0\rangle^* \end{aligned} \tag{IV.4}$$

and

$$\begin{aligned} K_{ij} &\equiv \langle 0|\mathbf{W}_i \hat{\mathbf{S}} \mathbf{W}_j|0\rangle \\ &= \langle 0|[\mathbf{W}_i, \mathbf{W}_j]|0\rangle \\ &= \langle 0|[\mathbf{W}_i^\dagger, \mathbf{W}_j^\dagger]|0\rangle^*. \end{aligned} \tag{IV.5}$$

We denote a general operator in $\hat{V}_p^{[\lambda]}$ by

$$\mathbf{F}^\dagger = \sum_i (F_i \mathbf{W}_i^\dagger + \bar{F}_i \mathbf{W}_i) \equiv \begin{bmatrix} F \\ \bar{F} \end{bmatrix} \tag{IV.6}$$

and the adjoint operator by

$$\mathbf{F} = \sum_i (F_i^* \mathbf{W}_i + \bar{F}_i^* \mathbf{W}_i^\dagger) \equiv \begin{bmatrix} F^* \\ \bar{F}^* \end{bmatrix}. \tag{IV.7}$$

The superoperator matric element for $\hat{S}$ between $F^\dagger$ and $G^\dagger$ is then

$$\begin{aligned} \langle 0|\mathbf{F}^\dagger \hat{\mathbf{S}} \mathbf{G}^\dagger|0\rangle &\equiv \langle 0|[\mathbf{F}^\dagger, \mathbf{G}^\dagger]|0\rangle \\ &\equiv [\bar{F} F] \begin{bmatrix} C_W & K_W \\ K_W^* & -C_W^* \end{bmatrix} \begin{bmatrix} G \\ \bar{G} \end{bmatrix}. \end{aligned} \tag{IV.8}$$

The superoperator representation of $\hat{H}$ in the primary basis is defined by

$$[\hat{H}]_W = \begin{bmatrix} A_W & L_W \\ L_W^* & A_W^* \end{bmatrix}, \tag{IV.9}$$

where

$$\begin{aligned} A_{ij} &\equiv \langle 0|\mathbf{W}_i \hat{\mathbf{H}} \mathbf{W}_j^\dagger|0\rangle \\ &= \langle 0|[[\mathbf{W}_i, \mathbf{H}], \mathbf{W}_j^\dagger]|0\rangle \\ &= \langle 0|[[\mathbf{W}_i^\dagger, \mathbf{H}], \mathbf{W}_j]|0\rangle^* \end{aligned} \tag{IV.10}$$

and

$$\begin{aligned} L_{ij} &\equiv \langle 0|\mathbf{W}_i \hat{\mathbf{H}} \mathbf{W}_j|0\rangle \\ &= \langle 0|[[\mathbf{W}_i, \mathbf{H}], \mathbf{W}_j]|0\rangle \\ &= \langle 0|[[\mathbf{W}_i^\dagger, \mathbf{H}], \mathbf{W}_j^\dagger]|0\rangle^*. \end{aligned} \tag{IV.11}$$

The superoperator matrix element for $\hat{H}$ between $F^\dagger$ and $G^\dagger$ is

$$\begin{aligned} \langle 0|\mathbf{F}^\dagger \hat{\mathbf{H}} \mathbf{G}^\dagger|0\rangle &\equiv \langle 0|[[\mathbf{F}^\dagger, \mathbf{H}], \mathbf{G}]|0\rangle \\ &\equiv [\overline{F}, F] \begin{bmatrix} A_W & L_W \\ L_W^* & A_W^* \end{bmatrix} \begin{bmatrix} G \\ \overline{G} \end{bmatrix}. \end{aligned} \tag{IV.12}$$

We seek a set of operators that are eigenoperators to $\hat{H}$ and which we denote by

$$\mathbf{Q}_\nu^\dagger = \sum_i (Q_i^\nu \mathbf{W}_i^\dagger + \overline{Q}_i^\nu \mathbf{W}_i) \equiv \begin{bmatrix} Q^\nu \\ \overline{Q}^\nu \end{bmatrix} \tag{IV.13}$$

with adjoint operators that we denote by

$$\mathbf{Q}_\nu = \sum_i (Q_i^{\nu*} \mathbf{W}_i + \overline{Q}_i^{\nu*} \mathbf{W}_i^\dagger) \equiv \begin{bmatrix} Q^{\nu*} \\ \overline{Q}^{\nu*} \end{bmatrix}. \tag{IV.14}$$

The orthonormality condition on the eigenoperators is

$$\begin{aligned} \delta(\mu, \nu) &\equiv C_{\mu\nu} \\ &\equiv \langle 0|\mathbf{Q}_\mu \hat{\mathbf{S}} \mathbf{Q}_\nu^\dagger|0\rangle \\ &= \langle 0|[\mathbf{Q}_\mu, \mathbf{Q}_\nu^\dagger]|0\rangle \\ &= -\langle 0|[\mathbf{Q}_\mu^\dagger, \mathbf{Q}_\nu]|0\rangle^* \\ &= -C_{\mu\nu}^* \end{aligned} \tag{IV.15}$$

and

$$\begin{aligned} 0 &\equiv K_{\mu\nu} \\ &\equiv \langle 0|\mathbf{Q}_\mu \hat{\mathbf{S}} \mathbf{Q}_\nu|0\rangle \\ &= \langle 0|[\mathbf{Q}_\mu, \mathbf{Q}_\nu]|0\rangle \\ &= \langle 0|[\mathbf{Q}_\mu^\dagger, \mathbf{Q}_\nu^\dagger]|0\rangle^* \\ &= K_{\mu\nu}^*. \end{aligned} \tag{IV.16}$$

So the metric in the eigenoperator basis is

$$\begin{aligned} [\hat{S}]_Q &= \begin{bmatrix} C_Q & K_Q \\ K_Q^* & -C_Q^* \end{bmatrix} \\ &= \begin{bmatrix} 1 & 0 \\ 0 & -1 \end{bmatrix}, \end{aligned} \tag{IV.17}$$

where 1 represents a $\gamma \times \gamma$ unit matrix. The eigenvalue condition is for real eigenvalues

$$\begin{aligned} \delta(\mu, \nu) w_\nu &= A_{\mu\nu} \\ &\equiv \langle 0 | \mathbf{Q}_\mu \hat{\mathbf{H}} \mathbf{Q}_\nu^\dagger | 0 \rangle \\ &= \langle 0 | [[\mathbf{Q}_\mu, \mathbf{H}], \mathbf{Q}_\nu^\dagger] | 0 \rangle \\ &= \langle 0 | [[\mathbf{Q}_\mu^\dagger, \mathbf{H}], \mathbf{Q}_\nu] | 0 \rangle^* \\ &= A_{\mu\nu}^* \end{aligned} \tag{IV.18}$$

and

$$\begin{aligned} 0 &= L_{\mu\nu} \\ &\equiv \langle 0 | \mathbf{Q}_\mu \hat{\mathbf{H}} \mathbf{Q}_\nu | 0 \rangle \\ &= \langle 0 | [[\mathbf{Q}_\mu, \mathbf{H}], \mathbf{Q}_\nu] | 0 \rangle \\ &= \langle 0 | [[\mathbf{Q}_\mu^\dagger, \mathbf{H}], \mathbf{Q}_\nu^\dagger] | 0 \rangle^* \\ &= L_{\mu\nu}^* . \end{aligned} \tag{IV.19}$$

So the representation of $\hat{H}$ in the eigenvector basis is

$$\begin{aligned} [\hat{H}]_Q &= \begin{bmatrix} A_Q & L_Q \\ L_Q^* & A_Q^* \end{bmatrix} \\ &= \begin{bmatrix} w & 0 \\ 0 & w \end{bmatrix}, \end{aligned} \tag{IV.20}$$

where

$$w = \text{diag}\, \{w_\gamma\}. \tag{IV.21}$$

The secular equation in the eigenoperator basis is

$$\begin{aligned} \det([\hat{\mathbf{H}}]_Q - \mathcal{E}[\mathbf{S}]_Q) &= \det\left(\begin{bmatrix} w & 0 \\ 0 & w \end{bmatrix} - \mathcal{E} \begin{bmatrix} 1 & 0 \\ 0 & -1 \end{bmatrix} \right) \\ &= 0 \end{aligned} \tag{IV.22}$$

so the eigenvalues are

$$\mathscr{E} = \begin{Bmatrix} +w \\ -w \end{Bmatrix}. \tag{IV.23}$$

In the primary basis, the secular equation is

$$\begin{aligned} \det([\hat{\mathbf{H}}]_w - \mathscr{E}[\hat{\mathbf{S}}]_w) &= \det\left(\begin{bmatrix} A_W & L_W \\ L_W^* & A_W^* \end{bmatrix} - \mathscr{E} \begin{bmatrix} C_W & K_W \\ K_W^* & -C_W^* \end{bmatrix} \right) \\ &= 0 \end{aligned} \tag{IV.24}$$

and the corresponding eigenoperator equation is

$$\begin{bmatrix} A_W & L_W \\ L_W^* & A_W^* \end{bmatrix} \begin{bmatrix} Q \\ \overline{Q} \end{bmatrix} = w \begin{bmatrix} C_W & K_W \\ K_W^* & -C_W^* \end{bmatrix} \begin{bmatrix} Q \\ \overline{Q} \end{bmatrix}. \tag{IV.25}$$

The inverse transformations of Eqs. (IV.13) and (IV.14) are formally

$$\mathbf{W}_i^\dagger = \sum_\nu (W_\nu^i \mathbf{Q}_\nu^\dagger + \overline{W}_\nu^i \mathbf{Q}_\nu) \equiv \begin{bmatrix} W \\ \overline{W} \end{bmatrix} \tag{IV.26}$$

and

$$\mathbf{W}_i = \sum_\nu W_\nu^{i*} \mathbf{Q}_\nu + \overline{W}_\nu^{i*} \mathbf{Q}_\nu^\dagger) \equiv \begin{bmatrix} W^* \\ \overline{W}^* \end{bmatrix}. \tag{IV.27}$$

Then

$$\begin{aligned} \langle 0|[\mathbf{Q}_\mu, \mathbf{W}_i^\dagger]|0\rangle &= \sum_\nu [W_\nu^i \langle 0|[\mathbf{Q}_\mu, \mathbf{Q}_\nu^\dagger]|0\rangle \\ &\qquad + \overline{W}_\nu^i \langle 0|[\mathbf{Q}_\mu, \mathbf{Q}_\nu]|0\rangle] \\ &= \sum_\nu \delta(\mu, \nu) W_\nu^i . \end{aligned} \tag{IV.28}$$

So

$$\begin{aligned} W_\nu^i &= \langle 0|[\mathbf{Q}_\nu, \mathbf{W}_i^\dagger]|0\rangle \\ &= \sum_j (\overline{Q}_j^{\nu *} \langle 0|[\mathbf{W}_j^\dagger, \mathbf{W}_i^\dagger]|0\rangle + Q_j^{\nu *} \langle 0|[\mathbf{W}_j, \mathbf{W}_i^\dagger]|0\rangle) \\ &= \sum_j \overline{Q}_j^{\nu *} K_{ji}^* + Q_j^{\nu *} C_{ji} \end{aligned} \tag{IV.29}$$

and

$$\begin{aligned} W_\nu^{i*} &= \langle 0|[\mathbf{W}_i, \mathbf{Q}_\nu^\dagger]|0\rangle \\ &= \sum_j (Q_j^\nu \langle 0|[\mathbf{W}_i, \mathbf{W}_j^\dagger]|0\rangle + \overline{Q}_j^\nu \langle 0|[\mathbf{W}_i, \mathbf{W}_j]|0\rangle) \\ &= \sum_j (Q_j^\nu C_{ij} + \overline{Q}_j^\nu K_{ij}). \end{aligned} \tag{IV.30}$$

Similarly,

$$\begin{aligned}\langle 0|[\mathbf{Q}_\mu, \mathbf{W}_i]|0\rangle &= \sum_\nu [W_\nu^{i*}\langle 0|[\mathbf{Q}_\mu, \mathbf{Q}_\nu]|0\rangle \\ &\qquad + \overline{W}_\nu^{i*}\langle 0|[\mathbf{Q}_\mu, \mathbf{Q}_\nu^\dagger]|0\rangle] \qquad \text{(IV.31)} \\ &= \sum_\nu \delta(\mu, \nu)\overline{W}_\nu^{i*}.\end{aligned}$$

So

$$\begin{aligned}\overline{W}_\nu^{i*} &= \langle 0|[\mathbf{Q}_\nu, \mathbf{W}_i]|0\rangle \\ &= \sum_j (Q_j^{\nu*}\langle 0|[\mathbf{W}_j, \mathbf{W}_i]|0\rangle + \overline{Q}_j^{\nu*}\langle 0|[\mathbf{W}_j^\dagger, \mathbf{W}_i]|0\rangle) \\ &= \sum_j (Q_j^{\nu*}K_{ji} - \overline{Q}_j^{\nu*}C_{ji}^*) \qquad \text{(IV.32)}\end{aligned}$$

and

$$\overline{W}_\nu^i = \sum_j (\overline{Q}_j^\nu K_{ji}^* + \overline{Q}_j^\nu C_{ij}). \qquad \text{(IV.33)}$$

We see that $\hat{V}_\rho^{[\lambda]}$ exhibits closure under the superoperator metric and thus either $\{\mathbf{W}_i, \mathbf{W}_i^\dagger\}$ or $\{\mathbf{Q}_\mu, \mathbf{Q}_\nu^\dagger\}$ constitute a complete basis. As a consequence of the foregoing, Eq. (IV.24) is a self-consistent set of equations for the operator space $\hat{V}_\rho^{[\lambda]}$, Eq. (IV.2), and can be solved by conventional means for the eigenvalues ω_ν and the eigenvectors $\mathbf{Q}_\nu^\dagger$.

We need now to show that the ω_ν and $\mathbf{Q}_\nu^\dagger$ are excitation energies and excitation operators with respect to the exact ground state, $|0\rangle$. Let us assume that, for $w_\nu > 0$,

$$|\nu\rangle \equiv \mathbf{Q}_\nu^\dagger|0\rangle \qquad \text{(IV.34)}$$

is an exact eigenvector to H in the space V_ρ with an eigenvalue E_ν. We note parenthetically that it is not normalized since

$$\begin{aligned}\langle \nu|\nu\rangle &= \langle 0|\mathbf{Q}_\nu \mathbf{Q}_\nu^\dagger|0\rangle \\ &= \overset{\gamma}{\sum_i \sum_j} (Q_i^{\nu*}Q_j^\nu\langle 0|\mathbf{W}_i \mathbf{W}_j^\dagger|0\rangle \\ &\qquad + Q_i^{\nu*}\overline{Q}_j^\nu\langle 0|\mathbf{W}_i \mathbf{W}_j|0\rangle \\ &\qquad + \overline{Q}_i^{\nu*}Q_j^\nu\langle 0|\mathbf{W}_i^\dagger \mathbf{W}_j^\dagger|0\rangle \\ &\qquad + \overline{Q}_i^{\nu*}\overline{Q}_j^\nu\langle 0|\mathbf{W}_i^\dagger \mathbf{W}_j|0\rangle. \qquad \text{(IV.35)}\end{aligned}$$

If $|\nu\rangle$ and $|0\rangle$ are exact eigenvectors, then

$$\langle 0|\nu\rangle = \langle 0|\mathbf{Q}_\nu^\dagger|0\rangle = 0, \qquad \text{(IV.36)}$$

but since $Q_\nu^\dagger|0\rangle \neq 0$, it follows that

$$\langle 0|\mathbf{Q}_\nu^\dagger = \mathbf{Q}_\nu|0\rangle = 0. \tag{IV.37}$$

We now compute the matrix elements in Eqs. (IV.15), (IV.16), (IV.18), and (IV.19) using Eqs. (IV.13), (IV.34), and (IV.37). Thus

$$\begin{aligned} C_{\mu\nu} &\equiv \langle 0|[\mathbf{Q}_\mu, \mathbf{Q}_\nu^\dagger]|0\rangle \\ &= \langle 0|\mathbf{Q}_\mu, \mathbf{Q}_\nu^\dagger|0\rangle - \langle 0|Q_\nu^\dagger Q_\mu|0\rangle \\ &= \langle \mu|\nu\rangle - 0 \\ &= \delta(\mu, \nu), \end{aligned} \tag{IV.38}$$

$$\begin{aligned} K_{\mu\nu} &\equiv \langle 0|[\mathbf{Q}_\mu, \mathbf{Q}_\nu]|0\rangle \\ &= 0, \end{aligned} \tag{IV.39}$$

$$\begin{aligned} A_{\mu\nu} &= \langle 0|[[\mathbf{Q}_\mu, \mathbf{H}], Q_\nu^\dagger]|0\rangle \\ &= \langle 0|[\mathbf{Q}_\mu, \mathbf{H}]Q_\nu^\dagger|0\rangle - \langle 0|Q_\nu^\dagger[Q_\mu, H]|0\rangle \\ &= \langle 0|\mathbf{Q}_\mu\mathbf{H}\mathbf{Q}_\nu^\dagger|0\rangle - \langle 0|\mathbf{H}\mathbf{Q}_\mu\mathbf{Q}_\nu^\dagger|0\rangle - 0 \\ &= \delta(\mu, \nu)(E_\nu - E_0) \\ &= \delta(\mu, \nu)w_\nu, \end{aligned} \tag{IV.40}$$

where ω_ν is the excitation energy from $|0\rangle \to |\nu\rangle$

$$\begin{aligned} L_{\mu\nu} &= \langle 0|[[\mathbf{Q}_\mu, \mathbf{H}], \mathbf{Q}_\nu]|0\rangle \\ &= 0. \end{aligned} \tag{IV.41}$$

It follows that w_ν and $\mathbf{Q}_\nu^\dagger$ computed by the superoperator formation are, indeed, excitation energies and excitation operators, respectively.

A superoperator hypervirial theorem follows trivially by multiplying (IV.25) from the left by any operator (say $F^\dagger$) in $\hat{V}_\rho^{[\lambda]}$.

$$[\bar{F}F]\begin{bmatrix} A_W & L_W \\ L_W^* & A_W^* \end{bmatrix}\begin{bmatrix} Q \\ \bar{Q} \end{bmatrix} = w[\bar{F}F]\begin{bmatrix} C_W & K_W \\ K_W^* & -C_W^* \end{bmatrix}\begin{bmatrix} Q \\ \bar{Q} \end{bmatrix} \tag{IV.42}$$

the Vth component of which is

$$\langle 0|[[\mathbf{F}^\dagger, \mathbf{H}], \mathbf{Q}_\nu^\dagger]|0\rangle = w_\nu\langle 0|[\mathbf{F}^\dagger, \mathbf{Q}_\nu^\dagger]|0\rangle. \tag{IV.43}$$

If we now substitute Eqs. (IV.34) and (IV.37) into (IV.43), we obtain the conventional hypervirial theorem

$$\langle 0|[\mathbf{F}, \mathbf{H}]|\nu\rangle = w_\nu\langle 0|\mathbf{F}|\nu\rangle. \tag{IV.44}$$

Finally, we construct a superoperator equivalent to the energy-weighted sum rule. For M, a dipole operator,

$$
\begin{aligned}
S &\equiv \tfrac{1}{2}\langle 0|\mathbf{M}\hat{\mathbf{H}}\mathbf{M}^\dagger|0\rangle \\
&= \tfrac{1}{2}\langle 0|[[\mathbf{M}, \mathbf{H}], \mathbf{M}^\dagger]|0\rangle \\
&= \tfrac{1}{2}(\langle 0|[\mathbf{M}, \mathbf{H}]\mathbf{M}^\dagger|0\rangle - \langle 0|\mathbf{M}^\dagger[\mathbf{M}, \mathbf{H}]|0\rangle) \\
&= \tfrac{1}{2}\sum_{\nu}(\langle 0|[\mathbf{M}, \mathbf{H}]|\nu\rangle\langle\nu|\mathbf{M}^\dagger|0\rangle - \langle 0|\mathbf{M}^\dagger|\nu\rangle\langle\nu|[\mathbf{M}, \mathbf{H}]|0\rangle) \\
&= \tfrac{1}{2}\sum_{\nu}\omega_\nu(\langle 0|\mathbf{M}|\nu\rangle\langle\nu|\mathbf{M}^\dagger|0\rangle + \langle 0|\mathbf{M}^\dagger|\nu\rangle\langle\nu|\mathbf{M}|0\rangle) \\
&= \sum_{\nu}\omega_\nu|\langle 0|\mathbf{M}|\nu\rangle|^2.
\end{aligned}
\tag{IV.45}
$$

In terms of the primary operators,

$$
\begin{aligned}
S &= \tfrac{1}{2}\langle 0|[[\mathbf{M}, \mathbf{H}], \mathbf{M}^\dagger]|0\rangle \\
&= \tfrac{1}{2}[\overline{M}^* M]\begin{bmatrix} A & L \\ L^* & A^* \end{bmatrix}\begin{bmatrix} M \\ \overline{M} \end{bmatrix}.
\end{aligned}
\tag{IV.46}
$$

How does SOF differ from full configuration interaction (CI)? The latter consists of the diagonalization of H in the $\gamma + 1$-dimensional vector space, which yields the exact ground state $|0\rangle$ and the exact excited states $|\nu\rangle$. We can express these exact states by a CI excitation operator

$$|\nu\rangle = \mathbf{Q}_\nu^\dagger(\mathrm{CI})|0\rangle, \tag{IV.47}$$

where

$$\mathbf{Q}_\nu^\dagger(\mathrm{CI}) = \sum_{i=1}^{\gamma} Q_i^\nu(\mathrm{CI})\mathbf{W}_i^\dagger, \tag{IV.48}$$

and where $w_\nu > 0$ the $\mathbf{Q}_\nu^\dagger(\mathrm{CI})$ can also be obtained by diagonalizing the submatrix $[A_w]$. If one diagonalizes $[A_w]$, one obtains

$$\mathbf{Q}_\nu(\mathrm{CI}) = \sum_{i=1}^{\gamma} Q_i^{\nu *}(\mathrm{CI})\mathbf{W}_i \tag{IV.49}$$

with $w_\nu < 0$.

An interpretation of the positive and negative eigenvalues can be obtained from the time-dependence of the eigenoperators by means of the equations of motion. Thus, for w_ν real,

$$
\begin{aligned}
A_{\mu\nu} &= \langle 0|[[\mathbf{Q}_\mu, \mathbf{H}], \mathbf{Q}_\nu^\dagger]|0\rangle \\
&= -i\langle 0|[\dot{\mathbf{Q}}_\mu, \mathbf{Q}_\nu^\dagger]|0\rangle \\
&= w_\nu\langle 0|[\mathbf{Q}_\mu, \mathbf{Q}_\nu^\dagger]|0\rangle \\
&= \delta(\mu, \nu)w_\nu
\end{aligned}
\tag{IV.50}
$$

for which a solution is

$$\mathbf{Q}_\nu(t) = \mathbf{Q}_\nu(0)e^{iw_\nu t}, \tag{IV.51}$$

and

$$\begin{aligned} A^*_{\mu\nu} &= \langle 0|[[\mathbf{Q}^\dagger_\mu, \mathbf{H}], \mathbf{Q}_\nu]|0\rangle \\ &= -i\langle 0|[\dot{\mathbf{Q}}^\dagger_\mu, \mathbf{Q}_\nu]|0\rangle \\ &= w_\nu\langle 0|[\mathbf{Q}^\dagger_\mu, \mathbf{Q}_\nu]|0\rangle \\ &= \delta(\mu, \nu)w_\nu \end{aligned} \tag{IV.52}$$

for which a solution is

$$\mathbf{Q}^\dagger_\nu(t) = \mathbf{Q}^\dagger_\nu(0)e^{-iw_\nu t}. \tag{IV.53}$$

It is customary to interpret $w_\nu > 0$ as representing a motion forward in time, and $\mathbf{Q}^\dagger_\nu$ and $\mathbf{Q}_\nu$ as excitation creation and annihilation operators, respectively. The interpretation is revised for $w_\nu < 0$.

Is SOF useful? If the full CI eigenvalues and eigenvectors are in hand the answer is no. In fact, if SOF were carried out for the exact ground state, one would obtain two sets of solutions, one with $w_\nu > 0$, which would be physical, and one with $w_\nu < 0$, which would be nonphysical and useless. However, full CI can rarely be executed and most calculations are carried out with limited CI(LCI). It is here that SOF may have application since the SOF extension of the space may partially compensate for the omission of configurations in LCI. To show this, we write for the LCI ground state

$$|0(\mathrm{LCI})\rangle = \sum_j^{\gamma-\delta} \lambda_j \mathbf{W}^\dagger_j |\rangle. \tag{IV.54}$$

Then by SOF

$$\begin{aligned} |\nu\rangle &= \mathbf{Q}^\dagger_\nu |0(\mathrm{LCI})\rangle \\ &= \sum_i^{\gamma-\delta} \sum_j^{\gamma-\delta} (\lambda_j Q^\nu_i \mathbf{W}^\dagger_i \mathbf{W}^\dagger_j |\rangle + \lambda_j \overline{Q}^\nu_i \mathbf{W}_i \mathbf{W}^\dagger_j |\rangle). \end{aligned} \tag{IV.55}$$

Now, whereas $\mathbf{W}_i|\rangle$ vanishes, $\mathbf{W}_i \mathbf{W}^\dagger_j|\rangle$ generally does not, so that in effect SOF has added configurations defined by the $\mathbf{W}_i \mathbf{W}^\dagger_j|\rangle$ terms to the CI space. Additional support for the superiority of SOF over LCI comes from the fact the SOF saturates the energy-weighted sum rule more completely than does the LCI sum rule:

$$S = \overline{M}^* A M. \tag{IV.56}$$

We close this section with a definition of the higher moments of the superoperator $\hat{H}$. We define the moments as powers of the excitation energies w_ν. Thus

$$\langle 0|\mathbf{Q}_\mu \hat{H}^n \mathbf{Q}^\dagger_\nu|0\rangle = \delta(\mu, \nu)w^n_\nu \tag{IV.57}$$

so that

$$\begin{aligned}\hat{H}^0_{ij} &= \langle 0|[\mathbf{W}_i, \mathbf{W}_j^\dagger]|0\rangle,\\ \hat{H}^1_{ij} &= \langle 0|[[\mathbf{W}_i, \mathbf{H}], \mathbf{W}_j^\dagger]|0\rangle,\\ \hat{H}^2_{ij} &= \langle 0|[[[\mathbf{W}_i, \mathbf{H}], \mathbf{H}], \mathbf{W}_j^\dagger]|0\rangle, \qquad \text{(IV.58)}\end{aligned}$$

etc.

V. The Random-Phase Approximation

The random-phase approximation (RPA) is an approximate procedure for the calculation of excitation operators and excitation energies. It can be formulated as time-dependent Hartree–Fock theory (TDHF) or in the superoperator formulation. Reality of the RPA excitation energies is imposed by the Hartree–Fock stability condition, Eq. (III.22), which is conveniently expressed in SOF. The RPA consists of two steps that must be taken in order. If the order is reversed, one obtains a second (but poorer) approximation, the Tamm–Dancoff approximation (TDA).

Step 1. Truncation of $\hat{V}^{[\lambda]}_\rho$ to the space of single-particle generators:

$$V^{[\lambda]}_\rho(\mathrm{RPA}) : \{\mathbf{E}_{\mathrm{ph}}, \mathbf{E}_{\mathrm{hp}}\}, \qquad \text{(V.1)}$$

where p and h refer to the highest-weight state [as in Eq. (II.5)]. The RPA excitation operators are

$$\mathbf{Q}^\dagger_\nu = \sum_{\mathrm{p}} \sum_{\mathrm{h}} Q^\nu_{\mathrm{ph}} \mathbf{E}_{\mathrm{ph}} + \bar{Q}^\nu_{\mathrm{ph}} \mathbf{E}_{\mathrm{hp}} \qquad \text{(V.2)}$$

and

$$\mathbf{Q}_\nu = \sum_{\mathrm{p}} \sum_{\mathrm{h}} Q^{\nu *}_{\mathrm{ph}} \mathbf{E}_{\mathrm{hp}} + \bar{Q}^{\nu *}_{\mathrm{ph}} \mathbf{E}_{\mathrm{ph}} \qquad \text{(V.3)}$$

and the excited states are formally

$$|\nu\rangle = \sum_{\mathrm{p}} \sum_{\mathrm{h}} Q^\nu_{\mathrm{ph}} \mathbf{E}_{\mathrm{ph}} |0\rangle + \bar{Q}^\nu_{\mathrm{ph}} \mathbf{E}_{\mathrm{hp}} |0\rangle \qquad \text{(V.4)}$$

but

$$0 \neq \mathbf{Q}_\nu |0\rangle. \qquad \text{(V.5)}$$

Step 2. Replace the exact ground state $|0\rangle$ by the highest-weight state in the evaluation of superoperator matrix elements. Thus, for the superoperator metric matrix

$$\begin{aligned}C_{\mathrm{php'h'}} &\equiv \langle |\mathbf{E}_{\mathrm{hp}} \hat{\mathbf{S}} \mathbf{E}_{\mathrm{p'h'}}| \rangle\\ &= \langle |\mathbf{E}_{\mathrm{hp}}, \mathbf{E}_{\mathrm{p'h'}}]| \rangle\\ &= \delta(\mathrm{h}, \mathrm{h'})\, \delta(\mathrm{p}, \mathrm{p'}) g_{\mathrm{h}}, \qquad \text{(V.6)}\end{aligned}$$

$$K_{\mathrm{ph,\, p'h'}} = 0$$

so

$$[\hat{S}]_W = \begin{bmatrix} g & 0 \\ 0 & -g \end{bmatrix} \tag{V.7}$$

where

$$g = \operatorname{diag}\{g_{\mathrm{h}}\}.$$

The transformations inverse to (V.2) and (V.3) are

$$\mathbf{E}_{\mathrm{ph}} = \sum_{\nu} (E_{\nu}^{\mathrm{ph}}\mathbf{Q}_{\nu}^{\dagger} + \overline{E}_{\nu}^{\mathrm{ph}}\mathbf{Q}_{\nu}) \tag{V.8}$$

and

$$\mathbf{E}_{\mathrm{hp}} = \sum_{\nu} (E_{\nu}^{\mathrm{ph}*}\mathbf{Q}_{\nu} + \overline{E}_{\nu}^{\mathrm{ph}*}\mathbf{Q}_{\nu}^{\dagger}). \tag{V.9}$$

On substituting the RPA metric into (IV.29), (IV.30), (IV.32), and (IV.33), we have

$$E_{\nu}^{\mathrm{ph}} = Q_{\mathrm{ph}}^{\nu*} g_{\mathrm{h}}, \tag{V.10}$$

$$E_{\nu}^{\mathrm{ph}*} = Q_{\mathrm{ph}}^{\nu} g_{\mathrm{h}}, \tag{V.11}$$

$$\overline{E}_{\nu}^{\mathrm{ph}*} = -\overline{Q}_{\mathrm{ph}}^{\nu*} g_{\mathrm{h}}, \tag{V.12}$$

$$\overline{E}_{\nu}^{\mathrm{ph}} = \overline{Q}_{\mathrm{ph}}^{\nu} g_{\mathrm{h}}. \tag{V.13}$$

Consequently, $\hat{V}_{\rho}^{[\lambda]}$(RPA) is closed so either $\{\mathbf{E}_{\mathrm{ph}}, \mathbf{E}_{\mathrm{hp}}\}$ or $\{\mathbf{Q}_{\nu}^{\dagger}, \mathbf{Q}_{\nu}\}$ constitute a complete basis. The RPA eigenoperator equation is then

$$\begin{bmatrix} A & L \\ L^* & A \end{bmatrix} \begin{bmatrix} Q \\ \overline{Q} \end{bmatrix} = w \begin{bmatrix} g & Q \\ -g & \overline{Q} \end{bmatrix}. \tag{V.14}$$

The RPA $[\hat{H}]$ is evaluated below. By the methods of Section IV, we obtain an RPA hypervirial theory

$$\langle | [F, H] | \nu \rangle = w \langle | F | \nu \rangle \tag{V.15}$$

and an RPA sum rule

$$S = \tfrac{1}{2}[M^* \; \overline{M}^*] \begin{bmatrix} A & L \\ L^* & A^* \end{bmatrix} \begin{bmatrix} M \\ \overline{M} \end{bmatrix}. \tag{V.16}$$

We now show that the RPA approximation can also be obtained from TDHF theory. The first nonvanishing variation term in the Baker–Campbell–Hausdorff expansion, Eq. (III.4), is (since $\mathbf{Z}^{\dagger} = -\mathbf{Z}$ and using the equation of motion)

$$\begin{aligned} \langle | [[\mathbf{Z}, \mathbf{H}], \mathbf{Z}^{\dagger}] | \rangle &= \langle | [\mathbf{Z}, [\mathbf{H}, \mathbf{Z}^{\dagger}]] | \rangle \\ &= \langle | [\mathbf{Z}, i\dot{\mathbf{Z}}^{\dagger}] | \rangle \\ &= [Z^* \overline{Z}^*] \begin{bmatrix} g & 0 \\ 0 & -g \end{bmatrix} \begin{bmatrix} i & \dot{Z} \\ i & \dot{\overline{Z}} \end{bmatrix} \end{aligned} \tag{V.17}$$

so that the TDHF equations are

$$\begin{bmatrix} A & L \\ L^* & A^* \end{bmatrix} \begin{bmatrix} Z \\ \bar{Z} \end{bmatrix} = \begin{bmatrix} ig \ \dot{Z} \\ -ig \ \dot{\bar{Z}} \end{bmatrix}. \tag{V.18}$$

We recover the RPA equation (V.14) by the substitution of

$$Z = Qe^{-iwt} + \bar{Q}e^{iwt}$$

and

$$\bar{Z} = \bar{Q}^* e^{-iwt} + Q^* e^{iwt} \tag{V.19}$$

into Eq. (V.18) and equating separately their coefficients e^{-iwt} and e^{iwt}. Thus the time variation of the Hartree–Fock orbitals can be expressed in terms of excitation operators. Note that if w is real, the Hartree–Fock state is a stable (oscillating) state and, if w is imaginary, then the Hartree–Fock state is unstable and will evolve to some non-Hartree–Fock minimum-energy state. This is consistent with the Hartree–Fock stability condition, Eq. (III.21):

$$\begin{aligned} \langle | [[\mathbf{Z}, \mathbf{H}], \mathbf{Z}^\dagger] | \rangle &= [\bar{Z}^* \ Z^*] \begin{bmatrix} A & L \\ L^* & A^* \end{bmatrix} \begin{bmatrix} Z \\ \bar{Z} \end{bmatrix} \\ &\geq 0 \end{aligned} \tag{V.20}$$

or

$$\begin{bmatrix} A & L \\ L^* & A^* \end{bmatrix} \begin{bmatrix} Z \\ \bar{Z} \end{bmatrix} = \lambda \begin{bmatrix} Z \\ \bar{Z} \end{bmatrix}, \qquad \lambda \geq 0. \tag{V.21}$$

Since $[\hat{\mathbf{H}}]$ is Hermitian the eigenvalues are real. If we equate the right sides of Eqs. (V.18) and (V.21) and substitute Eq. (V.19), we have

$$w = \pm \lambda \text{ (real).} \tag{V.22}$$

We turn now to the evaluation of $[\hat{\mathbf{H}}]$ in the RPA approximation, limiting ourselves to closed shells and applying the extremum condition, Eq. (III.10),

$$\begin{aligned} A_{\mathrm{php'h'}} &= \langle | [[\mathbf{E}_{\mathrm{hp}}, \mathbf{H}], \mathbf{E}_{\mathrm{p'h'}}] | \rangle \\ &= g_{\mathrm{h}}(\delta(\mathrm{p}, \mathrm{p'})\, \delta(\mathrm{h}, \mathrm{h'})(\varepsilon(\mathrm{p}) - \varepsilon(\mathrm{h})) \\ &\quad + g v_{\mathrm{hpp'h'}} - v_{\mathrm{hh'p'p}}), \end{aligned} \tag{V.23}$$

$$L_{\mathrm{php'h'}} = -g_{\mathrm{h}}(g v_{\mathrm{php'h'}} - v_{\mathrm{ph'p'h}}). \tag{V.24}$$

For fermions $g = 1$,

$$A_{\mathrm{php'h'}} = \delta(\mathrm{p}, \mathrm{p'})\,\delta(\mathrm{h}, \mathrm{h'})(\varepsilon(\mathrm{p}) - \varepsilon(\mathrm{h})) + v_{\mathrm{hpp'h'}} - v_{\mathrm{hh'p'p}} \tag{V.25}$$

$$L_{\mathrm{php'h'}} = -(v_{\mathrm{php'h'}} - v_{\mathrm{ph'p'h}}). \tag{V.26}$$

For freon singlet states $g = 2$,

$${}^{1}A_{\mathrm{php'h'}} = 2(\delta(\mathrm{p}, \mathrm{p'})\,\delta(\mathrm{h}, \mathrm{h'})(\varepsilon(\mathrm{p}) - \varepsilon(\mathrm{h})) + (2v_{\mathrm{hpp'h'}} - v_{\mathrm{hh'p'p}}), \tag{V.27}$$

$${}^{1}L_{\mathrm{php'h'}} = -2(2v_{\mathrm{php'h'}} - v_{\mathrm{ph'p'h}}). \tag{V.28}$$

Excited freon triplet states can also be obtained in the unitary group RPA from a freon ground triplet state, as will be discussed elsewhere.

Singlet and triplet RPA states are conventionally obtained in the fermion formulation from a singlet (freon orbitals doubly occupied) ground state. The fermion orbital excitation generates an equal mixture of an excited singlet and the three components of a triplet. The singlet RPA equations are identical to Eqs. (V.25) and (V.26), whereas the triplet RRA equations, which are independent of M_s, can be obtained by taking the third of the difference between the fermion and the freon singlet equations:

$${}^{3}A_{\mathrm{php'h'}} = g(\delta(\mathrm{p}, \mathrm{p'})\,\delta(\mathrm{h}, \mathrm{h'})(\varepsilon(\mathrm{p}) - \varepsilon(\mathrm{h})) - v_{\mathrm{hh'p'p}}), \tag{V.29}$$

$${}^{3}L_{\mathrm{php'h'}} = g v_{\mathrm{ph'p'h}}\,. \tag{V.30}$$

These triplet equations differ from the unitary group triplets mentioned in the foregoing: they are easier to compute but apparently less accurate.

If the order of approximation is reversed, the RPA excited states are

$$|v\rangle = \sum_{\mathrm{p}} \sum_{\mathrm{h}} (Q_{\mathrm{ph}}\,\mathbf{E}_{\mathrm{ph}}\,|\rangle + \bar{Q}_{\mathrm{ph}}\,\mathbf{E}_{\mathrm{hp}}\,|\rangle). \tag{V.31}$$

The second term is zero so that effectively

$$\bar{Q}_{\mathrm{ph}} = 0 \tag{V.32}$$

and Eq. (V.14) becomes

$$AQ = w^{\mathrm{TDA}}Q. \tag{V.33}$$

As a consequence of Brillouin's theorem, Eq. (V.33) is equivalent to a single-particle CI calculation and is called the Tamm–Dancoff approximation. The RPA differs from TDA in that it employs an extended Hilbert space and includes in the excited state calculation some of the correlation present in the exact ground state. Further, by Eqs. (IV.46) and (IV.56), TDA is farther from exhausting the sum rule than is RPA so that it can be anticipated that its intensities are poorer; this has been shown to be the case.

If we again drop the restriction to closed freon shells and decompose h into c (closed) and o (open) orbitals the RPA excitation operators become

$$\begin{aligned} Q_\nu^\dagger = {} & \sum_{\mathrm{p}} \sum_{\mathrm{c}} Q_{\mathrm{pc}}^\nu E_{\mathrm{pc}} + \overline{Q}_{\mathrm{pc}}^\nu E_{\mathrm{cp}} + \sum_{\mathrm{p}} \sum_{\mathrm{c}} Q_{\mathrm{po}}^\nu E_{\mathrm{po}} + \overline{Q}_{\mathrm{po}}^\nu E_{\mathrm{op}} \\ & + \sum_{\mathrm{c}} \sum_{0} Q_{\mathrm{oc}}^\nu E_{\mathrm{oc}} + \overline{Q}_{\mathrm{oc}}^\nu E_{\mathrm{co}} \end{aligned} \tag{V.34}$$

and

$$\begin{aligned} Q_\nu = {} & \sum_{\mathrm{p}} \sum_{\mathrm{c}} Q_{\mathrm{pc}}^{\nu *} E_{\mathrm{cp}} + \overline{Q}_{\mathrm{pc}}^{\nu *} E_{\mathrm{pc}} + \sum_{\mathrm{p}} \sum_{\mathrm{o}} Q_{\mathrm{po}}^{\nu *} E_{\mathrm{op}} + \overline{Q}_{\mathrm{po}}^{\nu *} E_{\mathrm{po}} \\ & + \sum_{\mathrm{o}} \sum_{\mathrm{c}} Q_{\mathrm{oc}}^{\nu *} E_{\mathrm{co}} + \overline{Q}_{\mathrm{oc}}^{\nu *} E_{\mathrm{oc}} \,. \end{aligned} \tag{V.35}$$

This leads to an RPA eigenoperator equation similar to (V.14) with three types of A's and Ls and both g_{c} and g_{o} occupations from the C's. This formalism will calculate an excited state spectrum from an open shell reference state, rather than a closed shell reference state as in triple RPA. For doublets, see Paldus and Cizek (1969).

The RPA approximation has been subjected to careful analysis; improvements have been suggested and calculations made (e.g., Oddershede and Elander, 1976; Rescingo, Bender and McKoy, 1977; Hansen and Bouman, 1977; Worth, Bartlett and Matsen, 1978).

VI. Green's Function

A Green's function (or propagator) in its time-independent form is a function of a complex variable whose poles predict excitation energies and whose residues predict transition probabilities. We develop Green's functions in the superoperator formulation rather than in the conventional time-dependent one. In the RPA approximation, we obtain the particle-hole propagator. We take as the superoperator the resolvent

$$\mathscr{G}(\mathscr{E}) = \frac{1}{\mathscr{E} - \hat{H}} \,. \tag{VI.1}$$

We define a superoperator Green's matrix in the primary basis,

$$\hat{V}_\rho^{[\lambda]} : \{\mathbf{W}, \mathbf{W}^\dagger\} \equiv \{\mathbf{W}_i, \mathbf{W}_j^\dagger, \ldots\}, \tag{VI.2}$$

$$[\hat{\mathscr{G}}(\mathscr{E})]_W \equiv \begin{bmatrix} \langle\langle \mathbf{W}; \mathbf{W}^\dagger \rangle\rangle_{\mathscr{E}} & \langle\langle \mathbf{W}; \mathbf{W} \rangle\rangle_{\mathscr{E}} \\ \langle\langle \mathbf{W}^\dagger; \mathbf{W}^\dagger \rangle\rangle_{\mathscr{E}} & \langle\langle \mathbf{W}^\dagger; \mathbf{W} \rangle\rangle_{\mathscr{E}} \end{bmatrix}, \tag{VI.3}$$

where

$$\begin{aligned}\langle\langle \mathbf{W}_i; \mathbf{W}_j^\dagger\rangle\rangle_{\mathscr{E}} &\equiv \langle 0|\mathbf{W}_i\mathscr{G}(\mathscr{E})\mathbf{W}_j^\dagger|0\rangle\\ &\equiv \langle 0|[[\mathbf{W}_i, \mathscr{G}(\mathscr{E})], \mathbf{W}_j^\dagger]|0\rangle,\end{aligned} \tag{VI.4}$$

etc.

The superoperator has a moment expansion, Eq. (IV.56),

$$\hat{\mathscr{G}}(\mathscr{E}) = \frac{1}{\mathscr{E}}\sum_n \frac{\hat{\mathbf{H}}^n}{\mathscr{E}^n} \tag{VI.5}$$

so

$$\begin{aligned}\mathscr{E}\langle\langle W_i; W_j^\dagger\rangle\rangle_{\mathscr{E}} &= \sum_n \frac{1}{\mathscr{E}^n}\langle 0|\mathbf{W}_i\hat{\mathbf{H}}^n\mathbf{W}_j^\dagger|0\rangle\\ &= \sum_n \frac{1}{\mathscr{E}^n}\langle 0|[\ldots[\mathbf{W}_i, \mathbf{H}], \ldots \mathbf{H}]_n, \mathbf{W}_j^\dagger]|0\rangle.\end{aligned} \tag{VI.6}$$

The moment expansion has a convenient recursion form

$$\mathscr{E}\langle\langle \mathbf{W}_i; \mathbf{W}_j^\dagger\rangle\rangle_{\mathscr{E}} = \langle 0|[\mathbf{W}_i, \mathbf{W}_j^\dagger]|0\rangle + \langle\langle[\mathbf{W}_i, \mathbf{H}]; \mathbf{W}_j^\dagger\rangle\rangle_{\mathscr{E}}, \tag{VI.7}$$

where

$$\begin{aligned}\mathscr{E}\langle\langle[\mathbf{W}_i, \mathbf{H}]; \mathbf{W}_j^\dagger\rangle\rangle_{\mathscr{E}} &= \langle 0|[[\mathbf{W}_i, \mathbf{H}], \mathbf{W}_j^\dagger]|0\rangle\\ &\quad + \langle\langle[[\mathbf{W}_i, \mathbf{H}], \mathbf{H}]; \mathbf{W}_j^\dagger\rangle\rangle_{\mathscr{E}},\end{aligned} \tag{VI.8}$$

etc.

Since $\hat{V}_p^{[\lambda]}$ is a complete superoperator space, we can represent the inverse of the resolvent as the inverse of its representation:

$$\begin{aligned}[\hat{\mathscr{G}}(\mathscr{E})]_W^{-1} &= [\hat{G}(\mathscr{E})^{-1}]_W\\ &= \mathscr{E}[\hat{S}]_W - [\hat{\mathbf{H}}]_W\end{aligned} \tag{VI.9}$$

or

$$[\mathscr{G}(\mathscr{E})]_W = [\hat{\mathbf{S}}]_W(\varepsilon[\hat{\mathbf{S}}]_W - [\mathbf{H}]_W)^{-1}[\hat{\mathbf{S}}_W]. \tag{VI.10}$$

Here $[\hat{\mathbf{S}}]$ and $[\hat{\mathbf{H}}]$ are given in Eqs. (IV.3) and (IV.9). The poles are determined by

$$\det(\varepsilon[\hat{\mathbf{S}}] - [\hat{\mathbf{H}}]) = 0, \tag{VI.11}$$

which by Eq. (IV.42) occur at the excitation energies $\pm w_\nu$.

In the excitation operator basis,

$$\hat{V}_p^{[\lambda]}: \{\mathbf{Q}, \mathbf{Q}^\dagger\} \equiv \{\mathbf{Q}_\mu, \mathbf{Q}_\nu^\dagger, \ldots\}, \tag{VI.12}$$

Green's matrix is

$$[\hat{\mathscr{G}}(\mathscr{E})]_Q \equiv \begin{bmatrix} \langle\langle \mathbf{Q}; \mathbf{Q}^\dagger\rangle\rangle_{\mathscr{E}} & \langle\langle \mathbf{Q}; \mathbf{Q}\rangle\rangle_{\mathscr{E}} \\ \langle\langle \mathbf{Q}^\dagger; \mathbf{Q}^\dagger\rangle\rangle_{\mathscr{E}} & \langle\langle \mathbf{Q}^\dagger; \mathbf{Q}\rangle\rangle_{\mathscr{E}} \end{bmatrix}. \tag{VI.13}$$

The excitation operator Green's function can be evaluated straightforwardly by the moment expansion:

$$\begin{aligned} \langle\langle \mathbf{Q}_\mu, \mathbf{Q}_\nu^\dagger\rangle\rangle_{\mathscr{E}} &\equiv \langle 0|\mathbf{Q}_\mu \hat{\mathscr{G}}(\mathscr{E})\mathbf{Q}_\nu^\dagger|0\rangle \\ &= \frac{1}{\mathscr{E}}\sum_n \frac{1}{\mathscr{E}^n}\langle 0|\mathbf{Q}_\mu \hat{H}^n \mathbf{Q}_\nu^\dagger|0\rangle \\ &= \frac{1}{\mathscr{E}}\sum_n \frac{w_\nu^n}{\mathscr{E}^n}\delta(\mu, \nu) \\ &= \frac{\delta(\mu, \nu)}{\mathscr{E} - w_\nu} \\ &\equiv \delta(\mu, \nu) G_\nu^+(\mathscr{E}), \end{aligned} \tag{VI.14}$$

etc.
So

$$[\hat{\mathscr{G}}(\mathscr{E})]_Q = \begin{bmatrix} G^+(\mathscr{E}) & 0 \\ 0 & G^-(\mathscr{E}) \end{bmatrix},$$

where

$$G^\pm(\mathscr{E}) = \left\{ G_\nu^\pm(\mathscr{E}) = \frac{1}{\mathscr{E} \mp w_\nu} \right\}. \tag{VI.15}$$

According to the discussion in Section IV, we can regard $G_\nu^\pm$ as propagators acting forward and backward in time.

We now compute the spectral representation of a primary Green's function by expanding the primary operators in terms of the excitation operators [Eqs. (IV.41) and (IV.13)]:

$$\begin{aligned} \langle\langle \mathbf{W}_i; \mathbf{W}_j^\dagger\rangle\rangle_{\mathscr{E}} &= \langle 0|\mathbf{W}_i \hat{\mathscr{G}}(\mathscr{E})\mathbf{W}_j^\dagger|0\rangle \\ &= \langle 0|[[\mathbf{W}_i, \hat{\mathscr{G}}(\mathscr{E})], \mathbf{W}_j^\dagger]|0\rangle \\ &= [W_i^* \bar{W}_i^*] \begin{bmatrix} G^+(\mathscr{E}) & 0 \\ 0 & G^-(\mathscr{E}) \end{bmatrix} \begin{bmatrix} W_j \\ \bar{W}_j \end{bmatrix} \\ &= \sum_\nu \left(\frac{\langle 0|\mathbf{W}_i|\nu\rangle\langle\nu|\mathbf{W}_j^\dagger|0\rangle}{\mathscr{E} - w_\nu} + \frac{\langle 0|\mathbf{W}_j^\dagger|\nu\rangle\langle\nu|\mathbf{W}_i|0\rangle}{\mathscr{E} + w_\nu} \right) \end{aligned} \tag{VI.16}$$

so that the poles of a primary Green's function are at the excitation energies ${}^{\dagger}w_\nu$. A double-time Green's function $\langle\langle \mathbf{W}(t);\ \mathbf{W}^\dagger(t')\rangle\rangle$ is obtained by a

Fourier transformation. The integral over $\mathscr{E}$ can be converted to a contour integral in the complex plane with residues that determine the transition probabilities.

Green's function for $\mathbf{W}_i \equiv \mathbf{E}_{rs}$, and $\mathbf{W}_j^\dagger \equiv \mathbf{E}_{tu}$ is called a two-body Green's function and is denoted

$$\langle\langle \mathbf{E}_{rs} ; \mathbf{E}_{tu}^\dagger \rangle\rangle_{\mathscr{E}} \equiv \langle 0 | [[\mathbf{E}_{rs}, \mathscr{G}(\mathscr{E})], \mathbf{E}_{tu}^\dagger] | 0 \rangle. \qquad \text{(VI.17)}$$

In the RPA approximation the generators become particle-hole operators and the Green's function is called a particle-hole propagator with a matrix denoted

$$[\hat{G}(\mathscr{E})]_{\mathrm{ph}} = \begin{bmatrix} \langle\langle E_{\mathrm{hp}} ; E_{\mathrm{p'h'}} \rangle\rangle_{\mathscr{E}} & \langle\langle E_{\mathrm{hp}} ; E_{\mathrm{h'p'}} \rangle\rangle_{\mathscr{E}} \\ \langle\langle E_{\mathrm{ph}} ; E_{\mathrm{p'h'}} \rangle\rangle_{\mathscr{E}} & \langle\langle E_{\mathrm{ph}} ; E_{\mathrm{h'p'}} \rangle\rangle_{\mathscr{E}} \end{bmatrix}. \qquad \text{(VI.18)}$$

The RPA space is complete so we can again employ the representation of the inverse:

$$[\hat{G}(\mathscr{E})]_{\mathrm{ph}} = [\hat{\mathbf{S}}]_{\mathrm{ph}} \left(\mathscr{E} \begin{bmatrix} g & 0 \\ 0 & -g \end{bmatrix} - \begin{bmatrix} A & L \\ L^* & A^* \end{bmatrix} \right)^{-1} [\hat{\mathbf{S}}]_{\mathrm{ph}} \qquad \text{(VI.19)}$$

with poles defined by

$$\det \begin{bmatrix} \mathscr{E} g - A & -L \\ -L^* & -\mathscr{E} g - A^* \end{bmatrix} = 0, \qquad \text{(VI.20)}$$

i.e., the RPA excitation energies.

VII. Summary

We have treated only a very small fraction of many-body theory, but the fraction is probably representative enough to show how the unitary group formulation is applied. Some of the features are (*1*) the employment of finite Hilbert subspaces; (*2*) the use of generators as operators that are bounded on these subspaces; (*3*) time-independent matrix evaluation and derivation of the $(-1)^{\mathrm{H}+\mathrm{L}}$ rule.

In addition, we have employed the superoperator formulation, which is particularly well suited to the unitary group, permitting a straightforward development of the random-phase approximation and hence a time-independent development of the time-independent Green's function.

ACKNOWLEDGMENT

I wish to acknowledge the extensive help of Connie Nelin in the preparation of this manuscript.

REFERENCES

Biedenharn, L. C. (1963). *J. Math. Phys.* **4**, 436.

Brown, G. E. (1973), "Many-Body Problems." Am. Elsevier, New York.

Feshbach, H., and de Shalit, A. (1974). "Theoretical Nuclear Physics," Vol. 1. Wiley, New York.

Gel'fand, I. M., and Tsetlin, M. L. (1950). *Dokl. Akad. Nauk USSR.* **71** 825, 1070; Gel'fand, I. M., and Graev, M. I. (1967). *Am. Math. Soc. Transl.* **64**, 116.

Goscinski, O., and Lukman, B. (1970). *Chem. Phys. Lett.* **7**, 573.

Hansen, A. E., and Bowman, T. D. (1977). *Chem. Phys. Lett.* **45**, 326.

Harter, W. G. (1973). *Phys. Rev. A* **8**, 2819.

Harter, W. G., and Patterson, C. W. (1976). *Phys. Rev. A* **13**, 1067.

Jones, W., and March, N. H. (1973). "Theoretical Solid State Physics." Academic Press, New York.

Jørgensen, P. (1975). *Annu. Rev. Phys. Chem.* **26**, 359.

Linderberg, J., and Öhrn, Y. (1973). "Propagators in Quantum Chemistry." Academic Press, New York.

Linderberg, J., and Ratner, M. (1970). *Chem. Phys. Lett.* **6**, 37.

Louck, J. D. (1970). *Am. J. Phys.* **38**, 3.

Matsen, F. A., (1974). *Int. J. Quantum Chem.* **S8**, 379.

Matsen, F. A. (1976a). *Int. J. Quantum Chem.* **10**, 511.

Matsen, F. A. (1976b). *Int. J. Quantum Chem.* **10**, 525.

Matsen, F. A., and Nelin, C. N. (1978). *Int. J. Quantum Chem.* (to be submitted).

Moshinsky, J. "Group Theory and the Many-Body Problem." Gordon & Breach, New York.

Moshinsky, M. (1963). *J. Math Phys.* **4**, 1128.

Moshinsky, M. (1965). *J. Math. Phys.* **6**, 682.

Oddershede, J., and Elander, N. (1976). *J. Chem. Phys.* **65**, 3495.

Paldus, J. (1974). *J. Chem. Phys.* **61**, 5321.

Paldus, J. (1976). *Theor. Chem.: Adv. Perspect.* **2**, 131.

Paldus, J., and Cizek, J. (1969). *J. Chem. Phys.* **52**, 2919.

Patterson, C. W., and Harter, W. G. (1976). "Unitary Calculus for Electronic Orbitals." Springer-Verlag, Berlin and New York.

Rescingo, T. N., Bender, C. F., and McKoy, B. V. (1977). *Chem. Phys. Lett.* **45**, 307.

Roothaan, C. C. J. (1960). *Rev. Mod. Phys.* **32**, 179.

Rowe, D. J. (1970) "Nuclear Collective Motion." Methuen, London.

Shavit, I. (1977). *Int. J. Quantum Chem. Symp.*, **11**, 131.

Thouless, D. J. (1972). "The Quantum Mechanics of Many-Body Systems," 2nd ed. Academic Press, New York.

Weyl, H. (1931). "The Theory of Groups and Quantum Mechanics." Dover, New York.

Weyl, H. (1939) "The Classical Groups." Princeton Univ. Press , Princeton, New Jersey.

Worth, G. T., Bartlett, B. L., and Matsen, F. A. (1978). *Chem. Phys. Lett.* **53**, 294.

ADVANCES IN QUANTUM CHEMISTRY, VOLUME 11

The Zero-Range Potential Model and Its Application in Atomic and Molecular Physics

G. DRUKAREV
Leningrad State University
Leningrad, USSR

I. Introduction

The zero-range potential model (ZRPM) is a method of treating the problem of a particle in the field of a short-range potential well when there is a shallow energy level near the boundary of the continuum spectrum. The short-range potential well should not be taken too literally. In fact, it is merely a schematic description of the interaction of a particle with an object that in itself can be a rather complicated system. However, we consider these problems for cases in which the details of internal structure of the object are not significant. A negative atomic ion is an example of such a system.

The basic idea of ZRPM is to replace the Schrödinger equation inside the well by a certain boundary condition on the wavefunction at the center of the well. This approach can be extended to the case when there is no shallow level, but it may appear if we make the well a little bit wider and deeper. This situation is often referred to as a "virtual level." The ZRPM can be easily generalized for the case when there are several potential wells

ISBN 0-12-034811-X

at rest or moving and also when, besides the wells, there are electric and magnetic fields. The great advantage of ZRPM is the possibility of obtaining an exact solution in closed form of many important and very difficult problems where other methods fail.

The boundary condition for the wavefunction was first used by Bethe and Peierls (1935) in the theory of deutron. For the scattering of neutrons the simplified version of ZRPM was used by Fermi (1934). For many years this method was used mainly in nuclear physics.

The use of the ZRPM in atomic physics was first reported in 1964 in three papers (Firsov and Smirnov, 1964; Demkov, 1964; Demkov and Drukarev, 1964).

In the following years there was a very intense and rapid development of applications of ZRPM to various problems of atomic and molecular physics. This work was recently summarized by Demkov and Ostrovsky (1975) in a first monograph on this subject. In this book one can find an extensive bibliography (the number of papers cited is about 170).

The aim of present review is to introduce the basic relations and show with several selected one- and two-center problems how ZRPM is used and what kind of results can be obtained.

II. Basic Relations

A. Boundary Conditions in One-Center Problems

1. Let us consider a particle in a field of a short-range spherical potential well in an S-state. Outside the potential well at a distance larger than the range of potential r_0, the wavefunction ψ satisfies the Schrödinger equation,

$$\frac{d^2}{dr^2}(r\psi) + \frac{2m}{\hbar^2} E(r\psi) = 0. \tag{II.1}$$

Inside the potential well,

$$\frac{d^2}{dr^2}(r\psi_1) + \frac{2m}{\hbar^2}(E - V)(r_1\psi) = 0. \tag{II.2}$$

At a distance comparable with the range r_0, the outside wavefunction ψ should be smoothly joined to the inside wavefunction ψ_1.

This matching can be formulated as a boundary condition

$$\frac{1}{(r\psi)}\frac{d}{dr}(r\psi)\bigg|_{r=r_0} = \frac{1}{(r\psi_1)}\frac{d}{dr}(r\psi_1)\bigg|_{r=r_0}. \tag{II.3}$$

Now if the potential well can just hold one shallow S-level, then the right-hand side of Eq. (II.3) in the region

$$-\hbar^2/2mr_0^2 \ll E \ll \hbar^2/2mr_0^2 \tag{II.4}$$

can be replaced without a large error by an energy-independent constant that we denote $-\alpha$. The outside wavefunction ψ in this energy region will change very slowly over the distance of the order r_0. We will then replace r_0 in the left-hand side of Eq. (II.3) by 0 and write

$$\frac{d}{dr}(r\psi)\bigg|_{r=0} = -\alpha(r\psi)_{r=0}. \tag{II.5}$$

This is the boundary condition of the ZRPM. It is used instead of Eq. (II.2) inside the well. After going to the limit $r = 0$, we can use Eq. (II.5) even if ψ is not spherical symmetrical.

Constant α is the only parameter of the model. In terms of it, one can express the energy of the bound state in the field of the short-range well (or, vice versa, express α in terms of the energy of a bound state). This approach was generalized for the states with nonzero angular momentum by Huang (1963) (one potential well) and by Andreeva and Rudakov (1977) (several nonoverlapping potential wells).

2. Let us first consider the bound state. The solution of Eq. (II.1) at negative energies will be

$$\psi = c\frac{1}{r}\exp\left[-\sqrt{-\frac{2mE}{\hbar^2}}\,r\right]. \tag{II.6}$$

By inserting Eq. (II.6) into Eq. (II.5), we get for the energy level

$$E = -\frac{\hbar^2\alpha^2}{2m}. \tag{II.7}$$

Consider now the scattering of the particle. The energy will be positive and we will write

$$E = \frac{\hbar^2 k^2}{2m}.$$

The expression for the outside wavefunction in the scattering problem is well known:

$$\psi = e^{i\bar{k}\bar{r}} + A\frac{e^{ikr}}{r}. \tag{II.8}$$

Here A is the scattering amplitude.

By inserting Eq. (II.8) into Eq. (II.5), we have for the scattering amplitude

$$A = -\frac{1}{\alpha + ik}. \tag{II.9}$$

For the scattering cross section, $\sigma = 4\pi|A|^2$, we get the familiar Wigner formula

$$\sigma = \frac{4\pi}{\alpha^2 + k^2}. \tag{II.10}$$

The value of the scattering amplitude at zero energy with a minus sign is called the scattering length a:

$$a = -A(0). \tag{II.11}$$

From Eq. (II.9) we see that

$$a = \frac{1}{\alpha}. \tag{II.12}$$

This result suggests the generalization of the boundary condition to the case when there is no bound state of the particle in the well: replace α by $1/a$ in Eq. (II.5). When there is a bound state, then $a > 0$. When there is no bound state, then $a < 0$. The case when $a < 0$ and $|a|$ is large (in comparison with the range r_0) is referred as a "virtual state." So we will write the boundary condition in the form

$$\frac{d}{dr}(r\psi)_0 = -\frac{1}{a}(r\psi)_0, \tag{II.13}$$

which holds both for bound and virtual states.

3. Sometimes the spin of the particle and of the object with which the particle interacts can play an important role. For this case we should generalize the boundary conditions and include spin variables. Consider, for example, the interaction of an electron with the hydrogen atom. To a certain extent we can replace the short-range interaction between these particles by the boundary condition of the electronic wavefunction at the center of the atom. However, the scattering length depends on the total spin of the system "electron + atom." In order to take this into account, instead of Eq. (II.13) we will write the boundary conditions in the form

$$\frac{d}{dr}(r\psi)_0 = -\left(\frac{1}{a_s}\hat{P}_s + \frac{1}{a_t}\hat{P}_t\right)(r\psi)_0, \tag{II.14}$$

where a_s, a_t are the scattering lengths in the singlet and triplet states of the system, and $\hat{P}_s$, $\hat{P}_t$ are the corresponding projection operators acting on the spin variables of the wavefunction. They can be expressed in terms of Pauli spin matrices by the well-known relations

$$\hat{P}_s = \frac{1 - \bar{\sigma}_1\bar{\sigma}_2}{4}; \qquad \hat{P}_t = \frac{3 + \bar{\sigma}_1\bar{\sigma}_2}{4}. \tag{II.15}$$

We will denote

$$\frac{1}{a_s}\hat{P}_s + \frac{1}{a_t}\hat{P}_t = \frac{\hat{1}}{a}. \tag{II.16}$$

It is interesting to note that at the same time

$$\hat{a} = a_s\hat{P}_s + a_t\hat{P}_t. \tag{II.17}$$

To verify this one should form a product

$$\left(\frac{1}{a_s}\hat{P}_s + \frac{1}{a_t}\hat{P}_t\right)(a_s\hat{P}_s + a_t\hat{P}_t).$$

Using the known properties of the projection operators $\hat{P}_s$, $\hat{P}_t$, it is easy to see that this product equals unity. Now, if the system is in a definite spin state (as, for example, the singlet state of the negative hydrogen ion H^-), then one of the operators $\hat{P}_t$, $\hat{P}_s$ ($\hat{P}_s$ in our example) will equal unity and the other zero.

4. An interesting modification and generalization of ZRPM in which the logarithmic derivative is a function of time was developed by Demkov (1964). Instead of Eq. (II.13), in this case we write

$$\frac{d}{dr}(r\psi(r, t))_{r=0} = -\alpha(t)(r\psi(r, t))_{r=0}.$$

This nonstationary boundary condition was applied by Demkov to the problem of electron detachment from a negative ion in collision with an atom.

5. There is also a generalization of the boundary conditions with the aim to account for various excited states of the object with which the particle interacts (Dalitz, 1962).

In this generalization, ψ is considered as a multicomponent function (a matrix column) and in Eq. (II.5) instead of the numerical coefficient α we have a matrix. This approach can be used to demonstrate in the simplest way the effects of channel coupling in many-channel problems.

B. Formulation of ZRPM in Terms of Green's Function

The wavefunction ψ subjected to the boundary conditions Eq. (II.13) is singular at the origin. Its behavior at $r \to 0$ is

$$\psi \sim c\left(\frac{1}{r} - \frac{1}{a}\right). \tag{II.18}$$

To account for this singularity, we should write the equation for the wavefunction in the form

$$\Delta\psi + \frac{2mE}{\hbar^2}\psi = -4\pi c\,\delta(\bar{r}). \tag{II.19}$$

If we choose

$$c = -\frac{1}{4\pi}, \tag{II.20}$$

we have for ψ the equation

$$\Delta\psi + \frac{2mE}{\hbar^2}\psi = \delta(\bar{r}), \tag{II.21}$$

which is indeed an equation for Green's function.

By comparing Eq. (II.21) with Eq. (II.2), we see that the ZRPM is equivalent to replacement

$$\frac{2m}{\hbar^2}V\psi \to \delta(\bar{r}). \tag{II.22}$$

Instead of Eq. (II.22), Fermi (1934) used the replacement

$$V \to \text{const} \times \delta(\bar{r}).$$

When used in the problem of scattering of a particle by several centers, Fermi's prescription leads to complete neglect of multiple scattering effects [which can be accounted for by using Eq. (II.22)]. There are cases for which multiple scattering effects are not very important (e.g., scattering of a neutron from the molecule).

The formulation (II.21) can be generalized to the case when, besides the short-range well, we have also a long-range potential U acting on the particle.

Then, instead of Eq. (II.21), we get the equation for Green's function in the field U,

$$\Delta\psi + \frac{2m}{\hbar^2}(E - U)\psi = \delta(\bar{r}) \tag{II.23}$$

subject to the boundary condition [incorporating Eq. (II.20)]

$$\frac{d}{dr}(r\psi)_0 = \frac{1}{4\pi a}. \tag{II.24}$$

C. Boundary Conditions for Many-Center Problems

1. Let us consider N nonoverlapping short-range potential wells, centered at the points $r_1 \cdots r_N$. In ZRPM, instead of the wells, we introduce N boundary conditions:

$$\frac{d}{d\rho_i}(\rho_i\psi)_{\rho_i=0} = -\frac{1}{a_i}(\rho_i\psi)_{\rho_i=0}, \tag{II.25}$$

where

$$\rho_i = |\bar{r} - \bar{r}_i|. \tag{II.26}$$

2. We did not take the spin into account. Now, we will consider a system such as $H + H^-$ and show by this example how the boundary conditions should be modified to include spin.

According to Eqs. (II.14) and (II.15) we will have for the function ψ, which depends on coordinates and spin variables,

$$\frac{d}{d\rho_1}(\rho_1\psi)_{\rho_1=0} = -\left\{\left(\frac{3}{4a_t} + \frac{1}{4a_s}\right) + \frac{1}{4}\left(\frac{1}{a_t} - \frac{1}{a_s}\right)\bar{\sigma}_1\bar{\sigma}\right\}(\rho_1\psi)_{\rho_1=0} \tag{II.27}$$

$$\frac{d}{d\rho_2}(\rho_2\psi)_{\rho_2=0} = -\left\{\left(\frac{3}{4a_t} + \frac{1}{4a_s}\right) + \frac{1}{4}\left(\frac{1}{a_t} - \frac{1}{a_s}\right)\bar{\sigma}_2\bar{\sigma}\right\}(\rho_2\psi)_{\rho_2=0}. \tag{II.28}$$

Here $\bar{\sigma}_1$ and $\bar{\sigma}_2$ act on the spin variables of atoms, and $\bar{\sigma}$ on the spin variable of electrons.

In order to separate the spin variables and obtain the relations only for coordinate part of the wavefunction, one should calculate the matrix elements of the spin operators $\bar{\sigma}_1\bar{\sigma}$ and $\bar{\sigma}_2\bar{\sigma}$.

The total spin and its projection of the system is conserved. So in the total spin representation, we should calculate only the diagonal matrix elements.

Let us consider the state in which the total spin and its projection is $\frac{1}{2}$. Now there are two different ways of constructing such a state. One is to combine the electron spin state with the singlet state of both atoms; the other is to combine the electron spin state with the triplet spin state of both atoms.

The first is described by the spin wavefunction

$$\chi_1 = \frac{1}{\sqrt{2}}u(u_1v_2 - u_2v_1), \tag{II.29}$$

and the second by the function

$$\chi_2 = \frac{1}{\sqrt{6}}\{2vu_1u_2 - u(u_1v_2 + u_2v_1)\}. \tag{II.30}$$

Here u corresponds to the spin projection $\frac{1}{2}$, and v corresponds to the spin projection $-\frac{1}{2}$. But the singlet and triplet states of a pair of hydrogen atoms have different energies. We then came to the conclusion that we have to deal with two-channel problems, which should be treated as suggested in Section II, A, 5. This approach was used by Demkov and Ostrovsky (1970).

The situation could be simplified if we neglect the coupling between the singlet and triplet channels of atoms. Then the problem is reduced to one channel, and we have only to calculate the matrix element $\langle\chi_1|\bar{\sigma}_i\bar{\sigma}|\chi_1\rangle$, which is equal to 0. The final result is that, for this one-channel approximation, we can use ordinary boundary conditions in which, instead of $1/a$, we substitute

$$\left\langle\frac{1}{a}\right\rangle = \frac{1}{4}\left(\frac{3}{a_t} + \frac{1}{a_s}\right). \tag{II.31}$$

3. Unlike the one-center problems, the boundary conditions, Eq. (II.25) should be modified in the presence of a magnetic field (Adamov *et al.*, 1968):

$$\frac{d}{d\rho_i}(\rho_i\psi)_{\rho_i=0} = \left[-\frac{1}{a} + \frac{i}{c}(\bar{A}(\bar{r}_i), \bar{n}_i)\right](\rho_i\psi)_{\rho_i=0}. \tag{II.32}$$

Here $\bar{A}$ is the vector potential of the magnetic field, and $\bar{n}_i$ is the unit vector in the direction $\bar{r} - \bar{r}_i$.

4. One more modification of the boundary condition was suggested recently by Rebane and Sharibdjanov (1975). It is connected with the behavior of the wavefunction when two centers are at a very small distance from each other. Then clearly we cannot consider the two potential wells as nonoverlapping. Just the contrary, in this case it is more appropriate to use the picture of "united atoms," that is, to introduce one potential well instead of two overlapping ones.

The problem is to construct some interpolation procedure that connects two limiting cases: one united well and two separate wells.

We will not reproduce here the details, but refer the reader to the original paper.

Finally, we mention the generalization of the boundary conditions to the case when the centers are moving with some velocities v_i, so that (Demkov, 1965; E. Solovjev, private communication)

$$\bar{r}_i = \bar{r}_i(t).$$

Then

$$\frac{d}{d\rho_i}(\rho_i\psi)_{\rho_i=0} = (-\alpha_i(t) + i\bar{v}_i\bar{n})(\rho_i\psi)_{\rho_i=0}, \qquad \text{(II.33)}$$

where

$$\bar{\rho}_i = \bar{r} - \bar{r}_i(t) \qquad \text{(II.34)}$$

$$\bar{n} = \frac{\bar{r}}{r}. \qquad \text{(II.35)}$$

III. Applications

A. References in the Literature to Various Applications

We list here some applications of Eqs. (II.23) and (II.24) and of the one- and many-center boundary conditions in atomic and molecular physics. The references are by no means complete. Further references may be found in the papers cited and in the book by Demkov and Ostrovsky (1975).

Several applications will be considered as examples in the subsequent sections of this paper.

Equations (II.23) and (II.24) were used to study a charged particle under the action of a short-range potential well and (*a*) a homogeneous electric field (Demkov and Drukarev, 1964), (*b*) a homogeneous magnetic field (Demkov and Drukarev, 1965), (*c*) crossed electric and magnetic fields (Drukarev and Monozon, 1971), (*d*) a rotating electric field (Manakov and Rapoport, 1975), (*e*) a Coulomb field of a point charge (Komarov, 1969; Presnyakov, 1970). The results of latter works are closely related to the properties of the system $A^- + B^+$ (where A^- is a negative atomic ion and B^+, positive atomic ion). Problems *a*, *b*, and *c* are discussed in this review.

The many-center boundary conditions were used in the following:

1. Energy terms of the system $H + H^-$ (Firsov and Smirnov, 1964; Demkov and Ostrovsky, 1975). The simplified version without account for spin effects is given here.

2. Energy terms of a particle in the field of N centers, including perturbation due to the weak electric and magnetic fields; application to the molecular systems (Adamov *et al.*, 1968).

3. Scattering of a particle on two centers; application to the problem of e-H_2 scattering (Subramanjan, 1968; see also this chapter, Section II, E).

4. Scattering on N centers; development of the method of partial waves (Demkov and Rudakov, 1970).

5. Particle in the field of infinite number of centers forming a periodical linear chain (Demkov and Subramanjan, 1969).

6. Scattering of an electron on long linear molecules (Demkov *et al.*, 1974).

7. Particle in a field of a three-dimensional lattice of zero-range potential centers (Goldberger and Seitz, 1947; Maleev, 1965).

8. Nonstationary version of ZRPM and its application to the theory of electron detachment from negative atomic ion (Demkov, 1965; Demkov and Ostrovsky, 1975).

9. Application of ZRPM to the electron-molecular scattering, including vibrational excitation and dissociative attachment. General theory (Drukarev, 1974); application to the vibrational and rotational excitation (Drukarev and Yurova 1977; also see this chapter, Section III, F).

B. Particle with Low-Binding Energy in the Electric Field

This problem is reduced to the equation

$$\Delta\psi + (-\alpha^2 - Fz)\psi = \delta(\vec{r}), \tag{III.1}$$

where

$$\alpha^2 = -\frac{2mE}{\hbar^2}, \qquad F = \frac{2me\mathscr{E}}{\hbar^2} \tag{III.2}$$

($\mathscr{E}$ is the electric field), and the boundary condition

$$\frac{d}{dr}(r\psi)_{r=0} = \frac{\alpha_0}{4\pi}, \tag{III.3}$$

the binding energy in the absence of the field being $-\hbar^2\alpha_0^2/2m$.

In the presence of the field there will be no bound stationary state but instead there will be a quasistationary state. As is well known, this state will be characterized by a complex energy

$$E = E_0 - i\frac{\Gamma}{2}, \tag{III.4}$$

where the imaginary part is directly related to the lifetime.

To find this complex energy, we will require that the solution of Eq. (III.1), which is Green's function of a free particle in an electric field, will behave at large distances as an outgoing wave.

By using cylindrical coordinates ρ and z and assuming that there is no angular momentum, we can represent ψ in form

$$\psi = \frac{1}{2\pi}\int_0^\infty J_0(\lambda\rho)g(p, z)\lambda\, d\lambda; \qquad p^2 = \alpha^2 + \lambda^2, \tag{III.5}$$

where J_0 is the Bessel function, and g is the one-dimensional Green function

$$\frac{d^2g}{dz^2} + (Fz - p^2)g = \delta(z), \tag{III.6}$$

which can be expressed in terms of Airy functions of the variable

$$\xi = (p^2 - Fz)F^{-2/3}. \tag{III.7}$$

Denote by u and v the independent solutions of the equation

$$\frac{d^2u}{d\xi^2} + \xi u = 0 \tag{III.8}$$

which at $\xi \to \infty$ has the following asymptotical behavior:

$$\begin{aligned} u &\sim \xi^{-1/4} \exp(\tfrac{2}{3}\xi^{3/2}) \cdot (1 + \tfrac{5}{48}\xi^{-3/2} + \cdots), \\ v &\sim \tfrac{1}{2}\xi^{-1/4} \exp(-\tfrac{2}{3}\xi^{3/2}) \cdot (1 - \tfrac{5}{48}\xi^{-3/2} + \cdots). \end{aligned} \tag{III.9}$$

Then

$$g = \begin{cases} F^{-1/3}v(\xi)[u(\xi_0) + 2iv(\xi_0)] & \xi > \xi_0 \\ F^{-1/3}v(\xi_0)[u(\xi) + 2iv(\xi)] & \xi < \xi_0 \end{cases}, \tag{III.10}$$

where $\xi_0 = p^2F^{-2/3}$.

Now, we should realize that use of ZRPM can be justified for not too strong a field F (otherwise the wavefunction will change rapidly over the small distances). We will assume that

$$\frac{1}{\alpha_0^2} F^{2/3} \ll 1. \tag{III.11}$$

For almost all cases of practical interest this condition is satisfied. For example, $E_0 = 0.75$ eV for H^-, and, at $\mathscr{E} = 2.5 \times 10^6$ V/cm, we have $F^{2/3}\alpha_0^{-2} = 0.18$.

Then we can use the asymptotic expression for the Airy functions. Referring to the original paper for details of computations, we write down here the approximate expression for g at small z:

$$g = \frac{1}{2p}\left\{\exp[-p|z|]\left(1 + \frac{5F^2}{32p^6}\right) + \frac{i}{2}\exp\left(p|z| - \frac{4p^3}{3F}\right)\right\}. \tag{III.12}$$

By substituting this expression in Eq. (III.5), we obtain an expression for ψ with small z. In particular, on the z axis, at $\rho = 0$, we have (after going over to integration with respect to p)

$$\psi = \frac{1}{4\pi}\int_{\alpha}^{\infty}\left\{\exp[-p|z|]\left(1 + \frac{5F^2}{32p^6}\right) + \frac{i}{2}\exp\left(p|z| - \frac{4p^3}{3F}\right)\right\} dp. \tag{III.13}$$

Now the term $(1/4\pi)\int_\alpha^\infty \exp[-p|z|]\,dp$ at $z \to 0$ diverges just as $1/4\pi|z|$. By applying the boundary condition, Eq. (III.3) and going to the limit $r \to 0$ along the z axis, we obtain an equation for α:

$$\alpha - \alpha_0 = -\frac{F^2}{32\alpha^5} + \frac{i}{2}\int_\alpha^\infty e^{-4p^3/3F}\,dp. \tag{III.14}$$

Again, taking into account Eq. (III.11), we can evaluate approximately the integral in Eq. (III.14). By replacing in the first approximation α by α_0 in the right-hand side of (III.14), we get

$$\alpha - \alpha_0 = -\frac{F^2}{32\alpha_0^5} + \frac{iF}{8\alpha_0^2}e^{-4\alpha_0^3/3F} \tag{III.15}$$

and, finally,

$$E = E_0 - \frac{\hbar^2 e^2 \mathscr{E}^2}{32 m E_0^2} + i\Gamma; \tag{III.16}$$

$$\Gamma = \frac{\hbar e \mathscr{E}}{4 \cdot (2mE_0)^{1/2}} \exp\left(-\frac{2^{5/2} m^{1/2} E_0^{3/2}}{3\hbar e \mathscr{E}}\right). \tag{III.17}$$

For a discussion of corrections due to finite range of a potential well and comparison with other calculations, we refer the reader to the original paper.

C. Particle with Low-Binding Energy in the Magnetic Field

Before entering the calculations, we will discuss some general features of this problem. First we consider the case of a shallow potential well, where in the absence of the field there is no bound state. If we switch on a magnetic field, the motion of the particle transverse to the field will be hindered and, consequently, the problem becomes similar to the one-dimensional problem. We know that for the one-dimensional problem there is a bound state in any well. We may, therefore, assume (and will prove later) that, for an arbitrarily shallow three-dimensional well, when we switch on an arbitrarily weak field, a bound state always appears. In first approximation the binding energy is proportional to the square of the field, so that the phenomenon is reminiscent of diamagnetism, but acts in the opposite direction, so that we might call it "antidiamagnetism."

The magnetic field thus appears to exert a stabilizing influence on the particle. Real magnetic fields are too weak for such an effect to be observable with free atoms or electrons. But in semiconductors at liquid helium temperatures and for low values of the effective mass of electrons or holes, we shall see that the binding energy may be comparable to kT, so that the bound states that are formed may be observed experimentally.

In addition to an antidiamagnetic downward shift of the energy, proportional to the square of the field, there is also an upward shift, linear in the field, of the boundary of the continuous spectrum, the shift being $\Delta E = \hbar\omega_L$ ($\omega_L = e\hbar/2mc$ is the Larmor frequency). This is related to the fact that, unlike a classical particle, a quantum particle with zero spin and sufficiently low energy cannot penetrate into a region of strong magnetic field, moving along a force line; the quantity ΔE is a sort of potential barrier and equal to the zero-point energy of a two-dimensional oscillator of frequency ω_L. The term ΔE increases the total energy and is analogous to a paramagnetic shift, but it also acts in the opposite direction (antiparamagnetism) and causes the system to be repelled from a region of the strong magnetic field. But if the particle has a spin and is oriented along the field then, for example, for an electron, the antiparamagnetic and paramagnetic terms compensate completely, and there remains only the quadratic antidiamagnetic term, which will lead to an attraction of the system into the field.

If the potential well is sufficiently deep so that there is a bound state in the absence of the magnetic field, there is the usual diamagnetic effect, which increases the total energy by an amount proportional to the square of the field and leads to expulsion of the system from the field. The linear shift of the edge of the continuous spectrum also appears, but it has no effect on the total energy, and only has the consequence that, despite the upward diamagnetic energy shift, the binding energy of the particle increases with the field, so that the magnetic field exerts a stabilizing influence on the particle in both the cases considered.

Now we pass to the mathematical formulation of the problem. The equation for the wavefunction is

$$\Delta\psi + (\varepsilon - \lambda^2\rho^2)\psi = \delta(\bar{r}), \qquad \text{(III.18)}$$

where

$$\varepsilon = \frac{2mE}{\hbar^2}; \qquad \lambda = \frac{e\mathscr{H}}{2\hbar c}; \qquad \rho^2 = x^2 + y^2; \qquad \text{(III.19)}$$

$\mathscr{H}$ is the strength of magnetic field. The solution of Eq. (III.18) can be represented in the form

$$\psi(\rho, z) = \sum_n \varphi_n(\rho)\varphi_n(0)g_n(z). \qquad \text{(III.20)}$$

Here φ_n is the regular normalized solution of the equation

$$\frac{d^2\varphi_n}{d\rho^2} + \frac{1}{\rho}\frac{d\varphi_n}{d\rho} + (\beta_n - \lambda^2\rho^2)\varphi_n = 0, \qquad \text{(III.21)}$$

i.e., eigenfunctions of the two-dimensional isotropic oscillator, having cylindrical symmetry,

$$\varphi_n = \sqrt{\frac{\lambda}{\pi}}\, e^{-\lambda^2\rho^2/2} L_n(\lambda\rho^2), \tag{III.22}$$

where the L_n are Laguerre polynomials. Eigenvalues β_n are

$$\beta_n = 4\lambda(n + \tfrac{1}{2}). \tag{III.23}$$

Functions g_n are one-dimensional Green's functions satisfying the equations

$$\frac{d^2 g_n}{dz^2} - \alpha_n^2 g_n = \delta(z); \qquad \alpha_n^2 = \beta_n - \varepsilon \tag{III.24}$$

and vanishing for $|z| \to \infty$ (since we are considering only bound states). Functions g_n have the form

$$g_n = \frac{1}{2\alpha_n}\, e^{-\alpha_n|z|} \tag{III.25}$$

and, consequently, the required wavefunction can be represented as a sum

$$\psi = \frac{\lambda}{2\pi} \sum_n e^{-\lambda\rho^2/2} L_n(\lambda\rho^2)\, \frac{1}{\alpha_n}\, e^{-\alpha_n|z|}. \tag{III.26}$$

For what follows, we need only consider the behavior of ψ for $\rho = 0$ on the z axis. We have

$$\psi = \frac{\lambda}{2\pi} \sum_n \frac{e^{-\alpha_n|z|}}{\alpha_n}, \tag{III.27}$$

$$\alpha_n = \sqrt{\lambda(4n + \xi)}; \qquad \xi = 2 - \frac{\varepsilon}{\lambda}. \tag{III.28}$$

In this case the series can be summed using the formula

$$\int_0^\infty \exp\left[-\beta t^2 - \frac{c}{t^2}\right] dt = \frac{1}{2}\sqrt{\frac{\pi}{\beta}}\, \exp[-2\sqrt{c\beta}] \tag{III.29}$$

and setting $c = \lambda z^2$, $\beta = n + \xi/4$. Then, interchanging the order of summation and integration and summing the geometrical progression under the integral, we get

$$\psi = \frac{\lambda^{1/2}}{2\pi^{3/2}} \int_0^\infty \frac{\exp\left[-\dfrac{\xi t^2}{4} - \dfrac{\lambda z^2}{t^2}\right]}{1 - \exp[-t^2]}\, dt. \tag{III.30}$$

When $z \to 0$ the integral diverges at its lower limit. If we separate the divergent part, then we obtain

$$\psi = \frac{1}{4\pi|z|}\exp[-\sqrt{\lambda\xi}|z|] + \frac{\lambda^{1/2}}{2\pi^{3/2}}\int_0^\infty \left(\frac{1}{2}\coth\frac{t^2}{2} + \frac{1}{2} - \frac{1}{t^2}\right)\exp\left[-\frac{\xi t^2}{4} - \frac{\lambda^2 z^2}{t^2}\right] dt. \qquad \text{(III.31)}$$

For large z the factor multiplying the exponential in the integrand can be replaced by unity and, consequently,

$$\psi|_{z\to\infty} \sim \frac{1}{4\pi}\sqrt{\frac{\lambda}{\xi}}\exp[-\sqrt{\lambda\xi}|z|]\left(1 + 0\left(\frac{1}{|z|}\right)\right), \qquad \text{(III.32)}$$

i.e., at infinity the behavior of ψ is determined by the first term of the sum Eq. (III.27) and is the same as in the one-dimensional case. It follows that the edge of the continuous spectrum is reached for $\xi = 0$, which coincides with the condition $E = \hbar\omega_L$.

By using the boundary conditions, we get an equation for determining the energy:

$$\frac{1}{a\sqrt{\lambda}} = \sqrt{\xi} - \frac{2}{\sqrt{\pi}}\int_0^\infty \left(\frac{1}{2}\coth\frac{t^2}{2} + \frac{1}{2} - \frac{1}{t^2}\right)e^{-\xi t^2/4}\, dt. \qquad \text{(III.33)}$$

The right side can be expressed in terms of the generalized Riemann ζ-function,

$$\frac{1}{a\sqrt{\lambda}} = -\zeta\left(\frac{1}{2}, \frac{\xi}{4}\right) = F(\xi), \qquad \text{(III.34)}$$

and can be represented to high accuracy by the expression

$$F(\xi) \approx (\xi + 4)^{1/2} - 2\xi^{-1/2} - (\xi + 4)^{-1/2} - \tfrac{1}{3}(\xi + 4)^{-3/2}. \qquad \text{(III.35)}$$

Finally, we get

$$\frac{1}{a\sqrt{\lambda}} = -2\xi^{-1/2} - \zeta(\tfrac{1}{2}) + 0(\xi) \qquad \xi \ll 1, \qquad \text{(III.36)}$$

$$\frac{1}{a\sqrt{\lambda}} = \xi^{1/2} - \xi^{-1/2} - \tfrac{1}{3}\xi^{-3/2} + 0(\xi^{-7/2}) \qquad \xi \gg 1, \qquad \text{(III.37)}$$

where $\zeta(s)$ is the usual Riemann ζ-function.

As we see from these expressions, the case $\xi \gg 1$ occurs when $a > 0$, where there is a bound state in the well even in the absence of the magnetic field. The case $\xi \ll 1$ occurs for $a < 0$, when there are no bound states in the absence of the field. In both cases, the right side of the equation is a large number and, consequently, $a\sqrt{\lambda} \ll 1$, i.e., the radius of the first Larmor orbit is much greater than the dimensions of the electron cloud in the absence of the field. We shall regard such a field as weak, whereas a field for which the opposite criterion $a\sqrt{\lambda} \gg 1$ is satisfied will be considered strong.

Now let us consider various limiting cases.

1. $a > 0$, weak field. By using formula (III.37), we get

$$\varepsilon a^2 = -1 + \tfrac{1}{3}\lambda^2 a^4 + 0(\lambda^4 a^8) \tag{III.38}$$

or, changing to the usual units,

$$E = E_0 + \frac{e^2 \mathscr{H}^2 a^2}{24mc^2}. \tag{III.39}$$

Using the equation

$$\langle r^2 \rangle = \tfrac{1}{2}a^2, \tag{III.40}$$

which comes from the expression for the wavefunction in the absence of the field,

$$\psi = \frac{1}{4\pi r} e^{-r/a}, \tag{III.41}$$

we get

$$E = E_0 + \frac{e^2 \mathscr{H}^2}{12mc^2} \langle r^2 \rangle, \tag{III.42}$$

the familiar result for the diamagnetic energy shift.

2. $a < 0$, weak field. By using Eq. (III.36), we get

$$2\lambda - \varepsilon = \frac{4\lambda^2 a^2}{[1 + a\lambda^{1/2}\zeta(\frac{1}{2})]^2} + 0(\lambda^{7/2}a^7). \tag{III.43}$$

From our earlier remarks, the value $\varepsilon = 2\lambda$ is the edge of the continuous spectrum, so that the difference $2\lambda - \varepsilon$ gives us the binding energy E_0. In ordinary units this quantity is equal to

$$E_0 = \frac{e^2 \mathscr{H}^2 a^2}{2mc^2} \left[1 + 1.46|a|\left(\frac{e\mathscr{H}}{2\hbar c}\right)^{1/2}\right]^{-2}. \tag{III.44}$$

3. $|a| = \infty$, arbitrary field. This is the limiting case where in zero field there is no bound state, but such a state appears for an arbitrarily small increase in the well depth. In this case the left side of Eq. (III.34) is zero, and we must find the value of ξ_0 for which the right side vanishes. With

the approximate formula (III.35), we can easily find $\xi_0 = 1.21$. Thus in this limiting case the binding energy E_0 increases linearly with the field:

$$2\lambda - \varepsilon = \xi_0 \lambda \quad \text{or} \quad E_0 = 0.3\,\frac{e\hbar\mathscr{H}}{mc}. \tag{III.45}$$

4. a arbitrary, strong field. In this case we must expand the function $F(\xi)$ in series in the neighborhood of the point ξ_0:

$$F(\xi) = F'(\xi_0)(\xi - \xi_0) + \tfrac{1}{2}F''(\xi_0)(\xi - \xi_0)^2 + \cdots. \tag{III.46}$$

By using the approximate formula (III.35), we easily find

$$F'(\xi_0) = 1.02, \qquad F''(\xi_0) = -0.95.$$

For the total energy of the bound state in the magnetic field, we then obtain the formula

$$\varepsilon a^2 = 0.79\lambda a^2 - 0.98a\sqrt{\lambda} - 0.45 + 0\left(\frac{1}{a\sqrt{\lambda}}\right). \tag{III.47}$$

The present approximate treatment is applicable if the following two conditions are satisfied.

A. The dimensions of the electron cloud should be much greater than the radius r_0 of the potential well. It follows that, if $a > 0$ for a bound state in the absence of a field, the inequality $a \gg r_0$ must be satisfied. This condition does not contain the magnetic field $\mathscr{H}$ and is a general condition for all cases in which one uses the zero-range approximation. If $a < 0$, then it is not necessary to require that $|a| \gg r_0$. In this case the wavefunction of the bound state will fall off very slowly in reasonably strong fields. If $E_0(\mathscr{H})$ is the binding energy, our condition can be written as

$$\sqrt{\frac{2mE_0(\mathscr{H})}{\hbar^2}}\, r_0 \ll 1 \tag{III.48}$$

or, replacing $E_0(\mathscr{H})$ by the first term in Eq. (III.44), we get

$$e\mathscr{H}ar_0/\hbar c \ll 1. \tag{III.49}$$

This condition is practically always satisfied: for example, if $a = 10^{-7}$ cm, $r_0 = 10^{-8}$ cm, we get $\mathscr{H} \ll 10^8$. A bound state near the edge of the continuous spectrum will always appear in a magnetic field if the scattering length a is negative, even if the well is deep and contains other bound states with large binding energies.

B. The radius of the first Larmor orbit should be much greater than the size of the well r_0, i.e.,

$$r_0\sqrt{\lambda} \ll 1. \tag{III.50}$$

This condition is surely satisfied for actual fields and not too large r_0. Even assuming $r_0 \sim 10^{-7}$ cm, we get $\mathscr{H} \ll 10^7$.

D. Particle with Low-Binding Energy in Crossed Electric and Magnetic Fields

Such a problem arises, for example, in the study of ionization of highly excited atoms or negative ions moving in a strong magnetic field. In a coordinate system connected with the moving particle, there will exist besides the magnetic field also an electric field, perpendicular to the latter and smaller in magnitude. Under the influence of the electric field, the electron can become detached by tunneling through the potential barrier. This process has come to be known in the literature as Lorentz ionization. When the velocity of the particle is comparatively large (indicating a large electric field), then one can neglect the influence of magnetic field in a coordinate system bounded with particle. But when the velocity tends to zero (this means that the electric field tends to zero) the influence of the magnetic field becomes important. The magnetic field can lead to complete stabilization of the particle when tunneling is impossible, as we will see.

The wavefunction now satisfies the equation

$$\Delta\psi + 2i\frac{e\mathscr{H}}{\hbar c}\frac{\partial\psi}{\partial x} + \left(-\frac{e^2\mathscr{H}^2}{\hbar^2 c^2}y^2 + \frac{2me\varepsilon}{\hbar^2}y + \frac{2mE}{\hbar^2}\right)\psi = \delta(\bar{r}). \qquad \text{(III.51)}$$

The magnetic field is directed along the z axis, and the electric field along the y axis.

Let us consider the expression

$$u = -e\mathscr{E}y + \frac{e^2\mathscr{H}^2}{2mc^2}y^2, \qquad \text{(III.52)}$$

which can be called the potential energy along the y direction. Its shape is parabolic, the position of the bottom of the well on the energy scale is given by the expression

$$u_0 = -\frac{mc^2}{e}\left(\frac{\mathscr{E}}{\mathscr{H}}\right)^2. \qquad \text{(III.53)}$$

Let us consider the ratio

$$\gamma = \sqrt{\left|\frac{E}{u_0}\right|}. \qquad \text{(III.54)}$$

If $\gamma > 1$, the tunneling is impossible and we have the stable state. If $\gamma < 1$, then the tunneling is possible and we will have a quasistationary state similar to the one described in 1.

The solution of Eq. (III.51) as a function of z at $x = y = 0$ can be represented in the form

$$\psi = \frac{1}{i(4\pi i)^{3/2}\lambda}\int_0^\infty \frac{dt}{t^{1/2}\sin(t/2)}\exp\left[i\left(-\frac{\alpha^2\lambda^2}{4}t - \frac{s^2}{\lambda^2}t + \frac{z^2}{\lambda^2 t} + \frac{s^2t^2}{2\lambda^2}\operatorname{ctg}\left(\frac{t}{2}\right)\right)\right] \tag{III.55}$$

where $\alpha^2 = -2mE/\hbar^2$; $\lambda = \sqrt{e\mathscr{H}/2\hbar c}$ is the Larmor radius; $s = mc^2\mathscr{E}/e\mathscr{H}^2$.

By inserting Eq. (III.55) in the boundary conditions, we obtain

$$-\alpha_0\lambda = -\alpha\lambda - \frac{1}{\sqrt{\pi i}}\int_0^\infty \frac{dt}{t^{3/2}}$$
$$\times\left\{\frac{t}{2\sin(t/2)}\exp\left[i\left(-\frac{\alpha^2\lambda^2 t}{4} - \frac{s^2}{\lambda^2}t + \frac{s^2t^2}{2\lambda^2}\operatorname{ctg}\left(\frac{t}{2}\right)\right)\right] - \exp\left(-i\frac{\alpha^2\lambda^2 t}{4}\right)\right\}\cdots. \tag{III.56}$$

In the case $\gamma \gg 1$, Eq. (III.56) can be used to calculate corrections to the energy level in pure magnetic fields due to the electric field. In the case $\gamma \ll 1$, Eq. (III.56) can be used to calculate the correction to the imaginary part of the complex energy Γ (which would be in the pure electric field) due to the magnetic field.

Referring to the original paper for details, we reproduce here only the expression for the ionization probability in the case when $\gamma \lesssim 1$:

$$W = \frac{E_0}{2\hbar}\frac{\mathscr{E}}{\mathscr{E}_0}\sqrt{\frac{E-u_0}{E}}\,e^{-\mathscr{E}/\mathscr{E}_0}, \tag{III.57}$$

where $\mathscr{E}_0$ is the atomic unit of the electric field, and u_0 is given by Eq. (III.53).

E. Particle in the Field of Two Centers

According to Eq. (II.25), we will have two boundary conditions:

$$\frac{d}{d\rho_1}(\rho_1\psi)_{\rho_1=0} = -\frac{1}{a_1}(\rho_1\psi)_{\rho_1=0}, \tag{III.58}$$

$$\frac{d}{d\rho_2}(\rho_2\psi)_{\rho_2=0} = -\frac{1}{a_2}(\rho_2\psi)_{\rho_2=0} \tag{III.59}$$

(r_1 is the position of the center of the first well and r_2 is the position of the center of the second well).

Now, in the absence of the second well, outside the first well we would have

$$\psi = c_1 \frac{e^{-\alpha\rho_1}}{\rho_1},$$

where α would be equal to $1/a_1$. Similarly, outside the second well in the absence of the first, we would have

$$\psi = c_2 \frac{e^{-\alpha\rho_2}}{\rho_2}$$

with $\alpha = 1/a_2$.

If both wells are present, we write (Firsov and Smirnov, 1964)

$$\psi = c_1 \frac{e^{-\alpha\rho_1}}{\rho_1} + c_2 \frac{e^{-\alpha\rho_2}}{\rho_2}, \tag{III.60}$$

where α should be calculated with the help of boundary conditions Eqs. (III.58) and (III.59).

By inserting Eq. (III.60) into Eqs. (III.58) and (III.59) and denoting

$$|\bar{r}_1 - \bar{r}_2| = R, \tag{III.61}$$

we get a system of equations for c_1, c_2:

$$\begin{aligned} \left(\alpha - \frac{1}{a_1}\right)c_1 + \frac{e^{-\alpha R}}{R} c_2 &= 0, \\ c_1 \frac{e^{-\alpha R}}{R} + \left(\alpha - \frac{1}{a_2}\right)c_2 &= 0. \end{aligned} \tag{III.62}$$

System (III.62) will have a nontrivial solution c_1, c_2 under the condition

$$\begin{vmatrix} \alpha - \dfrac{1}{a_1} & e^{-\alpha R}/R \\ e^{-\alpha R}/R & \alpha - \dfrac{1}{a_2} \end{vmatrix} = 0. \tag{III.63}$$

From this follows an equation for α:

$$\left(\alpha - \frac{1}{a_1}\right)\left(\alpha - \frac{1}{a_2}\right) - \frac{e^{-2\alpha R}}{R^2} = 0. \tag{III.64}$$

Let us denote by $\alpha_i(R)$ the roots of Eq. (III.64). Then from the relation,

$$E_i(R) = -\frac{\hbar^2\alpha_i^2(R)}{2m}, \tag{III.65}$$

we get the *energy terms* of the particle in the field of two centers.

The simplest case is two similar centers when $a_1 = a_2 > 0$. Then Eq. (III.64) reduces to

$$\frac{1}{\alpha} - \frac{1}{a} \pm \frac{e^{-\alpha R}}{R} = 0. \qquad \text{(III.66)}$$

We have two terms that are degenerate at $R = \infty$. As R decreases, one of the terms will go up, another down. The term that is going down is obviously a g term; the upgoing term is a u term. In the limit $R \rightarrow 0$ the energy of the g term becomes $-\infty$. But one should not take this result too literally. When the distance R becomes too small, the two potential wells begin to overlap and we can no longer replace them by two separate point centers, so that at small R the g term must be replaced by a more realistic term. One can say that ZRPM gives the asymptotic of the term.

The u term, which is going up, can reach the point $\alpha = 0$ (which corresponds to $E = 0$). From Eq. (III.26) it follows that this will happen at a distance

$$R_0 = a. \qquad \text{(III.67)}$$

If a is large, then R_0 is large and the ZRPM can be applied.

The situation when $\alpha = 0$ corresponds, for example, to a system $(AB) + e$, the electron being at rest. This result suggests that the cross section of the detachment of an electron from a negative atomic ion A^- in slow collision with a similar neutral atom A will be of the order πa^2.

What happens with the u term at $R < R_0$? The answer is almost obvious.

It will turn into the *quasistationary term* of the particle in the field of two centers. Such quasistationary terms are very important for the interpretation of the resonance phenomena in electron-molecular collisions (Schulz, 1973).

It is interesting to note that even in the case $a_1 = a_2 < 0$, when there is no bound states on the separate centers, there can be a g term at a distance

$$R \leq |a|. \qquad \text{(III.68)}$$

If $|a|$ is large enough, then the distance R will be in the limit of applicability of the ZRPM.

If $a_1 \neq a_2$, then one can deduce from Eq. (III.25) that in the case $a_1 > 0$, $a_2 > 0$ there will be two terms—one going up when $R \rightarrow 0$, the other going down. If $a_1 < 0$, $a_2 > 0$, there will be only one term at all distances R. If $a_1 < 0$, $a_2 < 0$, then there will be one term at the distances $R \leq \sqrt{a_1 a_2}$.

F. Scattering of a Particle by Two Centers

To calculate the scattering amplitude of a particle, we represent the wavefunction in form

$$\psi = e^{i\bar{k}\bar{r}} + A_1 \frac{e^{ik|\bar{r}-\bar{r}_1|}}{|\bar{r}-\bar{r}_1|} + A_2 \frac{e^{ik|\bar{r}-\bar{r}_2|}}{|\bar{r}-\bar{r}_2|} \tag{III.69}$$

and use the boundary conditions Eqs. (III.58) and (III.59).

We will suppose that the centers are located at the points

$$\bar{r}_1 = \frac{\bar{R}}{2}; \qquad \bar{r}_2 = -\frac{\bar{R}}{2} \tag{III.70}$$

and consider the simplest case of equal scattering length. Then we get for the determination of A_1 and A_2 a system of equations

$$\left(\frac{1}{a} + ik\right)A_1 + \frac{e^{ikR}}{R} A_2 = -e^{i(\bar{k}\bar{R}/2)}, \tag{III.71}$$

$$\left(\frac{1}{a} + ik\right)A_2 + \frac{e^{ikR}}{R} A_1 = -e^{-i(\bar{k}\bar{R}/2)}, \tag{III.72}$$

the solution of which is

$$A_1 = -\left[\frac{\cos(\bar{k}\bar{R}/2)}{\frac{1}{a} + ik + \frac{e^{ikR}}{R}} + i\frac{\sin(\bar{k}\bar{R}/2)}{\frac{1}{a} + ik - \frac{e^{ik\bar{R}}}{R}}\right] \tag{III.73}$$

$$A_2 = -\left[\frac{\cos(\bar{k}\bar{R}/2)}{\frac{1}{a} + ik + \frac{e^{ikR}}{R}} - i\frac{\sin(\bar{k}\bar{R}/2)}{\frac{1}{a} + ik - \frac{e^{ikR}}{R}}\right]. \tag{III.74}$$

Now, to obtain the expression for the scattering amplitude, we consider Eq. (III.69) at large r. Then

$$\psi \sim e^{i\bar{k}\bar{r}} + \left(A_1 e^{i(k/2)\bar{R}\bar{n}} + A_2 e^{-i(k/2)\bar{R}\bar{n}}\right)\frac{e^{ikr}}{r}. \tag{III.75}$$

From Eq. (III.75) follows the expression for the amplitude

$$A = A_1 e^{i(k/2)\bar{R}\bar{n}} + A_2 e^{-i(k/2)\bar{R}\bar{n}}, \tag{III.76}$$

where

$$\bar{n} = \frac{\bar{r}}{r}. \tag{III.77}$$

By inserting Eqs. (III.73) and (III.74) into Eq. (III.76) and introducing the notation

$$\bar{n}_0 = \frac{\bar{k}}{k}, \qquad \text{(III.78)}$$

we get

$$-A = \frac{\cos\left(\frac{k}{2}\,\bar{R}\bar{n}\right)\cos\left(\frac{k}{2}\,\bar{R}\bar{n}_0\right)}{\frac{1}{a} + ik + \frac{e^{ikR}}{R}} + \frac{\sin\left(\frac{k}{2}\,\bar{R}\bar{n}\right)\sin\left(\frac{k}{2}\,\bar{R}\bar{n}_0\right)}{\frac{1}{a} + ik - \frac{e^{ik\bar{R}}}{R}}. \qquad \text{(III.79)}$$

The term e^{ikR}/R represents in explicit form the influence of multiple scattering.

Note that the amplitude has a pole at some imaginary (or complex) value of k. This pole is just the energy of the particle in the bound (or quasistationary) state, as follows from Eq. (III.66).

Expression (III.79) for the amplitude A can be used to calculate the amplitude of vibrational and rotational excitation of a molecule in adiabatic approximation.

If we denote by φ_i, φ_f the initial and final wavefunction of nuclear motion, we have for the transition amplitude A_{fi} the approximate expression

$$A_{fi} = \int \varphi_f^* A(R) \varphi_i \, d\bar{R}. \qquad \text{(III.80)}$$

Expression (II.31) should be used for a.

The adiabatic approximation can be derived directly from the Faddeev theory of collisions in three-body systems (Drukarev, 1974) as a consequence of the small ratio of electronic mass to that of atom, provided the electronic energy exceeds significantly the average spacing of vibrational levels in the molecule.

If we use Eq. (III.79) in Eq. (III.80), we take into account only the short-range interaction of the electron with the molecule and obviously neglect all long-range interactions that should be added.

ACKNOWLEDGMENT

This review is an extended version of lectures given at the Institute of Theoretical Physics, Uppsala University, Sweden. The author wishes to thank Professors N. Fröman and P. O. Fröman for the invitation and their hospitality.

REFERENCES

Adamov, M., Demkov, Y., Obyedkov, V., and Rebane, T. (1968). *Teor. Eksp. Khim.* **4**, 147–153.

Andreeva, T., and Rudakov, V. (1977). *Vestn. Leningr. Univ.*, No. 22, p. 12.

Bethe, H., and Peierls, R. (1935). *Proc. R. Soc. London, Ser. A* **148**, 146.

Dalitz, R. (1962). "Strange Particles and Strong Interactions." Oxford Univ. Press, London and New York.

Demkov, Y. (1964). *Zh. Eksp. Teor. Fiz.* **46**, 1126–1135.

Demkov, Y. (1965). *Zh. Eksp. Teor. Fiz.* **49**, 885–894.

Demkov, Y., and Drukarev, G. (1964). *Zh. Eksp. Teor. Fiz.* **47**, 918–924.

Demkov, Y., and Drukarev, G. (1965). *Zh. Eksp. Teor. Fiz.* **49**, 257–264.

Demkov, Y., and Ostrovsky, V. (1970). *Zh. Eksp. Teor. Fiz.* **59**, 1765–1774.

Demkov, Y., and Ostrovsky, V. (1975). "Application of ZRPM in Atomic Physics." Leningrad Univ. Press, Leningrad. (English translation to be published by Plenum Press.)

Demkov, Y., and Rudakov, V. (1970). *Zh. Eksp. Teor. Fiz.* **59**, 2035–2047.

Demkov, Y., and Subramanjan, R. (1969). *Zh. Eksp. Teor. Fiz.* **57**, 698–702.

Demkov, Y., Ostrovsky, V., and Solovyev, E. (1974). *Zh. Eksp. Teor. Fiz.* **62**, 501–508.

Drukarev, G. (1974). *Zh. Eksp. Teor. Fiz.* **67**, 38–46.

Drukarev, G., and Monozon, B. (1971). *Zh. Eksp. Teor. Fiz.* **61**, 956–967.

Drukarev, G., and Yurova, I. (1977). *J. Phys. B* **10**, 3551–3558.

Fermi, E. (1934). *Nuovo Cimento* **11**, 157–166.

Firsov, O., and Smirnov, B. (1964). *Zh. Eksp. Teor. Fiz.* **47**, 232–239.

Goldberger, M., and Seitz, F. (1947). *Phys. Rev.* **71**, 294–310.

Huang, K. (1963). "Statistical Mechanics." Wiley (Interscience), New York.

Komarov, I. (1969). *Abstr. Pap., JCPEAC, 6th, 1969* pp. 1015–1017.

Maleev, S. (1965). *Phys. Solid State* **7**, 2990–2994.

Manakov, N., and Rapoport, L. (1975). *Zh. Eksp. Teor. Fiz.* **69**, 842–852.

Presnyakov, L. (1970). *Phys. Rev. A* **2**, 1720–1725.

Rebane, T., and Sharibdjanov, R. (1975). *Teor. Eksp. Khim.* **11**, 291–299.

Schulz, G. (1973). *Rev. Mod. Phys.* **45**, 423.

Subramanjan, R. (1968). *Zh. Eksp. Teor. Fiz.* **55**, 363–366.

ADVANCES IN QUANTUM CHEMISTRY, VOLUME 11

Polarization Propagator Calculations

JENS ODDERSHEDE
Department of Chemistry
Odense University
Odense, Denmark

I. Introduction

Since the early days of quantum mechanics the wavefunction concept, i.e., the Schrödinger (1926) picture, has played a dominant role in the description of the electronic structure of matter. The equivalent operator or Heisenberg formulation has received less attention. It has received its name because of its similarity with original Heisenberg (1925) matrix formulation of quantum theory. The fundamental dynamical dynamical variables in this formulation are the field operators, $\psi(\mathbf{r}, t)$. They are many particle operators and are represented in terms of expansions

$$\psi(\mathbf{r}, t) = \sum_j u_j(\mathbf{r}) a_j(t)$$

$$\psi^+(\mathbf{r}, t) = \sum a_j^+(t) u_j^*(\mathbf{r}) \tag{1a}$$

ISBN 0-12-034811-X

where $\{u_j\}$ is a complete and orthonormal set of one-electron functions which depend on the space–spin coordinate, **r**. The expansion coefficient are time-dependent operators. The antisymmetry principle in the Schrödinger picture is replaced by the requirement that the time-dependent operators must satisfy the following anticommutation relations:

$$\begin{aligned}[a_i(t), a_j(t')]_+ &= [a_i^+(t), a_j^+(t')]_+ = 0,\\ [a_i^+(t), a_j(t)]_+ &= \delta_{ij}\delta(t-t').\end{aligned} \tag{1b}$$

This "second-quantization" formalism was introduced in the early days of quantum theory by Jordan and Klein (1927), Jordan and Wigner (1928), and Dirac (1927), but has not until rather recently been used much in practical application of quantum mechanics [for reviews, see the books by Judd (1963, 1967), Linderberg and Öhrn (1973), and Avery (1976)].

In second quantization, the Schrödinger equation is replaced by the Heisenberg equation of motion

$$i\frac{da_j}{dt} = [a_j, H] \qquad (\hbar = 1), \tag{2}$$

where H is the total Hamiltonian of the system. It is not necessary to study the time evolution of the *individual* creation (a_j^+) and annihilation (a_j) operators. Average values of the type $\langle A(t)B(t')C(t'')\cdots\rangle$, where A, B, C, etc., can be any combination of creation and annihilation operators, contain all physical information about the system. In the nonrelativistic limit, it is sufficient to consider double time-average values $\langle A(t)B(t')\rangle$. Combinations of these form *double-time Green's function* (Zubarev, 1960), and we can thus use these functions as the dynamic variables of the system, i.e., they replace the wavefunction in the Schrödinger formulation. The one-electron Green's function, often called the "electron propagator" (Linderberg and Öhrn, 1973), is a combination of elementary creation and annihilation operators. Several important physical phenomena, such as addition and removal of an electron from an interacting system, are most conveniently described by means of this propagator. Öhrn (1976) has given a comprehensive review of the present status of electron propagator calculations.

In this review, I will discuss the properties of the *polarization propagator*. This is the double-time Green's function that describes the propagation of a density disturbance through an interacting system and which is a combination of average values of the type $\langle a_i^+(t)a_j(t)a_k^+(t')a_l(t')\rangle$ (Linderberg and Öhrn, 1973). This two-particle Green's function is particularly useful for calculation of *excitation properties* of the system.

Most of the fundamental theory for the polarization propagator can be found in the book by Linderberg and Öhrn (1973) and in the review by Jørgensen (1975). Only the relations that are needed to discuss the latest theoretical developments of the polarization propagator method will be repeated here (Section II). The main purpose of the present review is, however, to show how the polarization propagator can be used advantageously in practical calculations of excitation properties of atomic, molecular, and metallic systems. The properties that will be discussed represent the author's personal choice and are not an exhaustive account of the potential of the polarization propagator method.

II. Polarization Propagator Method

A. Fundamental Relations

The propagation of a density disturbance through an interacting system is described by the density fluctuation (or correlation) function (Zubarev, 1960, 1974):

$$\chi(t, t') = \langle\langle[\rho(t) - \langle\rho(t)\rangle]; [\rho(t') - \langle\rho(t')\rangle]\rangle\rangle, \tag{3}$$

where $\rho(t)$ is the density operator

$$\rho(t) = \sum_{ij} \rho_{ij} a_i^+(t) a_j(t), \tag{4}$$

and the (unspecified) average values are taken with respect to the exact N-electron ground state $|0\rangle$. The fluctuation function is a causal two-electron Green's function and is defined as (Zubarev, 1960; Linderberg and Öhrn, 1973)

$$\begin{aligned}\chi(t, t') = &-i\theta(t - t')\langle[\rho(t) - \langle\rho(t)\rangle][\rho(t') - \langle\rho(t')\rangle]\rangle \\ &-i\theta(t' - t)\langle[\rho(t') - \langle\rho(t')\rangle][\rho(t) - \langle\rho(t)\rangle]\rangle,\end{aligned} \tag{5}$$

where $\theta(t)$ is the Heaviside step function

$$\theta(t) = \begin{cases} 1 & t \geq 0 \\ 0 & t < 0. \end{cases} \tag{6}$$

Alternatively, we may write

$$\begin{aligned}\chi(t, t') = &-i\theta(t - t')\{\langle\rho(t)\rho(t')\rangle - \langle\rho(t)\rangle\langle\rho(t')\rangle\} \\ &-i\theta(t' - t)\{\langle\rho(t')\rho(t)\rangle - \langle\rho(t')\rangle\langle\rho(t)\rangle\}.\end{aligned} \tag{7}$$

It is often advantageous to consider the energy or Lehman (1954) representation, $\chi(E)$, of the fluctuation function. Since $|0\rangle$ in the exact ground state $\chi(t, t')$ depends only on the difference $t - t'$ (Zubarev, 1960) and we can write its Fourier transform as

$$\chi(E) = \int_{-\infty}^{\infty} d(t - t')\chi(t - t')e^{iE(t-t')}, \tag{8}$$

and we find for a pure-state density operator (Linderberg and Öhrn, 1973),

$$\chi(E) \equiv \langle\langle \rho; \rho \rangle\rangle_E = \lim_{\eta \to 0} \sum_{M \neq 0} \left\{ \frac{\langle 0|\rho|M\rangle\langle M|\rho|0\rangle}{E - \omega_{0M} + i\eta} - \frac{\langle 0|\rho|M\rangle\langle M|\rho|0\rangle}{E + \omega_{0M} - i\eta} \right\} \tag{9}$$

or in component form,

$$\langle\langle a_i^+ a_j; a_k^+ a_l \rangle\rangle_E = \lim_{\eta \to 0} \sum_{M \neq 0} \left\{ \frac{\langle 0|a_i^+ a_j|M\rangle\langle M|a_k^+ a_l|0\rangle}{E - \omega_{0M} + i\eta} - \frac{\langle 0|a_k^+ a_l|M\rangle\langle M|a_i^+ a_j|0\rangle}{E + \omega_{0M} - i\eta} \right\}. \tag{10}$$

The summations in Eqs. (9) and (10) extend over all excited states, and

$$\omega_{0M} = E_M - E_0 \tag{11}$$

is the exact energy difference between the ground, $|0\rangle$, and excited state, $|M\rangle$. Equation (10) thus clearly exhibits the physical interpretation of spectral Green's function: *the poles are the excitation energies and the residues give the corresponding one-electron transition matrix elements.* The last part of the statement follows from the fact that any one-electron operator $\hat{O}$ in second quantization is expressable as

$$\hat{O} = \sum_{ij} O_{ij} a_i^+ a_j, \tag{12}$$

and matrix elements of $\hat{O}$ between the ground and excited states are thus combinations of $\langle 0|a_i^+ a_j|M\rangle$ which are the residues of the spectral fluctuation function. Specific examples will be discussed in Sections III and IV.

The equation of motion for the density fluctuation function can be derived by taking the time derivative of $\chi(t, t')$ and using the Heisenberg equation of motion [Eq. (2)]. In the energy representation we find that $\chi(E)$ satisfies the relation (Linderberg and Öhrn, 1973)

$$E\langle\langle a_i^+ a_j; a_k^+ a_l \rangle\rangle_E = \langle [a_i^+ a_j, a_k^+ a_l] \rangle + \langle\langle a_i^+ a_j; [H, a_k^+ a_l] \rangle\rangle_E, \tag{13}$$

where H is the nonrelativistic, electronic Hamiltonian for the system

$$H = \sum_{ij} h_{ij} a_i^+ a_j + \tfrac{1}{4} \sum_{\substack{ij\\kl}} (ij\|kl) a_i^+ a_k^+ a_l a_j. \tag{14}$$

We have used the Mulliken (1944) notation for the two-electron integrals and $(ij\|kl) = (ij|kl) - (il|kj)$. The original Green's function is thus given in terms of another Green's function, and if we use Eq. (13) again, we see that a Green's function can be expressed as a power series in $1/E$. In Sections II,B and C, we will discuss how this equation can be solved approximately.

Before doing so, it is useful to discuss a boundary condition for the

Green's function. If we take the (positive) zero-time limit of $\chi(t, t')$ in Eq. (7), we obtain

$$\lim_{t-t'\to+0} \chi(t,t') = \frac{1}{i}\{\langle\rho\rho\rangle - \langle\rho\rangle\langle\rho\rangle\}. \tag{15}$$

By using the inverse of the Fourier transformation in Eq. (8), we find that the components of $\chi(E)$ must fulfill the constraints

$$\langle a_i^+ a_j a_k^+ a_l\rangle = \frac{i}{2\pi}\lim_{t\to+0}\int_{-\infty}^{\infty} e^{-iEt}\langle\langle a_i^+ a_j; a_k^+ a_l\rangle\rangle_E \, dE + \langle a_i^+ a_j\rangle\langle a_k^+ a_l\rangle. \tag{16}$$

This relation between the two-electron density matrix and the fluctuation function is of fundamental importance, and will be used in Sections II.B and V.A.

So far we have not employed any special properties of the one-electron states. In the remainder of this chapter we will, however, assume that $\{u_i\}$ is the set of ground-state Hartree–Fock (HF) spin orbitals. We will adapt the convention that indices a, b, c, d, etc. (α, β, γ, δ, etc.) refer to spin orbitals that are unoccupied (occupied) in the HF ground state. Spin orbitals with unspecified occupation will be labelled by i, j, k, and l. We will also define the *particle-hole* creation

$$q_{a\alpha}^+ = a_a^+ a_\alpha$$

and annihilation operators

$$q_{a\alpha} = a_\alpha^+ a_a. \tag{17}$$

The *particle-hole propagator*,

$$\mathbf{P}_{\mathrm{PH}}(E) = \langle\langle \tilde{\mathbf{q}}; \mathbf{q}^+\rangle\rangle_E, \tag{18}$$

is a special density fluctuation function and both this propagator and the *polarization propagator*,

$$\mathbf{P}(E) = \begin{Bmatrix} \langle\langle \tilde{\mathbf{q}}; \mathbf{q}^+\rangle\rangle_E & \langle\langle \tilde{\mathbf{q}}; \mathbf{q}\rangle\rangle_E \\ \langle\langle \tilde{\mathbf{q}}^+; \mathbf{q}^+\rangle\rangle_E & \langle\langle \tilde{\mathbf{q}}^+; \mathbf{q}\rangle\rangle_E \end{Bmatrix}, \tag{19}$$

satisfy the relations derived for the more general fluctuation function. In Eqs. (18) and (19), $\mathbf{q}$ and $\mathbf{q}^+$ are row vectors with elements $q_{a\alpha}$ and $q_{a\alpha}^+$, respectively. $\tilde{\mathbf{q}}$ is the transpose of $\mathbf{q}$. If we introduce in Eqs. (18) and (19), the singlet,

$${}^1Q_{a\alpha} = \frac{1}{\sqrt{2}}\{q_{a+\alpha+} + q_{a-\alpha-}\},$$

and triplet ($M_S = 0$)

$${}^3Q_{a\alpha}^0 = \frac{1}{\sqrt{2}}\{q_{a+\alpha+} - q_{a-\alpha-}\}, \tag{20}$$

spin components of the particle-hole operators, we obtain the so-called *singlet* and *triplet* propagators. For a singlet ground state these two spin components of the propagator determine the singlet and triplet excitation properties, respectively, and they can be evaluated independently of each other (see Section II.C).

B. Decoupling Schemes

Historically, the first approximate solutions to the equation of motion were obtained by means of decoupling schemes. The molecular applications of this approach were pioneered by Linderberg and Öhrn (1965, 1967) who calculated the total energy of the linear chain (Linderberg and Öhrn, 1968) and the π-spectrum of benzene (Linderberg and Thulstrup, 1968) using the electron propagator.

A similar decoupling approach was applied to the two-electron propagator by Linderberg and Ratner (1970), Jørgensen and Linderberg (1970), Linderberg *et al.* (1972), and Jørgensen and Oddershede (1972). The chain of equations resulting from iteration on expression (13) is decoupled by assuming

$$[H, a_k^+ a_l]|0\rangle = \sum_{k'l'} V_{kl,k'l'}\, a_{k'}^+ a_{l'}|0\rangle, \tag{21}$$

and the equivalent adjoint relations. The equation of motion takes the form

$$E\langle\langle a_i^+ a_j; a_k^+ a_l\rangle\rangle_E = \langle[a_i^+ a_j, a_k^+ a_l]\rangle + \sum_{k'l'} V_{kl,k'l'}\langle\langle a_i^+ a_j; a_{k'}^+ a_{l'}\rangle\rangle_E. \tag{22}$$

The formal solution of Eq. (22) is most conveniently expressed using the superoperator formalism. Following Goscinski and Lukman (1970) the superoperator Hamiltonian, $\hat{H}$, and identity operator, $\hat{I}$, are defined as

$$\hat{H}X_i = [H, X_i] \qquad \hat{I}X_i = X_i, \tag{23}$$

where $\{X_i\}$ is an operator space in which the binary product is given as

$$(X_i|X_j) = \langle[X_i^+, X_j]\rangle = \mathrm{Tr}[X_i^+, X_j]\rho. \tag{24}$$

The choice of density operator, ρ, specifies the nature of the average value to be used. Defining matrices **A**, **B**, and $\boldsymbol{\lambda}$ as

$$\begin{aligned} \mathbf{A} &= (\mathbf{q}^+|\hat{H}|\mathbf{q}^+), \\ \mathbf{B} &= (\mathbf{q}^+|\hat{H}|\mathbf{q}), \\ \boldsymbol{\lambda} &= (\mathbf{q}^+|\mathbf{q}^+) = -(\mathbf{q}|\mathbf{q})^*, \end{aligned} \tag{25}$$

implies that the V matrix in Eq. (21) is

$$\mathbf{V} = \left\{\begin{matrix} \mathbf{A} & \mathbf{B} \\ \mathbf{B}^* & \mathbf{A}^* \end{matrix}\right\}\left\{\begin{matrix} \boldsymbol{\lambda}^{-1} & \mathbf{0} \\ \mathbf{0} & -[\boldsymbol{\lambda}^*]^{-1} \end{matrix}\right\}, \tag{26}$$

where **V** is written in the same block form as the polarization propagator in Eq. (19). By using Eq. (22), we find the following expression for the polarization propagator:

$$\mathbf{P}(E) = \begin{pmatrix} \boldsymbol{\lambda} & \mathbf{0} \\ \mathbf{0} & -\boldsymbol{\lambda}^* \end{pmatrix} \begin{pmatrix} E\boldsymbol{\lambda} - \mathbf{A} & -\mathbf{B} \\ -\mathbf{B}^* & -E\boldsymbol{\lambda}^* - \mathbf{A}^* \end{pmatrix}^{-1} \begin{pmatrix} \boldsymbol{\lambda} & \mathbf{0} \\ \mathbf{0} & -\boldsymbol{\lambda}^* \end{pmatrix} \tag{27}$$

where according to Eq. (10) the positive and negative poles are placed below and above the real axis, respectively. It should be mentioned that the same approximate form for the polarization propagator can be obtained if we assume that the moment expansion of the particle-hole propagator forms a geometric series (Linderberg and Ratner, 1970; Linderberg *et al.*, 1972).

For a given reference state, $|0\rangle$, the matrix elements in Eq. (25) can be evaluated and excitation energies and response properties determined from a diagonalization of $\mathbf{P}^{-1}(E)$. This is a non-Hermitian eigenvalue problem which, however, for real matrices can be transformed into two Hermitian eigenvalue problems for $\mathbf{A} \pm \mathbf{B}$ (Jørgensen and Linderberg, 1970). For complex matrices, it is also possible to find the eigenvalues from two Hermitian eigenvalue problems of half the size (Linderberg and Öhrn, 1977). Through a series of transformations we can express $\mathbf{P}(E)$ in a spectral form

$$\mathbf{P}(E) = \begin{pmatrix} \mathbf{Z} & \mathbf{Y}^* \\ \mathbf{Y} & \mathbf{Z}^* \end{pmatrix} \begin{pmatrix} (E\mathbf{1} - \boldsymbol{\omega})^{-1} & \mathbf{0} \\ \mathbf{0} & -(E\mathbf{1} + \boldsymbol{\omega})^{-1} \end{pmatrix} \begin{pmatrix} \mathbf{Z}^+ & \mathbf{Y}^+ \\ \tilde{\mathbf{Y}} & \tilde{\mathbf{Z}} \end{pmatrix} \tag{28}$$

where the eigenvectors fulfill the normalization condition

$$\begin{pmatrix} \mathbf{Z} & -\mathbf{Y}^* \\ -\mathbf{Y} & \mathbf{Z}^* \end{pmatrix} \begin{pmatrix} \mathbf{Z}^+ & \mathbf{Y}^+ \\ \tilde{\mathbf{Y}} & \tilde{\mathbf{Z}} \end{pmatrix} = \begin{pmatrix} \boldsymbol{\lambda} & \mathbf{0} \\ \mathbf{0} & -\boldsymbol{\lambda}^* \end{pmatrix}. \tag{29}$$

The relations among the eigenvectors **Z**, **Y**, the eigenvalues $\boldsymbol{\omega}$, and the matrices **A** and **B** can for real matrices be found in Linderberg and Jørgensen (1970) and for complex matrices the relations are given by Linderberg and Öhrn (1977). By using Eqs. (10), (19), and (28), we can identify the residues of the polarization propagator as

$$Z_{a\alpha,\,M} = \langle 0 | a_\alpha^+ a_a | M \rangle$$

and

$$Y_{a\alpha,\,M} = \langle 0 | a_a^+ a_\alpha | M \rangle \tag{30}$$

where $|M\rangle \neq |0\rangle$. The terms for which $|M\rangle = |0\rangle$ are undetermined since the propagator in Eq. (10) is only defined for $|\mathrm{M}\rangle \neq |0\rangle$. Recalling the discussion following Eq. (12), it is thus possible to compute one-electron transition matrix elements from the eigenvectors of the polarization propagator.

In the time-dependent Hartree–Fock (TDHF) or random-phase approximation (RPA), average values are taken with respect to the Hartree–Fock ground state (Thouless, 1961; Dunning and McKoy, 1967, 1968; Rowe, 1968; Ball and McLachlan, 1964; McLachlan and Ball, 1964; Jørgensen and Linderberg, 1970). For a closed-shell ground state this means that $\lambda = 1$ and Eq. (27) reduces to

$$\mathbf{P}_{\text{TDHF}}(E) = \begin{Bmatrix} E\mathbf{1} - \mathbf{A} & \mathbf{B} \\ \mathbf{B}^* & -E\mathbf{1} - \mathbf{A}^* \end{Bmatrix}^{-1}. \tag{31}$$

This definition of RPA is identical to the diagrammatic (Gell-Mann and Brueckner, 1957) and dielectric (Lindhard, 1954) formulations. Jørgensen (1975) has recently reviewed the application of TDHF to atomic and molecular systems, and here we will repeat only a few fundamental properties of TDHF, which we shall make use of later.

The Hartree–Fock ground state is used to evaluate the **A** and **B** matrices in TDHF, but $|\text{HF}\rangle$ is not the ground state for the TDHF excitation operators (Rowe, 1968; Linderberg and Öhrn, 1977; Öhrn and Linderberg, 1978)

$$O_M^+ = \sum_{a\alpha} \{q_{a\alpha}^+ Z_{a\alpha,M} - q_{a\alpha} Y_{a\alpha,M}\}. \tag{32}$$

The *true* TDHF ground state, $|\text{TDHF}\rangle$, must fulfill the "killer condition" (Rowe, 1968),

$$O_M |\text{TDHF}\rangle = 0, \tag{33}$$

which is obviously not the case for $|\text{HF}\rangle$. This observation has led to consideration of higher RPA schemes (Rowe, 1968) in which $|\text{TDHF}\rangle$ is given as a sum of the HF ground state and doubly excited states (Shibuya and McKoy, 1970),

$$|\text{TDHF}\rangle = \left\{1 + \sum_{\substack{ab \\ \alpha\beta}} \kappa_{\alpha\beta}^{ab} q_{a\alpha}^+ q_{b\beta}^+ \right\} |\text{HF}\rangle, \tag{34}$$

and the correlation coefficients κ are determined such that Eq. (33) is fulfilled to a given order.

The inconsistency of the TDHF method can also be observed in the change in the two-electron density matrix. In TDHF, the **A** and **B** matrices are constructed from the HF two-electron density matrix, but the two-matrix calculated from the TDHF propagator using Eq. (16) is very different from the HF two matrix. This is illustrated in Table I. The

TABLE I

TYPICAL INDIVIDUAL ELEMENTS OF THE SINGLET AND TRIPLET TWO-ELECTRON DENSITY MATRIX, ⟨qq⟩, IN THE HARTREE-FOCK (HF), TIME-DEPENDENT HF (TDHF), THE SELF-CONSISTENT TDHF (SPPA), AND THE SECOND-ORDER POLARIZATION PROPAGATOR APPROXIMATION (SOPPA)

System	Symmetry[a]	HF (a.u.)	TDHF (a.u.)	SPPA (a.u.)	SOPPA[b] (a.u.)
Ethylene (PPP)[c]	Sing	0.0	−0.093	−0.107	−0.114
	Trip	0.0	0.150	0.112	0.114
	Sing + trip[d]	0.0	0.057	0.005	0.0
trans-Butadiene (PPP)[c]	Sing	0.0	−0.113	−0.149	−0.153
	Trip	0.0	0.391	0.164	0.153
	Sing + trip[d]	0.0	0.278	0.015	0.0
Hydrogen fluoride[e] (20 STO's)	Sing	0.0	−0.0514	−0.0463	−0.0487
	Trip	0.0	0.0563	0.0461	0.0487
	Sing + trip[d]	0.0	0.0049	0.0002	0.0
Helium[e] (48 STO's)	Sing	0.0	−0.0173	−0.0177	−0.0176
	Trip	0.0	0.0234	0.0177	0.0176
	Sing + trip[d]	0.0	0.0062	0.0000	0.0

[a] Sing—singlet; trip—triplet.

[b] The two-matrix elements are calculated from the Rayleigh-Schrödinger correlation coefficients (see Section II,C).

[c] Semiempirical calculations using the Pariser-Parr-Popple (PPP) model.

[d] This sum should be zero for a consistent solution (see Jørgensen *et al.*, 1974).

[e] *Ab initio* calculations using Slater-type orbital (STO) basis sets of the indicated size.

triplet two-matrix changes drastically from HF to TDHF, and it is well known that triplet properties generally are poorly described in the TDHF approximation (Dunning and McKoy, 1967, 1968; Jørgensen and Linderberg, 1970; Oddershede *et al.*, 1975). This problem is a consequence of the fact that the Hartree-Fock ground state often is triplet unstable (Čižek and Paldus, 1967), i.e., there exists another HF solution (which is not necessarily a pure spin state) with lower energy. If triplet instabilities occur, the normal TDHF procedure will give imaginary excitation frequencies (Jørgensen and Linderberg, 1970; Paldus and Čižek, 1970). The HF ground state for *trans*-butadiene in the Pariser-Parr-Pople (PPP) model (Parr, 1964) is nearly triplet instable (Jørgensen *et al.*, 1974) resulting in a substantial change between the TDHF and the self-consistent, triplet, two-electron, density matrix element (see Table I). For the other atoms and molecules in Table I, we are far from triplet (and singlet) instabilities and only moderate changes are found in the two matrix.

In an improved RPA method the large difference between the "input" and "output" two-matrix must be eliminated. In the self-consistent polarization propagator approximation (SPPA) we iterate on the two-matrix until a self-consistent solution is obtained (Linderberg and Ratner, 1970; Linderberg *et al.*, 1972; Jϕrgensen and Oddershede, 1972; Jϕrgensen *et al.*, 1974). The iterative scheme is based on the relation Eq. (16). By using Eq. (28), we find the following expression for the two-matrix:

$$\begin{Bmatrix} \langle \tilde{\mathbf{q}}\mathbf{q}^{+} \rangle & \langle \tilde{\mathbf{q}}\mathbf{q} \rangle \\ \langle \tilde{\mathbf{q}}^{+}\mathbf{q}^{+} \rangle & \langle \tilde{\mathbf{q}}^{+}\mathbf{q} \rangle \end{Bmatrix} = \begin{Bmatrix} \mathbf{ZZ}^{+} & \mathbf{ZY}^{+} \\ \mathbf{YZ}^{+} & \mathbf{YY}^{+} \end{Bmatrix}. \tag{35}$$

The zero-energy pole contributions, like, e.g., $\langle q \rangle \langle q^{+} \rangle$, cannot be determined from this equation; see the remarks following Eq. (30). They can, however, be calculated from other known two-matrix elements using certain sum rules (Jϕrgensen and Oddershede, 1972). If we perform the commutators in Eq. (25), the A and **B** matrices can be expressed as linear combination of two-electron integrals and two-matrix elements. The explicit formulas are given by Oddershede *et al.* (1975). From the TDHF two-matrix, new values for **A** and **B** can be calculated, giving new eigenvectors **Z** and **Y**, and an iterative procedure is thus established. The eigenvalue problem in SPPA is identical to the TDHF problem in Eq. (31). Only the actual expressions for the A and **B** matrix elements are different.

Examples of two-electron density matrix elements in SPPA are given in Table I. In the singlet case, only minor differences are found between the TDHF and the self-consistent two-matrix, whereas the changes in the triplet elements are more pronounced. The same effect is found for other properties calculated within the two approximations (see Sections III and IV). The two-matrix elements must in a consistent theory fulfill certain sum rules and internal constraints (Jørgensen and Oddershede, 1972; Jørgensen *et al.*, 1974), one of which is examined in Table I. Because the SPPA two-matrix is only approximately N-representable (Coleman, 1963), not even this approximation gives an exact fulfillment of the quoted sum rule.

The SPPA method is similar to the higher RPA(HRPA) method of Shibuya and McKoy (1970). Whereas Shibuya and McKoy (1970) iterate on the correlation coefficients $\boldsymbol{\kappa} = \mathbf{YZ}^{-1}$, we iterate on $\mathbf{YZ}^{+}$ (the rest of the two-matrix can be calculated from this block if we disregard the "small" $\mathbf{YY}^{+}$ block in the two-matrix; see, e.g., Oddershede *et al.*, 1975) and the difference between $\mathbf{YZ}^{-1}$ and $\mathbf{YZ}^{+}$ is of third order in **Y** (Jørgensen, 1975). This means that for all practical purposes the two methods are identical.

Experience shows that calculated excitation energies (especially the singlet excitation energies) are too high in the HRPA (Rose *et al.*, 1973; Rescigno *et al.*, 1977) and in the SPPA method (Oddershede *et al.*, 1975).

It is necessary to include the effect of two-particle, two-hole (2p-2h) excitations, $\mathbf{q}^+\mathbf{q}^+$, and de-excitations, $\mathbf{qq}$ (da Providencia, 1965, 1966, 1968; Shibuya *et al.*, 1973; Jørgensen *et al.*, 1975; Jordan, 1975) to obtain satisfactory agreement with experiment. The theoretical reason for the importance of the 2p − 2h terms will become more apparent later (Section II,D), but we will discuss here the derivation of the equation of motion with 2p − 2h corrections included, since these corrections were initially introduced in the decoupling procedure. The decoupling assumption in Eq. (21) is now replaced by

$$[H, a_k^+ a_l]|0\rangle = \sum_{k'l'} V_{kl,k'l'} a_{k'}^+ a_{l'}|0\rangle + \sum_{\substack{k'l'\\k''l''}} W_{kl,k'l'k''l''} a_{k'}^+ a_{l'} a_{k''}^+ a_{l''}|0\rangle \tag{36}$$

and a similar relation for $[H, a_k^+ a_l a_i^+ a_j]$. The equation of motion, Eq. (13), couples propagators of the particle-hole $\langle\langle q_{ij}; q_{kl}\rangle\rangle_E$, two-particle, two-hole $\langle\langle q_{ij} q_{i'j'}; q_{kl} q_{k'l'}\rangle\rangle_E$, and mixed-type $\langle\langle q_{ij}; q_{kl} q_{k'l'}\rangle\rangle_E$. The actual expression for the complete propagator is given by Jørgensen *et al.* (1975). If we partition (Löwdin, 1963, 1968) the effect of 2p − 2h excitations into the particle-hole space, we find the following expression for the polarization propagator (Jørgensen *et al.*, 1975):

$$\mathbf{P}^{-1}(E) = \mathbf{P}_{\mathrm{TDHF}}^{-1}(E) - \left\{\begin{matrix} \tilde{\mathbf{C}}(E\mathbf{1} - \mathbf{D})^{-1}\mathbf{C} & \mathbf{0} \\ \mathbf{0} & \mathbf{C}^+(-E\mathbf{1} - \mathbf{D}^*)^{-1}\mathbf{C}^* \end{matrix}\right\}, \tag{37}$$

where $\mathbf{P}_{\mathrm{TDHF}}(E)$ is defined in Eq. (31) and can be either the TDHF or the SPPA propagator. The last term in Eq. (37) is the 2p − 2h correction term, and matrices $\mathbf{C}$ and $\mathbf{D}$ are defined as

$$\mathbf{C} = (\mathbf{q}^+\mathbf{q}^+ | E\hat{I} - \hat{H} | \mathbf{q}^+), \tag{38}$$

$$\mathbf{D} = (\mathbf{q}^+\mathbf{q}^+ | \hat{H} | \mathbf{q}^+\mathbf{q}^+). \tag{39}$$

The Hartree–Fock ground state is used in Eqs. (38) and (39), and only the orbital energy difference is retained in the expression for $\mathbf{D}$ (Jørgensen *et al.*, 1975). This may seem inconsistent with the use of a correlated reference state for evaluating $\mathbf{A}$ and $\mathbf{B}$ matrices in SPPA, but we will show in Section II,D that this is actually the consistent approximation from the point of view of perturbation theory. We also defer the discussion of solution of the eigenvalue problem in Eq. (37) to Section III,A.

C. Perturbation Schemes

Using the operator relation

$$(E\hat{I} - \hat{H})^{-1} = E^{-1}\hat{I} + E^{-2}\hat{H} + E^{-3}\hat{H}\hat{H} + \cdots, \tag{40}$$

the equation of motion (13) can be written as (Pickup and Goscinski, 1973; Oddershede and Jørgensen, 1977a)

$$\langle\langle \mathbf{b}; \mathbf{b}^+ \rangle\rangle_E = (\mathbf{b}^+ |(E\hat{I} - \hat{H})^{-1}|\mathbf{b}^+), \tag{41}$$

where $\mathbf{b}^+(\mathbf{b})$ is a super-row (column) vector defined as

$$\mathbf{b}^+ = \{\mathbf{q}, \mathbf{q}^+\}. \tag{42}$$

The inner projection (Löwdin, 1965) technique allows us to replace the inverse of an operator with the inverse of a matrix, resulting in a very useful reformulation of Eq. (41),

$$\langle\langle \mathbf{b}; \mathbf{b}^+ \rangle\rangle_E = (\mathbf{b}^+ |\mathbf{h})(\mathbf{h}|E\hat{I} - \hat{H}|\mathbf{h})^{-1}(\mathbf{h}|\mathbf{b}^+). \tag{43}$$

The vector space $\mathbf{h}$ is a complete projection manifold. Approximate expressions for the propagator can now be obtained through truncating the projection manifold and approximating the reference state [i.e., the density operator ρ in Eq. (24)]. This approach has been used extensively for the electron propagator (Pickup and Goscinski, 1973; Simons and Smith, 1973; Purvis and Öhrn, 1974; Jørgensen and Simons, 1975). Appropriate choices of $\mathbf{h}$ and ρ lead to an electron propagator that is consistent through first, second, or third order in the electron repulsion (see, e.g., Öhrn, 1976, for a recent review).

In analogy with the treatment of the electron propagator, we choose for the projection manifold, $\mathbf{h}$, the set consisting of particle-hole, two-particle two-hole, etc., excitation operators, i.e.,

$$\mathbf{h} = \{\mathbf{h}_2, \mathbf{h}_4, \ldots\}, \tag{44}$$

where

$$\mathbf{h}_2 = \{\mathbf{q}, \mathbf{q}^+\}, \qquad \mathbf{h}_4 = \{\mathbf{q}\mathbf{q}, \mathbf{q}^+\mathbf{q}^+\}, \qquad \text{etc.} \tag{45}$$

This set forms a complete projection manifold (Dalgaard, 1978). To obtain a propagator consistent through *third* order in the electronic repulsion, it is only necessary to keep $\mathbf{h}_2$ and $\mathbf{h}_4$ (Oddershede and Jørgensen, 1977a) in which case the polarization propagator, Eq. (43), is

$$\begin{aligned}\langle\langle \mathbf{b}; \mathbf{b}^+ \rangle\rangle_E = (\mathbf{b}^+ |\mathbf{h}_2)\{&(\mathbf{h}_2|E\hat{I} - \hat{H}|\mathbf{h}_2) \\ &- (\mathbf{h}_2|\hat{H}|\mathbf{h}_4)(\mathbf{h}_4|E\hat{I} - \hat{H}|\mathbf{h}_4)^{-1}(\mathbf{h}_4|\hat{H}|\mathbf{h}_2)\}^{-1}(\mathbf{h}_2|\mathbf{b}^+),\end{aligned} \tag{46}$$

provided $\mathbf{h}_2$ is orthogonalized against $\mathbf{h}_4$. The inverse matrix in Eq. (43) is decomposed by means of the partitioning technique (Löwdin, 1963, 1968). It is possible to find renormalized expressions for $\mathbf{q}$ and $\mathbf{q}^+$ such that $\mathbf{b}$ and $\mathbf{h}_2$ fulfill (Oddershede and Jørgensen, 1977a)

$$(\mathbf{h}_2|\mathbf{h}_2) = (\mathbf{b}^+|\mathbf{h}_2) = \begin{Bmatrix} \mathbf{1} & \mathbf{0} \\ \mathbf{0} & -\mathbf{1} \end{Bmatrix}, \tag{47}$$

where the matrices are written in the same component form as the polarization propagator in Eq. (19). Defining

$$\hat{R} = \hat{H} + \hat{H}|\mathbf{h}_4)(\mathbf{h}_4|E\hat{I} - \hat{H}|\mathbf{h}_4)^{-1}(\mathbf{h}_4|\hat{H}, \tag{48}$$

the polarization propagator, Eq. (46), becomes

$$\mathbf{P}(E) = \begin{Bmatrix} E\mathbf{1} - (\mathbf{q}^+|\hat{R}|\mathbf{q}^+) & (\mathbf{q}^+|\hat{R}|\mathbf{q}) \\ (\mathbf{q}|\hat{R}|\mathbf{q}^+) & -E\mathbf{1} - (\mathbf{q}|\hat{R}|\mathbf{q}) \end{Bmatrix}^{-1}. \tag{49}$$

To proceed, it is necessary to define the *order concept* normally used in propagator calculations. The Hamiltonian, Eq. (14), is divided into a zeroth-order part, the Fock operator F, and a first-order part V, such that

$$H = F + V, \tag{50}$$

where for a closed-shell ground state

$$F = \sum_i \varepsilon_i a_i^+ a_i, \tag{51}$$

$$V = \tfrac{1}{4} \sum_{\substack{ij\\kl}} (ij\|kl) a_i^+ a_k^+ a_l a_j - \sum_{\alpha ij} (\alpha\alpha\| ij) a_i^+ s_j. \tag{52}$$

In the following we will talk about orders in the electronic repulsion, even though strictly speaking it should be referred to as orders in the fluctuation potential (Berry, 1966). The density operator is expanded using the Rayleigh–Schrödinger perturbation theory

$$\rho = \rho_0 + \rho_1 + \rho_2 + \cdots, \tag{53}$$

where ρ_0 is the Hartree–Fock density operator,

$$\rho_0 = |\mathrm{HF}\rangle\langle\mathrm{HF}|, \tag{54}$$

and ρ_1, ρ_2 are the first- and second-order Rayleigh–Schrödinger density operators,

$$\rho_1 = |\mathrm{HF}\rangle\langle 1| + |1\rangle\langle\mathrm{HF}\rangle, \tag{55}$$

$$\rho_2 = |\mathrm{HF}\rangle\langle 2| + |1\rangle\langle 1| + |2\rangle\langle\mathrm{HF}|. \tag{56}$$

The state $|1\rangle$ is expanded in doubly excited (HF$-$) configurations as indicated in Eq. (34), and $|2\rangle$ is in principle a combination of singly, doubly, triply, and quadruply excited configurations. To obtain the polarization propagator consistent through third order in the electronic repulsion, it is, however, not necessary to know $|2\rangle$ completely: only terms corresponding to singly and doubly excited configurations enter in the analysis (Oddershede and Jørgensen, 1977a).

Let us now return to the propagator in Eq. (49) and let us as an example determine the third-order expression for the $(\mathbf{q}^+|\hat{R}|\mathbf{q}^+)$ component of the polarization propagator. By using Eqs. (45), (48), and (50), we find that

$$(\mathbf{q}^+|\hat{R}|\mathbf{q}^+) = \mathbf{A} + \tilde{\mathbf{C}}(E\mathbf{1} - \mathbf{D})^{-1}\mathbf{C} + \tilde{\mathbf{G}}(-E\mathbf{1} - \mathbf{D}^*)^{-1}\mathbf{G}, \tag{57}$$

where the matrices **A**, **C**, and **D** are defined in Eqs. (25), (38), and (39), respectively, and

$$\mathbf{G} = (\mathbf{qq}|E\hat{I} - \hat{H}|\mathbf{q}^+). \tag{58}$$

If we use ρ_0, i.e., take Hartree–Fock average values, the matrices **A**, **C**, and **D** are nonvanishing, whereas ρ_1 is needed for **G**. Since $(\mathbf{qq}|\mathbf{q}^+) = \mathbf{0}$, matrix **G** is of at least second order in the electronic repulsion. Expanding the inverse matrix as

$$(-E\mathbf{1} - \mathbf{D}^*)^{-1} = -E^{-1}\mathbf{1} + E^{-2}\mathbf{D} - \cdots \tag{59}$$

shows that the leading term in $(-E\mathbf{1} - \mathbf{D}^*)^{-1}$ is of zeroth order, making the last term in Eq. (57) of at least fourth order. The first nonvanishing term in **C** is of first order and $(E\mathbf{1} - \mathbf{D})^{-1}$ is thus needed through first order to obtain the third-order expression for $(\mathbf{q}^+|\hat{R}|\mathbf{q}^+)$:

$$(\mathbf{q}^+|\hat{R}|\mathbf{q}^+) = \mathbf{A}(0, 1, 2, 3) + \tilde{\mathbf{C}}(1, 2)[E\mathbf{1} - \mathbf{D}(0, 1)]^{-1}\mathbf{C}(1, 2). \tag{60}$$

The numbers in the parentheses indicate the order of the matrices, e.g., **A** is needed in zeroth, first, second, and third order. In all expressions for the **A**, **B**, etc. matrices, we have kept both $\hat{F}$ and $\hat{V}$. This is necessary to ensure the proper hermiticity of the superoperator Hamiltonian (J. Linderberg, private communication, 1976; Nehrkorn *et al.*, 1976).[1]

A similar analysis can be carried out for the other components of the polarization propagator. If we require all blocks in Eq. (49) to be consistent through *third order* in the electronic repulsion, we find that $\mathbf{P}(E)$ can be expressed in the form (Oddershede and Jørgensen, 1977a)

$$\mathbf{P}^{(3)}(E) = \begin{Bmatrix} E\mathbf{1} - \mathbf{A} - \tilde{\mathbf{C}}(E\mathbf{1} - \mathbf{D})^{-1}\mathbf{C} & \mathbf{B} + \tilde{\mathbf{C}}(E\mathbf{1} - \mathbf{D})^{-1}\mathbf{G}^* + \tilde{\mathbf{G}}(-E\mathbf{1} - \mathbf{D}^*)^{-1}\mathbf{C}^* \\ \mathbf{B}^* + \mathbf{C}^*(-E\mathbf{1} - \mathbf{D}^*)^{-1}\mathbf{G} + \mathbf{G}^+(E\mathbf{1} - \mathbf{D})^{-1}\mathbf{C} & -E\mathbf{1} - \mathbf{A}^* - \mathbf{C}^+(-E\mathbf{1} - \mathbf{D}^*)^{-1}\mathbf{C}^* \end{Bmatrix}^{-1}. \tag{61}$$

---

[1] The proof for the hermiticity of $\hat{H}$ is repeated in the paper by Oddershede and Jørgensen (1977a).

In *second order* it reduces to

$$\mathbf{P}^{(2)}(E) = \begin{Bmatrix} E\mathbf{1} - \mathbf{A} - \tilde{\mathbf{C}}(E\mathbf{1} - \mathbf{D})^{-1}\mathbf{C} & \mathbf{B} \\ \mathbf{B}^* & -E\mathbf{1} - \mathbf{A}^* - \mathbf{C}^+(-E\mathbf{1} - \mathbf{D}^*)^{-1}\mathbf{C}^* \end{Bmatrix}^{-1}, \quad (62)$$

and in first order the 2p-2h terms are absent and we are left with the TDHF propagator in Eq. (31). The orders of the matrices in Eqs. (61) and (62) are given in Table II and the explicit expressions in the spin-orbital basis are given by Oddershede and Jørgensen (1977a).

TABLE II

MATRICES NEEDED TO OBTAIN THE POLARIZATION PROPAGATOR CONSISTENT THROUGH ZEROTH, FIRST, SECOND, AND THIRD ORDER IN THE ELECTRONIC REPULSION

Order of the polarization propagator	Matrices needed[a]	Order of the matrices
0	**A**	0
1	**A**	0–1
	B	1
2	**A**	0–2
	B	1–2
	C	1
	D	0
3	**A**	0–3
	B	1–3
	C	1–2
	D	0–1
	G	2

[a] Matrices **A**, **B**, **C**, **D**, and **G** are defined in Eqs. (25), (38), (39), and (58).

For a closed-shell ground state, singlet and triplet components of the **A**, **B**, etc. matrices are obtained by using the singlet and triplet components of the particle-hole [Eq. (20)] and 2p – 2h excitation operators. These combinations of the excitation operators and the corresponding matrix elements are given by Oddershede *et al.* (1978a) through second order and by Oddershede and Jørgensen (1976) for all elements needed through third order. It is thus possible to solve the singlet and triplet problem separately. A further reduction in the size of the matrix problem is obtained if (space-) symmetry-adapted excitation operators are used.

Extension of RPA and higher RPA methods to systems with open shell ground states is not a simple matter. It is rather straightforward to compute excitation energies corresponding to dipole-allowed transitions between spatially nondegenerate states with the same spin and space symmetry as the ground state (e.g., ${}^3\sum_g^-$ to ${}^3\sum_g^-$) transitions when the ground state has ${}^3\sum_g^-$ symmetry. These excitation energies can be obtained from the singlet polarization propagator where only totally symmetric singlet excitation operators, ${}^1Q_{a\pi}$, are used (see end of Section II,A). However, due to the symmetry coupling between the ground state and nontotally symmetric excitation operators, the poles of the propagator cannot, in general, be assigned unambiguously to excitations of a definite symmetry (Dalgaard, 1975). The triplet propagator will e.g. for a system with a doublet ground state have poles which are a mixture of excitations with doublet and quarter spin symmetry. This problem may be eliminated by proper use of projection operators. However, this has the effect of making the expressions for the **A**, **B**, etc. matrices quite complicated.

The RPA matrices for systems with open-shell ground states have been given by Jørgensen (1972), Dalgaard (1975), and Yeager and McKoy (1975). Recently, Swanstrøm and Jørgensen (1978) have shown how the RPA method can be extended through second order in the electronic repulsion in the open-shell case, provided the ground state has ${}^2\sum$ or ${}^2\prod$ symmetry.

D. Order Analysis

All four blocks of the polarization propagator, Eq. (19), contain the same information about excitation energies and one-electron transition matrix elements as can be seen from the spectral representation in Eq. (10). It is therefore often sufficient to know, e.g., the particle-hole propagator, Eq. (18). The particle-hole propagator, $\langle\langle \tilde{\mathbf{q}}; \mathbf{q}^+ \rangle\rangle_E$, can be found from $\mathbf{P}(E)$ in Eq. (49) using the partitioning technique,

$$\begin{aligned}\langle\langle \tilde{\mathbf{q}}; \mathbf{q}^+ \rangle\rangle_E^{-1} &= E\mathbf{1} - (\mathbf{q}^+|\hat{R}|\mathbf{q}^+) - (\mathbf{q}^+|\hat{R}|\mathbf{q})[-E\mathbf{1} - (\mathbf{q}|\hat{R}|\mathbf{q})]^{-1}(\mathbf{q}|\hat{R}|\mathbf{q}^+)\\ &= E\mathbf{1} - \mathbf{M}(E), \qquad (63)\end{aligned}$$

where $\mathbf{M}(E)$ is the proper particle-hole self-energy [also denoted the Bethe–Salpeter kernel (Ziman, 1969) or irreducible vertex part (Hedin and Lundqvist, 1969)]. To obtain $\mathbf{M}(E)$ consistent through third order, $(\mathbf{q}^+|\hat{R}|\mathbf{q}^+)$ must be consistent through the same order, whereas $(\mathbf{q}^+|\hat{R}|\mathbf{q})$ is needed through second order, and $(\mathbf{q}|\hat{R}|\mathbf{q})$ through first order only. Compared with the perturbation treatment of the polarization propagator this means that the latter two matrices can be calculated at a lower level of accuracy. Thus

$$\begin{aligned}\mathbf{M}^{(3)}(E) = \mathbf{A}(0, 1, 2, 3) &+ \tilde{\mathbf{C}}(1, 2)[E\mathbf{1} - \mathbf{D}(0, 1)]^{-1}\mathbf{C}(1, 2)\\ &- \mathbf{B}(1, 2)[-E\mathbf{1} - \mathbf{A}^*(0, 1)]^{-1}\mathbf{B}^*(1, 2), \qquad (64)\end{aligned}$$

TABLE III

MATRICES NEEDED TO OBTAIN THE PARTICLE-HOLE PROPAGATOR CONSISTENT THROUGH ZEROTH, FIRST, SECOND, AND THIRD ORDER IN THE ELECTRONIC REPULSION

Order of the particle-hole propagator	Matrices needed	Order of the matrices
0	**A**	0
1	**A**	0–1
2	**A**	0–2
	B	1
	C	1
	D	0
3	**A**	0–3
	B	1–2
	C	1–2
	D	0–1

where we have used the same notation as in Eq. (60). The order analysis of the particle-hole propagator is summarized in Table III.

The approximate polarization propagator through any order in electronic repulsion is symmetric under a transformation $E \rightarrow -E$, i.e., it can be represented in a spectral form. This is not the case for the corresponding particle-hole propagator [see, e.g., Eq. (64)] for which only the positive energy spectrum is treated consistently through the required order. Oddershede *et al.* (1977b) have shown that this deficiency of the particle-hole propagator has very little influence on the (positive) excitation energies, whereas the transition moments are rather poor in methods where the $E \rightarrow -E$ symmetry of the propagator is not preserved (see Section III,B for a more detailed discussion).

The particle-hole propagator written in the form of Eq. (63) can be compared directly with diagrammatic perturbation calculation of the proper particle-hole self-energy (Barrett, 1968; Paldus and Čížek, 1974). By expanding all inverse matrices, as indicated in Eq. (59), and retaining terms through third order, Oddershede and Jørgensen (1977a) have shown that an exact match is obtained for all first-, second-, and third-order irreducible particle-hole self-energy diagrams given by Paldus and Čížek (1974) and the irreducible diagrams generated by the analytic particle-hole self-energy in Eq. (64). This verifies that the particle-hole propagator in Eq. (64) in fact *is* consistent through third order in the electronic repulsion.

The particle-hole and polarization propagator contain, however, in addition to the finite-order diagrams also terms that represent diagram series summed to infinite order (Oddershede and Jørgensen, 1977a) and which are not present in the perturbation treatment of Paldus and Čižek (1974). These infinite series originate from the expansion of inverse matrices as indicated in Eq. (59) and are present in the polarization propagator in all orders (except zero) and in the particle-hole propagator in third and higher orders [cf. Eqs. (61) and (64)]. As an example, let us consider the first-order polarization propagator approach (FOPPA), i.e., TDHF. From Eq. (31) it follows that the corresponding particle-hole propagator is

$$\begin{aligned}\langle\langle \tilde{\mathbf{q}}; \mathbf{q}^{+} \rangle\rangle_{E}^{-1} &= E\mathbf{1} - \mathbf{A} - \mathbf{B}(1)[E\mathbf{1} - \mathbf{A}^{*}(0) - \mathbf{A}^{*}(1)]^{-1}\mathbf{B}^{*}(1) \\ &= E\mathbf{1} - \mathbf{A} - \mathbf{B}(1)[E\mathbf{1} - \mathbf{A}^{*}(0)]^{-1}\mathbf{B}^{*}(1) \\ &\quad - \mathbf{B}(1)[E\mathbf{1} - \mathbf{A}^{*}(0)]^{-1}\mathbf{B}^{*}(1) - \cdots. \end{aligned} \qquad (65)$$

The third, fourth, etc. terms in this equation represent the first, second, etc. RPA (or "ring") diagrams (Oddershede and Jørgensen, 1977a), and the partitioning technique offers thus a useful way to link together the diagrammatic (Gell-Mann and Brueckner, 1957) and the analytic definition of RPA normally used in molecular physics (McLachlan and Ball, 1964; Jørgensen and Linderberg, 1970).

The individual matrix elements $\mathbf{A}(1)$ and $\mathbf{B}(1)$ represent particle-hole interactions, and whole RPA series describe repeated particle-hole scattering events, which are often denoted as collective motions (Hedin and Lundqvist, 1969). The $\mathbf{A}(1)$ matrix contains the matrix elements between singly excited configurations. The first-order particle-hole propagator approach is therefore identical to the singly excited configuration interaction (SECI) or Tamm–Dancoff approximation (TDA). According to Eq. (65) the RPA method can be regarded as SECI augmented with terms describing collective motions. If we define in general the concept *collective effect* as the correlation contributions from sums of infinite series of diagrams (Oddershede *et al.*, 1978b), it is readily seen from Tables II and III that the difference between the polarization propagator and particle-hole propagator, both through second order, originates solely from the inclusion of collective effects in the former approach. This gives us a method for estimating the importance of collective effects (Oddershede *et al.*, 1978b), of which examples are given in Section III,B.

In Table IV we indicate the relations between propagator calculations and other similar methods. We have already discussed the connections between some of the methods. The equivalence between coupled HF (Lipscomb, 1966) and TDHF has been discussed by Linderberg and Öhrn (1973), and it will also become clear later (Sections IV,A and B) that we get identical expressions for response properties in TDHF and coupled HF.

TABLE IV

RELATIONS BETWEEN PERTURBATIVE-DETERMINED PROPAGATORS AND OTHER METHODS

	Polarization propagator			
Order	Abbreviated notation[b]	Identical methods	Particle-hole propagator (identical methods)	Diagonal elements of the particle-hole propagator[a] (identical methods)
1	FOPPA	RPA	SECI	Virtual HF
		TDHF	TDA	Single-transition approx. (STA)[c]
		Coupled HF		First-order Paldus-Čižek[d]
2	SOPPA	SPPA + 2p − 2h corr.	—	Second-order Paldus-Čižek[d]
		HRPA + 2p − 2h corr. = EOM		
3	TOPPA	Third-order EOM[e]	—	Third-order Paldus-Čižek[d]

[a] In the text this method is often referred to as the single-transition method.

[b] Abbreviations are defined in the text. TOPPA—third-order polarization propagator approach.

[c] See Dunning and McKoy (1967, 1968).

[d] The diagrammatic approach described by Paldus and Čižek (1974).

[e] Yeager and Freed (1977).

It was first pointed out by Shibuya and McKoy (1971) that the self-consistent pair correlation coefficient obtained in a HRPA calculation [see Eq. (34)] differed very little from the corresponding first-order Rayleigh–Schrödinger coefficient, and Williams and Poppinger (1975) have proposed a modified noniterative HRPA method in which the **A** and **B** matrices are constructed directly from the Rayleigh–Schrödinger correlation coefficients. Thus, except for a slightly different treatment of the 2p-2h corrections [compare Shibuya *et al.* (1973) and Jørgensen *et al.* (1975)], the Williams–Poppinger method is identical to the consistent second-order polarization propagator approach (SOPPA). Since SPPA is equivalent to the HRPA method (see Section II,B), we would expect the two-electron density matrix generated by SPPA to be similar to the Rayleigh–Schrödinger coefficients—a trend that can be observed in Table I. This is the reason for placing HRPA and SPPA under consistent second-order theories in Table IV. The fact that the self-consistent and the Rayleigh–Schrödinger correlation coefficients are so similar may be somewhat surprising, but it shows that the "classical" Rayleigh–Schrödinger coefficient deviates little from the "optimal," self-consistent expansion coefficients for doubly excited configurations.

This concludes our discussion of some theoretical aspects of the polarization propagator method, and we now turn to consider the applications of the method.

III. Electronic Spectra

A. The Eigenvalue Problem

The poles of the polarization and the particle-hole propagators are the electronic excitation energies, and the residues of the polarization propagator determine the transition moments, i.e., the electronic spectrum can be calculated by solving the eigenvalue problems for the inverse propagators (see Section II,A). The excitation energies are thus obtained *directly* from the propagator and no subtraction of (large) total energies is involved.

In time-dependent HF, this procedure results in a non-Hermitian eigenvalue problem, Eq. (31), the solution of which was discussed in Section II,B. In higher order theories, more complicated non-Hermitian energy-dependent matrix problems must be solved [see Eqs. (37), (61), (62), and (64)]. Through third order in the electronic repulsion it is, however, possible to write these propagators in a TDHF-like form (Oddershede *et al.*, 1978a) in the following way. The term $\mathbf{C}^{+}(-E\mathbf{1} - \mathbf{D}^{*})^{-1}\mathbf{C}^{*}$ is of at least second order in the electronic repulsion, and in a perturbation calculation it will be multiplied with "small" TDHF eigenvectors $\mathbf{Y}$, $\mathbf{Y}^{+}$, both of which are of first order (Oddershede and Jørgensen, 1977a). Changing $-E$ to $+E$ in this term will thus introduce error beyond third order in the electronic repulsion. Through third order it is similarly possible to change $-E$ to $+E$ in the off-diagonal blocks in Eq. (61). This last approximation is not necessary for bringing the propagator $\mathbf{P}^{(3)}(E)$ into a TDHF-like form but it simplifies the calculations.

The propagator in the TDHF-like form can be written in an energy-dependent spectral form equivalent to Eq. (28),

$$\mathbf{P}(E) = \begin{Bmatrix} \mathbf{Z}(E) & \mathbf{Y}(E) \\ \mathbf{Y}(E) & \mathbf{Z}(E) \end{Bmatrix} \begin{Bmatrix} (E\mathbf{1} - \boldsymbol{\omega}(E))^{-1} & \mathbf{0} \\ \mathbf{0} & -(E\mathbf{1} + \boldsymbol{\omega}(E))^{-1} \end{Bmatrix} \begin{Bmatrix} \tilde{\mathbf{Z}}(E) & \tilde{\mathbf{Y}}(E) \\ \tilde{\mathbf{Y}}(E) & \tilde{\mathbf{Z}}(E) \end{Bmatrix}. \tag{66}$$

For simplicity, we assumed that all matrices are real. The excitation energies, E_n, are the poles for the propagator, $E_n = \pm\omega_n(E_n)$. The residues, for example, at $E = E_n$, are determined as

$$\operatorname{Res}[E_n] = \lim_{E \to E_n} (E - E_n)[E - \omega_n(E)]^{-1} \begin{Bmatrix} \mathbf{Z}(E)\tilde{\mathbf{Z}}(E) & \mathbf{Z}(E)\tilde{\mathbf{Y}}(E) \\ \mathbf{Y}(E)\tilde{\mathbf{Z}}(E) & \mathbf{Y}(E)\tilde{\mathbf{Y}}(E) \end{Bmatrix}. \tag{67}$$

Assuming that $\mathbf{Z}(E)$ and $\mathbf{Y}(E)$ are analytic in the neighborhood of $E = E_n$,

$$\mathrm{Res}[E_n] = \Gamma_n \begin{Bmatrix} \mathbf{Z}(E_n)\tilde{\mathbf{Z}}(E_n) & \mathbf{Z}(E_n)\tilde{\mathbf{Y}}(E_n) \\ \mathbf{Y}(E_n)\tilde{\mathbf{Z}}(E_n) & \mathbf{Y}(E)\tilde{\mathbf{Y}}(E_n) \end{Bmatrix}, \tag{68}$$

where

$$\Gamma_n^{-1} = \left\{\frac{d}{dE}\left[E - \omega_n(\mathrm{E})\right]\right\}_{E=E_n} = 1 - \left(\frac{d\omega_n(E)}{dE}\right)_{E=E_n}. \tag{69}$$

The excitation energies in higher order theories are thus obtained by solving a TDHF-like eigenvalue problem at $E = E_n$, and the transition moments are calculated from the corresponding eigenvectors multiplied with the factor Γ_n (Oddershede *et al.*, 1978a). Similar expressions for the transition moments can be obtained from biorthogonal expansions of the particle-hole self-energy, an approach which has been used by Csanak *et al.* (1971) and Purvis and Öhrn (1974) to analyze the electronic self-energy appearing in the electron propagator.

Due to the energy dependence of the propagator matrix elements, iterative schemes must be used to solve for $E = E_n$. This means that the eigenvalue problem must be solved separately for every excitation energy, which is a rather time-consuming procedure. If, however, we put $E = 0$ in the two-particle, two-hole terms in Eqs. (61) and (62), the energy-dependent terms disappear, and we can determine all excitation energies from one diagonalization (Jørgensen *et al.*, 1975). We have collected in Table V typical results for various approximations to the two-particle, two-hole term. For small excitation energies, it is a good approximation to put $E = 0$ in the 2p − 2h terms, but for larger energies this can introduce errors of up to 1 eV in the excitation energy. The difference between the iterative solution and

TABLE V

EXCITATION ENERGIES FROM THE GROUND STATE CALCULATED AT VARIOUS LEVELS OF APPROXIMATION FOR THE TWO-PARTICLE, TWO-HOLE TERM $\tilde{\mathbf{C}}(E\mathbf{1} - \mathbf{D})^{-1}\mathbf{C}$ (SOPPA RESULTS)

System	Basis	Excited state	$E =$ 0 (eV)	E_{TDHF} (eV)	E_n[a] (eV)	Exact[b] (eV)
Be	50 STO's	$1s^22s2p(^1P)$	5.13	5.0242	5.0178	5.0225
FH	45 STO's	$B^1\Sigma_u^+$	14.31	13.25	13.4315	13.4321

[a] The self-consistent solution for which $-E$ has been changed into $+E$ in the term $\tilde{\mathbf{C}}(-E\mathbf{1} - \mathbf{D})^{-1}\mathbf{C}$.

[b] The excitation energy is determined as a pole for the polarizability and no approximation to the propagator matrix is involved (see Section IV,A).

the excitation energy obtained by putting $E = E_{\mathrm{TDHF}}$ in the 2p − 2h term is, however, very small and typically only one or two iterations are required to compute the self-consistent excitation energy. Shibuya *et al.* (1973) add the 2p − 2h corrections to the HRPA solution using first-order perturbation theory. Since the $\tilde{\mathbf{C}}(-E\mathbf{1} - \mathbf{D})^{-1}\mathbf{C}$ term is at least of fourth order, this method, often referred to as the equation-of-motion (EOM) approximation (see, e.g., McCurdy *et al.*, 1977), is very similar to the present approach. England *et al.* (1977) have also shown that an iterative EOM procedure gives a change in the excitation energy that is only slightly larger than the variations reported in Table V.

As discussed in Section II,B, the non-Hermitian TDHF eigenvalue problem can be replaced with two Hermitian eigenvalue problems for $\mathbf{A} \pm \mathbf{B}$, whereas in higher order theories, $\mathbf{A}$ and $\mathbf{B}$ are energy-dependent matrices. The size of the $\mathbf{A}$ and $\mathbf{B}$ matrices and hence of the eigenvalue problems is equal to the number of particle-hole excitations ($\mathbf{q}^{+}$) in the given basis set [see Eqs. (25) and (38)]. In practical application it is often necessary to limit the size of eigenvalue problem, and with our present programs we can treat a maximum of seventy-five particle-hole excitations of each spin symmetry (singlet and triplet). In the order calculation of the polarization propagator, an additional reduction of the secular problem is possible if we use the point-group symmetry (Σ, Π, etc. excitation spectra for diatomic molecules), and we can thus treat seventy-five excitations of each spin-space symmetry. In the iterative calculation of the propagator (SPPA), this latter reduction is greatly hindered by the fact that, e.g., the Π two-matrix is needed in the construction of the Σ-eigenvalue problem. This means that truncation of the $\mathbf{A}$, $\mathbf{B}$, and $\tilde{\mathbf{C}}(E\mathbf{1} - \mathbf{D})^{-1}\mathbf{C}$ matrices to 75 excitations often is a more serious approximation in SPPA than in SOPPA. The error introduced by truncation of the eigenvalue problem is examined in Fig. 1. This figure shows that truncation to less than half the size of the secular problem can cause serious errors in the excitation energies. Truncation of the matrix problem (for a given basis set) will always lead to larger excitation energies. This "variational" principle has been proven by Linderberg and Öhrn (1977).

In most applications of the EOM approximation, the particle-hole space is truncated to even less than 75 excitations [Rose *et al.*, 1973 (30 excitations of each symmetry) and McCurdy and McKoy, 1974], and England *et al.* (1977) have shown that the truncation error in the McCurdy and McKoy (1974) results for CO_2 were 0.3–0.4 eV. This error was, however, canceled by a similar error (with opposite sign) due to the limited-size basis set (England *et al.*, 1977). A peculiarity of the self-consistent polarization propagator approximation (and HRPA) might, however, in some cases result in truncation errors of the same size for both

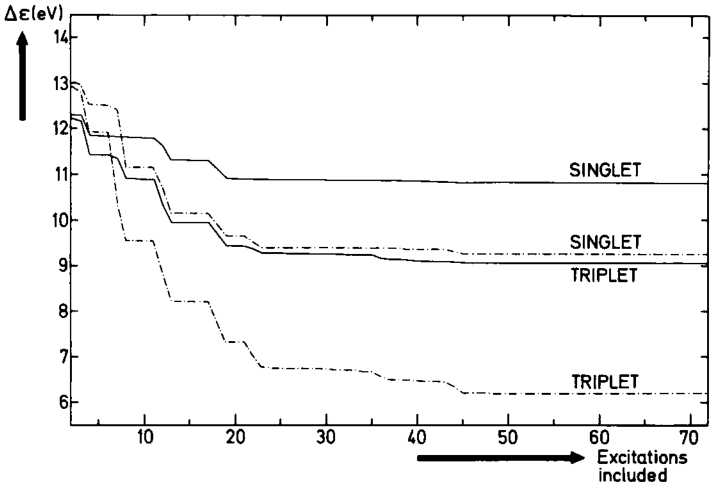

Fig. 1. The lowest sigma-excitations for CO of singlet ($X^1\Sigma^+$ to $I^1\Sigma^-$) and of triplet symmetry ($X^1\Sigma^+$ to $a'^3\Sigma^+$) in the random-phase approximation (dotted curves) and in the second-order polarization propagator approximation (solid curves) as a function of the size of the *sigma* secular problem. The excitations included in the calculation are arranged in order of increasing excitation energy, and seventy-four excitations are the maximum number of sigma-excitations in the given basis set (46 STO's).

SPPA and SOPPA, even though we can treat larger matrices in SOPPA due to the symmetry splitting. The truncation of **A** and **B** means that **Z** and **Y** and, hence, the two-matrix must be truncated too [see Eq. (35)]. Several (positive) contributions to the **A** and **B** matrices in SPPA are thus omitted [see Eqs. (14) and (15) in Oddershede *et al.* (1975)]. The negative error in the excitation energy may balance the positive error caused by the truncation of the eigenvalue problem, thus resulting in excitation energies of correct magnitudes. This cancellation is probably one of the reasons for the good results for SiO (Oddershede and Elander, 1976) for which substantial truncations in the SPPA matrices were required.

A polarization propagator calculation of the type outlined here must be preceded by a Hartree–Fock calculation [see Eqs. (51) and (52)] and the two-electron integrals must be transformed to the SCF basis. The HF and the transformation programs are in any applications the most time-consuming part of the total calculation, especially for large basis sets for systems with few electrons. The new integral transformation procedure of Beebe and Linderberg (1977) has, however, reduced the transformation time

TABLE VI

Computational Times (on a CDC 6400 Computer) for Polarization Propagator Calculations, Including Times for the "Satellite" Programs: Hartree-Fock and Integral Transformation to SCF Basis[a]

System (basis)	Hartree-Fock[b] (sec)				Transformation (sec)		Propagator calculation (sec)					
	Integral +	SCF +	misc.[c] =	total	Convent.[d]	distrib.[e]	TDHF[f] +	A(2), B(2)[g] +	2p − 2h[h] +	misc.[i] =	total (SOPPA);	total (SPPA)[j]
CH^+[k] (45 STO's)	1897	294	158	2349	10591	1780	Σ: 137	1022	96	146	1419	
							Π: 196	891	97	130	1314	
He (48 STO's)	277	234	9	520	9867	2067	Σ: 39	75	7	22	143	1606
							Π: 45	61	6	18	130	
FH[k] (45 STO's)	2055	612	95	2762	7968	1780	Σ: 279	1869	198	210	2556	
							Π: 363	1445	204	292	2304	

[a] The programs were compiled with the FTN 3 computer with highest optimization level (OPT = 2).

[b] For diatomic molecules the Harris and Michels (1967) program was used, and for atoms we used an atomic integral program written by N. H. F. Beebe and the SCF program of Harris and Michels (1967).

[c] Mainly integral retrival time.

[d] A conventional transformation procedure roughly proportional to N^5.

[e] The integral transformation procedure developed by Beebe and Linderberg (1977).

[f] Includes also the time for the virtual HF and the single-excited CI approximation.

[g] The difference between the TDHF and the second-order **A** and **B** matrices, see Eq. (62).

[h] The construction time for the two-particle, two-hole corrections, $\tilde{\mathbf{C}}(E\mathbf{1} - \mathbf{D})^{-1}\mathbf{C}$, see Eq. (62).

[i] Mainly diagonalization time.

[j] The iterative self-consistent polarization propagator method described in Section II,B.

[k] At one internuclear separation.

considerably. We find now as a rough rule-of-thumb that the ratio of the computational time for the atomic integrals +SCF, to the transformation and to the polarization propagator calculation is 1 : 1 : 1. A more detailed account for the computational effort involved in a propagator calculation is given in Table VI. The basis sets for CH^+ and FH are so large that the SPPA calculations would contain substantial truncation errors. We see, however, from the He calculation that the SPPA calculation, due to the iterative procedure, is much more expensive that the corresponding perturbation calculation of the second-order propagator (SOPPA).

In Sections III,B–E we now discuss some of the physical quantities that can be obtained from a solution of the propagator eigenvalue problem.

B. Excitation Energies

Historically, the first applications of RPA-like methods in nuclear (Green, 1965), atomic (Altick and Glassgold, 1964), and molecular physics (Ball and McLachlan, 1964) were directed toward the evaluation of vertical excitation energies. The literature in this area is extensive, and we refer the reader to Jørgensen (1975) and McCurdy *et al.* (1977) for recent reviews. In the present section, we discuss typical results obtained at various levels of approximation for the propagator. The excitation energies are calculated from the poles of the polarization propagator, but identical conclusions could have been reached from excitation energies calculated, for example, by the EOM approximation (McCurdy *et al.*, 1977). Appendix A contains a comprehensive list of calculations performed with these methods.

Excitation energies calculated through second order in the electronic repulsion are given in Table VII. The excitation energies obtained in consistent second-order theories are generally improved compared with those obtained in the corresponding first-order approximations. The single-excitation results are, however, unsatisfactory even in second order, except in the rare cases where a given state is well separated from all other states of the same symmetry (Oddershede and Jørgensen, 1977b; Oddershede *et al.*, 1978b). If the single-excitation scheme, in which only one particle-hole excitation is considered at a time, is carried to sufficiently high order in the electron repulsion, it must give the same excitation energy as that obtained from diagonalizing the inverse propagator. The single-excitation scheme is thus slowly convergent (Paldus and Čížek, 1974). Through second order in the electronic repulsion, Oddershede and Jørgensen (1977b) have shown that the excitation energy obtained from a single-excitation calculation and from separate self-consistent field calculations on both states (ΔSCF) (Bagus, 1965) plus first-order pair-correlation (Nesbet, 1969; Sinanoğlu, 1969) calculation are identical. This means that it is necessary to

TABLE VII

EXCITATION ENERGIES FROM THE GROUND STATE AT VARIOUS LEVELS OF APPROXIMATION FOR THE PARTICLE-HOLE AND THE POLARIZATION PROPAGATOR

	System/basis set/excited state:				
	Be	Be	He	FH[b]	FH[b]
	38 STO's	38 STO's	48 STO's	45 STO's	45 STO's
Method[a]	2s2p(^{1}P)	2s2p(^{3}P)	1s2s(^{1}S)	$^3\Pi(1)$	$B^1\Sigma_u^+$
Single-excitation schemes:					
STA(HF) (eV)	5.43	4.36	22.68	13.41	16.41
Second order (eV)	5.71	3.86	21.94	10.29	13.43
Strict diagrammatic approaches[c]:					
SECI(TDA) (eV)	5.04	1.70	21.13	11.11	15.46
Second order (eV)	5.21	2.23	20.66	9.73	13.43
Polarization propagator calculations:					
TDHF(RPA) (eV)	4.80	Unstable	21.10	10.95	15.43
SPPA(HRPA) (eV)	6.23	3.10	22.18	—	—
SPPA + 2p − 2h (eV)	5.57	2.91	20.82	—	—
SOPPA[**B**(2) = 0.0][d] (eV)	5.14	1.64	20.65	9.70	13.43
SOPPA (eV)	5.11	2.20	20.65	9.78	13.43
SOPPA + *E* shift[e] (eV)	5.03	1.83	21.09	9.22	13.43
Other calculations:					
Configuration interaction (eV)	—	—	—	10.13[h]	—
Bethe–Goldstone pairs[f] (eV)	5.29	—	—	—	—
Experiments	5.28[g]	2.72[g]	20.61[g]	—	13.63[i]

[a] The abbreviations are defined in the text.

[b] At the internuclear separation, $R = 1.733$ bohrs.

[c] The particle-hole propagator in Eq. (64) evaluated through first and second order.

[d] The **B**(2) matrix in Eq. (62) is set equal to zero.

[e] The second-order polarization propagator approximation with energy-shifted denominators (Oddershede *et al.*, 1978a).

[f] Moser *et al.* (1976).

[g] Moore (1949).

[h] Dunning (1976). At the internuclear separation, $R = 1.75$ bohrs.

[i] Interpolated value from DiLonardo and Douglas (1973).

include relaxation effects (ΔSCF) to a rather high order not only for the core states (Wendin, 1973b) but also for low-lying valence states. Born *et al.* (1978) have recently performed a similar identification of relaxation and correlation terms for an electron propagator calculation.

The difference between the single-excitation scheme and a *strict diagrammatic* approach is that both the off-diagonal and diagonal elements of the particle-hole self-energy matrix are calculated through the same order in the latter approximation. The inclusion of the off-diagonal elements has a noticeable effect on the excitation energies (see Table VII), and in the second-order diagrammatic approach they are of the same quality as those calculated in the polarization propagator method. This shows that collective effects (see Section II,D) are of little importance for a reliable description of excitation energies (Oddershede *et al.*, 1978b).

The SPPA (or HRPA) excitation energies in Table VII are much too high (Jørgensen *et al.*, 1974; Rescigno *et al.*, 1977), demonstrating that reliable results can only be expected from *consistent* approximations (cf. Table IV). The moderate changes from the first- to the second-order theory, together with the large differences between the TDHF and SPPA results, indicate that there is a considerable cancellation among individual second-order contributions (see Oddershede *et al.*, 1978b, for details). Even though the total change from TDHF to the second-order approach in absolute number is rather small, it is a large portion of the difference between the TDHF and experimental result. This is illustrated in Table VIII where we calculate the average deviation among the TDHF, SOPPA, and experimental excitation energies for all the systems considered so far. The agreement with experiment would improve in a third-order theory, but the major reason for the remaining difference between theory and experiment is the truncation of the size of the basis set. This is clearly demonstrated by the small error for He and H_2 for which it is possible to use basis sets that are relatively better than those used for larger systems.

TABLE VIII

AVERAGE DIFFERENCE BETWEEN EXPERIMENTAL[a] AND CALCULATED VERTICAL EXCITATION ENERGIES

System	No. of states[b]	Error (%)	
		TDHF	SOPPA
He	18	1.6	0.3
Be	4	6	4
Ne	16	9.1	2.4
H_2	6	1.7	1.4
CH^+	2	11	3
FH	4	10.0	2.7
CO	9	13.1	2.4

[a] When available, otherwise another very accurate calculation.

[b] Number of assigned states that are used in the calculation of the average error estimate.

We include in Table VII only SPPA results for systems for which it was unnecessary to truncate the **A**, **B**, etc. matrices. For He, the SOPPA and SPPA + 2p − 2h results are similar, whereas the difference between the corresponding Be results is rather large. For systems for which the HF ground state is triplet unstable (such as Be), substantial deviations can be observed between excitation energies calculated by the iterative and the perturbative methods. For systems without triplet instabilities (such as He), the two methods give very similar excitation energies [see e.g., the discussion in the Appendix to Rose *et al.* (1973)]. The quality of the spectra obtained with the two methods is, however, nearly the same also for systems with triplet unstable ground states. Thus, the much larger computational effort spent on an iterative calculation of the propagator (see Table VI) together with the additional truncation problem in SPPA (see Section III,A) suggests that the perturbation approach is a more effective way to obtain the same information. Many recent applications of RPA-like methods have indeed made use of direct calculations of the **A**, **B**, **C**, and **D** matrices (Williams, 1975; Elander *et al.*, 1977; Bouman and Hansen, 1977; Yeager and Freed, 1977; Oddershede *et al.*, 1978a).

In Table VII we also examine the effect of neglecting the second-order correction to the **B** matrix. It is very time-consuming to calculate the **B**(2) matrix [often more than 90% of the total time used to construct the **A**(2) and **B**(2) matrices, see Table VI]. Furthermore, **B**(2) does not enter in the second-order particle-hole propagator (see Table III) which might indicate that it can be ignored in the polarization propagator as well. We see from Table VII that this is a very good approximation in almost all cases. Only for systems that are nearly triplet unstable is the (small) contribution from **B**(2) of importance. This agrees with our earlier finding (Jørgensen *et al.*, 1974), namely that the rate of change of the lowest excitation energy is large when we approach an instability point.

Experience shows that introduction of energy-shifted denominators can improve the convergence of the perturbation expansions used in evaluating ground-state total energies (Kelly, 1969; Silver and Bartlett, 1976). This "shift" is accomplished by adding diagonal elements of the perturbation operator to the orbital energy difference in the denominators, and it corresponds diagrammatically to summing certain classes of diagrams to infinite orders (Kelly, 1969). Energy-shifted denominators can similarly be introduced in polarization propagator calculations (Yeager and Freed, 1977; Oddershede *et al.*, 1978a) by adding diagonal elements of the perturbation V [Eq. (52)] to the denominators of the Rayleigh–Schrödinger correlation coefficients and to the **D** matrix (2p − 2h term). We find (see Table VII) that denominator shifts have a relatively small effect on the excitation energies, especially in the singlet case where the shifts in the correlation coefficients and in the 2p – 2h term are of opposite sign and almost cancel each other (Oddershede *et al.*, 1978a). The changes reported by Oddershede *et al.* (1978a) are somewhat smaller than those found by Yeager and Freed (1977), but both investigations indicate that the agreement with experiments is worse *with* shifted denominators, i.e., the opposite conclusion of that reached for ground-state total energies (Silver and Bartlett, 1976). This discrepancy might be caused by an unbalanced treatment of ground and excited states in the shifted-SOPPA method. This approximation is not a consistent third- (or higher)order theory. Only a few of the third-order diagrams are included, and the larger disagreement between experimental and the shifted-SOPPA energies could be an effect similar to that found in SPPA without two-particle, two-hole corrections.

C. Potential Energy Surfaces

From the vertical excitation energies as a function of the internuclear coordinates and from the shape of one of the potential energy surfaces, e.g., the ground state, it is straightforward to compute adiabatic potential energy curves for excited states (Coughran *et al.*, 1973; Oddershede and Elander, 1976; Elander *et al.*, 1977). Several potential energy curves are thus obtained from *one* propagator calculation. A similar method has been used by Simons and co-workers to calculate potential energy surfaces for ions from the electron affinities and the ionization potentials obtained from the poles of the electron propagator (Griffing and Simons, 1975; Kenney and Simons, 1975; Anderson and Simons, 1977).

Rather accurate potential curves are obtained with this method. In Table IX, we give the average error of the spectroscopic constants derived from the potential curves for SiO (Oddershede and Elander, 1976) and CH^+ (Elander *et al.*, 1977). Only the molecular constants for the states that

TABLE IX

AVERAGE RELATIVE ERROR[a] OF THE SPECTROSCOPIC CONSTANTS CALCULATED WITH THE SECOND-ORDER POLARIZATION PROPAGATOR APPROXIMATION FOR SiO AND CH^+ [b]

δT_e	δr_e	$\delta \alpha_e$	$\delta \omega_e$	$\delta \omega_e x_e$
4.5%	1.7%	15.6%	8.9%	16.0%

[a] Relative to the experimental molecular constants [for SiO from Field *et al.* (1976, 1977) and for CH^+ from Botterud *et al.* (1973)].

[b] Original data can be found in the papers by Oddershede and Elander (1976) and Elander *et al.* (1977).

can be assigned unambiguously to measured states have been used in Table IX, i.e., seven states for SiO and two states for CH^+. Despite the limited number of states used in Table IX, the trends are probably typical for the accuracy of the propagator method: "equilibrium" spectroscopic constants, such as T_e and r_e, show satisfactory agreement with experiments, whereas molecular parameters that depend critically on the shape of the potential curves away from equilibrium (α_e and $\omega_e x_e$) are less accurate. This is caused by the fact that the reference state expansion used in the second-order polarization propagator calculation (Hartree–Fock plus doubly excited configurations) becomes worse when R is far from r_e for the ground state. In absolute numbers, the error bars in Table IX correspond to an error of about 0.2 eV in T_e and 0.03 Å in r_e. The actual size of, e.g., ω_e and α_e is quite different for SiO and CH^+, but the relative errors are the same for both molecules. Higher order propagator approaches *and* larger basis sets are required if the error bars on $\omega_e x_e$ and α_e are to be reduced compared with those given in Table IX.

As stated previously, the shape of one potential surface is needed to calculate potential curves with the present method. In all previous calculations (Coughran *et al.*, 1973; Oddershede and Elander, 1976; Elander *et al.*, 1977) an experimental ground or excited state has been used. This may not be the optimal choice since the experimental curve is often of higher accuracy than the calculated excitation energies. For example, in a second-order theory, it would be more natural to use a ground state calculated through second order in the electronic repulsion as a reference state. In Table X we examine the spectroscopic constants for the $A^1\Pi$ state in CH^+ calculated with various reference states. There is no clear tendency in the results in Table X, in agreement with the conclusion reached by Griffing and Simons (1975) in a similar investigation on BH, BH^+, and BH^-. It seems, however, as if the constants calculated from the second-order Rayleigh–Schrödinger ground state are slightly better than those obtained with the two other reference states. The equilibrium vibrational frequency, ω_e, especially, is improved. The calculated vertical excitation energies are too small for large R values and added to the experimental ground state this results in a value for ω_e, which is too large, whereas the second-order ground-state curve lies substantially above the experimental curve for large R, thus compensating for the too small excitation energy. Besides being consistent from a theoretical point of view (see Section V,B), the use of a second-order Rayleigh–Schrödinger ground state also allows us to make reliable calculations of potential curves for systems where detailed experimental information about individual states is not available. One such example is the $HeNe^{Z+}$ ($Z = 2$, 4, etc.) molecule for which we are

TABLE X

SPECTROSCOPIC CONSTANTS FOR THE $A^1\Pi$ STATE IN CH^+ CALCULATED FROM THE SOPPA EXCITATION ENERGY AND THE SHAPE OF THE GROUND STATE, $X^1\Sigma^+$, AT VARIOUS LEVELS OF APPROXIMATION

Calculations	T_e (cm^{-1})	r_e (Å)	B_e (cm^{-1})	α_e ($cm^{-1} \times 10^3$)	ω_e (cm^{-1})	$\omega_e x_e$ (cm^{-1})
Using $X^1\Sigma^+$ from:						
Hartree–Fock	22975	1.218	12.23	0.51	1979	55.1
Second-order perturbation[a]	22975	1.236	11.86	0.55	1759	54.5
Experiment[b]	22975	1.221	12.16	0.75	2214	100.6
Experimental constants for the $A^1\Pi$ state[b]	24073	1.234	11.90	0.94	1865	115.9

[a] Second-order Rayleigh–Schrödinger total energy.

[b] Botterud *et al.* (1973).

presently calculating excited states with the polarization propagator method (Sabin and Oddershede, 1978). It should be noted that the calculation of the second-order ground-state energy does not require extra computational effort when performed together with the propagator calculation.

The discussion in this section and most applications have concentrated on diatomic molecules. However, with a polyatomic Hartree–Fock program as a "satellite" program, it is equally straightforward to calculate force constants for large molecules.

D. Transition Moments

The electronic transition moments are calculated from the residues of the propagator, as discussed in Section III,A, and a few illustrative examples are given in Table XI. In the second-order theories with energy-dependent matrix elements, the directly calculated transition moments must be corrected with the factor Γ_n in Eq. (69), and we find that this causes a change of 1 (He) to 7 (FH)% in the transition moments.

The transition moments obtained from the *polarization* propagator at different levels of approximation are rather similar and in most cases distinctly different from those obtained from the *particle-hole* propagator through the same order in the electronic repulsion. This shows that inclusion of collective effects, i.e., diagram series summed to infinite orders (Section II,D), is important for a reliable description of transition moments (Oddershede *et al.*, 1978b) but not for excitation energies (see Section III,B). Furthermore, the small differences between the transition moments obtained

TABLE XI

THE SQUARE OF THE ELECTRONIC TRANSITION MOMENTS FROM GROUND TO EXCITED STATE AT VARIOUS LEVELS OF APPROXIMATIONS FOR THE PARTICLE-HOLE AND THE POLARIZATION PROPAGATOR

	System/basis set/excited state					
	Be 38 STO's 2s2p(^{1}P)		He 48 STO's 1s2p(^{1}P)		FH[b] 45 STO's $1\Pi(1)$	
Method[a]	Length	Velocity	Length	Velocity	Length	Velocity
Single-excitation scheme:						
STA(HF) (a.u.)	9.78	0.188	0.014	0.0052	0.055	0.0058
Strict diagrammatic approaches[c]:						
SECI (a.u.)	15.19	0.239	0.490	0.275	0.172	0.0515
Second order (a.u.)	15.48	0.238	0.493	0.278	0.160	0.0455
Polarization propagator calculations:						
TDHF(RPA) (a.u.)	11.67	0.363	0.474	0.301	0.172	0.0334
SPPA(HRPA) (a.u.)	11.99	0.346	0.473	0.293	—	—
SPPA + 2p − 2h (a.u.)	11.49	0.347	0.475	0.307	—	—
SOPPA[$B(2) = 0.0$][d] (a.u.)	11.65	0.347	0.473	0.301	0.164	0.0323
SOPPA (a.u.)	11.54	0.349	0.481	0.308	0.164	0.0352
SOPPA + E shift[e] (a.u.)	11.58	0.351	0.487	0.308	0.166	0.0362
Other calculations:						
Configuration interaction (a.u.)	—	—	0.531[f]	0.323[f]	—	—
Bethe–Goldstone pairs[g] (a.u.)	10.70	0.402	—	—	—	—
Experiments	10.37 ± 0.38[h]	0.390 ± 0.015[h]	0.529 ± 0.014[i]	0.322 ± 0.008[i]	—	—

[a] The abbreviations are defined in the text. [b] At the internuclear separation, $R = 1.733$ bohrs.

[c] The particle-hole propagator in Eq. (64) evaluated through first and second order in the electronic repulsion.

[d] The **B**(2) matrix in Eq. (62) is set equal to zero.

[e] The second-order polarization propagator approximation with energy-shifted denominators (Oddershede *et al.*, 1978a).

[f] Schiff *et al.* (1971). [g] Moser *et al.* (1976). [h] Martinson *et al.* (1974). [i] Burger and Lurio (1971).

in the first-order (TDHF) and second-order polarization propagator approximations indicate that the RPA series gives the most important contribution. Only minor improvements occur in second order.

Many of the trends in Table XI are similar to those observed for the excitation energies, e.g., the effect of neglecting **B**(2) and the effect of augmenting SOPPA with energy-shifted denominators. However, from the difference between the SPPA results with and without 2p – 2h corrections we see that the cancellation effects in second order are much more pronounced for the excitation energies than for the transition moments.

The intensities in UV spectra are proportional to the electronic oscillator strength:

$$f^L_{0M} = \tfrac{2}{3}\mathbf{M}_L^2\,\omega_{0M}; \qquad \mathbf{M}_L = \langle 0|\hat{\mathbf{r}}|M\rangle, \tag{70}$$

$$f^V_{0M} = \tfrac{2}{3}\mathbf{M}_V^2/\omega_{0M}; \qquad \mathbf{M}_V = \langle 0|\hat{\mathbf{p}}|M\rangle, \tag{71}$$

where $\mathbf{M}_L^2$ and $\mathbf{M}_V^2$ are the transition moments in the length and velocity formulation, respectively, and ω_{0M} is the electronic excitation energy, Eq. (11). Since both excitation energies and transition moments enter in Eqs. (70) and (71), it follows from the results in Tables VII and XI that reliable estimates of UV intensities require at least a second-order polarization propagator calculation. There is, however, a remaining error of a few percent in the transition moments even in the second-order polarization propagator approach (Jørgensen *et al.*, 1978b). The *first*-order Rayleigh–Schrödinger wavefunction determines the correction to the total energy through *third* order, and it is, therefore, likely that a third-order polarization propagator approximation would give a better and more consistent description of the wavefunctions for the ground and excited states and, hence, of the electronic transition moments.

Besides giving intensities in UV spectra, the electronic transition moments are also useful in other respects, e.g., in establishing the exact position of avoided crossings between adiabatic potential energy surfaces. This is of importance for calculating inelastic energy losses in atomic collisions (Mott and Massey, 1965). Oddershede and Elander (1976) have shown how the electronic transition moments are interchanged at avoided crossings between excited states in SiO, and we have found a similar behavior in HeNe^{2+} (Sabin and Oddershede, 1978). The reason for this variation of the transition moments is that the dominant configurations are interchanged at an avoided crossing, and it can be shown that the sum of the transition moments in a two-state picture must be the same before and after the avoided crossing (Nicolaides and Beck, 1978). We discuss next another application of the electronic transition moment.

E. Radiative Lifetimes

Most accurate experimental determinations of atomic and molecular transition probabilities are based on measurements of lifetimes for excited states. The radiative lifetime for an excited state $|K\rangle$ is given as

$$\tau_K^{-1} = \sum_{L<K} A_{KL}, \tag{72}$$

where A_{KL} is the Einstein coefficient for spontaneous emission from state $|K\rangle$ to $|L\rangle$,

$$A_{KL} = \frac{4}{3\hbar^4 c^3} \omega_{KL}^3 \mathbf{M}_{KL}^2, \tag{73}$$

and $\mathbf{M}_{KL}$ is the total transition moment in the dipole length formulation and ω_{KL} is defined in Eq. (11). From the radiative lifetime of the lowest excited state and the corresponding excitation energy, we can readily compute the transition moment. For higher lying states, several lifetimes must be known to calculate transition moments between various states, but for atoms this is a rather straightforward procedure and electronic transition probabilities for several thousand states have been measured using the preceding relation (Wiese *et al.*, 1966, 1969; Wiese and Fuhr, 1975; Biemont and Grevesse, 1977).

For molecules the situation is somewhat more complicated since in Eq. (72) we must sum over intermediate rotational and vibrational levels to obtain the lifetime of an excited electronic state. By measuring the lifetime of individual rovibronic levels, it is possible to compute the corresponding transition moments, but it is never possible to measure directly the *electronic* transition moment,

$$\mathbf{M}_e^{if}(R) = \langle \psi_i(R) | \mathbf{r} | \psi_f(R) \rangle, \tag{74}$$

which is the quantity calculated in the Born–Oppenheimer approximation. If we assume that the transition moment between two vibrational levels, $\mathbf{M}^2(v', v'')$, is given approximately by

$$\mathbf{M}^2(v', v'') \cong q(v', v'')\mathbf{M}_e^2(\bar{r}_{v'v''}), \tag{75}$$

where $q(v', v'')$ is the Frank–Condon factor and $\bar{r}_{v', v''}$ is the R centroid (Jarmain and Fraser, 1953; Fraser, 1954), then the resulting transition moment $\mathbf{M}_e$ represents a rather good approximation to the true electronic transition moment (Hinze *et al.*, 1975; Oddershede and Elander, 1976) and is often quoted as "the experimental electronic transition moment." A direct comparison between theory and experiment is, however, possible *only* if the theoreticians calculate the radiative lifetime, which in principle is straightforward (Hinze *et al.*, 1975; Oddershede and Elander, 1976) if the excitation energies and electronic transition moments are known as a function of the internuclear coordinates. Because most *ab initio* calculations concentrate on the energies, very few calculations of lifetimes for molecules are presently available. Besides our calculations on SiO (Oddershede and Elander, 1976) and CH^+ (Elander *et al.*, 1977) and the extensive study of H_2 by Dalgarno and co-workers (Allison and Dalgarno, 1969, 1970; Dalgarno and Stephens, 1970), only the configuration interaction calculations on LiH by Docken and Hinze (1972), on CH by Hinze *et al.* (1975), and on Na_2 by Stevens *et al.* (1977) are reported in the literature.

TABLE XII

COMPARISON OF CALCULATED WITH MEASURED RADIATIVE LIFETIMES

System	State	Calculated (SOPPA) [τ(nsec)]	Experiment [τ(nsec)]
He	$2p(^1P)$	0.591	0.557 ± 0.015[a]
Be	$2p(^1P)$	1.83	1.85 ± 0.07[b]
CH^+	$A^1\Pi(v' = 0)$[c]	598[d]	630 ± 50[e]
	$A^1\Pi(v' = 2)$[c]	845[d]	850 ± 70[e]
SiO	$A^1\Pi(v' = 0)$[c]	31.6[f]	9.6 ± 1.0[g]
	$A^1\Pi(v' = 3)$[c]	32.7[f]	9.6 ± 1.0[g]

[a] Burger and Lurio (1971).

[b] Martinson *et al.* (1974).

[c] The v' is the vibrational quantum number of the $A^1\Pi$ state.

[d] Elander *et al.* (1977).

[e] Erman (1977).

[f] Oddershede and Elander (1976). Using SPPA + 2p − 2*h* approximation.

[g] Smith and Liszt (1972).

In Table XII comparison is made between experimental radiative lifetimes and those calculated with the second-order polarization propagator approximations. The atomic lifetimes are calculated directly from the excitation energies in Table VII and the transition moments in Table XI and are, hence, of the same accuracy as these quantities. The molecular lifetimes are evaluated from the full potential curves as described by Oddershede and Elander (1976). For CH^+, excellent agreement is obtained with the high-frequency, deflection technique (Erman, 1975) measurements by Erman (1977). For SiO, our calculated values are approximately a factor of 3 higher than the lifetimes measured by Smith and Liszt (1972) using the phase-shift technique (Smith, 1971). The reason for this discrepancy is not clear but the phase-shift measurements on CH^+ (Brooks and Smith,

1975) are also about a factor of 3 smaller than the established value. However, the error in the CH^+ measurements is caused by the presence of Coulomb repulsion effects (Shemansky and Broadfoot, 1971; Möhlmann and de Heer, 1975; Curtis and Erman, 1977) that cannot be used to explain the deviation between theory and experiment in SiO.

The calculation of radiative lifetimes with the present approach (Oddershede and Elander, 1976) is only applicable to the lowest state which has a dipole allowed transition to the ground state. Transition moments between excited states which are needed to compute lifetimes for higher lying states can be calculated in RPA and (approximately) in higher order approaches from the eigenvectors **Y** and **Z** in Eq. (66) (Yeager *et al.*, 1975). It is thus straightforward to extend our methods to calculation of lifetimes for all excited states. It may, however, not be advantageous to compute all the individual contributions to the final lifetime but instead to evaluate the lifetime directly from the imaginary part of the polarization propagator as discussed by Dalgaard (1977). For atoms this is definitely the simplest approach, whereas the treatment of the nuclear Hamiltonian presents a problem for molecules. Cederbaum and Domcke (1976) have shown how the coupling between the electronic and vibrational motion can be treated approximately using only vibrational data for the *ground* electronic state, and they obtain very encouraging results for spectra of smaller molecules (Domcke and Cederbaum, 1976). Thus, a combination of the method of Dalgaard (1977) and the Cederbaum and Domcke (1976) treatment of the vibrational motion might give a direct and computationally feasible method for calculating radiative lifetimes of excited states of molecules.

I would like to end this section with a few personal comments. The calculation of radiative lifetimes for molecules seems to be an area almost overlooked by most theoreticians, even though it is rather straightforward and there is vigorous experimental activity in this field (Hefferlin, 1976; Erman, 1977). Comparison of theoretical and experimental predictions offers a possibility for detecting, e.g., systematic errors in either calculations or experiments, one example of which is the Coulomb repulsion effect in CH^+ (Elander *et al.*, 1977) and in other molecular ions.

The radiative lifetimes give information needed to determine abundances of molecules in interstellar space, which is of importance for deciding which processes take place where the density is so low that spontaneous emission is an important radiation process (see, e.g., Herbst and Klemperer, 1976). As an example of the importance of accurate lifetime determination, I would like to mention the work by Curtis *et al.* (1976) in which they conclude from measurements on the Swan band in C_2 that the earlier estimates of the solar carbon abundance must be decreased by 40%. Another important application of lifetimes is the calculation (measurement) of predissociation. Abrupt changes occur in the lifetimes for levels that are near a predissociation limit and this effect has been observed for both NO (Brzozowski *et al.*, 1976) and NH (W. H. Smith *et al.*, 1976).

The conclusion of my last remarks is that I strongly urge theoreticians to augment their large and expensive *ab initio* calculations on small molecules with a subsequent calculation of the radiative lifetimes.

IV. Second-Order Response Properties and Sum Rules

A. Frequency-Dependent Polarizabilities

Random-phase-type calculations have been used extensively to compute frequency-dependent (dynamic) dipole polarizabilities for atoms and diatomic molecules (Karplus and Kolker, 1964; Adamov and Evarestov, 1965; Victor *et al.*, 1967; Drake *et al.*, 1969; Drake and Dalgarno, 1970; Epstein, 1970; Martin *et al.*, 1974b, 1975; Oddershede *et al.*, 1975; Jørgensen *et al.*, 1978b). The dynamic polarizability tensor describes the energy change of a system caused by a time-varying external electric field, and the time-dependent and coupled Hartree–Fock methods (identical to the first-order polarization propagator method) are thus well suited for the calculation of this property (Dalgarno and Victor, 1966; Epstein and Lipscomb, 1970).

By using the propagator formalism, Linderberg and Öhrn (1973) have shown that the frequency-dependent polarizability is proportional to the negative value of the density fluctuation function defined in Eq. (9). This follows from Eq. (9) if, for example, we replace $\hat{\rho}$ by the dipole operator, $\hat{\mathbf{r}} = (\hat{x}, \hat{y}, \hat{x})$, and take the real and imaginary part of the $\langle\langle\hat{\mathbf{r}};\, \hat{\mathbf{r}}\rangle\rangle_E$ propagator

$$
\begin{aligned}
\operatorname{Re} \tfrac{1}{3} \operatorname{Tr}\langle\langle\hat{\mathbf{r}}; \hat{\mathbf{r}}\rangle\rangle_E &= -\frac{2}{3} \sum_{M \neq 0} \frac{\langle 0|\hat{\mathbf{r}}|M\rangle \cdot \langle M|\hat{\mathbf{r}}|0\rangle}{\omega_{0M}^2 - E^2}\, \omega_{0M} \\
&= -\sum_{M \neq 0} \frac{f_{0M}^L}{\omega_{0M}^2 - E^2} = -\alpha^L(E),
\end{aligned}
\tag{76}
$$

$$
\begin{aligned}
\operatorname{Im} \tfrac{1}{3} \operatorname{Tr}\langle\langle\hat{\mathbf{r}}; \hat{\mathbf{r}}\rangle\rangle_E &= -\frac{1}{3} \lim_{\eta \to 0} \sum_{M \neq 0} \left\{\frac{\eta}{(E - \omega_{0M})^2 + \eta^2} + \frac{\eta}{(E + \omega_{0M})^2 + \eta^2}\right\} \\
&\quad \times \langle 0|\hat{\mathbf{r}}|M\rangle \cdot \langle M|\hat{\mathbf{r}}|0\rangle \\
&= -\frac{\pi}{6} \sum_{M \neq 0} \langle 0|\hat{\mathbf{r}}|M\rangle \cdot \langle M|\hat{\mathbf{r}}|0\rangle \\
&\quad \times \{\delta(E - \omega_{0M}) + \delta(E + \omega_{0M})\}.
\end{aligned}
\tag{77}
$$

Equations (76) and (77) are readily recognized as the standard expressions for the real and imaginary part of the symmetric component of the frequency-dependent polarizability in the length formulation (Hirschfelder *et al.*, 1954). The operator $\hat{\mathbf{r}}$ is defined as [see Eq. (12)]

$$\hat{\mathbf{r}} = \sum_{ij} \mathbf{r}_{ij} a_i^+ a_j = \sqrt{2}\,(\mathbf{r}, \mathbf{r})\begin{pmatrix} {}^1\mathbf{Q} \\ {}^1\mathbf{Q}^+ \end{pmatrix}, \tag{78}$$

where ${}^1\mathbf{Q}$ and $\mathbf{r}$ are row vectors with elements ${}^1Q_{a\alpha}$ and $r_{a\alpha}$, respectively[2]. The singlet particle-hole operators are defined in Eq. (20). Introducing Eq. (78) into Eq. (76) gives

$$\alpha^L(E) = -\frac{2}{3}\,(\mathbf{r}, \mathbf{r})\ {}^1\mathbf{P}(E)\begin{pmatrix} \tilde{\mathbf{r}} \\ \tilde{\mathbf{r}} \end{pmatrix}, \tag{79}$$

where ${}^1\mathbf{P}(E)$ is the singlet component of the polarization propagator defined in Eq. (19). Similar expressions can be derived for the polarizability in the dipole velocity and in the mixed or $\hat{\mathbf{p}}\hat{\mathbf{r}}$ (Hansen, 1967) representation (Jørgensen *et al.*, 1978a).

The frequency-dependent polarizability can thus be calculated *directly* from the propagator by evaluating ${}^1\mathbf{P}(E)$ at the frequency, E_0, at which the polarizability is wanted. Depending on the level of sophistication of ${}^1\mathbf{P}(E_0)$, Eq. (79) yields $\alpha^L(E_0)$ without correlation, with first-order correlation, etc. [see Eqs. (61) and (62) and Table II]. No sum-over-states is required, but a truncation of the number of excitations included in the calculation of ${}^1\mathbf{P}(E_0)$ is equivalent to a truncation of the sum-over-states in Eq. (76). It is also possible to compute all individual excitation energies and oscillator strengths, as discussed in Section III,A and then perform the sum-over-states in Eq. (76). For TDHF and lower order approximations, this is straightforward and as simple as the direct evaluation from the polarization propagator. However, for higher order methods where energy-dependent matrix elements appear in the propagator, this approach becomes very clumsy and time-consuming and is not as accurate as a direct calculation.

Typical examples of results for $\alpha(E)$ can be found in Jørgensen *et al.* (1978b), and we have, as an illustration, plotted in Fig. 2 the isotropic part of the frequency-dependent polarizability for CH^+ calculated at two levels of approximation. The results using various formulations for $\alpha(E)$ (length, mixed, and velocity) cannot be distinguished with the scale used in Fig. 2. We have used a basis set consisting of 45 Slater-type orbitals (STO's) (Oddershede *et al.*, 1977). The TDHF (coupled HF) and the second-order

---

[2] The last equal sign in Eq. (79) is actually not strictly valid since we are omitting hole–hole, $a_\alpha^+ a_\beta$, and particle–particle, $a_a^+ a_b$, terms. These terms do not contribute to the first-order polarizability, but will enter beyond first order (Dalgaard, 1978) and we are presently investigating the sizes of these contributions to $\alpha(e)$ in a second-order theory.

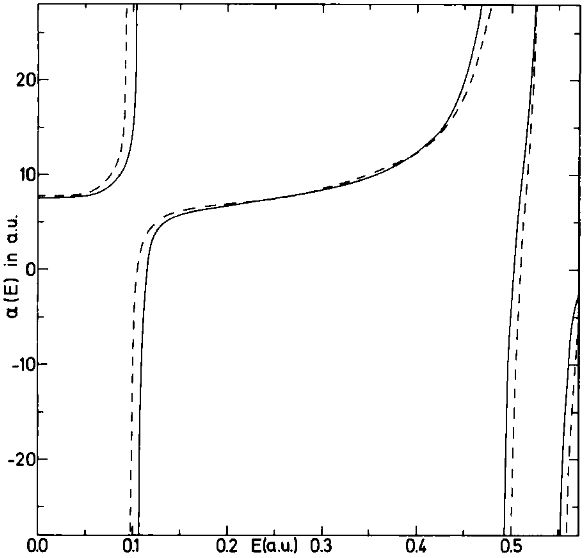

Fig. 2. The isotropic component of the dynamic polarizability for the $X^1\Sigma^+$ ground state of CH^+ calculated in the coupled HF (dashed curve) and the second-order polarization propagator approximation (solid curve).

curves follow each other closely except in regions close to an excitation threshold. The improvement in the SOPPA results near an excitation threshold is caused by the fact that the polarizability in this region is very sensitive to the position of the poles of the propagator, and the second-order polarization propagator gives a better description of the excitation spectrum (see Table VII). For other atoms and molecules, e.g., He, CO, and FH, this effect is much more pronounced (Jørgensen *et al.*, 1978b). The first pole for $\alpha(E)$ corresponds to the weak $X^1\Sigma^+$-$A^1\Pi$ transition ($f \approx 0.01$) and the second pole to the stronger ($f \approx 0.3$)$X^1\Sigma^+$-${}^1\Sigma^+(2)$ transition, and this intensity change is the reason for the difference in the derivative of $\alpha(E)$ in the neighborhood of the poles [cf. the discussion following Eq. (69)].

No experimental data on CH^+ polarizabilities have been reported in the literature, but it is our experience from calculations on similar systems (Jørgensen *et al.*, 1978b) that even though the changes from coupled HF to SOPPA in general are small, the latter results are always closer to the experimental results. In Table XIII, we compare our results for CH^+ with the TDHF calculation of $\alpha(0)$ by Watson *et al.* (1976). The difference between the length and velocity TDHF values for $\alpha_\perp$ (and α) in the present calculation is somewhat larger than normally found in this type of calculations (Oddershede *et al.*, 1975; Jørgensen *et al.*, 1978b), indicating the limitations of the present basis set (Harris, 1969). Even though the

TABLE XIII

STATIC POLARIZABILITIES FOR CH^+[a]

	Coupled Hartree–Fock						
			This calculation		SOPPA		
Parameter	Watson *et al.* (1976)	TM[b]	Length	Velocity	Length	Mixed	Velocity
$\alpha_{\parallel}$	8.68	6.53	7.98	8.04	7.91	8.03	8.21
$\alpha_{\perp}$	7.78	5.43	7.65	8.48	7.38	7.30	7.27
α	8.08	5.80	7.76	8.33	7.56	7.54	7.58

[a] In units of a_0^3.

[b] Minimum basis SCF calculation by Teixeira-Dias and Murrell (1970).

lowest transition in CH^+ is rather weak ($f \approx 0.01$), its excitation energy is also small (≈ 0.095 Hartree), which means that it gives an appreciable contribution to $\alpha_{\perp}$ in Table XIII. This transition is difficult to describe due to the small oscillator strength, and the deviation between $\alpha_{\perp}$ in length and velocity can be traced to a difference of 0.65 a.u. in the contribution from this weak transition.

B. Verdet Constants and Related Properties

A variety of macroscopic optical properties are related to the molecular frequency-dependent polarizability (see, e.g., Victor and Dalgarno, 1969; Langhoff, 1972; Ford and Browne, 1973; Zeiss and Meath, 1977). The *index of refraction*, $n(E)$, is obtained from $\alpha(E)$ through the Clausius–Mosotti relation (Hirschfelder *et al.*, 1954)

$$\frac{n^2(E) - 1}{n^2(E) + 2} = \tfrac{4}{3}\pi N\alpha(E), \tag{80}$$

where N is the number density of atoms or molecules. For gases, for which $n(E) \approx 1$, Eq. (80) reduces to

$$n(E) - 1 = 2\pi N\alpha(E). \tag{81}$$

Experimental values for the frequency-dependent polarizability are often obtained from measurements of $n(E)$ using the foregoing relations (P. L. Smith *et al.*, 1976).

From the anisotropy, i.e., the difference between the parallel, $\alpha_{\parallel}(E)$, and perpendicular, $\alpha_{\perp}(E)$, components of the polarizability,

$$\gamma(E) = \alpha_{\parallel}(E) - \alpha_{\perp}(E); \qquad \alpha(E) = \tfrac{1}{3}[\alpha_{\parallel}(E) + 2\alpha_{\perp}(E)], \tag{82}$$

it is possible to compute *Rayleigh scattering cross sections* (Dalgarno and Williams, 1962; Woodward, 1967),

$$\sigma(E) = \frac{128\pi^5}{9\lambda^4}\{3\alpha^2(E) + \tfrac{2}{3}\gamma^2(E)\}, \tag{83}$$

and the corresponding *Rayleigh depolarization ratio*,

$$\rho(E) = \frac{6\gamma^2(E)}{45\alpha^2(E) + 7\gamma^2(E)}. \tag{84}$$

Both $\sigma(E)$ and $\rho(E)$ are defined for unpolarized incident light. For molecules, equivalent expressions can be derived for plane-polarized incident light (Woodward, 1967; Ford and Browne, 1973). Expressions identical to Eqs. (83) and (84) hold for intensities and depolarization ratios in *Raman spectra*, provided $\alpha(E)$ and $\gamma(E)$ are replaced by their derivatives with respect to the normal coordinates for the vibrational modes in question (Woodward, 1967; Chantry, 1971).

A magnetic field applied parallel to the direction of propagation of incident light produces a rotation of the plane of polarization [the Faraday effect (Serber, 1932; Van Vleck, 1932)] and the angle of rotation is proportional to the magnetic field and the *Verdet constant*. This constant is determined from the energy derivative of $n(E)$, and for atoms in the gas phase it is given approximately by the Becquerel (1897) formula

$$V(E) = \frac{\pi e N}{mc^2} E \frac{d\alpha(E)}{dE}. \tag{85}$$

For molecules for frequencies far from excitation thresholds, Serber (1932) showed that Eq. (85) should be modified to

$$V(E) = r \frac{\pi e N}{mc^2} E \frac{d\alpha(E)}{dE}, \tag{86}$$

where r is an empirical, frequency-independent factor that varies between 1 (central field) and 0.5 (axial field). This means that the dispersion of the Faraday rotation is given by the Becquerel formula for molecules as well as atoms. According to Eqs. (79) and (86), $V(E)$ is proportional to the derivative of the polarization propagator, i.e., proportional to

$$\begin{aligned}\frac{d\mathbf{P}(E)}{dE} = -\mathbf{P}(E)\left\{\begin{matrix} 1 + \tilde{\mathbf{C}}(E\mathbf{1} - \mathbf{D})^{-2}\mathbf{C} \\ -\mathbf{C}^*(E\mathbf{1} + \mathbf{D}^*)^{-2}\mathbf{G} - \mathbf{G}^+(E\mathbf{1} - \mathbf{D})^{-2}\mathbf{C} \end{matrix}\right. \\ \left.\begin{matrix} -\tilde{\mathbf{C}}(E\mathbf{1} - \mathbf{D})^{-2}\mathbf{G}^* - \tilde{\mathbf{G}}(E\mathbf{1} + \mathbf{D}^*)^{-2}\mathbf{C}^* \\ -\mathbf{1} - \mathbf{C}^+(E\mathbf{1} + \mathbf{D}^*)^{-2}\mathbf{C} \end{matrix}\right\}\mathbf{P}(E),\end{aligned} \tag{87}$$

where we have used the third-order expression for the propagator in Eq. (61). Inserting Eq. (87) in Eqs. (79) and (86) gives an expression for *direct* evaluation of the Verdet constant in the dipole length approximation, and similar expression can be derived in the mixed and velocity formulations (Jørgensen *et al.*, 1978a). Numerical applications of these formulas have been reported by Jørgensen *et al.* (1978b). We find that the second-order polarization propagator approximation reproduces the experimental dispersion (Ingersoll and Liebenberg, 1954, 1956, 1958) of the Verdet constants for both the He atom and the CO molecule but that the absolute value for He is off by a few percent. The improvement from TDHF to SOPPA is, however, more pronounced for Verdet constants than for the corresponding dynamic polarizabilities (see Section IV,A), indicating that the dispersion of $\alpha(E)$ is better than its absolute size.

C. Energy-Weighted Sum Rules

The energy-weighted oscillator strength sum rules, or moments, are defined as

$$S(k) = \sum_{M \neq 0} f_{0M}\,\omega_{0M}^{k}, \tag{88}$$

where ω_{0M} and f_{0M} are given in Eqs. (11) and (70)–(71), respectively. For a linear molecule, $S(k)$ can be decomposed into a parallel ($\|$) and a perpendicular component ($\perp$). The sum rules are *static* quantities, but they are also of importance for calculation of dynamic properties such as the polarizability. For frequencies well below the first excitation threshold, $\alpha(E)$ is related to $S(k)$ through the expansion

$$\alpha(E) = \sum_{k=0}^{\infty} S(-2k-2)E^{2k}. \tag{89}$$

This relation is often used to determine "experimental" moments from measured refractive indices and Verdet constants (Langhoff and Karplus, 1969; Langhoff, 1972) but can, of course, also be used to compute $\alpha(E)$ from the moments.

A variety of important static properties of atomic and molecular systems can be calculated from the oscillator strength sum rules. Comprehensive reviews of this subject have been given by Levinger (1960) and Hirschfelder *et al.* (1964), and we shall restrict ourselves to mentioning a few examples. The Reiche–Thomas (1925)–Kuhn (1925) sum rule stating that

$$S(0) = N, \tag{90}$$

where N is the number of electrons in the system, is important because it can be used to check the internal consistency of a model (Harris, 1969) or a numerical calculation (Oddershede *et al.*, 1975). Other consistency relations require that $S(3)$ must be infinite for an S-state wavefunction and that $S(-3)$ must be the norm of the first-order perturbed wavefunctions (Vinti, 1932; Hirschfelder *et al.*, 1964). The mean excitation energies, $I(k)$, for passage of fast particles through matter are also given in terms of the oscillator strength distributions (Inokuti, 1971; Ford and Browne, 1973),

$$I(k) = \sum_{M \neq 0} \omega_{0M}^{k} f_{0M} S^{-1}(k) \ln(\omega_{0M}). \tag{91}$$

Parameter $I(0)$ is important in the Bethe (1930) theory of the stopping of high-velocity charged particles in gases, and Dalgarno and Stewart (1960) have determined this quantity for several atomic gases.

Thus, the calculation of oscillator strength sum rules is the basic problem in explaining several interesting physical phenomena. We have recently shown how the *even* sum rules, $S(2k)$, can be obtained from the zero-energy limit ($k \leq 0$) and the infinity-energy limit ($k \geq 0$) of the polarization propagator (Jørgensen *et al.*, 1978a). By differentiating the spectral representation of the propagator in Eq. (9) and comparing Eqs. (70) and (88), we find that ($k \geq 0$)

$$S^{L}(2k) = (-1)^{k} 2^{-k} (k!)^{-1} \lim_{E \to \infty} \left(E^{3} \frac{d}{dE} \right)^{k} E^{2} \tfrac{1}{3} \operatorname{Tr} \langle\langle \hat{\mathbf{r}}; \hat{\mathbf{r}} \rangle\rangle_{E}, \tag{92}$$

$$S^{L}(-2k-2) = -2^{-k} (k!)^{-1} \lim_{E \to 0} \left(\frac{1}{E} \frac{d}{dE} \right)^{k} \tfrac{1}{3} \operatorname{Tr} \langle\langle \hat{\mathbf{r}}; \hat{\mathbf{r}} \rangle\rangle_{E}, \tag{93}$$

and similar relations in the dipole velocity and mixed representation (Jørgensen *et al.*, 1978a). By using the relation between $\langle\langle \hat{\mathbf{r}}; \hat{\mathbf{r}} \rangle\rangle_{E}$ and ${}^{1}\mathbf{P}(E)$ [see Eqs. (78) and (79)] and the explicit expression for ${}^{1}\mathbf{P}(E)$, e.g., in Eq. (62), we obtain closed expressions for the even sum rules in terms of the matrices **A**, **B**, **C**, and **D**, provided suitable expansions are used for ${}^{1}\mathbf{P}(E)$ for large and small arguments. It is not necessary to evaluate the individual oscillator strengths and excitation energies that enter in $S(2k)$. The explicit expressions for the sum rules are given by Jørgensen *et al.* (1978a), and we will here repeat only a few of the simplest relations, all referring to the second-order polarization propagator.

The Reiche–Thomas–Kuhn sum rule in Eq. (90) takes the form

$$S^{\mathrm{L}}(0) = \tfrac{4}{3} \operatorname{Tr} \mathbf{r}(\mathbf{A} - \mathbf{B})\tilde{\mathbf{r}}, \tag{94}$$

$$S^{\mathrm{M}}(0) = -\frac{4i}{3} \operatorname{Tr} \mathbf{p}\tilde{\mathbf{r}}, \tag{95}$$

$$S^{\mathrm{V}}(0) = -\tfrac{4}{3} \operatorname{Tr} \mathbf{p}(\mathbf{A} - \tilde{\mathbf{C}}\mathbf{D}^{-1}\mathbf{C} - \mathbf{B})^{-1}\tilde{\mathbf{r}}, \tag{96}$$

in the three formulations, respectively. The **p** is the momentum vector array defined in analogy with **r** in Eq. (78). The length formula involves only the matrices **A** and **B**, whereas $S^V(0)$ requires knowledge of all second-order matrices but only in the combination obtained by putting $E = 0$ in the 2p – 2h term in Eq. (61). Thus, $S^L(0)$ can be determined from SOPPA *without* 2p – 2h corrections, and $S^V(0)$ from SOPPA where $E = 0$ in the 2p – 2h term, i.e., no iterative calculation is necessary (see Section III,A). The most interesting of the three expressions in Eqs. (94)–(96) is, however, the mixed expression that does not at all depend on the approximation level for the propagator but only on the basis set used in the calculation. This suggests that fulfillment of $S^M(0) = N$ could be used as a criterion for choice of basis set. This relation has also been proven by Hansen and Bouman (1977) for the single-transition (STA), SECI, and TDHF approximations, whereas they disagree with our finding for the second-order theory (HRPA).[3]

Examples of typical results obtained for $S(0)$ are given in Table XIV. The SECI approximation gives large deviations among the various formulations, whereas close agreement is found in TDHF. For complete basis sets the Reiche–Thomas–Kuhn sum rule should be fulfilled exactly in TDHF (Harris, 1969; Jørgensen and Linderberg, 1970) but not necessarily in SOPPA (Harris, 1969; Jørgensen and Linderberg, 1970; Jørgensen and Oddershede, 1972; Hansen and Bouman, 1977). The deviation of $S(0)$ from 2 in SOPPA for He is probably a consequence of this difference between SOPPA and TDHF approximations, whereas the difference between the exact and approximate results for the other atoms and molecules mostly reflects the limitations of the basis sets. Since all excitations, both discrete and continuum, are weighted equally in $S(0)$, this sum rules is hard to satisfy in finite basis sets, mainly due to an unsatisfactory description of the continuum states. This means that Eq. (90) is a good and relevant test of the quality of the wavefunction if we calculate properties that depend on the whole spectrum. If we are interested only in the bound-state properties (see, e.g., Section III,C), it is better to choose basis sets that give good agreement among the various formulations of the negative sum rules, $S(-2)$, $S(-4)$, etc.

Expressions similar to Eqs. (94)–(96) can be found for other simple energy-weighted sum rules, such as the static polarizability [$S(-2)$] and $S(2)$. We find that $S^V(2)$, like $S^L(0)$, can be calculated from **A** and **B** alone and that $S^L(-2)$ only requires knowledge of the frequency-dependent part of the 2p – 2h matrix (Jørgensen *et al.*, 1978a).

The rotatory strengths (Moscowitz, 1965) (in the length formulation),

---

[3] This disagreement might be explained by the absence in the present theory of the terms mentioned in footnote 2.

TABLE XIV

THE REICHE–THOMAS–KUHN SUM RULE, EQ. (90), FOR OSCILLATOR STRENGTHS IN THE DIPOLE LENGTH (l), MIXED (m), AND VELOCITY (v) FORMULATION

System (basis set) approximation[a]	$S_{\perp}(0)$			$S_{\parallel}(0)$			$S(0)$		
	l	m	v	l	m	v	l	m	v
He (48 STO's)									
SECI	—	—	—	—	—	—	2.17	2.00	1.84
TDHF	—	—	—	—	—	—	2.00	2.00	2.00
SOPPA	—	—	—	—	—	—	2.06	2.00	1.98
Exact	—	—	—	—	—	—	2	2	2
Be (38 STO's)									
SECI	—	—	—	—	—	—	4.88	3.97	3.42
TDHF	—	—	—	—	—	—	4.01	3.97	4.00
SOPPA	—	—	—	—	—	—	4.42	3.97	3.84
Exact	—	—	—	—	—	—	4	4	4
CH^+ (45 STO's)									
SECI	7.05	5.86	6.12	6.30	5.84	5.51	6.80	5.85	5.25
TDHF	5.88	5.86	5.87	5.85	5.84	5.87	5.87	5.85	5.87
SOPPA	6.14	5.86	5.78	6.09	5.84	5.85	6.12	5.85	5.80
Exact	6	6	6	6	6	6	6	6	6
FH (45 STO's)									
SECI	9.98	8.46	7.41	11.80	9.76	8.39	9.90	8.89	7.74
TDHF	8.52	8.46	8.57	9.77	9.76	9.89	8.94	8.89	9.01
SOPPA	9.03	8.46	8.48	10.38	9.76	9.88	9.48	8.89	8.95
Exact	10	10	10	10	10	10	10	10	10

[a] Abbreviations are defined in the text.

$$R_{0M} = \langle 0|\hat{\mathbf{r}}\times\hat{\mathbf{p}}|M\rangle \cdot \langle M|\mathbf{r}|0\rangle, \tag{97}$$

describe the difference between the absorption of left and right circularly polarized light, and the energy-weighted sum rules of these quantities play an important role in the theory of optical activity. The most well-known is the Condon (1937) sum rule stating that

$$\sum_{M\neq 0} R_{0M} = 0. \tag{98}$$

However, other very useful relations for higher sum rules have recently been derived by Hansen (1977) and Caldwell (1977). The propagator expressions for these sum rules are identical to those given for the oscillator strength sum rules, e.g., in Eqs. (94)–(96) except that **r** and **p** must be replaced by equivalent expressions for rotatory strengths.

D. Indirect Nuclear Spin–Spin Coupling Constants

Magnetic response phenomena described by second-order perturbation theory (Swanstrøm and Hegelund, 1975) can be obtained directly from the polarization propagator by means of relations similar to those used for electric response properties (Sections IV,A and B). Several static magnetic properties and their relation to propagator theory have been treated in Chapter 13 of the textbook by Linderberg and Öhrn (1973), and here we shall only mention one such quantity, namely the indirect nuclear spin–spin coupling constant.

The indirect nuclear spin–spin coupling is observed in high-resolution NMR spectra as the field-independent splitting of the NMR lines. Physically the energy shift originates from the indirect electron-coupled interaction between two (or more) nuclear spins and it is conventionally expressed as (Kowalewski, 1977)

$$\Delta E = \sum_{N>N'} \mathbf{I}_N \mathbf{J}_{NN'} \mathbf{I}_{N'}, \tag{99}$$

where $\mathbf{J}_{NN'}$ is the spin–spin coupling tensor. In nonviscous NMR experiments only the isotropic part of $\mathbf{J}_{NN'}$, i.e., the spin–spin coupling constant $J_{NN'}$, is measured. Following the original formulation by Ramsey (1953), we will assume that the most important contribution to the spin–spin coupling constant originates from the Fermi (1930) contact Hamiltonian, which may be written as (Oddershede and Linderberg, 1971)

$$H_F(N) = \sum_{ij} t_{ij}^N \, {}^3Q_{ij}^+ I_N, \tag{100}$$

where

$$t_{ij}^N = \frac{4\sqrt{2}\pi}{3} g\beta h\gamma_N u_i^*(\mathbf{R}_N) u_j(\mathbf{R}_N), \tag{101}$$

The triplet excitation operator ${}^3Q_{ij}^+$ is defined in Eq. (20) and $u_i(\mathbf{R}_N)$ is the amplitude of molecular orbital u_i at the position of nucleus N. According to Ramsey (1953),

$$I_N J_{NN'} I_{N'} = \sum_{M \neq 0} \frac{\langle 0|H_F(N)|M\rangle\langle M|H_F(N')|0\rangle + \text{compl. conj.}}{E_0 - E_M}. \tag{102}$$

Due to the appearance of ${}^3Q_{ij}^+$ in Eq. (100), the sum-over-states in Eq. (102) runs over all triplet excited states. Comparing Eqs. (9) and (102), the latter expression is readily recognized as the frequency-independent part of the $\langle\langle H_F(N); H_F(N')\rangle\rangle_E$ propagator, and, in analogy with the formulations that led to Eq. (79) for the polarizability, we find that (Oddershede *et al.*, 1975, 1977; Jørgensen, 1975);

$$J_{NN'} = 2(\mathbf{t}^N, \mathbf{t}^N)\, {}^3\mathbf{P}(E=0) \begin{pmatrix} \bar{\mathbf{t}}^{N'} \\ \bar{\mathbf{t}}^{N'} \end{pmatrix}, \tag{103}$$

where $\mathbf{t}^N$ is a vector array with elements $t^N_{a\pi}$. By using the *third-order* expression for the triplet polarization propagator (61), we find that

$$J_{NN'} = -4\mathbf{t}^N(\mathbf{A} - \tilde{\mathbf{C}}\mathbf{D}^{-1}\mathbf{C} - \mathbf{B} + \tilde{\mathbf{C}}\mathbf{D}^{-1}\mathbf{G} + \tilde{\mathbf{G}}\mathbf{D}^{-1}\mathbf{C})^{-1}\tilde{\mathbf{t}}^{N'} \quad (104)$$

which is the final expression to be used for *direct* evaluation of coupling constants.

We have used this expression to perform *ab initio* calculations of spin–spin coupling constants for a few diatomic molecules at various levels of approximation (Oddershede *et al.*, 1975, 1977c). We investigated three important issues, namely (i) Is it possible to truncate the sum-over-states in Eq. (102)?; (ii) How important are correlation effects?; and (iii) How large are the basis set effects? The numerical examples can be found in Oddershede *et al.* (1977), and we will here summarize only the conclusions. Even though the sum-over-states apparently has been eliminated in Eq. (102), it is concealed in the size of the matrix problem. By using successively larger and larger matrices, we can examine the effect of truncations in the sum-over-states. We find that the truncation according to the size of the triplet excitation energies may lead to meaningless results due to extremely large variations in the density on the magnetic nuclei [see Eq. (101)]. For example, for the HD molecule, the whole contribution to J_{HD} originates (for all basis sets) from the two transitions with the largest excitation energy (see Fig. 1 in Oddershede *et al.*, 1977).

Depending on the orders of the individual **A**, **B**, etc., matrices in Eq. (104), it is possible to calculate $J_{NN'}$ through zeroth, first, etc., order in the electronic repulsion (see Table II). The coupling constants calculated in the second-order approach are about 40% higher than the uncorrelated results, but the first-order (coupled HF) coupling constants are often more than 100% higher than the uncorrelated results and, in general, in very poor agreement with experiments (Oddershede *et al.*, 1977). This problem is connected with the possible triplet instability of the RPA solution (see the discussion in Section II,B). The coupled HF approximation (Pople *et al.*, 1967, 1968) has been the most widely used method for calculating the spin–spin coupling constants (Kowalewski, 1977). The reason for its unquestionable success is probably that some of the inherent problems discussed in the foregoing have been removed by the semiempirical parametrization proposed by Pople *et al.* (1967, 1968). *Ab initio* calculations with this method have also previously been shown to give very unsatisfactory results (Ostlund *et al.*, 1969).

For basis sets of "double zeta plus polarization function" quality, the variations of the coupling constant with the size of the basis set are not as dramatic as those caused, e.g., by truncation in the sum-over-states. However, it is in a sense more serious since the changes (about ±25%) are very unpredictable and elimination of those changes requires that the basis sets must be so large that the computational effort needed to evaluate coupling-coupling constants, even for small systems, becomes too large.

Thus, the indirect nuclear spin–spin coupling constants are one of the most difficult properties to calculate. The critical dependence on the density at the magnetic nuclei makes them very sensitive to the local quality of the wavefunction. Perhaps a new representation of the Fermi contact operator with the finite size of the nuclear taken into account is needed. It can safely be stated that *ab initio* calculation of the contact contribution to the spin–spin coupling constant is still in its infancy and new approaches are required. It will take some time before the calculation of coupling constants of interest to experimentalists can progress beyond the "semiempirical age."

V. Ground-State Correlation Energies

A. General Expressions

The ground-state total energy is

$$\begin{aligned} E_0 &= \langle H \rangle \\ &= \sum_{ij} \left\{ h_{ij} + \tfrac{1}{4} \sum_{k} (ij\|kk) \right\} \langle a_i^+ a_j \rangle - \tfrac{1}{4} \sum_{\substack{ij\\kl}} (ij\|kl) \langle a_i^+ a_l a_k^+ a_j \rangle. \end{aligned} \tag{105}$$

Average values are taken with respect to the exact reference state, and the Hamiltonian is given in Eq. (14). By using the relation (16) between the two-electron density matrix and the density fluctuation function, we find

$$\begin{aligned} E_0 = \sum_{ij} &\left\{ h_{ij} + \tfrac{1}{4} \sum_{k} (ij\|kk) + \tfrac{1}{4} \sum_{kl} (ij\|kl) \langle a_k^+ a_l \rangle \right\} \langle a_i^+ a_j \rangle \\ &- \frac{i}{8\pi} \sum_{\substack{ij\\kl}} (il\|kj) \lim_{t \to +0} \int_{-\infty}^{\infty} G_{ij,kl}(E)\, e^{-iEt}\, dE, \end{aligned} \tag{106}$$

where we have introduced the notation

$$G_{ij,kl}(E) \equiv \langle\langle a_i^+ a_j ; a_k^+ a_l \rangle\rangle_E \tag{107}$$

for the components of the density fluctuation function. If the unrestricted summations in the last term in Eq. (106) are divided into summations over occupied and unoccupied Hartree–Fock spin orbitals, we obtain an expression for E_0 in terms of the polarization propagator, Eq. (19). It is, however, convenient to keep E_0 in the form given in Eq. (106). Replacing

$|0\rangle$ by the Hartree–Fock reference state in Eq. (10) gives the following expression for the *zeroth-order* fluctuation function:

$$G^0_{ij,kl}(E) = \delta_{il}\,\delta_{jk}\lim_{\eta\to 0}\left\{\frac{n_l(1-n_k)}{E-\varepsilon_k+\varepsilon_l+i\eta} - \frac{n_k(1-n_l)}{E-\varepsilon_k+\varepsilon_l-i\eta}\right\}, \tag{108}$$

where ε_k is an HF orbital energy and the n_l are HF occupation numbers, i.e., $n_\alpha = 1$ and $n_a = 0$. Adding and subtracting G_0 in Eq. (106) gives

$$\begin{aligned} E_0 = {} & \sum_{ij}\left\{h_{ij} + \tfrac{1}{4}\sum_{k}(ij\|kk) + \tfrac{1}{4}\sum_{kl}(ij\|kl)\langle a_k^+ a_l\rangle\right\}\langle a_i^+ a_j\rangle - \tfrac{1}{4}\sum_{a\alpha}(\alpha\alpha\|aa) \\ & - \frac{1}{4\pi}\sum_{\substack{ij\\kl}}(ij\|kl)\int_0^\infty\{G_{ij,kl}(i\omega) - G^0_{ij,kl}(i\omega)\}\,d\omega. \end{aligned} \tag{109}$$

In the last term, we have replaced the integration along the real axis by an integration over the Coulson (1940) contour (see also Chapter 3 in Linderberg and Öhrn, 1973) and only the integration along the imaginary axis is nonvanishing. This transformation rests on the fact that only poles from the first term in Eq. (108) contribute to the integral in (106).

In the random-phase approximation, average values are taken with respect to the Hartree–Fock ground state (see Section II,B), and the total energy expression (109) reduces to

$$E_0^{\mathrm{RPA}} = E_0^{\mathrm{HF}} - \frac{1}{4\pi}\sum_{\substack{ij\\kl}}(ij\|kl)\int_0^\infty\{G^{\mathrm{RPA}}_{ij,kl}(i\omega) - G^0_{ij,kl}(i\omega)\}\,d\omega, \tag{110}$$

where E_0^{HF} is the Hartree–Fock ground-state energy and $G^{\mathrm{RPA}}(E)$ is given in Eq. (31). Comparison with diagrammatic perturbation theory shows that the expression in Eq. (110) gives the correct form for the ground-state energy, but that the factors on all diagrams are wrong (see Appendix B for details). It has been shown by Sawada (1957), Nozières and Pines (1958a), and Pines (1962) that introduction of an interaction strength parameter, g, will remedy this problem. Thus

$$\Delta E_{\mathrm{RPA}} = -\frac{1}{4\pi}\sum_{\substack{ij\\kl}}\int_0^1 dg(ij\|kl)\int_0^\infty\{G^{\mathrm{RPA}}_{ij,kl}(g;\,i\omega) - G^0_{ij,kl}(i\omega)\}\,d\omega, \tag{111}$$

where all bare interaction matrix elements must be multiplied by g and where we have defined the ground-state correlation energy (Löwdin, 1959) as

$$\Delta E_{\mathrm{RPA}} = E_0^{\mathrm{RPA}} - E_0^{\mathrm{HF}}. \tag{112}$$

Equation (111) is the well-known expression for the ground-state correlation in RPA, given in exactly the same form by Hubbard (1958), McLachlan and

Ball (1964), and Linderberg (1967). An equivalent expression for ΔE^{RPA} in terms of the imaginary part of the inverse, Lindhard (1954), dielectric function, i.e., $\mathrm{Im}(\varepsilon_{\mathrm{RPA}}^{-1})$, has been given by Nozières and Pines (1958a). A detailed comparison between the analytic expression (111) and the diagrammatic perturbation result (Gell-Mann and Brueckner, 1957) is given in Appendix B.

We can now use the explicit form for $\mathbf{G}^{\mathrm{RPA}}(E)$ in Eq. (31) to evaluate ΔE_{RPA}, and we will discuss this procedure in more detail in Section V,B. It is, however, also possible to use a Dyson-like equation for $\mathbf{G}(E)$ (Mattuck, 1976):

$$\mathbf{G}(g; E) = \mathbf{G}^0(E) + \mathbf{G}^0(E)\mathbf{M}(g; E)\mathbf{G}(g; E), \tag{113}$$

where $\mathbf{M}(E)$ is the irreducible vertex part, i.e., a generalization of the particle-hole self-energy defined in Eq. (63). With Eq. (113), ΔE_{RPA} becomes

$$\Delta E_{\mathrm{RPA}} = -\frac{1}{4\pi}\sum_{\substack{ij\\kl}}\int_0^1 dg(ij\|kl)\int_0^\infty \sum_{\substack{mn\\pq}} G^0_{ij,\,mn}(i\omega)M^{\mathrm{RPA}}_{mn,\,pq}(g)G^{\mathrm{RPA}}_{pq,\,kl}(g;\, i\omega)\, d\omega. \tag{114}$$

Under certain simplifying conditions, $\mathbf{G}^{\mathrm{RPA}}(E)$ can be determined in terms of $\mathbf{M}^{\mathrm{RPA}}$ and $\mathbf{G}^0$. We will return to this point in Section V,C.

The energy expression (109) can also be used to evaluate ground-state total energies in methods which go beyond RPA. More general expressions for $\mathbf{G}(E)$ such as those in Eqs. (61) and (62) must then be used. The treatment of the one-electron density matrix in Eq. (109) may, however, pose some problems. It is possible to express the one-matrix in terms of the two-matrix (Jørgensen and Oddershede, 1972), but because of the inconsistency of RPA (see Section II,B), the resulting one-matrix varies substantially depending on which sum rule has been used, thus making this approach less useful. We have previously shown that it is consistent to assume that the metric matrix in SPPA does not change during the iterations (Jørgensen *et al.*, 1974), i.e., it will always be the Hartree–Fock metric matrix. This means that it is also consistent with the iterative scheme to use the Hartree–Fock one-matrix in Eq. (109) for higher RPA methods. With this *approximation*, the resulting expression for the ground-state correlation energy is

$$\Delta E = -\frac{1}{4\pi}\sum_{\substack{ij\\kl}}\int_0^1 dg(ij\|kl)\int_0^\infty \sum_{\substack{mn\\pq}} G^0_{ij,\,mn}(i\omega)M_{mn,\,pq}(g;\, i\omega)G_{pq,\,kl}(g;\, i\omega)\, d\omega. \tag{115}$$

This general expression is very similar to ΔE_{RPA} in Eq. (114). The only difference is that the self-energy now is energy-dependent [see Eqs. (61) and (62)].

B. Application to Atomic and Molecular Systems

From the inverse of the polarization propagators in Eqs. (31), (61), and (62), we find that the corresponding irreducible vertex parts are [cf. Eqs. (63), (108), and (113)]

$$\mathbf{M}^{\mathrm{RPA}}(g) = g\begin{Bmatrix} \mathbf{A}(1) & -\mathbf{B}(1) \\ -\mathbf{B}(1) & \mathbf{A}(1) \end{Bmatrix} \tag{116}$$

$$\mathbf{M}^{(2)}(g; E) = \mathbf{M}^{\mathrm{RPA}}(g) + g^2$$
$$\begin{Bmatrix} \mathbf{A}(2) + \tilde{\mathbf{C}}(1)[E\mathbf{1} - \mathbf{D}(0)]^{-1}\mathbf{C}(1) & -\mathbf{B}(2) \\ -\mathbf{B}(2) & \mathbf{A}(2) + \tilde{\mathbf{C}}(1)[-E\mathbf{1} - \mathbf{D}(0)]^{-1}\mathbf{C}(1) \end{Bmatrix} \tag{117}$$

and similarly in higher orders. For simplicity we have assumed real matrices and we have used the fact that all bare interactions must be multiplied with the interaction strength parameter. The RPA irreducible vertex part is thus proportional to g. Since the leading term in $\mathbf{G}$ is $\mathbf{G}^0$ [see Eq. (113)], which is independent of g, we find from Eqs. (111) and (114) to *first nonvanishing order* in the interaction parameter that

$$\Delta E_{\mathrm{RPA}} \cong -\frac{1}{8\pi}\sum_{\substack{ij\\kl}} (ij\|kl) \int_0^\infty \{G^{\mathrm{RPA}}_{ij,\,kl}(g = 1; i\omega) - G^0_{ij,\,kl}(i\omega)\}\, d\omega. \tag{118}$$

By introducing the spectral representation for the RPA propagator, Eq. (28), and using the normalization condition for the eigenvectors, Eq. (29), we obtain

$$\Delta E_{\mathrm{RPA}} = -\tfrac{1}{4}\sum_{\substack{\alpha\beta\\ab}} \{(\alpha a\|\beta b)(\mathbf{Y}\mathbf{Z}^+)_{a\alpha,\,b\beta} + (ab\|\alpha\beta)(\mathbf{Y}\mathbf{Y}^+)_{a\alpha,\,b\beta}\}. \tag{119}$$

The last term is of second order in the "small" eigenvector component and therefore small compared with the first term (Oddershede and Jørgensen, 1977a), and

$$\Delta E_{\mathrm{RPA}} \cong -\tfrac{1}{4}\sum_{\substack{\alpha\beta\\ab}} (\alpha a\|\beta b)(\mathbf{Y}\mathbf{Z}^{-1})_{a\alpha,\,b\beta}\,. \tag{120}$$

We have also taken into consideration that the difference between $\mathbf{YZ}^+$ and $\mathbf{YZ}^{-1}$ is of third order in $\mathbf{Y}$ [see the discussion following Eq. (35)]. The electron-repulsion integral in Eq. (120) is $\mathbf{B}(1)$, i.e., the RPA value for the $\mathbf{B}$ matrix (Jørgensen and Linderberg, 1970). From the RPA eigenvalue problem, Eq. (28), or from the explicit relations between **Z**, **Y**, **A**, and **B** matrices (Jørgensen and Linderberg, 1970), we find that

$$-\sum_{\substack{\alpha\beta \\ ab}} \mathbf{B}(1)_{a\alpha,\, b\beta}(\mathbf{YZ}^{-1})_{a\alpha,\, b\beta} = \sum_{M} \omega_M^{\mathrm{RPA}} - \sum_{a\alpha} \mathbf{A}(1)_{a\alpha,\, a\alpha}, \tag{121}$$

where ω_M^{RPA} are the RPA excitation energies. The last term is the sum of the SECI excitation energies, and the final expression for ΔE^{RPA} is thus

$$\Delta E_{\mathrm{RPA}} = \tfrac{1}{4} \sum_{M \neq 0} \{\omega_M^{\mathrm{RPA}} - \omega_M^{\mathrm{SECI}}\}. \tag{122}$$

This is the correlation energy expression given by McLachlan and Ball (1964). They found ΔE_{RPA} by assuming that the elementary RPA excitation could be treated as a set of harmonic oscillators and that Eq. (122) is the zero-point energy of these oscillators. The argument given by McLachlan and Ball (1964) for preferring a factor of $\frac{1}{4}$ in Eq. (122) instead of $\frac{1}{2}$ is, however, rather loose. The present derivation shows that a factor of $\frac{1}{4}$ appears in ΔE_{RPA} if we solve Eq. (114) through first nonvanishing order in the interaction parameter. The resulting expressions are correct through second order in the electronic repulsion (see Appendix B) but will deviate already in third order from the diagrammatic expression due to the approximate treatment of the g dependence of $\mathbf{G}(E;\, g)$. If we do not at all consider the g dependence of **M** and **G** but instead use Eq. (110) to evaluate ΔE_{RPA}, we would have obtained exactly the same expression as Eq. (122) except that the factor in front would be $\frac{1}{2}$ rather than $\frac{1}{4}$ in which case not even the lowest order term in ΔE_{RPA} would agree with the diagrammatic perturbation expansion. A correct treatment of the g dependence of G would require solution of Eq. (113) which, even in RPA, can be done only approximately [see Section V,C and Linderberg (1964)].

If we keep only the leading term in the interaction strength parameter, the correlation energy in the *second*-order polarization propagator approximation is of the same form as the RPA expression in Eq. (120). The only difference is that the $\mathbf{YZ}^{-1}$ matrix must be calculated from the second-order polarization propagator, Eq. (66), in which case $(\mathbf{YZ}^{-1})_{a\alpha,\, b\beta}$ either is the first-order Rayleigh–Schrödinger coefficient $\kappa(1)_{\alpha\beta}^{ab}$ (in SOPPA) or very close to it (in SPPA with 2p-2h corrections). Thus, using the explicit expression for $\boldsymbol{\kappa}(1)$, we find that

$$\Delta E^{(2)} = -\frac{1}{4} \sum_{\substack{ab \\ \alpha\beta}} \frac{|(\alpha a||\beta b)|^2}{\varepsilon_a + \varepsilon_b - \varepsilon_\alpha - \varepsilon_\beta}. \tag{123}$$

This is the *second-order* polarization propagator expression for the correlation energy. It is derived in the same fashion as the McLachlan and

Ball (1964) formula for ΔE_{RPA} in Eq. (122). It is, furthermore, identical to the second-order Rayleigh–Schrödinger expression for the ground-state correlation energy.

The expression for ΔE_{RPA} given by Fukuda *et al.* (1964) is a combination of the two expressions in Eqs. (122) and (123). Fukuda *et al.* (1964) used the McLachlan and Ball (1964) expression in Eq. (122) with a factor $\frac{1}{2}$ in front rather than $\frac{1}{4}$. In order to obtain an expression correct through second order in perturbation theory, they subtracted the second-order Rayleigh–Schrödinger correlation energy (i.e., $\Delta E^{(2)}$) from this expression.

Expressions (120), (122), and (123) are given in the spin-orbital basis. By using Eq. (20), we find that the corresponding expression in the orbital basis is (Ball and McLachlan, 1964)

$$\Delta E_{\mathrm{RPA}} = \tfrac{1}{4} \sum_{M \neq 0} \sum_{S=0}^{1} (2S+1)\{\omega_M^{\mathrm{RPA}}(S) - \omega_M^{\mathrm{SECI}}(S)\}, \tag{124}$$

where $\omega(0)$ and $\omega(1)$ are the singlet and triplet excitation energies, respectively. We know that $\mathbf{YZ}^+$ in singlet must be equal to $-\mathbf{YZ}^+$ in triplet (see Table I). This means that we can eliminate either the triplet or the singlet two-matrix in the expression for the RPA correlation energy. For example, we can write Eq. (120) as

$$\Delta E_{\mathrm{RPA}} = -\tfrac{1}{2} \sum_{\substack{\alpha\beta \\ ab}} \{(\alpha a|\beta b) + (\alpha b|\beta a)\}\kappa_{\alpha\beta}^{ab}(\mathrm{singl.}), \tag{125}$$

where we have used the explicit expressions for $\mathbf{B}(1)$ in singlet and triplet (Oddershede *et al.*, 1975). In the *special case* of only one occupied orbital, i.e., a two-electron system, Eq. (125) can be simplified even further to

$$\Delta E_{\mathrm{RPA}} = \sum_{M \neq 0} \{\omega_M^{\mathrm{RPA}}(1) - \omega_M^{\mathrm{SECI}}(1)\}. \tag{126}$$

Another equivalent expression for the RPA correlation energy for closed-shell systems has been given by Szabo and Ostlund (1977a,b). Their expression for ΔE_{RPA} is size consistent, i.e., at long range it yields the RPA dispersion force between interacting systems.

Expressions (124) and (125) are in principle identical, but the inconsistency of RPA (see Section II,B) has the effect that the two equations give quite different correlation energies. This is illustrated in Table XV. The large difference between the two last columns is mainly a basis-set effect and is to a lesser extent caused by correlation effects beyond second order in the electronic repulsion (Eggarter and Eggarter, 1978a,b). The RPA results show the same behavior as the individual components of the two-matrix in Table I, namely that ΔE_{RPA} calculated from singlet alone is much closer to the "correct" second-order result. The deviation between the two RPA results

TABLE XV

GROUND-STATE CORRELATION ENERGIES

System (basis set)	RPA (a.u.) Eq. (123)[a]	RPA (a.u.) Eq. (125)[b]	Second-order RS[c] (a.u.)	Exact (a.u.)
He (48 STO's)	−0.0436	−0.0375	−0.0310	−0.0420[d]
H_2 (46 STO's)[e]	−0.0338	−0.0245	−0.0249	−0.0405[f]
FH (45 STO's)[g]	−0.308	–	−0.280	−0.460[h]

[a] Calculated from the singlet and triplet two-matrix.
[b] Calculated from the singlet two-matrix alone.
[c] The second-order Rayleigh–Schrödinger (RS) energy expression.
[d] Hibbert (1975).
[e] At the internuclear separation, $R = 1.40$ bohrs.
[f] Kolos and Roothaan (1960).
[g] At the internuclear separation, $R = 1.733$ bohrs.
[h] Cade and Huo (1967).

is very unsatisfactory. If we use other sum rules for the RPA two-matrix, we may obtain numerical results that are quite different from either of the two results in Table XV. This arbitrariness of the RPA approximation makes it less suitable for total energy calculations and only expressions that depend solely on the singlet two-matrix can be trusted (Adler, 1962; Wiser, 1963; Linderberg, 1964). A better but also more involved approach for calculating RPA total energies has been proposed by Linderberg and Öhrn (1977). They determine a ground state that is consistent with RPA and use this ground state to calculate the total energy, thus eliminating the arbitrariness caused by the approximate N representability of the RPA two-matrix.

C. Application to Metallic Systems

Due to the "infinite" extent of crystalline solids, alternative methods to those discussed in Section V,B must be used for metals. The Coulomb matrix element diverges as $\mathbf{q}^{-2}$, where $\mathbf{q}$ is the momentum difference between the particle and the hole state, and $\mathbf{q}$ can become infinitesimally small due to the large density of states near the Fermi level in metals. This means that all individual (Coulomb) RPA diagrams diverge. The second-order diagram in Fig. 3a diverges logarithmically, and the higher order diagrams have even more serious divergence. The arguments leading to the expression for ΔE_{RPA} in Eq. (118) is thus not applicable to metals. It is impossible to use concepts of "the leading term" when all contributions are infinite! We must instead go back to the exact expressions for ΔE_{RPA}, namely Eqs. (111)–(114).

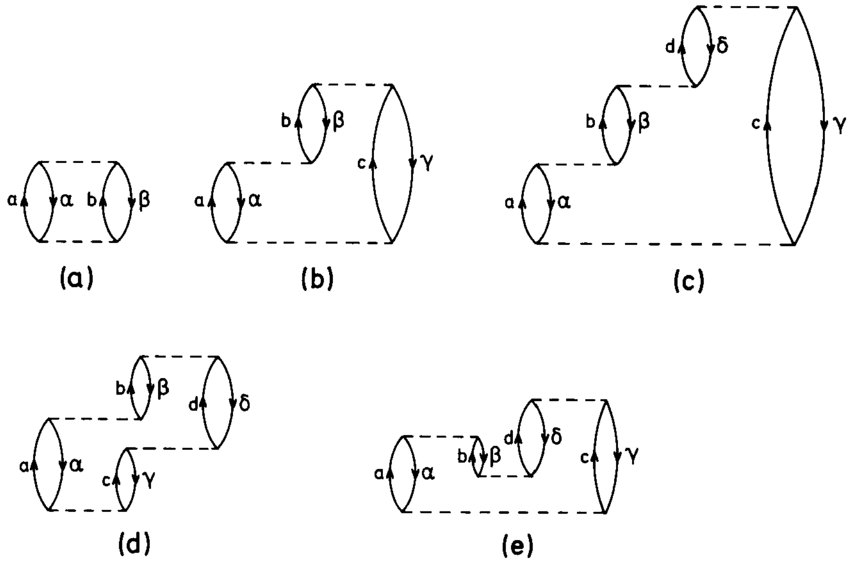

Fig. 3. Second- (a), third- (b), and fourth-order (c–e) energy Diagrams in the random-phase approximation. The convention introduced by Brandow (1967) is used, i.e., the dashed lines represent direct plus exchange interaction.

We will now briefly outline the derivation of an expression for the RPA correlation energy for a real metal. The particle and hole states are Hartree–Fock Bloch functions, and we define

$$\begin{aligned} |\alpha\rangle &= |\mathbf{k}\rangle, \\ |\beta\rangle &= |\mathbf{k}'\rangle, \\ |a\rangle &= |\mathbf{k}+\mathbf{q}\rangle, \\ |b\rangle &= |\mathbf{k}'-\mathbf{q}\rangle, \end{aligned} \tag{127}$$

where **k** and **k**′ are reciprocal lattice vectors inside the Fermi sea; we have made explicit use of momentum conservation. For convenience, the band indices have been suppressed. To repeat the present analysis in the multiband case poses no extra difficulties (Ehrenreich and Cohen, 1959; Monkhorst and Oddershede, 1973; Oddershede, 1978). Let us now consider the **B**(1) block of the RPA self-energy, Eq. (116). An element of the **B**(1) matrix is (Oddershede and Jørgensen, 1977a)

$$\mathbf{B}(1)_{a\alpha,b\beta} = (\mathbf{k}', \mathbf{k}+\mathbf{q}|\mathbf{k}, \mathbf{k}'-\mathbf{q}) - (\mathbf{k}', \mathbf{k}'-\mathbf{q}|\mathbf{k}, \mathbf{k}+\mathbf{q}). \tag{128}$$

The Bloch functions can, e.g. be of the form

$$|\mathbf{k}\rangle = \exp(2\pi i a^{-1}\mathbf{k}\cdot\mathbf{r}) \sum_{p} c_p(\mathbf{k}) \sum_{\mu} \phi_p(\mathbf{r}-a\mu), \tag{129}$$

where, for simplicity, we have assumed a simple-cubic crystal with lattice spacing a. The last sum runs over the whole reciprocal lattice, and p is an orbital index. These Bloch functions are very similar to those normally used in the tight-binding method (Ziman, 1965). In the electron gas model (Mattuck, 1976, p. 94), $|\mathbf{k}\rangle$ is equal to the exponential term alone. It turns out that the Bloch functions in Eq. (129) are particularly useful for *ab initio* band structure calculations of the type proposed by Harris and co-workers (Harris and Monkhorst, 1970; Harris *et al.*, 1973; Harris, 1975). It has been found (Harris *et al.*, 1973; Kumar *et al.*, 1977) that the coefficients $c_p(\mathbf{k})$ in general are weak functions of $\mathbf{k}$. Thus, inserting Eq. (129) into Eq. (128) shows that the last (Coulomb) term in Eq. (128) is almost independent of $\mathbf{k}$ and $\mathbf{k}'$. This is strictly so in the electron gas approximation, but the preceding argument indicates that this is also a good approximation for realistic band functions (Monkhorst and Oddershede, 1973). The first (exchange) term in Eq. (128) varies as $|\mathbf{k} - \mathbf{k}' + \mathbf{q}|^{-2}$. The $\mathbf{A}(1)$ elements entering in the RPA correlation energy beyond second order (see Appendix B) can similarly be divided into a Coulomb and an exchange part. If we now *disregard* all the exchange terms in $\mathbf{M}^{\mathrm{RPA}}(\mathbf{q}, g)$ and use the fact that $G_0(E)$ is diagonal [Eq. (108)], we find from Eq. (113) the following explicit solution for $G^{\mathrm{RPA}}(\mathbf{k}, \mathbf{q}, g; i\omega)$:

$$\int d^3\mathbf{k}\, G^{\mathrm{RPA}}(\mathbf{k}, \mathbf{q}, g; i\omega) = G_I^0(\mathbf{q}; i\omega)[1 - gG_I^0(\mathbf{q}; i\omega)v(\mathbf{q})]^{-1}, \tag{130}$$

where $v(\mathbf{q})$ is the Coulomb matrix, and G_I^0 is the integrated quantity

$$G_I^0(q; i\omega) = \int d^3\mathbf{k}\, G^0(\mathbf{k}, \mathbf{q}; i\omega). \tag{131}$$

If we insert Eq. (130) into Eq. (111) and integrate over the momentum $\mathbf{k}$, then

$$\begin{aligned} \Delta E_{\mathrm{RPA}} = -\frac{1}{2\pi} \int d^3\mathbf{q}\, v(\mathbf{q}) \int_0^1 g\, dg \int_0^\infty G_I^0(\mathbf{q}; i\omega) \\ \times [1 - gG_I^0(\mathbf{q}; i\omega)]^{-1} G_I^0(\mathbf{q}; i\omega) v(\mathbf{q})\, d\omega. \end{aligned} \tag{132}$$

The integration over the interaction strength parameter can now be performed, and we find

$$\Delta E_{\mathrm{RPA}} = \frac{1}{2\pi} \int d^3\mathbf{q} \int_0^\infty d\omega \{\mathrm{v}(\mathbf{q}) G_I^0(\mathbf{q}; i\omega) + \ln[1 - v(\mathbf{q}) G_I^0(\mathbf{q}; i\omega)]\}. \tag{133}$$

This is the standard expression for the correlation energy of a metal in the random-phase approximation *without* exchange (Bohm and Pines, 1953;

Hubbard, 1957; Nozières and Pines, 1958b; Carr and Maradudin, 1964; Singwi *et al.*, 1968; Monkhorst and Oddershede, 1973).

For the electron gas model system, Gell-Mann and Brueckner (1957) used Eq. (133) to find an analytic expression for the correlation energy in terms of the density parameter, r_s (i.e., the average interparticle distance in units of the Bohr radius). The Gell-Mann and Brueckner (1957) expression is only valid at high densities. Hubbard (1957) was the first to give numerical solutions to Eq. (133) for all values of r_s.

The infinite sum of divergent diagrams in Eq. (133) is thus *finite*. This is a numerical fact that may seem somewhat puzzling, and it has to the author's knowledge not yet been proven mathematically that the radius of convergence of the RPA series (see Fig. 3) is different from zero!

In deriving Eq. (133) we assumed that all exchange terms could be ignored. By doing so, we have taken into account the most divergent terms in the RPA series. This is, however, a rather crude approximation. A more accurate calculation shows that the exchange contribution for an electron gas in about 30% of the RPA result without exchange (Freeman, 1977). Gell-Mann and Brueckner (1957) calculated only the lowest order exchange diagram, i.e., the exchange counterpart of Fig. 3a. Hubbard (1957) argued that this would overestimate the importance of exchange and he suggested screening the Coulomb interaction to take into account the effect of exchange. Monkhorst and Oddershede (1973) have shown how the exchange terms can be calculated approximately for a real metal. It is also possible to obtain an expression for the sum of the most divergent exchange-energy diagrams that is of the same form as Eq. (133) (Oddershede, 1978).

Attempts to compute lattice corrections to the electron gas correlation energy are often based on the Hohenberg and Kohn (1964) theorem, stating that the total ground-state energy is a unique function of the charge density of the system. The metal is treated as an "inhomogeneous electron gas," and the correction to the electron gas result is obtained by means of *gradient expansions* of the correlation energy (Kohn and Sham, 1965; Sham and Kohn, 1966; Ma and Brueckner, 1968). This approach has been used extensively within the last few years, and much progress has been made (Rajagopal and Callaway, 1973; Kleinman, 1974; Geldart *et al.*, 1975; Rasolt and Geldart, 1975; Geldart and Rasolt, 1976; Singhal and Callaway, 1976; Rajagopal and Singhal, 1977). We have, however, chosen a different path. We still use Eq. (133) to compute the RPA correlation energy but we use realistic Hartree–Fock Bloch functions rather than plane waves as zeroth-order states. We have applied this method to simple-cubic metallic hydrogen (Monkhorst and Oddershede, 1973) for which accurate Hartree–Fock Bloch functions were available (Oddershede *et al.*, 1974; Kumar *et al.*, 1977). Correlation energies for this system, including contributions from excited

TABLE XVI

COMPARISON BETWEEN RANDOM-PHASE APPROXIMATION CORRELATION ENERGIES FOR SIMPLE CUBIC METALLIC HYDROGEN AND THE ELECTRON GAS

Lattice spacing a (bohrs)	Density parameter r_s	ΔE_{RPA}			
		Metallic hydrogen		Electron gas	
		HF[a]	Hartree[b]	PW[c]	GMB[d]
1.00	0.621	−0.041	−0.056	−0.071	−0.063
2.73	1.694	−0.024	−0.032	−0.053	−0.032
3.50	2.17	−0.020	−0.022	−0.040	−0.024

[a] Using the HF Bloch functions of Kumar *et al.* (1977) as zeroth-order states.

[b] Using zeroth-order states obtained from Kumar *et al.* (1977) by disregarding the exchange term.

[c] Using plane wave (PW) zeroth-order states. Except for a slightly different treatment of the exchange contribution, these correlation energies are identical to the Hubbard (1957) results.

[d] The high-density results of Gell-Mann and Brueckner (GMB) (1957).

bands, are summarized in Table XVI. We see that the lattice corrections give a considerable reduction of the electron gas results and the correlation energy per electron at the HF equilibrium ($a = 2.73$ bohrs) is of the same magnitude as that found for small atoms and molecules (Löwdin, 1959a,b; Clementi, 1963a,b). The shape of the conduction band in metallic hydrogen does not deviate much from that found for other simple metals (Kumar *et al.*, 1977). We believe, therefore, that the trends in Table XVI should be present also in correlation energies of other metallic systems. The band gaps for metallic hydrogen are, however, rather large (Kumar *et al.*, 1977) and the excited band contributions (and thus the *total* correlation energy) may be relatively larger for other metals.

The evaluation of exchange terms is the most time-consuming step in an *ab initio* Hartree–Fock band structure calculation (Harris and Monkhorst, 1971; Harris, 1975). It would, therefore, be computationally advantageous to use band quantities from simple *Hartree* calculations or statistical $X\alpha$-type calculations (Slater, 1951; Gáspár, 1954) to evaluate correlation energies. We have examined this possibility in Table XVI. We find that the effect of neglecting the exchange terms in the zeroth-order states is rather small compared with the total difference between the metallic hydrogen and electron gas correlation energy.

We have now demonstrated how to calculate *total* energies for metals by means of the polarization propagator method. The ground-state energy is, however, of limited value for solid-state physicists. Most interesting physical phenomena are related to the (quasi) one-particle spectrum (Ziman, 1965; Hedin and Lundqvist, 1969). The quasi-particle energies, $\varepsilon(\mathbf{k})$, can be obtained from the total energy by means of the Landau Fermi-liquid theory [for a review, see, e.g., Luttinger and Nozières (1962) and Chapter V in Hedin and Lundqvist (1969)]. Landau's (1956, 1958) key assumption is that the change in the total energy of a Fermi system can be expressed in terms of changes in the occupation numbers, $n(\mathbf{k})$, for the quasiparticles, i.e.,

$$\delta E = \sum_{\mathbf{k}} \varepsilon(\mathbf{k})\, \delta n(\mathbf{k}) \tag{134}$$

or

$$\varepsilon(\mathbf{k}) = \frac{\partial E}{\partial n(\mathbf{k})}. \tag{135}$$

The occupation numbers $n(\mathbf{k})$ must be those corresponding to the quasi-particle spectrum. If we take derivatives with respect to the Hartree–Fock occupation numbers, we exclude the interaction terms in $\varepsilon(\mathbf{k})$. In the random-phase approximation we can use Eq. (133) to estimate this zeroth-order approximation to the quasi-particle spectrum (Rice, 1965). It is, however, possible to use the new one-particle energies to calculate ΔE_{RPA} in Eq. (133) and thus establish an iterative RPA procedure. We have performed an iterative calculation for the electron gas, and we found that the self-consistent band energies varied little from the plane wave solutions. This can be seen, for example, from the fact that the difference between the zeroth-order and self-consistent RPA correlation energy was only 0.04% for $r_s = 0.1$ and 5% for $r_s = 5.0$. Similar small variations will probably be found for real metals.

Appendix A. Bibliography of *ab initio* RPA-like Calculations

This appendix contains a bibliography of *ab initio* atomic and molecular calculations performed with the *direct methods* discussed in the present communication. The coupled Hartree–Fock (CHF) approximation is the most frequently used direct method, and the literature in this area is rather extensive. Lipscomb (1966) has reviewed the CHF calculation of magnetic properties, and Werner and Meyer (1976a,b) have given a comprehensive list of applications of the CHF method to calculation of static polarizabilities for the first-row atoms (Li through Ne) and the molecules FH, CO, H_2O, NH_3, and CH_4. A summary of CHF calculations of various electric and magnetic properties for open shell atoms is provided by Mukherjee *et al.*

(1977). Kowalewski (1977) has recently reviewed the literature on *ab initio* calculations (including CHF calculations) of indirect nuclear spin–spin coupling constants, and Jamieson (1973) has given a review of TDHF calculations on small atoms. We will use these reviews as a "baseline" for the present survey of the literature on direct methods, and the material covered by these articles will not be repeated here.

In Table A-I we list the designations of the methods as given by the respective author(s), but we refer to Table IV for a comparison of the various methods. If calculations are performed at several levels of approximation, only the most advanced method is listed in the table. For basis sets consisting of Gaussian-type orbitals (GTO's) we have used the standard notation that square brackets, [ ], refer to contracted basis sets and parentheses, ( ), refer to uncontracted basis sets. For heteromolecules the functions for the heaviest atom are mentioned first. Floating spherical Gaussians are referred to as FSGO's.

The following shorthand notation is used in the table for the various excitation properties:

$\alpha(0)$	static polarizabilities
$\alpha(\omega)$	frequency-dependent polarizabilities
$V(\omega)$	Verdet constants
$\sigma(\omega)$	Rayleigh scattering cross sections
$\Delta\varepsilon$	vertical excitation energies
f	absorption oscillator strengths and photoionization cross sections
J_{AB}	nuclear spin–spin coupling constants between nuclei A and B
$S(n)$	oscillator strength sum rules
C_6	van der Waals coefficients
σ_N	nuclear magnetic shielding factor.

Appendix B. A Comparison of Analytic with Diagrammatic RPA

In this appendix we will demonstrate the equivalence between the analytic expressions for the RPA ground-state correlation energy [cf. Eqs. (110), (111), (114), (122), and (133) of the text] and the diagrammatic representation. Several authors have discussed the diagrammatic representation of some of the lowest order terms (Gell-Mann and Brueckner, 1957; McLachlan and Ball, 1964), but we treat here all terms through fourth order in the electronic repulsion, i.e., the diagrams in Fig. 3. Among other things, we will show how the "nonforward scattering" (or irregular time-ordered) ring diagrams, of which Fig. 3e is the lowest order term, are generated by the analytic expression (114). We use the diagrammatic rules given by Brandow (1967; see also Chapters 4 and 12 in Mattuck, 1976).

TABLE A-I

System	Method	Basis set	Property	Reference
He	RPA	Numer. V^{N-1}	f	Wendin (1970)
	TDHF	11 STO's	$\alpha(\omega)$, $V(\omega)$, $\Delta\varepsilon$	Epstein (1970)
	RPA	4 STO's	$\alpha(0)$	Gutschick and McKoy (1973)
	RPA	[10s13p]	$\alpha(\omega)$, $V(\omega)$, $\sigma(\omega)$, $\Delta\varepsilon, f$	Martin *et al.* (1974b, 1975)
	CHF	12 STO's	$\alpha(0)$	Fortune and Certain (1974)
	RPA	[10s13p]	$\Delta\varepsilon$, $S(n)$, f (photoioniz.)	Rescigno *et al.* (1974)
	EOM	[12s8p]	Incl. elec. scatt.	McCurdy and McKoy (1974)
	RPA	Numer. HF + WKB	$\alpha(\omega)$, $\Delta\varepsilon, f$	Linderberg and Prato (1974)
	RPA	?	f (photoioniz.)	Yeager *et al.* (1975)
	CHF	numerical method	Multip. polar. and shielding	McEachran *et al.* (1977)
	SOPPA	48 STO's	$\alpha(\omega)$, $V(\omega)$, $\Delta\varepsilon, f$, $S(n)$	Jørgensen *et al.* (1978b)
He series	CHF	4 STO's	$\alpha(\omega)$, $\Delta\varepsilon$	Arrighini *et al.* (1973)
	CHF	5 STO's	$\alpha(0)$	Bhattacharya *et al.* (1975)
	Rel. RPA	Iter. numer. proc.	$\Delta\varepsilon, f$	Johnson and Lin (1976); Johnson *et al.* (1976); Lin *et al.* (1977a,b)
	RPA	Numerical	$\Delta\varepsilon, f$ quadru- and octopole	Aldeen and Jamieson (1977)
Li	RPA	[10s8p]	$\Delta\varepsilon, f$	Yeager and McKoy (1975)
Li series	RPA	Iter. numer. proc.	$\alpha(\omega)$, $\Delta\varepsilon, f$, C_6	Stewart (1975a)
Be	TDHF	12 STO's	$\alpha(\omega)$, $V(\omega)$, $\Delta\varepsilon$	Epstein (1970)
	CHF	28 STO's	$\alpha(0)$	Fortune and Certain (1974)
	SOPPA	50 STO's	$\alpha(\omega)$, $V(\omega)$	Jørgensen *et al.* (1978b)
	SOPPA	50 STO's	$\Delta\varepsilon, f$	Oddershede *et al.* (1978a,b)
Be series	CHF	5 STO's	$\alpha(\omega)$, $\Delta\varepsilon$	Arrighini *et al.* (1973)
	RPA	Iter. num. proc.	$\alpha(\omega)$, $\Delta\varepsilon, f$, C_6	Stewart (1975a)
	RPA	5 STO's	$\Delta\varepsilon, f$	Stewart *et al.* (1975)
	rel. RPA	Iter. num. proc.	$\Delta\varepsilon, f$	Lin and Johnson (1977)

(*continued*)

TABLE A-I (*Continued*)

System	Method	Basis set	Property	Reference
Ne	TDHF	17 STO's	$\alpha(\omega)$, $V(\omega)$, $\Delta\varepsilon$	Epstein (1970)
	RPA	Numer. V^{N-1}	f	Ya'Amusia *et al.* (1971)
	RPA	Iter. num. proc.	$\alpha(\omega)$, $\Delta\varepsilon$, f, σ_N	Stewart (1975b)
	CHF	Numer. partial-wave	$\alpha_{\parallel}(0)$	Christiansen and McCullough (1977)
	CHF	Numer. method	Multipole polar. and shielding	McEachran *et al.* (1977)
Mg	Rel. RPA	Iter. numer. proc.	$\Delta\varepsilon$, f	Shorter *et al.* (1977)
Si	RPA	Numer. HF	f, $\Delta\varepsilon$	Dalgaard (1975)
Ar	RPA	Numer. V^{N-1}	f	Ya'Amusia *et al.* (1971)
	CHF	Numer. method	Multipole polar. and shielding	McEachran *et al.* (1977)
Zn series	Rel. RPA	Iter. numer. proc.	$\Delta\varepsilon$, f	Shorter and Dalgarno (1977)
Kr	RPA	Numer. V^{N-1}	f	Ya'Amusia *et al.* (1971)
Xe	RPA	Numer. V^{N-1}	f	Wendin (1971, 1972, 1973a)
	RPA	Numer. V^{N-1}	f	Ya'Amusia *et al.* (1971)
	RPA	Numer. V^{N-1}	f	Lin (1974)
Ba	RPA	Numer. V^{N-1}	f	Wendin (1973c, 1975)
	RPA	Numer. V^{N-1}	f	Fliflet *et al.* (1974)
H_2	TDHF	8 and 18 STO's	$\alpha(\omega)$, $V(\omega)$, $\Delta\varepsilon$	Epstein (1970)
	CHF	6 STO's	$\alpha(0)$, J_{HD}	Ditchfield *et al.* (1970)
	CHF	2 STO's	$\alpha(0)$	Teixeira-Das and Murrell (1970)
	CHF	Variable GTO's	$\alpha(0)$ for sev. R values	Lim and Linder (1970)
	CHF	6 STO's	$\alpha(0)$	Caves and Karplus (1969)
	CHF	12 FSGO's	Force const.	Swanstrøm *et al.* (1971)

	CHF	18 STO's	σ_N	Cook *et al.* (1971)
	SPPA	2 STO's	$\Delta\varepsilon$ for sev. R values	Ratner (1972)
	RPA	6 and 14 STO's	$\alpha(0)$	Gutschick and McKoy (1973)
	RPA	(8s5p)	$\alpha(\omega)$, $V(\omega)$, $\sigma(\omega)$, $S(n)$, C_6, $\Delta\varepsilon$, f	Martin *et al.* (1974b, 1975)
	RPA	? GTO's	f	Martin *et al.* (1974c)
	SPPA + 2p − 2h	14 STO's	f, $\Delta\varepsilon$	Jørgensen *et al.* (1975)
	SPPA + 2p − 2h	28 STO's	f, $\Delta\varepsilon$, $\alpha(0)$, $S(n)$, J_{HD}, C_6	Oddershede *et al.* (1975)
	TDHF	34 STO's	Potential curves, $f(R)$, $\alpha(0)$	Stewart *et al.* (1976)
	SOPPA	38 STO's	f, $\Delta\varepsilon$	Oddershede *et al.* (1978b)
	SOPPA	28–46 STO's	J_{HD}	Oddershede *et al.* (1977)
	RPA	$(20s5p_z)$	Elec. impact scat.	Resigno *et al.* (1976)
HeH^+	TDHF	34 STO's	Potential curves, $f(R)$, $\alpha(0)$	Stewart *et al.* (1976)
He	CHF	$(2s3p_x3p_y)$	$\alpha(0)$ for sev. R values	Lim *et al.* (1970)
	CHF	2 STO's + 14–16 FSGO's	$\alpha(0)$ for sev. R values	Buckingham and Watts (1970)
	CHF	$(5s4p_z4p_xd_{xz}d_{zz})$	$\alpha(0)$ for sev. R values	O'Brien *et al.* (1973)
	CHF	18 STO's	$\alpha(0)$ for sev. R values	Fortune and Certain (1974)
LiH	TDHF	8 and 12 STO's	$\alpha(0)$, $\Delta\varepsilon$	Epstein (1970)
	CHF	19 STO's	Magn. suscep., σ_N; hyperpol., $\alpha(0)$	Arrighini *et al.* (1970)
	CHF	11–27 FSGO's	Dipole moment deriv., force constants	Yde *et al.* (1972)
	CHF	4 STO's (gauge inv.) [STO-5G]	Spin-rot. const., σ_N	Ditchfield (1972a)
	RPA	13 STO's	$\alpha(0)$	Gutschick and McKoy (1973)
	TDHF	35 STO's	f, $\Delta\varepsilon$, $\alpha(\omega)$	Stewart *et al.* (1975)
BeH^+	TDHF	35 STO's	f, $\Delta\varepsilon$, $\alpha(0)$	Stewart *et al.* (1975)
BH	CHF	16–20 FSGO's	Dipole moment deriv., force constants	Yde *et al.* (1972)
	TDHF	46 STO's	$\Delta\varepsilon$, f, $\alpha(0)$	Watson *et al.* (1976)
	CHF	[bs4p/3s2p]	Magn. suscep.	Faszunski (1978)

(continued)

TABLE A-I (*Continued*)

System	Method	Basis set	Property	Reference
CH^+	CHF	3 STO's	$\alpha(0)$	Teixeira-Das and Murrell (1970)
	EOM	[3s2p1d/2s1p]	$\Delta\varepsilon, f$	Martin *et al.* (1974a)
	TDHF	46 STO's	$\Delta\varepsilon, f, \alpha(0)$	Watson *et al.* (1976)
	SOPPA	45 STO's	$f, \Delta\varepsilon$	Oddershede *et al.* (1978a,b)
	SOPPA	45 STO's	J_{CH^+}	Oddershede *et al.* (1977)
	SOPPA	30 STO's	Spect. constants rad. lifetimes	Elander *et al.* (1977)
Li_2	TDHF	14 and 22 STO's	$\Delta\varepsilon, \alpha(0)$	Epstein (1970)
	CHF	14–20 FSGO's	Dipole moment deriv., force constants	Yde *et al.* (1972)
	TDHF	44 STO's	$\Delta\varepsilon, f, \alpha(0)$	Watson *et al.* (1976)
FH	TDHF	17 and 19 STO's	$\alpha(\omega), \Delta\varepsilon$	Epstein (1970)
	CHF	6 STO's, gauge inv. [STO-5G]	σ_N, spin-rotation	Ditchfield (1972a)
	SPPA + 2p − 2h	33 STO's	$f, \Delta\varepsilon, \alpha(\omega), J_{HF}, C_6$	Oddershede *et al.* (1975)
	CHF	Numer. partial-wave	$\alpha_{\parallel}(0)$	Christiansen and McCullough (1977)
	SOPPA	20–45 STO's	J_{HF}	Oddershede *et al.* (1977)
	SOPPA	45 STO's	$\alpha(\omega), V(\omega), \Delta\varepsilon$	Jørgensen *et al.* (1977b)
	CHF	69 STO-3G	Hyperpolarizabilities	Raidy and Santry (1978)
AlH	CHF	36 STO's	σ_N, magn. suscep.	Laws *et al.* (1969)
CO	CHF	52 STO's	Dipole moment (R), various magn. prop.	Stevens and Karplus (1968)
	EOM	$[5s3p1p_z/5s3p1p_z]$	$\Delta\varepsilon, f$	Rose *et al.* (1973)
	EOM	[3s2p/3s2p] + (1s1pσ/1s1pσ) + (1s1pσ) at center	potent. curves, $f(R)$	Coughran *et al.* (1973)
	CHF	Numer. partial-wave	$\alpha_{\parallel}(0)$	Christiansen and McCullough (1977)

	SOPPA	45 STO's	J_{CO}	Oddershede *et al.* (1977)
	SOPPA	46 STO's	$\alpha(\omega)$, $\Delta\varepsilon$, $V(\omega)$	Jørgensen *et al.* (1978b)
N_2	CHF	52 STO's	σ_N, magn. suscep.	Laws *et al.* (1971)
	RPA	[4s3p] + (1s2p3d)	$\alpha(0)$	Gutshick and McKoy (1973)
	EOM	[4s3p] + ($2p_z 2d_\pi$) at center	$\Delta\varepsilon, f$	Rose *et al.* (1973)
	EOM	[4s3p] + ($2p_z 2d_\pi$) at center	Pot. curves, $f(R)$	Coughran *et al.* (1973)
	Third-order EOM	[3s2p] + ($2p_z 2d_\pi$) at center	$\Delta\varepsilon$	Yeager and Freed (1977)
	RPA	54 STO's	$\alpha(0)$, magn. prop.	Lamanna *et al.* (1977)
	HRPA	[4s3p] + ($p\sigma$ $d\pi$) at center	f between exc. states	Yeager and McKoy (1977)
O_2	RPA	[4s3p]	f, $\Delta\varepsilon$	Yeager and McKoy (1975)
F_2	HRPA	[3s2p] + (1s2p?d)	f, $\Delta\varepsilon$	Rescigno *et al.* (1977)
SiO	SPPA + 2p − 2h	33 STO's	Spectrosc. constants, radiative lifetimes	Oddershede and Elander (1976)
H_2O	CHF	27 STO's	$\alpha(0)$, hyperpolariz.	Arrighini *et al.* (1967, 1968a)
	CHF	7–27 STO's	Magn. suscep.	Arrighini *et al.* (1968b)
	CHF	29 STO's	$\alpha(0)$, magn. suscep.	Arrighini *et al.* (1970a)
	CHF	29 STO's	σ_N, spin-rot.	Arrighini and Guidotti (1970)
	CHF	7–27 STO's	σ_N	Arrighini *et al.* (1970b)
	CHF	[5s4p1d/3s1p]	Force const., $\alpha(0)$; magn. suscep., σ_N	Thomsen and Swanstrøm (1973)
	EOM	[3s2p/1s] + (2s2p/1s)	$\Delta\varepsilon, f$	Yeager *et al.* (1974)
	RPA	47 STO's	$\alpha(0)$, magn. prop.	Lamanna *et al.* (1977)
	CHF	(11s7p2d/5s1p)	σ_N	Lazzeretti and Zanasi (1977)
CO_2	EOM	[3s2p/3s2p] + (1s1p/1s1p)	$\Delta\varepsilon, f$	McCurdy and McKoy (1974)
	EOM	[4s3p/4s3p] + (1d/1d)	$\Delta\varepsilon$	England *et al.* (1977)
HCN	CHF	Min. STO-5G [gauge inv.]	σ_N	Ditchfield (1972b)
NH_3	CHF	32 STO's	$\alpha(0)$, hyperpolariz.	Arrighini *et al.* (1967, 1968a)
	CHF	8–32 STO's	Magn. suscep.	Arrighini *et al.* (1968b)
	CHF	8–32 STO's	σ_N, spin-rot.	Arrighini *et al.* (1970b)
	CHF	(11s7p2d/5s1p)	σ_N	Lazzeretti and Zanasi (1977)

(*continued*)

TABLE A-I *Continued*)

System	Method	Basis set	Property	Reference
C_2H_2	CHF	Min. STO-5G [gauge inv.]	σ_N	Ditchfield (1972b)
HCHO	RPA	Min. STO	$\Delta\varepsilon, f$	Dunning and McKoy (1968)
	CHF	Min. STO-5G [gauge inv.]	σ_N	Ditchfield (1972b)
	EOM	[3s2p/1s] + (1s1p/1s1p/1s) + (1s1p1p$_x$ 1p$_y$) at center	$\Delta\varepsilon, f$	Yeager and McKoy (1974)
H_2O_2	CHF	30 STO's	$\alpha(0)$	Arrighini *et al.* (1967)
	CHF	12–30 STO's	Magn. suscep.	Arrighini *et al.* (1968b)
CH_4	CHF	9–18 STO's	$\alpha(0)$, hyperpolariz.	Arrighini *et al.* (1967, 1968a)
	CHF	39 STO's	$\alpha(0)$, magn. suscep.	Arrighini *et al.* (1968c)
	CHF	9–18 STO's	Magn. suscep.	Arrighini *et al.* (1968b)
	CHF	9–18 STO's	σ_N, spin-rot.	Arrighini *et al.* (1970b)
	CHF	Min. STO	$\alpha(0)$	Teixeira-Das and Murrell (1970)
	CHF	Min. STO-5G [gauge inv.]	σ_N	Ditchfield (1972b)
	CHF	(11s7p2d/5s1p)	σ_N	Lazzeretti and Zanasi (1977)
CH_3F	CHF	Min. STO-5G [gauge inv.]	σ_N	Ditchfield (1972b)
C_2H_4	RPA	Min. STO	$f, \Delta\varepsilon$	Dunning and McKoy (1967)
	HRPA	[3s2p/1s]	$f, \Delta\varepsilon$	Shibuya and McKoy (1971)
	CHF	Min. STO-5G [gauge inv.]	σ_N	Ditchfield (1972b)
	EOM	[4s2p/2s] + (3p$_c$)	$\Delta\varepsilon, f$	Rose *et al.* (1973)
	EOM	[3s2p/1s] + (2pπ_2)	Potent. curves, $f(R)$	Coughran *et al.* (1973)
	HRPA	Single and double zeta STO-5G	f, rotatory strengths	Bouman and Hansen (1977)
C_3H_4	CHF	Min. STO-5G [gauge inv.]	σ_N	Ditchfield (1972b)
C_4H_6	RPA	Min. STO-4G	f, rotatory strengths	Bouman and Hansen (1978)
C_4H_8	HRPA	Single and double zeta STO-5G	f, rotatory strengths	Bouman and Hansen (1977)
C_2H_6	CHF	Min. STO-5G [gauge inv.]	σ_N	Ditchfield (1972b)
C_3H_5DN	RPA	Min. STO-3G	rotatory strengths	Yamakawa *et al.* (1976)
C_6H_6	EOM	[3s2p/1s]	$\Delta\varepsilon$	Rose *et al.* (1974)

The analysis is most conveniently carried out starting from the expression for E$_{\mathrm{RPA}}$ in Eq. (114). The zeroth-order propagator, $G^0_{a\alpha,\,\alpha a}(i\omega) \equiv G^0_{a\alpha}(i\omega)$, is diagonal and has poles at

$$\omega \equiv \omega_- = -\eta - i(\varepsilon_a - \varepsilon_\alpha) \tag{B.1}$$

and

$$\omega \equiv \omega_+ = \eta + i(\varepsilon_a - \varepsilon_\alpha) \tag{B.2}$$

for the first and the last term in Eq. (108), respectively. We have used the standard notation for particle and hole states [see after Eq. (16)]. The exponential factor in Eq. (106) allows us to replace the ω-integration in Eq. (114) with an integration over a semicircle closed in the lower half-plane. This means that only the $\mathbf{G}^0$ pole in Eq. (B.1) is inside the contour. The RPA self-energy is given in Eq. (116) and

$$A(1)_{a\alpha,\,b\beta} = (ab\|\beta\alpha), \tag{B.3}$$

$$B(1)_{a\alpha,\,b\beta} = (\beta a\|\alpha b). \tag{B.4}$$

Substituting Eqs. (108), (113), and (116) into Eq. (114) gives the following expression for the lowest order contribution to ΔE_{RPA}:

$$\Delta E^{(2)}_{\mathrm{RPA}} = \Delta E^{(2a)}_{\mathrm{RPA}} + \Delta E^{(2b)}_{\mathrm{RPA}} \tag{B.5}$$

where

$$\Delta E^{(2a)}_{\mathrm{RPA}} = -\frac{1}{16\pi} \sum_{\substack{ab\\ \alpha\beta}} (a\alpha\|\beta b) \int d\omega G^{0+}_{a\alpha}(i\omega) A(1)_{a\alpha,\,b\beta}\, G^{0+}_{b\beta}(i\omega)\, d\omega, \tag{B.6}$$

$$\Delta E^{(2b)}_{\mathrm{RPA}} = \frac{1}{8\pi} \sum_{\substack{ab\\ \alpha\beta}} (a\alpha\|b\beta) \int d\omega G^{0+}_{a\alpha}(i\omega) B(1)_{a\alpha,\,b\beta}\, G^{0-}_{b\beta}(i\omega)\, d\omega. \tag{B.7}$$

The integration over the interaction strength parameter gives a factor $\frac{1}{2}$, and we have divided $\mathbf{G}^0(i\omega)$ into two parts:

$$\mathbf{G}^0(i\omega) = \mathbf{G}^{0-}(i\omega) + \mathbf{G}^{0+}(i\omega) \tag{B.8}$$

that have poles at $\omega = \omega_-$ and ω_+, respectively. Two identical terms are included in $\Delta E^{(2b)}_{\mathrm{RPA}}$, and we have utilized the fact that $\mathbf{G}^{0+}(i\omega)$ has no poles inside the contour. By performing the contour integration, we find

$$\Delta E^{(2a)}_{\mathrm{RPA}} = 0 \tag{B.9}$$

and

$$\Delta E^{(2)}_{\mathrm{RPA}} = \Delta E^{(2b)}_{\mathrm{RPA}} = -\frac{1}{4}\sum_{\substack{ab\\ \alpha\beta}} \frac{(a\alpha\|b\beta)(\beta a\|\alpha b)}{\varepsilon_\alpha + \varepsilon_\beta - \varepsilon_a - \varepsilon_b}$$

$$= \frac{1}{4}\sum_{\substack{ab\\ \alpha\beta}} \frac{|(a\alpha\|\beta b)|^2}{\varepsilon_\alpha + \varepsilon_\beta - \varepsilon_a - \varepsilon_b}. \tag{B.10}$$

Equation (B.10) is an analytic representation of the second-order energy diagram in Fig. 3a, and it is identical to the second-order Rayleigh–Schrödinger expression in Eq. (123). The integration over the interaction strength parameter gave a factor $\frac{1}{2}$, which means that the lowest order term in Eq. (110) is twice the second-order perturbation term.

The third-order contribution to ΔE_{RPA} is obtained from Eq. (114) by retaining the first-order term in Eq. (113):

$$\Delta E^{(3)}_{\mathrm{RPA}} = -\frac{1}{8\pi}\int_0^1 g^2\,dg \sum_{\substack{ij\\ kl\\ mn}} (ij\|kl)$$

$$\times \int G^0_{ij}(i\omega) M^{\mathrm{RPA}}_{ij,mn}(g=1) G^0_{mn}(i\omega) M^{\mathrm{RPA}}_{mn,kl}(g=1) G^0_{kl}(i\omega)\,d\omega$$

$$= -\frac{12}{8\pi}\int_0^1 g^2\,dg \sum_{\substack{abc\\ \alpha\beta\gamma}} (a\alpha\|\beta b) B(1)_{a\alpha,c\gamma} B^*(1)_{c\gamma,b\beta}$$

$$\times \int G^{0+}_{a\alpha}(i\omega) G^{0-}_{c\gamma}(i\omega) G^{0+}_{b\beta}(i\omega)\,d\omega. \tag{B.11}$$

In the last expression the arbitrary summation indices are replaced with summations over particle and hole indices. Only terms containing at least one factor $\mathbf{G}^{0-}$ contribute to $\Delta E^{(3)}_{\mathrm{RPA}}$, and we find in analogy with the result in Eq. (B.9) that the term involving three factors $\mathbf{G}^{0-}$ also vanishes. The rest of the terms gives twelve identical contributions, one of which is listed in Eq. (B.11). By using Eqs. (108) and (B.4), we find that

$$E^{(3)}_{\mathrm{RPA}} = \sum_{\substack{abc\\ \alpha\beta\gamma}} \frac{(a\alpha\|\beta b)(\gamma a\|\alpha c)(b\gamma\|c\beta)}{(\varepsilon_\gamma + \varepsilon_\alpha - \varepsilon_a - \varepsilon_c)(\varepsilon_\gamma + \varepsilon_\beta - \varepsilon_c - \varepsilon_b)} \tag{B.12}$$

or

$$E^{(3)}_{\mathrm{RPA}} = \sum_{\substack{abc\\ \alpha\beta\gamma}} \frac{(a\alpha\|\beta b)(\gamma c\|\alpha a)(c\gamma\|b\beta)}{(\varepsilon_\alpha + \varepsilon_\gamma - \varepsilon_a - \varepsilon_c)(\varepsilon_\beta + \varepsilon_\gamma - \varepsilon_b - \varepsilon_c)} \tag{B.13}$$

which is an analytic representation of the energy diagram in Fig. 3b.

In fourth order, we find that

$$\Delta E^{(4)}_{\mathrm{RPA}} = -\frac{1}{32\pi} \sum_{\substack{ij\\kl\\mn\\pq}} (ij\|kl) \int G^0_{ij}(i\omega) M^{\mathrm{RPA}}_{ij,\,mn}(g=1) G^0_{mn}(i\omega)$$

$$\times M^{\mathrm{RPA}}_{mn,\,pq}(g=1) G^0_{pq}(i\omega) M^{\mathrm{RPA}}_{pq,\,kl}(g=1) G^0_{kl}(i\omega)\, d\omega, \qquad \text{(B.14)}$$

where we have integrated over the interaction strength parameter. In splitting the summation indices up into particle and hole indices, it is revealed that three different types of terms are present in Eq. (B.14). By collecting terms of the same type, we find that

$$\Delta E^{(4)}_{\mathrm{RPA}} = \Delta E^{(4a)}_{\mathrm{RPA}} + \Delta E^{(4b)}_{\mathrm{RPA}} + \Delta E^{(4c)}_{\mathrm{RPA}}, \qquad \text{(B.15)}$$

where

$$\Delta E^{(4a)}_{\mathrm{RPA}} = -\frac{1}{2\pi} \sum_{\substack{abcd\\ \alpha\beta\gamma\delta}} (a\alpha\|\beta b) B(1)_{a\alpha,\,c\gamma} B^*(1)_{c\gamma,\,d\delta} A^*(1)_{a\delta,\,b\beta}$$

$$\times \int G^{0+}_{a\alpha}(i\omega) G^{0-}_{c\gamma}(i\omega) G^{0+}_{d\delta}(i\omega) G^{0+}_{b\beta}(i\omega)\, d\omega, \qquad \text{(B.16)}$$

$$\Delta E^{(4b)}_{\mathrm{RPA}} = -\frac{1}{4\pi} \sum_{\substack{abcd\\ \alpha\beta\gamma\delta}} (a\alpha\|\beta b) B(1)_{a\alpha,\,c\gamma} A(1)_{c\gamma,\,d\delta} B^*(1)_{d\delta,\,b\beta}$$

$$\times \int G^{0+}_{a\alpha}(i\omega) G^{0-}_{c\gamma}(i\omega) G^{0-}_{d\delta}(i\omega) G^{0+}_{b\beta}(i\omega)\, d\omega, \qquad \text{(B.17)}$$

$$\Delta E^{(4c)}_{\mathrm{RPA}} = -\frac{1}{8\pi} \sum_{\substack{abcd\\ \alpha\beta\gamma\delta}} (a\alpha\|b\beta) B(1)_{a\alpha,\,c\gamma} B^*(1)_{c\gamma,\,d\delta} B(1)_{a\delta,\,b\beta}$$

$$\times \int G^{0+}_{a\alpha}(i\omega) G^{0-}_{c\gamma}(i\omega) G^{0+}_{d\delta}(i\omega) G^{0-}_{b\beta}(i\omega)\, d\omega. \qquad \text{(B.18)}$$

With the explicit expressions for **A**(1), **B**(1), $\mathbf{G}^{0+}$, and $\mathbf{G}^{0-}$, the $\Delta E^{(4a)}_{\mathrm{RPA}}$ can be reduced to

$$\Delta E^{(4a)}_{\mathrm{RPA}} = \sum_{\substack{abcd\\ \alpha\beta\gamma\delta}} \frac{(a\alpha\|\beta b)(\gamma c\|\alpha a)(d\delta\|c\gamma)(b\beta\|\delta d)}{(\varepsilon_\gamma + \varepsilon_\alpha - \varepsilon_c - \varepsilon_a)(\varepsilon_\gamma + \varepsilon_\beta - \varepsilon_c - \varepsilon_b)(\varepsilon_\gamma + \varepsilon_\delta - \varepsilon_c - \varepsilon_d)}. \qquad \text{(B.19)}$$

By using the identity,

$$(x - z)^{-1}(x + y)^{-1}(x + v)^{-1} + (z - x)^{-1}(z + v)^{-1}(z + y)^{-1}$$

$$= -(x + y)^{-1}(v + z)^{-1}\{(y + z)^{-1} + (v + x)^{-1}\}, \qquad \text{(B.20)}$$

where x, y, v, and z are orbital energy differences of the form, $\varepsilon_\alpha - \varepsilon_a$, $\varepsilon_\beta - \varepsilon_b$, etc., we find that

$$\Delta E_{\mathrm{RPA}}^{(4b)} = \sum_{\substack{abcd \\ \alpha\beta\gamma\delta}} \frac{(a\alpha\|\beta b)(\gamma c\|\alpha a)(\delta d\|c\gamma)(b\beta\|d\delta)}{(\varepsilon_\alpha + \varepsilon_\gamma - \varepsilon_a - \varepsilon_c)(\varepsilon_\alpha + \varepsilon_\delta - \varepsilon_a - \varepsilon_d)(\varepsilon_\beta + \varepsilon_\delta - \varepsilon_b - \varepsilon_d)}. \tag{B.21}$$

The energy integration in Eq. (B.18) gives two contributions which can be added together by means of the relation

$$\begin{aligned}
&(x+y)^{-1}(x-v)^{-1}(x+z)^{-1} + (v-x)^{-1}(v+y)^{-1}(v+z)^{-1} \\
&\quad = (x+y+v+z)(x+y)^{-1}(x+z)^{-1}(v+y)^{-1}(v+z)^{-1} \\
&\quad = (x+y+v+z)^{-1} \\
&\qquad \times \{(x+y)^{-1}(x+z)^{-1} + (x+y)^{-1}(v+y)^{-1} + (x+z)^{-1}(v+z)^{-1} \\
&\qquad + (v+y)(v+z)\}.
\end{aligned} \tag{B.22}$$

Collecting all factors and rearranging the terms gives

$$E_{\mathrm{RPA}}^{(4c)} = \sum_{\substack{abcd \\ \alpha\beta\gamma\delta}} \frac{(\alpha a\|\gamma c)(a\alpha\|b\beta)(\beta b\|\delta d)(d\delta\|c\gamma)}{\begin{array}{r}(\varepsilon_\alpha + \varepsilon_\beta + \varepsilon_\gamma + \varepsilon_\delta - \varepsilon_a - \varepsilon_b - \varepsilon_c - \varepsilon_d) \\ (\varepsilon_\alpha + \varepsilon_\gamma - \varepsilon_a - \varepsilon_a - \varepsilon_c)(\varepsilon_\gamma + \varepsilon_\delta - \varepsilon_c - \varepsilon_d)\end{array}}. \tag{B.23}$$

Applying the diagrammatic rules given by Brandow (1967), the expressions in Eqs. (B.19), (B.21), and (B.23) are readily recognized as an analytic representation of the energy diagrams in Fig. 3c, d, and e, respectively.

We end this appendix by giving the following simple rule for analytic representation of ground-state RPA energy diagrams: the **B**(1) [**B***(1)] matrix element is represented diagrammatically by an interaction line with all four external lines pointing upward [downward] (Brandow, 1967), whereas the A(1) matrix element is represented by an interaction line with two external particle-hole lines pointed downward and two particle-hole lines pointing upward. With these rules, it is easy to generate any RPA energy diagram from Eqs. (113), (114), and (116). For example, we see that the diagram in Fig. 3*e* consists of four **B**(1) matrix elements, in agreement with the analytic expression in Eq. (B.18).

ACKNOWLEDGMENTS

The polarization propagator method has been developed in close cooperation with Poul Jørgensen, and I wish to thank him for eight years of stimulating collaboration. I would also like to thank Jan Linderberg, Nelson Beebe, Nils Elander, Mark Ratner, John Sabin, and Henk Monkhorst for helping me with various aspects of the research reported here and for useful comments during the preparation of this manuscript. Financial support from the Danish Natural Science Research Council is gratefully acknowledged.

REFERENCES

Adamov, M. N., and Evarestov, R. A. (1965). *Opt. Spektrosk.* **19**, 648; *Opt. Spectrosc.* (*USSR*) **19**, 362 (1965).

Adler, S. L. (1962). *Phys. Rev.* **126**, 413.

Aldeen, I. H., and Jamieson, M. J. (1977) *J. Phys. B* **10**, 3591.

Allison, A. C., and Dalgarno, A. (1969). *J. Quant. Spectrosc. Radiat. Transfer* **9**, 1543.

Allison, A. C., and Dalgarno, A. (1970). *At. Data* **1**, 289.

Altick, P. L., and Glassgold, A. E. (1964). *Phys. Rev.* **133**, A632.

Anderson, E., and Simons, J. (1977). *J. Chem. Phys.* **66**, 2427.

Arrighini, G. P., and Guidotti, C. (1970). *Chem. Phys. Lett.* **6**, 435.

Arrighini, G. P., Maestro, M., and Moccia, R. (1967). *Chem. Phys. Lett.* **1**, 242.

Arrighini, G. P., Maestro, M., and Moccia, R. (1968a). *Symp. Faraday Soc.* **2**, 48.

Arrighini, G. P., Maestro, M., and Moccia, R. (1968b). *J. Chem. Phys.* **49**, 882.

Arrighini, G. P., Maestro, M., Moccia, R., and Salvetti, O. (1968c). *J. Chem. Phys.* **49**, 2224.

Arrighini, G. P., Guidotti, C., and Salvetti, O. (1970a). *J. Chem. Phys.* **52**, 1037.

Arrighini, G. P., Maestro, M., and Moccia, R. (1970b). *Chem. Phys. Lett.* **7**, 351.

Arrighini, G. P., Tomasi, J., and Petrongolo, C. (1970c). *Theor. Chim. Acta* **18**, 341.

Arrighini, G. P., Biondi, F., and Guidotti, C. (1973). *Phys. Rev. A* **8**, 577.

Avery, J. (1976). "Creation and Annihilation Operators." McGraw-Hill, New York.

Bagus, P. S. (1965). *Phys. Rev.* **139**, 619.

Ball, M. A., and McLachlan, A. D. (1964). *Mol. Phys.* **7**, 501.

Barrett, B. R. (1968). *Nucl. Phys. A* **109**, 129.

Becquerel, H. (1897). *C. R. Hebd. Seances Acad. Sci.* **125**, 679.

Beebe, N. H. F., and Linderberg, J. (1977). *Int. J. Quantum Chem.* **12**, 683.

Berry, R. S. (1966). *J. Chem. Educ.* **43**, 283.

Bethe, H. A. (1930). *Ann. Phys.* (*Leipzig*) [5] **5**, 325.

Bhattacharya, A. K., Moitra, R. K., and Mukherji, A. (1975). *Int. J. Quantum Chem.* **9**, 385.

Biemont, E., and Grevesse, N. (1978). *Phys. Scr.* **16**, 39.

Bohm, D., and Pines, D. (1953). *Phys. Rev.* **92**, 609.

Born, G., Kurtz, A., and Öhrn, Y. (1978). *J. Chem. Phys.* **68**, 74.

Botterud, I., Lofthus, A., and Veseth, L. (1973). *Phys. Scr.* **8**, 218.

Bouman, T. D., and Hansen, Aa. E. (1977). *J. Chem. Phys.* **66**, 3460.

Bouman, T. D., and Hansen, Aa. E. (1978). *Chem. Phys. Lett.* **53**, 160.

Brandow, B. H. (1967). *Rev. Mod. Phys.* **39**, 771.

Brooks, N. H., and Smith, W. H. (1975). *Astrophys. J.* **196**, 307.

Brzozowski, J., Erman, P., and Lyyra, M. (1976). *Phys. Scr.* **14**, 290.

Buckingham, A. D., and Watts, R. S. (1970). *Mol. Phys.* **26**, 7.

Burger, J. M., and Lurio, A. (1971). *Phys. Rev. A* **3**, 64.

Cade, P. E., and Huo, W. M. (1967). *J. Chem. Phys.* **47**, 614.

Caldwell, D. (1977). *Mol. Phys.* **33**, 495.

Carr, W. J., and Maradudin, A. A. (1964). *Phys. Rev.* **133**, A371.

Caves, T. C., and Karplus, M. (1969). *J. Chem. Phys.* **50**, 3849.

Cederbaum, L. S., and Domcke, W. (1976). *J. Chem. Phys.* **64**, 603.

Chantry, G. W. (1971). *In* "The Raman Effect" (A. Anderson, ed.), Vol. I, p. 48. Dekker, New York.

Christiansen, P. A., and McCullough, E. A. (1977). *Chem. Phys. Lett.* **51**, 468.

Čižek, J., and Paldus, J. (1967). *J. Chem. Phys.* **47**, 3976.

Clementi, E. (1963a). *J. Chem. Phys.* **38**, 2248.

Clementi, E. (1963b). *J. Chem. Phys.* **39**, 175.

Coleman, A. J. (1963). *Rev. Mod. Phys.* **35**, 668.

Condon, E. U. (1937). *Rev. Mod. Phys.* **9**, 432.

Cook, D. B., Davies, A. M., and Raynes, N. T. (1971). *Mol. Phys.* **21**, 113.

Coughran, R. J., Shibuya, T., and McKoy, V. (1973). *J. Chem. Phys.* **58**, 2699.

Coulson, C. A. (1940). *Proc. Cambridge Philos. Soc.* **40**, 201.

Csanak, Gy., Taylor, H. S., and Yaris, R. (1971). *Adv. At. Mol. Phys.* **7**, 287.

Curtis, L. J., and Erman, P. (1977). *J. Opt. Soc. Am.* **67**, 1218.

Curtis, L. J., Engman, B., and Erman, P. (1976). *Phys. Scr.* **13**, 270.

da Providencia, J. (1965). *Nucl. Phys.* **61**, 87.

da Providencia, J. (1966). *Nucl. Phys.* **83**, 209.

da Providencia, J. (1968). *Nucl. Phys.* **A108**, 589.

Dalgaard, E. (1975). *J. Phys. B* **8**, 695.

Dalgaard, E. (1977). *J. Phys. B* **10**, 147.

Dalgaard, E. (1978). *Int. J. Quantum Chem.* (to be published).

Dalgarno, A., and Stephens, T. L. (1970). *Astrophys. J.* **160**, L107.

Dalgarno, A., and Stewart, A. L. (1960). *Proc. R. Soc. London, Ser. A* **257**, 534.

Dalgarno, A., and Victor, G. A. (1966). *Proc. R. Soc. London, Ser. A* **291**, 291.

Dalgarno, A., and Williams, D. A. (1962). *Mon. Not. R. Astron. Soc.* **124**, 313.

DiLonardo, G., and Douglas, A. E. (1973). *Can. J. Phys.* **51**, 434.

Dirac, P. A. M. (1927). *Proc. R. Soc. London, Ser. A* **114**, 243.

Ditchfield, R. (1972a). *J. Chem. Phys.* **56**, 5688.

Ditchfield, R. (1972b). *Chem. Phys. Lett.* **15**, 203.

Ditchfield, R., Ostlund, N. S., Murrell, J. N., and Turpin, M. A. (1970). *Mol. Phys.* **18**, 433.

Docken, K. K., and Hinze, J. (1972). *J. Chem. Phys.* **57**, 4936.

Domcke, W., and Cederbaum, L. S. (1976). *J. Chem. Phys.* **64**, 612.

Drake, G. W. F., and Dalgarno, A. (1970). *Phys. Rev. A* **1**, 1325.

Drake, G. W. F., Victor, G. A., and Dalgarno, A. (1969). *Phys. Rev.* **180**, 25.

Dunning, T. H., and McKoy, V. (1967). *J. Chem. Phys.* **47**, 1735.

Dunning, T. H., and McKoy, V. (1968). *J. Chem. Phys.* **48**, 5263.

Dunning, T. H. (1976). *J. Chem. Phys.* **65**, 3854.

Eggarter, E., and Eggarter, T. P. (1978a). *J. Phys. B* **11**, 1157.

Eggarter, E., and Eggarter, T. P. (1978b). *J. Phys. B* **11**, 2069.

Enrenreich, H., and Cohen, M. H. (1959). *Phys. Rev.* **115**, 786.

Elander, N., Oddershede, J., and Beebe, N. H. F. (1977). *Astrophys. J.* **216**, 165.

England, W., Yeager, D., and Wahl, A. C. (1977). *J. Chem. Phys.* **66**, 2344.

Epstein, I. R. (1970). *J. Chem. Phys.* **53**, 1881.

Epstein, I. R., and Lipscomb, W. N. (1970). *Chem. Phys. Lett.* **4**, 479.

Erman, P. (1975). *Phys. Scr.* **11**, 65.

Erman, P. (1977). *Nukleonika* **22**, 607.

Erman, P. (1977). *Astrophys. J.* **213**, L89.

Fermi, E. (1930). *Z. Phys.* **60**, 320.

Field, R. W., Lagerqvist, A., and Renhorn, I. (1976). *Phys. Scr.* **14**, 298.

Field, R. W., Lagerqvist, A., and Renhorn, I. (1977). *J. Chem. Phys.* **66**, 868.

Fliflet, A. W., Chase, R. L., and Kelly, H. P. (1974). *J. Phys. B* **7**, L443.

Ford, A. L., and Browne, J. C. (1973). *Phys. Rev. A* **7**, 418.

Fortune, P. J., and Certain, P. R. (1974). *J. Chem. Phys.* **61**, 2620.

Fraser, P. A. (1954). *Can. J. Phys.* **32**, 515.

Freeman, D. L. (1977). *Phys. Rev. B* **15**, 5512.

Fukuda, N., Iwamoto, F., and Sawada, K. (1964). *Phys. Rev.* **135**, A932.

Gáspár, R. (1954). *Acta Phys. Acad. Sci. Hung.* **3**, 263.

Geldart, D. J. W., and Rasolt, M. (1976). *Phys. Rev. B* **13**, 1477.

Geldart, D. J. W., Rasolt, M., and Almbladh, C.-O. (1975). *Solid State Commun.* **16**, 243.

Gell-Mann, M., and Brueckner, K. A. (1957). *Phys. Rev.* **106**, 364.

Goscinski, O., and Lukman, B. (1970). *Chem. Phys. Lett.* **7**, 573.

Green, A. M. (1965). *Rep. Prog. Phys.* **28**, 113.

Griffing, K. M., and Simons, J. (1975). *J. Chem. Phys.* **62**, 535.

Gutschick, V. P., and McKoy, V. (1973). *J. Chem. Phys.* **58**, 2397.

Hansen, Aa. E. (1967). *Mol. Phys.* **13**, 425.

Hansen, Aa. E. (1977). *Mol. Phys.* **33**, 483.

Hansen, Aa. E., and Bouman, T. D. (1977). *Chem. Phys. Lett.* **45**, 326.

Harris, F. E. (1975). *In* "Theoretical Chemistry, Advances and Perspectives" (H. Eyring and D. Henderson, eds.), Vol. 1, p. 147. Academic Press, New York.

Harris, F. E., and Michels, H. H. (1967). *Adv. Chem. Phys.* **13**, 205.

Harris, F. E., and Monkhorst, H. J. (1970). *Phys. Rev. B* **2**, 4400.

Harris, F. E., and Monkhorst, H. J. (1971). *In* "Computational Methods in Band Theory" (P. M. Marcus, J. F. Janak, and A. R. Williams, eds.), p. 517. Plenum, New York.

Harris, F. E., Kumar, L., and Monkhorst, H. J. (1973). *Phys. Rev. B* **7**, 2850.

Harris, R. A. (1969). *J. Chem. Phys.* **50**, 3947.

Hedin, L., and Lundqvist, S. (1969). *Solid State Phys.* **23**, 1.

Hefferlin, R. (1976). *J. Quant. Spectrosc. Radiat. Transfer* **16**, 1101.

Heisenberg, W. (1925). *Z. Phys.* **33**, 879.

Herbst, E., and Klemperer, W. (1976). *Phys. Today* **29** No. 6, 32.

Hibbert, A. (1975). *Rep. Prog. Phys.* **38**, 1217.

Hinze, J., Lie, G. C., and Liu, B. (1975). *Astrophys. J.* **196**, 621.

Hirschfelder, J. O., Curtiss, C. F., and Bird, R. B. (1954). "Molecular Theory of Gases and Liquids." Wiley, New York.

Hirschfelder, J. O., Byers-Brown, W., and Epstein, S. T. (1964). *Adv. Quantum Chem.* **1**, 255.

Hohenberg, P., and Kohn, W. (1964). *Phys. Rev.* **136**, B864.

Hubbard, J. (1957). *Proc. R. Soc. London, Ser. A* **243**, 336.

Hubbard, J. (1958). *Proc. R. Soc. London, Ser. A* **244**, 199.

Ingersoll, L. R., and Liebenberg, D. H. (1954). *J. Opt. Soc. Am.* **44**, 566.

Ingersoll, L. R., and Liebenberg, D. H. (1956). *J. Opt. Soc. Am.* **46**, 538.

Ingersoll, L. R., and Liebenberg, D. H. (1958). *J. Opt. Soc. Am.* **48**, 339.

Inokuti, M. (1971). *Rev. Mod. Phys.* **43**, 297.

Jamieson, M. J. (1973). *In* "Wave Mechanics, the First Fifty Years" (W. C. Price, S. S. Chissick, and T. Ravensdale, eds.), p. 133. Butterworth, London.

Jarmain, W. R., and Fraser, P. A. (1953). *Proc. Phys. Soc. London, Ser. A* **66**, 1153.

Jaszunski, M. (1978). *Theor. Chim. Acta*, **48**, 323.

Johnson, W. R., and Lin, C. D. (1976). *Phys. Rev. A* **14**, 565.

Johnson, W. R., Lin, C. D., and Dalgarno, A. (1976). *J. Phys. B* **9**, L303.

Jordan, K. D. (1975). *Chem. Phys. Lett.* **36**, 264.

Jordan, P., and Klein, O. (1927). *Z. Phys.* **45**, 751.

Jordan, P., and Wigner, E. P. (1928). *Z. Phys.* **47**, 631.

Jørgensen, P. (1972). *J. Chem. Phys.* **57**, 4884.

Jørgensen, P. (1975). *Annu. Rev. Phys. Chem.* **26**, 359.

Jørgensen, P., and Linderberg, J. (1970). *Int. J. Quantum Chem.* **4**, 587.

Jørgensen, P., and Oddershede, J. (1972). *J. Chem. Phys.* **57**, 277.

Jørgensen, P., and Simons, J. (1975). *J. Chem. Phys.* **63**, 5302.

Jørgensen, P., Oddershede, J., and Ratner, M. (1974). *J. Chem. Phys.* **61**, 710.

Jørgensen, P., Oddershede, J., and Ratner, M. (1975). *Chem. Phys. Lett.* **32**, 111.

Jørgensen, P., Oddershede, J., and Beebe, N. H. F. (1978a). *J. Chem. Phys.* **68**, 2527.

Jørgensen, P., Oddershede, J., Albertsen, P., and Beebe, N. H. F. (1978b). *J. Chem. Phys.* **68**, 2533.

Judd, B. R. (1963). "Operator Techniques in Atomic Spectroscopy." McGraw-Hill, New York.

Judd, B. R. (1967). "Second Quantization and Atomic Spectroscopy." The Johns Hopkins Press, Baltimore, Maryland.

Karplus, M., and Kolker, H. J. (1964). *J. Chem. Phys.* **41**, 3955.

Kelly, H. P. (1969). *Adv. Chem. Phys.* **14**, 129.

Kenney, J., and Simons, J. (1975). *J. Chem. Phys.* **62**, 592.

Kleinman, L. (1974). *Phys. Rev. B* **10**, 2221.

Kohn, W., and Sham, L. J. (1965). *Phys. Rev.* **140**, A1133.

Kolos, W., and Roothaan, C. C. (1960). *Rev. Mod. Phys.* **32**, 219.

Kowalewski, J. (1977). *Prog. Nucl. Magn. Reson. Spectrosc.* **11**, 1.

Kuhn, W. (1925). *Z. Phys.* **33**, 408.

Kumar, L., Monkhorst, H. J., and Oddershede, J. (1977). *Int. J. Quantum Chem.* **12**, 145.

Lamanna, T., Guidotti, C., and Arrighini, G. P. (1977). *J. Chem. Phys.* **67**, 604.

Landau, L. D. (1956). *Zh. Eksp. Teor. Fiz.* **30**, 1058; *Sov. Phys.—JETP* (*Engl. Transl.*) **3**, 920 (1956).

Landau, L. D. (1958). *Zh. Eksp. Teor. Fiz.* **34**, 262; *Sov. Phys.—JETP* (*Engl. Transl.*) **7**, 182, (1958).

Langhoff, P. W. (1972). *J. Chem. Phys.* **57**, 2604.

Langhoff, P. W., and Karplus, M. (1969). *J. Opt. Soc. Am.* **59**, 863.

Laws, E. A., Stevens, R. M., and Lipscomb, W. N. (1969). *Chem. Phys. Lett.* **4**, 159.

Laws, E. A., Stevens, R. M., and Lipscomb, W. N. (1971). *J. Chem. Phys.* **54**, 4269.

Lazzaretti, P., and Zanasi, R. (1977). *Int. J. Quantum Chem.* **12**, 93.

Lehman, H. (1954). *Nuovo Cimento* [9] **11**, 342.

Levinger, J. S. (1960). "Nuclear Photo-Disintegration." Oxford Univ. Press, London and New York.

Lim, T. K., and Linder, B. (1970). *Theor. Chim. Acta* **19**, 38.

Lim, T. K., Linder, B., and Kromhout, R. A. (1970). *J. Chem. Phys.* **52**, 3831.

Lin, C. D. (1974). *Phys. Rev. A* **9**, 181.

Lin, C. D., and Johnson, W. R. (1977). *Phys. Rev. A* **15**, 1046.

Lin, C. D., Johnson, W. R., and Dalgarno, A. (1977a). *Phys. Rev. A* **15**, 154.

Lin, C. D., Johnson, W. R., and Dalgarno, A. (1977b). *Astrophys. J.* **217**, 1011.

Linderberg, J. (1964). *Ark. Fys.* **26**, 323.

Linderberg, J. (1967). *Int. J. Quantum Chem., Symp.* **S1**, 719.

Linderberg, J. (1976). Private communication.

Linderberg, J., and Öhrn, Y. (1965). *Proc. R. Soc. Ser. A* **285**, 445.

Linderberg, J., and Öhrn, Y. (1967). *Chem. Phys. Lett.* **1**, 295.

Linderberg, J., and Öhrn, Y. (1968). *J. Chem. Phys.* **49**, 716.

Linderberg, J., and Öhrn, Y. (1973). "Propagators in Quantum Chemistry." Academic Press, New York.

Linderberg, J., and Öhrn, Y. (1977). *Int. J. Quantum Chem.* **12**, 161.

Linderberg, J., and Prato, D. (1974). *Int. J. Quantum Chem.* **8**, 901.

Linderberg, J., and Ratner, M. (1970). *Chem. Phys. Lett.* **6**, 37.

Linderberg, J., and Thulstrup, E. W. (1968). *J. Chem. Phys.* **49**, 710.

Linderberg, J., Jørgensen, P., Oddershede, J., and Ratner, M. (1972). *J. Chem. Phys.* **56**, 6213.

Lindhard, J. (1954). *K. Dan. Vidensk. Selsk., Mat.-Fys. Medd.* **28**, 8.

Lipscomb, W. N. (1966). *Adv. Magn. Reson.* **2**, 137.

Löwdin, P,-O. (1959a). *Adv. Chem. Phys.* **2**, 207.

Löwdin, P.-O. (1959b). *J. Mol. Spectrosc.* **3**, 46.

Löwdin, P.-O. (1963). *J. Mol. Spectrosc.* **10**, 12.

Löwdin, P.-O. (1965). *Phys. Rev. A* **139**, 357.

Löwdin, P.-O. (1968). *Int. J. Quantum Chem.* **2**, 867.

Luttinger, J. M., and Nozières, P. (1962). *Phys. Rev.* **127**, 1423 and 1431.

Ma, S. K., and Brueckner, K. A. (1968). *Phys. Rev.* **165**, 18.

McCurdy, C. W., and McKoy, V. (1974). *J. Chem. Phys.* **61**, 2820.

McCurdy, C. W., Rescigno, T. N., Yeager, D. L., and McKoy, V. (1977). *Mod. Theor. Chem.* **3**, 339.

McEachran, R. P., Ryman, A. G., and Stauffer, A. D. (1977). *J. Phys. B* **10**, L681.

McLachlan, A. D., and Ball, M. A. (1964). *Rev. Mod. Phys.* **36**, 844.

Martin, P. H. S., Yeager, D. L., and McKoy, V. (1974a). *Chem. Phys. Lett.* **25**, 182.

Martin, P. H. S., Henneker, W. H., and McKoy, V. (1974b). *Chem. Phys. Lett.* **27**, 52.

Martin, P. H. S., Rescigno, T. N., McKoy, V., and Henneker, W. H. (1974c). *Chem. Phys. Lett.* **29**, 496.

Martin, P. H. S., Henneker, W. H., and McKoy, V. (1975). *J. Chem. Phys.* **62**, 69.

Martinson, I., Gaupp, A., and Curtis, L. J. (1974). *J. Phys. B* **7**, L463.

Mattuck, R. D. (1976). "A Guide to Feynman Diagrams in the Many-Body Problem," 2nd ed. McGraw-Hill, New York.

Möhlmann, G. R., and de Heer, F. (1975). *Chem. Phys. Lett.* **36**, 353.

Monkhorst, H. J., and Oddershede, J. (1973). *Phys. Rev. Lett.* **30**, 797.

Moore, P. E. (1949). *Natl. Bur. Std. (U.S.), Circ.* **467**, 1.

Moscowitz, A. (1965). *In* "Modern Quantum Chemistry" (O. Sinanoğlu, ed.), Part III, p.120. Academic Press, New York.

Moser, C. M., Nesbet, R. K., and Gupta, M. N. (1976). *Phys. Rev. A* **13**, 107.

Mott, N. F., and Massey, H. S. W. (1965). "The Theory of Atomic Collisions." Oxford Univ. Press (Clarendon), London and New York.

Mukherjee, P. K., Roy, H. P., and Gupta, A. (1977). *Phys. Rev. A* **17**, 30.

Mulliken, R. S. (1944). *J. Chem. Phys.* **46**, 497.

Nehrkorn, C., Purvis, G., and Öhrn, Y. (1976). *J. Chem. Phys.* **64**, 1752.

Nesbet, R. K. (1969). *Adv. Chem. Phys.* **14**, 1.

Nicolaides, C. A., and Beck, D. R. (1978). *Chem. Phys. Lett.* **12**, 655.

Nozières, P., and Pines, D. (1958a). *Nuovo Cimento* [10] **9**, 470.

Nozières, P., and Pines, D. (1958b). *Phys. Rev.* **111**, 442.

O'Brien, E. F., Gutschick, V. P., McKoy, V., and McTague, J. P. (1973). *Phys. Rev. A* **8**, 690.

Oddershede, J. (1978). In preparation.

Oddershede, J., and Elander, N. (1976). *J. Chem. Phys.* **65**, 3495.

Oddershede, J., and Jørgensen, P. (1976). "Notes on the Spin-adapted Matrix Elements which Appear in the Evaluation of the Polarization Propagator Through Third Order." Department of Chemistry, Aarhus University, Aarhus, Denmark (unpublished).

Oddershede, J., and Jørgensen, P. (1977a). *J. Chem. Phys.* **66**, 1541.

Oddershede, J., and Jørgensen, P. (1977b). *Chem. Phys. Lett.* **47**, 61.

Oddershede, J., and Linderberg, J. (1971). *Chem. Phys. Lett.* **8**, 165.

Oddershede, J., Kumar, L., and Monkhorst, H. J. (1974). *Int. J. Quantum Chem., Symp.* **S8**, 447.

Oddershede, J., Jørgensen, P., and Beebe, N. H. F. (1975). *J. Chem. Phys.* **63**, 2996.

Oddershede, J., Jørgensen, P., and Beebe, N. H. F. (1978a). *Int. J. Quantum Chem.* (in press).

Oddershede, J., Jørgensen, P., and Beebe, N. H. F. (1978b). *J. Phys. B* **11**, 1.

Oddershede, J., Jørgensen, P., and Beebe, N. H. F. (1977). *Chem. Phys.* **25**, 451.

Öhrn, Y. (1976). *In* "The World of Quantum Chemistry" (B. Pullman and R. Parr, eds.), p. 57. Reidel, Boston, Massachusetts.

Öhrn, Y., and Linderberg, J. (1978). *Int. J. Quantum Chem.* (to be published).

Ostlund, N. S., Newton, M. D., McIver, J. W., and Pople, J. A. (1969). *J. Magn. Reson.* **1**, 298.

Paldus, J., and Čižek, J. (1970). *J. Polym. Sci., Part C* **29**, 199.

Paldus, J., and Čižek, J. (1974). *J. Chem. Phys.* **60**, 149.

Parr, R. G. (1964). "The Quantum Theory of Molecular Electronic Structure." Benjamin, New York.

Pickup, B. T., and Goscinski, O. (1973). *Mol. Phys.* **26**, 1013.

Pines, D. (1962). "The Many-Body Problem." Benjamin, New York.

Pople, J. A., McIver, J. W., and Ostlund, N. S. (1967). *Chem. Phys. Lett.* **1**, 465.

Pople, J. A., McIver, J. W., and Ostlund, N. S. (1968). *J. Chem. Phys.* **49**, 2960 and 2965.

Purvis, G., and Öhrn, Y. (1974). *J. Chem. Phys.* **60**, 4063.

Raidy, T. E., and Santry, D. P. (1978). *Chem. Phys. Lett.* **53**, 568.

Rajagopal, A. K., and Callaway, J. (1973). *Phys. Rev. B* **7**, 1912.

Rajagopal, A. K., and Singhal, S. P. (1977). *Phys. Rev. B* **16**, 601.

Ramsey, N. F. (1953). *Phys. Rev.* **91**, 303.

Rasolt, M., and Geldart, D. J. W. (1975). *Phys. Rev. Lett.* **35**, 1234.

Ratner, M. (1972). *Int. J. Quantum Chem.* **6**, 1165.

Reiche, F., and Thomas, W. (1925). *Z. Phys.* **34**, 510.

Rescigno, T. N., McCurdy, C. W., and McKoy, V. (1974). *Phys. Rev. A* **9**, 2409.

Rescigno, T. N., McCurdy, C. W., McKoy, V., and Bender, C. F. (1976). *Phys. Rev. A* **13**, 216.

Rescigno, T. N., Bender, C. F., and McKoy, V. (1977). *Chem. Phys. Lett.* **45**, 307.

Rice, T. M. (1965). *Ann. Phys. (Leipzig)* [7] **31**, 100.

Rose, J. B., Shibuya, T., and McKoy, V. (1973). *J. Chem. Phys.* **58**, 74.

Rose, J. B., Shibuya, T., and McKoy, V. (1974). *J. Chem. Phys.* **60**, 2700.

Rowe, D. J. (1968). *Rev. Mod. Phys.* **40**, 153.

Sabin, J. R., and Oddershede, J. (1978). In preparation.

Sawada, K. (1957). *Phys. Rev.* **106**, 372.

Schiff, B., Pekeris, C. L., and Accad, Y. (1971). *Phys. Rev. A* **7**, 885.

Schrödinger, E. (1926). *Ann. Phys. (Leipzig)* [4] **79**, 361, 489, and 734.

Serber, R. (1932). *Phys. Rev.* **41**, 489.

Sham, L. J., and Kohn, W. (1966). *Phys. Rev.* **145**, 561.

Shemansky, D. E., and Broadfoot, A. L. (1971). *J. Quant. Spectrosc. Radiat. Transfer* **11**, 1401.

Shibuya, T., and McKoy, V. (1970). *Phys. Rev. A* **2**, 2208.

Shibuya, T., and McKoy, V. (1971). *J. Chem. Phys.* **54**, 1738.

Shibuya, T., Rose, J., and McKoy, V. (1973). *J. Chem. Phys.* **58**, 500.

Shorter, P., and Dalgarno, A. (1977). *Phys. Rev. A* **16**, 1502.

Shorter, P., Lin, C. D., and Johnson, W. R. (1977). *Phys. Rev. A* **16**, 1109.

Silver, D. M., and Bartlett, R. J. (1976). *Phys. Rev. A* **13**, 1.

Simons, J., and Smith, W. D. (1973). *J. Chem. Phys.* **58**, 4899.

Sinanoğlu, O. (1969). *Adv. Chem. Phys.* **14**, 237.

Singhal, S. P., and Callaway, J. (1976). *Phys. Rev. B* **14**, 2347.

Singwi, K. S., Tosi, M. P., Land, R. H., and Sjölander, A. (1968) *Phys. Rev.* **176**, 589.

Slater, J. C. (1951). *Phys. Rev.* **81**, 385.

Smith, P. L., Huber, M. C. E., and Parkinson, W. H. (1976). *Phys. Rev. A* **13**, 1422.

Smith, W. H. (1971). *Nucl. Instrum. & Methods* **90**, 115.

Smith, W. H., and Liszt, H. S. (1972). *J. Quant. Spectrosc. Radiat. Transfer* **12**, 505.

Smith, W. H., Brzozowski, J., and Erman, P. (1976). *J. Chem. Phys.* **64**, 4628.

Stevens, R. M., and Karplus, M. (1968). *J. Chem. Phys.* **49**, 1094.

Stevens, W. J., Hessel, M. M., Bertoncini, P. J., and Wahl, A. C. (1977). *J. Chem. Phys.* **66**, 1477.

Stewart, R. F. (1975a). *J. Phys. B* **8**, 1.

Stewart, R. F. (1975b). *Mol. Phys.* **29**, 1577.

Stewart, R. F., Watson, D. K., and Dalgarno, A. (1975). *J. Chem. Phys.* **63**, 3222.

Stewart, R. F., Watson, D. K., and Dalgarno, A. (1976). *J. Chem. Phys.* **65**, 2104.

Swanstrøm, P., and Hegelund, F. (1975). *In* "Computational Techniques in Quantum Chemistry and Molecular Physics" (G. H. F. Diercksen, B. T. Sutcliffe, and A. Veillard, eds.), p. 299. Reidel Publ., Dordrecht, The Netherlands.

Swanstrøm, P., and Jørgensen, P. (1978). To be published.

Swanstrøm, P., Thomsen, K. T., and Yde, P. B. (1971). *Mol. Phys.* **20**, 1135.

Szabo, A., and Ostlund, N. S. (1977a). *Int. J. Quantum Chem.* **S11**, 389.

Szabo, A., and Ostlund, N. S. (1977b). *J. Chem. Phys.* **67**, 4351.

Teixeira-Das, J. J. C., and Murrell, J. N. (1970). *Mol. Phys.* **19**, 329.

Thomsen, K. T., and Swanstrøm, P. (1973). *Mol. Phys.* **26**, 751.

Thouless, D. J. (1961). "Quantum Mechanics of Many Body Systems," 1st ed. Academic Press, New York.

Van Vleck, J. H. (1932). "The Theory of Electric and Magnetic Susceptibilities." Oxford Univ. Press, London and New York.

Victor, G. A., and Dalgarno, A. (1969). *J. Chem. Phys.* **50**, 2535.

Victor, G. A., Browne, J. C., and Dalgarno, A. (1967). *Proc. Phys. Soc., London* **92**, 42.

Vinti, J. P. (1932). *Phys. Rev.* **41**, 432.

Watson, D. K., Stewart, R. F., and Dalgarno, A. (1976). *J. Chem. Phys.* **64**, 4995.

Wendin, G. (1970). *Phys. Lett. A* **33**, 16.

Wendin, G. (1971). *Phys. Lett. A* **37**, 445.

Wendin, G. (1972). *J. Phys. B* **5**, 110.

Wendin, G. (1973a). *J. Phys. B* **6**, 42.

Wendin, G. (1973b). *Phys. Lett. A* **46**, 101.

Wendin, G. (1973c). *Phys. Lett. A* **46**, 119.

Wendin, G. (1975). *Phys. Lett. A* **51**, 291.

Werner, H.-J., and Meyer, W. (1976a). *Mol. Phys.* **31**, 855.

Werner, H.-J., and Meyer, W. (1976b). *Phys. Rev. A* **13**, 13.

Wiese, W. L., and Fuhr, J. R. (1975). *J. Phys. Chem. Ref. Data* **4**, 263.

Wiese, W. L., Smith, M. W., and Glennon, B. M. (1966). *Natl. Bur. Stand. (U.S.), Ref. Data. Ser.* 1.

Wiese, W. L., Smith, M. W., and Miles, B. M. (1969). *Natl. Bur. Stand. (U.S.), Ref. Data Ser.* **2**, 1.

Williams, G. R. J. (1975). *Chem. Phys. Lett.* **33**, 582.

Williams, G. R. J., and Poppinger, D. (1975). *Mol. Phys.* **30**, 1005.

Wiser, N. (1963). *Phys. Rev.* **129**, 62.

Woodward, L. A. (1967). *In* "Raman Spectroscopy, Theory and Practice" (H. A. Szymanski, ed.), p. 1. Plenum, New York.

Yamakawa, H., Aoyama, T., Inamoto, N., and Ichikawa, H. (1976). *Chem. Phys. Lett.* **41**, 143.

Ya'Amusia, M., Cherepkov, N. A., and Chernysheva, L. V. (1971). *Zh. Eksp. Teor. Fiz.* **60**, 160; *Sov. Phys.—JETP (Engl. Transl.)* **33**, 90 (1971).

Yde, P. B., Thomsen, K. T., and Swanstrøm, P. (1972). *Mol. Phys.* **23**, 691.

Yeager, D. L., and Freed, K. F. (1977). *Chem. Phys.* **22**, 415.

Yeager, D. L., and McKoy, V. (1974). *J. Chem. Phys.* **60**, 2714.

Yeager, D. L., and McKoy, V. (1975). *J. Chem. Phys.* **63**, 4861.

Yeager, D. L., and McKoy, V. (1977). *F. Chem. Phys.* **67**, 2473.

Yeager, D. L., McKoy, V., and Segal, G. A. (1974). *J. Chem. Phys.* **61**, 755.

Yeager, D. L., Nascimento, M. A. C., and McKoy, V. (1975). *Phys. Rev. A* **11**, 1168.

Zeiss, G. D., and Meath, W. J. (1977). *Mol. Phys.* **33**, 1155.

Ziman, J. M. (1965). "Principles of the Theory of Solids." Cambridge Univ. Press, London and New York.

Ziman, J. M. (1969). "Elements of Advanced Quantum Theory." Cambridge Univ. Press, London and New York.

Zubarev, D. N. (1960). *Usp. Fiz. Nauk* **71**, 71; *Sov. Phys.—Usp.* (*Engl. Transl.*) **3**, 320 (1960).

Zubarev, D. N. (1974). "Nonequilibrium Statistical Thermodynamics." Consultants Bureau, New York.

ADVANCES IN QUANTUM CHEMISTRY, VOLUME 11

Relativistic Quantum Chemistry

PEKKA PYYKKÖ
Department of Physical Chemistry
Åbo Akademi
Åbo (Turku), Finland

ISBN 0-12-034811-X

I. Introduction

A. Order-of-Magnitude Estimates

The speed of light is only

$$c = \alpha^{-1} = 137.037 \text{ a.u.} \tag{I.1}$$

and therefore the electron rest mass equals

$$E_0 = m_e c^2 = 18{,}799 \text{ a.u.} \tag{I.2}$$

As the nonrelativistic binding energy for a 1s electron is

$$E_{1s} = -\tfrac{1}{2}Z^2 = -3200 \text{ a.u.} \tag{I.3}$$

for a hydrogen-like atom having $Z = 80$, we see that the binding energy reaches in this case about 17 % of the rest mass.

One may also estimate the average radial velocity using the nonrelativistic result.

$$\langle v_r \rangle = \langle 1s | v_r | 1s \rangle = Z. \tag{I.4}$$

Thus the average 1s velocity is about 58 % of the speed of light in this case.

For this velocity, the electron mass has increased to the value

$$\begin{aligned} m &= m_e/\sqrt{1 - (v/c)^2} \\ &= 1.23 m_e . \end{aligned} \tag{I.5}$$

As the mass enters the denominator of the Bohr radius

$$a_0 = \hbar^2/m_e e^2, \tag{I.6}$$

we may expect a *relativistic contraction* of the order of 20 % for the 1s shell of Hg^{79+} or even for Hg.

All the other ns shells contract quite as much, both in the hydrogen-like and in the many-electron atom. This can be made plausible by the orthogonality requirement

$$\int_0^\infty R_{1s}(r) R_{ns}(r) r^2 \, dr = 0, \tag{I.7}$$

demanding that we move the nodes inward, pulling even the tails in. The p shells and the innermost d shells contract in the same way.

The *spin–orbit splitting* of the *nl* state in a hydrogen-like atom at the nonrelativistic limit is

$$\Delta E(nl) = \alpha^2 Z^4/(2n^3 l(l+1)). \tag{I.8}$$

In addition to these two direct relativistic effects, there exists a third, indirect one: the *relativistic SCF expansion* of the outer d shells and the f shells. It is caused by the contraction of the s and p shells, which leads to a more efficient screening of the nuclear attraction "seen" by the d's and the f's. The magnitude of these expansions is comparable to that of the contractions. In an SCF calculation, and evidently in nature, these two effects are mutually reinforcing, making them particularly large for the valence shell.

B. Historical Outline

The relativistic contraction and the relativistic splitting were first derived by Sommerfeld using the old quantum theory (Sommerfeld, 1916, p. 55). After the relativistic one-electron equation was proposed by Dirac (1928), it was analytically solved for a Coulomb field by Darwin (1928) and by Gordon (1928). A relativistic Hartree–Fock scheme involving four-component, Dirac, single-particle states and a single Slater determinant was proposed by Swirles (1935). Her proposal was first followed, omitting exchange, by Williams (1940) for Cu^+, by Mayers (1957) for Hg, and by Cohen (1960) for W. Pt, Hg, and U.

The relativistic Hartree–Fock or "Dirac–Fock" (DF) equations were cast into a more efficient form using Racah algebra by Grant (1961). Spin–orbit effects on the band structure of solids were discussed quite early (e.g., Elliott, 1954a,b; Lehman, 1959, 1960). The importance of the other relativistic effects on the band structure of solids was observed by Herman *et al.* (1963) and Johnson *et al.* (1963). Several independent relativistic atomic and band-structure programs were developed in the 1960s. They are discussed in Section III. The relativistic SCF expansion was observed by Mayers (1957) and by Boyd *et al.* (1963). Multiconfiguration Dirac–Fock (MCDF) atomic calculations were reported by Desclaux (1975) and by Grant *et al.* (1976).

Relativistic corrections were first introduced as first-order corrections to an *ab initio* molecular calculation by Ladik (1959, 1961a) for H_2. Corrected results of much higher accuracy were obtained for H_2 by Kołos and Wolniewicz (1964). Matcha (1973, 1976) used the first-order perturbation approach for studying the dissociation energies of diatomic alkali halides.

Dirac–Fock one-center expansion (DF-OCE) calculations on hydrides up to SnH_4 and HI were reported by Mackrodt (1970). The same approach was used by Desclaux and Pyykkö (1974, and later work) for studying relativistic effects on bond lengths, bond strengths, and other molecular properties of hydrides of a large number of elements, up to $(114)H_4$.

A relativistic Hartree–Fock–Slater or "Dirac–Slater" discrete variational method (DS-DVM) was presented by Rosén and Ellis (1974) and has since been applied to many molecules and collision systems, mainly to interpret electronic energy levels. The first relativistic multiple scattering (MS) $X\alpha$

results were published by Yang (1976) for C_2 and I_2. Extended Hückel calculations including a spin–orbit Hamiltonian in the diagonalized matrix were published by Manne *et al.* (1975). This method has proven useful in the interpretation of photoelectron spectra.

A nonrelativistic linear combination of atomic orbitals–configuration interaction (LCAO–CI) calculation using a pseudopotential from a relativistic atomic calculation and finally adding the spin–orbit splitting as a perturbation was presented for three states of HgH by Das and Wahl (1976).

C. Purpose of This Review

The purpose of the present article is to give a concise summary of relativistic calculations on multielectron or multicenter problems for the theoretical chemist. In Section II the Dirac–Fock Hamiltonian and the main quantum electrodynamical (QED) corrections are discussed. High-precision tests of QED on one- and two-electron systems fall outside the present review. So do relativistic effects on the long-distance intermolecular interactions [for this topic, see Certain and Bruch (1972, p. 119), Hirschfelder (1967), and Michels (1976)]. Section III is devoted to atomic and band-structure calculations. Only results of interest in the present context are touched upon.

Section IV describes the construction of relativistic molecular orbitals, and Section V the solvable one-electron molecular and solid-state models. The Dirac–Fock and Dirac–Slater molecular calculations are discussed in Sections VI and VII, respectively, the relativistic semiempirical methods in Section VIII, and the perturbation treatments of relativistic effects in Section IX. In relativistic treatments of several spectroscopic properties, the entire formulation must be changed if relativistic wavefunctions are used. Some examples are considered in Section X. Finally, Section XI gives a very tentative preliminary account of the relativistic effects on the chemical properties of the periodic system of elements.

II. The Hamiltonian

A. The Dirac–Fock Hamiltonian

The Dirac equation for a single electron is

$$h\psi = \left(c\boldsymbol{\alpha}\cdot\left(\mathbf{p} + \frac{e}{c}\mathbf{A}\right) + \beta mc^2 - eV\right)\psi = E\psi, \tag{II.1}$$

where $\mathbf{A}$ is the magnetic vector potential, V the electric potential, and ψ a four-component spinor. When deriving wavefunctions, the Dirac matrices

$\boldsymbol{\alpha}$ and β can be conveniently written as

$$\boldsymbol{\alpha} = \begin{pmatrix} 0 & \boldsymbol{\sigma} \\ \boldsymbol{\sigma} & 0 \end{pmatrix} \tag{II.2}$$

with the Pauli spin matrices

$$\sigma_x = \begin{pmatrix} 0 & 1 \\ 1 & 0 \end{pmatrix}, \quad \sigma_y = \begin{pmatrix} 0 & -i \\ i & 0 \end{pmatrix}, \quad \sigma_z = \begin{pmatrix} 1 & 0 \\ 0 & -1 \end{pmatrix}, \tag{II.3}$$

and

$$\beta = \begin{pmatrix} 1 & 0 \\ 0 & -1 \end{pmatrix} \tag{II.4}$$

where the 1 imply two-dimensional identity matrices. Then the Dirac–Fock Hamiltonian for a molecule becomes

$$H = \sum_i h_i + \sum_{i>j} e^2/r_{ij} \tag{II.5}$$

with

$$V = \sum_K eZ_K/r_K \tag{II.6}$$

and $\mathbf{A} = 0$. Thus the one-electron relativistic effects are treated exactly, but the electron–electron interaction is replaced by its nonrelativistic limit. The Dirac–Fock equations for atoms are normally solved using Racah algebra for the angular part and numerical methods for the radial part (see Grant, 1961, 1970). The single-particle states for a central field are of the form

$$\psi_{n\kappa m}(r, \theta, \phi) = \begin{pmatrix} g_{n\kappa}(r)\chi_{\kappa m}(\theta, \phi) \\ if_{n\kappa}(r)\chi_{-\kappa m}(\theta, \phi) \end{pmatrix}. \tag{II.7}$$

Here $g(r)$ and $f(r)$ are the radial functions for the "large" and the "small" components, respectively. The normalization condition is

$$\int_0^\infty (g^2 + f^2) r^2 \, dr = 1. \tag{II.8}$$

The $\chi_{\kappa m}$ are two-spinors:

$$\chi_{\kappa m} = \sum_{m_s = -1/2}^{1/2} C(l\tfrac{1}{2}j;\, m - m_s, m_s, m) \, |l, m - m_s\rangle \, |\tfrac{1}{2} m_s\rangle. \tag{II.9}$$

The relativistic quantum number

$$\kappa = \begin{cases} -l - 1, & j = l + \frac{1}{2} \\ l, & j = l - \frac{1}{2} \end{cases} \tag{II.10}$$

carries both l and j.

A series of interpretative studies on the Dirac equation was published by Hestenes (1975, and references therein) and by Dahl (1977). Virial theorems for Dirac particles were discussed by Rose and Welton (1952), Kim (1967), and Rosicky and Mark (1975).

B. Higher Order Corrections

1. Two-Electron Interaction

The corrections to the electron–electron Coulomb repulsion are summarized in Table I. For slowly moving electrons they are of the order $(v/c)^2$ compared with the Coulomb interaction. The magnetic Gaunt (1929) term is a purely classical one and describes the magnetic interaction between the spin current of one electron and the orbital current of the other one. The retardation term was added to it by Breit (1929, 1930b, 1932a). A derivation of H_{Br} from QED was presented by Bethe and Fermi (1932). Several other derivations were discussed by Bethe and Salpeter (1957), Brown and Ravenhall (1951), Gupta (1964), Nambu (1950), and Wadzinski (1970). [See also Buchmüller (1978) and Leiter (1978).]

For heavier atoms $(v/c)^2 \simeq (\alpha Z)^2$ approaches 1. Brown (1952) derived the expression H''_{Br} appropriate for heavy atoms using α rather than $Z\alpha$ as the expansion parameter and including the nuclear Coulomb attraction in the unperturbed part H_0. An independent derivation leading to the same result was published by Mittleman (1972). An expression, valid to order α^4, was also presented by Nambu (1950). A nonlocal generalization of H_{Br}, H'_{Br}, was derived by Bethe and Salpeter (1957). A detailed discussion of these various operators was published by Mann and Johnson (1971) who pointed out that H'_{Br} should be used in Dirac–Fock calculations. Safronova and Rudzikas (1976) carried out perturbation theoretical calculations going beyond the usual Breit Hamiltonian but omitting the QED corrections.

The derivation of H_{Br} implies that it should be added after the SCF phase as a first-order correction (Bethe and Salpeter, 1957), whereas the derivation of H''_{Br} (Mittleman, 1972) implies that it can be treated to infinite order, i.e., used during the SCF phase. In practice, the results are rather similar (J. P. Desclaux, unpublished calculations). Grant and Pyper (1976) propose that H_{Br} should be included in the CI matrix diagonalized in their MCDF atomic calculations. None of these corrections are fully covariant. The main justification for using them is the good agreement with experiment (see Table II for a typical example; several tens of other examples exist). So far as chemical properties of heavier elements are concerned, the Breit interaction appears to be an uninteresting quantity, compared with the other relativistic effects in Eq. (II.5) (Table III). For light systems, such as H_2 or He, the relativistic corrections derived from H_{Br} are rather more

TABLE I

CORRECTIONS TO THE ELECTRON–ELECTRON INTERACTION $H_{12} = 1/R$, $\mathbf{R} = \mathbf{r}_1 - \mathbf{r}_2$, $\mathbf{n} = \mathbf{R}/r$

Author(s)	Operator (a.u.)	Derived from	Later application	Comments
Gaunt (1929)	$H_G = \frac{-1}{R} \boldsymbol{\alpha}_1 \cdot \boldsymbol{\alpha}_2$	Two Dirac eqs.	Grant (1961)	Form proposed also by Heisenberg.
Breit (1929)	$H_{\mathrm{Br}} = H_G + H_{\mathrm{Ret}} = \frac{-1}{2R} (\boldsymbol{\alpha} \cdot \boldsymbol{\alpha}_2 + \boldsymbol{\alpha}_1 \cdot \mathbf{n}\boldsymbol{\alpha}_2 \cdot \mathbf{n})$ $+ 0((\alpha Z)^2)$	Two Dirac eqs. + retarded Hamiltonian of Darwin (1920)	Kim (1967)	Mann and Johnson (1971): $\langle H_{\mathrm{Ret}} \rangle \simeq -10^{-1} \langle H_G \rangle$
Brown (1952)	$H''_{\mathrm{Br}} = \frac{-1}{R} (\boldsymbol{\alpha}_1 \cdot \boldsymbol{\alpha}_2 \cos \omega R + 1 - \cos \omega R)$, $\omega = \varepsilon_1 - \varepsilon_2 = 0$ only for exchange matrix elements	QED. Include H_{12} + nuclear potential in unperturbed part	Smith and Johnson (1967)	Only α-expansion param., not any more $v/c \Rightarrow$ use for inner shells. $H''_{\mathrm{Br}} = H'_{\mathrm{Br}}$ for local potential
Bethe and Salpeter (1957)	$H'_{\mathrm{Br}} = -\alpha_{1i} \cdot \alpha_{2j} \left(\delta_{ij} \frac{\cos \omega R}{R} + \frac{\partial^2}{\partial R_i \, \partial R_j} \frac{\cos \omega R - 1}{\omega^2 R} \right)$	QED (non-cov.)	Mann and Johnson (1971)	Correct form for Dirac–Fock. Nonlocal generalization of H_{Br}

TABLE II

CONTRIBUTIONS TO THE 1s IONIZATION ENERGY OF Fm(Z = 100)[a]

Contribution[b]	(eV)
Electric	– 142,929
Magnetic (H_G)	715
Retardation (H_{Ret})	–41
Vacuum fluctuation	457
Vacuum polarization	– 155
Total theoretical	– 141,953 (26)
Experimental	– 141,963 (13)

[a] According to Fricke *et al.*, 1972.

[b] The first contribution represents the difference between two Dirac–Fock calculations. All contributions are calculated from first principles.

TABLE III

EFFECT OF THE BREIT CORRECTION, H_{Br}, ON THE EQUILIBRIUM Pb—H DISTANCE, R_e, ON THE FORCE CONSTANT, k_2, AND ON THE DISSOCIATION ENERGY, D_e (Morse) = $9k_2^3/2k_3^2$, FOR THE PROCESS $PbH_4 \rightarrow Pb + 4H$[a]

Quantity	Without H_{Br} (a.u.)	With H_{Br} (a.u.)	Change (%)
R_e	3.379	3.374	–0.17
k_2	0.468	0.475	1.5
D_e	0.858	0.891	3.8

[a] The results are from a third-order polynomial fit to the spherically symmetrical Dirac–Fock one-center expansion calculations of Desclaux and Pyykkö (1974) on PbH_4 at the five points $R = 3.1$, 3.3, 3.5, 3.7, and 4.03. The total relativistic contraction of R_e is 5.6% and the relativistic increase of k_2, 45%. Note that a quadratic fit was used in the original reference.

important than those coming from the Dirac equation (see Kołos and Wolniewicz, 1964; Das 1973, p. 156).

2. *Three-Electron Interaction*

The analogous three-electron energies are at the nonrelativistic limit of the order

$$E(3\text{-body}) \simeq \alpha^2(v/c)^2(1/r_{12})^2 \simeq \alpha^4 Z^4 \text{ a.u.} \qquad \text{(II.11)}$$

whereas the Breit correction H_{Br} and the electron–electron repulsion H_{12} were of the order of $\alpha^2 Z^3$ and Z a.u., respectively. Quantitative expressions for the three-electron interaction were presented in the nonrelativistic case by Primakoff and Holstein (1939) and by Chanmugam and Schweber (1970) and in the relativistic case by Mittleman (1971). The consequences of these three-body forces in chemical physics were reviewed by Jansen (1965). Three-body effects involving two electrons and one nucleus (i.e., diamagnetic shielding in hyperfine interactions) were considered by Labzovskii (1968, 1971).

3. *Other QED Effects*

The nuclear charge polarizes the vacuum, creating virtual electron–positron pairs (Akhiezer and Berestetskii, 1965; Bethe and Salpeter, 1957; Bjorken and Drell, 1964). This effect may be described by a vacuum polarization potential (Uehling, 1935; Wichmann and Kroll, 1956; Huang, 1976). The other lowest order effect is the vacuum fluctuation, or electron self-energy term corresponding to the zero-point oscillations of the electromagnetic field (see, e.g., Brown and Mayers, 1959; Cheng and Johnson, 1976; Desiderio and Johnson, 1971; Fricke, 1971; Fricke and Waber, 1972b; Huang *et al.*, 1976; Mohr, 1974, 1975). When these two QED effects are included, the calculated ionization energies typically deviate from experiment by a few electron volts implying four- or even five-figure agreement with experiment (Desiderio and Johnson, 1971; Fricke *et al.*, 1972; Mann and Johnson, 1971; see Table II). This suggests that the remaining QED effects and the correlation error are of the order of a few electron volts or less. The most notable exception so far is the result of Schreckenbach *et al.* (1977) for the $K\alpha_1^h$ hypersatellite of Hg. In that case a MCDF + H_{Br} + Lamb shift, calculation deviated from experiment by as much as 39 eV.

The QED corrections for the H_2 molecule were considered by Ladik (1961b, 1965) and by Garcia (1966).

4. *The Nonrelativistic Limit*

At the nonrelativistic limit, including terms of order $(v/c)^4$, the sum of the Dirac–Fock Hamiltonian [Eq. (II.5)] and H_{Br} reduces to the Breit–Pauli form (Itoh, 1965):

$$H = \sum_j \frac{1}{2m} \mathbf{p}_j^2 \qquad \text{(kinetic energy)} \qquad \text{(II.12a)}$$

$$-\sum_j \frac{1}{8m^3c^2} \mathbf{p}_j^4 \qquad \text{(mass velocity)} \qquad \text{(II.12b)}$$

$$+\sum_j \frac{e}{mc}\,\mathbf{p}_j \cdot \mathbf{A}_{\mathrm{ex}}(\mathbf{r}_j) \qquad \text{(external magnetic)} \tag{II.12c}$$

$$+\sum_j \frac{e^2}{2mc^2} \cdot \mathbf{A}_{\mathrm{ex}}^2(\mathbf{r}_j) \qquad \text{(external magnetic)} \tag{II.12d}$$

$$-\sum_j eV_{\mathrm{ex}}(\mathbf{r}_j) \qquad \text{(external electric)} \tag{II.12e}$$

$$+\sum_j \frac{e}{mc}\,\mathbf{s}_j \cdot \mathbf{H}_{\mathrm{ex}}(\mathbf{r}_j) \qquad \text{(spin–external magnetic)} \tag{II.12f}$$

$$+\sum_j \frac{e}{2m^2c^2}\,\mathbf{s}_j \cdot (\mathbf{E}_{\mathrm{ex}}(\mathbf{r}_j) \times \mathbf{p}_j) \qquad \text{(spin–orbit)} \tag{II.12g}$$

$$+\sum_j \frac{\pi e\hbar^2}{2m^2c^2}\,\rho_{\mathrm{ex}}(\mathbf{r}_j) \qquad \text{(Darwin)} \tag{II.12h}$$

$$+\sum_{j<k} e^2/r_{jk} \qquad \text{(Coulomb)} \tag{II.13a}$$

$$-\sum_{j<k} \frac{e^2}{2m^2c^2}\,\mathbf{p}_j \cdot \left(\frac{\mathbf{RR}}{R^3} + \frac{1}{R}\right) \cdot \mathbf{p}_k \qquad \text{(orbit–orbit)} \tag{II.13b}$$

$$+\sum_{j\neq k} \frac{e^2}{m^2c^2}\,\frac{1}{R^3}\,\mathbf{s}_j \cdot (\mathbf{R} \times \mathbf{p}_k) \qquad \text{(spin–other orbit)} \tag{II.13c}$$

$$-\sum_{j,\,k\neq j} \frac{e^2}{2m^2c^2}\,\frac{1}{R^3}\,\mathbf{s}_j \cdot (\mathbf{R} \times \mathbf{p}_j) \qquad \text{(spin–other orbit)} \tag{II.13d}$$

$$-\sum_{j<k} \frac{e^2}{m^2c^2}\,\mathbf{s}_j \cdot \left(\frac{3\mathbf{RR}}{R^5} - \frac{1}{R^3}\right) \cdot \mathbf{s}_k \qquad \text{(spin–spin)} \tag{II.13e}$$

$$-\sum_{j<k} \frac{8\pi e^2}{3m^2c^2}\,\delta(\mathbf{R})\,\mathbf{s}_j \cdot \mathbf{s}_k \qquad \text{(spin–spin)} \tag{II.13f}$$

$$-\sum_{j<k} \frac{\pi e^2\hbar^2}{m^2c^2}\,\delta(\mathbf{R}) \qquad \text{(Darwin).} \tag{II.13g}$$

Here $-e$ is the electron charge and $\mathbf{R} = \mathbf{r}_j - \mathbf{r}_k$, whereas

$$\mathbf{E}_{\mathrm{ex}}(\mathbf{r}) = -\nabla V_{\mathrm{ex}}(\mathbf{r}) \tag{II.14}$$

and

$$\mathbf{H}_{\mathrm{ex}}(\mathbf{r}) = \nabla \times \mathbf{A}_{\mathrm{ex}}(\mathbf{r}) \tag{II.15}$$

are the external electric and magnetic fields, respectively. The term $\rho_{ex}(\mathbf{r})$ is the charge density giving rise to the potential $V_{ex}(\mathbf{r})$,

$$\nabla^2 V_{ex}(\mathbf{r}) = -4\pi\rho_{ex}(\mathbf{r}). \tag{II.16}$$

For a point nucleus,

$$\rho_{ex}(\mathbf{r}) = Ze\,\delta(\mathbf{r}). \tag{II.17}$$

The Coulomb gauge,

$$\nabla \cdot \mathbf{A}_{ex}(\mathbf{r}) = 0, \tag{II.18}$$

is used.

The dominant relativistic corrections in heavier many-electron systems are the mass–velocity term, the spin–orbit term, and the Darwin term. The first one comes from the relativistic mass increase, Eq. (I.5). The Darwin term, Eqs. (II.12h) and (II.13g), can be interpreted as caused by the *Zitterbewegung*: when the four-component Dirac equation is reduced to a two-component form, the electron is no longer a point particle but rather a diffuse charge distribution whose typical dimensions are of the order of α a.u. This reduces the nuclear Coulomb attraction, Eq. (II.12e), and the electronic Coulomb repulsion, Eq. (II.13a). For a more detailed discussion of the nonrelativistic limit, see the Bibliography.

III. Atoms and Solids

A. Relativistic Atomic Calculations

Excellent reviews of relativistic atomic calculations were published by Grant (1970), Armstrong and Feneuille (1974), Lindgren and Rosén (1974), and Walker (1971). Doyle (1969) discussed Z-expansions and Jones (1975) the use of the Breit–Pauli approximation. A compilation of tables of atomic data is given in Table IV and a compilation of published programs in Table V.

1. *One-Electron Atoms*

An analytical solution for the Dirac equation in a Coulomb field was found by Darwin (1928) and by Gordon (1928). White (1931) presented pictorial representations of this solution. Didactic discussions were also published by Powell (1968) and by Szabo (1969). Burke and Grant (1967) prepared plots of the radial densities to demonstrate the relativistic contraction and studied various expectation values.

TABLE IV

RELATIVISTIC ATOMIC CALCULATIONS[a]

Authors	Atoms	Method	Comments
Herman and Skillman (1963)	$2 \lesssim Z \lesssim 102$	HFS + first-order rel. corr.[b]	—
Hartmann and Clementi (1964)	$2 \lesssim Z \lesssim 36$	HF + first-order rel. corr.	Analytic wavefunctions
Clementi (1964)	$2 \lesssim N \lesssim 18$	HF + first-order rel. corr.	Analytic wavefunctions
Fraga *et al.* (1976; Fraga and Karwowski, 1974)	$2 \lesssim Z \lesssim 102$[c]	HF + first-order rel. corr.	—
Fricke *et al.* (1971)	$104 \lesssim Z \lesssim 172$	DS	—
Lu *et al.* (1971a)	$2 \lesssim Z \lesssim 126$	DS	—
Huang *et al.* (1976)	$2 \lesssim Z \lesssim 106$	DS	Electron-binding energies including QED corrections
Carlson *et al.* (1969)	$96 \lesssim Z \lesssim 120$	DS	Electron-binding energies
Lu *et al.* (1971b)	$92 \lesssim Z \lesssim 126$	DS	X-Ray intensities
Scofield (1974)	$5 \lesssim Z \lesssim 104$	DS	X-Ray intensities
Cromer and Waber (1965)	$1 \lesssim Z \lesssim 102$[c]	DS	X-Ray scattering factors
Cromer (1965)	$10 \lesssim Z \lesssim 98$	DS	Anom. disp. corrections
Rosén and Lindgren (1968)	$Z \lesssim 95$	DS	Modified exchange
Chen *et al.* (1977)	$11 \lesssim Z \lesssim 103$	DS	*L*-Shell Coster-Kronig transition energies
Fricke and Soff (1977)	$100 \lesssim Z \lesssim 173$	DS	—
Desclaux *et al.* (1971a)	$3 \lesssim Z \lesssim 17$	DF	Excited states[d]
Desclaux (1973)	$1 \lesssim Z \lesssim 120$	DF	[d]
Malý and Hussonnois (1973a,b)	$1 \lesssim Z \lesssim 120$	DF	[e]
Mann and Waber (1970)	$118 \lesssim Z \lesssim 131$	DF	[d]
Mann and Waber (1973)	$57 \lesssim Z \lesssim 70$	DF	[e]
Carlson and Nestor (1977)	$95 \lesssim Z \lesssim 130$	MCDF	*K* and *L* X-ray spectra

[a] Z is the nuclear charge, and N the number of electrons.

[b] The mass-velocity, Darwin, and spin–orbit terms.

[c] Several ionic species included.

[d] Average of configuration.

[e] One *jj*-coupled configuration only.

TABLE V

PUBLISHED RELATIVISTIC ATOMIC PROGRAMS

Authors	Method
Herman and Skillman (1963)	HFS + first-order rel. corr.
Liberman *et al.* (1971)	DS
Eissner *et al.* (1974)	First-order rel. corr.; calculates radiative data.
Grant (1972, 1973, 1976)	Angular momentum coefficients for MCDF
Desclaux (1975)	MCDF

2. *Relativistic Thomas–Fermi Calculations*

A Thomas–Fermi equation using the relativistic equation between energy and momentum was first derived by Vallarta and Rosen (1932) and by Jensen (1933). The relativistic contraction of electronic charge was seen also here, but the corresponding charge density turned out to be non-normalizable for a point nucleus and normalizable for a finite nucleus. This error is due to neglect of a kinetic energy correction (Gombás, 1949, p. 122). Another charge density, derived by Rudkjøbing (1952) for a central potential, is normalizable for all Z (Gilvarry, 1954). Additional versions were derived by Braun (1975, 1976). Numerical calculations using the Gilvarry or Vallarta-Rosen expressions were published by Waber and Canfield (1975). No essential improvements were obtained for the radial charge densities. Gross and Rafelski (1977) announced relativistic Thomas–Fermi–Dirac (TFD) calculations for superheavy quasi molecules.

3. *Model Potentials*

Reitz (1950) solved numerically the Dirac equation for the Thomas–Fermi–Dirac field of several atoms. Later this became a standard way of initiating numerical SCF computations (see, e.g., Desclaux, 1975). Fogel (1954a,b) presented numerical solutions of the Dirac equation for the Hellmann potential

$$V(r) = -\frac{1}{r} - (Z-1)\frac{1}{r}e^{-kr}. \tag{III.1}$$

Darewych *et al.* (1971) found that Dirac–Fock wavefunctions and orbital energies could be closely simulated by the potential

$$V(r) = [(N-1)\gamma(r) - Z]/r, \tag{III.2}$$

$$\gamma(r) = 1 - [(e^{r/d} - 1)H + 1]^{-1}, \tag{III.3}$$

where d and H are parameters. Screening constants for approximating the radial wavefunctions of heavy atoms by Dirac–Coulomb wavefunctions were considered by Garstang and Mayers (1966) and by Denti (1968). Mande *et al.* (1977) presented a new electronegativity scale based on a screened Coulomb potential.

A more sophisticated model potential, based on angular quantum numbers, was proposed by Koenig (1972) and has since been applied to hyperfine structure (Luc-Koenig, 1972), transition probabilities (Luc-Koenig, 1974), and the inverted fine structure of alkali atoms (Luc-Koenig, 1976). McEnnan *et al.* (1977) presented analytic expressions for both bound and continuum wavefunctions for a screened Coulomb potential of the type

$$V(r) = -\frac{Z}{r}(1 + V_1\lambda r + V_2(\lambda r)^2 + V_3(\lambda r)^3 + \cdots). \tag{III.4}$$

Lee *et al.* (1977) deduced effective core potentials from DF calculations for Xe and Au and used an LCAO expansion for the valence electrons in them. Similar but analytic pseudopotentials were used by Hafner and Schwarz (1978) for a large number of atoms up to Ra. They included configuration interaction and obtained semiquantitative agreement with MCDF results for *LS* configuration mixing and for $\langle r^n \rangle$ with positive n.

4. *First-Order Perturbation Calculations*

Several calculations treating the relativistic effects as a first-order perturbation are mentioned in Table IV. This method evidently misses the self-consistent relativistic effects and is, therefore, rather inaccurate, particularly for the valence shells of heavier elements. The earliest first-order perturbation treatments of relativistic effects in many-electron ($N > 2$) systems seem to be those of Fröman (1958, 1960). The calculation of spin–orbit coupling constants in many-electron atoms was discussed by Blume and Watson (1962, 1963). Later the first-order method was used by Beck (1969), by Detrich (1972) using multiconfiguration functions, and by Griffin *et al.* (1969). Holmgren *et al.* (1976) interpreted the inverted fine structure of alkali atoms by using both the spin–orbit and correlation terms as perturbations in many-body theory. First-order results for the valence shells of Te and Pb are shown in Fig. 1. As seen, the Darwin term cancels about one-half of the relativistic contraction due to the mass-velocity term for the *s* states.

5. *Quasi-Relativistic Calculations*

In order to include the SCF relativistic effects, Cowan and Griffin (1976) carried out nonrelativistic calculations including the mass-velocity term, Eq. (II.12b), and the Darwin term, Eq. (II.12h), in the Hamiltonian during

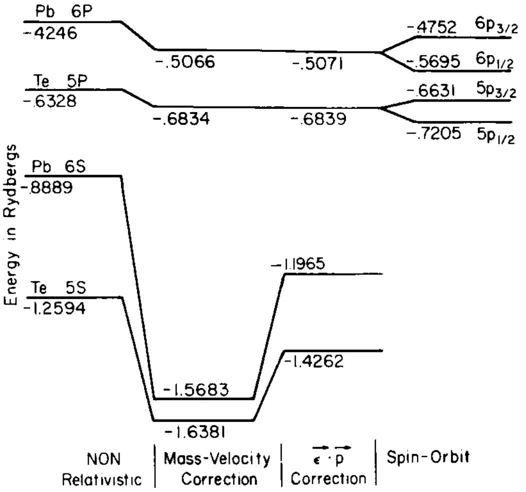

Fig. 1. First-order relativistic corrections for the valence orbitals of Te and Pb. The numbers are from the Hartree–Fock–Slater calculations of Herman and Skillman (1963) and the figure from Johnson *et al.* (1963).

the SCF phase and adding the spin–orbit terms, Eqs. (II.12g) and (II.13c–d) afterward as a first-order perturbations to avoid quadrupling the number of radial wavefunctions (a factor of 2 from spin–orbit splitting and a factor of 2 from large and small components). The theoretical justification of the method is not clear but the results must be deemed good. Rajnak (1976) applied the same code to several configurations of UI.

Inclusion of Breit–Pauli terms in the Schrödinger equation was also considered by Boys and Price (1954), Scherr (1972), Jones (1975), Huzinaga and Arnau (1971), and Feneuille and Luc-Koenig (1977).

Snijders and Baerends (1978) calculated the first-order relativistic wavefunction correction ψ_1 within a Hartree–Slater approach for several atoms. They found that the terms $\langle\psi_0(1)\psi_0(2)|r_{12}^{-1}|\psi_1(2)\psi_0(1)\rangle$ are comparable to the other $(v/c)^4$ corrections. This "first iteration in relativity" simulated DS calculations rather well and considerably improved the results of Herman and Skillman (1963).

6. *Dirac–Hartree Calculations*

The first relativistic SCF calculations by Williams (1940) for Cu^+, by Mayers (1957) for Hg, and by Cohen (1960) for W, Pt, Hg, and U omitted exchange entirely. Schonfelder (1966) applied Dirac–Hartree wavefunctions to electron scattering.

7. *Dirac–Slater Calculations*

Several DS calculations are summarized in Table IV. In addition to the DS program published by Liberman *et al.* (1971), other DS programs were written by Bhalla (1967, 1970, 1973), the Oak Ridge group (Carlson *et al.*, 1969; Lu *et al.*, 1971a,b), and, with a modified exchange expression, by Rosén and Lindgren (1968). All these exchange potentials were nonrelativistic. Ellis (1977a,b) derived a Slater-like expression for a Dirac–Fock relativistic free-electron gas and found a small reduction in the exchange potential at densities corresponding to the innermost shells of heavy atoms. A local representation of the Dirac–Fock exchange potential was presented by Miller (1973). Migdałek (1976a–e) used a "Dirac–Hartree + partial statistical exchange" scheme for calculating oscillator strengths.

The earliest DS calculations were mainly used to discuss total energies (Snow *et al.*, 1964), orbital energies (Liberman *et al.*, 1965), and orbital radii (Waber and Cromer, 1965). These calculations were extended to translawrencium elements by Tucker *et al.* (1968) and by Waber *et al.* (1969). The later applications, in addition to those in Table IV, include hyperfine integrals and their relativistic correction factors (Lindgren and Rosén, 1966; Rosén, 1969, 1972; Amoruso and Johnson, 1971), isomer shifts (Tucker *et al.*, 1969), atomic photoelectric effect (Pratt *et al.*, 1973), radial and spin–orbit parameters for crystal-field theory (Lewis *et al.*, 1970; Varga *et al.*, 1971), electric and magnetic susceptibilities, and shielding factors (Feiock and Johnson, 1969). Continuum DS solutions were presented for Hg by Berkowitz *et al.* (1974).

8. *Dirac–Fock Calculations*

Numerical Dirac–Fock programs were written by Coulthard (1967a,b, 1973a,b), Smith and Johnson (1967), Mann (1969), and Rosén (1973). In addition, two independent programs were described by Desclaux *et al.* (1971b). Kim (1967) and Kagawa (1975) reported Dirac–Fock calculations using Slater-type basis sets. Analytical wavefunctions were optimized for the *K* shell already by Asaad (1960). The formal theory for them was discussed by Synek (1964) and Leclercq (1970). Of these two methods, the numerical one is both more accurate and much faster.

Unrestricted Dirac–Fock calculations of hyperfine properties were performed by Desclaux and Bessis (1970). Andriessen *et al.* (1977) also discussed the relativistic effects on the core-polarization contribution. It is well known that a single *jj*-coupled configuration is not a good description of most atoms, with the exception of the heaviest ones (for numerical data, see Cowan and Mann, 1971; Desclaux, 1972). A simple way to remedy this deficiency is an average-of-configuration treatment proposed in the relativistic case by Mayers (1970) and used by Desclaux *et al.* (1971a) and in the tables of Desclaux (1973). A second method of this type was proposed by Lindgren and Rosén (1974) and a third one by Andriessen and van Ormondt (1975) who also discussed the connections between these methods (see also Larkins, 1976). A more exact way of avoiding this difficulty is to use a multiconfiguration Dirac–Fock method. The program of Desclaux (1975) accepts up to forty configurations. It has been used for calculating oscillator strengths by Desclaux and Kim (1975), Kim and Desclaux (1976), and Armstrong *et al.* (1976). Grant *et al.* (1976) have presented an MCDF-AL (average level) method, where the energies of an entire group of atomic states are obtained from a single diagonalization.

Lin (1977) showed that the exchange part of the DF approximation violates the gauge invariance of the transition amplitude, whereas the random-phase approximation (RPA) does not. This explains the different oscillator strengths from the length and velocity formulas.

The *jj*-coupled equivalents to Hund's rules were discussed by Walker and Waber (1973) and Pyper and Grant (1977). Walker (1969) studied electron scattering from Hg at the DF level. Finally one may point out that mixed atoms containing both electrons and muons can also be treated by the DF method (Fricke and Desclaux, 1974). Rose *et al.* (1978) showed that the contraction of s and $p_{1/2}$ valence AO = s is a direct relativistic effect.

9. *Beyond Dirac–Fock*

The main purpose of the MCDF method was to get a decent description of an *LS*-coupled state using *jj*-coupled determinants. Some correlation can, however, also be included. Johnson and Lin (1976, 1977) presented a relativistic random-phase approximation for two-electron atoms using DF basis functions and applied it to transition probabilities. Due to CI, the naming of ground-state electron configurations for open-shell systems is not always physically interesting. Pyper and Grant (1977) used the MCDF method for interpreting Hund's rules in atomic spectra.

B. Relativistic Band-Structure Calculations

The importance of spin–orbit effects on electronic energy band structure was realized quite early [see, e.g., Elliott (1954a,b), Lehman (1959, 1960), or the extensive bibliography of Bradley and Cracknell (1972)].

The other (mass–velocity and Darwin) terms were brought in by Callaway *et al.* (1957), Herman *et al.* (1963), and Johnson *et al.* (1963). Relativistic versions were presented for the orthogonalized plane-wave method (ROPW) (Soven, 1965), the Korringa–Kohn–Rostocker method (RKKR) (Onodera and Okazaki, 1966a; Sommers and Amar, 1969; Inoue and Okazaki, 1971; Neto and Ferreira, 1976), and the augmented plane-wave method (RAPW) (Loucks, 1965; Koelling, 1969), and the pseudopotential method (Animalu, 1966). Loucks (1967), Davis, (1974), Freeman and Koelling (1972, 1974), Koelling and Freeman (1976), and Rössler and Treusch (1972) reviewed relativistic band-structure results (see also Dimmock, 1971).

The early two-component calculations (Conklin *et al.*, 1965; Rabii, 1968) include only the direct relativistic effects as first-order perturbations, whereas the later four-component calculations, starting from DS or DF atomic potentials, include both the direct and indirect relativistic effects (Christensen and Seraphin, 1971; Koelling and Freeman, 1973, 1975; Onodera *et al.*, 1966; Krogh Andersen, 1969; Tterlikkis *et al.*, 1968, 1969, 1970). A quasi-relativistic spin-polarized method and an application on Gd were announced by Koelling *et al.* (1977; Koelling and Harmon, 1977).

IV. Relativistic Molecular Orbitals

Bethe (1929) introduced the concept of a "double-symmetry group." It is obtained from symmetry group G by adding to it an element R, $R^2 = E$, $RA = AR$, $\forall A \varepsilon G$. Then the order of the group is doubled and "additional" irreducible representations are introduced. The symmetry orbitals, spanned by relativistic basis functions with half-integer j belong to these additional irreducible representations. Their number is in many cases smaller than that of the representations of the single group. Then several nonrelativistic symmetries will be mapped to a single relativistic symmetry. This phenomenon is called "spin–orbit-induced hybridization." For example, the single group C_{2v}, of order $g = 4$, has four one-dimensional irreducible representations, whereas the corresponding double group has one additional two-dimensional irreducible representation,

$$\sum_{i=1}^{5} n_i^2 = 1^2 + 1^2 + 1^2 + 1^2 + 2^2 = 8. \qquad \text{(IV.1)}$$

Thus all the relativistic molecular orbitals of C_{2v} belong to the same irreducible representation Γ_5.

The character tables, compatibility tables, and coupling constants for all thirty-two double-point groups were published by Koster *et al.* (1963). Bradley and Cracknell (1972) gave the corresponding representation matrices, a thorough theoretical discussion, and an extensive bibliography. For a general discussion of double groups, see, e.g., Griffith (1960).

The required relativistic molecular orbitals can be constructed by projection operator methods or coupling constant methods.

Let ϕ_λ^k be the basis function belonging to the λth row of the kth irreducible representation, and $\psi_{n\kappa m}(\mathbf{r})$ an arbitrary four-component basis function at site $\mathbf{t}$. Then the projection operator method yields (Rosén and Ellis, 1975)

$$\begin{aligned}\phi^k_\lambda &= P^k_{\lambda\nu}\psi_{n\kappa m}(\mathbf{r}-\mathbf{t})\\ &= \frac{n_k}{g}\sum_R \Gamma^k_{\lambda\nu}(R)^*\psi_{n\kappa m}(\mathbf{r}-\mathbf{t}_\mathrm{R})(-)^{l\tau_\mathrm{R}}D^j_{m'm}(\alpha,\beta,\gamma).\end{aligned} \tag{IV.2}$$

Here n_k is the dimension of k, $\Gamma(R)$ is the representation matrix for the group element R, $\mathbf{t}_\mathrm{R}$ denotes the vector into which $\mathbf{t}$ is transformed, τ_R is zero (unity) for proper (improper) rotations, $D^j_{m'm}$ is a rotation matrix element, and (α, β, γ) are the Euler angles of R.

In the coupling constant method, one first constructs the nonrelativistic symmetry orbitals u^k_λ in a $|lm_l\rangle$ basis. One then observes into which additional irreducible representation j the spin functions v^j_μ belong. The symmetry functions ϕ^k_λ are then obtained using the coupling constants $u^{ij,k}_{\lambda\mu,\nu}$ tabulated by Koster *et al.* (1963):

$$\phi^k_\nu = \sum_{\lambda\mu} u^{ij,k}_{\lambda\mu,\nu}\, u^i_\lambda\, v^j_\mu . \tag{IV.3}$$

This yields every ϕ^k_ν as a linear combination of states $|lm_l\tfrac{1}{2}m_s\rangle$.

Finally, one may use Clebsch–Gordan coefficients to express them as states $|jm\rangle$ or $\psi_{n\kappa m}$. This method has the advantage of automatically giving the correct relative phase for the two states $j = l \pm \frac{1}{2}$.

Mulliken (1934) discussed *jj* coupling in molecules. Relativistic symmetry orbitals and explicit representation matrices were published for the double groups O, O_h, T_d, $D_{4\mathrm{h}}$, $C_{4\mathrm{v}}$, $D_{3\mathrm{d}}$, $C_{3\mathrm{v}}$, and $C_{2\mathrm{v}}$ by Onodera and Okazaki (1966b), for $D_{3\mathrm{h}}$ by Toivonen and Pyykkö (1977a; see also Teleman and Glodeanu, 1967), and for T and T_h by Toivonen and Pyykkö (1977b). General formulas for the "simple rotation groups" C_n, $C_{n\mathrm{h}}$, S_{2n}, $C_{n\mathrm{v}}$, D_n, $D_{n\mathrm{h}}$ and $D_{n\mathrm{d}}$ for any n were found by Oreg and Malli (1976a,b). Linear molecules were discussed by Nikitin (1961), Oreg and Malli (1974), and Desclaux and Pyykkö (1976). Basis functions at the $|lm_l\tfrac{1}{2}m_s\rangle$ level were derived for $D_{3\mathrm{h}}$ by Manne *et al.* (1975).

The symmetry coupling coefficients were also discussed by Golding for O (Golding, 1971) for the icosahedral group (Golding, 1973) and for C_n, D_n, and T (Golding and Newmarch, 1977). Lulek (1975) applied graphical methods on this problem.

A naive discussion of molecular binding at the *jj* limit was presented by Woods Halley and Shore (1965). Leushin (1968) published basis functions at the center of symmetry for all crystallographic point groups but did not discuss the influence of the orbital quantum number l. It seems that basis functions for the icosahedral groups have not yet been published.

V. One-Electron Systems

The simplest possible system for studying relativistic effects in chemical bonding is H_2^+. Pavlik and Blinder (1967) studied several variational LCAO-type solutions of the Dirac equation for H_2^+ and found that relativistic effects decrease the electronic energy by about -7×10^{-6} a.u.

Luke *et al.* (1969) used the exact nonrelativistic wavefunction of H_2^+ for calculating the relativistic correction exactly to the order α^2. Their result for the decrease of E_T is -7.38×10^{-6} a.u. and, for the increase of D_e, 1.2×10^{-6} a.u. or 12 ppm. They also found that relativistic effects shorten the bond length, R_e, by 3×10^{-5} a.u. or by 15 ppm. As the relativistic effects behave like Z^2, these results scale beautifully into a relativistic contraction of the order of 10% for the heaviest elements, in agreement with the Dirac–Fock one-center results discussed in Section IV,A. Bishop (1976, 1977) used a similar but more accurate solution for discussing the rotation-vibration energy levels for HD^+, HT^+, and HT^+.

Variational solutions of the one electron–two center problem at the particular eigenvalue diving to the lower continuum were considered by Popov (1971) and Marinov and Popov (1976, and references therein). Müller *et al.* (1973) solved the Dirac equation for two Coulomb centers using a large basis-set expansion in prolate spheroidal coordinates. An extended discussion of the same problem was given by Müller and Greiner (1976). Kaufmann and Wille (1976) used a Breit–Pauli perturbation scheme and conclude that their relativistic corrections agree within a few percent with the exact ones of Luke *et al.* for H_2^+, whereas larger deviations from those of Müller *et al.* were found for Br + Br, perhaps due to differences in the size of the basis sets.

The Kronig–Penney model for a Dirac electron in a one-dimensional crystal was considered independently by Wood and Callaway (1957), by Glasser and Davison (1970), by Avron and Grossman (1976), and by Kandilarov and Detcheva (1976).

VI. Dirac–Fock Calculations

A. One-Center Expansions

The nonrelativistic one-center expansion (OCE) calculations were reviewed by Bishop (1967), by Hayes and Parr (1967), and by Joshi (1965). This method is only applicable to hydrides XH_n^{m+} and even for them it is slowly converging if accurate results are required. On the other hand, even the crudest (spherically symmetrical) OCE's are known to give surprisingly good X—H bond lengths, R_e, and force constants, k_2. As most elements form chemical bonds with hydrogen, this is therefore a logical way to start investigating the effects of relativity on the length and strength of covalent chemical bonds and it is, indeed, almost the only method used for this purpose so far. [Exceptions are the first-order perturbation studies on H_2^+ by Luke *et al.* (1969) and on diatomic alkali halides by Matcha (1973, 1976).]

The central points of the DF-OCE method are as follows:

1. The wavefunction is expanded around the heavy atom.
2. The proton potential is expanded around the heavy atom X,

$$\frac{1}{r_H} = \sum_{l=0}^{\infty} \frac{r_<^l}{r_>^{l+1}} P_l(\cos \vartheta_X). \qquad \text{(VI.1)}$$

3. A full four-component Dirac equation is used for the single-particle states. Every single-particle state may consist of one or more $|nljm\rangle$ states. For example, the valence 6σ MO of AuH was expressed by Desclaux and Pyykkö (1976) in the form

$$\phi(m_j = \tfrac{1}{2}) = \chi(s_{1/2}\, m_j = \tfrac{1}{2}) - \chi(p_{1/2}\, m_j = \tfrac{1}{2}) + \chi(p_{3/2}\, m_j = \tfrac{1}{2}),$$
$$\phi(m_j = -\tfrac{1}{2}) = \chi(s_{1/2}\, m_j = -\tfrac{1}{2}) + \chi(p_{1/2}\, m_j = -\tfrac{1}{2}) + \chi(p_{3/2}\, m_j = -\tfrac{1}{2}). \qquad \text{(VI.2)}$$

4. The total wavefunction is expressed as a single Slater determinant.
5. Full exchange is used.
6. The radial wavefunctions are solved numerically. This gives automatically the best possible radial wavefunctions. The norms of the AO components, e.g., in Eq. (VI.2), are also optimized.
7. Finally, the Breit correction, H_{Br}, may be added after the SCF phase as a first-order correction. This was only done in one case (Desclaux and Pyykkö, 1974). As seen from Table III, H_{Br} seems to be a chemically uninteresting quantity, at least for the heavier elements.
8. The nonrelativistic results may be produced by the same program with exactly the same assumptions by changing the speed of light from 137 a.u. to a very high value.

Mackrodt (1970) published DF-OCE results within the spherically symmetrical approximation for the groups Ia and IVb to VIIb (NaH, RbH, CH_4 to SnH_4, ..., HF to HI). Unfortunately, his results seem to contain numerical errors that invalidate his conclusions. The same approximation was used for the group IVb hydrides CH_4 to PbH_4 (Desclaux and Pyykkö, 1974) and $(114)H_4$ (Pyykkö and Desclaux, 1977a). The relativistic effects shortened the X—H bond by 0.6, 1.8, and 5.6% and increased the stretching force constant by 10, 13, and 45% for GeH_4, SnH_4, and PbH_4, respectively. The R_e and k_2 for $(114)H_4$ were closely similar to those of PbH_4.

The symmetry functions, Eq. (VI.2), were added for the group Ib hydrides CuH, AgH, and AuH by Desclaux and Pyykkö (1976). The relativistic contraction[1] of R_e for AuH was 9.3 and 7.2% without and with the p-type symmetry functions, respectively. Relativistic effects increased the dissociation energy, D_e, by 0.002, 0.013, and 0.053 a.u., respectively. The last value is about 46% of the experimental D_e for AuH. The nonrelativistic orbital energies of AgH and AuH were strikingly similar, whereas the relativistic ones were not (see Fig. 3). The nonrelativistic bond lengths also agree within 3%, but the experimental R_e for AuH is 5.8% shorter than that for AgH. This suggested "that the chemical difference between silver and gold may mainly be a relativistic effect." In Part III of the DF-OCE series, Pyykkö and Desclaux (1976) found for the group IIIb series BH to TlH relativistic contractions

$$C = [R_e(\text{n.r.}) - R_e(\text{rel})]/R_e(\text{n.r.}) \qquad \text{(VI.3)}$$

of the same order of magnitude as for the IVb or Ib groups. Including the result of Luke *et al.* (1969) for H_2^+, a reasonable fit was found to be

$$C(\%) = 8.5 \times 10^{-4} Z^2, \qquad \text{(VI.4)}$$

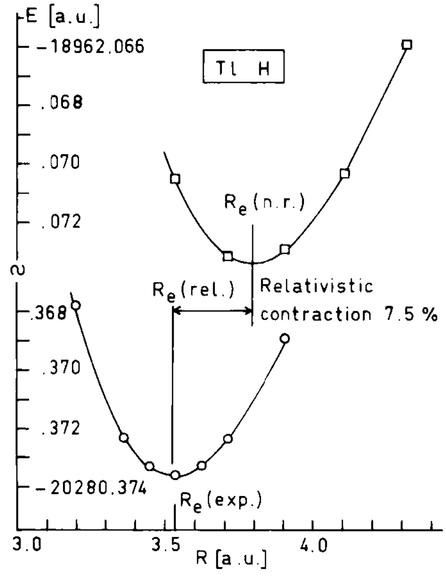

Fig. 2. The calculated relativistic and nonrelativistic total energies, E_T, as a function of the Tl—H bond length, R, for the TlH molecule (Pyykkö and Desclaux, 1976). The curves are fitted third-degree polynomials. The relativistic contraction is 7.5% of R(rel) or 7.0% of R(n.r.).

---

[1] The original values change slightly when a Morse potential fit is used (Pyykkö, 1979). Hay *et al.* (1978) find for AuH using pseudopotentials 14 to 17%.

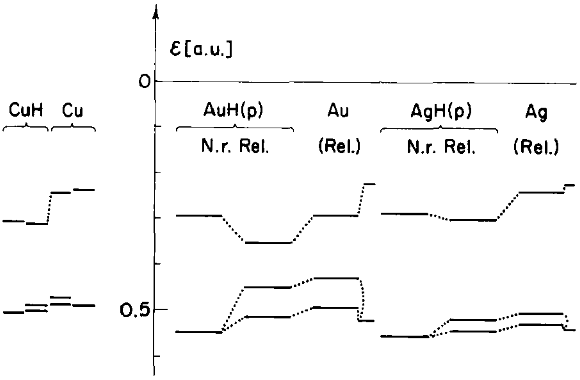

Fig. 3. The calculated nonrelativistic and relativistic Hartree–Fock orbital energies, ε, for molecules CuH, AuH, and AgH, according to Desclaux and Pyykkö (1976), and for atoms Cu, Au, and Ag, according to Desclaux (1973). The author observed the similarity of the nonrelativistic orbital energies for gold and silver while drawing this overhead transparency.

where Z is the central nuclear charge. The potential curves for TlH are shown in Fig. 2. A weak counterexample against a relativistic contraction of R_e of PbO was published by Schwenzer *et al.* (1973). They reported HF–LCAO calculations for both CO and PbO at the minimal Slater-type orbital (STO) level and found that the calculated R_e values deviated from R_e(exp) by +4 and −3 %, respectively. An error of this order of magnitude could, however, be explained by basis-set incompleteness and the usual correlation error.

A transition to predominant $p_{1/2}$ bonding instead of $p\sigma$ bonding was found for TlH. At the nonrelativistic limit, the ratio of the norms

$$N(p_{3/2})/N(p_{1/2}) = 2 \tag{VI.5}$$

for a $p\sigma$ orbital. For InH, this ratio has fallen to 1.46, and for TlH to only 0.65. The adopted model placed the 6s AO in the core and also neglected the *jj*-coupled Slater determinant with the AO's $|6p_{3/2}, m_j = 3/2\rangle$ and $|6p_{3/2}, m_j = -3/2\rangle$. With these reservations, the decoupling of the $6p_{3/2}$ AO from the chemical bond may, at least partially, explain the dominant monovalency of Tl as contrasted to the trivalency of B, Al, Ga, and In. The relativistic effects increased D_e for AlH, GaH, and InH and decreased D_e for TlH, presumably due to the lost directional characteristics of the $p\sigma$ bond.

At this point it is worthwhile to mention the experimental photoelectron spectroscopic evidence for an increased $p_{1/2}$ norm in the electronic ground state of Se_2 and Te_2 (Berkowitz, 1975; Lee *et al.*, 1976) and TeO (Potts and Williams, 1976).

In view of the large relativistic effects for the other groups, it is surprising that the group IVa elements Zr ($Z = 40$) and Hf ($Z = 72$) should be chemically and physically so similar. Pyykkö and Desclaux (1977b) carried out DF-OCE calculations for the tetrahedral model systems TiH_4, ZrH_4, HfH_4, and $(104)H_4$ including both p and d AO's in the t_2 MO's Γ_7 and Γ_8. About 50% p and 50% d character was found. The relativistic contraction C_r was an order of magnitude smaller than those predicted by Eq. (VI.4) and, in fact, negative for TiH_4 and ZrH_4. Thus the similarity of Zr and Hf seems to be due to an anomalous cancellation of the relativistic effects.

Pyykkö and Desclaux (1978) considered MH_4 (M = Ce, Th) and MH_6 (M = Cr, Mo, W, U, 106) and Pyykkö (1979) considered group II MH^+ and MH_2.

B. Linear Combination of Atomic Orbitals

The formal theory for a molecular DF-LCAO scheme was discussed by Malli and Oreg (1975), but numerical applications of this scheme have not yet been published.

VII. Dirac–Slater Calculations

A. Discrete Variational Method

The discrete variational method of Ellis and collaborators calculates the Hamiltonian and overlap matrix elements by using a discrete, three-dimensional set of N sampling points, $\mathbf{r}_p$, and weigths, W_p, e.g.,

$$\langle \chi_i | H | \chi_j \rangle = \frac{1}{2}\left[\sum_{p=1}^{N} W_p \int ds\, \chi_i^{+}(\mathbf{r}_p, s)(E_j^0 + U_j(\mathbf{r}_p))\chi_j(\mathbf{r}_p, s) + \text{Hermitian conjugate}\right]. \qquad \text{(VII.1)}$$

Here the $\chi_j(\mathbf{r})$ are relativistic symmetry orbitals, expressed as a linear combination of four-component AO's centered on the various atoms, s is the spin coordinate, E_j^0 is the eigenvalue of the single-site Dirac Hamiltonian for the basis orbital χ_j, and U_i is the Coulomb plus exchange potential generated as a superposition of the atomic densities. Then the secular equation

$$\mathrm{HC} = \mathrm{ESC} \qquad \text{(VII.2)}$$

can be solved in the usual way. Typical values of N are a few hundred points per atom for $Z < 50$ and up to 1500 points for heavy atoms such as U. The latter N gives an eigenvalue accuracy of about 0.01 eV (Koelling *et al.*, (1976). A minimal basis of numerical atomic DS solutions is used in the construction of the χ_j. Thus both the direct and indirect relativistic effects are included, even when no iterations are carried out.

Rosén and Ellis (1974) first applied this method to the linear molecule XeF_2 using both the DS-DVM eigenvalues and a transition-state procedure for determining the ionization energies. The dihydrides H_2X (X = O, S, Se, Te), diatomic indium halides InX (X = F, Cl, Br, I), and metal chlorides XCl (X = B, Al, Ga, In) were discussed by Rosén and Ellis (1975). The spin-orbit splitting is automatically obtained in the DS-DVM calculations. The value for InI, 0.7 eV, is in good agreement with the experimental value of 0.68 eV.

Ellis *et al.* (1975) presented results for UO_2^{2+}. They also introduced a moment-polarized exchange scheme, having separate values for the positive and negative m_j, and applied it to Os. The spin polarization and spin-orbit splittings were found to be nearly additive. [Unrestricted DF calculations by Desclaux and Bessis (1970) were already mentioned in Section III,A,8.]

The ionization potentials of the uranyl ion, UO_2^{2+}, including a D_{6h} crystal field were reported by Walch and Ellis (1976). One example is reproduced in Fig. 4. Koelling *et al.* (1976) gave results for the actinide hexafluorides UF_6, NpF_6, and PuF_6. The results were again used for predicting electronic spectra. The dioxides ThO_2 and UO_2 were discussed by Gubanov *et al.* (1977) using cluster models such as $(UO_6)^{10-}$. Adachi *et al.* (1977) considered the cesium halides, CsX, (X = F, Cl, Br, I). Both the spin-orbit splitting of the I and Cs 5p AO and the relativistic contraction

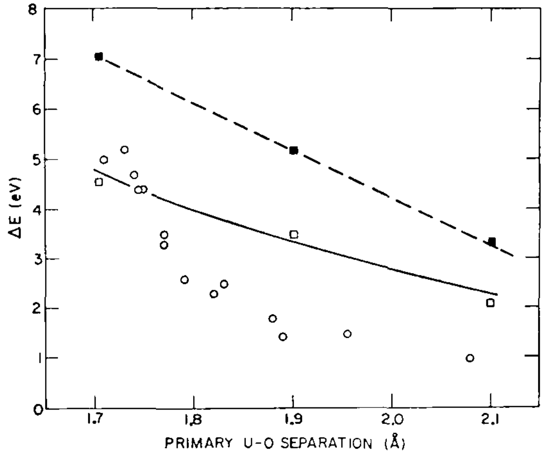

Fig. 4. Comparison of the experimental "$6p_{3/2}$" splitting versus primary U—O separation and the calculated 14S 1_u-7S 3_u splitting (Walch and Ellis, 1976). The dashed line stands for the free ion UO_2^{2+}, and the solid line for a UO_2^{2+} ion perturbed by a D_{6h} crystal field. The circles represent experimental data.

of the latter one were helpful in improving the agreement with experiment for CsI. Ellis (1977b) tested a moment-polarized version of his relativistic exchange potential on the open-shell molecule FeO, opening the way to simultaneous treatment of core-polarization effects, relativistic splittings, and level shifts in molecules containing heavy atoms. Ellis and Rosén (1977) applied their method on the hexafluorides of the 5d transition metals. Kim *et al.* (1977a,b) studied UF_6, Rosén (1978) InI, Rosén *et al.* (1978) $(110)F_6$, and Gubanov and Chirkov (1978) CmO_2.

The DS-DVM method was also applied on quite a different problem, namely, the colliding heavy ion systems such as $(Au—I)^{76+}$ at internuclear distances $0 < R < 0.3$ a.u. by Morović *et al.* (1976) and Fricke *et al.* (1976). The results were used for interpreting collision X-rays. Morović *et al.* (1977) presented a similar discussion for the Xe—Ag system.

B. Multiple Scattering Xα

The formalism for a DS-MS Xα scheme was discussed by Yang and Rabii (1975), Cartling and Whitmore (1975, 1976), Machado and Ferreira (1976), Neto and Ferreira (1976) and Rosicky *et al.* (1976). A quasi-relativistic scheme using the mass–velocity and Darwin terms and omitting the spin–orbit interaction was used for PbTe by Pratt (1973).

In this method the space is divided into N nonoverlapping spheres that are surrounded by an outer sphere O and the potential is taken as

$$V(\mathbf{r}) = \sum_{\alpha=O}^{N} V_\alpha(r_\alpha) + \bar{V}, \tag{VII.3}$$

where the V_α are spherically symmetrical, and $\bar{V}$ is a constant from which the energy $\varepsilon = E - \bar{V}$ is measured. This local potential $V(\mathbf{r})$ may include a local density approximation of exchange and correlation. The solution $\psi(\mathbf{r})$ satisfies the integral equation

$$\psi(\mathbf{r}) = \int d\mathbf{r}' G(\mathbf{r}, \mathbf{r}')[V(\mathbf{r}') - \bar{V}]\psi(\mathbf{r}'), \tag{VII.4}$$

where the Green's function $G(\mathbf{r}, \mathbf{r}')$ is defined by

$$[c\boldsymbol{\alpha} \cdot \mathbf{p} + \beta mc^2 - \varepsilon]G(\mathbf{r}, \mathbf{r}') = -I\,\delta(\mathbf{r} - \mathbf{r}'). \tag{VII.5}$$

Here I is a four-dimensional unit matrix.

The first numerical results using this scheme were published by Yang (1976) for C_2 and I_2. The calculated ionization energies for I_2 are shown in Fig. 5. One particular point of interest is the fact that the spin–orbit splitting of the $1\pi_g$ into $1e_{3/2g}$ and $3e_{1/2g}$ is smaller than the splitting of the $1\pi_u$ into $1e_{3/2u}$ and $2e_{1/2u}$. This effect was first interpreted by Wittel (1972) as arising from spin-orbit-induced hybridization. The $e_{1/2g}$ MO's arising from $1\pi_g$ and $2\sigma_g$ have the same symmetry and repel each other, diminishing

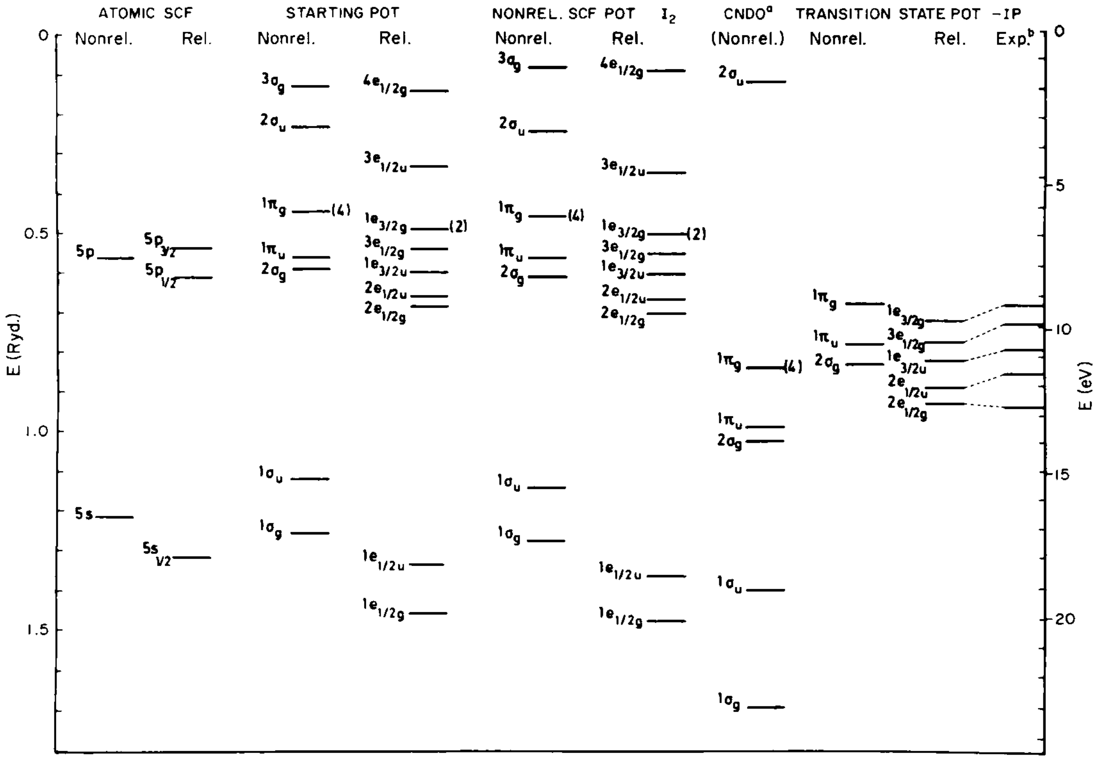

Fig. 5. Valence orbital energies of I and I_2 (Yang, 1976). The results under "Transition State Pot." come from three separate nonrelativistic and five separate relativistic SCF transition calculations. The relativistic calculations also use the nonrelativistic SCF transition state potential.

the $1\pi_g$ splitting. [The overlap effects may also contribute to the difference of the splittings; see Hall (1975).]

Dirac–Slater MS-Xα results for other molecules were announced by Yang *et al.* (1976). Critical remarks on the MS-Xα method, due to surface charges on the various spheres, were published by Grant and Whitehead (1976). For other applications, see Yang and Rabii (1976), Messmer *et al.* (1977), Yang (1978), and Yang *et al.* (1978).

VIII. Semiempirical Calculations

A. Crystal-Field Theory

Crystal-field theory is based on the assumption that the crystal-field parameters B_q^k may be factorized into a product

$$B_q^k = A_k^q\langle r^k\rangle = A_k^q \int_0^\infty R_{nl}(r) r^k R_{nl}(r) r^2\, dr. \qquad \text{(VIII.1)}$$

Here the A_k^q are determined by the point charges representing the ligands and the $R_{nl}(r)$ are the nonrelativistic wavefunctions of the open shell of the transition metal in question.

Wybourne (1965) observed that in the relativistic case the two radial wavefunctions g and f in Eq. (II.7) will be different for the two cases $j = l \pm \frac{1}{2}$. Then one must consider the integral,

$$R_{+-}^k = \int_0^\infty r^k(g_+ g_- + f_+ f_-) r^2\, dr, \qquad \text{(VIII.2)}$$

and the corresponding integrals R_{++}^k and R_{--}^k separately. Here + refers to $j = l + \frac{1}{2}$, and − to $j = l - \frac{1}{2}$. These integrals arise when an equivalent operator formalism is used to express the relativistic interactions in an *LS*-coupled formalism. A similar formalism was used for hyperfine effects in atoms by Sandars and Beck (1965).

Wybourne (1965, 1966) applied this method to the zero-field splitting of $Gd^{3+}(4f^7)$ and concluded that the relativistic contributions are important, although apparently not dominant. Chatterjee *et al.* (1973) included the effects of overlap and covalency to this model. Newman and Urban (1975) compared the DF $R_{\pm\pm}^k$ of Rosén and Waber (1974) with those obtained from HFS wavefunctions by allowing for $nl \rightarrow n'l$ CI due to the spin–orbit interaction. A similar comparison for Mn^{2+} was done by Andriessen *et al.* (1973, 1974). They found that the contribution to the difference of $R_{5/2,\,5/2}^2$ and $R_{3/2,\,3/2}^2$ from the continuum states is about half that of the bound states. A small difference between the CI and DF values was attributed to SCF relativistic effects. The Mn^{2+} zero-field splitting was studied earlier by Van Heuvelen (1967) and Hagston and Lowther (1973). The latter authors introduced double group theory to this problem.

Coulomb and spin–orbit parameters for crystal-field treatments of the actinides were calculated by Lewis *et al.* (1970) and Varga *et al.* (1971) from DS and DF wavefunctions. Parrot (1975) used the same effective operator formalism for discussing spin-forbidden transition probabilities of d^5 ions. Zevin *et al.* (1978) considered relativistic quadrupolar contributions in systems with nonvanishing orbital magnetism.

B. Extended Hückel Calculations

Due to spin–orbit-induced hybridization, higher order spin–orbit effects may considerably change the composition of molecular orbitals. A simple example are the different spin–orbit splittings of the $I_2^+ \Pi$ states, interpreted using second-order perturbation theory by Wittel (1972). Berkowitz *et al.* (1973) diagonalized the π-σ and spin–orbit splitting matrices for diatomic alkali halides. Wu and Fehlner (1966) discussed similar effects for some heavy group 4–6 diatomic molecules. A simple way to include these effects is to use Hückel or extended Hückel (EH) theory, including spin and thereby doubling the size of the matrix. Then some form of the spin–orbit Hamiltonian, $H_{S\text{–}O}$, may be included in the matrix before it is diagonalized.

Calculations of this type were reported for alkyl halides by Brogli and Heilbronner (1971), for halomethanes by Dixon *et al.* (1971), for the PX_3 (X = Cl, Br, I) and PYX_3 (X = Cl, Br; Y = O, S) series by Berkosky *et al.* (1973), for the dihalogens I_2, Br_2, ICl, and IBr by Hall (1975b), for the same molecules as well as several halomethanes, haloacetylenes, halocyanides, and haloborides by Manne *et al.* (1975), for mercury halides by Wittel *et al.* (1974b), for iodoethylenes by Wittel *et al.* (1974a), and for GaI_3 by Wittel and Manne (1975). The results of Manne *et al.* (1975) for the dihalogens are reproduced in Fig. 6.

It is interesting to observe that, e.g., for the $2b_1$ MO of CH_2I_2, having the C_{2v} symmetry, only 57% of the original symmetry is left after spin–orbit interaction, making the normal point-group classification of little meaning (Manne *et al.*, 1975).

A technical point of interest is that if the usual, real, basis functions $|l(xyz)m_s\rangle$ are used, the matrix to be diagonalized is a complex one (Hall, 1975a,b). If double-group basis functions are used, a real matrix may be used in the cases treated by Dixon *et al.* (1971) or Berkosky *et al.* (1973). Manne, Wittel, and collaborators first solve the usual EH problem and then diagonalize the doubled complex matrix.

Hafemeister (1967) pointed out that relativistic effects change the overlap integrals between two iodine ions in an alkali iodide crystal by as much as 10%. It would be interesting to see in which way such effects will influence the EH results. We emphasize that the calculations mentioned in the foregoing use one-component basis functions that are identical for $j = l \pm \frac{1}{2}$.

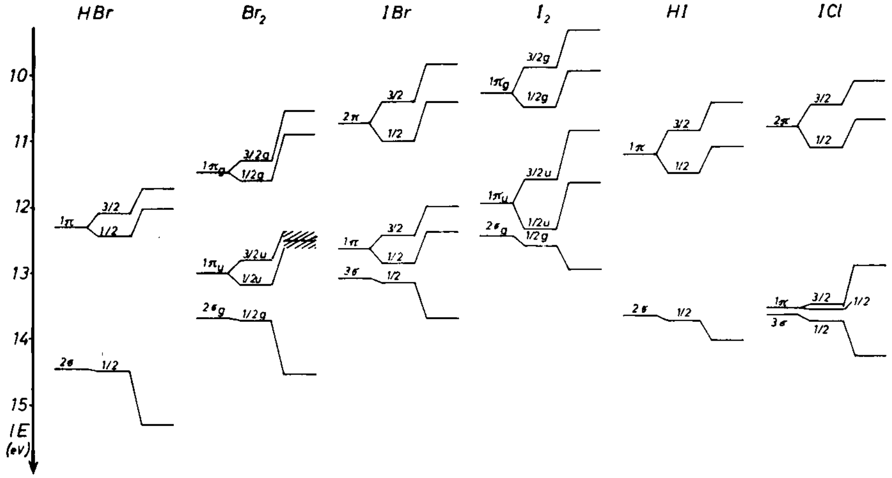

Fig. 6. Comparison of theoretical and experimental ionization energies for diatomic bromides and iodides, according to Manne *et al.* (1975). For each molecule the contributions from left to right are (i) and (ii) Extended Hückel calculations without and with spin–orbit interaction, respectively, and (iii) experimental ionization energies.

This question was recently studied in the relativistically parametrized extended Hückel theory (REX) of Lohr and Pyykkö (in press).

Hyde and Peel (1977) treated the spin–orbit splittings of tin and antimony halides in much the same way but within a nonempirical valence-electron (NEVE) pseudopotential framework.

IX. Perturbation Calculations

Spin–orbit splittings in atoms, molecules, and solids form a vast field that would require its own review. A concise summary of calculations of spin–orbit coupling constants and related quantities in molecules was given by Richards *et al.* (1974). The consequences of spin–orbit coupling extend from the strength and polarization of singlet–triplet transitions, zero-field splittings and intensities in the magnetic circular dichroism spectra to off-diagonal effects such as Λ-doubling, singlet–triplet perturbations for diatomic molecules, g tensors, and NMR pseudocontact effects and predissociation linewidths.

The singlet–triplet transition probabilities of aromatic systems were reviewed by Goodman and Laurenzi (1968) and those of transition metal complexes by Lohr (1972). An extensive discussion of spin–orbit effects for the triplet states of organic molecules was given by McGlynn *et al.* (1969) and by Becker (1969). Tully (1976) reviewed spin–orbit effects on potential surfaces for molecular collisions and McClure (1959) spin–orbit effects in optical spectra of solids.

A. Breit–Pauli *ab Initio* Calculations

Ladik (1959, 1961a) calculated various perturbation terms in Eqs. (II.12) and (II.13) using the simple Wang wavefunction for H_2. He concluded that relativistic effects decrease D_e by 18×10^{-6} a.u. This result seems to be too large by an order of magnitude, due to the omitted terms, the simple wavefunction or errors. Kołos and Wolniewicz (1964) found, using a fifty-four-term wavefunction, that the relativistic decrease of D_e is only 2.4×10^{-6} a.u.

Matcha (1973) used the Breit–Pauli first-order perturbation scheme in conjunction with his near-Hartree–Fock STO wavefunctions for several diatomic alkali halides. He found that the relativistic effects increase D_e for LiBr, the heaviest molecule studied, by 7.8%. The dominant term for the molecules was the mass-velocity one, Eq. (II.12b). Its effect was largely canceled by the Darwin term, Eq. (II.12h), rather like in Fig. 1. The spin–spin and spin–orbit corrections for the constituent atoms were larger still (see Table VI) and are, in fact, the dominant contribution to D_e^{rel}. The relativistic SCF effects are evidently missing from these calculations, but they demonstrate beautifully how large the relativistic effects on D_e are already for a relatively light atom such as Br ($Z = 35$). A more detailed discussion of the same results was published by Matcha (1976). A D_e^{rel} of the present magnitude for solid KCl would double the deviation of Löwdin (1948) from experiment.

TABLE VI

VARIOUS RELATIVISTIC FIRST-ORDER BREIT–PAULI CORRECTION TERMS TO THE DISSOCIATION ENERGIES, D_e, OF LiBr AND KCl[a]

Contribution[b]	LiBr	KCl
ΔM = Mass velocity, Eq. (II.12b), (a.u.)	+0.00394	+0.00371
ΔD = Darwin, Eqs. (II.12h) and (II.13g), (a.u.)	−0.00277	−0.00259
ΔF = Fermi contact part of spin–spin, Eqs. (II.13f), (a.u.)	+0.00004	+0.00003
ΔS = Spin–spin and spin–orbit, Eq. (II.12g), (a.u.)	+0.01119	+0.00267
D_e^{rel}(total) (a.u.)	+0.01240	+0.00382
D_e(exp.) (a.u.)	0.158	0.161
100 × D_e^{rel}(total)/D_e(exp.) (a.u.)	7.8	2.4

[a] According to Matcha, 1973, 1976.

[b] Symbol Δ refers to the difference between the molecule and the atoms. Contribution S vanishes for these closed-shell molecules, and ΔS thus arises from the atoms only. The orbit–orbit terms are omitted. The spin–spin terms, Eqs. (II.13c–e), vanish because the alkali ^2S and halogen ^2P states involve only one spin.

B. Quasi-Relativistic Methods

An interesting possibility would be to carry out molecular LCAO calculations using nonrelativistic wavefunctions but including some or all of the Breit–Pauli perturbation terms, Eqs. (II.12) and (II.13) in the Hamiltonian during the SCF phase. Such a method was proposed and formulated both omitting (Bersuker *et al.*, 1972) and including (Bersuker *et al.*, 1974) the two-electron terms of order $(v/c)^2$. Numerical results were reported for the single case of $PtCl_6^{2-}$ by Bersuker *et al.* (1977).

The theoretical foundations of this method are not clear. Its practical applications on atoms (see Section III,A,5) or solids (see Section III,B) would be sufficiently promising to merit a serious study.

C. Pseudopotential Methods[1]

A common method in band-structure calculations for heavy elements and their compounds is to use a pseudopotential that is supposed to include the other relativistic effects and to add the spin–orbit splitting afterward as a first-order perturbation (see, e.g., Schlüter and Schlüter, 1974). The first molecular application of this method was published by Das and Wahl (1976) for the lowest $^2\Sigma_{1/2}$, $^2\Pi_{1/2}$, and $^2\Pi_{3/2}$ states of HgH. The core potential for Hg was obtained by using the atomic DF program of Desclaux (1975). This pseudopotential is then inserted to a normal MCSCF LCAO calculation. One merit of this method is that it can describe the $^2\Sigma - {}^2\Pi_{1/2}$ mixing. The calculated R_e, D_e, the vibration frequency, ω_e, and the anharmonicity, $\omega_e x_e$, were in reasonable agreement with experiment.

One may expect this method to become quite popular, although it clearly contains more arbitrary elements than a fully self-consistent molecular DF or DS calculation. In this connection we also may mention the attempts of Gilbert *et al.* (1975) to deduce radii and softnesses for alkali and halide ions and rare gases from DF data.

D. Relativistic Corrections for Hyperfine Matrix Elements

The relativistic calculation of magnetic and electric hyperfine coupling constants in atoms was reviewed recently in great detail by Armstrong (1971) and by Lindgren and Rosén (1974). We, therefore, discuss here only the approximate, multiplicative, relativistic correction factors (RCF) that may be of some utility in molecular calculations.

1. *Magnetic Dipole Case*

An approximate correction for relativistic effects in a multielectron system can be obtained by multiplying the nonrelativistic matrix element of the hyperfine Hamiltonian, $H_{\mathrm{hfs}}^{\mathrm{n.r.}}$, by a relativistic correction factor

---

[1] Applied recently on diatomic rare gas compounds (Dunning and Hay, 1978; Ermler *et al.*, 1978; Wadt *et al.*, 1978), on I_2 (Das and Wahl, 1978), on PbO (Datta *et al.*, 1978), on AuH, HgH, and $HgCl_2$ (Hay *et al.*, 1978) and on Au_2 (Lee *et al.*, 1979).

$$B(n, \kappa, Z) = \frac{\langle \psi_{n\kappa}^{\mathrm{rel}} | H_{\mathrm{hfs}}^{\mathrm{rel}} | \psi_{n\kappa}^{\mathrm{rel}} \rangle}{\langle \psi_{nl}^{\mathrm{n.r.}} | H_{\mathrm{hfs}}^{\mathrm{n.r.}} | \psi_{nl}^{\mathrm{n.r.}} \rangle}. \tag{IX.1}$$

Here n and κ are the quantum numbers of the atomic orbital in question, and Z is the nuclear charge. Such correction factors were first evaluated by Breit (1930a) for $\kappa = -1$ (s electrons) and $n = 1,2$ using the Darwin–Gordon solution for a hydrogen-like atom. He already pointed out that this correction is a factor of 3.9 for the 2s shell of U. More approximate correction factors were derived by Racah (1931a,b) and Casimir (1936) and tabulated by Kopfermann (1958). Breit's original idea of n-dependent hydrogen-like correction factors $B(n, -1, Z)$ was generalized to arbitrary n by Inokuti and Usui (1957) and by Pyykkö and Pajanne (1971). As the latter authors found these corrections somewhat better than the n-independent ones of Racah (1931a,b) and Casimir (1936), the idea was generalized to arbitrary κ by Rosén and Lindgren (1973; Lindgren and Rosén, 1973) and by Pyykkö *et al.* (1973). The latter reference also gave numerical tables. These calculations were also compared with the corresponding DS RCF by Rosén (1972). The main conclusion was that the n-dependent corrections are an improvement over the Racah–Casimir ones for $\kappa = \pm 1$ but not for higher $|\kappa|$.

Such correction factors were used in otherwise nonrelativistic calculations of nuclear spin–spin coupling constants in molecules by Dalling and Gutowsky (1971) and by Pyykkö and Jokisaari (1975). A significant improvement was found for heavier elemenets such as Pb. Although these corrections are nearly 50 years old, surprisingly they are not well known to chemists or other NMR experimentalists. The failure to include them gives theoretical results that are too small by a factor of 2–3 for Hg (Henneike, 1972).

2. *Finite Nuclear Size*

The effect of the finite nuclear size on the magnetic hfs of $s_{1/2}$ states may rise to about 20% for the heaviest elements. This effect was discussed by Rosenthal and Breit (1932), Breit (1932b), Racah (1932), Crawford and Schawlow (1949), Bohr and Weisskopf (1950), Bohr (1951), and Rosenberg and Stroke (1972).

3. *The Self-coupling Problem*

Some confusion has been caused by the diverging second-order self-coupling energy $E_{\mathrm{HH}}^{(2)}$ of the Fermi-contact Hamiltonian,

$$H_3 = -\frac{8\pi}{3} g g_n \beta \beta_n \mathbf{I} \cdot \mathbf{s}\, \delta(\mathbf{r}_N), \tag{IX.2}$$

in calculations of nuclear spin–spin coupling constants, J. If the expressions for the internuclear spin–spin coupling are derived from second-order perturbation theory, the self-coupling terms are avoided entirely. If, however, variational methods are used, and an energy minimum, instead of a stationary condition, is used, the $E_{\mathrm{HH}}^{(2)}$ must be included.

We first have the problem of the correct order of magnitude of $E_{\mathrm{HH}}^{(2)}$. Gregson *et al.* (1970) found that a finite value could be obtained by using an exponential approximation to the function,

$$r_0/4\pi r^2(r + r_0)^2, \tag{IX.3}$$

appearing in Blinder's (1965) derivation of H_3. Here r_0 is of the order of the nuclear dimensions. A similar calculation using Eq. (IX.3) was carried out by Power and Pitzer (1971). Latvamaa *et al.* (1973) considered the same problem at the Dirac and QED levels of approximation and found that the Gregson self-coupling energies are over 100 times too large and totally unphysical. The reason was that introducing a variational function with sharp structure amounts to using second-order perturbation theory at high (in fact, ultrarelativistic) intermediate energies and evidently this cannot be done nonrelativistically. Later, Moore and Moss (1975a,b; 1976) found results of the correct order of magnitude if all the terms that are quadratic in the nuclear vector potential $\mathbf{A}_N$ are included. Their theory evidently still lacks quantitative meaning.

We then have the question how large an effect these intermediate states, corresponding to sharp structure in the perturbed wavefunction, have on J. According to Pyykkö and Jokisaari (1975) and Jansen *et al.* (1976; for a summary, see Pyykkö, 1975a) such contributions are less than 10^{-3} of the total for several X—H and X—X coupling constants. Sänger and Voitländer (1975) also found variationally that the self-coupling and heterocoupling energies are independent of each other to the order $O(10^{-6})$. We thus conclude that the self-coupling energy is not a relevant quantity in the present context.

Reiterating, we note that, due to the *Zitterbewegung*, the nonrelativistic one-component electron is not a point particle but rather a diffuse affair having dimensions of nearly 10^{-2} a.u. Any wavefunction introducing a sharper structure than this, is unphysical. A first-order correction for this effect is provided by the Darwin terms in Eqs. (II.12) and (II.13).

4. *Isotope and Isomer Shifts*

The theory for isotope shifts in atomic spectroscopy was reviewed by Breit (1958) and by Bauche and Champeau (1976). The theory for isomer shifts in Mössbauer spectroscopy was reviewed by Shirley (1964), who also gave numerical tables of the relevant relativistic correction factors $S'(Z)$, originally introduced by Bodmer (1953). Mallow *et al.* (1976) found from MCDF calculations "relativistic corrections" that agreed with the hydrogen-like $S'(Z)$ of Shirley to about 1% for Fe, 4% for Ru, and 15% for Ir. A combination of nonrelativistic EHT calculations and DF electronic densities at the nucleus was used for several iron compounds by Trautwein *et al.* (1975) and Reschke *et al.* (1977).

5. *Electric Quadrupole Effects*

The relativistic correction factors for nuclear quadrupole coupling were discussed by Casimir (1936) and Kopfermann (1958). An effective nuclear charge Z' must be used here. An n-dependent, hydrogen-like correction factor $C(n, \kappa, Z)$ was introduced (Lindgren and Rosén, 1973; Pyykkö *et al.*, 1973; Rosén and Lindgren, 1973), but the results were not encouraging.

X. Theories for Spectroscopic Properties

For several spectroscopic or other molecular properties the use of relativistic wavefunctions necessitates a change of the entire theory. In this section we mention some examples.

A. Compton Scattering

Mendelsohn *et al.* (1973, 1974) used DF wavefunctions together with a classical impulse profile,

$$J_{n\kappa}(q) = \tfrac{1}{2} \int_q^\infty (g_{n\kappa}^2(p) + f_{n\kappa}^2(p))p\,dp, \tag{X.1}$$

for calculating the Compton profile of several elements. The relativistic contraction manifests itself here as a relativistic decrease of $J(0)$. For U this decrease was 6.60%.

The relativistic expression for the Compton cross section was considered by Eisenberger and Reed (1974), by Manninen *et al.* (1974), and by Ribberfors (1975a,b). The relativistic theory becomes necessary for photon energies larger than about 20 keV. In that theory one loses the possibility of interpreting the results in terms of a simple momentum density.

B. Nuclear Spin–Spin Coupling Constants

Ramsey's (1953) nonrelativistic theory of nuclear spin–spin coupling in molecules assumed *LS* coupling and used a nonrelativistic hyperfine Hamiltonian consisting of the familiar nuclear spin–electron orbit, dipole–dipole, and Fermi-contact parts H_1, H_2, and H_3, respectively. For heavier molecules *LS* coupling breaks down, and the relativistic hfs Hamiltonian

$$H_{\text{hfs}}^{\text{rel}} = e\boldsymbol{\alpha} \cdot \mathbf{A}_N, \tag{X.2}$$

should be used. Here $\mathbf{A}_N$ is the vector potential due to the nuclear magnetic moment, and $\boldsymbol{\alpha}$ a Dirac matrix. Such a theory, using *jj*-coupling and $H_{\mathrm{hfs}}^{\mathrm{rel}}$, was formulated by Pyykkö (1977). A new isotropic coupling term, $J_{\mathrm{s-p}}$, was found. This term involves s AO's at one nucleus and p AO's at another. At the nonrelativistic limit, the theory of Pyykkö (1977) reduces to that of Ramsey (1953) and $J_{\mathrm{s-p}}$ vanishes.

A simple relativistic Pople–Santry-type model was constructed using the matrix elements of Lipas *et al.* (1973) and applied to $\mathrm{Hg(CH_3)_2}$. Relativistic effects increased the isotropic coupling constant $^1J(\mathrm{Hg—C})$ and its anisotropy by factors of 2.67 and 3.25, respectively. The new term $J_{\mathrm{s-p}}$ was only -1.7% of total. For coupling between two heavy $\mathrm{sp^3}$ hybridized elements, it should be 6 times larger. At this point it is interesting to note that Tterlikkis *et al.* (1969) found, in their ROPW calculations, a relativistic increase by a factor of 1.61 for the pseudodipolar coupling constant in Cs. The corresponding increase of the isotropic Knight shift was 1.32, whereas $B(6, -1, 55)$ would be 1.42. We are not aware of other examples of a possible relativistic increase of the relative coupling anisotropy,

$$\Delta' J = (J_{\parallel} - J_{\perp})/J. \tag{X.3}$$

Experimentally, the heaviest elements often show large values of $\Delta' J$. The predicted trend was confirmed for $\mathrm{Cd(CH_3)_2}$ by Jokisaari *et al.* (1978).

Relativistic corrections to the Zeeman effect in diatomic molecules were considered by Veseth (1977).

C. Magnetic Neutron Scattering

Stassis and Deckman (1976) considered the problem of magnetic scattering of neutrons by a relativistic atom. The interaction, responsible for the scattering, is again of the form Eq. (X.2), where $\mathbf{A}_N$ is now the vector potential of the neutron. This operator is "odd" in the sense of coupling the large components, g, to the small components, f. This leads to integrals of the type

$$\int_0^{\infty} j_k(qr) f(r) g(r)\, dr. \tag{X.4}$$

When such a straightforward formalism is used, toether with DF wavefunctions, the spin–orbit and other relativistic effects are all automatically included, just as in Section X,B.

The method was applied on tripositive rare-earth ions by Stassis *et al.* (1977). The differences between the nonrelativistic and relativistic formalisms were small (of the order of a few parts per thousand), since the velocities of the 4f electrons are small. It was estimated, however, that, for the conduction electron-polarization effects in Gd or Er, the difference between the two formalisms may rise to 10%.

D. Atomic Transition Probabilities

Hydrogen-like relativistic correction factors were introduced for atomic transition probabilities by Younger and Weiss (1975). Lin *et al.* (1977) concluded that these factors worked very well for the 3p–3d transitions but not for the 3p–4d or 3p–4s ones of the argon isoelectronic series.

XI. Relativity and the Periodic Table

Although relatively few firm and definitive conclusions on the effects of relativity on the chemical properties of the known elements exist, a certain preliminary understanding begins to emerge. With these reservations, we discuss in Section XI,A the elements 1–106 and summarize in Section XI,B the earlier, extensive discussions on the heavier elements.

A. Known Elements

1. *Groups Ia and IIa*

The alkalis $_3$Li, $_{11}$Na, $_{19}$K, $_{37}$Rb, $_{55}$Cs, and $_{87}$Fr and the alkaline earths $_4$Be, $_{12}$Mg, $_{20}$Ca, $_{38}$Sr, $_{56}$Ba, and $_{88}$Ra have the valence electron configurations $(\mathrm{ns})^1$ and $(\mathrm{ns})^2$, respectively. The principal relativistic effect, then, should be the relativistic contraction of the ns shell. As seen from Table VII, this contraction overtakes the shell structure expansion for I_1 of group Ia and both I_1 and I_2 of group IIa when going from fifth row (Cs, Ba) to sixth row (Fr, Ra).

Fricke and Waber (1972a) observed that the atomic radii begin to decrease when going from Cs to Fr or from Ba to Ra, making Cs the largest atom in nature. The question of relativistic contributions to the cohesive energies of the alkali metals was raised by Callaway *et al.* (1957). No definitive answers seem to exist.

2. *Group IIIa*

This group comprises the elements $_{21}$Sc, $_{39}$Y, $_{57}$La, and $_{89}$Ac. The electronic ground-state configuration is $(\mathrm{ns})^2((\mathrm{n}-1)\mathrm{d})^1$. In this case it is not clear from which orbital the first electron will be removed. We therefore give in Table VIII the first three experimental ionization potentials and the relaxed-orbital DS binding energies of Huang *et al.* (1976). One would expect that the s AO's would again contract from La to Ac and the d AO would expand. Experimentally, I_1 to I_3 are all larger for Ac than for La. If the experimental data are correct, a likely explanation is that, in contrast to the theoretical prediction, the first electron is removed from the 7s AO of Ac.

TABLE VII

DIRAC–FOCK ns ORBITAL ENERGIES, $-\varepsilon_{rel}$, THEIR RELATIVISTIC INCREASE, $\varepsilon_{rel}/\varepsilon_{n.r.}$ AND THE EXPERIMENTAL IONIZATION POTENTIALS, I_1 AND I_2, FOR THE ALKALI AND ALKALINE EARTH ELEMENTS

Element	n	$-\varepsilon_{rel}$ (eV)	$\varepsilon_{rel}/\varepsilon_{n.r.}$[a]	I_1[b] (eV)	I_2[b] (eV)
Li	2	5.343	1.0001	5.39	75.619
Na	3	4.962	1.0013	5.138	47.29
K	4	4.028	1.0038	4.339	31.81
Rb	5	3.811	1.0158	4.176	27.5
Cs	6	3.490	1.0370	3.893	25.1
Fr	7	3.611	1.1255	4	—
Be	2	8.417	1.0002	9.32	18.206
Mg	3	6.897	1.0015	7.644	15.031
Ca	4	5.342	1.0040	6.111	11.868
Sr	5	4.932	1.0157	5.692	11.027
Ba	6	4.440	1.0359	5.21	10.001
Ra	7	4.523	1.1174	5.277	10.144

[a] From Desclaux, 1973.

[b] From *Handbook of Chemistry and Physics*, 1975–1976.

TABLE VIII

RELAXED-ORBITAL DIRAC–SLATER IONIZATION ENERGIES I_1 AND THE FIRST THREE EXPERIMENTAL IONIZATION POTENTIALS FOR GROUP IIIa ELEMENTS.

	Theory[a]		Experiment[b]		
Element	I_1(ns) (eV)	$I_1((n-1)d_{3/2})$ (eV)	I_1 (eV)	I_2 (eV)	I_3 (eV)
Sc	5.469	7.163	6.54	12.8	24.75
Y	5.182	5.265	6.38	12.23	20.5
La	4.576	5.579	5.61	11.43	19.17
Ac	4.882	4.372	6.9	12.1	20

[a] From Huang *et al.*, 1976.

[b] From *Handbook of Chemistry and Physics*, 1975–1976.

3. *Group IVa*

This group consists of the elements $_{22}$Ti, $_{40}$Zr, $_{72}$Hf, and the element 104, which has been obtained and shown to behave chemically like Zr and Hf (Zvara *et al.*, 1966; Silva *et al.*, 1970). The principal valency of these elements is 4. The atomic radii and the ionic radii of Zr and Hf are closely similar and so are their chemical and physical properties, despite of the fact that Hf is a heavy element. This suggests that the relativistic effects somehow cancel in group IVa. Dirac–Fock one-center expansion calculations by Pyykkö and Desclaux (1977b) for the model systems TiH_4 to $(104)H_4$ show that this, indeed, is the case. The relativistic contractions of the X—H bond length are one order of magnitude smaller than those predicted by Eq. (VI.4). The valence t_2 MO consisted of about 50% np and 50% (n − 1)d character and their relativistic contractions and expansions cancel.

4. *Other 3d, 4d, and 5d Transition Elements*

As seen in the preceding, the chemical difference between the fifth row and the sixth row contains large, if not dominant, relativistic contributions. It then is interesting to note that the cohesive energies of the elements Ta to Pt are systematically larger than those of Nb to Pd (Kittel, 1971, p. 96). Similarly, the 5d transition elements generally give more stable hydrides than the 4d ones (Chatt, 1968). This may well be a relativistic effect. It is not evident which orbitals would be responsible. Dirac–Fock OCE calculations for the octahedral model systems MoH_6 and WH_6 suggest that the 6s and 6p contraction and an increasing $d_{3/2}$ character for the Γ_8^+ (5d) MO on W may provide the explanation (Pyykkö and Desclaux, 1978).

The ionization potentials increase from $_{72}$Hf(5d^2) to $_{74}$W(5d^4) and then drop for $_{75}$Re(5d^5). The experimental values are 7, 7.88, 7.98, and 7.87 eV, respectively. This was interpreted by Fricke *et al.* (1971) as a *j-j* coupling effect, due to the filling of the $5d_{3/2}$ shell for W.

5. *Lanthanoids and Actinoids*

The most conspicuous relativistic effect on the chemical and physical properties of the 4f and 5f transition metals is the relativistic SCF expansion of these very shells (see Table IX and Fig. 7). The decrease of $|\varepsilon_{4f}|$ is several tens of percent and that of $|\varepsilon_{5f}|$ roughly a factor of $\frac{1}{2}$. Again the orbital energies of a nonrelativistic lanthanoid $(4f)^n$ and the corresponding nonrelativistic actinoid $(5f)^n$ show a striking similarity, as seen in Fig. 7. Although extensive theoretical discussions of the actinoids exist (Freeman and Koelling, 1974; Davis, 1974), we are not aware of earlier discussions of this similarity of the $\varepsilon_{\text{n.r.}}$. On the other hand, the $\langle r^n \rangle_{\text{n.r.}}$ in Table IX are quite different. Therefore it is only partially correct to claim that the chemical difference between lanthanoids and actinoids would be a relativistic effect. The strong deviations from *LS* coupling in UO_2^{2+} were

TABLE IX

THE RELATIVISTIC AND NONRELATIVISTIC EXPECTATION VALUES $\langle r \rangle$ AND $\langle r^{-1} \rangle$ FOR Sm AND Pu[a]

			Orbital				
Atom	Case	Quantity	$5/6p_{1/2}$	$5/6p_{3/2}$	$4/5f_{5/2}$	$4/5f_{7/2}$	$6/7s_{1/2}$
Sm	Rel.	$\langle r \rangle$	1.615	1.709	0.946	0.960	4.645
Sm	N.r.		1.719	1.719	0.902	0.902	4.883
Pu	N.r.		1.894	1.894	1.220	1.220	5.177
Pu	Rel.		1.606	1.862	1.355	1.406	4.461
Sm	Rel.	$\langle r^{-1} \rangle$	0.807	0.757	1.398	1.382	0.266
Sm	N.r.		0.747	0.747	1.444	1.444	0.251
Pu	N.r.		0.670	0.670	1.078	1.078	0.235
Pu	Rel.		0.821	0.692	0.994	0.962	0.279

[a] The data are taken from Desclaux, 1973.

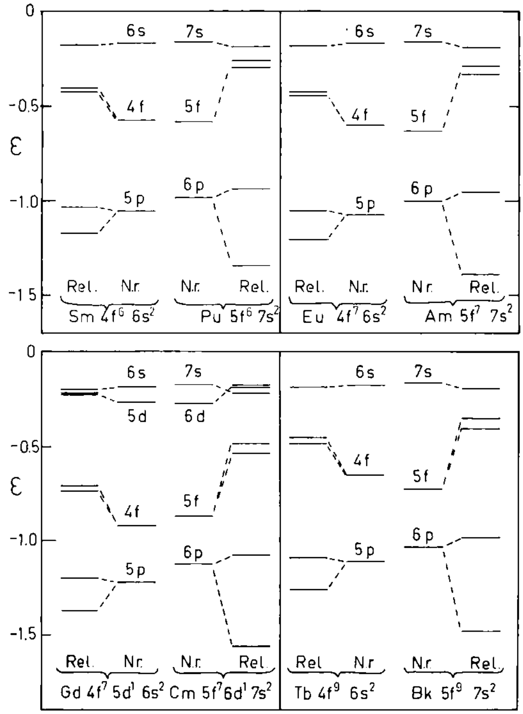

Fig. 7. The Dirac–Fock average-of-configuration orbital energies, ε, in atomic units for the lanthanoids Sm, Eu, Gd, Tb and for the corresponding actinoids Pu, Am, Cm, Bk. The data are taken from Desclaux (1973).

discussed by Jørgensen and Reisfeld (1975). Skriver *et al.* (1978) calculated the bulk properties of the actinoid metals.

6. *Group Ib*

The coinage metals $_{29}$Cu, $_{47}$Ag, and $_{79}$Au, with the electron configuration $((n-1)d)^{10}(ns)^1$, provide an unusually beautiful example of the effects of relativity (see Fig. 3). The chemical difference between Cu and the two others is caused by the shell structures, but the difference between Ag and Au seems to be mainly a relativistic effect.

a. Ionization Potentials. The experimental ionization potentials of Cu, Ag, and Au are shown in Table X. It is indeed seen that the first ionization potential of Au is larger than that of Ag, due to the relativistic contraction of the ns shell. This explains the redox nobility of gold and also the existence of an auride ion, Au^-, in CsAu or RbAu (Keller *et al.*, 1973). No such compounds are known for Ag. The second ionization potential of Au is smaller than that of Ag, due to the relativistic SCF expansion of the $(n-1)d$ shell. The relativistic contraction, $\varepsilon_{rel}/\varepsilon_{n.r.}$ for the 6s shell of $_{79}$Au, 1.3211, is much larger than that of the 6s shell of $_{87}$Fr, 1.1255. This can be attributed to an SCF relativistic effect with the 5d shell. The chemical difference between Ag and Au, and between the isoelectronic systems Cd^+ and Hg^+, was also discussed by Corbett (1962) who attributed the high first ionization potential of Hg to "poor nuclear shielding by the 5d and, particularly, the 4f electrons." We here find that this is indeed a partial explanation, the relativistic contraction of the s and p shells explaining the rest. In this sense the "inert pair effect" of Sidgwick (1950 and earlier work) is also a relativistic effect. It is quite possible that the higher valencies of Au are due to the 5d participation. Orgel (1958) proposed

TABLE X

Dirac-Fock Orbital Energies, ε_{rel}, and Their Relativistic Changes, $\varepsilon_{rel}/\varepsilon_{n.r.}$, and the Experimental Ionization Potentials for Cu, Ag, and Au

	$-\varepsilon_{rel}$[a]		$\varepsilon_{rel}/\varepsilon_{n.r.}$[a]				
Element	ns (eV)	$(n-1)d_{5/2}$ (eV)	ns	$(n-1)d_{5/2}$	I_1[b] (eV)	I_2[b] (eV)	I_3[b] (eV)
Cu	6.661	12.906	1.0263	0.9655	7.724	20.29	36.83
Ag	6.453	13.646	1.0781	0.9332	7.574	21.48	34.82
Au	7.937	11.667	1.3211	0.8229	9.22	20.5	—

[a] From Desclaux, 1973.

[b] From *Handbook of Chemistry and Physics*, 1975–1976.

that the extra stability of linear compounds of Hg^{2+} and the isoelectronic systems would be due to the diminished d-s separation.

b. Bond Lengths. The calculated relativistic contractions, *C*, of the bond length are about 2 and 5 % for AgH and AuH, respectively (Desclaux and Pyykkö, 1976). The experimental bond length (Herzberg, 1950) for AuH is 5.8 % shorter than that for AgH, which also supports the present argument. (See also the footnote on p. 374.)

c. Bond Strengths. The dissociation energies, D_0^0, are 2.5 and 3.1 eV for AgH and AuH, respectively (Herzberg, 1950). The difference of 0.6 eV is comparable with the relativistic increase of D_0^0, estimated for AuH by Desclaux and Pyykkö (1976). Likewise, the D_0^0 for Ag_2 and Au_2 are 1.67 and 2.34 eV, respectively (Taylor, 1975, p. 42) whereas those for the two metals are 2.96 and 3.78 eV, respectively (Kittel, 1971). The larger values for Au may be attributed to the 6s contraction. Lee *et al.* (1979) find for Au_2 a relativistic increase of D_e of about 1 eV.

d. Electronic Band Structure. Experimentally, Ag and Au have the same crystal structure and closely similar lattice parameters, in contrast to the shorter bonds for Au, discussed in Section XI,A,6,b. A likely explanation is provided by the increased, repulsive, overlap of the filled 5d shells of Au. According to the RAPW calculations of Christensen and Seraphin (1971), the d bandwidths are 0.120 and 0.210 a.u. for Ag and Au, respectively. The relativistic and nonrelativistic band structures of the two metals were recently compared by J. Keller (private communication), who came to the same conclusion as the author as shown in Fig. 3, that is, the difference between Ag and Au is mainly a relativistic effect.

e. Relativity or Lanthanoid Contraction? The traditional explanation for the contraction of Au compared to Ag has been a nonrelativistic effect, namely, the lanthanoid contraction. Bagus *et al.* (1975) tried to estimate this contribution by considering a "pseudo-Au" atom with $Z = 65$ and an empty 4f shell. This effect was found to be comparable to the relativistic contraction. The point is, however, that the lanthanoid contraction makes the 6s radii of Au and Ag equal; without it Au would be larger than Ag. The smaller valence s radius and greater nobility of Au may be attributed to relativity.

7. *Group IIb*

This group consists of the elements ${}_{30}Zn$, ${}_{48}Cd$, and ${}_{80}Hg$. The valence electron configuration is $((n-1)d)^{10}(ns)^2$. The interaction potential between two metal atoms is weak. The D_0^0 values for Cd_2 and Hg_2 are 0.12 and

0.18 eV, respectively (*Handbook of Chemistry and Physics*, 1975–1976). The first ionization potentials, I_1, for Cd and Hg are 8.991 and 10.43 eV, respectively, and the melting points 594 and 234 K, respectively. The chemical stability of the $(6s)^2$ family was interpreted as a relativistic effect by Jørgensen (1971, p. 489). In this sense one could loosely say that "mercury is pseudohelium" due to the relativistic contraction of the 6s shell. The relativistic effects on the Hg—Hg interaction potential were discussed in more detail by Pyper *et al.* (1977). In a Gordon–Kim model, relativistic effects diminish the interaction potential to 45% of the nonrelativistic value. Baylis (1977) reconsidered the problem including both the relativistic effects via a Dirac–Fock treatment and, approximately, the valence-core correlation effects via a polarization potential. He concluded that correlation is as important as relativity for the Hg—Hg potential.

Ions Cd_2^{2+} and Hg_2^{2+} are isoelectronic with Ag_2 and Au_2. The force constants, k, for these four systems are 110, 190, 118, and 211 Nm^{-1} (Taylor 1975, pp. 12 and 27; Kleeman and Lindkvist, 1954). In this case the relativistic contraction of the 6s shell makes the bond stronger.

8. *Group IIIb*

Elements $_5B$, $_{13}Al$, $_{31}Ga$, $_{49}In$, and $_{81}Tl$ have the valence electron configuration $(ns)^2(np)^1$. The principal valencies are 3 for B to In and 1 for Tl. The two traditional explanations for the change from In to Tl are that (1) the "inert pair effect" of Sidgwick (1950) pushes the 6s shell deeper and makes it unavailable for chemical bonding and (2) the shell-structure effects make the Tl atom more diffuse than In, giving less angular overlap with the ligands for "paying" for the hybridization (Drago, 1958). Phillips (1973) called explanation 1 a "relativistic dehybridization." A third explanation that was proposed on the basis of atomic (Fricke, 1975, p. 121) and molecular DF-OCE (Pyykkö and Desclaux, 1976) calculations is that the spin–orbit splitting of the 6p shells isolates the $6p_{3/2}$ subshell from the chemical bond leaving a half-filled, monovalent $6p_{1/2}$ shell. How much truth belongs to each of the three explanations, remains an open question.

The D_0^0 of the diatomic molecules In_2 and Tl_2 are 0.93 and 0.60 eV (Taylor, 1975, p. 49). The cohesive energies of the two metals are 2.6 and 1.87 eV, respectively (Kittel, 1971). Pyykkö and Desclaux (1976) found that relativistic effects make the bond stronger for InH and weaker for TlH. The experimental D_0^0 are 2.48 and 2.18 eV, respectively (Herzberg, 1950). This effect was interpreted by the weaker directional characteristics of the $p_{1/2}$ bond of Tl.

9. *Group IVb*

Elements $_6C$, $_{14}Si$, $_{32}Ge$, $_{50}Sn$, and $_{82}Pb$ have the valence electron configuration $(ns)^2(np)^2$. The principal valencies are 4 for C to Sn and

2 for Pb. The same qualitative explanations can be offered for the change from Sn to Pb as in Section XI,A,8. Fricke *et al.* (1971) observed that I_1 increases from p^1 to p^3 for rows 2–5, but only increases from p^1 to p^2 for the sixth row, dropping back for Bi(p^3). This is a manifestation of *j-j* coupling. Lead has a filled $6p_{1/2}$ shell that has a large I_1 and may, at least partially explain why Pb has so much smaller bond strengths than Sn. The experimental D_0^0 are 1.95 and 0.98 eV for the $^3\Sigma$ ground states of Sn_2 and Pb_2 (Taylor, 1975, p. 80). The D_0^0 for SnH and PbH are 3.2 and 1.59 eV, respectively, although the R_e and k_2 are quite similar (Herzberg, 1950). The cohesive energies of the elements are 3.12 and 2.04 eV, respectively (Kittel, 1971).

10. *Group Vb*

The group consists of the elements $_7N$, $_{15}P$, $_{33}As$, $_{51}Sb$, and $_{83}Bi$. The principal valencies are ± 3 for As and Sb and 3 for Bi. The D_0^0 again decrease from 3.05 to 2.00 eV for Sb_2 and Bi_2 (Taylor, 1975, p. 116) or from 2.7 to 2.15 eV for the elements.

11. *Groups VIb, VIIb, and VIIIb*

Not very much is known about the chemistries of $_{84}Po$, $_{85}At$, or $_{86}Rn$. The experimental I_1 exhibit a decrease from the fifth row to the sixth row (9.01 and 8.43 eV for Te and Po, 10.454 and 9.5 eV for I and At, 12.127 and 10.746 eV for Xe and Rn, respectively). It is not evident whether this decrease should be attributed to the $6p_{1/2}$–$6p_{3/2}$ spin–orbit splitting or to a shell-structure expansion for the sixth row. The dominant valencies for Se and Te are 4, whereas that for Po is 2. This may be due to a $(6p_{1/2})^2$ inert pair for Po.

12. *Valency Rule for Heavy Transition Metals*

As already stated, relativistic effects seem to explain the chemical difference between Ag and Au and contribute strongly to the difference between lanthanoids and actinoids. The main relativistic effects were (1) the relativistic contraction of s and p shells, (2) the spin–orbit splitting of the p, d, f, ..., and (3) the relativistic self-consistent expansion of the d and f shells. The relativistic effects overtake the shell-structure differences when going from the fifth row to the sixth row. The similarity of Zr and Hf is explained by a cancellation of effects 1 and 3 for the valence t_2 MO.

Going to the right from group IVB, we observe the following (Cotton and Wilkinson, 1972; Heslop and Jones, 1976):

a. Both Mo and W form the trihalides MF_3, MCl_3, MBr_3, and MI_3. As to the tetrahalides, only MoF_4, $MoCl_4$, and $MoBr_4$ are known, although WF_4, WCl_4, WBr_4, and WI_4 exist. Molybdenum forms MoF_5 and Mo_2Cl_{10}, but for W also the bromide WBr_5 is known. Only MoF_6 and, possibly, $MoCl_6$ are known, although WF_6, WCl_6, and WBr_6 exist.

b. Only $TcCl_4$ is known, although $ReCl_4$, $ReBr_4$, and ReI_4 exist. Only TcF_5 has been reported, whereas ReF_5, $ReCl_5$, and $ReBr_5$ are known. Of the hexahalides, TcF_6, ReF_6, and $ReCl_6$ exist, whereas the only known heptahalide is ReF_7.

c. Both Ru and Os have trihalides up to RuI_3 and OsI_3; the only tetrahalide of Ru is the fluoride RuF_4, but Os forms OsF_4, $OsCl_4$, and $OsBr_4$.

d. Both Rh and Ir form the trihalides MF_3, MCl_3, MBr_3, and MI_3; the only tetrahalide of Rh is RhF_4, whereas Ir may form $IrCl_4$, $IrBr_4$, and IrI_4.

e. Both Pd and Pt form the dihalides MCl_2, MBr_2, and MI_2. No trihalides are known for Pd, but $PtCl_3$, and, possibly, PtI_3 are known. The only tetrahalide of Pd is PdF_4, whereas PtF_4, $PtCl_4$, $PtBr_4$, and PtI_4 as well as $(PtF_5)_4$ and PtF_6 are known. The principal oxides are PdO and PtO_2.

f. Both AgF_4^- and AuF_4^- are known, whereas only Au forms $AuCl_4^-$ and $AuBr_4^-$.

g. Lanthanoids from trihalides, with the exception of Ce, Pr, and Tb that also exhibit MF_4. Of the actinoids, Pa forms $PaCl_4$ and PaI_5; U forms UF_4, UCl_4, UBr_4, UI_4, UF_5, U_2Cl_{10}, UF_6, and UCl_6; Np forms NpF_3 to NpI_3, NpF_4 to $NpBr_4$ and NpF_6; Pu forms PuF_3 to PuI_3, PuF_4 and PuF_6; Am forms AmF_3 to AmI_3 and AmF_4.

All these trends can be collected in the rule: *for predominantly ionic compounds of two transition elements belonging to the same column, the heavier one exhibits the higher valency.* The explanation is the relativistic SCF expansion that makes it easier to remove electrons from 5d or 5f shells than from 4d or 4f, respectively. As observed above for Ag and Au or for lanthanoids and actinoids, the nonrelativistic orbital energies of the fifth-row and sixth-row elements are closely similar. The analogous similarity between Tc and Re is shown in Table XI.

In addition to the foregoing orbital energy argument, the larger radii of the less electronegative halogens may give steric repulsion contributions in the same direction. The fact that already the nonrelativistic 5d and 5f radii are larger than the 4d or 4f ones (see Table IX) may also have an effect. Again it is not clear how much truth belongs to each explanation.

Perhaps the most striking example of the present rule is the existence of UF_6 as compared to lanthanoid trifluorides. According to the SCF molecular calculation of Kim *et al.* (1977a,b), the 5f charge falls from -3.35 to -1.76 e and the net U charge increases from -1.48 to $+2.84$ e when going from the nonrelativistic case to the relativistic one.

TABLE XI

NONRELATIVISTIC AND RELATIVISTIC ORBITAL ENERGIES ε FOR Tc $4d^5 5s^2$ AND Re $5d^5 6s^2$ [a]

Atom	Method	n	Orbital $(n-1)d_{3/2}$ (a.u.)	 $(n-1)d_{5/2}$ (a.u.)	 $ns_{1/2}$ (a.u.)
Tc	Rel.	5	0.4597	0.4493	0.2454
Tc	N.r.	5	0.4807	0.4807	0.2350
Re	N.r.	6	0.4538	0.4538	0.2347
Re	Rel.	6	0.3972	0.3661	0.2783

[a] The data are taken from Desclaux, 1973.

B. Superheavy Elements

Several excellent reviews exist on the predicted chemical properties of the superheavy elements (Waber, 1969; Cowan and Mann, 1971; Fricke and Waber, 1971; Fricke, 1975; Mann, 1975). More recently, Pitzer (1975a,b) used the Desclaux atomic calculations, assuming nonrelativistic hybridization ratios, to discuss the chemical properties of Rn, 112, 114, and 118. This method was criticized by Pyykkö and Desclaux (1976) who pointed out that the hybridization ratios (e.g. $N(p_{3/2})/N(p_{1/2})$ for pσ) change due to relativistic effects. Waber and Fricke (1976) discussed the ions of the superheavy elements under vacuum and in solution. Grant and Pyper (1977) used MCDF atomic calculations together with a simple ionic model or Pauling's semiempirical VB resonance model for discussing the heats of formation of the compounds of 114 and 116. Pyykkö and Desclaux (1977a) carried out a DF-OCE calculation on $(114)H_4$ and found nearly the same R_e and k_2 as for the isoelectronic PbH_4. The average orbital energy, $[2\varepsilon(np_{3/2}) + \varepsilon(np_{1/2})]/3$, was found to be closely similar for the two molecules. If the average of the $np_{3/2}$ and $np_{1/2}$ is the important quantity, the often used method of estimating atomic radii from the last maximum of the outermost orbital (here $np_{3/2}$) becomes somewhat suspicious.

XII. Conclusion

The point of view adopted in this article is that relativistic calculations are only a factor of 4 more difficult than nonrelativistic ones: a factor of 2 from having large and small components and almost a factor of 2 from spin–orbit splitting. Having learned to think in terms of an abstract quantity, namely, the wavefunction, it is not a major step to learn to think in terms of two quantities, the large and the small components. In the valence region, the small component is, indeed, vanishingly small. Therefore pseudopotential and quasi-relativistic methods show some promise, although a straightforward Dirac–Fock or Dirac–Slater method is more coherent.

The chemical difference between the fifth row and the sixth row seems to have strong, if not dominant, relativistic contributions that, however, enter in an individualistic manner for the various columns of the periodic system. A detailed understanding of these effects will form the impact of relativity on chemistry.

ACKNOWLEDGMENTS

I wish to thank Professor Per-Olov Löwdin for proposing that this article be written. Besides my quoted coauthors, I want to thank, R. F. Barrow, I. Fischer-Hjalmars, H. B. Jansen, J. Linderberg, L. L. Lohr, Jr., K. Ruedenberg, R. A. van Santen, and Y. Yafet for intelligent questions, useful proposals, or vehement opposition. While accepting the responsibility for any remaining omissions or errors, I am indebted to H. Adachi, B. Fricke, I. P. Grant, C. K. Jørgensen, R. Manne, K. S. Pitzer, W. H. E. Schwarz, J. T. Waber, and K. Wittel for supplementary material and corrections.

REFERENCES

Adachi, H., Rosén, A., and Ellis, D. E. (1977). *Mol. Phys.* **33**, 199.

Akhiezer, A. I., and Berestetskii, V. B. (1965). "Quantum Electrodynamics." Wiley (Interscience), New York.

Amoruso, M. J., and Johnson, W. R. (1971). *Phys. Rev. A* **3**, 6.

Andriessen, J., and van Ormondt, D. (1975). *J. Phys. B* **8**, 1993.

Andriessen, J., Chatterjee, R., and van Ormondt, D. (1973). *J. Phys. C* **6**, L288.

Andriessen, J., Chatterjee, R., and van Ormondt, D. (1974). *J. Phys. C* **7**, L339.

Andriessen, J., van Ormondt, D., Ray S. N., Raghunatan, K., and Das, T. P. (1977). *J. Phys. B* **10**, 1979.

Animalu, A. O. E. (1966). *Philos. Mag.* [8] **13**, 53.

Armstrong, L., Jr. (1971). "Theory of Hyperfine Structure of Free Atoms." Wiley (Interscience), New York.

Armstrong, L., Jr., and Feneuille, S. (1974). *Adv. At. Mol. Phys.* **10**, 1–52.

Armstrong, L., Jr., Fielder, W. R., and Dong, L. L. (1976). *Phys. Rev. A* **14**, 1114.

Asaad, W. N. (1960). *Proc. Phys. Soc., London* **76**, 641.

Avron, J. E., and Grossman, A. (1976). *Phys. Lett A* **56**, 55.

Bagus, P. S., Lee, Y. S., and Pitzer, K. S. (1975). *Chem. Phys. Lett.* **33**, 408.

Bauche, J., and Champeau, R.-J. (1976). *Adv. At. Mol. Phys.* **12**, 39.

Baylis, W. E. (1977). *J. Phys. B* **10**, L583.

Beck, D. R. (1969). *J. Chem. Phys.* **51**, 2171.

Becker, R. S. (1969). "Theory and Interpretation of Fluorescence and Phosphorescence." Wiley, New York.

Berkosky, J. L., Ellison, F. O., Lee, T. H., and Rabalais, J. W. (1973). *J. Chem. Phys.* **59**, 5342.

Berkowitz, J. (1975). *J. Chem. Phys.* **62**, 4074.

Berkowitz, J., Dehmer, J. L., Kim, Y.-K., and Desclaux, J. P. (1974). *J. Chem. Phys.* **61**, 2556.

Berkowitz, S., Dehmer, J. L., and Walker, T. E. H. (1973). *J. Chem. Phys.* **59**, 3645.

Bersuker, I. B., Budnikov, S. S., and Leizerov, B. A. (1972). *Int. J. Quantum Chem.* **6**, 849.

Bersuker, I. B., Budnikov, S. S., and Leizerov, B. A. (1974). *Teor. Eksp. Khim.* **10**, 586.

Bersuker, I. B., Budnikov, S. S., and Leizerov, B. A. (1977). *Int. J. Quantum Chem.* **11**, 543.

Bethe, H. (1929). *Ann. Phys.* (Leipzig) [5] **3**, 133.

Bethe, H. A., and Fermi, E. (1932). *Z. Phys.* **77**, 296.

Bethe, H. A., and Salpeter, E. E. (1957). "Quantum Mechanics of One- and Two-Electron Systems." Springer-Verlag, Berlin and New York.

Bhalla, C. P. (1967). *Phys. Rev.* **157**, 1136.

Bhalla, C. P. (1970). *Nucl. Instrum. & Methods* **90**, 149.

Bhalla, C. P. (1973). *Nucl. Instrum. & Methods* **110**, 227.

Bishop, D. M. (1967). *Adv. Quantum Chem.* **3**, 25.

Bishop, D. M. (1976). *At. Data Nucl. Data Tables* **18**, 521.

Bishop, D. M. (1977). *J. Chem. Phys.* **66**, 3842.

Bjorken, J. D., and Drell, S. D. (1964). "Relativistic Quantum Mechanics." McGraw-Hill, New York.

Blinder, S. M. (1965). *Adv. Quantum Chem.* **2**, 47.

Blume, M., and Watson, R. E. (1962). *Proc. R. Soc. London, Ser. A* **270**, 127.

Blume, M., and Watson, R. E. (1963). *Proc. R. Soc. London, Ser. A* **271**, 565.

Bodmer, A. R. (1953). *Proc. Phys. Soc., London, Sect. A* **66**, 1041.

Bohr, A. (1951). *Phys. Rev.* **81**, 331.

Bohr, A., and Weisskopf, V. F. (1950). *Phys. Rev.* **77**, 94.

Boyd, R. G., Larson, A. C., and Waber, J. T. (1963). *Phys. Rev.* **129**, 1629.

Boys, S. F., and Price, V. E. (1954). *Philos. Trans. R. Soc. London, Ser. A* **246**, 451.

Bradley, C. J., and Cracknell, A. P. (1972). "The Mathematical Theory of Symmetry in Solids." Oxford Univ. Press (Clarendon), London and New York.

Braun, J. J. (1975). Ph.D. Thesis, Oklahoma State University, Stillwater; Braun, J. J. (1976). *Diss. Abstr. B* **36**, 5092.

Breit, G. (1929). *Phys. Rev.* **34**, 553.

Breit, G. (1930a). *Phys. Rev.* **35**, 1447.

Breit, G. (1930b). *Phys. Rev.* **36**, 383.

Breit, G. (1932a). *Phys. Rev.* **39**, 616.

Breit, G. (1932b). *Phys. Rev.* **42**, 348.

Breit, G. (1958). *Rev. Mod. Phys.* **30**, 507.

Brogli, F., and Heilbronner, E. (1971). *Helv. Chim. Acta* **54**, 1423.

Brown, G. E. (1952). *Philos. Mag.* [7] **43**, 467.

Brown, G. E., and Mayers, D. F. (1959). *Proc. R. Soc. London, Ser. A* **251**, 105.

Brown, G. E., and Ravenhall, D. G. (1951). *Proc. R. Soc. London, Ser. A* **208**, 552.

Burke, V. M., and Grant, I. P. (1967). *Proc. Phys. Soc., London* **90**, 297.

Callaway, J., Woods, R. D., and Sirounian, V. (1957). *Phys. Rev.* **107**, 934.

Carlson, T. A., and Nestor, C. W., Jr. (1977). *At. Data Nucl. Data Tables* **19**, 153.

Carlson, T. A., Nestor, C. W., Jr., Malik, F. B., and Tucker, T. C. (1969). *Nucl. Phys. A* **135**, 57.

Cartling, B. G., and Whitmore, D. M. (1975). *Chem. Phys. Lett.* **35**, 51.

Cartling, B. G., and Whitmore, D. M. (1976). *Int. J. Quantum Chem.* **10**, 393.

Casimir, H. B. G. (1936). "On the Interaction between Atomic Nuclei and Electrons." Teyler, Haarlem (reprinted, Freeman, San Francisco, California, 1963).

Certain, P. R., and Bruch, L. W. (1972). *In* "Theoretical Chemistry" (W. Byers Brown, ed.), pp. 113–165. Butterworth, London.

Chanmugam, G., and Schweber, S. S. (1970). *Phys. Rev. A* **1**, 1369.

Chatt, J. (1968). *Science* **160**, 723.

Chatterjee, R., Newman, D. J., and Taylor, C. D. (1973). *J. Phys. C* **6**, 706.

Chen, M. H., Crasemann, B., Huang, K.-N., Ayoagi, M., and Mark, H. (1977). *At. Data Nucl. Data Tables* **19**, 97.

Cheng, K. T., and Johnson, W. R. (1976). *Phys. Rev. A* **14**, 1943.

Christensen, N. E., and Seraphin, B. O. (1971). *Phys. Rev. B* **4**, 3321.

Clementi, E. (1964). *J. Mol. Spectrosc.* **12**, 18.

Cohen, S. (1960). *Phys. Rev.* **118**, 489.

Conklin, J. B., Jr., Johnson, L. E., and Pratt, G. W., Jr. (1965). *Phys. Rev.* **137**, A1282.

Corbett, J. D. (1962). *Inorg. Chem.* **1**, 700.

Coulthard, M. A. (1967a). *Proc. Phys. Soc., London* **90**, 615.

Coulthard, M. A. (1967b). *Proc. Phys. Soc., London* **91**, 44.

Coulthard, M. A. (1973a). *J. Phys. B* **6**, 23.

Coulthard, M. A. (1973b). *J. Phys. B* **6**, 2224.

Cowan, R. D., and Griffin, D. C. (1976). *J. Opt. Soc. Am.* **66**, 1010.

Cowan, R. D., and Mann, J. B. (1971). *At. Phys., Proc. Int. Conf. At. Phys., 2nd, 1970* p. 215.

Crawford, M. F., and Schawlow, A. L. (1949). *Phys. Rev.* **76**, 1310.

Cromer, D. T. (1965). *Acta Crystallogr.* **18**, 17.

Cromer, D. T., and Waber, J. T. (1965). *Acta Crystallogr.* **18**, 104.

Dahl, J. P. (1977). *K. Dan. Vidensk. Selsk., Mat.-Fys. Medd.* **39**, No. 12.

Dalling, D. K., and Gutowsky, H. S. (1971). *J. Chem. Phys.* **55**, 4959.

Darewych, J. W., Green, A. E. S., and Sellin, D. L. (1971). *Phys. Rev. A* **3**, 502.

Darwin, C. G. (1920). *Philos. Mag.* [6] **39**, 537.

Darwin, C. G. (1928). *Proc. R. Soc. London, Ser. A* **118**, 654.

Das, T. P. (1973). "Relativistic Quantum Mechanics of Electrons." Harper, New York.

Das, G., and Wahl, A. C. (1976). *J. Chem. Phys.* **64**, 4672.

Davis, H. L. (1974). *In* "The Actinides: Electronic Structure and Properties" (A. J. Freeman, and J. B. Darby, Jr., eds.), Vol. 2, pp. 1–49. Academic Press, New York.

Denti, P. (1968). *Nuovo Cimento B* **56**, 105.

Desclaux, J. P. (1972). *Int. J. Quantum Chem.* **6**, 25.

Desclaux, J. P. (1973). *At. Data Nucl. Data Tables* **12**, 311.

Desclaux, J. P. (1975). *Comput. Phys. Commun.* **9**, 31; erratum **13**, 71 (1977).

Desclaux, J. P., and Bessis, N. (1970). *Phys. Rev. A* **2**, 1623.

Desclaux, J. P., and Kim, Y.-K. (1975). *J. Phys. B* **8**, 1177.

Desclaux, J. P., and Pyykkö, P. (1974). *Chem. Phys. Lett.* **29**, 534.

Desclaux, J. P., and Pyykkö, P. (1976). *Chem. Phys. Lett.* **39**, 300.

Desclaux, J. P., Moser, C. M., and Verhaegen, G. (1971a). *J. Phys. B* **4**, 296.

Desclaux, J. P., Mayers, D. F., and O'Brien, F. (1971b). *J. Phys. B* **4**, 631.

Desiderio, A. M., and Johnson, W. R. (1971). *Phys. Rev. A* **3**, 1267.

Detrich, J. (1972). *Phys. Rev. A* **5**, 2014.

Dimmock, J. O. (1971). *Solid State Phys.* **26**, 103.

Dirac, P. A. M. (1928). *Proc. R. Soc. London* **117**, 610.

Dixon, R. N., Murrell, J. N., and Narayan, B. (1971). *Mol. Phys.* **20**, 611.

Doyle, H. T. (1969). *Adv. At. Mol. Phys.* **5**, 337–413.

Drago, R. S. (1958). *J. Phys. Chem.* **62**, 353.
Eisenberger, P., and Reed, W. A. (1974). *Phys. Rev. B* **9**, 3237.
Eissner, W., Jones, M., and Nussbaumer, H. (1974). *Comput. Phys. Commun.* **8**, 270.
Elliot, R. J. (1954a). *Phys. Rev.* **96**, 266.
Elliot, R. J. (1954b). *Phys. Rev.* **96**, 280.
Ellis, D. E. (1977a). *J. Phys. B* **10**, 1.
Ellis, D. E. (1977b). *Int. J. Quantum Chem.* **S11**, 201.
Ellis, D. E., and Rosén, A. (1977). *Z. Phys. A* **283**, 3.
Ellis, D. E. Rosen, A., and Walch, P. F. (1975). *Int. J. Quantum Chem.* **S9**, 351.
Feiock, F. D., and Johnson, W. R. (1969). *Phys. Rev.* **187**, 39.
Feneuille, S., and Luc-Koenig, E. (1977). *Comments At. Mol. Phys.* **6**, 151.
Fogel, K.-G. (1954a). *Acta Acad. Abo., Ser. B* **19**, No. 8.
Fogel, K.-G. (1954b). *Acta Acad. Abo., Ser. B* **19**, No. 9.
Fraga, S., and Karwowski, J. (1974). "Tables of Hartree-Fock Atomic Data." University of Alberta, Edmonton.
Fraga, S., Karwowski, J., and Saxena, K. M. S. (1976). "Handbook of Atomic Data." Elsevier, Amsterdam.
Freeman, A. J., and Koelling, D. D. (1972). *J. Phys. (Paris), Colloq.* **33**, C3-C57.
Freeman, A. J., and Koelling, D. D. (1974). *In* "The Actinides: Electronic Structure and Related Properties" (A. J. Freeman and J. B. Darby, Jr., eds.), Vol. I, pp. 51-108. Academic Press, New York.
Fricke, B. (1971). *Lett. Nuovo Cimento* **2**, 293.
Fricke, B. (1975). *Struct. Bonding (Berlin)* **21**, 89.
Fricke, B., and Desclaux, J. P. (1974). *Phys. Lett. B* **51**, 317.
Fricke, B., and Soff, G. (1977). *At. Data Nucl. Data Tables* **19**, 83.
Fricke, B., and Waber, J. T. (1971). *Actinides Rev.* **1**, 433.
Fricke, B., and Waber, J. T. (1972a). *J. Chem. Phys.* **56**, 3246.
Fricke, B., and Waber, J. T. (1972b). *J. Chem. Phys.* **57**, 371.
Fricke, B., Greiner, W., and Waber, J. T. (1971). *Theor. Chim. Acta* **21**, 235.
Fricke, B., Desclaux, J. P., and Waber, J. T. (1972). *Phys. Rev. Lett.* **28**, 714.
Fricke, B., Morović, T., Sepp, W.-D., Rosén, A., and Ellis, D. E. (1976). *Phys. Lett. A* **59**, 375.
Fröman, A. (1958). *Phys. Rev.* **112**, 870.
Fröman, A. (1960). *Rev. Mod. Phys.* **32**, 317.
Garcia, J. D. (1966). *Phys. Rev.* **147**, 66.
Garstang, R. H., and Mayers, D. F. (1966). *Proc. Cambridge Philos. Soc.* **62**, 777.
Gaunt, J. A. (1929). *Proc. R. Soc. London* **122**, 513.
Gilbert, T. L., Simpson, O. C., and Williamson, M. A. (1975). *J. Chem. Phys.* **63**, 4061.
Gilvarry, J. J. (1954). *Phys. Rev.* **95**, 71.
Glasser, M. L., and Davison, S. G. (1970). *Int. J. Quantum Chem.* **S3**, 867.
Golding, R. M. (1971). *Mol. Phys.* **21**, 157.
Golding, R. M. (1973). *Mol. Phys.* **26**, 661.
Golding, R. M., and Newmarch, J. D. (1977). *Mol. Phys.* **33**, 1301.
Gombás, P. (1949). "Die statistische Theorie des Atoms und ihre Anwendungen." Springer-Verlag, Berlin and New York.
Goodman, L., and Laurenzi, B. J. (1968). *Adv. Quantum Chem.* **4**, 153.
Gordon, W. (1928). *Z. Phys.* **48**, 11.
Grant, I. P. (1961). *Proc. R. Soc. London, Ser. A* **262**, 555.
Grant, I. P. (1970). *Adv. Phys.* **19**, 747.
Grant, I. P. (1972). *Comput. Phys. Commun.* **4**, 377.
Grant, I. P. (1973). *Comput. Phys. Commun.* **5**, 263.

Grant, I. P. (1976). *Comput. Phys. Commun.* **11**, 397.

Grant, I. P., and Pyper, N. C. (1976). *J. Phys. B* **9**, 761.

Grant, I. P., and Pyper, N. C. (1977). *Nature (London)* **265**, 715.

Grant, I. P., and Whitehead, M. A. (1976). *Mol. Phys.* **32**, 1181.

Grant, I. P., Mayers, D. F., and Pyper, N. C. (1976). *J. Phys. B* **9**, 2777.

Gregson, M. J., Hall, G. G., and Rees, D. (1970). *J. Phys. B* **3**, 1195.

Griffin, D. C., Andrew, K. L., and Cowan, R. D. (1969). *Phys. Rev.* **177**, 62.

Griffith, J. S. (1960). "The Theory of Transition Metal Ions." Cambridge Univ. Press, London and New York.

Gross, E. K. U., and Rafelski, J. (1977). *Bull. Am. Phys. Soc.* [2] **22**, 83.

Gubanov, V. A., Rosén, A., and Ellis, D. E. (1977). *Solid State Commun.* **22**, 219.

Gupta, S. N. (1964). *Nucl. Phys.* **57**, 19.

Hafemeister, D. W. (1967). *J. Chem. Phys.* **46**, 1929.

Hafner, P., and Schwarz, W. H. E. (1978). *J. Phys. B* **11**, 217.

Hagston, W. E., and Lowther, J. E. (1973). *J. Phys. Chem. Solids* **34**, 1773.

Hall, M. B. (1975a). *J. Am. Chem. Soc.* **97**, 2057.

Hall, M. B. (1975b). *Int. J. Quantum Chem.* **S9**, 237.

Hartmann, H., and Clementi, E. (1964). *Phys. Rev.* **133**, A1295.

Hayes, E. F., and Parr, R. G. (1967). *Prog. Theor. Phys., Suppl.* **40**, 78.

Henneike, H. F. (1972). *J. Am. Chem. Soc.* **94**, 5945.

Herman, F., and Skillman, S. (1963). "Atomic Structure Calculations." Prentice-Hall, Englewood Cliffs, New Jersey.

Herman, F., Kuglin, C. D., Cuff, K. F., and Kortum, R. L. (1963). *Phys. Rev. Lett.* **11**, 541.

Herzberg, G. (1950). "Molecular Spectra and Molecular Structure I." Van Nostrand-Reinhold, Princeton, New Jersey.

Hestenes, D. (1975). *J. Math. Phys.* **16**, 556.

Hirschfelder, J. O., ed. (1967). "Intermolecular Forces," *Adv. Chem. Phys.*, Vol. 12. Wiley (Interscience), New York.

Holmgren, L., Lindgren, I., Morrison, J., and Mårtensson, A.-M. (1976). *Z. Phys. A* **276**, 179.

Huang, K.-N. (1976). *Phys. Rev. A* **14**, 1311.

Huang, K.-N., Aoyagi, M., Chen, M. H., Crasemann, B., and Mark, H. (1976). *At. Data Nucl. Data Tables* **18**, 243.

Huzinaga, S., and Arnau, C. (1971). *Mol. Phys.* **20**, 895.

Hyde, R. G., and Peel, J. B. (1977). *Mol. Phys.* **33**, 887.

Inokuti, M., and Usui, T. (1957). *Busseiron Kenkyu* **105**, No. 2, 40.

Inoue, M., and Okazaki, M. (1971). *J. Phys. Soc. Jpn.* **30**, 1575.

Itoh, T. (1965). *Rev. Mod. Phys.* **37**, 157.

Jansen, H. B., Lohman, J. A. B., and Pyykkö, P. (1976). *Chem. Phys.* **12**, 273.

Jansen, L. (1965). *Adv. Quantum Chem.* **2**, 119.

Jensen, H. (1933). *Z. Phys.* **82**, 794.

Johnson, L. E., Conklin, J. B., and Pratt, G. W., Jr., (1963). *Phys. Rev. Lett.* **11**, 538.

Johnson, W. R., and Lin, C. D. (1976). *Phys. Rev. A* **14**, 565.

Johnson, W. R., and Lin, C. D. (1977). *J. Phys. B* **10**, L331.

Jones, M. (1975). *Philos. Trans. R. Soc. London, Ser. A* **277**, 587.

Jørgensen, C. K. (1971). "Modern Aspects of Ligand Field Theory." North-Holland Publ., Amsterdam.

Jørgensen, C. K., and Reisfeld, R. (1975). *Chem. Phys. Lett.* **35**, 441.

Joshi, B. D. (1965). *J. Chem. Phys.* **43S**, 40.

Kagawa, T. (1975). *Phys. Rev. A* **12**, 2245.

Kandilarov, B. D., and Detcheva, V. (1976). *J. Phys. C* **9**, L107.

Kaufmann, P., and Wille, U. (1976). *Z. Phys. A* **279**, 259.

Keller, O. L., Jr., Nestor, C. W., Jr., Carlson, T. A., and Fricke, B. (1973). *J. Phys. Chem.* **77**, 1806.

Kim, B.-I., Adachi, H., and Imoto, S. (1977a). *Chem. Lett.* p. 109.

Kim, B.-I., Adachi, H., and Imoto, S. (1977b). *Mol. Phys.* (in press).

Kim, Y.-K. (1967). *Phys. Rev.* **154**, 17; errata: *Phys. Rev.* **159**, 190 (1967).

Kim, Y.-K., and Desclaux, J. P. (1976). *Phys. Rev. Lett.* **36**, 139.

Kittel, C. (1971). "Introduction to Solid State Physics," 4th ed. Wiley, New York.

Kleeman, B., and Lindkvist, S. (1954). *Ark. Fys.* **9**, 385.

Koelling, D. D. (1969). *Phys. Rev.* **188**, 1049.

Koelling, D. D., and Freeman, A. J. (1973). *Phys. Rev. B* **7**, 4454.

Koelling, D. D., and Freeman, A. J. (1975). *Phys. Rev. B* **12**, 5622.

Koelling, D. D., and Freeman, A. J. (1976). *In* "Plutonium and Other Actinides" (H. Blank and R. Lindner, eds.), p. 291. North-Holland Publ. Amsterdam.

Koelling, D. D., and Harmon, B. N. (1977). *J. Phys. C* **10**, 3107.

Koelling, D. D., Harmon, B. N., and Schirber, J. (1977). *Bull. Am. Phys. Soc.* **22**, 411.

Koelling, D. D., Ellis, D. E., and Bartlett, R. J. (1976). *J. Chem. Phys.* **65**, 3331.

Koenig, E. (1972). *Physica (Utrecht)* **62**, 393.

Kołos, W., and Wolniewicz, L. (1964). *J. Chem. Phys.* **41**, 3663.

Kopfermann, H. (1958). "Nuclear Moments." Academic Press, New York.

Koster, G. F., Dimmock, J. O., Wheeler, R. G., and Statz, H. (1963). "Properties of the Thirty-Two Point Groups." MIT Press, Cambridge, Massachusetts.

Krogh Andersen, O. (1969). Thesis, Technical University of Denmark.

Labzovskii, L. N. (1968). *Opt. Spektrosk.* **24**, 322; *Opt. Spectrosc. (Engl. Transl.)* **24**, 169 (1968).

Labzovskii, L. N. (1971). *Zh. Eksp. Teor. Fiz.* **61**, 1410; *Sov. Phys.—JETP (Engl. Transl.)* **34**, 749 (1972).

Ladik, J. (1959). *Acta Phys. Acad. Sci. Hung.* **10**, 271.

Ladik, J. (1961a). *Acta Phys. Acad. Sci. Hung.* **13**, 123.

Ladik, J. (1961b). *Acta Phys. Acad. Sci. Hung.* **13**, 139.

Ladik, J. (1965). *J. Chem. Phys.* **42**, 3340.

Larkins, F. P. (1976). *J. Phys. B* **9**, 37.

Latvamaa, E., Kurittu, L., Pyykkö, P., and Tataru, L. (1973). *J. Phys. B* **6**, 591.

Leclercq, J. M. (1970). *Phys. Rev. A* **1**, 1358.

Lee, S.-T., Süzer, S., and Shirley, D. A. (1976). *Chem. Phys. Lett.* **41**, 25.

Lee, Y. S., Ermler, W. C., and Pitzer, K. S. (1977). *J. Chem. Phys.* **67**, 5861.

Lehman, G. W. (1959). *Phys. Rev.* **116**, 846.

Lehman, G. W. (1960). *Phys. Rev.* **117**, 1493.

Leushin, A. M. (1968). "Tables of Functions Transforming according to Irreducible Representations of Crystallographic Point Groups." Nauka, Moscow (in Russian).

Lewis, W. B., Mann, J. B., Liberman, D. A., and Cromer, D. T. (1970). *J. Chem. Phys.* **53**, 809.

Liberman, D. A., Waber, J. T., and Cromer, D. T. (1965). *Phys. Rev.* **137**, A27.

Liberman, D. A., Cromer, D. T., and Waber, J. T. (1971). *Comput. Phys. Commun.* **2**, 107.

Lin, D. L. (1977). *Phys. Rev. A* **16**, 600.

Lin, D. L., Fielder, W., Jr., and Armstrong, L., Jr. (1977). *Phys. Rev. A* **16**, 589.

Lindgren, I., and Rosén, A. (1966). Report UUIP-491. Dept. of Physics, University of Uppsala.

Lindgren, J., and Rosén, A. (1973). *Phys. Scr.* **8**, 119.

Lindgren, I., and Rosén, A. (1974). *Case Stud. At. Phys.* **4**, 93.

Lipas, P. O., Pyykkö, P., and Pajanne, E. (1973). *J. Chem. Phys.* **58**, 3248.

Lohr, L. L., Jr. (1972). *Coord. Chem. Rev.* **8**, 241.

Loucks, T. L. (1965). *Phys. Rev.* **139**, A1333.

Loucks, T. L. (1967). "Augmented Plane Wave Method." Benjamin, New York.

Löwdin, P.-O. (1948). Thesis, University of Uppsala.

Lu, C. C., Carlson, T. A., Malik, F. B., Tucker, T. C., and Nestor, C. W., Jr., (1971a). *At. Data* **3**, 1.

Lu, C. C., Malik, F. B., and Carlson, T. A. (1971b). *Nucl. Phys. A* **175**, 289.

Luc-Koenig, E. (1972). *J. Phys. (Paris)* **33**, 847.

Luc-Koenig, E. (1974). *J. Phys. B* **7**, 1052.

Luc-Koenig, E. (1976). *Phys. Rev. A* **13**, 2114.

Luke, S. K., Hunter, G., McEachran, R. P., and Cohen, M. (1969). *J. Chem. Phys.* **50**, 1644.

Lulek, T. (1975). *Acta Phys. Pol. A* **48**, 513.

McClure, D. S. (1959). *Solid State Phys.* **9**, 399.

McEnnan, J., Botto, D. J., Pratt, R. H., Bunaciu, D., and Florescu, V. (1977). *Phys. Rev. A* **16**, 1768.

McGlynn, S. P., Azumi, T., and Kinoshita, M. (1969). "Molecular Spectroscopy of the Triplet State." Prentice-Hall, Englewood Cliffs, New Jersey.

Machado, W. V. M., and Ferreira, L. G. (1976). *Chem. Phys. Lett.* **37**, 51.

Mackrodt, W. C. (1970). *Mol. Phys.* **18**, 697.

Malli, G., and Oreg, J. (1975). *J. Chem. Phys.* **63**, 830.

Mallow, J. V., Freeman, A. J., and Desclaux, J. P. (1976). *Phys. Rev. B* **13**, 1884.

Malý, J., and Hussonnois, M. (1973a). *Theor. Chim. Acta* **28**, 363.

Malý, J., and Hussonnois, M. (1973b). *Theor. Chim. Acta* **31**, 137.

Mande, C., Desmukh, P., and Desmukh, P. (1977). *J. Phys. B* **10**, 2293.

Mann, J. B. (1969). *J. Chem. Phys.* **51**, 841.

Mann, J. B. (1975). "The 1975 Centenary Volume of the Discovery of Gallium." USSR Acad. Sci.

Mann, J. B., and Johnson, W. R. (1971). *Phys. Rev. A* **4**, 41.

Mann, J. B., and Waber, J. T. (1970). *J. Chem. Phys.* **53**, 2397.

Mann, J. B., and Waber, J. T. (1973). *At. Data* **5**, 201.

Manne, R., Wittel, K., and Mohanty, B. A. (1975). *Mol. Phys.* **29**, 485.

Manninen, S., Paakkari, T., and Kajantie, K. (1974). *Philos. Mag.* [8] **29**, 167.

Marinov, M. S., and Popov, V. S. (1976). *Yad. Fiz.* **23**, 479; *Sov. J. Nucl. Phys. (Engl. Transl.)* **23**, 251 (1976).

Matcha, R. L. (1973). *J. Am. Chem. Soc.* **95**, 7505.

Matcha, R. L. (1976). *J. Chem. Phys.* **65**, 1962.

Mayers, D. F. (1957). *Proc. R. Soc. London, Ser. A* **241**, 93.

Mayers, D. F. (1970). *J. Phys. (Paris)* **31S**, C4-C221.

Mendelsohn, L. B., Biggs, F., and Mann, J. B. (1973). *Int. J. Quantum Chem.* **S7**, 395.

Mendelsohn, L. B., Biggs, F., and Mann, J. B. (1974). *Chem. Phys. Lett.* **26**, 521.

Michels, M. A. J. (1976). Thesis, University of Amsterdam.

Migdałek, J. (1976a). *Can. J. Phys.* **54**, 118.

Migdałek, J. (1976b). *Can. J. Phys.* **54**, 130.

Migdałek, J. (1976c). *Can. J. Phys.* **54**, 2272.

Migdałek, J. (1976d). *J. Quant. Spectrosc. Radiat. Tranfer* **16**, 265.

Migdałek, J. (1976e). *J. Quant. Spectrosc. Radiat. Transfer* **16**, 385.

Miller, L. D. (1973). *Phys. Rev. A* **7**, 1433.

Mittleman, M. (1971). *Phys. Rev. A* **4**, 893.

Mittleman, M. (1972). *Phys. Rev. A* **6**, 2395.

Mohr, P. J. (1974). *Ann. Phys. (N.Y.)* **88**, 52.

Mohr, P. J. (1975). *Phys. Rev. Lett.* **34**, 1050.

Moore, E. A., and Moss, R. E. (1975a). *Mol. Phys.* **30**, 1297.

Moore, E. A., and Moss, R. E. (1975b). *Mol. Phys.* **30**, 1315.
Moore, E. A., and Moss, R. E. (1976). *Mol. Phys.* **31**, 1599.
Morović, T., Fricke, B., Rosén, A., and Ellis, D. E. (1976). *Int. J. Quantum Chem.* **S10**, 227.
Morović, T., Fricke, B., Sepp, W.-D., Rosén, A. and Ellis, D. E. (1977). *Phys. Lett. A* **63**, 12.
Müller, B., and Greiner, W. (1976). *Z. Naturforsch., Teil A* **31**, 1.
Müller, B., Rafelski, J., and Greiner, W. (1973). *Phys. Lett. B* **47**, 5.
Mulliken, R. S. (1934). *Phys. Rev.* **46**, 549.
Nambu, Y. (1950). *Prog. Theor. Phys.* **5**, 614.
Neto, A. A., and Ferreira, L. G. (1976). *Phys. Rev. B* **14**, 4390.
Newman, D. J., and Urban, W. (1975). *Adv. Phys.* **24**, 793.
Nikitin, E. E. (1961). *Opt. Spektrosk.* **10**, 443; *Opt. Spectrosc. (Engl. Transl.)* **10**, 227 (1961).
Onodera, Y., and Okazaki, M. (1966a). *J. Phys. Soc. Jpn.* **21**, 1273.
Onodera, Y., and Okazaki, M. (1966b). *J. Phys. Soc. Jpn.* **21**, 2400.
Onodera, Y., Okazaki, M., and Inui, T. (1966). *J. Phys. Soc. Jpn.* **21**, 816.
Oreg, J., and Malli, G. (1974). *J. Chem. Phys.* **61**, 4349.
Oreg, J., and Malli, G. (1976a). *J. Chem. Phys.* **65**, 1746.
Oreg, J., and Malli, G. (1976b). *J. Chem. Phys.* **65**, 1755.
Orgel, L. E. (1958). *J. Chem. Soc.* p. 4186.
Parrot, R. (1975). *Phys. Lett. A* **54**, 75.
Pavlik, P. I., and Blinder, S. M. (1967). *J. Chem. Phys.* **46**, 2749.
Phillips, J. C. (1973). "Bonds and Bands in Semiconductors." Academic Press, New York.
Pitzer, K. S. (1975a). *J. Chem. Phys.* **63**, 1032.
Pitzer, K. S. (1975b). *J. Chem. Soc. Chem. Commun.* p. 760.
Popov, V. S. (1971). *Yad. Fiz.* **14**, 458.
Potts, A. W., and Williams, T. A. (1976). *Chem. Phys. Lett.* **42**, 550.
Powell, R. E. (1968). *J. Chem. Educ.* **45**, 558.
Power, J. D., and Pitzer, R. M. (1971). *Chem. Phys. Lett.* **8**, 615.
Pratt, G. W., Jr. (1973). *J. Nonmetals* **1**, 103.
Pratt, R. H., Ron, A., and Tseng, H. K. (1973). *Rev. Mod. Phys.* **45**, 273.
Primakoff, H., and Holstein, T. (1939). *Phys. Rev.* **55**, 1218.
Pyper, N. C., and Grant, I. P. (1977). *J. Phys. B* **10**, 1803.
Pyper, N. C., Grant, I. P., and Gerber, R. B. (1977). *Chem. Phys. Lett.* **49**, 479.
Pyykkö, P. (1975a). *Theor. Chim. Acta* **39**, 185.
Pyykkö, P. (1975b). "Relativistic Theory of Atoms and Molecules," Lecture Notes. Scheikundig Laboratorium, Vrije Universiteit, Amsterdam.
Pyykkö, P. (1977). *Chem. Phys.* **22**, 289.
Pyykkö, P., and Desclaux, J. P. (1976). *Chem. Phys. Lett.* **42**, 545.
Pyykkö, P., and Desclaux, J. P. (1977a). *Nature (London)* **266**, 336.
Pyykkö, P., and Desclaux, J. P. (1977b). *Chem. Phys. Lett.* **50**, 503.
Pyykkö, P., and Jokisaari, J. (1975). *Chem. Phys.* **10**, 293.
Pyykkö, P., and Pajanne, E. (1971). *Phys. Lett. A* **35**, 53; Erratum: *ibid.* **38**, 218 (1972).
Pyykkö, P., Pajanne, E., and Inokuti, M. (1973). *Int. J. Quantum Chem.* **7**, 785.
Rabii, S. (1968). *Phys. Rev.* **167**, 801.
Racah, G. (1931a). *Nuovo Cimento* **8**, 178.
Racah, G. (1931b). *Z. Phys.* **71**, 431.
Racah, G. (1932). *Nature (London)* **129**, 723.
Rajnak, K. (1976). *Phys. Rev. A* **14**, 1979.
Ramsey, N. F. (1953). *Phys. Rev.* **91**, 303.
Reitz, J. R. (1950). *Phys. Rev.* **77**, 10.
Reschke, R., Trautwein, A., and Desclaux, J. P. (1977). *J. Phys. Chem. Solids* **38**, 837.

Ribberfors, R. (1975a). *Phys. Rev. B* **12**, 2067.

Ribberfors, R. (1975b). *Phys. Rev. B* **12**, 3136.

Richards, W. G., Raftery, J., and Hinkley, R. K. (1974). *Chem. Soc. Spec. Period. Rep., Theor. Chem.* **1**, 1–33.

Rose, M. E., and Welton, T. A. (1952). *Phys. Rev.* **86**, 432.

Rosén, A. (1969). *J. Phys. B* **2**, 1257.

Rosén, A. (1972). *Phys. Scr.* **6**, 37.

Rosén, A. (1973). *Phys. Scr.* **8**, 154.

Rosén, A., and Ellis, D. E. (1974). *Chem. Phys. Lett.* **27**, 595.

Rosén, A., and Ellis, D. E. (1975). *J. Chem. Phys.* **62**, 3039.

Rosén, A., and Lindgren, I. (1968). *Phys. Rev.* **176**, 114.

Rosén, A., and Lindgren, J. (1973). *Phys. Scr.* **8**, 45.

Rosén, A., and Waber, J. T. (1974). *Int. J. Quantum Chem.* **S8**, 127.

Rosenberg, H. J., and Stroke, H. H. (1972). *Phys. Rev. A* **5**, 1992.

Rosenthal, J. E., and Breit, G. (1932). *Phys. Rev.* **41**, 459.

Rosicky, F., and Mark, F. (1975). *J. Phys. B* **8**, 2581.

Rosicky, F., Weinberger, P., and Mark, F. (1976). *J. Phys. B* **9**, 2971.

Rössler, U., and Treusch, J. (1972). *Rep. Prog. Phys.* **35**, 883–947.

Rudkjøbing, M. (1952). *K. Dan. Vidensk. Selsk., Mat.-fys. Medd.* **27**, No. 5.

Safronova, U. I., and Rudzikas, Z. B. (1976). *J. Phys. B* **9**, 1989.

Sandars, P. G. H., and Beck, J. (1965). *Proc. R. Soc. London, Ser. A* **289**, 97.

Sänger, W., and Voitländer, J. (1975). *Z. Naturforsch., Teil A* **30**, 1491.

Scherr, C. W. (1972). *Mol. Phys.* **24**, 283.

Schlüter, I. C., and Schlüter, M. (1974). *Phys. Rev. B* **9**, 1652.

Schonfelder, J. L. (1966). *Proc. Phys. Soc., London* **87**, 163.

Schreckenbach, K., Börner, H. G., and Desclaux, J. P. (1977). *Phys. Lett. A* **63**, 330.

Schwenzer, G. M., Liskow, D. H., Schaefer, H. F., III, Bagus, P. S., Liu, B., McLean, A. D., and Yoshimine, M. (1973). *J. Chem. Phys.* **58**, 3181.

Scofield, J. H. (1974). *At. Data Nucl. Data Tables* **14**, 121.

Shirley, D. A. (1964). *Rev. Mod. Phys.* **36**, 339.

Sidgwick, N. V. (1950). "The Chemical Elements and Their Compounds," p. 286. Oxford Univ. Press, London and New York.

Silva, R., Harris, J., Nurmia, M., Eskola, K., and Ghiorso, A. (1970). *Inorg. Nucl. Chem. Lett.* **6**, 871.

Smith, F. C., and Johnson, W. R. (1967). *Phys. Rev.* **160**, 136.

Snijders, J. G., and Baerends, E. J. (1978). To be published.

Snow, E. C., Canfield, J. M., and Waber, J. T. (1964). *Phys. Rev.* **135**, A969.

Sommerfeld, A. (1916). *Ann. Phys. (Leipzig)* [4] **51**, 1–94 and 125–167.

Sommers, C. B., and Amar, H. (1969). *Phys. Rev.* **188**, 1117.

Soven, P. (1965). *Phys. Rev.* **137**, A1706.

Stassis, C., and Deckman, H. W. (1976). *Phys. Rev. B* **13**, 4934.

Stassis, C., Deckman, H. W., Harmon, B. N., Desclaux, J. P., and Freeman, A. J. (1977). *Phys. Rev. B* **15**, 369.

Swirles, B. (1935). *Proc. R. Soc. London, Ser. A* **152**, 625.

Synek, M. (1964). *Phys. Rev.* **136**, A1552.

Szabo, A. (1969). *J. Chem. Educ.* **46**, 678.

Taylor, M. J. (1975). "Metal-to-Metal Bonded States of the Main Group Elements." Academic Press, New York.

Teleman, E., and Glodeanu, A. (1967). *Rev. Roum. Sci. Tech., Ser. Electrotech. Energ.* **12**, 551–560 (as quoted by Bradley and Cracknell, 1972).

Toivonen, H. T., and Pyykkö, P. (1977a). *Int. J. Quantum Chem.* **11**, 695.

Toivonen, H. T., and Pyykkö, P. (1977b). Report No. B79. Dept. Phys. Chem., Åbo Akademi., Åbo (Turku), Finland.

Trautwein, A., Harris, F. E., Freeman, A. J., and Desclaux, J. P. (1975). *Phys. Rev. B* **11**, 4101.

Tterlikkis, L., Mahanti, S. D., and Das, T. P. (1968). *Phys. Rev. Lett.* **21**, 1796.

Tterlikkis, L., Mahanti, S. D., and Das, T. P. (1969). *Phys. Rev.* **178**, A630.

Tterlikkis, L., Mahanti, S. D., and Das, T. P. (1970). *Phys. Rev. B* **1**, 2041.

Tucker, T. C., Roberts, L. D., Nestor, C. W., Jr., Carlson, T. A., and Malik, F. B. (1968). *Phys. Rev.* **174**, 118.

Tucker, T. C., Roberts, L. D., Nestor, C. W., Jr., Carlson, T. A., and Malik, F. B. (1969). *Phys. Rev.* **178**, 998.

Tully, J. C. (1976). *In* "Dynamics of Molecular Collisions" (W. H. Miller, ed.), Part B, pp. 217–267. Plenum, New York.

Uehling, E. A. (1935). *Phys. Rev.* **48**, 55.

Vallarta, M. S., and Rosen, N. (1932). *Phys. Rev.* **41**, 708.

Van Heuvelen, A. (1967). *J. Chem. Phys.* **46**, 4903.

Varga, L. P., Mann, J. B., Asprey, L. B., and Reisfeld, M. J. (1971). *J. Chem. Phys.* **55**, 4230.

Veseth, L. (1977). *J. Mol. Spectrosc.* **66**, 259.

Waber, J. T. (1969). *Proc. Robert A. Welch Found. Conf. Chem. Res.* **13**, 353.

Waber, J. T., and Canfield, J. M. (1975). *Int. J. Quantum Chem.* **S9**, 51.

Waber, J. T., and Cromer, D. T. (1965). *J. Chem. Phys.* **42**, 4116.

Waber J. T., and Fricke, B. (1976). *J. Inorg. Nucl. Chem., Suppl.* pp. 13–24.

Waber, J. T., Cromer, D. T., and Liberman, D. (1969). *J. Chem. Phys.* **51**, 664.

Wadzinski, H. T. (1970). *J. Phys. (Paris)* **31S**, C4–C213.

Walch, P. F., and Ellis, D. E. (1976). *J. Chem. Phys.* **65**, 2387.

Walker, D. W. (1969). *J. Phys. B* **2**, 356.

Walker, D. W. (1971). *Adv. Phys.* **20**, 257.

Walker, T. E. H., and Waber, J. T. (1973). *Phys. Rev. A* **7**, 1218.

White, H. E. (1931). *Phys. Rev.* **38**, 513.

Wichmann, E. A., and Kroll, N. M. (1956). *Phys. Rev.* **101**, 843.

Williams, A. O., Jr. (1940). *Phys. Rev.* **58**, 723.

Wittel, K. (1972). *Chem. Phys. Lett.* **15**, 555.

Wittel, K., and Manne, R. (1975). *J. Chem. Phys.* **63**, 1322.

Wittel, K., Bock, H., and Manne, R. (1974a). *Tetrahedron* **30**, 651.

Wittel, K., Mohanty, B. S., and Manne, R. (1974b). *J. Electron Spectrosc. Relat. Phenom.* **5**, 1115.

Wood, R. D., and Callaway, J. (1957). *Bull. Am. Phys. Soc.* [2] **2**, 18.

Woods Halley, J., and Shore, H. (1965). *J. Chem. Phys.* **42**, 597.

Wu, M., and Fehlner, T. P. (1976). *J. Am. Chem. Soc.* **98**, 7578.

Wybourne, B. G. (1965). *J. Chem. Phys.* **43**, 4506.

Wybourne, B. G. (1966). *Phys. Rev.* **148**, 317.

Yang, C. Y. (1976). *Chem. Phys. Lett.* **41**, 588.

Yang, C. Y., and Rabii, S. (1975). *Phys. Rev. A* **12**, 362.

Yang, C. Y., Johnson, K. H., and Horsley, J. A. (1976). *Bull. Am. Phys. Soc.* [2] **21**, 382.

Zvara, I., Chuburkov, Y. T., Tsaletka, R., Zvarova, T. S., Shalevskii, M. R., and Shilov, B. V. (1966). *At. Energ.* **21**, 709.

BIBLIOGRAPHY

Berestetskii, V. B., Lifshitz, E. M., and Pitaevskii, L. P. (1971). "Relativistic Quantum Theory," Part 1. Pergamon, Oxford.

Corinaldesi, E., and Strocchi, F. (1963). "Relativistic Wave Mechanics." North-Holland Publ., Amsterdam.
Desclaux, J. P., and Pyykkö, P. "Relativistic Theory of Atoms and Molecules" (to be published).
Grant, I. P. "Relativistic Theory of Atomic Structure." Oxford Univ. Press, London and New York (to be published).
Jauch, J. M., and Rohrlich, F. (1976). "The Theory of Photons and Electrons," 2nd ed. Springer-Verlag, Berlin and New York.
Moss, R. E. (1973). "Advanced Molecular Quantum Mechanics: An Introduction to Relativistic Quantum Mechanics and the Quantum Theory of Radiation." Chapman & Hall, London.
Mott, N. F., and Massey, H. S. W. (1965). "The Theory of Atomic Collisions," 3rd ed. Oxford Univ. Press (Clarendon), London and New York.
Rose, M. E. (1961). "Relativistic Electron Theory." Wiley, New York.
Sokolov, A. A., and Ternov, I. M. (1974). "Relativistic Electron." Nauka, Moscow (in Russian).

REFERENCES ADDED IN PROOF

Buchmüller, W. (1978). Report Bonn-HE-78-4. Bonn University (to be published).
Cotton, F. A., and Wilkinson, G. (1972). "Advanced Inorganic Chemistry," 3rd ed. Interscience, New York.
Das, G., and Wahl, A. C. (1978). *J. Chem. Phys.* **69**, 53.
Datta, S. N., Ewig, C. S., and Van Wazer, J. R. (1978). *Chem. Phys. Lett.* **57**, 83.
Dunning, T. H., Jr., and Hay, P. J. (1978). *J. Chem. Phys.* **69**, 134.
Ermler, W. C., Lee, Y. S., Pitzer, K. S., and Winter, N. W. (1978). (to be published).
Gubanov, V. A., and Chirkov, A. K. (1978). *Inorg. Nucl. Chem. Lett.* **14**, 139.
Hay, P. J., Wadt, W. R., Kahn, L. R., and Bobrowicz, F. W. (1978). Report LA-UR 78-13. Los Alamos Scientific Laboratory, *J. Chem. Phys.* (to be published).
Heslop, R. B., and Jones, K. (1976). "Inorganic Chemistry." Elsevier, Amsterdam.
Jokisaari, J., Räisänen, K., Lajunen, L., Passoja, A., and Pyykkö, P. (1978). *J. Magn. Reson.* **31**, 121.
Lee, Y. S., Ermler, W. C., Pitzer, K. S., and McLean, A. D. (1979). (to be published).
Leiter, D. (1978). *Nuovo Cimento B* **43**, 13.
Messmer, R. P., Salahub, D. R., Johnson, K. H., and Yang, C. Y. (1977). *Chem. Phys. Lett.* **51**, 84.
Pyykkö, P., and Desclaux, J. P. (1978). *Chem. Phys.* (to be published).
Rose, S. J., Grant, I. P., and Pyper, N. C. (1978). *J. Phys. B* **11**, 1171.
Rosén, A. (1978). *Int. J. Quantum Chem.* **13**, 509.
Rosén, A., Fricke, B., and Morović, T. (1978). *Phys. Rev. Lett.* **40**, 856.
Skriver, H. L., Andersen, O. K., and Johansson, B. (1978). *Phys. Rev. Lett.* **41**, 42.
Wadt, W. R., Hay, P. J., and Kahn, L. R. (1978). *J. Chem. Phys.* **68**, 1752.
Yang, C. Y. (1978). *J. Chem. Phys.* **68**, 2626.
Yang, C. Y., and Rabii, S. (1976). *Int. J. Quantum Chem.* **S10**, 313.
Yang, C. Y., Johnson, K. H., and Horsley, J. A. (1978). *J. Chem. Phys.* **68**, 1001.
Younger, S. M., and Weiss, A. W. (1975). *J. Res. Nat. Bur. Stand. A* **79**, 629.
Zevin, V., Fekete, D., and Kaplan, N. (1978). *Phys. Rev. B* **17**, 355.

ADVANCES IN QUANTUM CHEMISTRY, VOLUME 11

Fundamentals of Equilibrium Thermodynamics and Statistical Mechanics

GUNNAR SPERBER*

Quantum Chemistry Group
University of Uppsala
Uppsala, Sweden

The present article is a "reduced version" of a stencilled report available from the Uppsala Quantum Chemistry Group (1973). This report is referred to as TN 401 throughout. Among the material in TN 401 not included here are the sections on "Equilibrium conditions in complex isolated systems," "Transformations of thermodynamic variables," "Heat and work," and "Classical statistical mechanics" (which we regard just as an approximation to quantum statistical mechanics).

I. Fundamental Concepts of Equilibrium Thermodynamics

There is considerable disagreement among authors about how to define and delimit the subject of thermodynamics (as well as statistical mechanics). This confusion has its roots in the history of the subject. We choose to define *thermodynamics* as the study of the states of macroscopic systems and of the interconversion between these states under various conditions, without quantitative consideration of the rates of change. Qualitative consideration

---

* Present address: Åkervägen 2, S-752 51 Uppsala, Sweden.

ISBN 0-12-034811-X

of the rates of change, on the other hand, is very important, entailing a separation of rates into different classes ("rapid" and "slow" processes). Thermodynamics is characterized by the particular study of a quantity known as entropy, whose fundamental property is that it cannot decrease measurably for an isolated macroscopic system.

The branch of science in which the rates of processes in macroscopic systems are subjected to quantitative study is called *kinetics* (from the Greek word *kinein* "to move"). Kinetics is so far essentially an empirical science, whose formulas are (with certain exceptions, such as the "Onsager relations") of a limited and approximate validity. As might be expected from the fundamental role played by entropy in thermodynamics, consideration of the rate of change in entropy is of importance in modern kinetics (see, e.g., Yourgrau *et al.*, 1966).

Kinetics in a wide sense is clearly a very general science; it includes, for instance, thermodynamics itself (by "removal" of those formulas that explicitly include rates of change). There is also a branch of science where one considers only processes in which the entropy of the participating subsystems is nearly constant (or the changes in entropy are of no importance to the problem). This part of kinetics is more-or-less identical with classical mechanics and field theory (including also nonviscous hydrodynamics, theory of elasticity, etc.), or rather with that part of it which can be put in a Lagrange–Hamilton form (cf. Landau and Lifshitz, 1959, p. 232). If we remove from this part those formulas which explicitly include nonzero time derivatives, we obtain a "core" that is common to thermodynamics and classical mechanics (Scheme 1). It includes the mechanical conservation laws and the theory of mechanical equilibrium (statics).

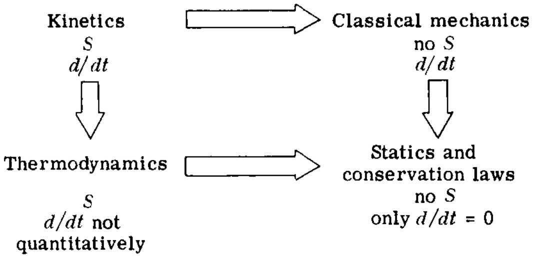

Scheme 1

The name "thermodynamics" is something of a misnomer, since "dynamics" elsewhere in physics is usually understood to imply explicit consideration of rates. "Thermostatics" might be more appropriate but could be misunderstood as excluding altogether the consideration of nonequilibrium situations. Some authors, however, define thermodynamics as dealing only with equilibrium conditions.

Conservation laws are of great importance in thermodynamics as well as in classical mechanics and quantum mechanics. Such laws state that certain quantities do not change with time in an isolated system and that any change in a nonisolated (sub)system must be linked by some physical process to an opposing change somewhere else. First, quantum theory tells us that certain basic quantum numbers, such as total charge, total baryon number, and total lepton number, are strictly conserved. Next, we have the law of energy conservation, which can take various forms, depending on the circumstances. For an isolated system in a static external field the conserved total energy can be written (in the nonrelativistic approximation):

$$E^{\mathrm{t}} = E^{\mathrm{i}} + \tfrac{1}{2}mv_{\mathrm{m}}^2 + U, \tag{I.1}$$

where E^{i} is the internal energy of the system, which includes the "kinetic energy of relative motion" of its parts, and v_{m} is the velocity of the center of mass of the system; U is the potential energy of interaction with the external field, which is usually a function of the position of the system and of its internal distribution of mass or charge.

In relativistic theory the corresponding equation is

$$E^{\mathrm{t}} = \frac{m_0 c^2}{\sqrt{1 - v_{\mathrm{m}}^2/c^2}} + U \tag{I.2}$$

so that E^{i} in Eq. (I.1) is identified as $E^{\mathrm{r}} = m_0 c^2$, the "rest energy."

It may happen that it is not appropriate to consider the external field as static. We should then regard our system as nonisolated, being a subsystem of a larger system that consists of three parts: (*a*) the object system (we use this term throughout for denoting a subsystem that is the principal object of interest in a given situation; (*b*) the body producing the field; and (*c*) the field itself. Assuming now that this larger system is not itself in some external field, we can find a Lorentz frame in which its center of mass is at rest, and in this frame the total energy takes the form of a rest energy $M_0 c^2$ that is a sum of several terms,

$$E^{\mathrm{t}} = E_a^{\mathrm{r}} + E_a^{\mathrm{k}} + E_b^{\mathrm{r}} + E_b^{\mathrm{k}} + E_{\mathrm{f}}, \tag{I.3}$$

where E_a^{r} is the rest energy of the object system, E_a^{k} its kinetic energy, and E_{f} is the energy of the field itself.

Since conservation laws are so important in thermodynamics, we often use a trick when we deal with a nonisolated system: we imagine it to be enclosed, together with a sufficient part of its surroundings, in a large isolating box with rigid, heat-isolating and impenetrable walls. We suppose the box to be so large that its presence does not matter for the "object system" in which we are really interested. If radiation processes are of importance, we must suppose the walls of the box to be equipped with suitable absorbers, emitters, or reflectors so that the actual radiation conditions near the object subsystem are simulated. We have thus constructed an isolated system to which the fundamental conservation laws can be directly applied:

$$\frac{dE^{\mathrm{t}}}{dt} = 0 \tag{I.4a}$$

$$\frac{dN_{\mathrm{A}}}{dt} = 0, \qquad \frac{dN_{\mathrm{B}}}{dt} = 0, \qquad \text{etc.,} \tag{I.4b}$$

where N_{A}, N_{B}, etc., are the relevant conserved particle numbers, and

$$\frac{dV}{dt} = 0, \tag{I.4c}$$

where V is the volume of the isolating box.

Although we do not consider the actual values of nonzero time derivatives in thermodynamics, their relative orders of magnitude are very important. In fact, we make a mental subdivision of processes, and of the time derivatives of state variables, into different "rate classes" to which we may attach arbitrary names: "very rapid processes," "rapid processes," "slow processes," "very slow processes," etc. We will usually consider systems in which the rate classes are well separated, so that a "rapid" process in an isolated system runs almost to completion in a time interval during which a "slow" process leads only to a negligible change. (Strictly speaking, we should perhaps consider the orders of magnitude of kinetic coefficients rather than of time derivatives, but it would take us too deeply into kinetics to attempt precise definitions here.)

Corresponding to the different rate classes in a system there are various classes of *quasi-equilibrium states.* A state of an isolated macroscopic system is called a state of quasi equilibrium with respect to processes belonging to a particular rate class if all such processes have run to completion or nearly so, so that only processes belonging to slower rate classes are going on in the system. We will frequently refer just to "states of quasi-equilibrium," assuming that it is clear from the context which rate class we are referring to.

By definition, it is clear that during a slow process the macroscopic state variables vary slowly (conserved variables of an isolated system do not vary at all, of course). During a rapid process most state variables vary rapidly. However, in an isolated system there are certain state variables that vary slowly (or not at all) even during a rapid process. We call these variables *quasi-conserved quantities*. More precisely, quantities that during processes of a certain rate class vary only with a speed belonging to a slower rate class are quasi-conserved with respect to the first rate class. Among these quantities are obviously the strictly conserved quantities.

Let us consider a concrete example. We take a vessel, pour into it two liquids of very different density, and put the vessel into an isolating container. At first the liquids move about rapidly in the vessel, but this motion soon ceases because of friction and viscosity. During this rapid process, several quantities vary slowly and are thus quasi-conserved with respect to this process, for instance, the variables defining the composition and amount of each liquid phase, and the total energy of the subsystem consisting of the vessel plus its contents. After the initial rapid relaxation process the system is in a state of quasi equilibrium with respect to such rapid processes, in which state the lighter liquid forms a layer above the heavier liquid. However, slow processes, such as diffusion and evaporation, will continue, taking the system through successive states that are quasi-equilibrium states with respect to rapid processes but not with respect to such slower processes. The number of independent quantities that are quasi-conserved with respect to slow processes is naturally smaller than the number of quantities that are quasi-conserved with respect to rapid processes. The variables just mentioned are not quasi-conserved in the new sense, but the chemical composition (mole numbers) of the whole isolated system is, as are the variables defining the shape of the vessel (there are many such variables, but usually not all of them are of interest). After a few days, the diffusion processes, evaporation of the liquids, etc., may have also effectively ceased, and the system is in a state of quasi equilibrium of "higher rank," in which the liquids have mixed with each other (partially or completely, depending on the particular nature of the system) and the temperature and vapor pressures are uniform throughout the container. Now, suppose that a very slow chemical reaction can take place between the liquids. This is then a process of an even slower rate class, with respect to which the variables defining the chemical composition (numbers of moles of various substances present in the system) are not quasi-conserved. This process may cease in quasi equilibrium, say, after a few years.

The system may further contain a certain amount of uranium that undergoes radioactive decay. This decay process belongs to an even slower rate class, with respect to which quasi equilibrium would not be reached until after millions of years, if it were practicable to wait that long. With respect to this process, not even the numbers of atoms of each species are conserved. Even after all those millions of years the system would not really be in "absolute" equilibrium since there would remain various possible nuclear reactions, etc., whose rates under ordinary conditions are immeasurably small. If we could suppose that all possible processes would run to completion, the system still remaining isolated, the result would be a state of absolute equilibrium. The only quantities that are quasi-conserved with respect to all theoretically possible processes are the strictly conserved quantities (total energy, baryon number, etc.).

Concerning the question of isolation, it seems clear that no actual physical system is completely isolated; the completely isolating box is just an idealization that we can use without harm in most cases. An actual system can only be "quasi-isolated": a wall can be described as quasi-isolating with respect to a particular quantity if its presence causes this quantity to be quasi-conserved although it would not be in the absence of the wall. For instance, a vessel with a solid wall of steel can usually be regarded as quasi-isolating with respect to the volume and mole numbers of its contents but not with respect to energy, since heat can easily be exchanged through it. However, under certain circumstances, one may be able to effect a "state of de facto isolation" also with respect to energy by carefully regulating the temperature outside the vessel so that it is constantly equal to the temperature inside.

A state of quasi equilibrium can "be changed" in either one of three ways:

a. If one just waits sufficiently long so that slow processes become important.

b. If the (quasi) isolation ceases because of some process occurring outside the system, for instance human interference, rapid processes may start again. We will then have to regard our object system as a part (subsystem) of some larger system that relaxes toward a state of quasi equilibrium of its own.

c. Certain quasi-equilibrium states, called metastable states, have the property that after a certain interval of time rapid processes start again because some process inside the system has triggered the change. The triggering process may either be a microscopic one, in which case the length of the "latency interval" cannot be predicted exactly (for example, a supercooled liquid in which spontaneous crystallization may occur), or some slow macroscopic process (for example, a time bomb).

When we speak about "states" in thermodynamics, it is normally understood that two distinct states can be distinguished from each other by the value of some macroscopically observable quantity. Likewise, when we speak about a process, we suppose that it can be followed on the macroscopic level (an exception is the microscopic triggering process mentioned in the last paragraph). A macroscopic system has, in general, a very large number of macroscopically distinct states (macrostates). To specify completely and uniquely every macrostate, one would need a large number of physical parameters (state variables). However, one can usually be content with studying some special subset of macrostates (very often they are states of quasi equilibrium in some sense), and then a smaller number of state variables, often just a few of them, are necessary.

One of the fundamental mathematical tools of thermodynamics is that of a state space for a system, which is just an n-dimensional linear space in which a possible state of the system is represented by a point (one point may sometimes correspond to many possible macrostates) whose coordinates are given by the values (for the state in question) of n selected state variables. The development in time of the system will be represented by some curve in the state space. It is obvious that "the state space of a system" can be defined in many ways. First, there is the question of which kinds of states to include. Second, the choice of state variables is, of course, not unique. However, we will actually prefer certain choices as being more "fundamental" than others (see the following). In practice, the choice of state space is usually made on the basis of convenience.

To each macrostate of a macroscopic system there belongs a certain nonnegative number S, called the entropy of the state. It can be regarded as a function of the variables that define the state or, alternatively, it can itself be regarded as an independent variable (we will usually choose the former alternative in this treatise). It is characterized by the following property: if an *isolated* macroscopic system is in a state P_1 at the time t_1, with entropy $S(P_1)$, and in a state P_2 with entropy $S(P_2)$ at some later time t_2, so that $t_2 > t_1$, then $S(P_2) \geq S(P_1)$. In other words, we have

$$\frac{dS}{dt} \geq 0 \qquad \text{for an isolated system,} \tag{I.5}$$

which is sometimes shortened to read: $dS \geq 0$ for an isolated system.

More generally, we may say that any measurable entropy decrease that occurs in a nonisolated macroscopic (sub)system is always coupled through some physical process to an entropy increase (which at least balances the decrease) somewhere else, usually in the immediate surroundings, unless radiation takes place.

Strictly speaking, we should perhaps admit the possibility of a momentary decrease in entropy for an isolated system, due to a fluctuation (see Section XI). Such decreases, however, are in practice always too small to be measurable (see Section VI for a discussion of the measurement of entropy).

It follows that if an isolated system goes from a state P_1 to a state P_2 and back to the state P_1, we must have $S(P_1) = S(P_2)$. Any process in an isolated system during which its entropy remains constant is called reversible, since the opposite process can then, in principle, occur even if the system remains in isolation. A process during which the entropy of an isolated system increases is called irreversible, since the opposite process is not possible unless the isolation of the system ceases. In practice, processes are seldom strictly reversible, but many processes are accompanied by very small entropy increases. (It should be noted that in the chemical, especially the biochemical, literature, the phrase "reversible chemical reaction" is used to denote something quite different, namely a reaction that can fairly easily be made to go in the other direction by changing the conditions, for instance by addition of other substances that themselves react with one of the reacting species.)

The entropy of a body has the fundamental property that (like the internal energy, but unlike the total energy) it does not depend explicitly on the position or velocity of the body. Ordinary electrostatic and gravitational fields have zero entropy, but "incoherent" radiation fields have positive entropy.

The following theorem links the concepts of quasi-equilibrium states, quasi-conserved variables, and entropy: in a state of quasi equilibrium of an isolated system the nonconserved state variables have values such that the entropy of the system attains a maximum with respect to variation of the nonconserved variables, the quasi-conserved variables remaining fixed during the variation.

We illustrate this theorem by a diagram (Fig. 1). It refers to a hypothetical isolated system whose states are defined by just one nonconserved variable R and one quasi-conserved variable Q; the entropy values are illustrated by means of contours. We suppose that the system is initially in the state P_0. The system undergoes a rapid process during the initial phase; the entropy increases rapidly, but variable Q changes little. When the system has reached state P_1, the entropy can only increase further if Q changes, so that the remainder of the process is slow. It is also clear

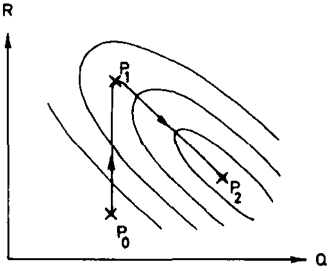

Fig. 1. Diagram illustrating the theorem about quasi-equilibrium states.

that all the states through which the system travels during this slow phase are approximately at the maximum of entropy with respect to variable R but fixed Q. For if the system should stray from this path the rapid process will tend to steer it back again. This presupposes that R remains nonconserved and Q quasi-conserved so that the system does not enter any region where R is quasi-conserved or Q nonconserved. If both variables were quasi-conserved or both nonconserved, thermodynamics would not tell us anything about the intermediate path of the system except that the entropy must never decrease in the direction of development. In any case, the path ends at the final equilibrium state P_2.

The choice of quasi-conserved variables for a system is not unique, as we pointed out before. Any smooth function of quasi-conserved variables is also a quasi-conserved variable. We can narrow the choice considerably by requiring that they be additive (extensive) as far as possible. Additivity means (using an admittedly loose definition) that if the states of two systems are characterized by values Q_1 and Q_2 of the variable in question, and these systems are juxtaposed to form a larger system, without change in the states of the two subsystems, the corresponding variable for this larger system has the value $Q_1 + Q_2$.

Of the usual conserved variables, volume and quantum numbers (particle numbers) are additive more or less by definition. The additivity of energy is a bit more problematic. If there are charged bodies in the system the total energy is certainly not additive unless the electromagnetic field is counted as a separate system with its own energy, cf. Eq. (I.3). Even when the bodies are uncharged, the Van der Waals forces between bodies in contact must be taken into account in many problems, although in others it can be neglected. One often regards the surfaces of bodies as separate systems with their own energy, in order to ensure additivity of the energy. Note also that the *internal* energy of bodies in relative motion is not additive, even if the total energy is.

It is of great importance that the entropy is also an additive quantity. Any monotone increasing function of S is nondecreasing in time, like S itself, but it is not additive unless it is of the form, const. $\times S$.

Note that the additivity laws are valid only when we add two systems by juxtaposition, not when we allow, e.g., two fluids to mix. In a mixture of two substances, A and B, say, we therefore cannot regard the assembly of molecules of type A and the assembly of molecules of type B as separate subsystems in the ordinary sense.

Suppose that we want to study a certain class of quasi-equilibrium states. As a "standard option" we will describe the states by means of a "complete set" of functionally independent quasi-conserved quantities $Q_1, Q_2, Q_3, \ldots$, which have been chosen to be additive as far as this is possible. By "complete" we mean that a set of fixed values Q_1^0, $Q_2^0, \ldots,$ (which must in general satisfy certain restricting inequalities, for instance $V > 0$) is sufficient to specify uniquely one macrostate of quasi equilibrium out of the class being considered. Often, however, one chooses to ignore some of these variables by regarding states that differ only in the values of these variables as equivalent; it is meaningful to do so only if they have the same entropy (within the accuracy considered). As an example we may think of the horizontal position variables of a chunk of ice that is floating in a glass of water; it makes sense to consider states that differ only in the position of the ice chunk on the surface as thermodynamically equivalent. After "equivalencing" there will remain a set of variables that we will refer to as "basic thermodynamic parameters" for the class of states we are considering. (The selection of such parameters is not unique, since linear combinations of additive state variables are again additive.) The values of these parameters will be considered as coordinates in a certain state space in which there is one more coordinate, namely the entropy value, which we think of as being marked along the "vertical axis." Thus, if there are n basic thermodynamic parameters $Q_1 \cdots Q_n$, their values $Q_1^0 \cdots Q_n^0$ in a state define a certain point in the "basal coordinate hyperplane" of the space. The entropy value is the $(n+1)$st coordinate of the point $(Q_1^0, \ldots, Q_n^0, S_{\max}(Q_1^0, \ldots, Q_n^0))$ describing our state in the $(n+1)$-dimensional state space. We write $S_{\max}$ to remind ourselves that there exist nonequilibrium states with the same values of the Q but lower values of S.

When the values of $Q_1 \cdots Q_n$ vary over the set of permitted values, the set of points $(Q_1, \ldots, Q_n, S_{\max}(Q_1, \ldots, Q_n))$ defines a hypersurface (of dimensionality n) in the state space, a so-called quasi-equilibrium surface. We will regard the equation,

$$S = S_{\max}(Q_1, \ldots, Q_n), \tag{I.6}$$

of this surface as the fundamental form of the "equation of state" for the set of states we are considering. If we wish to consider nonequilibrium states, they will correspond to points below the quasi-equilibrium surface but above the basal coordinate hyperplane, since the entropy of such a state is less than $S_{\max}$ but larger than zero.

If within the set of quasi-equilibrium states corresponding to a particular rate class we want to find those states which are quasi-equilibrium states also with respect to a "slower" rate class, we proceed as follows: among the basic thermodynamic parameters we select (usually after a linear transformation) those which are quasi-conserved also with respect to the new rate class (among these will obviously be those strictly conserved quantities which are being considered in the problem). We fix a set of values, say $Q_1^0, \ldots, Q_m^0$, of these new parameters, and find the maximum of entropy with respect to the other parameters $Q_{m+1}, \ldots, Q_n$. We thus find

$$\begin{aligned} S_{\max_{\max}}(Q_1^0, \ldots, Q_m^0) &= \max_{Q_{m+1}, \ldots, Q_n} S_{\max}(Q_1^0, \ldots, Q_m^0, Q_{m+1}, \ldots, Q_n) \\ &= S_{\max}(Q_1^0, \ldots, Q_m^0, Q_{m+1}^*, \ldots, Q_n^*). \end{aligned} \tag{I.7}$$

This defines a new quasi-equilibrium surface in a state space of $m + 1$ dimensions. (Here $Q_{m+1}^* \cdots Q_n^*$ are the equilibrium values of $Q_{m+1} \cdots Q_n$.)

It is clear that the considerations have so far been of a rather formal nature; they have been aimed at setting up a convenient mathematical framework for thermodynamics. Physics enters the subject when we consider the problem of identifying a complete set of quasi-conserved parameters for an actual system, and the concomitant problem of measuring them experimentally, or the problem of measuring the entropy of a system, or of calculating it from "first principles" when the values of a complete set of quasi-conserved variables are known. The last problem belongs in the domain of equilibrium statistical mechanics. The identification of quasi-conserved quantities is (except for the strictly conserved ones) either a problem of kinetics or of empirical observation. However, there are some general rules that tell us which quantities are possible candidates for "quasi conservedness" in specific kinds of systems. Variables defining the chemical composition (molecule numbers) are always among the candidates; for a pure substance these reduce to one nonzero quantity, namely, the total number of molecules in the system.

Note that the number of photons in a system is not conserved and usually cannot be regarded as quasi-conserved either, since absorption and emission events are so frequent that this number rapidly adjusts itself to any change in the rest of the system.

We will henceforward usually suppose that it is understood beforehand what particular kind of quasi equilibrium (rate class) we have in mind. Therefore we can drop the prefix "quasi-" and just speak of equilibrium states, equilibrium surfaces, and conserved quantities.

II. State Derivatives

As we have seen, the problem of finding the equilibrium state of an isolated system reduces to the problem of finding the state of maximum entropy for fixed values of the conserved variables. We thus get a mathematical problem of maximizing a certain function with respect to nonconserved variables that vary over a certain domain of definition. We must first distinguish between the usual two cases: the maximum may be located in the interior of the domain or at its boundary. In the first case we know that the partial derivatives of the entropy with respect to the nonconserved variables must be zero at the maximum, if they exist. It seems, however, to be a general law of thermodynamics that the first partial derivatives with respect to additive state variables exist and are continuous in the interior of the domain of definition (at the boundaries they may approach infinity or become ill-defined). Furthermore, the entropy is normally a convex function of the additive state variables (see Section III). This has the consequence that, if there is a maximum in the interior of the domain, it must be the absolute (global) maximum, which may be attained either in a single point or in a connected convex set of points in the domain. If the domain is also convex, there can be no local maxima of the entropy. Therefore we can usually be content with trying to find a point where the first partial derivatives of the entropy with respect to the nonconserved variables are zero. Only if no such points exist do we need to search on the boundary of the domain of definition.

These derivatives are quantities of considerable physical importance, not only because they are zero at equilibrium, but also because it is often easier to measure them than to measure the entropy (cf. Section VI). They are also important in kinetics. In this context we should point out that the nonconserved variables to be varied very often include the energies, volumes, etc. of subsystems to the isolated system under consideration. Therefore, for subsystems, derivatives of the entropy with respect to variables that would be conserved if the subsystem were isolated are of great importance (see in the following). We will refer collectively to first-order partial derivatives of the entropy with respect to additive state variables as "state derivatives." A more descriptive name is "entropic intensive parameters" (Callen, 1960). Obviously, they can themselves be regarded as functions of the additive state variables.

Let us now consider a set of states of some system that are defined by the values of some nonconserved variables $R_1 \cdots R_m$ and some conserved variables $Q_1 \cdots Q_n$. The conserved variables define a subset of equilibrium states with entropy values given by

$$S_{\max}(Q_1, \ldots, Q_n) = S(R_1^*(Q_1 \cdots Q_n), \ldots, R_m^*(Q_1 \cdots Q_n), Q_1, \ldots, Q_n), \quad \text{(II.1)}$$

where $S(R_1, \ldots, Q_n)$ is the entropy of an arbitrary state in the set, and $R_1^* \cdots R_m^*$ are the equilibrium values of $R_1 \cdots R_m$ for given values of $Q_1 \cdots Q_n$. We assume that the entropy maximum is of the "interior" kind so that, for each equilibrium state, we have

$$\left(\frac{\partial S}{\partial R_i}\right)_{\not{R}, Q} = 0 \qquad \text{for } i = 1 \cdots m, \quad \text{(II.2)}$$

where by $\not{R}$, Q we mean that all the R and Q except R_i are to be held constant.

We now consider the derivatives of the *equilibrium* entropy. It is easily shown (see TN 401) that we have

$$\left(\frac{\partial S_{\max}}{\partial Q_j}\right)_{\not{Q}} = \left(\frac{\partial S}{\partial Q_j}\right)_{R,\not{Q}} \tag{II.3}$$

This theorem is important because it permits us to define state derivatives without always specifying the particular kind of quasi equilibrium (rate class) we have in mind. Variables $R_1 \cdots R_m$ might, in their turn, be quasi-conserved with respect to some faster class of processes, so that the function $S(R_1 \cdots Q_n)$ defines a quasi-equilibrium surface in a state space where the coordinates are $(R_1, \dots, R_m, Q_1, \dots, Q_n, S)$. We see that at a point of "real" equilibrium, where we have $R_i = R_i^*(Q_1 \cdots Q_n)$, we can define the state derivatives $\partial S/\partial Q_j$ *either* by reference to the quasi-equilibrium surface as $(\partial S/\partial Q_j)_{R,\not{Q}}$ *or* by reference to the real equilibrium surface as $(\partial S_{\max}/\partial Q_j)_{\not{Q}}$. We stress that this holds in general only if the equilibrium values R_i^* are in the interior of the domain of permissible values of R_i.

We can state essentially the same theorem without explicitly referring to any nonconserved variables, as follows:

Consider a "one-dimensional" set of states labeled by a parameter t, which is such that the entropy $S(t)$ and the conserved variables $Q_1(t), \dots, Q_n(t)$ are differentiable functions of t. Furthermore, suppose that for $t = t_0$ the corresponding state is an equilibrium state. For other values of t this need not be the case. However, we consider for each t also the equilibrium state into which our given state relaxes if the system is isolated. It has the same values $Q_j(t)$ of the conserved variables but a value $S_{\max}(t)$ of the entropy. We have

$$S_{\max}(t) \geq S(t) \qquad \text{with equality for } t = t_0. \tag{II.4}$$

Consider a small increment Δt in the variable t (corresponding to small shifts ΔQ_j in the variables Q_j). We have then

$$\Delta S_{\max} = S_{\max}(t_0 + \Delta t) - S_{\max}(t_0) \geq S(t_0 + \Delta t) - S(t_0) = \Delta S. \tag{II.5}$$

We assume that t_0 is in the interior of the interval of definition for t so that we can choose Δt to be either positive or negative. We find

$$\begin{aligned} \frac{\Delta S_{\max}}{\Delta t} &\geq \frac{\Delta S}{\Delta t} \qquad \text{if } \Delta t \geq 0, \\ \frac{\Delta S_{\max}}{\Delta t} &\leq \frac{\Delta S}{\Delta t} \qquad \text{if } \Delta t \leq 0. \end{aligned} \tag{II.6}$$

Letting Δt tend to zero, we obtain

$$\frac{dS_{\max}}{dt} = \frac{dS}{dt}. \tag{II.7}$$

In other words, suppose that we start with a state of equilibrium and that the variables Q_j receive small increments ΔQ_j (for instance because of contact with the environment). The corresponding small shift in entropy ΔS (which may be of either sign) is then to first order equal to $(\partial S_{\max}/\partial Q_1) \cdot \Delta Q_1 + \cdots$ whether the new state is also an equilibrium state or a nonequilibrium state belonging to some differentiable set of states through the initial equilibrium state. The difference in entropy $S(t_0 + \Delta t) - S_{\max}(t_0 + \Delta t)$ between such a nonequilibrium state and the corresponding equilibrium state is of at least second order (it is obviously negative). Therefore the first derivatives of the entropy with respect to conserved variables have a somewhat wider significance than their definition would indicate.

In what follows we will usually be concerned with a "standard" type of system in which the basic thermodynamic parameters are the internal energy E, the volume V, and a set of composition variables (mole numbers) $N_A, N_B, \ldots$. We will suppose that external fields can be neglected and that the shape of the system is either nonconserved or thermodynamically unimportant. This is the case if the system is fluid (a liquid, gas, or easily deformable plastic solid). If we want to consider elastic deformation of solid bodies the shape also becomes of importance, which makes the formalism much more complicated. We use S (omitting the index "max") to denote the equilibrium entropy for a specified set of parameters.

Derivative $(\partial S/\partial E)_{V, N_A, N_B, \ldots}$ is by definition equal to $1/T$ where T is the thermodynamic absolute temperature. Derivative $(\partial S/\partial V)_{E, N_A, N_B, \ldots}$ is written as p/T, where p is the pressure in the system (see TN 401). The derivatives of type $(\partial S/\partial N_A)_{E, V, N_B, \ldots}$ are written as $-(\mu_A/T)$, where the numbers u_A, μ_B, etc. are chemical potentials (osmotic potentials) for the constituent substances A, B, etc.

These quantities T, p, μ_A, etc. are more directly defined in terms of a picture in which we use the same state variables to describe the same equilibrium surface but regard S as one of the *independent* variables and E as the dependent variable. By applying a well-known formula derived from the chain rule, we find:

$$
\begin{aligned}
\left(\frac{\partial E}{\partial S}\right)_{V, N_A, N_B, \ldots} &= T \\
\left(\frac{\partial E}{\partial V}\right)_{S, N_A, N_B, \ldots} &= -p \\
\left(\frac{\partial E}{\partial N_A}\right)_{S, V, N_B, \ldots} &= \mu_A \\
&\ldots
\end{aligned}
\tag{II.8}
$$

(energetic intensive parameters).

We will sometimes speak somewhat loosely about T, p, and μ also as "state derivatives." Equation (II.8) is often condensed into the symbolic form:

$$T\,dS - dE - p\,dV + \mu_{\mathrm{A}}\,dN_{\mathrm{A}} + \mu_{\mathrm{B}}\,dN_{\mathrm{B}} + \cdots = 0, \tag{II.9}$$

which is sometimes called Gibbs' fundamental equation.

Although nothing prevents us in principle from using the total rest energy $E^{\mathrm{r}} = m_0 c^2$ in thermodynamic calculations, it is usually not very practical to do so, since the variations in rest mass during any actual process (except for nuclear reactions) are exceedingly small compared to the rest mass itself. Normally, one therefore subtracts from E^{r} a suitable "fiducial energy" E_0^{r} that may be (but need not be) equal to the rest energy of the system in a certain "fiducial state." As the fiducial state of a mixture of substances one generally chooses a state in which the constituents have been separated into pure form. This means that the fiducial energy will be of the form

$$E_0^{\mathrm{r}} = e_{\mathrm{A}0}^{\mathrm{r}} N_{\mathrm{A}} + e_{\mathrm{B}0}^{\mathrm{r}} N_{\mathrm{B}} + \cdots, \tag{II.10}$$

where $e_{\mathrm{A}0}^{\mathrm{r}}$ is the rest energy of 1 mole of pure substance A in its fiducial state, etc. The internal energy E is defined as $E^{\mathrm{r}} - E_0^{\mathrm{r}}$. It is clear that E_0^{r} and, therefore, E are usually not conserved during chemical reactions in an isolated system, although E^{r} itself is of course conserved.

In statistical mechanics the fiducial energy is often chosen as the sum of the ground-state energies of all the molecules present in the system (see Sections V and X).

The derivative $\partial S/\partial E = 1/T$ is not affected by the choice of fiducial energy, neither is $\partial S/\partial V$ as long as the fiducial energy is independent of the volume. The chemical potential, on the other hand, does depend on the choice of fiducial energy.

Let us define an "absolute chemical potential" $\mu_{\mathrm{A}}^{\mathrm{r}}$ by

$$\mu_{\mathrm{A}}^{\mathrm{r}} = \left(\frac{\partial E^{\mathrm{r}}}{\partial N_{\mathrm{A}}}\right)_{S,\,V,\,N_{\mathrm{B}},\,\ldots}. \tag{II.11}$$

We find immediately

$$\begin{aligned}\mu_{\mathrm{A}} = \left(\frac{\partial E}{\partial N_{\mathrm{A}}}\right)_{S,\,V,\,N_{\mathrm{B}},\,\ldots} &= \mu_{\mathrm{A}}^{\mathrm{r}} - \left(\frac{\partial E_0^{\mathrm{r}}}{\partial N_{\mathrm{A}}}\right)_{N_{\mathrm{B}},\,\ldots}\\ &= \mu_{\mathrm{A}}^{\mathrm{r}} - e_{\mathrm{A}0}^{\mathrm{r}}.\end{aligned} \tag{II.12}$$

The difference in chemical potential between two states of the same system is clearly independent of the choice of fiducial energy.

III. General Properties of Equilibrium Surfaces. Phase Transformations

The character of an equilibrium surface obviously depends on the system. However, equilibrium surfaces have certain properties in common, as we will show in this section.

We will assume that we are dealing with a system of the "standard type" so that the basic thermodynamic parameters are E, V, and some composition variables N_A, N_B, etc. The essential thing is that all the relevant parameters are additive. The additional coordinate in our basic state space is S, and the equation of the equilibrium surface is

$$S = S(E, V, N_A, \ldots) \tag{III.1}$$

[we omit the index "max", cf. Eq. (I.6)].

We consider an arbitrary equilibrium state defined by $(E_1, V_1, \ldots)$ and with entropy $S_1 = S(E_1, V_1, \ldots)$. The corresponding point in state space has coordinates $(S_1, E_1, V_1, \ldots)$ (we write the entropy coordinate first in this section). It is clear that we can form other states of equilibrium by just taking "t times as much of everything." Therefore, to the parameter values $(tE_1, tV_1, tN_{A1}, \ldots)$, there corresponds a state of equilibrium whose entropy is tS_1. The corresponding points in state space,

$$(tS_1, tE_1, tV_1, tN_{A1}, \ldots) \qquad \text{where } t > 0, \tag{III.2}$$

form a ray in state space that starts at the origin and, in principle, extends to infinity. We will refer to states that differ only by such an "amount factor" t as "states of the same kind." The entire ray of states of the same kind lies in the equilibrium surface. Note that it is essential here that the parameters include the mole numbers; often these are omitted and understood to be constant, and in that case only one of the states on the ray is in the "reduced state space" corresponding to a hyperplane $N = \text{const.}$ in the "full state space."

We thus find that the equilibrium surface must fulfill a "homogeneity equation":

$$S(tE_1, tV_1, tN_{A1}, \ldots) = tS(E_1, V_1, N_{A1}, \ldots). \tag{III.3}$$

By differentiating Eq. (III.3) with respect to E_1, V_1, etc., we find that the state derivatives (pressure, temperature, etc.) are independent of t, as expected. By differentiating Eq. (III.3) with respect to t, we obtain the important formula

$$E\frac{\partial S}{\partial E} + V\frac{\partial S}{\partial V} + N_A\frac{\partial S}{\partial N_A} + \cdots = S. \tag{III.4}$$

By applying the definitions of temperature, etc., we reformulate this equation as

$$E + pV - \mu_A N_A - \cdots - TS = 0, \tag{III.5}$$

which is known as the thermodynamic identity or Euler's relation.

We now consider a further equilibrium state $(S_2, E_2, V_2, \ldots)$ which we represent by the symbol P_2. With this and the state $P_1 = (S_1, E_1, V_1)$, we form first the two equilibrium states, $tP_1 = (tS_1, tE_1, tV_1, \ldots)$ and $(1-t)P_2 = ((1-t)S_2, (1-t)E_2, (1-t)V_2, \ldots)$. Then we take one subsystem in state tP_1 and one in state $(1-t)P_2$ and juxtapose these to form a system whose state point is $(tS_1 + (1-t)S_2, tE_1 + (1-t)E_2, tV_1 + (1-t)V_2, \ldots)$ which we represent as $tP_1 + (1-t)P_2$. For each t between 0 and 1, there is one such state; together these states form a line segment in state space connecting the two points P_1 and P_2. We suppose that P_1 and P_2 are not of the same kind (on the same ray; see the foregoing).

The states in the interior of the segment are usually not equilibrium states; such a state decays irreversibly (if the system is isolated) into some equilibrium state that has the same values of the basic parameters E, V, etc. as the initial state $tP_1 + (1-t)P_2$ but a larger value of the entropy. This equilibrium state is (normally) on the same equilibrium surface as P_1 and P_2. We thus find the following basic inequality for the equilibrium entropy:

$$\begin{aligned} S(tE_1 + (1-t)E_2, tV_1 + (1-t)V_2, \ldots) &\geq tS(E_1, V_1, \ldots) \\ + (1-t)S(E_2, V_2, \ldots) &\qquad \text{for } 0 \leq t \leq 1, \end{aligned} \tag{III.6}$$

where the equality sign holds in case $tP_1 + (1-t)P_2$ is an equilibrium state.

In other words, the equilibrium surface lies above any line segment connecting any two points on it. This is a well-known mathematical property called convexity. We can therefore say: an equilibrium surface is normally (upward) convex if the thermodynamic parameters are additive.

From Eq. (III.6) follow a number of inequalities for the derivatives of the entropy. For instance, the first partial derivative of the equilibrium entropy with respect to any direction in the basal coordinate hyperplane is itself nonincreasing in this direction. Thus $1/T$ is nonincreasing, that is, T is nondecreasing when the energy increases but the volume and the composition remain constant, and p/T is nonincreasing when the volume increases but the energy and the composition remain constant, etc. The second derivative of the equilibrium entropy with respect to any direction in the basal hyperplane is negative or zero. In the particular direction given by a ray through the origin it is zero, since the entropy is linear in this direction.

The matrix,

$$\begin{matrix} \dfrac{\partial^2 S}{\partial E^2} & \dfrac{\partial^2 S}{\partial E\,\partial V} & \cdots \\ \dfrac{\partial^2 S}{\partial V\,\partial E} & \dfrac{\partial^2 S}{\partial V^2} & \cdots \\ & \cdots, & \end{matrix}$$

is symmetric and negative semidefinite (has only nonpositive eigenvalues). This means that its odd-order principal minors (including the diagonal elements) are nonpositive, the even-order minors, nonnegative. The determinant is zero everywhere.

It also follows that the derivative of the entropy with respect to any direction in which the state surface can be extended *ad infinitum* must be positive or zero. For suppose that, say, $\partial S/\partial V$ were negative and equal to $-a$ at some point $(E_0, V_0, \ldots)$. Then it must be less than or equal to $-a$ in all points $(E_0, V_0 + \Delta V, \ldots)$ also, since it is nonincreasing in the direction of increasing V (see the foregoing). Thus we find

$$S(E_0, V_0 + \Delta V, N_{A0}, \ldots) \leq S(E_0, V_0, N_{A0}, \ldots) - a\,\Delta V. \qquad \text{(III.7)}$$

If ΔV can be increased without limit, S would eventually become negative, which is impossible. Therefore $\partial S/\partial V$ cannot be negative. This proof is applicable for E (that is, T must be positive) and V (p must be positive or zero). It cannot always be applied for N, although this depends on the system and on the choice of fiducial energy. In particular, if the internal energy parameter is chosen to be the total rest energy E^r, it is normally only possible to increase N very little while keeping E^r constant, since any substantial increase in N will inevitably increase the mass and therefore E^r much more than can be compensated for by removing heat from the system. Therefore the proof does not apply at all, and one finds that μ^r is in fact very large and positive, although it would be negative or zero if the proof were valid. For a system of noninteracting bosons, it is possible to make a choice of fiducial energy such that N can be increased without limit for constant E and V; then the proof does apply and μ is always negative or zero (cf. Section X).

If one selects two arbitrary points on an equilibrium surface one will usually find that the surface lies above the line segment joining them, in the strict sense, so that the inequality sign holds in Eq. (III.6) whenever $0 < t < 1$. However, the opposite case when the line is in the surface is of great importance. We already know one trivial case of this, namely when the two points lie on a "ray" through the origin and thus correspond to different amounts of the same substance in the same kind of state. The interesting case is when the two points do not lie on a ray. Let us examine this case in more detail.

It may be possible to extend the line segment beyond the points initially selected; if we do that as far as is possible without leaving the equilibrium surface, we find two end points P_1 and P_2 (unless the segment can be extended *ad infinitum* in either direction), which represent two states that are not of the same kind. The states $tP_1 + (1 - t)P_2$ in the interior of the line segment represent inhomogeneous states of the system, in which "t parts of P_1 and $(1 - t)$ parts of P_2" have been juxtaposed and are in equilibrium with each other. This situation is called phase equilibrium. Obviously any state of the form $t_1 P_1 + t_2 P_2$, where t_1 and t_2 are arbitrary positive numbers, is also a state of phase equilibrium. This corresponds to drawing rays from the origin through all the points on the segment, thus extending it into an "infinite triangle" that forms part of the equilibrium hypersurface. (If, however, one "reduces" the state space by keeping the mole numbers constant, the "triangle" is again reduced into a line segment; cf. the foregoing.)

Equilibrium states also exist in which more than two phases are present. If there are, e.g., three phases in equilibrium, we can select three points representing the pure phases and let them define the corners of a triangle; then we extend this triangle into an "infinite triangular pyramid" by drawing rays through all the points. This pyramid is a "three-phase equilibrium part" of the equilibrium hypersurface.

Since the entropy is linear in p directions when p phases are present, the matrix of second derivatives of the entropy has (at least) p eigenvalues that are zero; the other eigenvalues are negative. At the boundary of a phase equilibrium zone, the second derivatives are in general discontinuous, one or more of the zero eigenvalues jumping abruptly to a nonzero value. The first derivatives, on the other hand, are continuous. The situation is referred to as a "first-order phase transition." There also exist "second-order phase transitions" in which the second-order derivatives of the entropy are continuous but the third-order derivatives discontinuous.

It follows from the convexity of the equilibrium surface that *all* the first partial derivatives are constant along any linear segment that lies in the surface (see also TN 401). This constancy of the state derivatives along rays and phase equilibrium line segments has the consequence that the number of "effective parameters" determining the values of the state derivatives is lessened. Thus, for instance, the temperature is certainly a function $T(E, V, N_A, \ldots)$ of all the basic thermodynamic parameters, but it depends in fact only on the ratios between these quantities. If more than one phase is present there is a further reduction in the number of essential parameters within the multiphase part of the equilibrium surface. The number of essential parameters is equal to the total number of basic thermodynamic parameters minus the number of phases; in the standard case, it is thus equal to $n + 2 - p$, where n is the number of independent conserved mole numbers $N_A, N_B, \ldots$, and p is the number of homogeneous phases present in the system at equilibrium. This formula is known as Gibbs' phase rule. If the number of phases is equal to $n + 2$ (the maximum possible) the state derivatives are completely fixed at equilibrium, since no essential variable is left. Thus, for a pure substance in a state of three-phase equilibrium, the temperature, pressure, and chemical potential cannot be varied at all unless one of the phases disappears. If two phases are present, all the state derivatives are functions of a single variable; two of them can be expressed as functions of the third one, for instance μ and p as functions of T. If only one phase is present two of the state derivatives are independent and the third one is a function of them; for instance μ may be expressed as a function of T and p.

Unfortunately, it is rather difficult to make a satisfactory drawing of an equilibrium surface for a realistic system even if one is content with, e.g., making a contour map of S as a function of E and V at constant N. We will therefore not attempt this, but just make some remarks about what happens in the simplest case: a pure substance with one solid phase, one liquid phase, and one gaseous phase. A certain triangular region in the (E, V) plane (see Fig. 2) will correspond to states where all the phases coexist; each

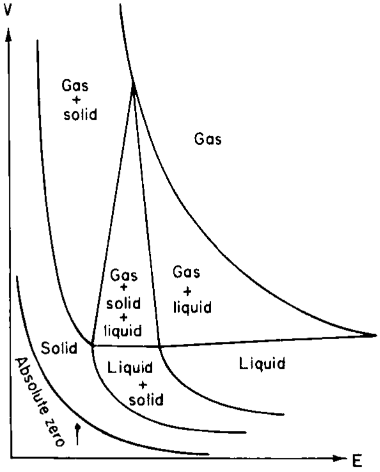

Fig. 2. Diagram showing the topology of the (E, V) plane (N fixed) for a pure substance of the ordinary kind. (The metrical relations in the figure have no significance whatsoever.)

corner of the triangle represents one phase in a definite state. Inside this triangle the entropy is a "planar" function of E and V. [The triangle is an intersection of an "infinite triangular pyramid" with a coordinate hyperplane $N = \text{const.}$ in the full (S, E, V, N) state space.] Adjoining the sides of this three-phase (triple-point) part of the surface there are "pseudocylindrical" parts representing sets of states in which two phases are in equilibrium. These parts can be thought of as made up of linear segments, the end points of which represent pure phases. One of the two-phase parts represents liquid and gas in equilibrium; toward high energies this part becomes narrower and finally ends at a certain "critical point."

The remainder of the equilibrium surface consists of two one-phase parts. One of these represents states where the whole system is solid, whereas the other one-phase region represents states in which the system is either liquid or gaseous. The "liquid" and "gaseous" parts of this region merge gradually into each other beyond the critical point; one can therefore take a pure substance gradually from a liquid to a gaseous state or vice versa by passing through states above the critical temperature. Toward low energies the equilibrium surface ends at the ground-state energy which is a function $E_{\min}(V)$ of V for fixed N. At this boundary, T is zero ($\partial S/\partial E$ is infinite) and S is usually zero also, although cases are known when the entropy is extremely rapidly increasing near $E_{\min}$ and the practically measurable limit of S as $E \rightarrow E_{\min}$ is larger than zero. The character of the equilibrium surface near $E_{\min}$ can often be easily predicted from statistical mechanics.

In parts of the multiphase regions there may exist metastable states in which only one phase is present (supercooled liquids, etc.). The set of such states will then be represented by a further surface in state space below the true equilibrium surface (since the entropy of such a state is lower than that of the corresponding stable equilibrium state). At the boundary to the true one-phase region, the surface of metastable states joins the true equilibrium surface smoothly, with continuous second derivatives (see Fig. 3).

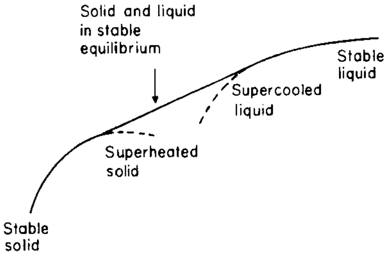

Fig. 3. Diagram showing behavior of state surfaces in "true" equilibrium and in metastable equilibrium.

IV. Fundamental Concepts of Equilibrium Statistical Mechanics

In the foregoing exposition of equilibrium thermodynamics, we left out two very important issues that must be clarified if the theory is not to hang in the air. One is how to measure thermodynamic quantities experimentally; we postpone this until Section VI. The other is to find some way of calculating from "first principles" the equilibrium properties of a system for prescribed values of the basic thermodynamic parameters E, V, etc. This is one of the aims of the science of statistical mechanics.

During the second half of the nineteenth century, this was attempted on the basis of regarding macroscopic systems as composed of particles obeying ordinary Lagrange–Hamilton classical mechanics. Although the development of classical statistical mechanics by Maxwell, Boltzmann, Gibbs, etc. is now recognized as a great scientific feat, the resulting theory had several unsatisfactory features and was at that time believed by many scientists to be nonsense. The "old quantum theory" improved the situation considerably. After quantum mechanics was proposed, it soon became clear that a much more satisfactory theory could be found by retaining the general framework of classical statistical mechanics but substituting the concept of a quantum-mechanical pure state for the concept of a "cell" in phase space. From this "quantum statistical mechanics," improved formulas corresponding to those of classical statistical mechanics can be derived as approximations. Although quantum statistical mechanics is widely believed to be "exact" there is, strictly speaking, no experimental proof that this is the case. The reason is that the calculations required to find accurate values of physical properties by statistical mechanics are in most cases impossible to perform at present. This is quite natural, since the situation is similar in the "parent science" of quantum statistical mechanics, namely the quantum mechanics of many-particle systems.

We will expound the basic postulates of equilibrium statistical mechanics (in its quantum version) without trying to find any deeper reasons for their validity, except that we try to show that they encounter no obvious objections that cannot be overcome. There have been many attempts to find a more satisfactory foundation for statistical mechanics; we will just mention the following watchwords in this connection: ergodic theory, master equations, statistical independence of subsystems, information theory, coarse-graining procedures. We refer the reader wishing more information about this subject to some textbooks (Landau and Lifshitz, 1959; Gibbs, 1902; von Neumann, 1955; Tolman, 1938; Mayer and Mayer, 1940; Chintschin, 1956; Fowler and Guggenheim, 1952; Kittel, 1958; Huang, 1963) and articles (Jaynes, 1957; Löwdin, 1967; Hatsopoulos and Gyftopoulos, 1976). The author of the present treatise is inclined to take a rather skeptical attitude (Sperber, 1974) toward these attempts at justification. We point out, however, that even if any or all of them should turn out to be unfounded this would not necessarily affect the validity of the basic postulates of equilibrium statistical mechanics. On the other hand, we cannot rest completely assured of the general validity of these postulates either, as long as experimental verification is scarce and quantum mechanics itself has its troubles.

When we spoke in earlier sections of states of a macroscopic system, it has been understood that different "macrostates" can be distinguished from each other by some macroscopically observable characteristic. In statistical mechanics the concept of a macrostate is still important, but we encounter also the concept of a "microstate" or "quantum state" (pure state). As we know from quantum mechanics, the quantum states of a system (or rather the "state vectors" or wavefunctions representing them) form a Hilbert space, and "physical observables" correspond to linear operators on this space.

The fundamental idea of quantum statistical mechanics is that to a macrostate of an isolated system there corresponds a certain finite-dimensional subspace of the Hilbert space, called the subspace of accessible microstates for the macrostate in question. As we know, in any such subspace an orthonormal basis of state vectors φ_i, $i = 1, 2, \ldots, \Gamma$, can be selected; the number of basis vectors, Γ, is the dimension of the subspace.

If a physical property (observable) corresponds to an operator A, its expectation value in a microstate ψ is $\langle\psi|A|\psi\rangle$ according to the principles of quantum mechanics. In practice, it is usually true (see particularly, Chintschin, 1956) for quantities of physical interest that almost all the microstates in a subspace of accessible states yield expectation values that are almost equal from the macroscopic point of view. (In fact, if the relevant subspaces did not have this kind of "almost uniformity," statistical mechanics would lose most of its cogency and intuitive appeal.) However, in order to make a definite general assumption, we postulate that the expectation value of A in the macrostate (macroscopic mean value) is to be found as an arithmetic mean with equal weights over a set of orthonormal basis functions in the subspace:

$$\overline{\overline{A}} = \sum_{i=1}^{\Gamma} \langle\varphi_i|A|\varphi_i\rangle/\Gamma. \tag{IV.1}$$

This is often referred to as the postulate of equal *a priori* probabilities and random phases. (See Section XI for some further remarks on the physical meaning of this postulate.) The particular choice of orthonormal basis in Eq. (IV.1) is immaterial, since the result is independent of the choice. We can write the formula in an explicitly invariant manner if we introduce the self-adjoint projection operator O that projects onto the subspace of accessible microstates; we then have

$$\begin{aligned} O &= \sum_{i=1}^{\Gamma} |\varphi_i\rangle\langle\varphi_i| \\ \Gamma &= \operatorname{Tr} O \qquad\qquad \text{(IV.2)} \\ \overline{\overline{A}} &= \operatorname{Tr}(AO)/\Gamma. \end{aligned}$$

We can also introduce the normalized statistical operator (density matrix) $\rho = O/\Gamma$, so that

$$\overline{\overline{A}} = \operatorname{Tr}(A\rho). \qquad \text{(IV.3)}$$

Operator O or ρ is often supposed to represent a large ensemble of systems in different quantum states; this particular kind of ensemble is called a "microcanonical ensemble." We will, however, speak freely about O or ρ as representing a single isolated macroscopic system in quasi equilibrium, and sometimes speak of O or ρ itself as "the microcanonical ensemble." Quantity Γ might be called the "microcanonical partition function," although this name does not seem to be in wide use (cf. Section IX).

Although one would perhaps expect that the entropy of a macrostate should be an observable and correspond to some positive definite operator S that would be independent of the state under consideration, quantum statistical mechanics does not make use of any such operator. Instead it is postulated that the entropy is related to the dimension Γ of the space of accessible microstates by the following fundamental equation (Boltzmann's equation in its quantum form):

$$S = k \ln \Gamma, \qquad \text{(IV.4)}$$

where k is a dimensional constant (Boltzmann's constant) whose value depends on the unit used for measuring entropy. Another form of the fundamental equation is

$$S = -k \operatorname{Tr}(\rho \ln \rho). \qquad \text{(IV.4a)}$$

Supposing now that the postulates, Eqs. (IV.1) and (IV.4) are accepted, the fundamental problem of statistical mechanics is (in principle) to find the subspace of accessible microstates corresponding to an equilibrium macrostate given by certain values of the basic thermodynamic parameters. We will suppose at first that these quantities correspond to a set of mutually commuting self-adjoint operators $(B_1, B_2, \ldots, B_n)$. There exists a set of orthonormal state vectors $\{\psi_j\}$ that are simultaneous eigenfunctions to all the operators B_k with eigenvalues $(b_{1j}, b_{2j}, \ldots, b_{nj})$ so that

$$B_1\psi_j = b_{1j}\psi_j, \ldots, B_n\psi_j = b_{nj}\psi_j \qquad \text{for all } j. \tag{IV.5}$$

In order to get any sense out of the formalism we must suppose that to a given macroscopically observed value B_k^0 of the quantity B_k there corresponds a small interval $(B_k^1; B_k^2)$ that contains B_k^0. Since the equilibrium macrostate is the state of largest entropy for the given values B_k^0 of the parameters, and a larger entropy clearly corresponds to a larger subspace because of Eq. (IV.4), it is natural to assume that the subspace of accessible microstates for the equilibrium state is the largest subspace that is compatible with these values. We therefore postulate that the subset $\{\psi_i\}$ consisting of all those eigenfunctions whose eigenvalues b_{ki} fulfil the relations $B_k^1 < b_{ki} < B_k^2$ for $k = 1, \ldots, n$ forms a basis set for the subspace we seek, and that the number of such eigenfunctions is our wanted $\Gamma_{\max} = \exp(S_{\max}/k)$. The projection operator O is then the "spectral projection" belonging to the given set of intervals:

$$O = O_{B_1}^{(B_1^1;\, B_1^2)} O_{B_2}^{(B_2^1;\, B_2^2)} \cdots O_{B_n}^{(B_n^1;\, B_n^2)}, \tag{IV.6}$$

where $O_{B_k}^{(B_k^1;\, B_k^2)}$ is a projection operator from the spectral resolution of B_k belonging to the interval $(B_k^1; B_k^2)$. In general, we must presuppose here that the equilibrium macrostate is uniquely defined by the parameter values B_k^0. If this is not the case, further parameters should in principle be added until uniqueness is attained.

To nonequilibrium macrostates with the same values of the B_k but lower entropy values than the equilibrium macrostate, there should correspond smaller subspaces that, strictly speaking, are included in the "equilibrium subspace" defined earlier. However, their presence is immaterial, since their dimensions are very much smaller than the dimension of the equilibrium subspace (cf. in the following). In Section XI, we shall explore the hypothesis that their presence corresponds to the occurrence of very infrequent fluctuations away from the equilibrium state. The situation is somewhat strange: to the many different nonequilibrium states, there corresponds a collection of microstates that forms just a tiny fraction of the accessible microstates; the overwhelming majority of these correspond to the single macrostate of equilibrium. This is just the "almost uniformity" of which we spoke earlier in this section.

It might seem at first that the results computed from Eqs. (IV.2) and (IV.4) with O given by Eq. (IV.6) would be greatly dependent on the magnitude of the interval widths $B_k^2 - B_k^1$; in particular, this is clearly the case with the number Γ. However, we will now try to convince the reader of the plausibility of the statement that the physically important results, in particular the entropy value, are essentially unaffected by the choice of interval widths as long as these have any kind of sensible magnitude.

We will make use of the obvious inequality,

$$\max_l \ln \Gamma_l \leq \ln(\Gamma_1 + \Gamma_2 + \cdots + \Gamma_m) \leq \max_l \ln \Gamma_l + \ln m, \qquad \text{(IV.7)}$$

which is valid for any set of positive numbers Γ_l.

For simplicity we will consider a case where there are just two basic thermodynamic parameters, B and C. We suppose that the "larger intervals" (B^1; B^3) and (C^1; C^3) are given; they yield a certain subspace spanned by those simultaneous eigenfunctions of B and C whose eigenvalues are within these intervals. We also consider the "smaller intervals" (B^1; B^2); (B^2; B^3) and (C^1; C^2); (C^2; C^3) that together yield four subspaces (see Fig. 4).

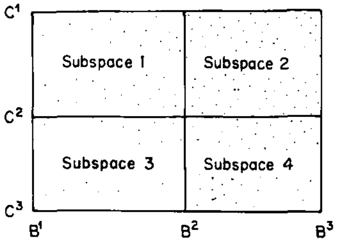

Fig. 4. Distribution of eigenvalues of thermodynamic parameters.

The projection operators O_1, O_2, O_3, O_4 onto the smaller subspaces commute, and their sum is the projection onto the bigger subspace corresponding to the larger intervals. The sum of the dimensions $\Gamma_1 \cdots \Gamma_4$ is the dimension Γ of the larger subspace. To an observable A, we get four expectation values, $\overline{A}_1 = \mathrm{Tr}(AO_1)/\Gamma_1$, etc. for the smaller subspaces, and one expectation value

$$\overline{A} = (\Gamma_1 \overline{A}_1 + \Gamma_2 \overline{A}_2 + \Gamma_3 \overline{A}_3 + \Gamma_4 \overline{A}_4)/\Gamma$$

for the larger subspace; this is a weighted mean of the values $\overline{A}_1 \cdots \overline{A}_4$.

We suppose that the intervals are small in the macroscopic sense. We must also suppose that the operator A is such that the expectation values $\overline{A}_1 \cdots \overline{A}_4$ are close together when the intervals are small. One might argue that operators that do not have this "macroscopic continuity" property are simply outside the domain of statistical mechanics. However, the critical reader may wish to see some proof that "ordinary" operators do have this property. For certain simple model systems, such as an ideal gas, such proofs can be given, but in general this seems to be very difficult (cf. later).

If $\overline{\overline{A}}_1 \cdots \overline{\overline{A}}_4$ are nearly equal, then their mean $\overline{\overline{A}}$ must also be nearly equal to these other values. We can, therefore, conclude that the interval sizes are of no importance so long as the intervals contain the macroscopic values B^0, C^0 of B and C and are small in the macroscopic sense, since it does not matter whether we use the larger or the smaller intervals.

The entropy must also have the "macroscopic continuity property," so that the four values $S_1 = k \ln \Gamma_1, \ldots, S_4 = k \ln \Gamma_4$ are, macroscopically speaking, almost equal to one another. This certainly does not imply that the numbers $\Gamma_1 \cdots \Gamma_4$ themselves are nearly equal. The entropy is usually of the general order of magnitude of kN, where N is the number of atoms in the macroscopic system. Thus we might have, e.g., $S_1 = k \times 10^{16}$, $S_2 = k(10^{16} + 10^7)$ which is a relative difference of only 10^{-9}. We find that Γ_2/Γ_1 is equal to $\exp 10^7$ so that Γ_1 and Γ_2 are of completely different orders of magnitude. This may seem surprising at first, but it is necessary for the reader to understand what is going on here, since it is crucial for the validity of statistical mechanics.

For the entropy value $S = k \ln(\Gamma_1 + \cdots + \Gamma_4)$ that corresponds to the larger intervals, we find from Eq. (IV.7) that

$$\max_{l=1\cdots 4} S_l \leq S \leq \max_{l=1\cdots 4} S_l + k \ln 4. \tag{IV.8}$$

In a more general case we might have n thermodynamic parameters and, say, p smaller intervals to one large interval. Then the number m in Eq. (IV.7) is p^n so that we would get

$$\max_l S_l \leq S \leq \max_l S_l + k \cdot n \cdot \ln p. \tag{IV.9}$$

If $n \cdot \ln p$ is small relative to N, we can neglect the term $k \cdot n \cdot \ln p$ and find that S is equal to the largest of the nearly equal numbers S_l. If N is, say, 10^{16} so that we want $n \cdot \ln p$ to be less than, say, 10^7 this will hold so long as

$$p \leq \exp\left(\frac{10^7}{n}\right). \tag{IV.10}$$

Because n is a fairly small number, we find that, if the larger intervals are small in the macroscopic sense, we need only require that the smaller intervals should be of reasonable size, e.g., not much smaller than quantities ascribable to single particles. The entropy values calculated will be practically unaffected by the interval sizes as long as these are reasonable. In particular we may choose the widths for quantities of the particle number type to be unity (1.6×10^{-24} mole) so that the particle numbers can be taken as completely fixed.

Summing up, we can say that as long as the intervals are small enough so that the expectation values of physically interesting quantities vary only negligibly over the intervals, but not so small as to be very much smaller than any reasonable number, the choice of widths for the thermodynamic parameters is physically immaterial. This holds only for macroscopic systems, indicating that the entropy is probably not well defined for microscopic systems.

In fact, microcanonical ensembles with intervals of macroscopically significant size can often be used also. This depends on the fact that, if the entropy function $S(B_1, B_2, \ldots, B_n)$ has a well-defined maximum in the region defined by some macroscopically large intervals $(B_k^1; B_k^2)$, the microcanonical ensemble defined by these large intervals will in effect be almost identical to a microcanonical (sub)ensemble defined by some small intervals around the values B_k^0 that yield the entropy maximum—because almost all the eigenfunctions in the larger ensemble will actually be within the subensemble. Further comments on this follow later, and some specific instances are mentioned.

In principle, the flow scheme of a computation in quantum statistical mechanics should be as shown in Scheme 2.

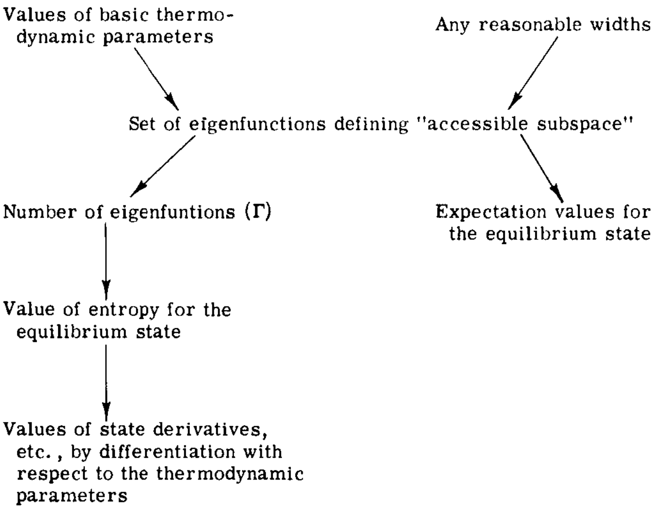

Scheme 2

Clearly, the number Γ need not be found with any accuracy to speak of. As we saw already, one may err by an enormously large factor in the computation of Γ without making more than a completely negligible error in the entropy value itself. In spite of this fact, it is usually an exceedingly difficult problem to find accurate values of S for realistic systems. In Section IX, we speak about a mathematical reformulation of the theory (the canonical ensemble formalism) that makes the problem somewhat more tractable.

We have now stated our basic postulates and would like to find out whether or not they are true. As we said before, the best proof, namely direct experimental verification in a sufficient number of nontrivial cases, is more or less out of reach for us. The next best validation would be mathematical proof that the results have certain properties that we know from experiment that they should have if they are correct. For instance, we would like to have general proof that the equilibrium entropy has continuous first derivatives with respect to the parameters, but that it can have discontinuities in the higher derivatives such as are connected with phase transformations (see Section III). We would also like to prove that the entropy is additive, or at least fulfills Eq. (III.3). The latter task is fairly easy, although by no means trivial, for ideal gases (see Sections V and X). The same may be true for systems of particles interacting by weak, short-range forces (the author cannot pretend to be an expert in these matters). For particles interacting by means of long-range forces, such as Coulomb forces, the additivity of entropy must probably be related to the tendency toward screening of the long-range forces by quasi-particle formation (cf. Section X) that occurs in such systems. To sum up the situation, we can perhaps say that the required continuity-discontinuity and additivity properties have been demonstrated in various simplified model systems and that there are good reasons to think that they are generally valid.

We would also like to be assured that Eq. (I.7) is valid when the number of basic thermodynamic parameters is changed as a result of a change in the time scale under consideration (different "rate class"). This is also connected with the "uniformity problem" mentioned earlier. Let us again discuss a model system with two thermodynamic parameters B and C and entropy $S(B, C)$, which is supposed to be computed according to the prescriptions made earlier in this section. Let C^* be such that $S(B, C^*) = \max_c S(B, C)$. What we need to show is that $S(B, C^*)$ is identical (within a negligible error) to the value $S(B)$ that we find if we ignore the parameter C altogether, which is equivalent to putting the "interval of accessible eigenvalues" for C equal to the whole range of all possible values of C.

To show this, let us subdivide the range of possible values of C (which must be finite, as is indeed found in practice in cases of this nature) into small intervals that we number with an index i that goes from 1 to m, where m is a large number. Let C_i be some value within the ith interval. We also select a fixed value of B, surround it with some small interval and thus get a finite set of eigenfunctions for each i. Each such set contains Γ_i eigenfunctions, where, according to Eq. (IV.4), we have

$$\Gamma_i = \exp\left(\frac{S(B, C_i)}{k}\right). \tag{IV.11}$$

If we allow arbitrary values of C, we get a number

$$\Gamma = \sum_{i=1}^{m} \Gamma_i \tag{IV.12}$$

with

$$\Gamma = \exp\left(\frac{S(B)}{k}\right)$$

Again, we apply Eq. (IV.7) and find that $S(B)$ is indeed equal to $\max_i S(B, C_i)$ within a negligible error limit $k \ln m$.

Suppose now that there is one unique value I of i for which $S(B, C_i)$ assumes its maximum value, and that this value is significantly larger than the next largest value $S(B, C_J)$. We have then

$$\Gamma_I = \Gamma_J \exp\left(\frac{S(B, C_I) - S(B, C_J)}{k}\right) \tag{IV.13}$$

and

$$\sum_{i \neq I} \Gamma_i \leq (m-1)\Gamma_J. \tag{IV.14}$$

Therefore the number Γ_I is much larger than the sum of all the other Γ_i, which means that the states in the "restricted" microcanonical ensemble defined by a small interval around C_I dominate the "full" microcanonical ensemble where all values of C are permitted.

We now finally come to the really crucial question: Can we prove that S as computed from Eq. (IV.4) is nondecreasing in time? Here we encounter at once an obvious objection: according to the principles of quantum mechanics, the time development of the statistical operator ρ of a system should be given by some law of the form

$$\rho(t) = U(t)\rho(t_0)U^\dagger(t), \tag{IV.15}$$

where the unitary operator $U(t)$ is called an evolution operator. Now it is easy to show that quantities such as $\mathrm{Tr}(\rho \ln \rho)$ are invariant under unitary transformations of the type Eq. (IV.15), so that the entropy ought to be conserved and never increase for an isolated system.

There are various possible ways out of this difficulty. One may argue that the postulates may need some formal modification but that the "true" formulas may lead to the same physical results as our postulates. One may also argue that the law, Eq. (IV.15) may not be strictly valid for macroscopic systems, perhaps because "observation processes" intervene (cf. Sperber, 1974).

In this connection we must confess to a certain amount of cheating when we stated the basic postulates. We assumed that the basic thermodynamic parameters, one of which is normally the energy E, correspond to commuting operators on Hilbert space. Now it is a well-known theorem of quantum mechanics that any operator that commutes with the energy operator (Hamiltonian) of an isolated system corresponds to a strictly conserved quantity. Since in practice some of the parameters are usually just quasi-conserved, these should correspond to operators that do not commute exactly but only approximately with the Hamiltonian. For statistical mechanics, this fact causes difficulties that are really of a rather fundamental nature but can, in practice, often be overcome by a somewhat heuristic "stretching" of the formalism, involving adding terms to the Hamiltonian to take the other parameters into account. We will go into some detail about this for the standard type of systems whose thermodynamic parameters are the total energy (which is in this case equal to the internal energy), the volume, and some "particle numbers."

The volume parameter is handled simply by assuming that the system is surrounded by an infinitely high potential wall that does not allow any particles to escape. Thus the Hamiltonian is augmented by potential terms (one for each particle) which are zero inside the system, but infinite outside it. As we know, the "augmented" Hamiltonian will have an entirely discrete spectrum with a finite number of eigenvalues in each finite energy interval (this number depends on the volume, of course). There is no need to consider a separate "volume operator." Strictly speaking, the interval of possible volumes for the system extends all the way from zero to the volume of the box, since the potential wall does not prevent the system from shrinking into a smaller volume. Normally, however, the entropy is an increasing function of the volume, and, therefore, almost all the states in the microcanonical ensemble will correspond to volumes very near the maximum allowed (cf. the foregoing).

The treatment of other kinds of quasi-conserved quantities may cause more difficulty sometimes. Systems of reacting molecules at high concentration is one instance. Another one is supercooled liquids, in which case we would have to consider the system to be restricted to states in which the solid phase is absent from the system—it does not appear too easy to formulate such a restriction quantum-mechanically. Suppose, anyway, that we have found a self-adjoint projection operator Q projecting onto a subspace of states that, for some reason, seem suitable for representing macrostates that have some particular macroscopic property. We can then form the "outer projection" QHQ of the full Hamiltonian H. This operator commutes with Q, and we may take it as our modified Hamiltonian—the undesirable quantum states have already been eliminated from it. It may even be possible to consider the remainder $H - QHQ$ of the Hamiltonian as a perturbation that is responsible for the slow changes (chemical reactions, for instance) that continue even in a state of quasi equilibrium. However, this question is outside the domain of this article.

We will also consider another, more explicit kind of modified Hamiltonian for the case of a system of composite particles where the average distance between the "particles" (which are in fact bound systems composed of elementary particles) is much larger than the size of the particles themselves. We will think of the bound systems as molecules in a dilute gas, but the discussion applies equally well to nuclei, which are bound systems of nucleons. We need not assume in this context that the interaction between the molecules is weak.

Suppose that the total macroscopic system is composed of N_a elementary particles of type a, N_b elementary particles of type b, etc., that form various bound systems (molecules) of types A, B, etc. Let a molecule of type A be composed of N_{Aa} particles a, N_{Ab} particles b, etc. We have obviously $N_a = N_{Aa} N_A + N_{Ba} N_B + \cdots$. To the Hamiltonian of the system (including the external potential wall), we add a further term that serves the purpose of separating the system exactly into well-defined molecules of the desired kinds and numbers. It is a many-particle potential (a multiplicative operator in the coordinate representation),

$$V(\mathbf{r}_{a1}, \mathbf{r}_{a2}, \ldots, \mathbf{r}_{aN_a}, \mathbf{r}_{b1}, \mathbf{r}_{b2}, \ldots, \mathbf{r}_{bN_b}, \mathbf{r}_{c1}, \ldots), \tag{IV.16}$$

which is zero when the elementary particle coordinates $\mathbf{r}$ form well-defined groups of the right composition, N_A groups of type A, N_B of type B etc.; otherwise the potential is infinite. More specifically, we assign a "limiting radius" R_A to molecules A, R_B to molecules B, etc. To satisfy the "general group requirement," so that potential V will be zero, a configuration of particle positions $\mathbf{r}$ must be such that N_{Aa} of the elementary particles a, N_{Ab} particles b, etc., together form a group in space such that all these particles are at a distance less than R_A from the center of gravity of the group. Furthermore, all the elementary particles in the system must fall into such groups, exactly N_A groups of type N_A, N_B of type B, etc., otherwise function V will be infinite. Finally, the groups must not overlap, which means that the centers of gravity of one group of type I and one of type J must be at a distance greater than $R_I + R_J$ in all cases; if this is not the case, V is infinite. Thus V prevents the molecules from reacting with one another.

As a result of manipulations of this kind, we may arrive at a situation in which all the thermodynamic parameters except the energy have, so to say, been built into the Hamiltonian, and the only thing left to do in order to set up the microcanonical ensemble is to select those eigenstates (stationary states) of the modified Hamiltonian which have energies between two specified limits E_1 and E_2 (we use subscripts instead of superscripts here). The number $\Gamma(E_1, E_2)$ of states is related to the equilibrium entropy of the system by Boltzmann's equation. We define formally the function $S(E)$ by

$$S(E) = k \ln \Gamma(E_0, E), \tag{IV.17}$$

where E_0 is the ground-state energy of the Hamiltonian. Thus we have put the lower limit equal to its lowest possible value. (All basic thermodynamic parameters other than the energy are fixed and need not be referred to here.) Function $S(E)$ is quite smooth and can be regarded as differentiable; the derivative $dS(E)/dE$ is equal to the reciprocal temperature $1/T(E)$.

For $\Gamma(E_1, E_2)$, we find the following equation:

$$\begin{aligned}\Gamma(E_1, E_2) &= \exp\left(\frac{S(E_2)}{k}\right) - \exp\left(\frac{S(E_1)}{k}\right)\\ &= \exp\left(\frac{S(E_2)}{k}\right)\left[1 - \exp\left(-\frac{S(E_2) - S(E_1)}{k}\right)\right].\end{aligned} \tag{IV.18}$$

We assume that $S(E)$ is a convex function (see Section III); then it follows that, for $E_1 < E_2$, we have

$$\frac{S(E_2) - S(E_1)}{E_2 - E_1} \geq \left(\frac{dS(E)}{dE}\right)_{E=E_2} = \frac{1}{T(E_2)}. \tag{IV.19}$$

From Eqs. (IV.18) and (IV.19), we get

$$\Gamma(E_1, E_2) \geq \exp\left(\frac{S(E_2)}{k}\right)\left[1 - \exp\left(-\frac{E_2 - E_1}{kT(E_2)}\right)\right]. \tag{IV.20}$$

Now it is a fact that $kT(E_2)$ is a small positive quantity of the order of magnitude of the translational energy of a single molecule; it is thus much smaller than any macroscopically significant quantity. If we choose the interval length $E_2 - E_1$ to be $\gg kT(E_2)$, we get

$$\Gamma(E_1, E_2) \approx \exp\left(\frac{S(E_2)}{k}\right) = \Gamma(E_0, E_2). \tag{IV.21}$$

In fact, the overwhelming majority of all the microstates in the macroscopically large interval $(E_0;\ E_2)$ are "crowded" into the small interval

$(E_1;\ E_2)$ as long as this interval is larger than, say, $50kT$. The quantity $k \ln \Gamma(E_1, E_2)$ is practically unaffected by the width $E_2 - E_1$ down to extremely small widths, much smaller than any reasonable number such as kT.

We will also look at the "density of states" that is formally defined by

$$D(E_2) = \lim_{E_1 \to E_2} \frac{\Gamma(E_1, E_2)}{E_2 - E_1}. \tag{IV.22}$$

So long as $E_2 - E_1$ is $\gg kT(E_2)$, we have

$$\frac{\Gamma(E_1, E_2)}{E_2 - E_1} \approx \frac{\exp(S(E_2)/k)}{E_2 - E_1}, \tag{IV.23}$$

which does not appear to approach any finite limit. Not until $E_2 - E_1$ becomes $\ll kT(E_2)$ do we approach the formal limit

$$D(E_2) = \frac{\exp(S(E_2)/k)}{kT(E_2)}. \tag{IV.24}$$

We can, in fact, put

$$S(E_2) = k \ln D(E_2) \tag{IV.25}$$

with a completely negligible error, since, if we use any reasonable energy units, the term $k \ln kT$ will be very small. Strictly speaking, however, Eq. (IV.25) is not dimensionally correct.

V. The Ideal Gas under Maxwell–Boltzmann Conditions

We consider a macroscopic system composed of N_A molecules of type A with molecular mass M_A, N_B molecules of type B, etc., whose interaction we neglect. The system is enclosed in a rectangular box (infinite potential wall) whose sides have lengths L_x, L_y, L_z. We suppose that external fields can be neglected and that the volume $V = L_x L_y L_z$ is large enough so that the size of the molecules themselves is negligible in comparison to the volume available per molecule (V/N).

We also add a further restrictive assumption that will be removed in Section X: we assume that the ground state of molecule A has degeneracy D_A, the ground state of B degeneracy D_B, etc., and that the internally excited states of the molecules are so high-lying that they are of no interest for the problem at hand (this means in practice that the molecules must be monatomic, since polyatomic molecules have many low-lying rotational states).

To set up the stationary state wavefunctions, we may regard the system as composed of N_a elementary particles of type a, N_b of type b, etc., as we did in Section IV, and apply the formalism given there to construct a modified Hamiltonian containing a "separation term," Eq. (IV.16). However, it is more convenient to use a formalism whereby we regard the system as composed of fictitious elementary particles of type A, B, etc., with spin $(D_A - 1)/2$, $(D_B - 1)/2$, etc. In TN 401 a partial justification for using such a formalism is given. Quantum chemists are used to make an implicit transformation of a similar kind when they regard nuclei as "point particles" with one internal spin coordinate instead of treating them as systems of strongly interacting nucleons of spin $\frac{1}{2}$.

In the fictitious-particle representation, then, the independent variables are $\mathbf{R}_{A1}$, σ_{A1}, $\mathbf{R}_{A2}$, σ_{A2}, etc., where σ_{A1} can take D_A discrete values, etc. We set up approximate eigenfunctions of the Hamiltonian that are properly symmetrized–antisymmetrized products of free-particle functions:

$$\psi_{i_{A1}, i_{A2}, \ldots} = S_{op}\, e^{i\mathbf{k}_{A1} \cdot \mathbf{R}_{A1}} \chi_{m_{A1}}(\sigma_{A1}) e^{i\mathbf{k}_{A2} \cdot \mathbf{R}_{A2}} \chi_{m_{A2}}(\sigma_{A2}) \cdot \cdots \tag{V.1}$$

with

$$\chi_{m_{A1}} = \begin{cases} 1 & \text{when } \sigma_{A1} = m_{A1} \\ 0 & \text{otherwise} \end{cases}$$

(an "elementary spin function"). Here the wave vectors $\mathbf{k}$ have the following form:

$$\mathbf{k}_{A1} = 2\pi\left(\frac{n_{A1x}}{L_x}\hat{x} + \frac{n_{A1y}}{L_y}\hat{y} + \frac{n_{A1z}}{L_z}\hat{z}\right), \tag{V.2}$$

etc.

Each such total wavefunction ψ is labeled by a set of molecular indices i, one for each molecule. Each i stands for a combination of three translational indices n_x, n_y, n_z and one internal index m. Thus we have

$$i_{A1} = [n_{A1x}, n_{A1y}, n_{A1z}, m_{A1}] \tag{V.3}$$

etc.

The energy eigenvalue of a function $\psi_{i_{A1}, \ldots}$ is the sum of two parts, namely (*a*) the sum of the internal molecular energies, which, because of the restriction we made earlier, is a constant that depends only on the numbers N_A, N_B, etc., and which we take as our fiducial energy; and (*b*) the sum of the translational kinetic energies of the molecules, which will thus be our total energy eigenvalue e of the wavefunction,

$$e = \frac{\hbar^2 \mathbf{k}_{A1}^2}{2M_A} + \cdots = \frac{(2\pi\hbar)^2}{2} \sum_{J = A, B, \ldots} \left\{\frac{1}{M_J} \sum_{i = 1, 2, \ldots} \left[\frac{n_{Jix}^2}{L_x^2} + \frac{n_{Jiy}^2}{L_y^2} + \frac{n_{Jiz}^2}{L_z^2}\right]\right\}. \tag{V.4}$$

We now seek the number $\Gamma(E_0, E)$ (see Section IV), which is the number of different eigenfunctions, Eq. (V.1), that have eigenvalues, Eq.

(V.4), which are less than E, the macroscopic total (internal) energy of the system. Actually, as we saw, almost all such functions will have eigenvalues that are very close to E.

We can think of an eigenfunction Eq. (V.1) as a point in a Cartesian space whose coordinates are the quantum numbers $n_{\mathrm{J}ix}$, $n_{\mathrm{J}iy}$, $n_{\mathrm{J}iz}$, and $m_{\mathrm{J}i}$; the space has dimensionality $4N$, where N, the total number of molecules, is equal to $N_{\mathrm{A}} + N_{\mathrm{B}} + \cdots$. The allowed eigenfunctions form a lattice in this space. Since each point can be said to occupy a cube of unit volume in this space, our task becomes one of finding the volume occupied by the allowed part of the lattice. In general this is a very difficult problem. The trouble is caused by the presence of "exceptional points" for which two or more of the indices i are equal; these are exactly the points at which the difference between fermion and boson particles show up. If, however, we ignore these exceptional points, in the hope that the crude estimate of Γ that we obtain will still give us a good value of S (cf. Section IV), we can easily derive the formula (see TN 401):

$$\Gamma \approx \frac{E^{3N/2} V^N \prod_{\mathrm{J}} M_{\mathrm{J}}^{3N_{\mathrm{J}}/2} \prod_{\mathrm{J}} D_{\mathrm{J}}^{N_{\mathrm{J}}}}{\hbar^{+3N} (2\pi)^{3N/2} (3N/2)! \prod_{\mathrm{J}} (N_{\mathrm{J}})!}. \tag{V.5}$$

We can expect this formula to be better the larger Γ is, since the "exceptional points" then become relatively fewer.

We now apply Stirling's formula $n! \approx n^n e^{-n} (2\pi n)^{1/2}$, take the logarithm, and neglect terms of order $k \ln N$ that are clearly not of macroscopic size. Under conditions when our approximate counting procedure is valid ("Maxwell–Boltzmann conditions"), we get the following formula for the entropy:

$$\begin{aligned} \frac{S}{k} = {} & \frac{3N}{2} \ln E + N \ln V - \frac{3N}{2} \ln N - \sum_{\mathrm{J}} N_{\mathrm{J}} \ln N_{\mathrm{J}} + \sum_{\mathrm{J}} N_{\mathrm{J}} \ln D_{\mathrm{J}} \\ & + \frac{3}{2} \sum_{\mathrm{J}} N_{\mathrm{J}} \ln M_{\mathrm{J}} + \frac{5N}{2} - 3N \ln \hbar - \frac{3N}{2} \ln 3\pi \end{aligned} \tag{V.6}$$

with

$$N = \sum_{\mathrm{J}} N_{\mathrm{J}}.$$

We find immediately that

$$\frac{1}{k} \frac{\partial S}{\partial E} = \frac{3N}{2E};$$

that is,

$$E = \tfrac{3}{2} k \cdot N \cdot T. \tag{V.7}$$

$$\frac{1}{k} \frac{\partial S}{\partial V} = \frac{N}{V};$$

that is,

$$pV = kNT = \tfrac{2}{3}E. \tag{V.8}$$

$$\frac{1}{k}\frac{\partial S}{\partial N_J} = \tfrac{3}{2}\ln E + \ln V - \tfrac{3}{2}\ln N - \ln N_J + \ln D_J + \tfrac{3}{2}\ln M_J$$
$$- 3\ln \hbar - \tfrac{3}{2}\ln 3\pi; \tag{V.9}$$

that is,

$$\mu_J = \frac{2E}{3N}\ln\left[\left(\frac{3\pi\hbar^2 \cdot N}{E \cdot M_J}\right)^{3/2} \cdot \frac{N_J}{VD_J}\right] = kT \ln c_J \frac{C_J}{(kT)^{3/2}}, \tag{V.10}$$

where C_J is the concentration N_J/V of substance J, and the constant c_J is

$$c_J = \frac{1}{D_J}\left(\frac{2\pi\hbar^2}{M_J}\right)^{3/2}. \tag{V.11}$$

From the average kinetic energy per molecule, $\varepsilon = E/N = \tfrac{3}{2}kT$, one can find a mean-square momentum per molecule $(2M_J\varepsilon)^{1/2}$ and its corresponding de Broglie wavelength $2\pi\hbar/(2M_J\varepsilon)^{1/2}$. The "thermal wavelength" λ_J for a molecule of type J is taken to be $(3/2\pi)^{1/2}$ times this quantity; that is

$$\lambda_J = \frac{\sqrt{2\pi} \cdot \hbar}{\sqrt{M_J \cdot kT}}. \tag{V.12}$$

The "thermal volume" of a molecule J is λ_J^3. One can express the chemical potential as follows:

$$\mu_J = k \cdot T \cdot \ln \frac{\lambda_J^3}{v_J D_J}, \tag{V.13}$$

where v_J is the volume V/N_J available per molecule J, ignoring the presence of molecules of other kinds.

If we multiply all the numbers E, V, N_J by the same factor t, the resulting entropy is also multiplied by t, as required for additivity (see Section III). From the additivity follows the thermodynamic identity, Eq. (III.5), which in our case yields a convenient expression for the entropy:

$$S = \sum_J N_J\left(\tfrac{5}{2}k - \frac{\mu_J}{T}\right). \tag{V.14}$$

According to formula (V.14) with (V.10), the entropy would be negative at sufficiently low temperatures, which is impossible. Therefore our formulas cannot be valid for low temperatures. In Section X, we derive our formulas as limiting approximations valid at "high" temperature, or, to be more precise, when $v_J \gg \lambda_J^3$.

VI. Measurement of Thermodynamic Quantities

In principle, the rest energy $E^r = m_0 c^2$ of a system can be determined by weighing; in practice, it is clear that the difference in rest mass between different states with the same particle numbers is too small to be determined by this method, and other methods must be found for measuring such energy differences.

We start by defining an energy unit as the difference in energy between two well-defined states of some system. Two energy units of this kind are commonly used in thermodynamics: (*1*) the joule, which is (apart from a very small relativistic correction) twice the difference between the total energy of a body weighing 1 kg that is traveling with a velocity of 1 meter/sec and the total energy of the same body at rest; (*2*) the (less accurately defined) calorie, which is the difference in energy between two particular states of 1 gm of water.

Now suppose that we have a large isolated system that contains the object system[1] and, for instance, a body weighing m kilograms. Suppose that initially the object system is in a state P_1 and the velocity of the body is 1 meter/sec. Now suppose a process occurs inside the isolated system, after which the object system is in a state P_2, the body is at rest but its state otherwise unchanged, and all other parts of the total system are in their initial states. It follows from the laws of additivity and conservation for the total energy that the energy difference $E(P_2) - E(P_1)$ for the object system is equal to $m/2$ joules. One can also use similar experiments where the body is replaced by other kinds of subsystems, provided that the energy difference between the initial and the final states of these subsystems are already known.

In principle, the difference in entropy between two states of a system could be determined in a similar way. We would then define the unit of entropy as the difference in entropy between two well-defined states of, say, 1 gm of some substance. Thereafter we might perform an experiment as follows. A certain isolated system contains initially the object system in state P_1, m grams of the reference substance in reference state 1, and some other subsystems. Suppose now that a *reversible* process occurs, after which the object subsystem is in state P_2, the reference substance in reference state 2, and the other subsystems have suffered only such changes that can lead to no change in entropy. (Such changes are, e.g., changes in the velocity of a body whose state remains otherwise unchanged, and changes in the strength of electrostatic and gravitational fields. It will in general be

---

[1] In this section, an *object system* means a subsystem on which a measurement is performed.

necessary to allow some such change to take place, since otherwise energy conservation would be violated.) It is then clear that we have $S(P_2) - S(P_1) = m$ entropy units.

In practice, it is usually not possible to effect a completely reversible transformation of this kind, or even reversible to a good enough approximation that the procedure will yield entropy values of acceptable accuracy (to try to achieve this ideal is a generalized problem of constructing an "ideal engine"). Therefore an indirect method based on the measurement of state derivatives is used instead. Suppose the two states P_1 and P_2 are (quasi)-equilibrium states located on some equilibrium surface. Let us join P_1 and P_2 by some curve C that lies in this surface. We can then find the entropy difference as a line integral:

$$S(P_2) - S(P_1) = \int_C \left[\frac{\partial S}{\partial E} dE + \frac{\partial S}{\partial V} dV + \cdots\right]. \tag{VI.1}$$

If we introduce some parameter u, $u_1 \le u \le u_2$, to label the points along the curve, we can rewrite the integral as

$$S(P_2) - S(P_1) = \int_{u_1}^{u_2} \left[\frac{1}{T(u)} \frac{dE}{du} + \frac{p(u)}{T(u)} \frac{dV}{du} + \cdots\right] du. \tag{VI.2}$$

The pressure in a system may be measured by means of an instrument known as a barometer (discussed in TN 401). Measurement of the thermodynamic absolute temperature T is somewhat more difficult. The most accurate instrument for this purpose is the gas thermometer; it contains a gas whose pressure is first determined, after which the temperature is calculated from Eq. (V.8) or whatever corresponding law is applicable for the gas used. The problem is that for no gas is the exact equation of state known except for photon gas, which is not very suitable for this kind of experiment, although "radiation thermometers," in which the intensity of the thermal radiation from an object is measured, are used at high temperatures. However, helium gas behaves very nearly as an ideal gas under a quite wide range of conditions, and the "practical temperature scale," which thus is not exactly identical to the thermodynamic temperature scale, is essentially based on the assumption that helium is an ideal gas. In practice, the gas thermometer is a very clumsy instrument, so various other instruments (some of which are well-known to everybody) are used instead, their scales being calibrated in such a way that the temperature of certain easily prepared states (melting ice at atmospheric pressure, etc.) agree with the gas-thermometer values.

VII. Equilibrium in Subsystems That Are in Contact with Reservoirs

If a system is not isolated, the question of which state of equilibrium it will evolve toward cannot in general be solved without taking its environment into account and treating both together as a larger system. In some very important cases, however, the properties of the environment enter the resulting calculation only through one or a few constant parameters. This happens when the environment is or can be regarded as a "reservoir." By a *reservoir* we mean a system that is in internal equilibrium and whose relevant state derivatives remain constant during all possible processes of interest.

As an example of this simplification, we consider an object system whose state is specified by the internal energy E_1 and a nonconserved quantity K_1 which may, for instance, tell how far a particular chemical reaction has proceeded (see Section VIII). The object subsystem is separated by a rigid, impenetrable, heat-conducting wall from a second system with internal energy E_2 and no other important parameters. Together these subsystems form an isolated system. Quantities E_1 and E_2 are not conserved, although $E = E_1 + E_2$ is.

The entropy of the total system is

$$S = S_1(E_1, K_1) + S_2(E - E_1). \tag{VII.1}$$

Quantities E_1 and K_1 will change until S becomes a maximum; at this maximum we have

$$\frac{\partial S}{\partial E_1} = \frac{1}{T_1} - \frac{1}{T_2} = 0; \qquad \frac{\partial S}{\partial K_1} = \frac{\partial S_1}{\partial K_1} = 0. \tag{VII.2}$$

Suppose now that S_2 is a linear function of E_2 for all values of $E_2 = E - E_1$ that are of interest in the problem. For instance, system 2 might consist of three phases of a pure substance in equilibrium (ice, water, and water vapor, for instance) in which case the entropy is a linear function of all the thermodynamic parameters as long as all three phases are actually present (see Section III). Alternatively, system 2 might simply be so large in relation to system 1 that it can absorb a "large" quantity of energy from system 1 without changing its temperature appreciably (its heat capacity is large). In practice, system 2 may be any medium whose temperature is held nearly constant by a thermostat or similar device. In all these cases, we refer to subsystem 2 as an energy reservoir (heat reservoir). For such a system we have (to sufficient accuracy)

$$S_2 = \frac{E_2}{T_2} + S_2^0, \tag{VII.3}$$

where T_2 is a constant and S_2^0 does not depend on E_2. We get

$$S = S_1(E_1, K_1) - \frac{E_1}{T_2} + \frac{E}{T_2} + S_2^0. \tag{VII.4}$$

We see that the last two terms in Eq. (VII.4) are constant during the approach to equilibrium, and the equilibrium condition of maximum S is equivalent to the condition that the quantity

$$S_1(E_1, K_1) - \frac{E_1}{T_2} \tag{VII.5}$$

shall be a maximum with respect to E_1 and K_1. Since T_2 is constant, we can replace this by the equivalent condition that

$$E_1 - T_2 S_1(E_1, K_1) \tag{VII.6}$$

be a minimum with respect to E_1 and K_1. The only property of system 2 entering these expressions is the constant T_2.

The differential equilibrium conditions are, of course, still of the same form, Eq. (VII.2):

$$\frac{1}{T_1} = \frac{1}{T_2}; \qquad \frac{\partial S_1}{\partial K_1} = 0, \tag{VII.7}$$

the special feature being that T_2 is a predetermined constant.

If the wall separating the object system and the reservoir conducts heat well and the process leading to change in K_1 is slow, one will find that E_1 adjusts rapidly until T_1 becomes equal to T_2, which will continue to be the case for the rest of the process, during which K_1 and E_1 change slowly (a slow heat flow will in general continue) until $\partial S_1/\partial K_1 = 0$ is also fulfilled. This slow part of the process can thus (because $T_1 = T_2$) be described as a minimization of the quantity (where, however, E_1 and K_1 are not to be varied independently),

$$E_1 - T_1 S_1(E_1, K_1). \tag{VII.8}$$

This is just the Helmholtz free energy of system 1 and does not contain anything explicitly referring to system 2 at all.

VIII. Chemical Equilibrium

We will now apply the methods of Sections I and II to the study of mixtures of substances that react chemically with each other. To be specific, we shall suppose that we are dealing with a mixture of four substances A, B, C, D, which can react according to the formula

$$a\mathrm{A} + b\mathrm{B} \rightleftharpoons c\mathrm{C} + d\mathrm{D} \tag{VIII.1}$$

where a, b, c, and d are some integers. We will suppose that no other reaction is of importance on the time scale we are considering, and to begin with we shall also suppose that the reaction is slow enough that one can measure the entropy of an arbitrary mixture containing N_A moles of substance A, N_B moles of B, etc. The other basic thermodynamic parameters are as usual the internal energy E and the volume V, so that we have an entropy function of the type

$$S = S(E, V, N_A, N_B, N_C, N_D). \tag{VIII.2}$$

The internal energy is measured relative to some fiducial state with the substances in pure form (see Section II) so that, according to Eq. (II.10), we have

$$E = E^r - e^r_{A0} N_A - e^r_{B0} N_B - e^r_{C0} N_C - e^r_{D0} N_D. \tag{VIII.3}$$

Here E^r is conserved for an isolated system, but E is not in general conserved during the reaction, nor are the individual quantities N_A, etc. In order to apply the formalism of Section II, we should find conserved linear combinations of our nonconserved quantities N_J. Such quantities are easily found. Consider a linear combination,

$$N_h = h_A N_A + \cdots + h_D N_D. \tag{VIII.4}$$

Suppose that a moles of A react with b moles of B to form c moles of C and d moles of D. After the reaction N_h has changed to $h_A(N_A - a) + \cdots + h_D(N_D + d)$ which is equal to the old N_h if and only if

$$ah_A + bh_B - ch_C - dh_D = 0 \tag{VIII.5}$$

which can be regarded as a vector orthogonality relation between a "reaction vector" $(a\ b\ -c\ -d)$ and the vector $(h_A\ h_B\ h_C\ h_D)$. We choose an arbitrary set of three, linearly independent vectors $(h^i_A\ h^i_B\ h^i_C\ h^i_D)$, $i = 1, 2, 3$, that are orthogonal to the reaction vector. The corresponding quantities

$$N^i_h = h^i_A N_A + h^i_B N_B + h^i_C N_C + h^i_D N_D \tag{VIII.6}$$

are conserved during the reaction.

We can now rewrite the entropy as a function

$$S = S(E^r, V, N^1_h, N^2_h, N^3_h, K), \tag{VIII.7}$$

where the "reaction variable" K changes during the reaction to attain a final equilibrium value K^*. We can use as K any linear combination of the N_J whose coefficient vector $(k_A\ k_B\ k_C\ k_D)$ is not orthogonal to the reaction vector. If the system is not isolated, E^r and V will also change in general, but in any case we have

$$\left(\frac{\partial S}{\partial K}\right)_{E^{\mathrm{r}}, V, N_h{}^1, N_h{}^2, N_h{}^3} = 0 \qquad \text{at equilibrium} \tag{VIII.8}$$

since the entropy of the environment is not a function of K (cf. also Section VII).

We will now convert the basic condition, Eq. (VIII.8) into other, more useful forms. By using the chain rule, we find (see TN 401) that Eq. (VIII.8) is equivalent to

$$a\mu_{\mathrm{A}}^{\mathrm{r}} + b\mu_{\mathrm{B}}^{\mathrm{r}} - c\mu_{\mathrm{C}}^{\mathrm{r}} - d\mu_{\mathrm{D}}^{\mathrm{r}} = 0. \tag{VIII.9}$$

Then by reformulating this in terms of ordinary chemical potentials, we get with Eq. (II.12):

$$a\mu_{\mathrm{A}} + b\mu_{\mathrm{B}} - c\mu_{\mathrm{C}} - d\mu_{\mathrm{D}} = -ae_{\mathrm{A}0}^{\mathrm{r}} - be_{\mathrm{B}0}^{\mathrm{r}} + ce_{\mathrm{C}0}^{\mathrm{r}} + de_{\mathrm{D}0}^{\mathrm{r}}. \tag{VIII.10}$$

The quantity on the right-hand side of Eq. (VIII.10) is easily seen to be the energy $\Delta e^{\mathrm{fiducial}}$ absorbed upon conversion of a moles of substance A plus b moles of B into c moles of C plus d moles of D, all substances being in their *fiducial* states.

One can obtain another, more familiar form of the equilibrium condition by choosing a certain reference state of chemical potential for each substance. This reference state need not have anything to do with the fiducial state used in defining the internal energy. We define $\mu_{\mathrm{A}}^{\mathrm{ref}}$ as the chemical potential of substance A in its reference state, etc.; $\mu_{\mathrm{A}}^{\mathrm{r,\,ref}}$ is the "absolute chemical potential" $\mu_{\mathrm{A}}^{\mathrm{ref}} + e_{\mathrm{A}0}^{\mathrm{r}}$ of substance A in its reference state; see Eq. (II.12). Since $\mu_{\mathrm{A}} - \mu_{\mathrm{A}}^{\mathrm{ref}} = \mu_{\mathrm{A}}^{\mathrm{r}} - \mu_{\mathrm{A}}^{\mathrm{r,\,ref}}$, etc., we get

$$a(\mu_{\mathrm{A}} - \mu_{\mathrm{A}}^{\mathrm{ref}}) + \cdots - d(\mu_{\mathrm{D}} - \mu_{\mathrm{D}}^{\mathrm{ref}}) = a(\mu_{\mathrm{A}}^{\mathrm{r}} - \mu_{\mathrm{A}}^{\mathrm{r,\,ref}}) + \cdots - d(\mu_{\mathrm{D}}^{\mathrm{r}} - \mu_{\mathrm{D}}^{\mathrm{r,\,ref}}). \tag{VIII.11}$$

With Eq. (VIII.9), we get

$$a(\mu_{\mathrm{A}} - \mu_{\mathrm{A}}^{\mathrm{ref}}) + \cdots - d(\mu_{\mathrm{D}} - \mu_{\mathrm{D}}^{\mathrm{ref}}) = -a\mu_{\mathrm{A}}^{\mathrm{r,\,ref}} \cdots + d\mu_{\mathrm{D}}^{\mathrm{r,\,ref}}. \tag{VIII.12}$$

If the reference states are chosen as states of the pure substances, the thermodynamic identity, Eq. (III.5) applied to 1 mole of pure substance J in its reference state yields

$$\mu_{\mathrm{J}}^{\mathrm{r,\,ref}} = g_{\mathrm{J}}^{\mathrm{r,\,ref}} = e_{\mathrm{J}}^{\mathrm{r,\,ref}} + p_{\mathrm{J}}^{\mathrm{ref}}v_{\mathrm{J}}^{\mathrm{ref}} - T_{\mathrm{J}}^{\mathrm{ref}}s_{\mathrm{J}}^{\mathrm{ref}}, \tag{VIII.13}$$

where we have used small letters g_{J}, e_{J}, v_{J}, and s_{J} to denote the Gibbs free energy, etc., of 1 mole of substance J.

We can then rewrite Eq. (VIII.12) as

$$a(\mu_{\mathrm{A}} - \mu_{\mathrm{A}}^{\mathrm{ref}}) + \cdots - d(\mu_{\mathrm{D}} - \mu_{\mathrm{D}}^{\mathrm{ref}}) = \Delta g^{\mathrm{ref}}, \tag{VIII.14}$$

where we should note that the appearance of the Gibbs free energy has nothing directly to do with whether the reaction takes place at constant temperature and pressure or under other conditions (cf. Section VII).

Often the reference states are chosen to have the same temperature as the equilibrium state (especially when this temperature is fixed, e.g., because the system is in contact with a heat reservoir). It is then customary to define the "chemical activity" α_J of substance J by the equation

$$\alpha_J = \exp \frac{\mu_J - \mu_J^{\text{ref}}}{RT}. \tag{VIII.15}$$

So at equilibrium, we have

$$\frac{\alpha_A^a \alpha_B^b}{\alpha_C^c \alpha_D^d} = \exp \frac{\Delta g^{\text{ref}}}{RT}. \tag{VIII.16}$$

If our system happens to be a dilute gas to which the Maxwell–Boltzmann approximation is applicable, we get from Eq. (V.10) or the more general equation (X.30)

$$\alpha_J = \frac{C_J}{C_J^{\text{ref}}}, \tag{VIII.17}$$

for any state with the same temperature as the reference state; here C_J is the concentration of substance J. By inserting Eq. (VIII.17) into Eq. (VIII.16), we get the ordinary "law of chemical equilibrium" that can also be derived from suitable assumptions about the rates of reactions on the molecular level.

Up to now we have been regarding the entropy as a function, Eq. (VIII.2), of the "momentary" numbers N_J. This means that the chemical potentials μ_J have been defined in the following way. We add a small amount ΔN_A of substance A, say, to the system in question and let it mix into the system, but do not allow a reaction to occur. We measure the entropy increase ΔS and apply the equation (valid to first order)

$$\Delta S \approx -\frac{\mu_A}{T}\Delta N_A + \frac{1}{T}\Delta E + \frac{p}{T}\Delta V. \tag{VIII.18}$$

In practice, this scheme may be impossible to carry out, e.g., if the reaction is too swift (see also the following). However, we can then usually still find the chemical potentials in a state of chemical *equilibrium* (although not in other states) by using a slightly different scheme. By starting from the equilibrium state at hand, we add a small amount ΔN_A of substance A, and mix it into the system. Then we isolate the system and let the reaction proceed until a new state of equilibrium is reached. The entropy increase

ΔS^* relative to the initial equilibrium state is larger than ΔS. According to the theorem we proved at the beginning of Section II, however, the difference $\Delta S^* - \Delta S$ is of second order in the quantities ΔN_A, etc., so that Eq. (VIII.18) is still valid to first order if we substitute ΔS^* instead of ΔS:

$$\Delta S^* \approx -\frac{\mu_A}{T}\Delta N_A + \frac{1}{T}\Delta E + \frac{p}{T}\Delta V. \qquad \text{(VIII.19)}$$

This equation is then used to define our μ_A.

This definition is of particular interest when the equilibrium concentration of one or more of the reactants is extremely small (students of chemistry may remember the solution of HgS in water that supposedly contains about one ion per bathtub). In such cases the definition of μ_A (we suppose that A is the component with the small equilibrium concentration) by means of Eq. (VIII.18) does not work, because we would have to take $|\Delta N_A| \ll N_A$ to make the higher order corrections negligible. If we use Eq. (VIII.19) instead, we can use a macroscopic ΔN_A. This is shown in TN 401 for the case of a mixture of ideal gases under Maxwell–Boltzmann conditions.

IX. The Canonical Ensemble Formalism in Statistical Mechanics

We indicated in Section IV that the choice of weights for the microstates in an ensemble is to a large extent arbitrary, since the ensemble is dominated by a group of microstates that are in practice almost indistinguishable from one another (and which correspond to the macrostate of largest entropy compatible with the given restrictions on the thermodynamics parameters). One can, therefore, choose weights in other ways than the microcanonical one of taking the weights to be equal for "allowed" microstates and zero for other microstates. Hence one can set up other kinds of ensembles that can normally also be used to represent a single macrostate but which are easier to handle mathematically than the microcanonical ensembles.

It will be assumed throughout the remainder of this treatise that Boltzmann's equation (IV.4) is universally valid.

We consider a system whose basic thermodynamic parameters are $B_1, B_2, \ldots, B_m$; we assume that the corresponding operators commute and thus have a set of simultaneous eigenfunctions $\{\psi_i\}$ [see Eq. (IV.5)]. We subdivide the set of parameters into two groups: $B_1, B_2, \ldots, B_l$ and $B_{l+1}, B_{l+2}, \ldots, B_m$. The quantities in the second group are to be treated in the "microcanonical manner," i.e., if their macroscopic values are $B_{l+1}^0, \ldots, B_m^0$, we surround these values with small intervals $(B_{l+1}^1; B_{l+1}^2)$, etc., and declare that all those eigenfunctions whose eigenvalues $b_{(l+1)i}, \ldots, b_{mi}$ do not all lie within the corresponding intervals are to be assigned zero weight in the ensemble. The eigenstates that do fulfill these restrictions are all assigned positive weights that depend smoothly on the eigenvalues $b_{1i}, \ldots, b_{li}$ of the first group of variables according to a formula of the type

$$w_i = \frac{1}{P} e^{-f(b_{1i}, b_{2i}, \ldots, b_{li})/k}, \tag{IX.1}$$

where k is Boltzmann's constant and f is a smooth function that has the dimension of entropy and which approaches plus infinity in every direction in which the domain of possible values of its arguments extends toward infinity. [The last requirement must be satisfied if constant P, as defined in the next equation (IX.2), is to exist.]

In practice, f will usually be chosen as a linear function $c_1 \cdot b_{1i} + \cdots + c_l \cdot b_{li}$, in which case we speak about a canonical- or Gibbs-type ensemble. We will then refer to the first group of parameters as the "canonical group," and to the second as the "microcanonical group."

Constant P is a normalization constant that is chosen such that the sum of the normalized weights is unity:

$$P = \sum_i \exp[-f(b_{1i}, \ldots, b_{li})/k]. \tag{IX.2}$$

Constant P is called the partition function of the ensemble; in the canonical case, it is a function of variables $c_1, c_2, \ldots, c_l$ and $B_{l+1}^1, \ldots, B_m^2$. Its name is a bit unfortunate insofar as it may be confused with the "distribution function," which is the function in Eq. (IX.1).

The statistical operator of the ensemble is

$$\rho = \sum_i w_i |\psi_i\rangle\langle\psi_i| = \frac{1}{P} \exp\left[\frac{-f(B_1^{\mathrm{op}}, \ldots, B_l^{\mathrm{op}})}{k}\right] O_{B_{l+1}}^{(B_{l+1}^1;\, B_{l+1}^2)}, \ldots, O_{B_m}^{(B_m^1;\, B_m^2)}, \tag{IX.3}$$

cf. Eq. (IV.6).

The expectation value $\overline{\overline{A}}$ of an operator A with respect to the ensemble is

$$\overline{\overline{A}} = \mathrm{Tr}(A\rho) = \sum_i w_i \langle\psi_i| A |\psi_i\rangle. \tag{IX.4}$$

Our next task is to try to show that for "decent" operators this value is almost equal to the expectation value with respect to a certain microcanonical ensemble, provided that the function $f(B_1, \ldots, B_l)$ fulfills a certain condition. This condition is that the function

$$g(B_1, \ldots, B_l) = S(B_1, \ldots, B_l, B_{l+1}^0, \ldots, B_m^0) - f(B_1, \ldots, B_l) \tag{IX.5}$$

which we regard as a function of $B_1 \cdots B_l$ only, should have a unique absolute maximum that is not too flat, and that g should approach minus infinity with sufficient speed in any direction in which its domain extends to infinity (cf. the foregoing).

We will look a little closer at the maximum condition. We suppose for simplicity that the first group of parameters contains just one member that is the internal energy E of the system, and that function f is a linear function cE, where c is a positive number. The ensemble is then a canonical ensemble in the restricted sense.

The entropy function is convex but may have a flat part, as indicated in Fig. 5, for instance when the equilibrium surface has a three-phase equilibrium part (see Section III). Normally, function $g = S - f$ will clearly have a unique maximum with respect to E. This maximum occurs at a value E^* such that

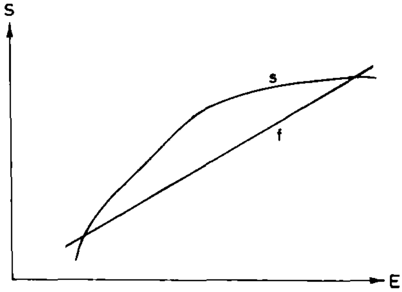

Fig. 5. Relation of S and f for a canonical ensemble (cf. Fig. 3).

$$\left(\frac{\partial S}{\partial E}\right)_{E=E^*} = \frac{1}{T(E^*)} = c. \tag{IX.6}$$

If, however, c happens to be equal to the slope $\partial S/\partial E$ in the "flat" part, the maximum is not unique and E^* is not well defined. In this exceptional case the canonical ensemble cannot be used to describe a single macrostate (at least not directly).

The function

$$I(B_1, \ldots, B_l) = e^{g/k}\frac{1}{P} = e^{(S-f)/k}\cdot\frac{1}{P} \tag{IX.7}$$

might be called the "importance function"; it is the product of the weight function (distribution function) $e^{-f/k}/P$ and the function $\Gamma = e^{S/k}$, which is essentially the "density of microstates" at the point $(B_1, \ldots, B_l, B^0_{l+1}, \ldots, B^0_m)$ (see Section IV).

Our maximum condition on g implies that function I has a very sharp peak at point $(B_1^*, \ldots, B_l^*)$, where g has its maximum. It is this sharpness that makes our ensemble physically (although not mathematically) almost indistinguishable from a microcanonical ensemble constructed by letting the weights be nonzero (and equal) only for eigenstates whose eigenvalues $b_{1i}, \ldots, b_{li}$ are nearly equal to $B_1^*, \ldots, B_l^*$ (see the following). Close to the maximum, we can approximate g by its second-order part,

$$g(B_1, \ldots, B_l) \approx \tfrac{1}{2} \sum_{j=1}^{l} \sum_{k=1}^{l} h_{jk}(B_j - B_j^*)(B_k - B_k^*), \tag{IX.8}$$

where

$$h_{jk} = \left[\frac{\partial^2 g}{\partial B_j\, \partial B_k}\right]_{B_1 = B_1^*,\, B_2 = B_2^*,\, \ldots,\, B_l = B_l^*}. \tag{IX.9}$$

Therefore the importance function $e^{g/k}/P$ behaves essentially like a multidimensional Gaussian function whose width in the "broadest direction" is of the order $(k/|h|)^{1/2}$, where h is the numerically smallest eigenvalue of the matrix h_{jk}. Since k is very small the distribution is (macroscopically speaking) very sharp unless h is also very small.

If f is a linear function, we will have

$$h_{jk} = \left[\frac{\partial^2 S}{\partial B_j\, \partial B_k}\right]_{B_1 = B_1^*, \ldots}. \tag{IX.10}$$

These derivatives are inversely proportional to the "amount parameter" t (see Section III); as a consequence the absolute widths of type $\Delta B = [\overline{\overline{B^2}} - (\overline{\overline{B}})^2]^{1/2}$ are proportional to $t^{1/2}$ and the relative widths of type $\Delta B/\overline{\overline{B}}$ to $1/t^{1/2}$ (see later).

At the maximum point $(B_1^*, \ldots, B_l^*)$, we have, of course,

$$\frac{\partial g}{\partial B_j} = \frac{\partial S}{\partial B_j} - \frac{\partial f}{\partial B_j} = 0, \qquad j = 1, \ldots, l \tag{IX.11}$$

unless the maximum should happen to occur at a boundary of the domain of definition. For a canonical-type ensemble, we have

$$f = \sum_{j}^{l} c_j B_j \tag{IX.12}$$

so that the maximum condition becomes

$$\frac{\partial S}{\partial B_j} = c_j, \qquad j = 1, \ldots, l \tag{IX.13}$$

of which Eq. (IX.6) is a special case. Note, however, that it is advisable to avoid constructing a canonical-type ensemble for which the canonical group includes the whole set of basic thermodynamic parameters so that $l = m$ (at least if they are all additive). If we try to do that, then the following occurs. There exists a functional relation

$$F\left(\frac{\partial S}{\partial B_1}, \frac{\partial S}{\partial B_2}, \ldots, \frac{\partial S}{\partial B_m}\right) = 0 \tag{IX.14}$$

between the state derivatives (see Section III). If we choose the coefficients c_j in such a way that they do not fulfill the relation $F(c_1, \ldots, c_m) = 0$, then the maximum of g either does not exist at all or occurs for the physically meaningless values $B_1 = \cdots = B_m = 0$ (no system at all). If the c_j do fulfill this relation, the maximum occurs along a whole "ray" in state space, Eq. (III.2). This means that function g does not go to minus infinity when t goes to infinity and, therefore, the partition function P is infinite (see in the following). Constructing a canonical-type ensemble is therefore in general meaningful only if $l < m$.

We will now find a formula for the logarithm of the partition function P [in a way, a generalization of formula (IV.4) for the logarithm of the "microcanonical partition function" Γ]. Let us subdivide the "allowed part" of the hyperplane $(B_1, \ldots, B_l)$ (i.e., the domain of definition for these variables) into many small "hyper-rectangles" R_p (cf. Fig. 4, Section IV). The sum in Eq. (IX.2) is thus subdivided into partial sums

$$P_p = \sum_i{}' e^{-f(b_{1i}, \ldots, b_{li})/k}, \tag{IX.15}$$

where the prime indicates summation over those eigenstates that lie within the rectangle R_p. The number Γ_p of such eigenstates satisfies a Boltzmann equation,

$$k \ln \Gamma_p = S(B_1^p, B_2^p, \ldots, B_l^p, B_{l+1}^0, \ldots, B_m^0), \tag{IX.16}$$

where $(B_1^p \cdots B_l^p)$ is some point in the rectangle R_p. Because functions S and f are macroscopically smooth, we can also write

$$P_p = \Gamma_p \cdot e^{-f(B_1^p, \ldots, B_l^p)/k} \tag{IX.17}$$

if the rectangles are chosen small enough. Taking the logarithm, we get

$$k \ln P_p = S(B_1^p, B_2^p, \ldots, B_l^p, B_{l+1}^0, \ldots, B_m^0) - f(B_1^p, \ldots, B_l^p). \tag{IX.18}$$

Since $P = P_1 + P_2 + \cdots$, we can apply Eq. (IV.7) and conclude that

$$k \ln P = \max_p g(B_1^p, \ldots, B_l^p) = g(B_1^*, \ldots, B_l^*) \tag{IX.19}$$

provided that only a reasonable number of rectangles contribute appreciably to the (in principle infinite) sum over P_p. This will be the case if g decreases sufficiently rapidly (e.g., linearly) when the arguments approach infinity (we will not bother with giving a formal proof). Equation (IX.19) will then be valid whether the maximum of g is unique or not (within a macroscopically negligible error, of course).

If our ensemble is of canonical type, we get an alternative expression for $k \ln P$ with the aid of Eqs. (IX.12), (IX.13), and the formula corresponding to Eq. (III.4) (we suppose here that all the B are additive):

$$k \ln P = S(B_1^*, \ldots, B_m^0) - \sum_{j=1}^{l} \frac{\partial S}{\partial B_j} \cdot B_j^* = \sum_{j=l+1}^{m} \frac{\partial S}{\partial B_j} \cdot B_j^0, \qquad \text{(IX.20)}$$

where the derivatives are to be taken at the point $(B_1^*, \ldots, B_m^0)$.

We will now estimate expectation values of the type, Eq. (IX.4). Once more, we decompose the sum into partial sums over small rectangles:

$$\bar{\bar{A}} = \sum_p \frac{P_p}{P} \bar{\bar{A}}_p \qquad \text{(IX.21)}$$

with

$$\bar{\bar{A}}_p = \frac{\sum_i' e^{-f(b_{1i}, \ldots, b_{li})/k} \langle \psi_i | A | \psi_i \rangle}{P_p}. \qquad \text{(IX.22)}$$

Now, if the rectangles are small enough, we will have

$$\frac{P_p}{P} = I(B_1^p, \ldots, B_l^p) \qquad \text{(IX.23)}$$

because of Eqs. (IX.18) and (IX.7). We also get

$$\bar{\bar{A}}_p = \bar{\bar{A}}_{\text{microcan}}(B_1^p, \ldots, B_l^p) \qquad \text{(IX.24)}$$

because function $e^{-f/k}$ varies little relative to itself over a sufficiently small rectangle, and also because nearly all the pure-state expectation values $\langle \psi_i | A | \psi_i \rangle$ are normally almost equal to one another. If I is a very sharply peaked function and $\bar{\bar{A}}_{\text{microcan}}$ is a smooth function of the B_j, then all the $\bar{\bar{A}}_p$ that contribute appreciably in the sum Eq. (IX.21) will be almost equal, and we get

$$\bar{\bar{A}} = \bar{\bar{A}}_{\text{microcan}}(B_1^*, \ldots, B_l^*) \qquad \text{(IX.25)}$$

with macroscopically negligible error.

We will briefly study the ensemble width ΔA of the quantity A. We can show (cf. Section XI) that

$$(\Delta A)^2 = \sum_p \frac{P_p}{P} (\Delta A_p)^2 + \sum_p \frac{P_p}{P} (\bar{\bar{A}}_p - \bar{\bar{A}})^2, \qquad \text{(IX.26)}$$

where the first term can be regarded as a weighted average over squared "microcanonical widths" (i.e., widths calculated from a microcanonical ensemble) and the second term is an extra squared width that we will interpret in Section XI as possibly being due to fluctuations in A that occur because our system is not isolated but is in contact with some other system (a "reservoir" if the ensemble is of canonical type). The microcanonical width should then be due to fluctuations that would occur even for an isolated system.

The second term in Eq. (IX.26) can be expressed as an integral quotient:

$$\frac{\int I(B_1,\ldots,B_l)[\overline{\overline{A}}_{\text{microcan}}(B_1,\ldots,B_l)-\overline{\overline{A}}_{\text{microcan}}(B_1^*\cdots B_l^*)]^2\,dB_1\cdots dB_l}{\int I(B_1,\ldots,B_l)\,dB_1\cdots dB_l}. \tag{IX.27}$$

This can sometimes be estimated using expression (IX.8) for g and the first-order terms in the Taylor expansion of $\overline{\overline{A}}_{\text{microcan}}$ about the point $(B_1^*,\ldots,B_l^*)$. The result is

$$k\sum_j^l\sum_k^l a_j(\mathbf{h}^{-1})_{jk}a_k, \tag{IX.28}$$

where

$$a_j=\left[\frac{\partial\overline{\overline{A}}_{\text{microcan}}}{\partial B_j}\right]_{B_1=B_1^*,\ldots} \tag{IX.29}$$

and $\mathbf{h}^{-1}$ is the inverse matrix to matrix $\mathbf{h}$ given by Eq. (IX.9).

We will finally evaluate the quantity $-k\operatorname{Tr}(\rho\ln\rho)$ [cf. Eq. (IV.4a)]. From Eq. (IX.3) we find

$$-\ln\rho=\ln P+\frac{1}{k}f(B_1^{\text{op}},\ldots,B_l^{\text{op}})-\ln O_{B_{l+1}}-\ln O_{B_{l+2}}-\cdots, \tag{IX.30}$$

and, since $O\ln O=0$ for a projection operator O, we get

$$-\rho\ln\rho=\frac{1}{P}\left[\ln P+\frac{1}{k}f(B_1^{\text{op}},\ldots,B_l^{\text{op}})\right]\exp\left[-\frac{1}{k}f(\cdots)\right]O_{B_{l+1}}\cdots, \tag{IX.31}$$

and, with the aid of Eqs. (IX.3), (IX.4), and (IX.19)

$$-k\operatorname{Tr}(\rho\ln\rho)=g(B_1^*,\ldots,B_l^*)+\overline{\overline{f(B_1^{\text{op}},\ldots,B_l^{\text{op}})}}. \tag{IX.32}$$

In the normal case when g has a unique maximum the ensemble average $\overline{\overline{f(B_1,\ldots,B_l)}}$ is equal to $f(B_1^*,\ldots,B_l^*)$, so that

$$-k\operatorname{Tr}(\rho\ln\rho)=S(B_1^*,\ldots,B_l^*,B_{l+1}^0,\ldots,B_m^0), \tag{IX.33}$$

which shows that Eq. (IV.4a) is valid for more general ensembles than microcanonical ones.

When one uses the canonical ensemble formalism to compute equilibrium properties of a system, the independent variables that specify the state of the system are, in the first instance, the numbers $c_1, \ldots, c_l$ and $B_{l+1}^0, \ldots, B_m^0$. From these we are to calculate the values of $B_1^*, \ldots, B_l^*$ and of the equilibrium entropy $S(B_1^*, \ldots, B_m^0)$, as well as other physical quantities (state derivatives, expectation values). We note first that the values of the first group of state derivatives are given immediately by the c_j according to Eq. (IX.13) if these variables are given physically meaningful values.

The hard part of the computation is to find the logarithm of the partition function P. When we have found $\bar{g} = k \ln P$ as a function of our independent variables, the second group of state derivatives and the B_j^* of the first group can be found immediately by differentiation. We have by definition

$$\bar{g}(c_1, \ldots, c_l, B_{l+1}^0, \ldots, B_m^0) = S(B_1^*, \ldots, B_l^*, B_{l+1}^0, \ldots, B_m^0) - \sum_{j=1}^{l} c_j B_j^*, \tag{IX.34}$$

where the B_j^* are, in their turn, functions of our independent variables. We can prove (see TN 401) that

$$\left(\frac{\partial \bar{g}}{\partial B_k^0}\right)_{c_p,\, \not{B}_q^0} = \left(\frac{\partial S}{\partial B_k^0}\right)_{B_p^*,\, \not{B}_q}, \tag{IX.35}$$

which gives us the values of those state derivatives which are not given by Eq. (IX.13).

The B_j^*, if they are unique, can be found as ensemble expectation values or as partial derivatives of $\bar{g}$:

$$B_j^* = \bar{\bar{B}}_j = \frac{1}{P}\,\mathrm{Tr}(B_j^{\mathrm{op}} C^{\mathrm{op}}) = -\frac{k}{P}\frac{\partial\, \mathrm{Tr}\, C^{\mathrm{op}}}{\partial c_j} = -\frac{k}{P}\frac{\partial P}{\partial c_j} = -\left(\frac{\partial \bar{g}}{\partial c_j}\right)_{\not{c}_p,\, B_q^0}. \tag{IX.36}$$

The entropy itself can be found from Eq. (IX.34).

In the standard case the basic thermodynamic parameters are E, V, N_A, N_B, ... The most commonly used canonical-type ensembles are then as follows.

a. The "canonical group" of variables includes only the energy E. The ensemble operator is of the form

$$\rho_{\mathrm{can}} = \frac{1}{P_{\mathrm{can}}} \exp\left(-\frac{c_E}{k} E^{\mathrm{op}}\right), \tag{IX.37}$$

which is a "canonical ensemble" in the restricted sense. The Hamiltonian operator already contains implicitly the "built-in" values of the parameters: V^0, N_A^0, etc. (see Section IV).

Our formulas yield in this case:

$$\frac{\partial S}{\partial E^*} = \frac{1}{T^*} = c_E, \tag{IX.38}$$

$$-E^* = \frac{\partial(k \ln P_{\text{can}})}{\partial c_E}, \tag{IX.39}$$

$$S - \frac{E^*}{T^*} = -\frac{F^*}{T^*} = k \ln P_{\text{can}} = \frac{p^*}{T^*} V^0 - \sum_{\mathrm{J}} \frac{\mu_{\mathrm{J}}^*}{T^*} N_{\mathrm{J}}^0, \tag{IX.40}$$

$$\frac{\partial S}{\partial V^0} = \frac{p^*}{T^*} = \frac{\partial(k \ln P_{\text{can}})}{\partial V^0}, \tag{IX.41}$$

$$\frac{\partial S}{\partial N_{\mathrm{J}}^0} = -\frac{\mu_{\mathrm{J}}^*}{T^*} = \frac{\partial(k \ln P_{\text{can}})}{\partial N_{\mathrm{J}}^0}. \tag{IX.42}$$

b. The canonical group of parameters includes E and all the N_{J}. The ensemble

$$\rho_{g\text{can}} = \frac{1}{P_{g\text{can}}} \exp\left(-\frac{c_E}{k} \tilde{E}^{\text{op}} - \sum_{\mathrm{J}} \frac{c_{\mathrm{J}}}{k} N_{\mathrm{J}}^{\text{op}} \right) \tag{IX.43}$$

is called a grand-canonical ensemble. Here $\tilde{E}^{\text{op}}$ implicitly contains V^0, but the N_{J} can be arbitrary (a "second-quantization type" of Hamiltonian operator). We get in this case

$$\frac{\partial S}{\partial E^*} = \frac{1}{T^*} = c_E, \tag{IX.44}$$

$$\frac{\partial S}{\partial N_{\mathrm{J}}^*} = -\frac{\mu_{\mathrm{J}}^*}{T^*} = c_{\mathrm{J}}, \tag{IX.45}$$

$$-E^* = \frac{\partial(k \ln P_{g\text{can}})}{\partial c_E}, \tag{IX.46}$$

$$-N_{\mathrm{J}}^* = \frac{\partial(k \ln P_{g\text{can}})}{\partial c_{\mathrm{J}}}, \tag{IX.47}$$

$$S - \frac{E^*}{T^*} + \sum_{\mathrm{J}} \frac{\mu_{\mathrm{J}}^*}{T^*} N_{\mathrm{J}}^* = k \ln P_{g\text{can}} = \frac{p^*}{T^*} V^0, \tag{IX.48}$$

where in fact p^* does not depend on parameter V^0 but only on c_E and the c_{J} (T^* and the μ_{J}^*).

The following notations will be used in Section X:

$$\beta = \frac{c_E}{k} = \frac{1}{kT^*},$$

$$\gamma_J = \frac{c_J}{k} = -\frac{\mu_J^*}{kT^*}, \qquad \text{(IX.49)}$$

$$z_J = e^{-\gamma_J} = e^{\mu_J^*/kT^*}$$

(the so-called fugacity of substance J).

When we consider the practical side of such computations, we must realize that sums of the type Eqs. (IX.2) or (IX.4) are completely useless as they stand, because the number of states that contribute significantly to such sums is enormously large (namely of the order of $e^{S/k}$). Therefore the partition function cannot be computed by simple summation over microstates, but the sum must be rearranged. Fortunately, one does not need P itself but only its logarithm. Thus an attractive possibility is to try to rearrange the sum into an infinite product, so that its logarithm will have the form of an infinite sum that (hopefully) can be computed. We shall see in the next section that in the case of a mixture of ideal gases, the grand-canonical partition function is very easily rearranged into a convergent infinite product.

The so-called cluster expansion of the grand-canonical partition function for gases is a quite different type of infinite product than the one we use in Section X. The cluster expansion is such that ln P takes the form of a power series in the variables z_J defined by Eq. (IX.49). It can be formally derived from the following power series for $P_{g\text{can}}$ (we assume that we are dealing with a pure substance):

$$P_{g\text{can}} = \operatorname{Tr} e^{-\beta E^{\text{op}} - \gamma N^{\text{op}}} = 1 + \sum_{N=1}^{\infty} z^N P_{\text{can}}(N). \qquad \text{(IX.50)}$$

In principle, this series is convergent for all physically admissible values of z. However, it is dominated by terms for which N is of the order of N^* and is, therefore, of no use as it stands. We can now find the corresponding power series for the logarithm:

$$\ln P_{g\text{can}} = zP_{\text{can}}(1) + z^2[P_{\text{can}}(2) - \tfrac{1}{2}(P_{\text{can}}(1))^2] + \cdots. \qquad \text{(IX.51)}$$

One might perhaps be inclined to assume that this series would also be useless. However, it usually has good convergence properties when T and μ are well away from the region where the gas condenses into a liquid. Moreover, the low-order terms involve only few-particle canonical partition functions, which one may hope to be able to compute.

In Section X, we derive the cluster expansion for ideal gases in a different way; it turns out to be convergent whenever $\mu < 0$ (where the fiducial energy has been taken as the sum of the molecular ground-state energies).

Cluster expansions of grand-canonical expectation values of the form

$$\overline{\overline{A}} = \frac{\mathrm{Tr}(Ae^{-\beta E^{\mathrm{op}} - \gamma N^{\mathrm{op}}})}{P_{g\mathrm{can}}} = \frac{a_0 + za_1 + z^2a_2 + \cdots}{1 + zP_{\mathrm{can}}(1) + z^2P_{\mathrm{can}}(2) + \cdots} \tag{IX.52}$$

can be found by expanding the quotient of two power series as a new power series in z. The cluster expansions for $\overline{\overline{E}}$ and $\overline{\overline{N}}$ can of course also be found by differentiation of Eq. (IX.51) with respect to β and γ.

X. Treatment of Ideal Gases by Means of the Grand-Canonical Ensemble Method. Remarks on the Statistical Mechanics of Assemblies of Interacting Particles

We consider a system consisting of initially indeterminate numbers of "particles" of types A, B, etc., enclosed in a rectangular box (infinitely high potential wall) of dimensions L_x, L_y, L_z. The particles may actually be atoms, molecules, etc., whose interaction we neglect (see Section V). In general, every particle of kind J has a whole sequence (sometimes infinite) of possible "internal eigenstates" (including rotational states) whose corresponding "internal wavefunctions" χ_{m_J} depend only on the internal coordinates of the "particles." We number these states in order of ascending energy $\varepsilon_{m_\mathrm{J}}^{\mathrm{intl}}$ with $m_\mathrm{J} = 0$ denoting the internal state of lowest energy. (The question of what to do with "internal continuum states" of the "particles" is briefly discussed in TN 401.)

The "total one-particle state" of a particle of kind J is given by a combination index $i\mathrm{J}$ that stands for a set of four quantum numbers $n_{\mathrm{J}x}$, $n_{\mathrm{J}y}$, $n_{\mathrm{J}z}$, m_J [see Eq. (V.3)], where the first three are the translational quantum numbers; these can take any integer values (positive or negative). The one-particle energy of such a state is

$$\varepsilon_{i\mathrm{J}} = \frac{(2\pi\hbar)^2}{2M_\mathrm{J}} \left[\frac{n_{\mathrm{J}x}^2}{L_x^2} + \frac{n_{\mathrm{J}y}^2}{L_y^2} + \frac{n_{\mathrm{J}z}^2}{L_z^2}\right] + \varepsilon_{m_\mathrm{J}}^{\mathrm{intl}} = \varepsilon_{i\mathrm{J}}^{\mathrm{kin}} + \varepsilon_{m_\mathrm{J}}^{\mathrm{intl}}. \tag{X.1}$$

Usually, the energy scale is chosen such that the ground-state energy of a particle is zero:

$$\varepsilon_{0_\mathrm{J}}^{\mathrm{intl}} = 0. \tag{X.2}$$

We must now enumerate the possible stationary states of the total system of noninteracting particles. In Section V we did this by specification of the quantum numbers for each particle; we then had to exclude forbidden and superfluous states. Here we will use the "Fock way" instead: for each one-particle state we specify the *number of particles* that are in that state. Thus a quantum state (microstate) of the system is given by an infinite row of integers $\{n_{iJ}\}$ (occupation numbers) that must not be confused with the translational quantum numbers n_{Jx}, etc. The possible values of the n_{iJ} are

0 and 1	if J stands for a fermion particle (one that contains an odd number of elementary fermions);
0, 1, 2, 3, 4, ...	if J stands for a boson particle.

There are no other restrictions on the occupation numbers, since the total particle numbers N_J are arbitrary in the grand-canonical ensemble. Each microstate $\psi_{\{n_{iJ}\}}$ has its own set of total particle numbers (eigenvalues of the number operators); these are obviously sums of the n_{iJ}:

$$N_K^{\mathrm{op}}\psi_{\{n_{iJ}\}} = \left(\sum_i n_{iK}\right)\psi_{\{n_{iJ}\}}. \tag{X.3}$$

We choose our fiducial energy so that we have

$$\tilde{E}^{\mathrm{op}}\psi_{\{n_{iJ}\}} = \left(\sum_J \sum_i n_{iJ}\varepsilon_{iJ}\right)\psi_{\{n_{iJ}\}}. \tag{X.4}$$

If Eq. (X.2) is valid, this means that the fiducial energy is chosen equal to the sum of the ground-state energies of all the particles present in the state $\psi_{\{n_{iJ}\}}$. Note that if the system contains fermions the energy eigenvalue of the lowest state with specified particle numbers is then not zero but a positive number (which is a function of the volume of the system) since all the fermions cannot be in the one-particle ground state simultaneously.

We now set up the grand-canonical ensemble, where we must at first suppose the thermodynamic quantities $\beta = 1/kT$ and $\gamma_J = -\mu_J/kT$, along with the volume V, to be the independent variables. The weight of a state $\psi_{\{n_{iJ}\}}$ in the ensemble is

$$\begin{aligned} w_{\{n_{iJ}\}} &= \frac{1}{P}\exp\left[-\beta\sum_J\sum_i n_{iJ}\varepsilon_{iJ} - \sum_J \gamma_J \sum_i n_{iJ}\right] \\ &= \frac{1}{P}\prod_J\prod_i \exp[-n_{iJ}(\beta\varepsilon_{iJ} + \gamma_J)] = \frac{1}{P}\prod_J\prod_i f_{iJ}^{n_{iJ}}, \end{aligned} \tag{X.5}$$

where

$$f_{iJ} = \exp[-(\beta\varepsilon_{iJ} + \gamma_J)] = \exp\left(-\frac{\varepsilon_{iJ} - \mu_J}{kT}\right). \tag{X.6}$$

The partition function is

$$P = \sum_{\{n_{i\mathrm{J}}\}} \prod_{\mathrm{J}} \prod_{i} f_{i\mathrm{J}}^{n_{i\mathrm{J}}}. \tag{X.7}$$

We can easily reformulate this as an infinite product (cf. Section IX):

$$P = \prod_{\mathrm{J}} \prod_{i} g_{i\mathrm{J}}^{0}, \tag{X.8}$$

where

$$g_{i\mathrm{J}}^{0} = \sum_{k=0}^{k_\mathrm{J}} f_{i\mathrm{J}}^{k} \tag{X.9}$$

with

$$k_\mathrm{J} = \begin{cases} 1 & \text{for fermions} \\ \infty & \text{for bosons} \end{cases}$$

Proving the convergence of our infinite sums and products and the validity of the manipulations with them is fairly easy because of the presence of the strongly decreasing exponentials and the fact that the terms and factors are positive. The infinite sum in Eq. (X.9) in the boson case converges only if $f_{i\mathrm{J}} < 1$, that is,

$$\beta\varepsilon_{i\mathrm{J}} + \gamma_\mathrm{J} > 0 \qquad \text{for all } i \text{ in the boson case.} \tag{X.10}$$

This is true if and only if $\gamma_\mathrm{J} > -\beta\varepsilon_{0_\mathrm{J}}$, that is, $\mu_\mathrm{J} < \varepsilon_{0_\mathrm{J}}$. With the standard choice, Eq. (X.2), we thus have

$$\mu_\mathrm{J} < 0 \qquad \text{for bosons.}$$

[This follows also from the fact that N_J can increase without limit for constant E and V if the particles of type J are bosons (see Section III)].

Equation (X.9) is equivalent to

$$g_{i\mathrm{J}}^{0} = \begin{cases} 1 + f_{i\mathrm{J}} & \text{for fermions} \\ \dfrac{1}{1 - f_{i\mathrm{J}}} & \text{for bosons.} \end{cases} \tag{X.11}$$

Taking the logarithm of Eq. (X.8) gives us the pressure in the system according to Eq. (IX.48):

$$\frac{pV}{kT} = \ln P = \pm \sum_{\mathrm{J}} \sum_{i} \ln(1 \pm f_{i\mathrm{J}}) \tag{X.12}$$

with the upper sign in the fermion case, and the lower sign in the boson case.

Differentiating Eq. (X.12) yields the energy and the number of particles according to Eqs. (IX.46) and (IX.47). However, we can just as easily find these quantities as expectation values [cf. Eq. (IX.36)].

We are mostly interested in operators that are symmetric sums of one-particle operators (or two-particle operators). So let A be of the type

$$A_{\mathrm{K}} = \sum_{p=1}^{N_{\mathrm{K}}} A_p = A_1(\mathbf{r}_1, \sigma_1) + \cdots + A_{N_{\mathrm{K}}}(\mathbf{r}_{N_{\mathrm{K}}}, \sigma_{N_{\mathrm{K}}}), \tag{X.13}$$

where N_{K} varies according to the number of particles of type K in the wavefunction on which A operates. It is an exercise in elementary quantum mechanics to show that

$$\langle \psi_{\{n_{i\mathrm{J}}\}} | A_{\mathrm{K}} | \psi_{\{n_{i\mathrm{J}}\}} \rangle = \sum_i n_{i\mathrm{K}} \langle \varphi_{i\mathrm{K}} | A_1 | \varphi_{i\mathrm{K}} \rangle \tag{X.14}$$

when the $\varphi_{i\mathrm{J}}$ are orthonormal.

With Eq. (X.5) we thus get

$$\begin{aligned}
\overline{\overline{A}}_{\mathrm{K}} &= \frac{1}{P} \sum_{\{n_{i\mathrm{J}}\}} \left(\prod_{\mathrm{J}} \prod_i f_{i\mathrm{J}}^{n_{i\mathrm{J}}} \right) \left(\sum_j n_{j\mathrm{K}} \langle \varphi_{j\mathrm{K}} | A_1 | \varphi_{j\mathrm{K}} \rangle \right) \\
&= \sum_j \langle \varphi_{j\mathrm{K}} | A_1 | \varphi_{j\mathrm{K}} \rangle \frac{(\prod_{\mathrm{J} \neq \mathrm{K}} \prod_i g_{i\mathrm{J}}^0)(\prod_{i \neq j} g_{i\mathrm{K}}^0) g_{j\mathrm{K}}^1}{P} \\
&= \sum_j \langle \varphi_{j\mathrm{K}} | A_1 | \varphi_{j\mathrm{K}} \rangle \frac{g_{j\mathrm{K}}^1}{g_{j\mathrm{K}}^0}
\end{aligned} \tag{X.15}$$

with

$$g_{j\mathrm{K}}^1 = \sum_{k=0}^{k_{\mathrm{K}}} k \cdot f_{j\mathrm{K}}^k \tag{X.16}$$

and k_{K} is again 1 for fermions, and ∞ for bosons.

The average occupation number for the one-particle state $\varphi_{j\mathrm{K}}$ is

$$\overline{\overline{n}}_{j\mathrm{K}} = \frac{g_{j\mathrm{K}}^1}{g_{j\mathrm{K}}^0} = \frac{1}{(1/f_{j\mathrm{K}}) \pm 1} = \frac{1}{e^{(\beta\varepsilon_{j\mathrm{K}} + \gamma_{\mathrm{K}})} \pm 1} \tag{X.17}$$

which is the famous Fermi–Dirac (Bose–Einstein) one-particle distribution function.

If A_{K} is a symmetric sum, $\sum_{p<q} A_{pq}$, of two-particle operators we can also derive a formula for its expectation value; if particles of type K are fermions, the formula is

$$\begin{aligned}
\overline{\overline{A}}_{\mathrm{K}} = \sum_{i<j} [&\langle \varphi_{i\mathrm{K}}(1)\varphi_{j\mathrm{K}}(2) | A_{12} | \varphi_{i\mathrm{K}}(1)\varphi_{j\mathrm{K}}(2) \rangle \\
&- \langle \varphi_{i\mathrm{K}}(1)\varphi_{j\mathrm{K}}(2) | A_{12} | \varphi_{j\mathrm{K}}(1)\varphi_{j\mathrm{K}}(2) \rangle] \overline{\overline{n}}_{i\mathrm{K}} \overline{\overline{n}}_{j\mathrm{K}}.
\end{aligned} \tag{X.18}$$

It should be remarked that these formulas can be derived more elegantly with the aid of the formalism of second quantization.

Let us first put $A_1 = 1$ in Eq. (X.15); we get the obvious formula

$$N_{\mathrm{K}} = \overline{\overline{N_{\mathrm{K}}^{\mathrm{op}}}} = \sum_j \bar{\bar{n}}_{j\mathrm{K}}. \tag{X.19}$$

We can also let A_1 be the kinetic energy operator or the internal energy operator for a single particle of kind K; we then get

$$\overline{\overline{E_{\mathrm{K}}^{\mathrm{kin}}}} = \sum_j \bar{\bar{n}}_{j\mathrm{K}}\, \varepsilon_{j\mathrm{K}}^{\mathrm{kin}}, \tag{X.20}$$

$$\overline{\overline{E_{\mathrm{K}}^{\mathrm{intl}}}} = \sum_j \bar{\bar{n}}_{j\mathrm{K}}\, \varepsilon_{j\mathrm{K}}^{\mathrm{intl}} \tag{X.21}$$

[cf. Eq. (X.1)]. Quantity $\overline{\overline{E_{\mathrm{K}}^{\mathrm{intl}}}}$ (the sum of the internal one-particle energies of the particles of kind K) should not be confused with the internal energy of the total system, which is just

$$E = \overline{\overline{E^{\mathrm{op}}}} = \sum_{\mathrm{J}} \left(\overline{\overline{E_{\mathrm{J}}^{\mathrm{kin}}}} + \overline{\overline{E_{\mathrm{J}}^{\mathrm{intl}}}}\right) = \sum_{\mathrm{J}} \sum_i \bar{\bar{n}}_{i\mathrm{J}}\, \varepsilon_{i\mathrm{J}}. \tag{X.22}$$

We have now found p, N_{K}, and E, and we get the entropy S from the thermodynamic identity Eq. (IX.48). Let us also consider a sample of pure "J gas" with volume V, temperature T, and chemical potential μ_{J}. We can compute its pressure $p_{\mathrm{J,\,pure}}$ and the quantities $E_{\mathrm{J,\,pure}}^{\mathrm{kin}}$, $E_{\mathrm{J,\,pure}}^{\mathrm{intl}}$, and $N_{\mathrm{J,\,pure}}$. We find that the mixture quantities are related to the pure-gas quantities by the following formulas, which are valid only for ideal gases (we will henceforward leave out the bars over expectation values):

$$\begin{aligned} p &= \sum_{\mathrm{J}} p_{\mathrm{J,\,pure}}, \\ N_{\mathrm{J}} &= N_{\mathrm{J,\,pure}}, \\ E_{\mathrm{J}}^{\mathrm{kin}} &= E_{\mathrm{J,\,pure}}^{\mathrm{kin}}, \\ E_{\mathrm{J}}^{\mathrm{intl}} &= E_{\mathrm{J,\,pure}}^{\mathrm{intl}}. \end{aligned} \tag{X.23}$$

Our expressions (X.12), (X.19), (X.20), and (X.21) imply infinite summations over the indices n_x, n_y, n_z, and m for each kind of particle. Normally the summands are so smooth that the summations over the n can be replaced by integrations. The exception (Einstein condensation) occurs for bosons at very low temperatures, in which case the term for $n_x = n_y = n_z = 0$ must be considered separately. We will not treat this case here but refer to the special literature.

The integrations can be performed by a transformation to polar coordinates in "n space" ($\mathbf{k}$ space) and result in the following formulas, which are valid when Einstein condensation does not occur:

$$
\begin{aligned}
N_{\mathrm{K}} &= F_{\mathrm{K}} \sum_{m_{\mathrm{K}}} h_1^{\pm}(\beta\varepsilon_{m_{\mathrm{K}}}^{\mathrm{intl}} + \gamma_{\mathrm{K}}), \\
E_{\mathrm{K}}^{\mathrm{kin}} &= \frac{F_{\mathrm{K}}}{\beta} \sum_{m_{\mathrm{K}}} h_2^{\pm}(\beta\varepsilon_{m_{\mathrm{K}}}^{\mathrm{intl}} + \gamma_{\mathrm{K}}), \\
E_{\mathrm{K}}^{\mathrm{intl}} &= F_{\mathrm{K}} \sum_{m_{\mathrm{K}}} \varepsilon_{m_{\mathrm{K}}}^{\mathrm{intl}}\, h_1^{\pm}(\beta\varepsilon_{m_{\mathrm{K}}}^{\mathrm{intl}} + \gamma_{\mathrm{K}}), \\
p_{\mathrm{K}} V &= \frac{F_{\mathrm{K}}}{\beta} \sum_{m_{\mathrm{K}}} h_0^{\pm}(\beta\varepsilon_{m_{\mathrm{K}}}^{\mathrm{intl}} + \gamma_{\mathrm{K}}) = \frac{2}{3} E_{\mathrm{K}}^{\mathrm{kin}},
\end{aligned}
\tag{X.24}
$$

where

$$
\beta = \frac{1}{kT}; \quad \gamma_{\mathrm{K}} = -\frac{\mu_{\mathrm{K}}}{kT}; \quad F_{\mathrm{K}} = \frac{4\pi V}{(2\pi\hbar)^3}\left(\frac{2M_{\mathrm{K}}}{\beta}\right)^{3/2}; \tag{X.25}
$$

[see also Eqs. (X.22) and (X.23)]. The nonelementary functions $h_0^{\pm}$, $h_1^{\pm}$, and $h_2^{\pm}$ (plus sign for fermions; minus sign for bosons) are defined by

$$
\begin{aligned}
h_0^{\pm}(s) &= \pm\int_0^{\infty} \ln(1 \pm e^{-(r^2+s)})r^2\,dr = \tfrac{2}{3}h_2^{\pm}(s) \qquad \text{(by partial integration)}, \\
h_1^{\pm}(s) &= \int_0^{\infty} \frac{1}{e^{r^2+s} \pm 1}\, r^2\,dr, \\
h_2^{\pm}(s) &= \int_0^{\infty} \frac{1}{e^{r^2+s} \pm 1}\, r^4\,dr.
\end{aligned}
\tag{X.26}
$$

Note that factor F_{K} is a large dimensionless quantity that is of the order of magnitude of the ratio between the total volume V of the system and the "thermal volume" λ_{K}^3 of a single particle [see Eq. (V.11)]. Functions h_0, etc., are exponentially decreasing for large s. The summations in Eq. (X.24) run over the internal (including rotational) stationary states of the "particles" (molecules). The average number of molecules that are in internal state m_{K} is $F_{\mathrm{K}} h_1^{\pm}(\beta\varepsilon_{m_{\mathrm{K}}}^{\mathrm{intl}} + \gamma_{\mathrm{K}})$.

The "ideal gas laws," Eq. (X.24) are, of course, not yet of the form Eq. (III.1) that we have taken as the fundamental form of the equation of state in earlier sections. If the independent variables are E, V, and the N_{J}, one must in general solve for β and the γ_{J} in terms of the independent variables (which, of course, is not possible in closed form).

We now want to derive the Maxwell-Boltzmann formulas of Section V as approximations. This is easily done by deriving power series expansions valid for $\gamma_{\mathrm{K}} > 0$ and then neglecting all terms except the first.

When $\gamma_K > 0$, we have $\exp[-(r^2 + \beta\varepsilon^{\text{intl}}_{m_K} + \gamma_K)] < 1$. Therefore the integrands in Eq. (X.26) can be expanded:

$$\frac{1}{e^{r^2+s} \pm 1} = \frac{e^{-(r^2+s)}}{1 \pm e^{-(r^2+s)}} = e^{-(r^2+s)} \mp e^{-2(r^2+s)} + \cdots, \tag{X.27}$$

etc., and the termwise integrations over r are then easily performed, leading to infinite series. Since these have the form of power series in the z_K, they are, in fact, identical to the corresponding cluster expansions (see Section IX). Their first terms are

$$\begin{aligned} N_K &= \frac{\sqrt{\pi}}{4} F_K a_K z_K + \cdots, \\ E^{\text{kin}}_K &= \frac{3}{2}\frac{\sqrt{\pi}}{4} F_K \frac{1}{\beta} a_K z_K + \cdots, \\ E^{\text{intl}}_K &= \frac{\sqrt{\pi}}{4} F_K \varepsilon'_K z_K + \cdots, \\ p_K V &= \tfrac{2}{3} E^{\text{kin}}_K \end{aligned} \tag{X.28}$$

with

$$\begin{aligned} z_k = \exp(-\gamma_K); \qquad a_K &= \sum_{m_K} \exp(-\beta \cdot \varepsilon^{\text{intl}}_{m_K}); \\ \varepsilon'_K &= \sum_{m_K} \varepsilon^{\text{intl}}_{m_K} \exp(-\beta \cdot \varepsilon^{\text{intl}}_{m_K}). \end{aligned} \tag{X.29}$$

In the Maxwell-Boltzmann case, $z_K \ll 1$, that is, $N_k \ll F_K$, the higher terms can be neglected. The resulting simple formulas, which can be rewritten as

$$\begin{aligned} E^{\text{kin}}_K &= \tfrac{3}{2} kT \cdot N_K, \\ E^{\text{intl}}_K &= \frac{\varepsilon'_K}{a_K} \cdot N_K, \\ p_K V &= kT \cdot N_K, \\ \mu_K &= kT \cdot \ln \frac{4}{\sqrt{\pi}} \frac{N_K}{F_K \cdot a_K} = kT \ln \frac{(2\pi\hbar)^3 \cdot N_K}{\pi^{3/2} \cdot (kT)^{3/2} \cdot (2M_K)^{3/2} \cdot V \cdot a_K}, \end{aligned} \tag{X.30}$$

degenerate into the formulas of Section V when the internal spectrum of the particles contains only a ground-state level of degeneracy D_K plus high-lying levels for which the exponentials in Eq. (X.29) are negligible, so that $a_K \approx D_K$, $\varepsilon'_K \approx 0$ because of Eq. (X.2).

In the Maxwell–Boltzmann case we also get from Eq. (X.17)

$$\bar{\bar{n}}_{j\mathrm{K}} \approx e^{-(\beta\varepsilon_{i\mathrm{K}} + \gamma_{\mathrm{K}})} = z_{\mathrm{K}}\, e^{-\beta\varepsilon_{j\mathrm{K}}}; \tag{X.31}$$

the Maxwell–Boltzmann one-particle distribution. It is clear that the Maxwell–Boltzmann case is just the case in which all the $\bar{\bar{n}}_{i\mathrm{J}}$ are small.

Quantity a_{K} is sometimes called the "internal molecular partition function" since it formally looks like a canonical partition function for a system consisting of a single molecule (where only its internal states are taken into account). The average number of molecules in internal state m_{K} is proportional to the Boltzmann factor $\exp(-\beta\varepsilon_{m_{\mathrm{K}}}^{\mathrm{intl}})$; therefore, the average internal energy of one molecule K is $\varepsilon'_{\mathrm{K}}/a_{\mathrm{K}}$, in agreement with Eq. (X.30).

We will just say a few words about the treatment of systems composed of interacting particles. We can divide these into systems with weakly interacting particles and systems with strongly interacting particles (where "weak" and "strong" are not used in the quite specific sense that they have in the theory of elementary particles). Systems of strongly interacting particles are usually treated by means of some kind of formal transformation, sometimes explicitly exhibited or sometimes just implicitly supposed to exist, after which transformation the system can formally be regarded as a system of weakly interacting "quasi particles," or rather approximated or simulated (at least as regards certain of its properties) in a certain region of conditions by a "model system" of weakly interacting particles. One very well-known example of this is what we have done in Sections V and X, namely to regard a system composed of strongly interacting nucleons and electrons as a system of weakly interacting molecules. Another case is when one regards the vibrational states of a solid as states of an assembly of weakly interacting phonons. Many other formalisms of this type have been developed more recently; we just mention the band theory of the electronic properties of solids, the Debye–Hückel theory of ionic solutions, the Landau theory of superfluidity, and the BCS theory of superconductivity.

Weakly interacting systems are usually treated by means of the basic formulas (X.17), etc., where the "quasi-particle state spectra" may, however, be quite different from the free-particle spectra considered in Section X; they may, for instance, show band gaps. The interactions may be corrected for by various more-or-less *ad hoc* corrections containing adjustable parameters (for instance in the van der Waal's equation) or by cluster expansions (see Section IX), Green's function techniques, etc. The coefficients in the resulting approximate formulas may sometimes be calculated explicitly or they may sometimes be adjusted to fit experimental data.

When one is treating dilute systems of weakly interacting particles at "high temperature," one often starts the treatment by going over to the approximation of classical statistical mechanics (see TN 401).

XI. Equilibrium Fluctuations in Nonconserved Quantities

Earlier we stressed that in the normal case nearly all the wavefunctions in a microcanonical ensemble yield almost the same expectation values for operators of physical interest. In this final section, we discuss, in a rather loose and heuristic manner, the deviations from this rule and their possible physical significance.

According to the principles of quantum mechanics, the probability that a quantity A attains a value between the limits a_1 and a_2 is

$$P_A^{(a_1, a_2)} = \mathrm{Tr}(O_A^{(a_1, a_2)}\rho), \tag{XI.1}$$

where ρ is the statistical operator and $O_A^{(a_1, a_2)}$ is the spectral projection operator from the spectral resolution of A belonging to the interval (a_1, a_2); O_{A} projects onto the subspace spanned by those eigenfunctions of A whose eigenvalues lie in this interval. As a measure of the "statistical spread" of the values of A, we take the quantity $(\Delta A)^2$ defined by

$$\begin{aligned}(\Delta A)^2 &= \overline{A^2} - \overline{\overline{A}}^2 = \mathrm{Tr}(A^2\rho) - (\mathrm{Tr}(A\rho))^2 \\ &= \mathrm{Tr}((A - \overline{\overline{A}})^2\rho).\end{aligned} \tag{XI.2}$$

For a microcanonical ensemble,

$$\rho = \sum_i{}' \, |\psi_i\rangle\langle\psi_i|. \tag{XI.3}$$

This becomes

$$(\Delta A)^2 = \frac{1}{\Gamma}\sum_i{}' \, (\Delta A_i^q)^2 + (\Delta\overline{A}^{\mathrm{ens}})^2, \tag{XI.4}$$

where the first term is an ensemble average over the "squared quantum width" of A in each state i,

$$(\Delta A_i^q)^2 = \langle\psi_i|A^2|\psi_i\rangle - (\langle\psi_i|A|\psi_i\rangle)^2, \tag{XI.5}$$

and the second term is a measure of the spread in expectation values within the ensemble,

$$\begin{aligned}(\Delta\overline{A}^{\mathrm{ens}})^2 &= \frac{1}{\Gamma}\sum_i{}' \, (\langle\psi_i|A|\psi_i\rangle)^2 - \overline{\overline{A}}^2 \\ &= \frac{1}{\Gamma}\sum_i{}' \, (\langle\psi_i|A|\psi_i\rangle - \overline{\overline{A}})^2.\end{aligned} \tag{XI.6}$$

The two terms are not separately invariant under unitary transformations among the ψ_i, although their sum is. If, however, A should happen to commute with ρ, the ψ_i can be chosen as eigenfunctions of A, in which case the first term will be zero, and the statistical spread of A values can be ascribed entirely to the spread in expectation values within the ensemble. We will deal here essentially with cases where A nearly, but not quite, commutes with ρ. We will assume that choosing the ψ_i as "near eigenfunctions" of A will yield a separation of $(\Delta A)^2$ in which the ensemble spread in expectation values is more important than the "quantum spread."

We suppose (see Section IV) that the microcanonical ensemble represents an isolated system in a state of quasi equilibrium with certain values B_k^0 of the quasi-conserved variables B_k, so that

$$\begin{aligned} \rho &= \frac{1}{\Gamma} \prod_k O_{B_k}^{(B_k^1,\, B_k^2)}, \\ \Gamma &= \operatorname{Tr}\left(\prod_k O_{B_k}^{(B_k^1,\, B_k^2)} \right). \end{aligned} \tag{XI.7}$$

We further suppose that A represents a quantity that is not quasi-conserved but, nevertheless, commutes approximately with ρ. Often it may represent a quantity belonging to some subsystem of our isolated system. Equation (XI.1) gives us the probability of finding a value of A between a_1 and a_2; we will assume that this probability is essentially independent of the size of the other intervals (B_k^1, B_k^2) that we use to define our microcanonical ensemble, although it must obviously depend on the size of (a_1, a_2).

Primarily, this probability refers to the probability of finding a value of A between a_1 and a_2 if we make an observation on a system chosen at random from an appropriate statistical ensemble of similar systems. However, one usually makes a certain rather tenuous "ergodic hypothesis." We suppose that the value of A in an individual macroscopic system will execute "random oscillations" (fluctuations) about its mean value $\overline{\overline{A}}$. The postulate states that, if we follow an isolated system over a sufficiently long time, we will find that the value of A lies in (a_1, a_2) a fraction of the total time that is equal to the said probability $P_A^{(a_1, a_2)}$.

The experimental evidence for the quantitative validity of this postulate would hardly seem to be overwhelming. Strictly speaking, however, it is hardly possible to disprove it experimentally, since the ergodic postulate per se says nothing whatsoever about *how* long the "long time" must be taken; this is a kinetic problem belonging outside the domain of equilibrium statistical mechanics. In practice, it seems to be the rule that if the spread ΔA is large, the time necessary will be very long (often longer than the quasi-equilibrium character of the macrostate is really valid) when A is a macroscopic quantity such as the energy of a macroscopic subsystem. As an example, we may take operator A to represent the position of a small body floating on a liquid surface. The Brownian motion will eventually carry it around the whole surface, but the time that will pass before the body has moved even, say, 1 cm will be long if the body is of macroscopic size, and the time that will elapse before it has been close to every part of the surface is, of course, much longer.

The so-called quasi-thermodynamic theory of fluctuations aims at providing us with quantitative estimates of probabilities of type $P_A^{(a_1, a_2)}$. We first notice that the operator,

$$O_A^{(a_1, a_2)} O_B^{(B_1{}^1, B_1{}^2)} O_B^{(B_2{}^1, B_2{}^2)} \ldots, \tag{XI.8}$$

has the form of a new microcanonical ensemble operator, where A is now among the defining variables. Its trace can formally be used to define an entropy $\tilde{S}_{\Delta a}$ according to (we put $a_0 = (a_1 + a_2)/2$; $\Delta a = a_2 - a_1$)

$$\exp\left[\frac{1}{k}\tilde{S}_{\Delta a}(a_0, B_1^0, B_2^0, \ldots)\right] = \mathrm{Tr}(O_A^{(a_1, a_2)} \cdots) = \Gamma \cdot P_A^{(a_1, a_2)}, \tag{XI.9}$$

where we have used Eqs. (XI.1) and (XI.7). For the ratios between probabilities belonging to different intervals, we find

$$\frac{P_A^{(a_1, a_2)}}{P_A^{(a_3, a_4)}} = \exp\left\{\frac{1}{k}\left[\tilde{S}_{a_2 - a_1}\left(\frac{a_1 + a_2}{2}, B_1^0, \ldots\right) - \tilde{S}_{a_4 - a_3}\left(\frac{a_3 + a_4}{2}, \ldots\right)\right]\right\} \tag{XI.10}$$

which according to the "ergodic postulate" should govern the ratios between the probabilities that the quantity A "fluctuates into" this or that interval. However, insofar as these ratios are measurable in practice, they must correspond to entropy differences that are far too small to be measured as such.

We assume that $\tilde{S}_{\Delta a}(a_0, \ldots)$ is a smooth function of a_0 for constant Δa. "Normally" this function has a well-defined maximum so that $\exp(\tilde{S}(a_0)/k)$ takes the form of a sharp Gaussian distribution (cf. Section IX). This fact can be used to obtain an approximate formula for the dispersion ΔA with respect to our original ensemble ρ. Let us divide the range of A into small intervals of equal size Δa, separated by a net of points $\{a_i\}$. According to the spectral theorem, we have

$$A^n \approx \sum_i \left(\frac{a_i + a_{i+1}}{2}\right)^n O_A^{(a_i, a_{i+1})} \tag{XI.11}$$

and, therefore,

$$(\Delta A)^2 = \overline{\overline{A^2}} - \overline{\overline{A}}^2 \approx \frac{1}{\Gamma}\sum_i \left(\frac{a_i + a_{i+1}}{2}\right)^2 \exp\left[\tilde{S}_{\Delta a}\left(\frac{a_i + a_{i+1}}{2}, \ldots\right)\Big/k\right]$$
$$- \left\{\frac{1}{\Gamma}\sum_i \frac{a_i + a_{i+1}}{2} \exp\left[\tilde{S}_{\Delta a}\left(\frac{a_i + a_{i+1}}{2}, \ldots\right)\Big/k\right]\right\}^2. \qquad \text{(XI.12)}$$
$$1 = \frac{1}{\Gamma}\sum_i \exp\left[\tilde{S}_{\Delta a}\left(\frac{a_i + a_{i+1}}{2}, \ldots\right)\Big/k\right].$$

If we take Δa small enough, our sums become integrals:

$$(\Delta A)^2 \approx \frac{\int a^2 e^{S_{\Delta a}(a, \ldots)/k}\, da}{\int e^{S_{\Delta a}(a, \ldots)/k}\, da} - \left[\frac{\int a e^{S_{\Delta a}(a, \ldots)/k}\, da}{\int e^{S_{\Delta a}(a, \ldots)/k}\, da}\right]^2. \qquad \text{(XI.13)}$$

We expand $\tilde{S}_{\Delta a}(a)$ around its maximum at a^*:

$$\tilde{S}_{\Delta a}(a) = \tilde{S}_{\Delta a}(a^*) + \frac{1}{2}\left[\frac{\partial^2 \tilde{S}}{\partial a^2}\right]_{a=a^*}(a - a^*)^2 + \cdots. \qquad \text{(XI.14)}$$

Here it will sometimes be sufficient to consider only the second-order term. For the integrals will receive contributions essentially from the region where $|a - a^*|$ is of the order of magnitude of $(k/|\partial^2\tilde{S}/\partial a^2|)^{1/2}$. This is a very small quantity unless the second derivative is itself very small so that the maximum is very flat; we provisionally exclude this case. The higher order terms will be negligible in the important region; for instance, the third-order term in Eq. (XI.14) is of order $\sqrt{k^3}$, leading to a factor of order $\exp(\sqrt{k})$ in the integrands of Eq. (XI.13), which factor is so nearly unity that it can be neglected. Therefore the distribution of A values is a simple Gaussian one. The dispersion (width) ΔA is found from Eq. (XI.13) to be just

$$\Delta A = \sqrt{\frac{k}{|\partial^2\tilde{S}/\partial a^2|_{a=a^*}}}. \qquad \text{(XI.15)}$$

We note that it is proportional to the square root of the "amount parameter" t (see Section III); the relative width $\Delta A/\overline{\overline{A}}$ is proportional to $1/\sqrt{t}$ (cf. also Section IX). (We get of course also $\overline{\overline{A}} = a^*$.)

Usually, however, the fluctuations become quantitatively measurable only when $|\partial^2\tilde{S}/\partial a^2|$ is small, so that higher order terms in the expansion of $\tilde{S}$ may become important. Therefore the simple formula (XI.15) is perhaps mostly of theoretical interest.

The derivatives of $\tilde{S}$ can often be estimated by studying states $(a, B_1^0, B_2^0, \ldots)$ of the system that are defined by values of a that are sufficiently different from a^* so that the entropy differences between the states are thermodynamically measurable. This, of course, presupposes that such states exist and are amenable to experimental study. If this is the case, it follows from Eq. (XI.9) that the macroscopically measurable entropy $S(a, B_1^0, \ldots)$ is equal to $\tilde{S}_{\Delta a}(a, \ldots)$ to within a macroscopically negligible error. Since $\tilde{S}_{\Delta a}(a, \ldots)$ must presumably be a microscopically and macroscopically smooth function of a, it seems reasonable to conclude that the "microscopic derivatives" of $\tilde{S}_{\Delta a}$ must be equal to the macroscopically measurable derivatives of S.

One case in which it may be possible to apply this kind of reasoning is when we deal with a subsystem of a larger subsystem that is isolated and in equilibrium; the thermodynamic parameters of the subsystem can then show fluctuations. Let us consider a specific instance. Subsystem 1 is the contents of a certain arbitrarily delimited constant "zone" in space; its energy E_1 and mole numbers N_{A1}, etc., can clearly fluctuate. Subsystem 2 is the rest of our isolated system; we assume that the usual additivity laws are valid. According to the principles stated in the foregoing, the probability of finding a given set of values E_1^0, $N_{A1}^0, \ldots$ of the parameters should be proportional to

$$\exp\left\{\frac{1}{k}\left[S_1(E_1^0, V_1, N_{A1}^0, \ldots) + S_2(E - E_1^0, V_2, N_A - N_{A1}^0, \ldots)\right]\right\}. \tag{XI.16}$$

The same result, however, can be obtained from an ensemble that refers only to system 1, if we let it be a weighted ensemble of the type discussed in Section IX, with

$$f(E_1, N_{A1}, \ldots) = -S_2(E - E_1, V_2, N_A - N_{A1}, \ldots) + \text{const.} \tag{XI.17}$$

It is, therefore, plausible that we can use such an ensemble to describe a subsystem of an isolated system in equilibrium, although the argument given is admittedly far from sufficient to prove this. A more detailed motivation can undoubtedly be given, but since we do not consider this point to be of central importance in statistical mechanics, we will not discuss it further.

We see from Eq. (XI.17) that if subsystem 2 has the character of an "energy-particle reservoir" (cf. Section VII) so that the entropy S_2 is linear in its arguments, the ensemble describing subsystem 1 will be a grand-canonical ensemble. However, we should be careful to apply such arguments only in the case of macroscopic subsystems. One might try to apply the canonical ensemble formalism to a subsystem consisting of a single molecule that is part of a macroscopic sample of an ideal gas. This would lead to the conclusion that the state of the molecule could be described by an ensemble (one-particle density matrix) of the form

$$\rho = \text{const.} \sum_i e^{-\beta\varepsilon_i} |\phi_i\rangle\langle\phi_i|. \tag{XI.18}$$

As we see from Section X, this is in general not true; the one-particle density matrix is of the Fermi or Bose type:

$$\rho = \text{const.} \sum_i \frac{1}{e^{\beta\varepsilon_i + \gamma} \pm 1} |\phi_i\rangle\langle\phi_i|. \tag{XI.19}$$

Only under Maxwell–Boltzmann conditions can this be approximated by Eq. (XI.18).

ACKNOWLEDGMENTS

The author is indebted to Dr. E. G. Larson for valuable discussions, to P. Kaijser for reading through the original manuscript and suggesting various improvements, and to the editor for suggesting that the article be cut to reasonable size.

REFERENCES

Callen, H. B. (1960). "Thermodynamics." Wiley, New York.

Chintschin, A. J. (1956). "Mathematische Grundlagen der Quantenstatistik." Akademie-Verlag, Berlin.

Fowler, R., and Guggenheim, E. A. (1952). "Statistical Thermodynamics." Cambridge Univ. Press, London and New York.

Gibbs, J. W. (1902). "Elementary Principles in Statistical Mechanics." Yale Univ. Press, New Haven, Connecticut (reprinted by Dover, New York, 1960).

Hatsopoulos, G. N., and Gyftopoulos, E. P. (1976). *Found. Phys.* **6**, 15, 127, 439, and 561.

Huang, K. (1963). "Statistical Mechanics." Wiley, New York.

Jaynes, E. T. (1957). *Phys. Rev.* **106**, 620.

Kittel, C. (1958). "Elementary Statistical Physics." Wiley, New York.

Landau, L. D., and Lifshitz, E. M. (1959). "Statistical Physics." Pergamon, Oxford.

Löwdin, P. O. (1967). *Adv. Quantum Chem.* **3**, 323.

Mayer, J. E., and Mayer, M. G. (1940). "Statistical Mechanics." Wiley, New York.

Sperber, G. (1974). *Found. Phys.* **4**, 163.

Tolman, R. C. (1938). "The Principles of Statistical Mechanics." Oxford Univ. Press, London and New York.

Uppsala Quantum Chemistry Group. (1973). "An Introduction for Quantum Chemists to Equilibrium Thermodynamics and Statistical Mechanics," Tech. Note No. 401 (unpublished).

von Neumann, J. (1955). "Mathematical Foundations of Quantum Mechanics." Princeton Univ. Press, Princeton, New Jersey.

Yourgrau, W., van der Merwe, A., and Raw, G. (1966). "Treatise on Irreversible and Statistical Thermophysics." Macmillan, New York.

Subject Index